東京帝國大學

地震研究所彙報

第六號

昭和四年四月發行

目次

論文

方位的分布を持つレーレー波の續研究（英文）……所員 妹澤克惟
水中衝撃による深海波の生成（英文）……所員 妹澤克惟
方位的及帶狀的に分布せる表面應力を受ける彈性球體の平衡（英文）……所員 妹澤克惟／所員 西村源六郎
矯狀體の減衰振動（英文）……所員 末廣恭二
昭和二年丹後地震後の水準測量成果の一解釋（英文）……所員 坪井忠二
潮汐の負荷による地殼の傾斜運動（英文）……所員 高橋龍太郎
砂層の崩壞に關する實驗（第二報）（英文）……所員 寺田寅彦／所員 宮部直巳
地震發生の機巧に就いて（邦文）……所員 石本巳四雄
大正十二年相模灘大地震の機巧に就いて（英文）……所員 藤原咲平／所員 高山威雄
最近の二三の大地震の觀測及其走時曲線（第二回）（英文）……所員 松澤武雄
最近の二三の大地震の觀測及其走時曲線（第三回）（英文）……所員 松澤武雄
最近の二三の大地震の觀測及其走時曲線（第四回）（英文）……所員 松澤武雄
地震の震源の位置と地震波の傳播速度とを求める圖法（英文）……所員 高橋龍太郎
丹後地震の餘震觀測調査報告（第一報）（邦文）……囑託 那須信治
地球上に於ける地震活動地域平均緯度の長期移動（英文）……所員 寺田寅彦／所員 宮部直巳
東京帝國大學法學部、文學部及經濟學部講義室鐵骨架構の振動觀測に就いて（邦文）……所員 内田詳三／囑託 齋田時太郎／武藤清

報告

東京天文臺におけるリーフラー時計の遲速度變化と地震發生（英文）……所員 石本巳四雄／囑託 辻光之助

所報

(The titles in occidental languages are given on the back cover.)

本彙報ハ不定期ニ發行ス.

本彙報掲載ノ報告ニ關シテハ著者ノミニ責任アルモノトス.

本彙報ニ關スル照會通信ハ東京帝國大學地震研究所長ニ宛テラレタシ.

The bulletin is published at irregular intervals.

The authors of the papers alone are responsible for the statements and opinions.

All communications relating to this bulletin should be addressed to the Director of the Earthquake Research Institute, Tokyo Imperial University.

地震研究所彙報　第六號　目次

論　文

頁

方位的分布を持つレーレー波の續研究（英文）…… 所員　妹澤克惟… 1

水中衝撃による深海波の生成（英文）…… 所員　妹澤克惟… 19

方位的及帶狀的に分布せる表面應力を受ける彈性球體の平衡（英文）……（所員　妹澤克惟／所員　西村源六郎）… 47

壔狀體の減衰振動（英文）…… 所員　末廣恭二… 63

昭和二年丹後地震後の水準測量成果の一解釋（英文）…… 所員　坪井忠二… 71

潮汐の負荷による地殼の傾斜運動（英文）…… 所員　高橋龍太郎… 85

砂層の崩壞に關する實驗（第二報）（英文）……（所員　寺田寅彦／所員　宮部直巳）… 109

地震發生の機巧に就いて（邦文）…… 所員　石本巳四雄… 127

大正十二年相模灘大地震の機巧に就いて（英文）……（所員　藤原咲平／所員　高山威雄）… 149

最近の二三の大地震の觀測及其走時曲線（第二回）（英文）…… 所員　松澤武雄… 177

最近の二三の大地震の觀測及其走時曲線（第三回）（英文）…… 所員　松澤武雄… 205

最近の二三の大地震の觀測及其走時曲線（第四回）（英文）…… 所員　松澤武雄… 213

地震の震源の位置と地震波の傳播速度とを求める圖法（英文）…… 所員　高橋龍太郎… 231

丹後地震の餘震觀測調査報告（第一報）（邦文）…… 囑託　那須信治… 245

地球上に於ける地震活動地域平均緯度の長期移動（英文）……（所員　寺田寅彦／所員　宮部直巳）… 333

東京帝國大學法學部，文學部及經濟學部講義室鐵骨架構の振動觀測に就いて（邦文）……（所員　内田詳三／囑託　齋田時太郎／武藤清）… 345

報　告

東京天文臺におけるリーフラー時計の遲速度變化と地震發生……（所員　石本巳四雄／囑託　辻光之助）… 354

所　報 …… 359

CONTENTS OF VOLUME VI

Papers Contributed

		Page
Further Studies on Rayleigh-waves having Some Azimuthal Distribution. (in English)	K. Sezawa	1
Formation of Deep-Water Waves due to Subaqueous Shocks. (in English)	K. Sezawa	19
Elastic Equilibrium of a Spherical Body under Surface Tractions of a Certain Zonal and Azimuthal Distribution. (in English)	K. Sezawa, G. Nishimura	47
On the Damped Transversal Vibration of Prismatic Bars. (in English)	K. Suyehiro	63
An Interpretation of the Results of the Repeated Precise Levellings in the Tango District after the Tango Earthquake in 1927. (in English)	C. Tsuboi	71
Tilting Motion of the Earth Crust caused by Tidal Loading. (in English)	R. Takahashi	85
Experiment Investigations of the Deformation of Sand Mass by Lateral Pressure. (with an Appendix.) (in English)	T. Terada, N. Miyabe	109
Sur le mécanisme de la production des ondes sismiques. (in Japanese)	M. Ishimoto	127
On the Mechanism of the Great Sagami Bay Earthquake on September 1, 1923. (in English)	S. Fujiwhara, T. Takayama	149
Observation of Some Recent Earthquakes and their Time-distance Curves. (Part II) (in English)	T. Matuzawa	177
Observation of Some Recent Earthquakes and their Time-distance Curves. (Part III) (in English)	T. Matuzawa	205
Observation of Some Recent Earthquakes and their Time-distance Curves. (Part IV) (in English)	T. Matuzawa	213
A Graphical Determination of the Position of the Hypocenter of an Earthquake and the Velocity of the Propagation of the Seismic Waves. (in English)	R. Takahashi	231
On the Aftershocks of the Tango Earthquake. (in Japanese)	N. Nasu	245
A Long Period Fluctuation in Latitude of the Seismic Activity of the Earth. (in Engiish)	T. Terada, N. Miyabe	333
An Investigation of the Vibration of a Steel Frame. (in Japanese)	Y. Uchida, T. Saida, K. Muto	345

Report

Monthly Means of the Daily Rates of the Riefler Clock in the Tôkyô Astronomical Observatory and their Bearing on the Occurrence of Earthquakes.	M. Ishimoto, K. Tuzi	354

Institute Notes 359

東京帝國大學

地震研究所彙報

第　六　號

Further Studies on Rayleigh-waves having Some Azimuthal Distribution.

By **Katsutada SEZAWA,**

Member of the Institute.

方位的分布を持つレーレー波の續研究

所員　妹澤克惟

彈性體の內部を傳はる波が變位分布の方向性を示す如く、表面波にも斯る性質があつてよい筈である。其序說は旣に發表してあるが、この論文では其委細と延長とを述べる事にした。さて地震學上で問題となる所の押し引きの法則が表面波にあてはまるかどうかと言ふ事や、遠距離地震波の主要部に橫波の優勢な事や、又地殼內部の振動型が遠方の表面で如何なる特性を示すかと言ふ問題等は、すべてこの研究の結果によつて、可なりの程度まで明かにされる樣に思はれる。それのみでなく彈性力學其自身の問題としても多少重要であらう。

論文は二部に分れ、第一部では、半無限體の表面に方位的分布を持つて波動するレーレー波の解と、其一般問題及び彈性體の內部に振動原がある時斯るレーレー波が生ずる場合等が說明され、第二部では球面上に於て、方位的分布を持つレーレー波が傳はる機構を示した。

主要な結果を摘錄すれば、

（1）方位的分布を持つレーレー波は平面上でも、球面上でも其方位的分布が其波線上に擴散される事なく、傳播される。

（2）固體平面上をレーレー波が傳はる場合に、普通のレーレー波に似た變位はどこまでも保たれるが夫に直角な變位は、波動が原點から遠ざかるに從つて次第に消滅する。この性質はあらゆる方向に擴がる彈性體中の波動とは大分違つてゐる。

（3） 地震の押しと引きの法則は横の變位さへ考へなければ、やはり成立する。
（4） 半無限體の内部に振動原がある時も、遠方の表面波の方位性は或程度まで原點のものと一致する。
（5） 球の曲率が考慮に入る程の長波では、震波赤道に於てさへも可なりの横變位が殘り、震原近所では寧ろ横變位の方がレーレー波の普通の變位よりも勝つてゐる。
（6） 短波長の波でも震原附近だけは可なりの横振動がある。

In a previous paper(1) the author had the occasion of studying the propagation of Rayleigh-waves having a certain azimuthal distribution on the surface of a semi-infinite solid body. Although that investigation has been carried out for a simple case where the harmonic waves of varying fronts along the azimuthal direction are generated from a source on the surface of the body, yet some natures different from the surface waves of symmetrical distribution have been discovered. The present problem has been given for the purpose of studying, together with the detailed explanation of the foregoing solution, the more extended cases such as the motion due to an arbitrary initial disturbance, waves due to the source in the interior of the body or the transmission of these waves on a spherical surface.

The question how the shocks of unsymmetrical type in the vicinity of the epicentre will be transmitted on the surface of the elastic body is very important, besides on the theoretical problem of radiation of waves of such a type, on the law of pull and push concerning the surface waves. The case(2) of pull and push for bodily elastic waves had already been employed by many seismologists to find the mechanism of the disturbance at the epicentral region. Though it is not easy to select the leading part of the surface waves of the present type from the seismic records, the application of the present theory on such leading part, if possible, will be much significant for the determination of the disturbance at the epicentral region. The case of the transmission of waves in some dispersive medium should be excluded from the practical application, because in this the leading

(1) *Proc. Imp. Acad.* **4** (1928) p. 267.
(2) Prof. Shida's idea.

parts at a distance cannot give the nature[1] of the waves in the neighbourhood of the region. At a distance not so far from the disturbed region, the law of pull and push will, of course, be consistent even though the material of the earth has a slight dispersive property.

The present paper consists of two parts: the first part deals with the problems concerning the transmission of waves on the surface of a semi-infinite solid body and the other treats of the propagation on a spherical surface. Throughout this paper the effect of gravity or the hypothesis of stratum has not been taken into consideration. The former is known to give very little effect on the transmission of waves and the latter is not so essential for the present purpose.

I. Transmission on a Semi-infinite Body.[2]

1. Let us suppose, in the first instance, that the axis of z is directed downwards from the surface of the body perpendicular to the plane of the boundary. The senses of r, θ being horizontal, let u, v, w be the components of displacement in radial, azimuthal and vertical directions, and ρ, λ, μ be the density and Lamé's elastic constants. The equations of motion of the solid body in cylindrical coordinates are expressed by

$$\left.\begin{aligned}
\rho\frac{\partial^2 u}{\partial t^2} &= (\lambda+2\mu)\frac{\partial \Delta}{\partial r} - \frac{2\mu}{r}\frac{\partial \varpi_z}{\partial \theta} + 2\mu\frac{\partial \varpi_\theta}{\partial z}, \\
\rho\frac{\partial^2 v}{\partial t^2} &= (\lambda+2\mu)\frac{1}{r}\frac{\partial \Delta}{\partial \theta} - 2\mu\frac{\partial \varpi_r}{\partial z} + 2\mu\frac{\partial \varpi_z}{\partial r}, \\
\rho\frac{\partial^2 w}{\partial t^2} &= (\lambda+2\mu)\frac{\partial \Delta}{\partial z} - \frac{2\mu}{r}\frac{1}{\partial r}(r\varpi_\theta) + \frac{2\mu}{r}\frac{\partial \varpi_r}{\partial \theta}.
\end{aligned}\right\} \quad \cdots\cdots\cdots (1)$$

where

$$\left.\begin{aligned}
\Delta &= \frac{1}{r}\frac{\partial (r)u}{\partial r} + \frac{1}{r}\frac{\partial v}{\partial \theta} + \frac{\partial w}{\partial z}, & 2\varpi_r &= \frac{1}{r}\frac{\partial w}{\partial \theta} - \frac{\partial v}{\partial z}, \\
2\varpi_\theta &= \frac{\partial u}{\partial z} - \frac{\partial w}{\partial r}, & 2\varpi_z &= \frac{1}{r}\left(\frac{\partial (rv)}{\partial r} - \frac{\partial u}{\partial \theta}\right).
\end{aligned}\right\} \quad \cdots\cdots (2)$$

(1) "Propagation of the Leading and Trailing Parts of a Train of Elastic Waves," *Bull. Ear. Res. Inst.* **4** (1928) p. 107.

(2) The author read similar papers so ago as Oct. 1924 at the Colloq. of the Seism. Inst. and May 1926 at the Meeting of the Earth. Res. Inst., the latter paper being on plane Rayleigh-waves having some amplitude-distribution in each wave-front. Dr. H. Nakano also studied some case of cylindrical (not annular) Rayleigh-waves in different manners, *Geophys. Mag.* **6** (1928).

If we eliminate u, v, w in (1) by means of (2), we find

$$\left.\begin{aligned}
\rho\frac{\partial^2 \Delta}{\partial t^2}&=(\lambda+2\mu)\left[\frac{\partial^2 \Delta}{\partial r^2}+\frac{1}{r}\frac{\partial \Delta}{\partial r}+\frac{1}{r^2}\frac{\partial^2 \Delta}{\partial \theta^2}+\frac{\partial^2 \Delta}{\partial z^2}\right],\\
\rho\frac{\partial^2 \varpi_r}{\partial t^2}&=\mu\left[\frac{\partial^2 \varpi_r}{\partial r^2}+\frac{3}{r}\frac{\partial \varpi_r}{\partial r}+\frac{\varpi_r}{r^2}+\frac{1}{r^2}\frac{\partial^2 \varpi_r}{\partial \theta^2}+\frac{\partial^2 \varpi_r}{\partial z^2}+\frac{2}{r}\frac{\partial \varpi_z}{\partial z}\right],\\
\rho\frac{\partial^2 \varpi_\theta}{\partial t^2}&=\mu\left[\frac{\partial^2 \varpi_\theta}{\partial r^2}+\frac{1}{r}\frac{\partial \varpi_\theta}{\partial r}-\frac{\varpi_\theta}{r^2}+\frac{1}{r^2}\frac{\partial^2 \varpi_\theta}{\partial \theta^2}+\frac{\partial^2 \varpi_\theta}{\partial z^2}+\frac{2}{r^2}\frac{\partial \varpi_r}{\partial \theta}\right],\\
\rho\frac{\partial^2 \varpi_z}{\partial t^2}&=\mu\left[\frac{\partial^2 \varpi_z}{\partial r^2}+\frac{1}{r}\frac{\partial \varpi_z}{\partial r}+\frac{1}{r^2}\frac{\partial^2 \varpi_z}{\partial \theta^2}+\frac{\partial^2 \varpi_z}{\partial z^2}\right].
\end{aligned}\right\}\quad\cdots\cdots(3)$$

As it is difficult to solve the original equations in (1), we shall now treat of the equations in (3), whose forms are somewhat simple in comparison with those in (1). From the first and the last equations in (3), we get the following solutions without difficulty:

$$\left.\begin{aligned}
\Delta&=A_m H_m^{(2)}(kr)\, e^{-\alpha z+ipt}\begin{Bmatrix}\cos\\ \sin\end{Bmatrix} m\theta,\\
2\varpi_z&=B_m H_m^{(2)}(kr)\, e^{-\beta z+ipt}\begin{Bmatrix}\sin\\ -\cos\end{Bmatrix} m\theta,
\end{aligned}\right\}\quad\cdots\cdots(4)$$

in which

$$k^2=\alpha^2+h^2=\beta^2+j^2,$$

$$h^2=\frac{\rho p^2}{\lambda+2\mu},\qquad j^2=\frac{\rho p^2}{\mu}.$$

$\frac{2\pi}{k}$ gives the wave length approximately corresponding to the period of the harmonic waves, namely $\frac{2\pi}{p}$.

Substituting the solution in the second of (4) in the second of the equations (3) and finding the particular and complementary solutions, both in appropriate forms, we obtain

$$2\varpi_r=\left\{C_m\frac{H_m^{(2)}(kr)}{r}-\frac{\beta}{k^2}B_m\frac{\partial H_m^{(2)}(kr)}{\partial r}\right\}e^{-\beta z+ipt}\begin{Bmatrix}\sin\\ -\cos\end{Bmatrix} m\theta.\quad\cdots\cdots(5)$$

Again, substituting this in the third of (3) and proceeding as before, we find

$$2\varpi_\theta=\left\{C_m\frac{1}{m}\frac{\partial H_m^{(2)}(kr)}{\partial r}-\frac{\beta_m}{k^2}B_m\frac{H_m^{(2)}(kr)}{r}\right\}e^{-\beta z+ipt}\begin{Bmatrix}\cos\\ \sin\end{Bmatrix} m\theta.\quad\cdots\cdots(6)$$

Equations (4), (5), (6) give us the general expression of Δ, ϖ_r, ϖ_θ, ϖ_z. We shall now find the expressions of displacements from these values under the conditions written by (2).

Displacement (u_1, v_1, w_1), answering to Δ in (4) and satisfying $\varpi_z = \varpi_r = \varpi_\theta = 0$ in (2), is expressed by

$$\left.\begin{aligned} u_1 &= -A_m \frac{1}{h^2} \frac{\partial H_m^{(2)}(kr)}{\partial r} e^{-\alpha z + ipt} \left.\begin{matrix}\cos\\ \sin\end{matrix}\right\} m\theta, \\ v_1 &= A_m \frac{m}{h^2} \frac{H_m^{(2)}(kr)}{r} e^{-\alpha z + ipt} \left.\begin{matrix}\sin\\ -\cos\end{matrix}\right\} m\theta, \\ w_1 &= A_m \frac{\alpha}{h^2} H_m^{(2)}(kr)\, e^{-\alpha z + ipt} \left.\begin{matrix}\cos\\ \sin\end{matrix}\right\} m\theta \end{aligned}\right\} \quad \cdots\cdots\cdots\cdots (7)$$

Displacement (u_2, v_2, w_2), answering to ϖ_z in (4) besides the second terms of the right hand sides of ϖ_r and ϖ_θ, both given in (5) and (6), under the condition that $\Delta = 0$ in (2), is expressed by

$$\left.\begin{aligned} u_2 &= B_m \frac{m}{k^2} \frac{H_m^{(2)}(kr)}{r} e^{-\beta z + ipt} \left.\begin{matrix}\cos\\ \sin\end{matrix}\right\} m\theta, \\ v_2 &= -B_m \frac{1}{k^2} \frac{\partial H_m^{(2)}(kr)}{\partial r} e^{-\beta z + ipt} \left.\begin{matrix}\sin\\ -\cos\end{matrix}\right\} m\theta, \\ w_2 &= 0. \end{aligned}\right\} \quad \cdots\cdots\cdots\cdots (8)$$

Though this type of solution is not suited for the present problem because of the factors $\frac{H_m^{(2)}(kr)}{r}$ and $\frac{\partial H_m^{(2)}(kr)}{\partial r}$ involved in the expressions of u_2 and v_2, yet we should obtain this solution for the consideration of the generality and also for the future use in complex cases. In the present case both types of solutions in (7) and in the expressions below suffice for the complete determination of the problem.

Displacement (u_3, v_3, w_3) derived from the values of the first terms of the right hand sides of the expressions of ϖ_r and ϖ_θ, both given in (5) and (6), and fulfilling the conditions $\Delta = \varpi_z = 0$ in (2), is written by

$$\left.\begin{aligned} u &= C_m \frac{\beta}{mj^2} \frac{\partial H_m^{(2)}(kr)}{\partial r} e^{-\beta z + ipt} \left.\begin{matrix}\cos\\ \sin\end{matrix}\right\} m\theta, \\ v_3 &= -C_m \frac{\beta}{j^2} \frac{H_m^{(2)}(kr)}{r} e^{-\beta z + ipt} \left.\begin{matrix}\sin\\ -\cos\end{matrix}\right\} m\theta, \\ w_3 &= -C_m \frac{k^2}{mj^2} H_m^{(2)}(kr)\, e^{-\beta z + ipt} \left.\begin{matrix}\cos\\ \sin\end{matrix}\right\} m\theta. \end{aligned}\right\} \quad \cdots\cdots\cdots\cdots (9)$$

The surface, $z = 0$, being free from tractions, the equations

$$\lambda\Delta + 2\mu \frac{\partial w}{\partial z} = 0, \quad \frac{1}{r}\frac{\partial w}{\partial \theta} + \frac{\partial v}{\partial z} = 0, \quad \frac{\partial u}{\partial z} + \frac{\partial w}{\partial r} = 0, \cdots\cdots\cdots (10)$$

in which $u=v_1+v_3$, $v=v_1+v_3$, $w=w_1+w_3$, must hold on that surface. It may seem that two types of solutions are not sufficient for three conditions as expressed by (10); the second and the third terms of (10), however, are equivalent for the present special problem.

These equations give us the following relations:

$$\left(\frac{C_m}{m}\right)\Bigg| A_m=\frac{2j^2\sqrt{k^2-h^2}}{h^2(2k^2-j^2)}, \quad B_m=0 \qquad \cdots\cdots\cdots\cdots (11)$$

The velocity of propagation is the same as that of the ordinary Rayleigh-waves, though the azimuthal distribution of displacements is not uniform.

The distribution of displacement (taking $\lambda=\mu$, $z=0$) is, though roughly, expressed by

$$\left.\begin{aligned} u&=-\frac{1.50\,A_m}{k}\frac{\partial H_m^{(2)}(kr)}{\partial(kr)}e^{ipt}\begin{matrix}\cos\\ \sin\end{matrix}\Big\}m\theta,\\ v&=\frac{1.50m\,A_m}{k}\frac{H_m^{(2)}(kr)}{kr}e^{ipt}\begin{matrix}\sin\\ -\cos\end{matrix}\Big\}m\theta,\\ w&=-\frac{2.21\,A_m}{k}H_m^{(2)}(kr)\,e^{ipt}\begin{matrix}\cos\\ \sin\end{matrix}\Big\}m\theta. \end{aligned}\right\} \cdots\cdots\cdots\cdots (12)$$

We have now seen that, when $\lambda=\mu$, the ratio of the vertical and the radial components of displacement given by (12), that is w/u, is about $3/2$ for all azimuth. This conforms with the nature of the ordinary Rayleigh-waves of the symmetrical type. Again, the ratio of the azimuthal displacement at the azimuth θ_2, where $\begin{matrix}\cos\\ \sin\end{matrix}\Big\}m\theta_2=1$, and the radial displacement at the azimuth θ_1, where $\begin{matrix}\cos\\ \sin\end{matrix}\Big\}m\theta_1=1$, is approximately $ml/2\pi r$, l being the wave length. This shows that, in spite of the maintenance of the natures of the vertical and the horizontal components of displacement in wave profile and in azimuthal distribution, the azimuthal component of displacement quickly disappears as the distance from the origin increases. Thus these natures will be understood by the following simple expressions:

$$\left.\begin{aligned} u&=-\frac{1.50\,A_m}{k}\frac{\partial H_m^{(2)}(kr)}{\partial(kr)}e^{ipt}\begin{matrix}\cos\\ \sin\end{matrix}\Big\}m\theta,\\ v&=0,\\ w&=-\frac{2.21\,A_m}{k}H_m^{(2)}(kr)\,e^{ipt}\begin{matrix}\cos\\ \sin\end{matrix}\Big\}m\theta. \end{aligned}\right\} \cdots\cdots\cdots\cdots (13)$$

at $r\to\infty$.

Such qualities cannot exist in the propagation of bodily waves, in which the ratios of the azimuthal component of displacement to other components are maintained for all distances.

As the radial and the vertical movements are, thus, maintained during the propagation, the law of pull and push due to Prof. Shida is applicable even to the transmission of surface waves in a restricted sense that the azimuthal movement is out of consideration.

2. We may now proceed to the case in which the waves due to some arbitrary disturbance having azimuthal distribution are transmitted on the surface of a semi-infinite solid. The elementary solutions which should be needed here are obtained from rewriting $H_m^{(2)}(kr)$ in Δ, u_1, v_1, w_1, u_3, v_3, w_3 by $J_m(kr)$. Thus we get

$$\left.\begin{aligned}
\Delta &= A_m J_m(kr)\, e^{-\alpha z}\begin{Bmatrix}\cos\\ \sin\end{Bmatrix} pt \begin{Bmatrix}\cos\\ \sin\end{Bmatrix} m\theta,\\
u_1 &= -A_m \frac{1}{h^2}\frac{\partial J_m(kr)}{\partial r} e^{-\alpha z}\begin{Bmatrix}\cos\\ \sin\end{Bmatrix} pt \begin{Bmatrix}\cos\\ \sin\end{Bmatrix} m\theta,\\
v_1 &= A_m \frac{m}{h^2}\frac{J_m(kr)}{r} e^{-\alpha z}\begin{Bmatrix}\cos\\ \sin\end{Bmatrix} pt \begin{Bmatrix}\sin\\ -\cos\end{Bmatrix} m\theta,\\
w_1 &= A_m \frac{\alpha}{h^2} J_m(kr)\, e^{-\alpha z}\begin{Bmatrix}\cos\\ \sin\end{Bmatrix} pt \begin{Bmatrix}\cos\\ \sin\end{Bmatrix} m\theta.\\
u_3 &= C_m \frac{\beta}{m_j{}^2}\frac{\partial J_m(kr)}{\partial r} e^{-\beta z}\begin{Bmatrix}\cos\\ \sin\end{Bmatrix} pt \begin{Bmatrix}\cos\\ \sin\end{Bmatrix} m\theta,\\
v_3 &= -C_m \frac{\beta}{j^2}\frac{J_m(kr)}{r} e^{-\beta z}\begin{Bmatrix}\cos\\ \sin\end{Bmatrix} pt \begin{Bmatrix}\sin\\ -\cos\end{Bmatrix} m\theta,\\
w_3 &= -C_m \frac{k^2}{mj^2} J_m(kr)\, e^{-\beta z}\begin{Bmatrix}\cos\\ \sin\end{Bmatrix} pt \begin{Bmatrix}\cos\\ \sin\end{Bmatrix} m\theta,
\end{aligned}\right\} \quad \cdots\cdots\cdots\cdots (14)$$

in which $\dfrac{C_m}{m} = A_m \dfrac{2\alpha j^2}{h^2(2k^2-j^2)}$ (condition of zero tangential stress).

Hence the elementary solutions of displacements are expressed by the following simple forms:

When $z=0$,

$$\left.\begin{aligned}
u &= -\frac{\{(2k^2-j^2)-2\alpha\beta\}}{h^2(2k^2-j^2)} A_m \frac{\partial J_m(kr)}{\partial r}\begin{Bmatrix}\cos\\ \sin\end{Bmatrix} pt \cos m\theta,\\
v &= \frac{m\{(2k^2-j^2)-2\alpha\beta\}}{h^2(2k^2-j^2)} A_m \frac{J_m(kr)}{r}\begin{Bmatrix}\cos\\ \sin\end{Bmatrix} pt \sin m\theta.
\end{aligned}\right\} \quad \cdots\cdots\cdots (15)$$

$$w=-\frac{\alpha j^2}{h^2(2k^2-j^2)}A_m J_m(kr)\begin{matrix}\cos\\ \sin\end{matrix}\Big\}pt\cos m\theta.$$

To generalise this, we use Fourier's double integral theorem, namely

$$f(r)=\int_0^\infty J_m(kr)\,kdk\int_0^\infty f(\alpha)\,J_m(k\alpha)\,\alpha d\alpha. \quad \ldots\ldots\ldots (16)$$

Thus, for the initial disturbance on the surface such that

$$t=0,\quad z=0,\quad w=f(r)\cos m\theta,\quad \frac{\partial w}{\partial t}=0, \quad \ldots\ldots\ldots\ldots (17)$$

we get on the surface, $z=0$, the expressions of the displacement in the forms:

$$\left.\begin{aligned} u&=\cos m\theta\int_0^\infty\frac{(2k^2-j^2)-2\alpha\beta}{\alpha j^2}\frac{\partial J_m(kr)}{\partial r}\cos kVt\cdot kdk\int_0^\infty f(\alpha)J_m(k\alpha)\alpha d\alpha,\\ v&=-m\sin m\theta\int_0^\infty\frac{(2k^2-j^2)-2\alpha\beta}{\alpha j^2}\frac{J_m(kr)}{r}\cos kVt\cdot kdk\int_0^\infty f(\alpha)J_m(k\alpha)\alpha d\alpha,\\ w&=\cos m\theta\int_0^\infty J_m(kr)\cos kVt\cdot kdk\int_0^\infty f(\alpha)\,J_m(k\alpha)\,\alpha d\alpha, \end{aligned}\right\}$$

$$\ldots\ldots\ldots\ldots\ldots\ldots\ldots\ldots (18)$$

in which V is the velocity of propagation of Rayleigh-waves. Evaluating these, we find the behaviour of waves due to the arbitrary initial disturbance.

We now consider a simplest case where

$$t=0\quad z=0,\quad w=\frac{Ca^2r}{(a^2+r^2)^{\frac{3}{2}}}\cos\theta,\quad \frac{\partial w}{\partial t}=0. \ldots\ldots\ldots\ldots (19)$$

By the adjustment of C and a, we may obtain different kind of disturbance at the origin.

As we know the integral formula,

$$Ca\int_0^\infty\frac{\alpha J_0(k\alpha)}{(a^2+\alpha^2)^{\frac{3}{2}}}d\alpha=Ce^{-ak}. \ldots\ldots\ldots\ldots\ldots\ldots (20)$$

we have

$$\begin{aligned} w&=-Ca\cos\theta\int_0^\infty J_1(kr)\cos kVt\,\frac{\partial}{\partial k}(e^{-ak})\,kdk\\ &=-Ca^2\cos\theta\frac{\partial}{\partial r}\int_0^\infty J_0(kr)\cos kVt\,e^{-ak}dk. \ldots\ldots\ldots\ldots\ldots (21)\end{aligned}$$

Expanding $\cos kVt$ in ascending power of kVt, we get

$$w=-Ca^2\frac{\partial}{\partial r}\int_0^\infty e^{-ak}J_0(kr)\left(1-\frac{k^2\overline{Vt}^2}{2!}+\frac{k^4\overline{Vt}^4}{4!}-\ldots\ldots\right)dk. \ldots\ldots (22)$$

Substituting the relations,

$$\int_0^\infty e^{-ak} J_0(kr)\,dk = \frac{1}{R}, \quad \int_0^\infty e^{-ak} J_0(kr)\, k^n\, dk = n! \frac{P_n(\cos\theta)}{R^{n+1}}, \quad \ldots\ldots (23)$$

in which $a = R\cos\theta$, $r = R\sin\theta$, we obtain

$$w = -Ca^2\cos\theta \frac{\partial}{\partial r}\left[\frac{1}{\sqrt{a^2+r^2}}\left\{1 - \frac{\overline{Vt}^2}{(a^2+r^2)} P_2\left(\frac{a}{\sqrt{a^2+r^2}}\right)\right.\right.$$
$$\left.\left. + \frac{\overline{Vt}^4}{(a^2+r^2)^2} P_4\left(\frac{a}{\sqrt{a^2+r^2}}\right) - \ldots\ldots\right\}\right]. \quad \ldots\ldots (24)$$

The treatment of u and v has been omitted in the present case. It is worthy of notice that, in spite of the continuous displacement of the initial disturbance at the origin, the waves do not appear to be transmitted over the point, $r = 0$, at the origin in the direction of other quadrants. Such a nature can never occur in two-dimensional propagation of waves. In two-dimensional propagation of surface waves the original patterns of displacements are transmitted in both directions along the surface without modification of the type.

3. The theory of the formation of the surface waves in three dimentions, when periodic disturbances act on a point in the interior of the solid body, was studied by Professor H. Lamb.[1] The present section of this investigation, being a certain modification of Lamb's paper, deals with the propagation of such waves having some azimuthal distribution.

We shall take the free surface of a semi-infinite solid body to be $z = 0$. and shall suppose that the positive sense of the axis of z is directed towords the interior of the body. Again, in three-dimensional problems where the disturbing origin is a doublet oscillating horizontally, we must first find the solution of

$$\rho \frac{\partial^2 \Delta_0}{\partial t^2} = (\lambda + 2\mu)\left(\frac{\partial^2 \Delta_0}{\partial R^2} + \frac{2}{R}\frac{\partial \Delta_0}{\partial R} + \frac{1}{R^2}\frac{\partial^2 \Delta_0}{\partial \omega^2} + \frac{1}{R^2}\frac{\partial \Delta_0}{\partial \omega}\right), \quad \ldots\ldots (25)$$

where ω is the co-latitude at the origin.

The expression of the primary waves are thus given by

---

(1) H. Lamb, *Phil. Trans. Roy. Soc.*, **203** (1904).

$$\Delta_0 = e^{ipt}\frac{\partial}{\partial x}\frac{e^{-ihR}}{R} \quad \cdots\cdots (26)$$

$$= e^{ipt}\cos\omega\frac{\partial}{\partial R}\frac{e^{ihR}}{R}, \quad \cdots\cdots (26')$$

where

$$R = \sqrt{x^2+y^2+z^2}.$$

The radial displacement near the origin is written by

$$u_R = -\frac{1}{h^2}\frac{\partial \Delta_0}{\partial R}, \quad \cdots\cdots (27)$$

so that the real form of displacement is approximately written by

$$u_R = -\frac{1}{R}\sin(pt-hR)\cos\omega \cdots\cdots (28)$$

Now we know the expression

$$\frac{e^{-ihR}}{R} = \int_0^\infty \frac{e^{-\alpha z}}{\alpha} J_0(kr)\,k\,dk, \cdots\cdots (29)$$

which is due to H. Lamb.[1] In this $\alpha = \sqrt{k^2-h^2}$ or $i\sqrt{h^2-k^2}$ according as $k^2 \gtrless h^2$. Modifying (29), we find

$$\cos\omega\frac{\partial}{\partial R}\frac{e^{-ihR}}{R} = -\cos\theta\int_0^\infty \frac{e^{-\alpha z}}{\alpha} J_1(kr)\,k^2\,dk,^{(2)} \cdots\cdots (30)$$

where θ is the azimuth with respect to z-axis.

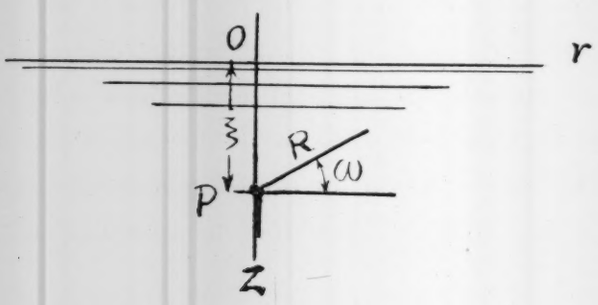

In the case of an internal source of disturbance at $(r=0,\ z=\xi)$, the dilatation is expressed by

(1) Prof. H. Lamb, "On the Propagation of Tremors over the Surface of an Elastic Solid", *Phil. Trans. Roy. Soc.*, **203**(1904); also *Math Tripos Paper* (1905).

(2) More complex cases of waves due to multiplets will soon be published in Bull. **7** of the Institute. These cases are studied by the assistance of Mr. G. Nishimura.

$$\left.\begin{aligned} \Delta_0 &= -e^{ipt}\cos\theta\left[\int_0^\infty \frac{e^{\alpha(z-\xi)}}{\alpha} J_1(kr)\,k^2\,dk + \int_0^\infty \frac{e^{-\alpha(z+\xi)}}{\alpha} J_1(kr)\,k^2\,dk\right] \\ &= -2e^{ipt}\cos\theta\int_0^\infty \frac{\operatorname{ch}\alpha z}{\alpha} e^{-\alpha\xi} J_1(kr)\,k^2\,dk, \qquad [z<\xi] \\ \Delta_0 &= -2e^{ipt}\cos\theta\int_0^\infty \frac{\operatorname{ch}\alpha\xi}{\alpha} e^{-\alpha z} J_1(kr)\,k^2\,dk. \qquad [z>\xi] \end{aligned}\right\} \ldots (31)$$

The expressions of displacement are given by

$$\left.\begin{aligned} u_0 &= -\frac{1}{h^2}\frac{\partial \Delta_0}{\partial r} = \frac{2e^{ipt}\cos\theta}{h^2}\int_0^\infty \frac{\operatorname{ch}\alpha z}{\alpha} e^{-\alpha\xi}\frac{\partial J_1(kr)}{\partial r} k^2\,dk, \\ v_0 &= -\frac{1}{h^2 r}\frac{\partial \Delta_0}{\partial \theta} = -\frac{2e^{ipt}\sin\theta}{h^2}\int_0^\infty \frac{\operatorname{ch}\alpha z}{\alpha} e^{-\alpha\xi}\frac{J_1(kr)}{r} k^2\,dk, \\ w_0 &= -\frac{1}{h^2}\frac{\partial \Delta_0}{\partial z} = \frac{2e^{ipt}\cos\theta}{h^2}\int_0^\infty \operatorname{sh}\alpha z\, e^{-\alpha\xi} J\ (kr)\,k^2 dk. \end{aligned}\right\} [z<\xi] \ldots (32)$$

The stress-components at the surface are expressed by

$$\left.\begin{aligned} \widehat{zr} &= 0, \qquad \widehat{z\theta} = 0, \\ \widehat{zz} &= 2\mu\, e^{ipt}\frac{\cos\theta}{h^2}\int_0^\infty \frac{(2k^2-j^2)}{\alpha} e^{-\alpha\xi} J_1(kr)\,k^2\,dk. \end{aligned}\right\} \ldots\ldots\ldots (33)$$

Now, for free surface waves, we have the typical solutions expressed by (15). Summing up the solutions of the type (15) so as to annihilate the stress $\widehat{zz}$ in (33) when combined with (32), we find the complete solutions of the free surface waves as below:

$$\left.\begin{aligned} u_1 &= -\frac{2e^{ipt}\cos\theta}{h^2}\int_0^\infty \frac{(2k^2-j^2-2\alpha\beta)}{F(k)}\,\frac{(2k^2-j^2)}{\alpha} e^{-\alpha\xi}\frac{\partial J_1(kr)}{\partial r} k^2\,dk, \\ v_1 &= \frac{2e^{ipt}\sin\theta}{h^2}\int_0^\infty \frac{(2k^2-j^2-2\alpha\beta)}{F(k)}\,\frac{(2k^2-j^2)}{\alpha} e^{-\alpha\xi}\frac{J_1(kr)}{r} k^2\,dk, \\ w_1 &= -\frac{2e^{ipt}\cos\theta}{h^2}\int_0^\infty \frac{\alpha j^2}{F(k)}\,\frac{(2k^2-j^2)}{\alpha} e^{-\alpha\xi} J_1(kr)\,k^2\,dk, \end{aligned}\right\} [z=0] \quad (34)$$

in which

$$F(k) = (2k^2-j^2)^2 - 4k^2\alpha\beta. \qquad \ldots\ldots\ldots\ldots (35)$$

The resultant displalcement $u = u_0 + u_1$, $v = v_0 + v_1$, $w = w_0 + w_1$ gives the movement of the surface of the body. These processes are quite similar to what H. Lamb had employed. Thus, the further calculation is also very like to Lamb's method. We may superpose on the solutions Bessel's function of the second kind to obtain progressive waves.

The final solutions can be expressed by

$$\left.\begin{aligned} u&=-\frac{4i\pi\cos\theta}{h^2}\frac{j^2\kappa^2\beta_1}{F'(\kappa)}e^{-\alpha_1\xi}\frac{\partial H_1^{(2)}(\kappa r)}{\partial r}e^{-ipt}\\ &\qquad +\text{asymptotically vanishing terms},\\ v&=\frac{4i\pi\sin\theta}{h^2}\frac{j^2\kappa^2\beta_1}{F'(\kappa)}e^{-\alpha_1\xi}\frac{H_1^{(2)}(\kappa r)}{r}e^{ipt}+\cdots,\\ w&=-\frac{2i\pi\cos\theta}{h^2}\frac{j^2\kappa^2(2\kappa^2-j^2)}{F'(\kappa)}e^{-\alpha_1\xi}H_1^{(2)}(\kappa r)\,e^{ipt}+\cdots\cdots \end{aligned}\right\}\cdots\cdots(36)$$

In these, κ is the real positive root of

$$F(k)=(2k^2-j^2)^2-4k^2\alpha\beta,$$

such that

$$\left.\begin{aligned} \frac{\kappa}{j}&=1.04678, \quad [\lambda=\infty]\\ &=1.087664, \quad [\lambda=\mu] \end{aligned}\right\}\cdots\cdots\cdots\cdots\cdots\cdots(37)$$

α_1, β_1 being the corresponding values of α, β, while the "asymptotically vanishing terms" are meant that these terms tend to vanish (compared with the first terms) as r is increased indefinitely.

It is worthy of notice that, in spite of the maintenance of the natures of the vertical and the horizontal components of displacement in wave profile and in azimuthal distribution, the azimuthal component of displacement quickly disappears as the distance from the origin increases. Thus, the quite similar nature as on the plane surface occurs.

II. Transmission on a Spherical Surface.

4. We shall suppose that the origin of the disturbance is at some portion of the axis $\theta=0$, and suppose that the waves are transmitted in the direction of the colatitude. Let u, v, w be radial, colatitudinal and azimuthal components of the displacement. The equations of motion of the solid body in spherical coordinates are expressed by

$$\left.\begin{aligned} \rho\frac{\partial^2 u}{\partial t^2}&=(\lambda+2\mu)\frac{\partial\Delta}{\partial r}-\frac{2\mu}{r\sin\theta}\frac{\partial(\varpi_\phi\sin\theta)}{\partial\theta}+\frac{2\mu}{r\sin\theta}\frac{\partial\varpi_\theta}{\partial\phi},\\ \rho\frac{\partial^2 v}{\partial t^2}&=(\lambda+2\mu)\frac{1}{r}\frac{\partial\Delta}{\partial\theta}-\frac{2\mu}{r\sin\theta}\frac{\partial\varpi_r}{\partial\phi}+\frac{2\mu}{r}\frac{\partial(r\varpi_\phi)}{\partial r},\\ \rho\frac{\partial^2 w}{\partial t^2}&=(\lambda+2\mu)\frac{1}{r\sin\theta}\frac{\partial\Delta}{\partial\phi}-\frac{2\mu}{r}\frac{\partial(r\varpi_\theta)}{\partial r}+\frac{2\mu}{r}\frac{\partial\varpi_r}{\partial\theta}, \end{aligned}\right\}\cdots\cdots(38)$$

where
$$\left.\begin{aligned}
\Delta &= \frac{1}{r^2\sin\theta}\left[\frac{\partial(ur^2\sin\theta)}{\partial r}+\frac{\partial(vr\sin\theta)}{\partial\theta}+\frac{\partial(wr)}{\partial\phi}\right],\\
2\varpi_r &= \frac{1}{r^2\sin\theta}\left[\frac{\partial}{\partial\theta}(wr\sin\theta)-\frac{\partial}{\partial\phi}(vr)\right],\\
2\varpi_\theta &= \frac{1}{r\sin\theta}\left[\frac{\partial u}{\partial\phi}-\frac{\partial(wr\sin\theta)}{\partial r}\right],\\
2\varpi_\phi &= \frac{1}{r}\left[\frac{\partial(vr)}{\partial r}-\frac{\partial u}{\partial\theta}\right].
\end{aligned}\right\}\quad\ldots\ldots(39)$$

Eliminating u, v, w in (38) by means of (39), we get

$$\left.\begin{aligned}
\rho\frac{\partial^2\Delta}{\partial t^2} &= (\lambda+2\mu)\left[\frac{1}{r^2}\frac{\partial}{\partial r}\left(r^2\frac{\partial\Delta}{\partial r}\right)\right.\\
&\qquad\left.+\frac{1}{r^2}\frac{\partial}{\sin\theta\partial\theta}\left(\sin\theta\frac{\partial\Delta}{\partial\theta}\right)+\frac{1}{r^2\sin^2\theta}\frac{\partial^2\Delta}{\partial\phi^2}\right],\\
\rho\frac{\partial^2\varpi_r}{\partial t^2} &= \mu\left[\frac{\partial^2\varpi_r}{\partial r^2}+\frac{4}{r}\frac{\partial\varpi_r}{\partial r}+\frac{2}{r^2}\varpi_r\right.\\
&\qquad\left.+\frac{1}{r^2\sin\theta}\frac{\partial}{\partial\theta}\left(\sin\theta\frac{\partial\varpi_r}{\partial\theta}\right)+\frac{1}{r^2\sin^2\theta}\frac{\partial^2\varpi_r}{\partial\phi^2}\right],\\
\rho\frac{\partial^2\varpi_\theta}{\partial t^2} &= \mu\left[\frac{1}{r}\frac{\partial^2(\varpi_\theta r)}{\partial r^2}+\frac{1}{r^2\sin^2\theta}\frac{\partial^2\varpi_\theta}{\partial\phi^2}\right.\\
&\qquad\left.-\frac{1}{r^2\sin^2\theta}\frac{\partial^2(\varpi_\phi\sin\theta)}{\partial\phi\,\partial\theta}-\frac{1}{r}\frac{\partial^2\varpi_r}{\partial r\partial\theta}\right],\\
\rho\frac{\partial^2\varpi_\phi}{\partial t^2} &= \mu\left[\frac{1}{r}\frac{\partial^2(\varpi_\phi r)}{\partial r^2}+\frac{1}{r^2}\frac{\partial}{\partial\theta}\frac{1}{\sin\theta}\frac{\partial(\varpi_\phi\sin\theta)}{\partial\theta}\right.\\
&\qquad\left.-\frac{1}{r^2}\frac{\partial}{\partial\theta}\frac{1}{\sin\theta}\frac{\partial\varpi_\theta}{\partial\phi}-\frac{1}{r\sin\theta}\frac{\partial^2\varpi_r}{\partial r\partial\phi}\right]
\end{aligned}\right\}\quad\ldots\ldots(40)$$

These give us as in the former case,

$$\left.\begin{aligned}
\Delta &= \frac{J_{n+\frac{1}{2}}(hr)}{\sqrt{r}}\left\{A_{mn}P_n^m(\cos\theta)+A'_{mn}Q_n^m(\cos\theta)\right\}\begin{Bmatrix}\cos\\ \sin\end{Bmatrix}m\phi\,e^{ipt},\\
2\varpi_r &= \frac{J_{n+\frac{1}{2}}(kr)}{r^{\frac{3}{2}}}\left\{B_{mn}P_n^m(\cos\theta)+B'_{mn}Q_n^m(\cos\theta)\right\}\begin{Bmatrix}\sin\\ -\cos\end{Bmatrix}m\phi\,e^{ipt},\\
2\varpi_\theta &= \left[\frac{J_{n+\frac{1}{2}}(kr)}{\sqrt{r}}\left\{C_{mn}\frac{P_n^m(\cos\theta)}{\sin\theta}+C'_{mn}\frac{Q_n^m(\cos\theta)}{\sin\theta}\right\}\right.\\
&\qquad+\frac{1}{n(n+1)}\frac{1}{r}\frac{d}{dr}\left(\sqrt{r}\,J_{n+\frac{1}{2}}(kr)\right)\left\{B_{mn}\frac{dP_n^m(\cos\theta)}{d\theta}\right.\\
&\qquad\left.\left.+B'_{mn}\frac{dQ_n^m(\cos\theta)}{d\theta}\right\}\right]\begin{Bmatrix}\sin\\ -\cos\end{Bmatrix}m\phi\,e^{ipt},
\end{aligned}\right\}\quad(41)$$

$$2\varpi_\phi=\Big[\frac{1}{m}\frac{J_{n+\frac{1}{2}}(kr)}{\sqrt{r}}\Big\{C_{mn}\frac{dP_n^m(\cos\theta)}{d\theta}+C'_{mn}\frac{dQ_n^m(\cos\theta)}{d\theta}\Big\}$$
$$+\frac{m}{n(n+1)}\frac{1}{r}\frac{d}{dr}\Big(\sqrt{r}\,J_{n+\frac{1}{2}}(kr)\Big)\Big\{B_{mn}\frac{P_n^m(\cos\theta)}{\sin\theta}$$
$$+B'_{mn}\frac{Q_n^m(\cos\theta)}{\sin\theta}\Big\}\Big]\begin{Bmatrix}\cos\\ \sin\end{Bmatrix}m\phi\,e^{ipt},$$

in which $h^2=\dfrac{\rho p^2}{\lambda+2\mu}$, $k^2=\dfrac{\rho p^2}{\mu}$.

Displacement $(u_1,\ v_1,\ w_1)$ answering to Δ in (41) and satisfying $\varpi_r=\varpi_\theta=\varpi_\phi=0$ is expressed by

$$\left.\begin{aligned}
u_1&=-\frac{1}{h^2}\frac{d}{dr}\frac{J_{n+\frac{1}{2}}(hr)}{\sqrt{r}}\Big\{A_{mn}P_n^m(\cos\theta)+A'_{mn}Q_n^m(\cos\theta)\Big\}\begin{Bmatrix}\cos\\ \sin\end{Bmatrix}m\phi\,e^{ipt},\\
v_1&=-\frac{1}{h^2}\frac{J_{n+\frac{1}{2}}(hr)}{r^{\frac{3}{2}}}\Big\{A_{mn}\frac{dP_n^m(\cos\theta)}{d\theta}+A'_{mn}\frac{dQ_n^m(\cos\theta)}{d\theta}\Big\}\begin{Bmatrix}\cos\\ \sin\end{Bmatrix}m\phi\,e^{ipt},\\
w_1&=\frac{m}{h^2}\frac{J_{n+\frac{1}{2}}(hr)}{r^{\frac{3}{2}}}\Big\{A_{mn}\frac{P_n^m(\cos\theta)}{\sin\theta}+A'_{mn}\frac{Q_n^m(\cos\theta)}{\sin\theta}\Big\}\begin{Bmatrix}\sin\\ -\cos\end{Bmatrix}m\phi\,e^{ipt}.
\end{aligned}\right\}\quad(42)$$

Displacement $(u_2,\ v_2,\ w_2)$ answering to ϖ_r together with the second terms in the expressions of ϖ_θ and ϖ_ϕ, under the condition that $\Delta=0$, is expressed by

$$\left.\begin{aligned}
u_2&=0,\\
v_2&=\frac{m}{n(n+1)}\frac{J_{n+\frac{1}{2}}(kr)}{\sqrt{r}}\Big\{B_{mn}\frac{P_n^m(\cos\theta)}{\sin\theta}+B'_{mn}\frac{Q_n^m(\cos\theta)}{\sin\theta}\Big\}\begin{Bmatrix}\cos\\ \sin\end{Bmatrix}m\phi\,e^{ipt},\\
w_2&=-\frac{1}{n(n+1)}\frac{J_{n+\frac{1}{2}}(kr)}{\sqrt{r}}\Big\{B_{mn}\frac{dP_n^m(\cos\theta)}{d\theta}+B'_{mn}\frac{dQ_n^m(\cos\theta)}{d\theta}\Big\}\begin{Bmatrix}\sin\\ -\cos\end{Bmatrix}m\phi\,e^{ipt}.
\end{aligned}\right\}\quad(43)$$

Displacement $(u_3,\ v_3,\ w_3)$ derived from the values of the first terms of ϖ_θ and ϖ_ϕ and fulfilling the conditions, $\Delta=\varpi_r=0$, is written by

$$\left.\begin{aligned}
u_3&=-\frac{n(n+1)}{mk^2}\frac{J_{n+\frac{1}{2}}(kr)}{r^{\frac{3}{2}}}\Big\{C_{mn}P_n^m(\cos\theta)\\
&\qquad+C'_{mn}Q_n^m(\cos\theta)\Big\}\begin{Bmatrix}\cos\\ \sin\end{Bmatrix}m\phi\,e^{ipt},\\
v_3&=-\frac{1}{mk^2}\frac{1}{r}\frac{d}{dr}\Big(\sqrt{r}\,J_{n+\frac{1}{2}}(kr)\Big\{C_{mn}\frac{dP_n^m(\cos\theta)}{d\theta}\\
&\qquad+C'_{mn}\frac{dQ_n^m(\cos\theta)}{d\theta}\Big\}\begin{Bmatrix}\cos\\ \sin\end{Bmatrix}m\phi\,e^{ipt},
\end{aligned}\right\}\quad\cdots\cdots(44)$$

$$w_3=\frac{1}{k^2}\frac{1}{r}\frac{d}{dr}\left(\sqrt{r}J_{n+\frac{1}{2}}(kr)\right)\left\{C_{mn}\frac{P_n^m(\cos\theta)}{\sin\theta}+C'_{mn}\frac{Q_n^m(\cos\theta)}{\sin\theta}\right\}\begin{matrix}\sin\\-\cos\end{matrix}\Big\}m\phi\, e^{ipt}.$$

The surface, $r=a$, being free from traction, three equations,

$$\left.\begin{aligned}\lambda\Delta+2\mu\frac{\partial u}{\partial r}&=0,\\ \frac{\partial v}{\partial r}-\frac{v}{r}+\frac{1}{r}\frac{\partial u}{\partial\theta}&=0,\\ \frac{1}{r\sin\theta}\frac{\partial u}{\partial\phi}+\frac{\partial w}{\partial r}-\frac{w}{r}&=0,\end{aligned}\right\}\quad\cdots\cdots\cdots\cdots\cdots\cdots(45)$$

in which $u=u_1+u_2+u_3$, $v=v_1+v_2+v_3$, $w=w_1+w_2+w_3$ must hold on that surface.

In the present case, the type of solutions in (43) is not needed; and we have to solve the following two equations:

$$\left.\begin{aligned}&[B_{mn}=0],\\ &\left[\lambda\frac{J_{n+\frac{1}{2}}(ha)}{\sqrt{a}}-2\mu\frac{1}{h^2}\frac{d^2}{da^2}\frac{J_{n+\frac{1}{2}}(ha)}{\sqrt{a}}\right]A_{mn}\\ &\qquad-2\mu\frac{n(n+1)}{k^2}\frac{d}{da}\frac{J_{n+\frac{1}{2}}(ka)}{a^{\frac{3}{2}}}\frac{C_{mn}}{m}=0,\\ &\left[-\frac{1}{h^2}\left(a\frac{d}{da}\frac{J_{n+\frac{1}{2}}(ha)}{a^{\frac{5}{2}}}+\frac{1}{a}\frac{d}{da}\frac{J_{n+\frac{1}{2}}(ha)}{\sqrt{a}}\right)A_{mn}\right.\\ &\qquad-\frac{1}{k^2}\left(a\frac{d}{da}\frac{1}{a^2}\frac{d}{da}\sqrt{a}\,J_{n+\frac{1}{2}}(ka)\right.\\ &\qquad\left.\left.+\frac{n(n+1)}{a}\frac{J_{n+\frac{1}{2}}(ka)}{a^{\frac{3}{2}}}\right)\frac{C_{mn}}{m}\right]=0.\end{aligned}\right\}\quad\cdots\cdots\cdots(46)$$

These equations are too complicated to study the nature of the motion, so that we must be contented with the following simflified form:

$$\left(\frac{k^2}{f^2}-2\right)^4=16\left(1-\frac{h^2}{f^2}\right)\left(1-\frac{k^2}{f^2}\right),\quad\cdots\cdots\cdots\cdots\cdots(47)$$

where

$$\frac{h}{f}=\frac{ha}{n},\quad\frac{k}{f}=\frac{ka}{n}.\quad\cdots\cdots\cdots\cdots\cdots(48)$$

In this equation the largeness of n is taken into consideration; even

when $n=100$, the wave length on the surface of the earth is so large as 360 kilometers. Also, for the sake of simplicity, for the values of Bessel's functions in (46), the first term of the asymptotic expansion due to P. Debye, namely

$$J_n(x)=\frac{1}{\pi}\,e^{-x(\tau\cosh\tau-\sinh\tau)}\sum_{q=0}^{q=l}B_q(\tau)\,\frac{\Gamma\left(q+\frac{1}{2}\right)}{\left(\frac{x}{2}\sinh\tau\right)^{q+\frac{1}{2}}}, \qquad \cdots\cdots\cdots (49)$$

in which $\cosh\tau=\dfrac{n}{x}>1$, is taken.

The equation (47) is of the same form as that derived by Lord Rayleigh to determine the velocity of propagation of plane surface waves.

The velocity of propagation excepting near the origin, when n is large, is given by

$$\frac{2\pi/f}{2\pi/p}=q\sqrt{\frac{\mu}{\rho}}, \qquad \cdots\cdots\cdots\cdots\cdots (50)$$

where $q=0.9553$ for incompressible material and 0.9194 for materials whose Poisson's ratio is $\frac{1}{4}$.

The value of C_{mn}/A_{mn} is obtained from one of the relations in (46). If the second relation is used,

$$\frac{C_{mn}}{mA_{mn}}=\left\{-\frac{k^2}{h^2}\,\frac{\left[\frac{1}{r}\frac{d}{dr}\frac{J_n(hr)}{\sqrt{r}}-\frac{1}{r^2}\frac{J_n(hr)}{\sqrt{r}}\right]}{\left(-k^2+\frac{2(n^2+n-1)}{r^2}\right)\frac{J_n(kr)}{\sqrt{r}}-\frac{2}{r}\frac{d}{dr}\frac{J_n(kr)}{\sqrt{r}}}\right\}_{r=a} \qquad \cdots\cdots (51)$$

Thus, the expressions of the displacement are given by

$$\left.\begin{aligned} u &\fallingdotseq A_{mn}\left[\frac{1}{h^2}\frac{d}{da}\frac{J_{n+\frac{1}{2}}(ha)}{\sqrt{a}}+\left(\frac{C_{mn}}{mA_{mn}}\right)\frac{n(n+1)}{k^2}\frac{J_{n+\frac{1}{2}}(ka)}{a^{\frac{3}{2}}}\right]\left[P_n^m(\cos\theta)\right.\\ &\qquad\left.-iD_{mn}Q_n^m(\cos\theta)\right]_{\sin}^{\cos}\Big\}m\phi\,e^{ipt},\\ v &\fallingdotseq A_{mn}\left[\frac{1}{h^2}\frac{J_{n+\frac{1}{2}}(ha)}{a^{\frac{3}{2}}}+\left(\frac{C_{mn}}{mA_{mn}}\right)\frac{1}{k^2a}\frac{d}{da}\left(\sqrt{a}\,J_{n+\frac{1}{2}}(ka)\right)\right]\left[\frac{dP_n^m(\cos\theta)}{d\theta}\right.\\ &\qquad\left.-iD_{mn}\frac{dQ_n^m(\cos\theta)}{d\theta}\right]_{\sin}^{\cos}\Big\}m\phi\,e^{ipt}. \end{aligned}\right\} \qquad (52)$$

$$w \fallingdotseq -mA_{mn}\left[\frac{1}{h^2}\frac{\mathrm{J}_{n+\frac{1}{2}}(ha)}{a^{\frac{3}{2}}}+\left(\frac{C_{mn}}{mA_{mn}}\right)\frac{1}{k^2 a}\frac{d}{da}\left(\sqrt{a}\,\mathrm{J}_{n+\frac{1}{2}}(ka)\right)\right]\left[\frac{dP_n^m(\cos\theta)}{\sin\theta}\right.$$
$$\left.-iD_{mn}\frac{Q_n^n(\cos\theta)}{d\theta}\right]\begin{matrix}\cos\\-\sin\end{matrix}\Big\}\, m\phi\, e^{ipt},$$

where D_{mn} is a positive number, whose value is constant for a given n and which is to be so adjusted that $P_n^m(\cos\theta)$ and $D_{mn}Q_n^m(\cos\theta)$ may have enveloping curves in common, excepting near the antipode as well as the origin within a zenith distance corresponding to, say, $\frac{1}{4}$ wave length. Motions in these regions must be excluded from the consideration.

Here, in this case where the curvature of the surface should not be neglected and hence the wave length is not so small, it seems unlikely that the azimuthal component of displacement disappears as the waves proceed towards the equatorial circle. It appears that even at the equatorial circle long Rayleigh-waves as affected by the curvature of the earth have the azimuthal and ordinary components of displacement, each component of comparable magnitude; in the vicinity of the seismic pole these waves have the large azimuthal component compared with the vertical and the radial components. This can be also known from the transmission on a semi-infinite solid body where in very vicinity of the epicentre the azimuthal component is much larger than the radial and vertical ones.

Now we have seen that long waves on the surface of the earth have the component of displacement like Love-type waves besides other components, while short waves at some distance from the origin appear to be Rayleigh-type.

Summary.

We have now obtained by the use of mathematical theory of elasticity some results having the practical importance on the seismological problems; the principal results are enumerated as follows:

(1) Rayleigh-waves having azimuthal distribution can be transmitted on the surface of a semi-infinite solid or a spherical surface without diffusion of displacements in each wave front.

(2) Though in the case of the propagation of Rayleigh-waves on

plane surface, the nature of the vertical and the horizontal components of displacement in wave profile and in azimuthal distribution is maintained for all distances, the azimuthal component of displacement quickly disappears as the distance from the origin increases, shewing the nature quite different from the bodily elastic waves.

(3) The law of pull and push is applicable even to the surface waves, with the condition that the azimuthal component is out of consideration. This law is also valid in the case of the transmission of waves caused by the arbitrary disturbance.

(4) When the disturbance acts on an interior point of the body the azimuthal distribution of displacement on the surface is in conformity with the motion of the source to a certain extent.

(5) Even at the equatorial circle of the sphere long Rayleigh-waves as affected by the curvature of the surface have the azimuthal and the ordinary components of comparable magnitudes; in the vicinity of the seismic pole these waves have the large azimuthal component compared with the vertical and the radial components.

(6) Short waves show the nature of giving the large azimuthal component only in very vicinity of the seismic epicentre.

In concluding this paper, the author is indebted to Professors Suyehiro and Terada for their kind advices and also to Mr. G. Nishimura who has assisted him in preparing this paper.[1]

July, 1928.

---

(1) Generation of Rayleigh-waves due to internal multiplet nuclei will be published in Proc. Imp. Acad. 5 No. 2 and Bull. 7 of our Institute. In the former paper some symbol has been misemployed though the final results are correct; in the latter paper it is correctly employed.

Formation of Deep-water Waves due to Subaqueous Shocks.

By **Katsutada SEZAWA,**

Member of the Institute.

水中衝撃による深海波の生成

所員　妹澤克惟

海底地震がある場合に如何なる海嘯が起るであらうかといふ問題は、其の海底の變動の如きものを推定する爲めに大切なわけであるが、其第一歩として深海中の適當な深さで衝撃が働く場合に表面に現はれる波動を算定してみた。勿論次の機會（彙報第七號）には淺海の底に衝撃が働く場合の研究を試みようと思ふがこの論文は寧ろ其準備である。

さて波動の概念は、水中の一點で働く調和振動が壓縮波として水に傳へられ、表面に達した部分が反射する時に表面に壓力の不平衡が起り、其を消す爲めに、其所に重力表面波が現はれ、これが水面上の遠距離へ送られるものとした。但し注意すべきは、この重力波は主として振動原より餘り遠からぬ上部の水面で發生する事と、始めの衝撃による波動は波長が相當に長い爲、多くの場合には其慣性を看過してもよい事とである。しかしこの論文では水深の大なる場合を考慮して慣性を其儘保存して置いた。

論文は六節に分れ、始めの三節では、二次元問題に於て原點が單原、水平に振動する複原、及び上下に振動する複原がある場合、他の三節はこれ等が三次元問題で行はれる場合とする。計算の重要な結果を拔萃すれば、

（1）原點の變位が極めて僅かであるにも拘らず水面に起る波は可なり大なる變位を持つ。

（2）表面に現はれる波動は主として普通の重力波であつて、原點の周期に相當した重力波の波長を持ち、且つ水點は圓形軌道を畫く。

（3）表面波の方位的分布は大體原點の運動に應ずるが、三次元の場合に原點が水平に振動するものでは、遠方の横變位が消滅する。

The problem of the propagation of deep-water waves in the case in which the waves are caused by some disturbing shocks acting on an interior point of the water, has the important bearings on the *tsunamis* as well as on the

general oceanography. Yet this problem has not been much studied for the reason that it involves mathematical difficulty and more probably has received very little attention from mathematical physicists in general. The problem itself, however, has been occasioned to be considered by a few students such as Prof. K. Terazawa,(1) H. Lamb,(2) K. Sano,(3) and R. Nomitsu,(4) though it is difficult to say that they have given the full satisfaction both in process and in result. The methods of analysis employed by Prof. K. Terazawa, H. Lamb and K. Sano seem to be some extensions of the problem of the ordinary water waves travelling horizontally from the start, while that appeared in Nomitsu's paper may be regarded as giving the flow of water from a source of stream. A conceivable problem arising in connection with the present investigation is on the wavy surface of water due to a submerged obstacle in running stream or conversely on the formation of water waves propagated with the same velocity as that of a submerged body moving uniformly. The case of the running stream attracted Lamb's attention,(5) and in a recent paper by T. H. Havelock,(6) the wave resistance of submerged moving body was considered from the same line of argument. Although it appears that our problem is related to these papers, they cannot be applied entirely to the present case. Because the nature of the original disturbance in this is quite different from those of Lamb and Havelock and accordingly the problem has been treated *ab initio* by a different method.

In the present analysis, an attempt is made to study the way in which the waves of the disturbing shocks acting on an interior point of the water are transmitted in all directions and in which these primary waves tend to excite the gravity waves travelling on the surface of the deep-water.

---

(1) Prof. K. Terazawa, "On Deep-sea Water Waves....," *Proc. Roy. Soc.*, **92** (1916).

(2) H. Lamb, *London Math. Soc. Proc.*, **21** (1922).

(3) Keizô Sano & Ken Hasegawa, "On the Waves produced by the Sudden Depression.....of the Bottom of the Sea.....", *Proc. Tokyo Math.-Phys. Soc.*, Ser. II **8** (1915–16).

(4) 理學博士 野満隆治「水中爆發の理論的研究」火兵學會誌、第十二卷（大正七年）。

(5) Prof. H. Lamb, "Waves due to Submerged Cylinder" *Ann. di math.*, **21**; also his *Hydrodynamics*, Chap. IX.

(6) Prof. T. H. Havelock, "Some Cases of Wave Motion due to a Submerged Obstacle." *Proc. Roy. Soc.*, **93** (1917).

The paper consists of two parts; the first part is on the propagation of shocks in two dimensions and the remaining part on that in three dimensions.

The method of analysis employed in this is to apply thoroughly the formulae which the eminent mathematician H. Lamb originally obtained by means of Green's theorem for the purpose of solving some problem of seismic waves. When the depth[1] of the point on which the disturbance acts is very small, the solution may otherwise be obtained approximately; when the depth is relatively large, it will be found that the transmission of shocks in the water wholly depends upon the waves of compression of the water and in effect the formulae quoted above play their important *roles*.

Part I. Two-dimensional Problems.

1. Among different types of motion at the origin special importance attaches to the simple harmonic type, by means of which the mathematical treatments are easily carried out. Generalising this type using Fourier's double integral theorem, complex cases such as the wave motion due to some arbitrary disturbances at the origin are obtained without difficulty. We shall take the free surface of deep water to be $y=0$, and shall suppose that the positive sense of the axis of y is directed towards the interior of the water.

Again, in two-dimensional problems where there is symmetry about a point, we must first find the solution of

$$\rho \frac{\partial^2 \psi}{\partial t^2} = \kappa \left(\frac{\partial^2 \psi}{\partial R^2} + \frac{1}{R} \frac{\partial \psi}{\partial R} \right), \quad \ldots\ldots\ldots\ldots\ldots\ldots (1)$$

where ψ is the dilatation, ρ is the active density of the water and κ is the volume elasticity of the water such that

$$\kappa = \rho_0 \left(\frac{dp}{d\rho} \right)_{\rho=\rho_0}, \qquad \kappa\psi = p_0 \quad \ldots\ldots\ldots\ldots\ldots\ldots (23)$$

For the ordinary water at 15°C the value of κ is 2.046×10^{10} dyne/cm^2.

In the case of simple-harmonic waves, the time factor being e^{ipt}, the

(1) The case of shallow-water waves due to bottom-shocks, in which the effect of the inertia of water is neglected or is not neglected, will appear in Bull. 7.

equation (1) takes the form

$$\nabla^2\psi+h^2\psi=0, \quad \ldots\ldots\ldots\ldots\ldots\ldots\ldots\ldots (3)$$

provided

$$h^2=\frac{\rho p^2}{\kappa} \quad \ldots\ldots\ldots\ldots\ldots\ldots\ldots\ldots (4)$$

The expression of the primary waves are, thus, expressed by

$$\psi=-ie^{ipt}H_0^{(2)}(hR), \quad \ldots\ldots\ldots\ldots\ldots\ldots (5)$$

where

$$R=\sqrt{x^2+y^2}. \quad \ldots\ldots\ldots\ldots\ldots\ldots\ldots\ldots (6)$$

The radial displacement near the origin is given by

$$u_R=-\frac{1}{h^2}\frac{\partial\psi}{\partial R}, \quad \ldots\ldots\ldots\ldots\ldots\ldots (7)$$

so that the real form of displacement is approximately written by

$$u_R\fallingdotseq\frac{1}{h}\sqrt{\frac{2}{\pi hR}}\cos\left(pt-hR+\frac{\pi}{4}\right) \quad \ldots\ldots\ldots\ldots\ldots\ldots (8)$$

Now we know the expression

$$H_0^{(2)}(hR)=\frac{i}{\pi}\int_{-\infty}^{\infty}\frac{e^{-\alpha y}e^{\mp ifx}}{\alpha}df, \quad \ldots\ldots\ldots\ldots\ldots\ldots (9)$$

which is first discovered by H. Lamb[2] using Green's theorem and recently renewed by H. Nakano[3] in proving this expression by means of the contour integration.

In the expression (9), $\mp$ of $e^{\mp ifx}$ should be taken for x-positive and α is taken such that

$$\alpha=\sqrt{f^2-h^2}, \quad \text{or} \quad i\sqrt{h^2-f^2} \quad \ldots\ldots\ldots\ldots\ldots\ldots (10)$$

according as $f^2\gtrless h^2$, the radical being taken positively.

In the case of an internal source of disturbance, resident at the point $x=0$, $y=\xi$, we may conveniently consider an image at $x=0$ and $y=-\xi$ The dilatation is therefore expressed by

---

(1) Exact solution at the origin will be seen in Lamb's paper, "The Early Stages of a Submarine Explosion," *Phil. Mag.*, **45** (1923).

(2) Prof. H. Lamb, "On the Propagation of Tremors over the Surface of an Elastic Solid", *Phil. Trans. Roy. Soc.*, **203** (1904).

(3) Dr. H. Nakano, "On Rayleigh Waves", *Jap. Journ. Astr. & Geophys*, **2** (1925).

$$\psi=\frac{e^{ipt}}{\pi}\left[\int_{-\infty}^{\infty}\frac{e^{\alpha(y-\xi)}\,e^{\mp ifx}}{\alpha}df+\int_{-\infty}^{\infty}\frac{e^{-\alpha(y+\xi)}\,e^{\mp ifx}}{\alpha}df\right]$$

$$=\frac{2e^{ipt}}{\pi}\int_{-\infty}^{\infty}\frac{\mathrm{ch}\,\alpha y}{\alpha}e^{-\alpha\xi}e^{\mp ifx}df, \qquad [y<\xi] \quad \ldots\ldots\ldots\ldots\ldots\ldots (11)$$

and similarly

$$=\frac{2e^{ipt}}{\pi}\int_{-\infty}^{\infty}\frac{\mathrm{ch}\,\alpha\xi}{\alpha}e^{-\alpha y}e^{\mp ifx}df. \qquad [y>\xi] \quad \ldots\ldots\ldots\ldots\ldots\ldots (12)$$

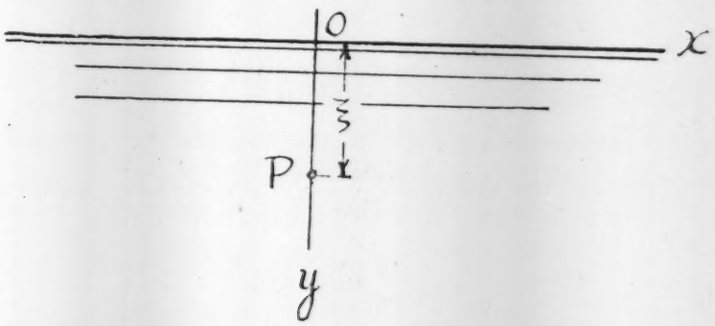

The expression of displacement is thus written by

$$\left.\begin{aligned} u_0&=-\frac{1}{h^2}\frac{\partial\psi}{\partial x}=\pm\frac{2ie^{ipt}}{\pi h^2}\int_{-\infty}^{\infty}\frac{\mathrm{ch}\,\alpha y}{\alpha}e^{-\alpha\xi}e^{\mp fx}f\,df,\\ v_0&=-\frac{1}{h^2}\frac{\partial\psi}{\partial y}=-\frac{2e^{ipt}}{\pi h^2}\int_{-\infty}^{\infty}\mathrm{sh}\,\alpha y\,e^{-\alpha\xi}e^{\mp ifx}df,\end{aligned}\right\}[y<\xi] \quad \ldots\ldots (13)$$

where u_0, v_0 are components of displacement in x- and y-directions.

The pressure-components at the surface are expressed by

$$[p_{xy}]_{y=0}=0, \quad [p_0]_{y=0}=\kappa\psi=\frac{2\kappa e^{ipt}}{\pi}\int_{-\infty}^{\infty}\frac{e^{-\alpha\xi}\,e^{\mp ifx}}{\alpha}df \quad \ldots\ldots\ldots (14)$$

Now, for gravity waves, the velocity potential ϕ will satisfy the equation of continuity such as

$$\frac{\partial^2\phi}{\partial x^2}+\frac{\partial^2\phi}{\partial y^2}=0 \quad \ldots\ldots\ldots\ldots\ldots\ldots\ldots (15)$$

the solution of which may be written by

$$\phi=Ce^{-fy}e^{i(pt\mp fx)}, \quad \ldots\ldots\ldots\ldots (16)$$

the upper and the lower signs being taken for x-positive and -negative respectively.

As the displacement (u_1, v_1) is connected with ϕ in the near forms,

$$\frac{\partial u_1}{\partial t}=-\frac{\partial \phi}{\partial x},\quad \frac{\partial v_1}{\partial t}=-\frac{\partial \phi}{\partial y}, \qquad \cdots\cdots(17)$$

we find

$$\left.\begin{aligned} u_1&=\pm\frac{f}{p}Ce^{-fy}e^{i(pt\mp fx)},\\ v_1&=-\frac{if}{p}Ce^{-fy}e^{i(pt\mp fx)}. \end{aligned}\right\} \qquad \cdots\cdots(18)$$

The integral of the equation of motion of the fluid is expressed by

$$\frac{p_1}{\rho}=\frac{\partial \phi}{\partial t}-gv_1-F(t), \qquad \cdots\cdots(19)$$

where p_1 is the pressure and $F(t)$ is the integration constant which may be supposed merged in the value of $\frac{\partial \phi}{\partial t}$. At the surface, we have

$$\frac{p_1}{p}=\left(\frac{\partial \phi}{\partial t}\right)_{y=0}+gv_1, \qquad \cdots\cdots(20)$$

in which v_1 is the surface elevation.

The kinematical relation at the surface is given by

$$\frac{\partial v_1}{\partial t}=-\left(\frac{\partial \phi}{\partial y}\right)_{y=0}, \qquad \cdots\cdots(21)$$

with the condition that the normal to the free surface makes very small angle with the vertical.

Differentiating (20) with respect to t and subsituting from (21), we obtain

$$\frac{1}{\rho}\frac{\partial p_1}{\partial t}=(-p^2+fg)C[e^{-fy}]_{y=0}e^{i(pt\mp fx)}, \qquad \cdots\cdots(22)$$

the integral of which is written by

$$[p_1]_{y=0}=i\rho C\frac{p^2-fg}{p}e^{i(pt\mp fx)}. \qquad \cdots\cdots(23)$$

The surface $y=0$ being free from traction, we have

$$[\text{the element of } p_0]_{y=0}+[p_1]_{y=0}=0, \qquad \cdots\cdots(24)$$

from which we find

$$C=-\frac{2\kappa}{\pi}\frac{e^{-\alpha\xi}p}{\alpha i\rho(p^2-fg)}. \qquad \cdots\cdots(25)$$

Thus u_1 and v_1 at the surface in the expressions of (18) can be written by

$$\left.\begin{aligned} u_1 &= \mp\frac{2\kappa f}{\pi}\frac{e^{-a\xi}}{\alpha i\rho(p^2-fg)}e^{i(pt\mp fx)}, \\ v_1 &= \frac{2\kappa f}{\pi}\frac{e^{-a\xi}}{\alpha\rho(p^2-fg)}e^{i(pt\mp fx)}. \end{aligned}\right\} \quad \cdots\cdots\cdots\cdots\cdots\cdots (26)$$

Multiplying these by df, integrating from $-\infty$ to ∞ and afterwards adding to u_0 and v_0, we get

$$\left.\begin{aligned} u = u_0 + u_1 &= \pm\frac{2ie^{ipt}}{\pi h^2\rho}\int_{-\infty}^{\infty}\frac{(\rho p^2-fg)+\kappa h^2}{p^2-fg}e^{-a\xi\mp ifx}\frac{f}{\alpha}df, \\ v = v_0 + v_1 &= \frac{2kc^{ipt}}{\pi\rho}\int_{-\infty}^{\infty}\frac{e^{-a\xi\mp ifx}}{p^2-fg}\frac{f}{\alpha}df. \end{aligned}\right\} \quad \cdots\cdots (27)$$

These expressions may be written by

$$\left.\begin{aligned} u = \mp\frac{2ie^{ipt}}{\pi h^2\rho}\Bigg[&\int_0^{\infty}\frac{\rho(p^2-fg)+\kappa h^2}{p^2-fg}e^{-a\xi\mp ifx}\frac{f}{\alpha}df \\ &-\int_0^{\infty}\frac{\rho(p^2+fg)+\kappa h^2}{p^2+fg}e^{-a\xi\pm ifx}\frac{f}{\alpha}df\Bigg], \\ v = \frac{2\kappa e^{ipt}}{\pi\rho}\Bigg[&\int_0^{\infty}\frac{e^{-a\xi\mp ifx}}{p^2-fg}\frac{f}{\alpha}df-\int_0^{\infty}\frac{e^{-a\xi\pm ifx}}{p^2+fg}\frac{f}{\alpha}df\Bigg]. \end{aligned}\right\} \quad \cdots\cdots (28)$$

These are the expressions of the wave motion on the surface of the water, when symmetrical shocks having the displacement expressed by (8) act on the origin ($x=0$, $y=\xi$).

To integrate the expressions in (28), we consider the integrals,

$$\left.\begin{aligned} &\int_c\frac{\rho(p^2-gZ)+\kappa h^2}{p^2-gZ}e^{-\xi\sqrt{Z^2-h^2}\mp iZx}\frac{Z}{\sqrt{Z^2-h^2}}dZ, \\ &\int_c\frac{e^{-\xi\sqrt{Z^2-h^2}\mp iZx}}{p^2-gZ}\frac{Z}{\sqrt{Z^2-h^2}}dZ, \\ &\int_c\frac{\rho(p^2+gZ)+\kappa h^2}{p^2+gZ}e^{-\xi\sqrt{Z^2-h^2}\pm iZx}\frac{Z}{\sqrt{Z^2-h^2}}dZ, \\ &\int_c\frac{e^{-\xi\sqrt{Z^2-h^2}\pm iZx}}{p^2+gZ}\frac{Z}{\sqrt{Z^2-h^2}}dZ, \end{aligned}\right\} \quad \cdots\cdots (29)$$

taken round some closed contours. In the present case, the first two integrals in (29) should be taken round a contour represented by the left

of the annexed drawings, while the remaining two should be taken round that of the right-hand side.

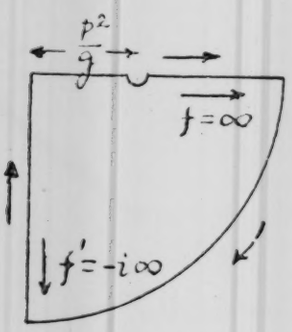

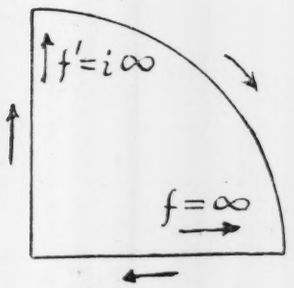

Equating each sum of the integrals taken round the contour to zero,[1] we find

$$\left.\begin{aligned} u=&\mp\frac{2k}{g\rho}e^{ipt}\left[\frac{1}{\sqrt{1-\left(\frac{hg}{p^2}\right)^2}}e^{-\xi\sqrt{\frac{p^4}{g^2}-h^2}\mp\frac{ip^2}{g}x}\right.\\ &\left.-\frac{2g}{\pi h^2\kappa}\int_0^\infty\frac{\rho(p^2+gf)+\kappa h^2}{(p^2+igf)}e^{-i\xi\sqrt{f^2+h^2}\mp fx}\frac{f}{\sqrt{f^2+h^2}}df\right],\\ v=&\frac{2i\kappa}{g\rho}e^{ipt}\left[\frac{1}{\sqrt{1-\left(\frac{hg}{p^2}\right)^2}}e^{-\xi\sqrt{\frac{p^4}{g^2}-h^2}\mp\frac{ip^2}{g}x}\right.\\ &\left.-\frac{2g}{i\pi}\int_0^\infty e^{-i\xi\sqrt{f^2+h^2}\mp fx}\frac{f}{\sqrt{f^2+h^2}}df\right].\end{aligned}\right\}\quad\ldots\ldots(30)$$

in which the upper and the lower signs are taken according as $x\gtrless 0$.

In this the "principal values" due to Cauchy are taken for the integration of the form,

$$\int_0^\infty\frac{F(f)}{p^2-fg}df,\qquad\ldots\ldots\ldots\ldots\ldots\ldots(31)$$

which is indeterminate in the ordinary sense of integration. In such a case the indeterminateness is avoided by inserting in the equations of motion small frictional terms proportional to the velocity and finally making the coefficients due to these terms vanish. In the present investigation this procedure has been omitted.

As the second terms on the right-hand sides of the expressions of u and

(1) Correction due to the branch point has been omitted in this deep-water problem; such effect will be considered in Bull. 7.

v in (30) tend to vanish as the distance on the surface from $x=0$ is increased in virtue of the factor $e^{\mp fx}$, we may disregard these second terms for large distances.

Thus we find the expressions of the horizontal and the vertical components of displacement of the surface of the water in the forms:

$$\left.\begin{aligned} u &\fallingdotseq \mp\frac{2\kappa}{g\rho}\frac{1}{\sqrt{1-\left(\frac{hg}{p^2}\right)^2}}e^{-\xi\sqrt{\frac{p^4}{g^2}-h^2}}\cos\left(pt\mp\frac{p^2}{g}x\right), \\ v &\fallingdotseq -\frac{2\kappa}{g\rho}\frac{1}{\sqrt{1-\left(\frac{hg}{p^2}\right)^2}}e^{-\xi\sqrt{\frac{p^4}{g^2}-h^2}}\sin\left(pt\mp\frac{p^2}{g}x\right), \end{aligned}\right\}[p^2>hg) \quad \ldots.(32)$$

and

$$\left.\begin{aligned} u &\fallingdotseq \pm\frac{2\kappa}{g\rho}\frac{1}{\sqrt{\left(\frac{hg}{p^2}\right)^2-1}}\sin\left(pt\mp\frac{p^2}{g}x-\xi\sqrt{h^2-\frac{p^4}{g^2}}\right), \\ v &\fallingdotseq \frac{2\kappa}{g\rho}\frac{1}{\sqrt{\left(\frac{hg}{p^2}\right)^2-1}}\cos\left(pt\mp\frac{p^2}{g}x-\xi\sqrt{h^2-\frac{p^4}{g^2}}\right), \end{aligned}\right\}[p^2<hg] \quad \ldots.(33)$$

corresponding to the displacement near the origin

$$u_R=\frac{1}{h}\sqrt{\frac{2}{\pi hR}}\cos\left(pt-hR+\frac{\pi}{4}\right). \quad [R^2=x^2+(y-\xi)^2] \ldots\ldots(34)$$

These give us the nature that the surface waves are propagated from the disturbed portion. The motion of the water particle on the surface is parfectly circular. The amplitude depends on the period and the depth of the focus. The figure in next page shews the ratio of the amplitude at x and that near the disturbed origin.

2. In two-dimensional motion where there is not symmetry about a point, but where the origin of the disturbance is a doublet oscillating horizontally, we must find the solution of the equation

$$\rho\frac{\partial^2\psi}{\partial t^2}=\kappa\left(\frac{\partial^2\psi}{\partial R^2}+\frac{1}{R}\frac{\partial\psi}{\partial R}+\frac{1}{R^2}\frac{\partial^2\psi}{\partial\theta^2}\right), \quad \ldots\ldots\ldots(35)$$

where θ is the agimuth at the origin of shocks.

In the case of a doublet oscillating horizontally, the primary waves may be written by

$$\psi = -ie^{ipt}\frac{\partial H_0^{(2)}(hR)}{\partial x} \quad \cdots\cdots\cdots\cdots\cdots\cdots\cdots\cdots (36)$$

$$= ihe^{ipt}H_1^{(2)}(hR)\cos\theta. \quad \cdots\cdots\cdots\cdots\cdots\cdots (36')$$

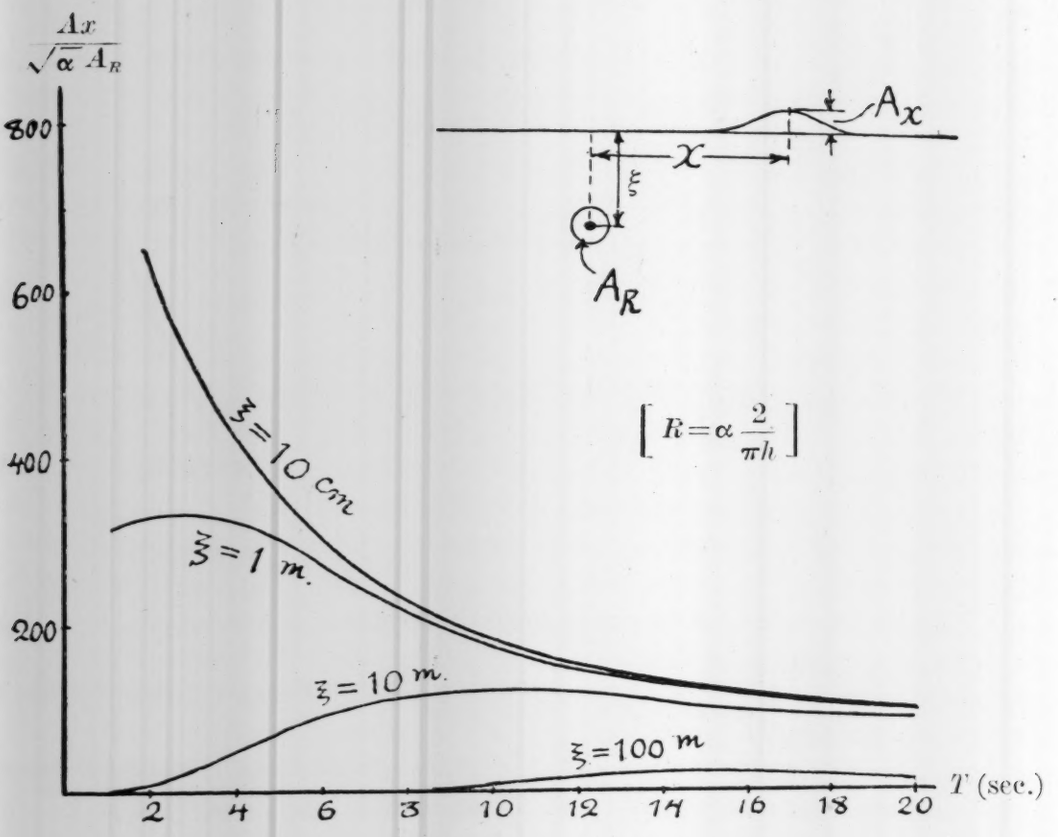

The radial displacement in real form is approximately writted by

$$u_R = -\sqrt{\frac{2}{\pi hR}}\cos\left(pt - hR + \frac{3\pi}{4}\right)\cos\theta. \quad \cdots\cdots\cdots\cdots (37)$$

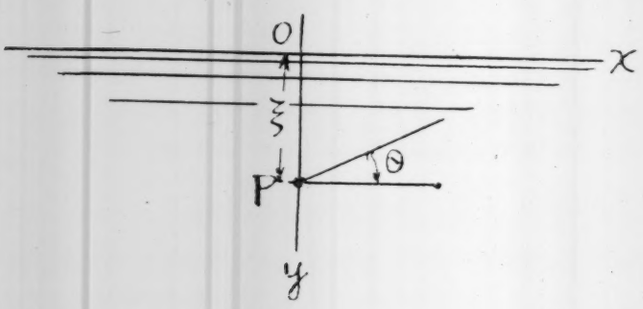

Modifying the relation written in (9), we find

$$ihH_1^{(2)}(hR)\cos\theta=\mp\int_{-\infty}^{\infty}\frac{e^{-\alpha y\mp ifx}}{\alpha}fdf \qquad (38)$$

Superposing the effect of the image for the source ($x=0$, $y=\xi$), we obtain

$$\left.\begin{aligned}\psi&=\mp\frac{2ie^{ipt}}{\pi}\int_{-\infty}^{\infty}\frac{\operatorname{ch}\alpha y}{\alpha}e^{-\alpha\xi\mp ifx}fdf, \qquad [y<\xi]\\ \psi&=\mp\frac{2ie^{ipt}}{\pi}\int_{-\infty}^{\infty}\frac{\operatorname{ch}\alpha\xi}{\alpha}e^{-\alpha y\mp ifx}fdf. \qquad [y>\xi]\end{aligned}\right\} \qquad (39)$$

The expressions of displacement are

$$\left.\begin{aligned}u_0&=-\frac{1}{h^2}\frac{\partial\psi}{\partial x}=\frac{2e^{ipt}}{\pi h^2}\int_{-\infty}^{\infty}\frac{\operatorname{ch}\alpha y}{\alpha}e^{-\alpha\xi\mp ifx}f^2df,\\ v_0&=-\frac{1}{h^2}\frac{\partial\psi}{\partial y}=\pm\frac{2ie^{ipt}}{\pi h^2}\int_{-\infty}^{\infty}\operatorname{sh}\alpha y e^{-\alpha\xi\mp ifx}fdf.\end{aligned}\right\}[y<\xi] \qquad (40)$$

The stress-components are given by

$$[p_{xy}]_{y=0}=0 \qquad [p_0]_{y=0}=\kappa\psi=\mp\frac{2i\kappa e^{ipt}}{\pi}\int_{-\infty}^{\infty}\frac{e^{-\alpha\xi\mp ifx}}{\alpha}fdf, \qquad (41)$$

the upper and the lower signs being taken for x-positive and -negative respectively.

Now, for gravity waves, a similar treatment as in section 1 being carried out, the results of the calculation of the pressure on the surface can be written by

$$[p_1]_{y=0}=i\rho C\frac{p^2-fg}{p}e^{i(pt\mp fx)}. \qquad (42)$$

Putting (41) and (42) in the surface conditions, we find

$$C=\pm\frac{2\kappa}{\pi}\frac{e^{-\alpha\xi}pf}{\alpha\rho(p^2-fg)} \qquad (43)$$

The displacement due to the gravity waves is therefore expressed by

$$\left.\begin{aligned}u_1&=\frac{2\kappa}{\pi}\frac{e^{-\alpha\xi}f^2}{\alpha\rho(p^2-fg)}e^{i(pt\mp fx)},\\ v_1&=\mp\frac{2i\kappa}{\pi}\frac{e^{-\alpha\xi}f^2}{\alpha\rho(p^2-fg)}e^{i(pt\mp fx)}.\end{aligned}\right\} \qquad (44)$$

Multiplying these by df, integrating from $-\infty$ to ∞ and afterwards adding to u_0 and v_0, we get

$$\left.\begin{aligned} u&=\frac{2e^{ipt}}{\pi h^2\rho}\int_{-\infty}^{\infty}\frac{\rho(p^2-fg)+\kappa h^2}{p^2-fg}e^{-\alpha\xi\mp ifx}\frac{f^2}{\alpha}df,\\ v&=\mp\frac{2i\kappa e^{ipt}}{\pi\rho}\int_{-\infty}^{\infty}\frac{e^{-\alpha\xi\mp ifx}}{p^2-fg}\frac{f^2}{\alpha}df. \end{aligned}\right\}\quad\cdots\cdots\cdots\cdots(45)$$

Following the same process of integration as in the former case, we find

$$\left.\begin{aligned} u&=\frac{2i\kappa}{g\rho}e^{ipt}\left[\frac{p^2}{g}\frac{1}{\sqrt{1-\left(\frac{hg}{p^2}\right)^2}}e^{-\xi\sqrt{\frac{p^4}{g^2}-h^2}\mp i\frac{p^2}{g}x}\right.\\ &\qquad\left.-\frac{2g}{\pi h^2\kappa}\int_0^{\infty}\frac{\rho(p^2+igf)+\kappa h^2}{p^2+igf}e^{-i\xi\sqrt{f^2+h^2}\mp fx}\frac{f^2}{\sqrt{f^2+h^2}}df\right],\\ v&=\pm\frac{2\kappa}{g\rho}e^{ipt}\left[\frac{p^2}{g}\frac{1}{\sqrt{1-\left(\frac{hg}{p^2}\right)^2}}e^{-\xi\sqrt{\frac{p^4}{g^2}-h^2}\mp i\frac{p^2}{g}x}\right.\\ &\qquad\left.-\frac{2g}{i\pi}\int_0^{\infty}\frac{e^{-i\xi\sqrt{f^2+h^2}+fx}}{p^2+igf}\frac{f^2}{\sqrt{f^2+h^2}}df\right]. \end{aligned}\right\}\quad\cdots\cdots(46)$$

in which the upper and the lower signs are taken according as $x\gtrless 0$. The principal values have been taken as in the former case. As the second terms in (46) become negligibly small as x tends to $\pm\infty$, we obtain at such a point,

$$\left.\begin{aligned} u&\fallingdotseq-\frac{2\kappa}{g\rho}\frac{p^2}{g}\frac{1}{\sqrt{1-\left(\frac{hg}{p^2}\right)^2}}e^{-\xi\sqrt{\frac{p^4}{g^2}-h^2}}\sin\left(pt\mp\frac{p^2}{g}x\right),\\ v&=\pm\frac{2\kappa}{g\rho}\frac{p^2}{g}\frac{1}{\sqrt{1-\left(\frac{hg}{p^2}\right)^2}}e^{-\xi\sqrt{\frac{p^4}{g^2}-h^2}}\cos\left(pt\mp\frac{p^2}{g}x\right), \end{aligned}\right\}[p^2>hg]\quad\cdots(47)$$

and

$$\left.\begin{aligned} u&\fallingdotseq\frac{2\kappa}{g\rho}\frac{p^2}{g}\frac{1}{\sqrt{\left(\frac{hg}{p^2}\right)^2-1}}\cos\left(pt\mp\frac{p^2}{g}x-\xi\sqrt{h^2-\frac{p^4}{g^2}}\right),\\ v&\fallingdotseq\frac{2\kappa}{g\rho}\frac{p^2}{g}\frac{1}{\sqrt{\left(\frac{hg}{p^2}\right)^2-1}}\sin\left(pt\mp\frac{p^2}{g}x-\xi\sqrt{h^2-\frac{p^4}{g^2}}\right), \end{aligned}\right\}[p^2<hg]\quad\cdots(48)$$

corresponding to the displacement near the origin,

$$u_R=-\sqrt{\frac{2}{\pi hR}}\cos\left(pt-hR+\frac{3\pi}{4}\right)\cos\theta. \quad [R^2=x^2+(y-\xi)^2]. \ldots (49)$$

These give us the nature that the surface waves are generated from the disturbed portion. The motion of the water particle in this case, too, is on a circular orbit. The amplitude at a large distance is p^2/gh times that of the former case, when the horizontal displacements at the origin are taken the same for both cases.

3. In two-dimensional motion where the disturbing origin is a doublet oscillating vertically, we find the solution of (35) for the primary waves in the following form:

$$\psi=-ie^{ipt}\frac{\partial H_0^{(2)}(hR)}{\partial y} \quad \ldots\ldots\ldots\ldots\ldots\ldots (50)$$

$$=ihe^{ipt}H_0^{(2)}(hR)\sin\theta \quad \ldots\ldots\ldots\ldots\ldots\ldots (50')$$

The radical displacement in real form is approximately written by

$$u_R=-\sqrt{\frac{2}{\pi hR}}\cos\left(pt-hR+\frac{3\pi}{4}\right)\text{in}\,\theta. \quad \ldots\ldots\ldots\ldots (51)$$

Considering the effect of the image for the source $(x=0,\ y=\xi)$, we find

$$\psi=-\frac{2}{\pi}e^{ipt}\int_{-\infty}^{\infty}\text{ch}\,\alpha y\,e^{-\alpha\xi\mp ifx}df, \quad [y<\xi] \quad \ldots\ldots\ldots (52)$$

so that the expressions of the displacement are given by

$$\left.\begin{aligned}u_0&=\mp\frac{2i}{\pi h^2}e^{ipt}\int_{-\infty}^{\infty}\text{ch}\,\alpha y\,e^{-\alpha\xi\mp ifx}f\,df,\\ v_0&=\frac{2}{\pi h^2}e^{ipt}\int_{-\infty}^{\infty}\alpha\,\text{sh}\,\alpha y\,e^{-\alpha\xi\mp ifx}df.\end{aligned}\right\}[y>\xi]\ldots\ldots\ldots (53)$$

The stress-components are

$$[p_{xy}]_{y=0}=0, \quad [p_0]_{y=0}=-\frac{2\kappa}{\pi}\int_{-\infty}^{\infty}e^{-\alpha\xi\mp ifx}df. \ldots\ldots\ldots (54)$$

Again, pursuing the same line of argument for the gravity waves as before, we find the value of the constant in (16) in the form:

$$C=\frac{2\kappa}{\pi}e^{-\alpha\xi}\frac{p}{i\rho(p^2-fg)}. \ldots\ldots\ldots\ldots\ldots\ldots (55)$$

The surface displacement due to gravity waves is, thus, expressed by

$$\left.\begin{aligned} u_1 &= \pm\frac{2\kappa}{\pi}\frac{e^{-\alpha\xi}f}{i\rho(p^2-fg)}e^{i(pt\mp fx)}, \\ v_1 &= -\frac{2\kappa}{\pi}\frac{e^{-\alpha\xi}f}{\rho(p^2-fg)}e^{i(pt\mp fx)}). \end{aligned}\right\} \quad \cdots\cdots\cdots\cdots (56)$$

The resultant displacement, when the contour integrations are performed, is expressed by

$$\left.\begin{aligned} u &= \mp\frac{2\kappa}{g\rho}e^{ipt}\left[\frac{p^2}{g}e^{-\xi\sqrt{\frac{p^4}{g^2}-h^2}\mp i\frac{p^2}{g}x}\right. \\ &\qquad \left. -\frac{2g}{\pi h^2\kappa}\int_0^\infty \frac{\rho(p^2+igf)+\kappa h^2}{p^2+igf}e^{-i\xi\sqrt{f^2+h^2}\mp fx}\,fdf\right], \\ v &= -\frac{2i\kappa}{g\rho}e^{ipt}\left[\frac{p^2}{g}e^{-\xi\sqrt{\frac{p^4}{g^2}-h^2}\mp i\frac{p^2}{g}x}\right. \\ &\qquad \left. -\frac{2g}{i\pi}\int_0^\infty e^{-i\xi\sqrt{f^2+h^2}\mp fx}\,fdf\right]. \end{aligned}\right\} \quad \cdots\cdots\cdots (57)$$

Neglecting the second terms for a large distance, we find

$$\left.\begin{aligned} u &\fallingdotseq \pm\frac{2\kappa}{g\rho}\frac{p^2}{g}e^{-\xi\sqrt{\frac{p^4}{g^2}-h^2}}\cos\left(pt\mp\frac{p^2}{g}x\right), \\ v &\fallingdotseq \frac{2\kappa}{g\rho}\frac{p^2}{g}e^{-\xi\sqrt{\frac{p^4}{g^2}-h^2}}\sin\left(pt\mp\frac{p^2}{g}x\right), \end{aligned}\right\} [p^2>hg] \quad \cdots\cdots (58)$$

and

$$\left.\begin{aligned} u &\fallingdotseq \pm\frac{2\kappa}{g\rho}\frac{p^2}{g}\cos\left(pt\mp\frac{p^2}{g}x-\xi\sqrt{\frac{p^4}{g^2}-h^2}\right), \\ v &\fallingdotseq \frac{2\kappa}{g\rho}\frac{p^2}{g}\sin\left(pt\mp\frac{p^2}{g}x-\xi\sqrt{\frac{p^4}{g^2}-h^2}\right), \end{aligned}\right\} [p^2<hg] \quad \cdots\cdots (59)$$

corresponding to the displacement in the neighbourhood of the origin,

$$u_R = -\sqrt{\frac{2}{\pi hR}}\cos\left(pt-hR+\frac{3\pi}{4}\right)\sin\theta. \quad [R^2=x^2+(y-\xi)^2] \quad \cdots\cdots (60)$$

We may conclude that the amplitude of waves at a large distance, when the origin is a doublet oscillating vertically, is $\sqrt{1-\left(\frac{hg}{p^2}\right)^2}$ times that of former case where the doublet prosecutes the horizontal oscillations. In these both cases the absolute amplitudes at the origins are taken the same.

Part II. Three-dimensional Problems.

4. We shall take the free surface of the water to be $z=0$, and shall

suppose that the positive sense of the axis of z is directed towards the interior of the water.

Again, in three-dimensional problems where there is symmetry about a point, we must first find the solution of

$$\rho \frac{\partial^2 \psi}{\partial t^2} = \kappa \left(\frac{\partial^2 \psi}{\partial R^2} + \frac{2}{R} \frac{\partial \psi}{\partial R} \right). \quad \ldots\ldots\ldots\ldots\ldots\ldots (61)$$

When the motion at the origin is of a simple-harmonic type, the equation (61) takes the form,

$$\frac{\partial^2 \psi}{\partial R^2} + \frac{2}{R} \frac{\partial \psi}{\partial R} + h^2 \psi = 0, \quad \ldots\ldots\ldots\ldots\ldots\ldots (62)$$

provided

$$h^2 = \frac{\rho p^2}{\kappa} \quad \ldots\ldots\ldots\ldots\ldots\ldots\ldots\ldots\ldots\ldots (63)$$

The expression of the primary waves are, thus, given by

$$\psi = e^{ipt} \frac{e^{-ihR}}{R}, \quad \ldots\ldots\ldots\ldots\ldots\ldots\ldots\ldots\ldots\ldots (64)$$

where $R = \sqrt{x^2+y^2+z^2}$.

The radial displacement near the origin is written by

$$u_R = -\frac{1}{h^2} \frac{\partial \psi}{\partial R}, \quad \ldots\ldots\ldots\ldots\ldots\ldots\ldots\ldots (65)$$

so that the real form of displacement is approximately expressed by

$$u_R = -\frac{1}{hR} \sin (pt - hR). \quad \ldots\ldots\ldots\ldots\ldots\ldots\ldots\ldots (66)$$

Now we know the expression

$$\frac{e^{-ihR}}{R} = \int_0^\infty \frac{e^{-\alpha z}}{\alpha} J_0(fr) f \, df, \quad \ldots\ldots\ldots\ldots\ldots\ldots (67)$$

which is due to H. Lamb.[1] In this $R = \sqrt{r^2+z^2}$ and α has the same meaning as in (10), i.e.

$$\alpha = \sqrt{f^2-h^2}, \quad \text{or} \quad i\sqrt{h^2-f^2}, \quad \ldots\ldots\ldots\ldots\ldots\ldots (68)$$

according as $f^2 \gtrless h^2$, the radical being taken positively.

---

(1) Prof. H. Lamb, *loc. cit.* p. 22; also *Math. Tripos Paper* (1905).

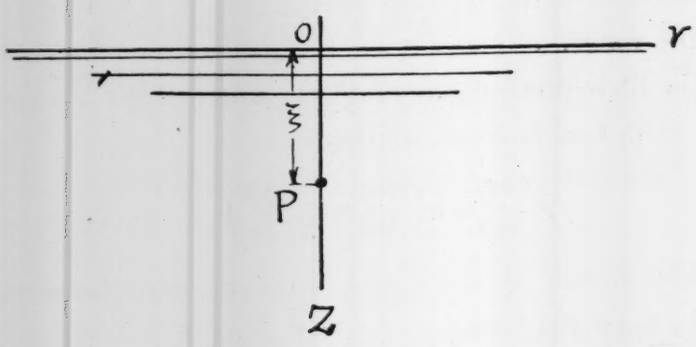

In the case of an internal source of disturbance, resident at the point $r=0$ and $z=\xi$, the dilatation is expressed by

$$\psi=e^{ipt}\left[\int_0^\infty \frac{e^{\alpha(z-\xi)}}{\alpha}J_0(fr)\,f\,df+\int_0^\infty \frac{e^{-\alpha(z+\xi)}}{\alpha}J_0(fr)\,f\,df\right]$$

$$=e2^{ipt}\int_0^\infty \frac{\mathrm{ch}\,\alpha z}{\alpha}e^{-\alpha\xi}J_0(fr)\,f\,df, \qquad [z<\xi] \quad \cdots\cdots\cdots\cdots\cdots\cdots (68)$$

and similarly

$$\psi=2e^{ipt}\int_0^\infty \frac{\mathrm{ch}\,\alpha\xi}{\alpha}\,e^{-\alpha z}J_0(fr)\,f\,df. \qquad [z>\xi] \quad \cdots\cdots\cdots\cdots\cdots\cdots (69)$$

The expressions of displacement are given by

$$\left.\begin{aligned} u_0&=-\frac{1}{h^2}\frac{\partial\psi}{\partial R}=\frac{2e^{ipt}}{h^2}\int_0^\infty \frac{\mathrm{ch}\,\alpha z}{\alpha}\,e^{-\alpha\xi}J_1(fr)\,f^2\,df,\\ v_0&=-\frac{1}{h^2 r}\frac{\partial\psi}{\partial\omega}=0,\\ w_0&=-\frac{1}{h^2}\frac{\partial\psi}{\partial z}=-\frac{2e^{ipt}}{h^2}\int_0^\infty \mathrm{sh}\,\alpha z e^{-\alpha\xi}J_0(fr)\,f\,df,\end{aligned}\right\} \cdots\cdots\cdots (70)$$

where u_0, v_0, w_0 are radial, azimuthal and vertical components of displacement respectively.

The stress-components at the surface are expressed by

$$[p_{zr}]_{z=0}=0, \qquad [p_{zw}]_{z=0}=0,$$

$$[p_0]_{z=0}=\kappa\psi=2\kappa\,e^{ipt}\int_0^\infty \frac{e^{-\alpha\xi}}{\alpha}J_0(fr)\,f\,df \quad \cdots\cdots\cdots\cdots\cdots (71)$$

Now, for gravity waves, the velocity potential ϕ will satisfy the equation of continuity such that

$$\frac{\partial^2\phi}{\partial r^2}+\frac{1}{r}\frac{\partial\phi}{\partial r}+\frac{\partial^2\phi}{\partial z^2}=0, \quad \ldots\ldots\ldots\ldots\ldots\ldots (72)$$

the solution of which may be written by

$$\phi=Ce^{-fz}e^{ipt}J_0(fr). \quad \ldots\ldots\ldots\ldots\ldots\ldots (73)$$

As the displacement (u_1, v_1, w_1) is connected with ϕ in the near forms,

$$\frac{\partial u_1}{\partial t}=-\frac{\partial\phi}{\partial r}, \quad \frac{\partial v_1}{\partial t}=-\frac{\partial\phi}{\partial\omega}, \quad \frac{\partial w_1}{\partial t}=-\frac{\partial\phi}{\partial z}, \quad \ldots\ldots\ldots\ldots (74)$$

we find

$$\left.\begin{aligned} u_1&=-\frac{if}{p}Ce^{-fz+ipt}J_1(fr), \\ v_1&=0, \\ w_1&=-\frac{if}{p}Ce^{-fz+ipt}J_0(fr). \end{aligned}\right\} \quad \ldots\ldots\ldots\ldots\ldots\ldots (75)$$

The integral of the equations of motion of the fluid is expressed by

$$\frac{p_1}{\rho}=\frac{\partial\phi}{\partial t}-gz-F(t), \quad \ldots\ldots\ldots\ldots\ldots\ldots (76)$$

where p_1 is the pressure and $F(t)$ is an integration constant which can be merged in the value of $\frac{\partial\phi}{\partial t}$. At the surface of the water we have

$$\frac{p_1}{\rho}=\left(\frac{\partial\phi}{\partial t}\right)_{z=0}+gw_1, \quad \ldots\ldots\ldots\ldots\ldots\ldots (77)$$

in which w_1 is the surface elevation.

The kinematical relation at the surface is given by

$$\frac{\partial w_1}{\partial t}=-\left(\frac{\partial\phi}{\partial z}\right)_{z=0}, \quad \ldots\ldots\ldots\ldots\ldots\ldots (78)$$

with the condition that the normal to the free surface makes very small angle with the vertical.

Differentiating (77) with respect t and substituting from (78), we obtain

$$\frac{1}{\rho}\frac{\partial p_1}{\partial t}=(-p^2+fg)C[e^{-fz}]_{z=0}e^{ipt}J_0(fr) \quad \ldots\ldots\ldots\ldots\ldots\ldots (79)$$

the integral of which is written by

$$[p_1]_{z=0}=i\rho C\frac{p^2-fg}{p}e^{ipt}J_0(fr) \quad \ldots\ldots\ldots\ldots\ldots\ldots (80)$$

The surface $z=0$ being free from traction, the equation,

$$(\text{element of } p_0)+p_1=0 \quad \cdots\cdots\cdots\cdots\cdots\cdots (81)$$

must hold on that surface. Thus we find

$$C=-2\kappa\frac{e^{-\alpha\xi}}{\alpha}\frac{pf}{i\rho(p^2-fg)} \quad \cdots\cdots\cdots\cdots\cdots\cdots (82)$$

The displacement given in (75) becomes

$$\left.\begin{aligned} u_1&=\frac{2\kappa f^2 e^{-\alpha\xi}}{\alpha\rho(p^2-fg)}e^{ipt}J_1(fr),\\ v_1&=0,\\ w_1&=\frac{2\kappa f^2 e^{-\alpha\xi}}{\alpha\rho(p^2-fg)}e^{ipt}J_0(fr). \end{aligned}\right\} \quad \cdots\cdots\cdots\cdots\cdots\cdots (83)$$

Multiplying these by df, integrating from 0 to ∞ and afterwards adding to u_0 and w_0, we get

$$\left.\begin{aligned} u=u_0+u_1&=\frac{2e^{ipt}}{h^2\rho}\int_0^\infty\frac{\rho(p^2-fg)+\kappa h^2}{p^2-fg}e^{-\alpha\xi}J_1(fr)\frac{f^2}{\alpha}df,\\ w=w_0+w_1&=\frac{2\kappa e^{ipt}}{\rho}\int_0^\infty\frac{e^{-\alpha\xi}}{p^2-fg}J_0(fr)\frac{f^2}{\alpha}df. \end{aligned}\right\} \quad \cdots\cdots (84)$$

These give us the oscillatory motion of a standing type at infinite distances, so that we may be justified if, following H. Lamb, we superpose on these some similar formulae of vibratory motion, whose phase only differs a quarter period from that of the expression in (84). This procedure, when r is increased, is not unreasonable. Thus we take the following formulae, in which a system of standing vibrations is superposed:

$$\left.\begin{aligned} u&=\frac{2e^{ipt}}{h^2\rho}\int_0^\infty\frac{\rho(p^2-fg)+\kappa h^2}{p^2-fg}e^{-\alpha\xi}H_1^{(2)}(fr)\frac{f^2}{\alpha}df,\\ w&=\frac{2\kappa e^{ipt}}{\rho}\int_0^\infty\frac{e^{-\alpha\xi}}{p^2-fg}H_0^{(2)}(fr)\frac{f^2}{\alpha}df. \end{aligned}\right\} \quad \cdots\cdots\cdots (85)$$

To integrate the expressions in (85), we consider the integrals,

$$\left.\begin{aligned} &\int_c\frac{\rho(p^2-gZ)+\kappa h^2}{p^2-gZ}e^{-\xi\sqrt{Z^2-h^2}}H_1^{(2)}(rZ)\frac{Z^2}{\sqrt{Z^2-h^2}}dZ,\\ &\int_c\frac{e^{-\xi\sqrt{Z^2-h^2}}}{p^2-gZ}H_0^{(2)}(rZ)\frac{Z^2}{\sqrt{Z^2-h^2}}dZ, \end{aligned}\right\} \quad \cdots\cdots\cdots (86)$$

taken round some closed contours. In the present case the integration is

to be taken round the contour below.

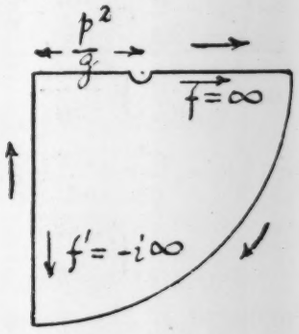

Equating each sum of the integrals taken round the contour to zero,[1] we find

$$\left.\begin{aligned} u=&\frac{2i\kappa e^{ipt}}{g\rho}\Bigg[\frac{p^2}{g}\frac{\pi}{\sqrt{1-\left(\frac{hg}{p^2}\right)^2}}e^{-\xi\sqrt{\frac{p^4}{g^2}-h^2}}H_1^{(2)}\left(\frac{p^2}{g}r\right)\\ &+\frac{g}{ih^2\kappa}\int_0^\infty\frac{\rho(p^2+igf)+\kappa h^2}{p^2+igf}e^{-i\xi\sqrt{f^2+h^2}}H_1^{(2)}(-ifr)\frac{f^2}{\sqrt{f^2+h^2}}df\Bigg],\\ w=&\frac{2i\kappa e^{ipt}}{g\rho}\Bigg[\frac{p^2}{g}\frac{\pi}{\sqrt{1-\left(\frac{hg}{p^2}\right)^2}}e^{-\xi\sqrt{\frac{p^4}{g^2}-h^2}}H_0^{(2)}\left(\frac{p^2}{g}r\right)\\ &+\frac{g}{i}\int_0^\infty\frac{e^{i\xi\sqrt{f^2+h^2}}}{p^2+igf}H_0^{(2)}(-ifr)\frac{f^2}{\sqrt{f^2+h^2}}df.\end{aligned}\right\}\quad(87)$$

In this the "principal values" has been taken in the process of integrations. As the second terms on the right-hand sides of the expressions of u and w in (87) become negligible, as r is increased, in virtue of $H_0^{(2)}(-ifr)$ and $H_1^{(2)}(-ifr)$, we may disregard these second terms.

Thus we find

$$\left.\begin{aligned} u\fallingdotseq&-\frac{2\kappa\pi}{g\rho}\frac{p^2}{g}\frac{1}{\sqrt{1-\left(\frac{hg}{p^2}\right)^2}}e^{-\xi\sqrt{\frac{p^4}{g^2}-h^2}}\frac{\sin\left(pt-\frac{p^2}{g}r+\frac{3\pi}{4}\right)}{\sqrt{\frac{\pi p^2 r}{2g}}},\\ w\fallingdotseq&\frac{2\kappa\pi}{g\rho}\frac{p^2}{g}\frac{1}{\sqrt{1-\left(\frac{hg}{p^2}\right)^2}}e^{-\xi\sqrt{\frac{p^2}{g^2}-h^2}}\frac{\cos\left(pt-\frac{p^2}{g}r+\frac{3\pi}{4}\right)}{\sqrt{\frac{\pi p^2 r}{2g}}},\end{aligned}\right\}\quad[p^2>hg]\quad(88)$$

(1) Correction due to branch point has been omitted; such effect will be considered in Bull. 7.

and

$$\left.\begin{aligned} u &\fallingdotseq \frac{2\kappa\pi}{g\rho}\frac{p^2}{g}\frac{1}{\sqrt{\left(\frac{hg}{p^2}\right)^2-1}}\frac{\cos\left(pt-\frac{p^2}{g}r+\frac{3\pi}{4}-\xi\sqrt{h^2-\frac{p^4}{g^2}}\right)}{\sqrt{\frac{\pi p^2 r}{2g}}}, \\ w &\fallingdotseq \frac{2\kappa\pi}{g\rho}\frac{p^2}{g}\frac{1}{\sqrt{\left(\frac{hg}{p^2}\right)^2-1}}\frac{\sin\left(pt-\frac{p^2}{g}r+\frac{3\pi}{4}-\xi\sqrt{h^2-\frac{p^4}{g^2}}\right)}{\sqrt{\frac{\pi p^2 r}{2g}}}, \end{aligned}\right\}[p^2<hg] \quad (89)$$

corresponding to the displacement in the vicinity of the origin as written by

$$u_R \fallingdotseq -\frac{1}{hR}\sin(pt-hR), \quad [R^2=r^2+(z-\xi)^2]. \quad \ldots\ldots\ldots (90)$$

The motion of the water particle is perfectly circular. The amplitude depends on the period of oscillations at the origin and the depth of that origin beneath the water level.

5. In three-dimensional motion where there is not symmetry about a point but where the disturbing origin is a doublet oscillating horizontally, we must find the solution of

$$\rho\frac{\partial^2\psi}{\partial t^2}=\kappa\left(\frac{\partial^2\psi}{\partial R^2}+\frac{2}{R}\frac{\partial\psi}{\partial R}+\frac{1}{R^2}\frac{\partial^2\psi}{\partial\theta^2}+\frac{1}{R^2}\frac{\partial\psi}{\partial\theta}\cot\theta\right), \quad \ldots\ldots (91)$$

where θ is the co-latitude at the origin.

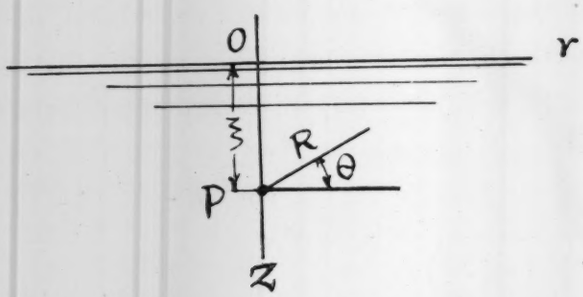

In the case of a doublet oscillating horizontally, the primary waves may be written by

$$\psi=e^{ipt}\frac{\partial}{\partial x}\frac{e^{-ihR}}{R} \quad \ldots\ldots\ldots\ldots\ldots\ldots (92)$$

$$=e^{ipt}\cos\theta\frac{\partial}{\partial R}\frac{e^{ihR}}{R}. \quad \ldots\ldots\ldots\ldots\ldots (92')$$

The radial displacement in real form is approximately written by

$$u_R=\frac{1}{R}\cos(pt-hR)\cos\theta. \quad \cdots\cdots\cdots\cdots\cdots\cdots (93)$$

Modifying the relation in (67), we find

$$\cos\theta\frac{\partial}{\partial R}\frac{e^{-ihR}}{R}=-\cos\omega\int_0^\infty\frac{e^{-\alpha z}}{\alpha}J_1(fr)\,f^2\,df, \quad \cdots\cdots\cdots\cdots (94)$$

where ω is the azimuth with respect to z-axis.

Supposing the effect of the image for the source $(r=0,\ z=\xi)$, we get

$$\left.\begin{aligned}\psi&=-2e^{ipt}\cos\omega\int_0^\infty\frac{\mathrm{ch}\,\alpha z}{\alpha}e^{-\alpha\xi}J_1(fr)\,f^2\,df, \quad [z<\xi]\\ \psi&=-2e^{ipt}\cos\omega\int_0^\infty\frac{\mathrm{ch}\,\alpha\xi}{\alpha}e^{-\alpha z}J_1(fr)\,f^2\,df. \quad [z>\xi]\end{aligned}\right\} \cdots\cdots\cdots (95)$$

The expressions of the displacement are given by

$$\left.\begin{aligned}u_0&=-\frac{1}{h^2}=\frac{2e^{ipt}\cos\omega}{h^2}\int_0^\infty\frac{\mathrm{ch}\,\alpha z}{\alpha}e^{-\alpha\xi}\frac{\partial J_1(fr)}{\partial r}f^2\,df,\\ v_0&=-\frac{1}{h^2r}\frac{\partial\Delta_0}{\partial\omega}=-\frac{2e^{ipt}\sin\omega}{h^2}\int_0^\infty\frac{\mathrm{ch}\,\alpha z}{\alpha}e^{-\alpha\xi}\frac{J_1(fr)}{r}f^2\,df,\\ w_0&=-\frac{1}{h^2}\frac{\partial\Delta_0}{\partial z}=\frac{2e^{ipt}\cos\omega}{h^2}\int_0^\infty\mathrm{sh}\,\alpha z\,e^{-\alpha\xi}J_1(fr)\,f^2\,df.\end{aligned}\right\}[z<\xi] \cdots (96)$$

The stress-components at the surface are expressed by

$$\left.\begin{aligned}[p_{zr}]_{z=0}&=0, \qquad [p_{z\omega}]_{z=0}=0,\\ [p_0]_{z=0}&=-2\kappa e^{ipt}\cos\omega\int_0^\infty\frac{e^{-\alpha\xi}}{\alpha}J_1(fr)\,f^2\,df.\end{aligned}\right\} \cdots\cdots\cdots (97)$$

Now, for gravity waves, the velocity potential ϕ will satisfy the equation of continuity such as

$$\frac{\partial^2\phi}{\partial r^2}+\frac{1}{r}\frac{\partial\phi}{\partial r}+\frac{\partial^2\phi}{\partial z^2}+\frac{1}{r^2}\frac{\partial^2\phi}{\partial\omega^2}=0, \quad \cdots\cdots\cdots\cdots (98)$$

the solution of which may be written by

$$\phi=-Ce^{-fz+ipt}J_1(fr)\cos\omega. \quad \cdots\cdots\cdots\cdots (99)$$

The displacement corresponding to this is expressed by

$$\left.\begin{aligned} u_1 &= -\frac{i}{p} C e^{-fz+ipt} \frac{\partial J_1(fr)}{\partial r} \cos\omega, \\ v_1 &= \frac{i}{p} C e^{-fz+ipt} \frac{J_1(fr)}{r} \sin\omega, \\ w_1 &= \frac{if}{p} C e^{-fz+ipt} J_1(fr) \cos\omega. \end{aligned}\right\} \quad \cdots\cdots\cdots\cdots (100)$$

From the integral of the equations of equilibrium and the kinematical condition at the surface, we find the surface pressure as below:

$$p_1 = -i\rho C \frac{p^2 - fg}{p} e^{-fz+ipt} J_1(fr) \cos\omega. \quad \cdots\cdots\cdots\cdots (101)$$

The condition at the surface gives us

$$C = -2\kappa \frac{e^{-a\xi}}{\alpha} \frac{pf^2}{i\rho(p^2 - fg)}. \quad \cdots\cdots\cdots\cdots (102)$$

The displacement in (100) is therefore written by

$$\left.\begin{aligned} u_1 &= \frac{2\kappa f^2 e^{-a\xi}}{\alpha\rho(p^2 - fg)} e^{ipt} \frac{\partial J_1(fr)}{\partial r} \cos\omega, \\ v_1 &= -\frac{2\kappa f^2 e^{-a\xi}}{\alpha\rho(p^2 - fg)} e^{ipt} \frac{J_1(fr)}{r} \sin\omega, \\ w^1 &= -\frac{2\kappa f^3 e^{-a\xi}}{\alpha\rho(p^2 - fg)} e^{ipt} J_1(fr) \cos\omega. \end{aligned}\right\} \quad \cdots\cdots\cdots\cdots (103)$$

Multiplying these by df, integrating from 0 to ∞ and afterwards adding to u_0, v_0 and w_0, besides the superposition of the terms due to Bessel's function of the second kind, we get

$$\left.\begin{aligned} u &= \frac{2\kappa e^{ipt} \cos\omega}{h^2\rho} \int_0^\infty \left[\frac{\rho}{\kappa} + \frac{h^2}{p^2 - fg}\right] e^{-a\xi} \frac{\partial H_1^{(2)}(fr)}{\partial r} \frac{f^2}{\alpha} df, \\ v &= -\frac{2\kappa e^{ipt} \sin\omega}{h^2\rho} \int_0^\infty \left[\frac{\rho}{\kappa} + \frac{h^2}{p^2 - fg}\right] e^{-a\xi} \frac{H_1^{(2)}(fr)}{r} \frac{f^2}{\alpha} df, \\ w &= -\frac{2\kappa e^{ipt} \cos\omega}{\rho} \int_0^\infty \frac{e^{-a\xi}}{p^2 - fg} H_1^{(2)}(fr) \frac{f^3}{\alpha} df. \end{aligned}\right\} \quad \cdots\cdots (104)$$

Considering the contour integrations similar to those in (86), we find

$$\left.\begin{aligned}
u=&\frac{2i\kappa e^{ipt}\cos\omega}{g\rho}\Bigg[\frac{p^2}{g}\frac{\pi}{\sqrt{1-\left(\frac{hg}{p^2}\right)^2}}e^{-\xi\sqrt{\frac{p^4}{g^2}-h^2}}\frac{\partial H_1^{(2)}\left(\frac{p^2}{g}r\right)}{\partial r}\\
&+\frac{g}{ih^2\kappa}\int_0^\infty\frac{\rho(p^2+igf)+\kappa h^2}{p^2+igf}e^{-i\xi\sqrt{f^2+h^2}}\frac{\partial H_1^{(2)}(-ifr)}{\partial r}\frac{f^2}{\sqrt{f^2+h^2}}df\Bigg],\\
v=&-\frac{2i\kappa e^{ipt}\sin\omega}{g\rho r}\Bigg[\frac{p^2}{g}\frac{\pi}{\sqrt{1-\left(\frac{hg}{p^2}\right)^2}}e^{-\xi\sqrt{\frac{p^4}{g^2}-h^2}}H_1^{(2)}\left(\frac{p^2}{g}r\right)\\
&+\frac{g}{ih^2\kappa}\int_0^\infty\frac{\rho(p^2+igf)+\kappa h^2}{p^2+igf}e^{-i\xi\sqrt{f^2+h^2}}H_1^{(2)}(-ifr)\frac{f^2}{\sqrt{f^2+h^2}}df\Bigg],\\
w=&-\frac{2i\kappa e^{ipt}\cos\omega}{g\rho}\Bigg[\frac{p^4}{g^2}\frac{\pi}{\sqrt{1-\left(\frac{hg}{p^2}\right)^2}}e^{-\xi\sqrt{\frac{p^4}{g^2}-h^2}}H_1^{(2)}\left(\frac{p^2}{g}r\right)\\
&+\frac{g}{i}\int_0^\infty\frac{e^{i\xi\sqrt{f^2+h^2}}}{p^2+igf}H_0^{(2)}(-ifr)\frac{f^3}{\sqrt{f^2+h^2}}df\Bigg].
\end{aligned}\right\}\quad(105)$$

Thus we find the components of displacement on the surface of the water in the forms:

$$\left.\begin{aligned}
u&\fallingdotseq\frac{2\kappa\pi}{g\rho}\frac{p^4}{g^2}e^{-\xi\sqrt{\frac{p^4}{g^2}-h^2}}\frac{\cos\left(pt-\frac{p^2}{g}r+\frac{3\pi}{4}\right)}{\sqrt{\frac{\pi p^2 r}{2g}}}\cos\omega,\\
v&\fallingdotseq\frac{2\kappa\pi}{g\rho r}\frac{p^2}{g}e^{-\xi\sqrt{\frac{p^4}{g^2}-h^2}}\frac{\sin\left(pt-\frac{p^2}{g}r+\frac{3\pi}{4}\right)}{\sqrt{\frac{\pi p^2 r}{2g}}}\sin\omega,\\
w&\fallingdotseq\frac{2\kappa\pi}{g\rho}\frac{p^4}{g^2}e^{-\xi\sqrt{\frac{p^4}{g^2}-h^2}}\frac{\sin\left(pt-\frac{p^2}{g}r+\frac{3\pi}{4}\right)}{\sqrt{\frac{\pi p^2 r}{2g}}}\cos\omega.
\end{aligned}\right\}\quad[p^2>hg]\quad\ldots.(106)$$

and

$$\left.u\fallingdotseq\frac{2\kappa\pi}{g\rho}\frac{p^4}{g^2}\frac{\sin\left(pt-\frac{p^2}{g}r+\frac{3\pi}{4}-\xi\sqrt{\frac{p^4}{g^2}-h^2}\right)}{\sqrt{\frac{\pi p^2 r}{2g}}}\cos\omega,\right.$$

$$\left.\begin{aligned} v &\fallingdotseq -\frac{2\kappa\pi}{g\rho r}\frac{p^2}{g}\frac{\cos\left(pt-\frac{p^2}{g}r+\frac{3\pi}{4}-\xi\sqrt{\frac{p^4}{g^2}-h^2}\right)}{\sqrt{\frac{\pi p^2 r}{2g}}}\sin\omega, \\ w &\fallingdotseq -\frac{2\kappa\pi}{g\rho}\frac{p^4}{g^2}\frac{\cos\left(pt-\frac{p^2}{g}r+\frac{3\pi}{4}-\xi\sqrt{\frac{p^4}{g^2}-h^2}\right)}{\sqrt{\frac{\pi p^2 r}{2g}}}\cos\omega, \end{aligned}\right\}[p^2<hg]\ldots(107)$$

corresponding to the displacement near the origin as written by

$$u_R \fallingdotseq \frac{1}{R}\cos(pt-hR)\cos\theta. \quad \ldots\ldots\ldots\ldots\ldots\ldots(108)$$

It is worthy of notice that in spite of the maintenance of the natures of the vertical and the horizontal components of displacement in wave profile and in azimuthal distribution, the azimuthal component of displacement quickly disappears as the distance from the origin increases.

6. In three-dimensional motion in which the origin of the disturbance is a doublet oscillating vertically, we find the solution of (91) in the following form:

$$\psi = e^{ipt}\frac{\partial}{\partial z}\frac{e^{-ihR}}{R}. \quad \ldots\ldots\ldots\ldots\ldots\ldots(109)$$

The radial displacement is approximately written by

$$u_R = \frac{1}{R}\cos(pt-hR)\sin\theta, \quad \ldots\ldots\ldots\ldots\ldots\ldots(110)$$

where θ is the latitude at the origin concerning the line of the oscillations.

Considering the effect of the image for the source $(r=0,\ z=\xi)$, we find

$$\psi = -2e^{ipt}\int_0^\infty \operatorname{ch}\alpha z\, e^{-\alpha\xi}J_0(fr)f\,df, \quad [y<\xi]\ldots\ldots\ldots(111)$$

so that the expressions of the displacement are givien by

$$\left.\begin{aligned} u_0 &= -\frac{2e^{ipt}}{h^2}\int_0^\infty \operatorname{ch}\alpha z\, e^{-\alpha\xi}J_1(fr)\,f^2\,df, \\ v_0 &= 0, \\ w_0 &= \frac{2e^{ipt}}{h^2}\int_0^\infty \alpha\operatorname{sh}\alpha z\, e^{-\alpha\xi}J_0(fr)f\,df. \end{aligned}\right\}[y<\xi] \quad \ldots\ldots(112)$$

The stress-components are expressed by

$$\left.\begin{aligned} &[p_{zr}]_{z=0}=0, \qquad [p_{z\omega}]_{z=0}=0, \\ &[p_0]_{z=0}=-2\kappa e^{ipt}\int_0^\infty e^{-\alpha\xi}J_0(fr)f\,df. \end{aligned}\right\} \quad \cdots\cdots\cdots\cdots\cdots\cdots (113)$$

Again, pursuing the same line of treatment as before, we find

$$C=2\kappa e^{-\alpha\xi}\frac{pf}{i\rho(p^2-fg)}. \quad \cdots\cdots\cdots\cdots\cdots\cdots (114)$$

The resultant displacement on the surface is expressed by

$$\left.\begin{aligned} u&=-\frac{2\kappa e^{ipt}}{h^2\rho}\int_0^\infty\left[\frac{\rho}{\kappa}+\frac{h^2}{p^2-fg}\right]e^{-\alpha\xi}J_1(fr)\,f^2\,df, \\ w&=-\frac{2\kappa e^{ipt}}{\rho}\int_0^\infty\frac{e^{-\alpha\xi}}{p^2-fg}J_0(fr)f^2\,df. \end{aligned}\right\} \quad \cdots\cdots\cdots (115)$$

Thus the results, when the contour integrations for the adjusted integrals are performed by means of the formulae similar to (86), are written by

$$\left.\begin{aligned} u=&-\frac{2i\kappa e^{ipt}}{g\rho}\left[\frac{p^4}{g^2}\pi e^{-\xi\sqrt{\frac{p^4}{g^2}-h^2}}H_1^{(2)}\left(\frac{p^2}{g}r\right)\right. \\ &\left.+\frac{g}{ih^2\kappa}\int_0^\infty\frac{\rho(p^2+igf)+\kappa h^2}{p^2+igf}e^{-i\xi\sqrt{f^2+h^2}}H_1^{(2)}(-ifr)\,f^2\,df\right], \\ w=&-\frac{2i\kappa e^{ipt}}{g\rho}\left[\frac{p^4}{g^2}\pi e^{-\xi\sqrt{\frac{p^4}{g^2}-h^2}}H_0^{(2)}\left(\frac{p^2}{g}r\right)\right. \\ &\left.+\frac{g}{i}\int_0^\infty\frac{e^{-i\xi\sqrt{f^2+h^2}}}{p^2-fg}H_0^{(2)}(-ifr)\,f^2\,df\right], \end{aligned}\right\} \quad \cdots (116)$$

Neglecting the second terms for a large distance, we obtain

$$\left.\begin{aligned} u&=\frac{2\kappa\pi}{g\rho}\frac{p^4}{g^2}e^{-\xi\sqrt{\frac{p^4}{g^2}-h^2}}\frac{\sin\left(pt-\frac{p^2}{g}r+\frac{3\pi}{4}\right)}{\sqrt{\frac{\pi p^2 r}{2g}}}, \\ w&=-\frac{2\kappa\pi}{g\rho}\frac{p^4}{g^2}e^{-\xi\sqrt{\frac{p^4}{g^2}-h^2}}\frac{\cos\left(pt-\frac{p^2}{g^2}r+\frac{3\pi}{4}\right)}{\sqrt{\frac{\pi p^2 r}{2g}}}, \end{aligned}\right\} [p^2>hg] \quad \cdots (117)$$

and

$$\left.\begin{aligned} u&=\frac{2\kappa\pi}{g\rho}\frac{p^4}{g^2}\frac{\sin\left(pt-\frac{p^2}{g}r+\frac{3\pi}{4}-\xi\sqrt{h^2-\frac{p^4}{g^2}}\right)}{\sqrt{\frac{\pi p^2 r}{2g}}},\\ w&=-\frac{2\kappa\pi}{g\rho}\frac{p^4}{g^2}\frac{\cos\left(pt-\frac{p^2}{g}r+\frac{3\pi}{4}-\xi\sqrt{h^2-\frac{p^4}{g^2}}\right)}{\sqrt{\frac{\pi p^2 r}{2g}}},\end{aligned}\right\}[p^2<hg]\quad\ldots(118)$$

corresponding to the displacement in the neighbourhood of the origin,

$$u_R=\frac{1}{R}\cos(pt-hR)\sin\theta,\quad[R^2=r^2+(z-\xi)^2]\quad\ldots\ldots(119)$$

Some notices which should be added here seem very like those in the preceding sections, so that we will complete this section without adding any remark.

Résumé.

The formation of deep water waves, when some disturbances act on a point in the interior of the water, has been studied. The compressional disturbances of the simple-harmonic type being propagated radially from the origin, a succession of gravity waves is gradually developed by the surface conditions of the water.

The method of analysis employed in this is, in the first place, to apply on the primary waves (the primary pressure having inertia effect) the mathematical results due to H. Lamb, i.e.

$$H_0^{(2)}(hR)=\frac{i}{\pi}\int_{-\infty}^{\infty}\frac{e^{-\alpha y}e^{\mp ifx}}{\alpha}df,\quad[R^2=x^2+y^2]$$

and

$$\frac{e^{-ihR}}{R}=\int_0^{\infty}\frac{e^{-\alpha z}}{\alpha}J_0(fr)\,fdf,\quad[R^2=x^2+y^2+z^2]$$

where

$$\alpha=\sqrt{f^2+h^2}\quad\text{or}\quad i\sqrt{h^2-f^2},$$

according as $f^2\gtrless h^2$. Some modified formulae have also been employed. In the second step, gravity waves, which are to be superposed on the primary waves, have been formulated to satisfy the boundary conditions.

The paper consists of six sections: the beginning three sections deal with the cases in which the origin is either a singlet, a doublet oscillating horizontally or a doublet moving vertically all in two dimensions, while the remaining three treat of the similar cases in three dimensions.

The principal results obtained by this investigation are enumerated as follows:

1. In spite of very small displacements of the compressional waves in the neighbourhood of the origin in the interior of the water, the excited surface waves have relatively large amplitudes.

2. The generated surface waves are chiefly the ordinary gravity waves having the same frequency as that of the origin together with their wave length proper to the period.

3. The distribution of the wave motion on the surface of water always conspires with the modes of oscillation at the origin.

4. This fails in a three-dimensional case where a doublet oscillates horizontally. In this, notwithstanding the maintenance of the natures of the vertical and the horizontal components of displacement in wave profile and in azimuthal distribution, the azimuthal component of displacement quickly disappears as the distance from the disturbed portion is increased.

Concluding Remarks.

We may now review some results of this mathematical investigation from the general consideration. Although the examples in the present paper are of some idealized kinds, yet we may say that the theory is an important guidance for the confirmation of the behaviours of the formation of deep-water waves under certain possible conditions. This can be clearly known in the light of other branches of siences in which highly idealized models contribute very often to the determination of the natures.

It has been necessary to idealize this problem in different manners to obtain the regorous solutions of the mathematical equations and to find the most important natures not in combined forms but in pure states. In the first place, the motion of both compressional and gravity waves has been taken to be small. The "small motion" is not meant that the amplitude of the motion is small, but it defines that the slope or the gradient of the motion is small. Secondly, the type of the motion is assumed to be simple-harmonic. Generalising this type by means of Fourier's double integral theorem the complicated cases such as the wave motion due to some arbitrary disturbances at the origin may be obtained without difficulty. This, however, has been omitted in this occasion and left for the future study.

The preceding solutions tell the fact that, in spite of very small displacements of the compressional waves in water, the generated surface waves proceed with large amplitudees. The figure in p. 28 is illustrated as an example. This example also shows that the deeper the origin of the disturbance and the quicker the period of the oscillations, the more quiescent become the surface waves at a certain distance. Not less important is the fact that at a large distance from the origin the generated surface waves due the compressional disturbances acting on the interior of the water are chiefly the ordinary gravity waves having the same frequency as that of the origin together with their wave length proper to the period. The orbital motion of the water particle is perfectly circular. An equally significant nature is that the distribution of the wave motion on the surface always conspires with the modes of the oscillations at the origin. An exceptional case is the three-dimensional motion due to a doublet oscillating horizontally. In this case, notwithstanding the maintenance of the natures of the vertical and the horizontal components of displacement in wave profile and in azimuthal distribution, the azimuthal component of displacement quickly disappears as the distance from the origin is increased.

The extended case of the present problem, in which the shallow-water waves are formed by the shocks at the bottom of the sea, is more significant on the practical seismology; this, however, will be left for future studies.(1)

In conclusion the author must express his sincere thanks to Professors Suyehiro and Terada for their kind advices.

September, 1928.

---

(1) The problem of shallow-water waves due to bottom shocks will be published in Bull. 7 of the Institute. The case of the pressure-distribution, in which the effect of inertia is neglected, will also be involved in that paper, because such a case is rather important on shallow-water problem.

Elastic Equilibrium of a Spherical Body under Surface Tractions of a Certain Zonal and Azimuthal Distribution.

By **Katsutada SEZAWA** and **Genrokuro NISHIMURA.**

Earthquake Research Institute.

方位的及帶狀的に分布せる表面應力を受ける彈性球體の平衡

所員 妹澤克惟
所員 西村源六郎

半無限體が一點の周圍に對稱をなさぬ荷重を受ける時の彈性平衡は寺澤博士などによつて既に解かれてゐるが、表面が球狀をなす場合は未だ考へられて居らぬ樣に思はれる。この問題が地形の複雜な部分例へばパナマの周圍の如き場所の潮汐荷重問題に大切な事は勿論であるが、尙海岸線の水陸分布による地殼の應力狀態の想像をも與へる。

この研究は完全な彈性體の場合に極めて嚴密な計算を施したものであるから、地球物理學の問題としては重力の影響（荷重自身の引力でなく）や、地球內部の物質分布及び物質の時間による變形の議論の必要があるが、前二者は計算の結果から見て唯其補正計算を別に行へば充分らしく、又時間による影響に就ては未だ一般物質の場合でさへ明瞭でないから猶研究の餘地があると思はれる。然し或る瞬間に於ける應力分布に對しては本文の結果が可成適用されるであらう。

計算の方法は球座標による彈性體平衡式から變容歪方程式と非變容歪方程式とを導出し、次に此等各に特有なる變位式を見出し、之に變容歪にも非變容歪にも無關係な變位式を加へて一般解式とする。上述の解式を境界條件によつて適當に調整しH調和分析によつて既與の荷重壓の爲めに生ずる內力の分布を得た次第である。

主要な結果を摘錄すれば、

（1） 球の一部に加へられた荷重が如何に集中する場合でも、球の內部の應力は全體に均一される傾向があり、これだけでも充分靜水壓の性質を示す。時によつて同じ半徑中にあつて異なる符號の應力の現はれる事もある。

（2） 表面では剪應力がなく、中心に向ふ垂直應力のみを與へても、他の直角方向の垂直應力が前述の垂直應力と略同じ値に達し、これが水底の固體應力の靜水平衡にある事と一致する傾向を示す。

（3） 本論文の第一章にある一般解式は其儘球の外部問題に應用され得る形、即ち張力、曲力、剪力を受ける無限彈性體に球窩や充塡物のある問題の解となる。但し具體的に係數等を決定する事は他の機會に殘した。

The theory of elastic equilibrium of a semi-infinite solid under a normal boundary pressure, which is distributed unsymmetrically about a point on the surface, was given by Prof. K. Terazawa,(1) leading to important results in regard to the geophysical problem such as the deflection of the vertical,(2) both in the tilting of the surface and in the sense of gravity, due to the tidal loading of the earth's surface. The present problem, which is somewhat similar to that of Prof. Terazawa, is related to the more extended case of the elastic equilibrium of a spherical body under surface tractions of a certain zonal and azimuthal distribution. Such a problem on the sphere in a simplest case, where there is symmetry about a point at the pole, was studied by many investigators, such as Lord Kelvin,(3) G. H. Darwin,(4) A. E. H. Love;(5) the case, in which the normal boundary pressure is not distributed symmetrically, has not yet been studied as far as the authors are aware.

The importance of dealing with the problem in the case, where there is no symmetry about a point on the surface, arises from the tidal loading in the aqueous region of the irregular form on the earth's surface, for instance, in the vicinity of Panama where there is a certain azimuthal distribution of land and sea. In fact, such distribution will be observed at various portions of the margin lines separating the continental block and th ocean basin or at the mountain ranges including volcanoes. Besides this, the equivalent stress distribution at some local point in the earth crust appears to exist everywhere, as supposed from the records of the

---

(1) K. Terazawa, *Phil Trans. Roy. Soc.* (A) **217** (1916); and also *J. Coll. Sci.*, Tokyo, **37** (1916).

(2) H Lamb, "On the Deflection of the Vertical by Tidal Loading of the Earth's Surface," *Roy. Soc. Proc.* (A) **93** (1917).

(3) Kelvin and Tait, *Nat. Phil.*, Part 2.

(4) G. H. Darwin, *Phil. Trans. Roy. Soc.*, **173** (1882).

(5) A. E. H. Love, *Some Problems of Geodynamics* (1911).

observation of the earthquake movements at different stations in the vicinity of the seismic origin.

The present paper treats of the problem of the elastic equilibrium of a non-gravitating spherical solid, whose elasticities and density are uniform. In the first section the general solutions of the problem have been obtained in the form of harmonic functions, while the second section deals with a certain example of polar loads of some azimuthal distribution.

The method of analysis employed in this paper is somewhat similar to that of the wave motion on the surface of an elastic sphere; in this case, however, a different component of displacement having a special meaning has been introduced. Moreover the azimuthal variation of the boundary pressure makes the treatment much difficult, yet the problem has been studied strictly throughout the whole paper.

In order to investigate the manner in which the elastic sphere is in equilibrium under the applied stress at the boundary, it will be necessary to consider the problem under certain simplifying assumptions. It will be assumed here that the earth may be treated as a homogeneous elastic body. The body will be supposed to be free from the effects of gravity and the rotation of the earth, as these effects are insignificant when the normal pressure on the boundary surface is not so small. The present study is some extension of the plane problem to the case where the effect of the curvature of the surface of the earth is taken into account; and the problems involving every geophysical element will be discussed in the further study.

1. General Solutions.

We shall use the spherical polar coordinates r, θ, ϕ, the origin being at the center of the sphere, the axis of $\theta=0$ being the radial line connecting the centre of the sphere and the poles, in the vicinity of which the normal pressure is distributed. We shall denote u, v, w as the components of displacement in the direction of the radius, colatitude and azimuth and λ, μ Lamé's elastic constants. Then the equations of equilibrium of the body are expressed by

$$\left.\begin{aligned}
&(\lambda+2\mu)\frac{\partial \Delta}{\partial r}-\frac{2\mu}{r\sin\theta}\frac{\partial(\varpi_\phi\sin\theta)}{\partial\theta}+\frac{2\mu}{r\sin\theta}\frac{\partial\varpi_\theta}{\partial\phi}=0,\\
&(\lambda+2\mu)\frac{1}{r}\frac{\partial \Delta}{\partial\theta}-\frac{2\mu}{r\sin\theta}\frac{\partial\varpi_r}{\partial\phi}+\frac{2\mu}{r}\frac{\partial(\varpi_\phi r)}{\partial r}=0,\\
&(\lambda+2\mu)\frac{1}{r\sin\theta}\frac{\partial \Delta}{\partial\phi}-\frac{2\mu}{r}\frac{\partial(\varpi_\theta r)}{\partial r}+\frac{2\mu}{r}\frac{\partial\varpi_r}{\partial\theta}=0,
\end{aligned}\right\}\quad\cdots\cdots\cdots(1)$$

where

$$\left.\begin{aligned}
\Delta&=\frac{1}{r^2\sin\theta}\left[\frac{\partial(ur^2\sin\theta)}{\partial r}+\frac{\partial(vr\sin\theta)}{\partial\theta}+\frac{\partial(wr)}{\partial\phi}\right],\\
2\varpi_r&=\frac{1}{r^2\sin\theta}\left[\frac{\partial}{\partial\theta}(wr\sin\theta)-\frac{\partial}{\partial\phi}(vr)\right],\\
2\varpi_\theta&=\frac{1}{r\sin\theta}\left[\frac{\partial u}{\partial\phi}-\frac{\partial(wr\,\mathrm{ins}\,\theta)}{\partial r}\right],\\
2\varpi_\phi&=\frac{1}{r}\left[\frac{\partial(vr)}{\partial r}-\frac{\partial u}{\partial\theta}\right].
\end{aligned}\right\}\quad\cdots\cdots\cdots(2)$$

The elimination of u, v, w among (1) and (2) gives us that

$$\left.\begin{aligned}
&\frac{1}{r^2}\frac{\partial}{\partial r}\left(r^2\frac{\partial \Delta}{\partial r}\right)+\frac{1}{r^2}\frac{\partial}{\partial\theta}\left(\sin\theta\frac{\partial \Delta}{\partial\theta}\right)+\frac{1}{r^2\sin^2\theta}\frac{\partial^2 \Delta}{\partial\phi^2}=0,\\
&\frac{\partial^2\varpi_r}{\partial r^2}+\frac{4}{r}\frac{\partial\varpi_r}{\partial r}+\frac{2}{r^2}\varpi_r+\frac{1}{r^2\sin\theta}\frac{\partial}{\partial\theta}\left(\sin\theta\frac{\partial\varpi}{\partial\theta}\right)+\frac{1}{r^2\sin^2\theta}\frac{\partial^2\varpi_r}{\partial\phi^2}=0,\\
&\frac{1}{r}\frac{\partial^2(\varpi_\theta r)}{\partial r^2}+\frac{1}{r^2\sin^2\theta}\frac{\partial^2\varpi_\theta}{\partial\phi^2}-\frac{1}{r^2\sin^2\theta}\frac{\partial^2\varpi(_\phi\sin\theta)}{\partial\phi\partial\theta}-\frac{1}{r}\frac{\partial^2\varpi_r}{\partial r\partial\theta}=0,\\
&\frac{1}{r}\frac{\partial^2(\varpi_\phi r)}{\partial r^2}+\frac{1}{r^2}\frac{\partial}{\partial\theta}\frac{1}{\sin\theta}\frac{\partial(\varpi_\phi\sin\theta)}{\partial\theta}-\frac{1}{r^2}\frac{\partial}{\partial\theta}\frac{1}{\sin\theta}\frac{\partial\varpi_\theta}{\partial\phi}-\frac{1}{r\sin\theta}\frac{\partial^2\varpi_r}{\partial r\partial\phi}=0.
\end{aligned}\right\}$$

$\cdots\cdots\cdots\cdots\cdots\cdots(3)$

These give us

$$\left.\begin{aligned}
\Delta&=\left(A_{mn}r^n+\frac{A'_{mn}}{r^{n+1}}\right)P_n^m(\cos\theta)\begin{matrix}\cos\\ \sin\end{matrix}\Big\}m\phi,\\
2\varpi_r&=\left(B_{mn}r^{n-1}+\frac{B'_{mn}}{r^{n+2}}\right)P_n^m(\cos\theta)\begin{matrix}\sin\\ -\cos\end{matrix}\Big\}m\phi,\\
2\varpi_\theta&=\left[\left(D_{mn}mr^n+\frac{D'_{mn}m}{r^{n+1}}\right)\frac{P_n^m(\cos\theta)}{\sin\theta}\right.\\
&\qquad\left.+\left(\frac{B_{mn}}{n},^{n-1}-\frac{B'_{mn}}{(n+1)\,r^{n+2}}\right)\frac{dP_n^m(\cos\theta)}{d\theta}\right]\begin{matrix}\sin\\ -\cos\end{matrix}\Big\}m\phi,
\end{aligned}\right\}\quad\cdots\cdots(4)$$

$$2\varpi_\phi=\left[\left(D_{mn}r^n+\frac{D'_{mn}}{r^{n+1}}\right)\frac{dP_n^m(\cos\theta)}{d\theta}\right.$$
$$\left.+\left(\frac{B_{mn}}{n}r^{n-1}-\frac{B'_{mn}}{(n+1)\,r^{n+2}}\right)\begin{matrix}\cos\\ \sin\end{matrix}\right\}m\phi,$$

in which A_{mn}, A'_{mn}, B_{mn}, B'_{mn}, C_{mn}, C'_{mn} are arbitrary constants.

Displacement (u_1, v_1, w_1) answering to Δ in (4) and satisfying $\varpi_r=\varpi_\theta=\varpi_\phi=0$ is expressed by

$$\left.\begin{aligned}
u_1&=\left[\frac{A_{mn}(n+2)}{2(2n+3)}r^{n+1}+\frac{A'_{mn}(n-1)}{2(2n-1)\,r^n}\right]P_n^m(\cos\theta)\begin{matrix}\cos\\ \sin\end{matrix}\Big\}m\phi,\\
v_1&=\left[\frac{A_{mn}}{2\,(2n+3)}r^{n+1}-\frac{A'_{mn}}{2(2n-1)\,r^n}\right]\frac{dP_n^m(\cos\theta)}{d\theta}\begin{matrix}\cos\\ \sin\end{matrix}\Big\}m\phi,\\
w_1&=-\left[\frac{A_{mn}m}{2\,(2n+3)}r^{n+1}-\frac{A'_{mn}}{2\,(2n-1)\,r^n}\right]\frac{P_n^m(\cos\theta)}{\sin\theta}\begin{matrix}\sin\\ -\cos\end{matrix}\Big\}m\phi.
\end{aligned}\right\}\quad\ldots\ldots(5)$$

Displacement (u_2, v_2, w_2) answering to ϖ_r together with the second terms in the expression of ϖ_θ, ϖ_ϕ, all given in (4) under the condition that $\Delta=0$, is expressed by

$$\left.\begin{aligned}
u_2&=0,\\
v_2&=\left[\frac{mB_{mn}}{n\,(n+1)}r^n+\frac{mB_{mn}}{n(n+1)\,r^{n+1}}\right]\frac{P_n^m(\cos\theta)}{\sin\theta}\begin{matrix}\cos\\ \sin\end{matrix}\Big\}m\phi,\\
w_2&=-\left[\frac{B_{mn}}{n\,(n+1)}r^n+\frac{B'_{mn}}{n(n+1)\,r^{n+1}}\right]\frac{dP_n^m(\cos\theta)}{d\theta}\begin{matrix}\sin\\ -\cos\end{matrix}\Big\}m\phi.
\end{aligned}\right\}\quad\ldots\ldots(6)$$

Displacement (u_4, v_4, w_4) derived from the values of the first terms of ϖ_θ, ϖ_ϕ, in (4) and fulfilling the conditions, $\Delta=\varpi_r=0$, is written by

$$\left.\begin{aligned}
u_4&=\left[\frac{D_{mn}n(n+1)}{2(2n+3)}r^{n+1}+\frac{D'_{mn}n(n+1)}{2(2n-1)\,r^n}\right]P_n^m(\cos\theta)\begin{matrix}\cos\\ \sin\end{matrix}\Big\}m\phi,\\
v_4&=\left[\frac{D_{mn}(n+3)}{2(2n+3)}r^{n+1}+\frac{D'_{mn}(n-2)}{2\,(2n-1)\,r^n}\right]\frac{1}{m}\,\frac{dP_n^m(\cos\theta)}{d\,\theta}\begin{matrix}\cos\\ \sin\end{matrix}\Big\}m\phi,\\
w_4&=-\left[\frac{D_{mn}\,m(n+3)}{2(2n+3)}r^{n+1}+\frac{D'_{mn}\,m(n-2)}{2(2n-1)\,r^n}\right]\frac{P_n^m(\cos\theta)}{\sin\theta}\begin{matrix}\sin\\ -\cos\end{matrix}\Big\}m\phi.
\end{aligned}\right\}\quad\ldots(7)$$

Displacement (u_3, v_3, w_3), which satisfies $\Delta=\varpi_r=\varpi_\theta=\varpi_\phi=0$, is expressed by

$$\left.\begin{aligned} u_3&=\left[C_{mn}\,nr^{n-1}-\frac{C'_{mn}\,(n+1)}{r^{n+2}}\right]P_n^m(\cos\theta)\begin{matrix}\cos\\ \sin\end{matrix}\Big\}m\phi,\\ v_3&=\left[C_{mn}\,r^{n-1}+\frac{C'_{mn}}{r^{n+2}}\right]\frac{dP_n^m(\cos\theta)}{d\theta}\begin{matrix}\cos\\ \sin\end{matrix}\Big\}m\phi,\\ w_3&=-m\left[C_{mn}\,r^{n-1}+\frac{C'_{mn}}{r^{n+2}}\right]\frac{P_n^m(\cos\theta)}{\sin\theta}\begin{matrix}\sin\\ -\cos\end{matrix}\Big\}m\phi. \end{aligned}\right\}\quad\cdots\cdots\cdots(8)$$

From the equations in (1) we have the identical relations such that

$$\frac{D_{mn}}{A_{mn}}=-\frac{(\lambda+2\mu)}{\mu(n+1)},\qquad \frac{D'_{mn}}{A'_{mn}}=\frac{\lambda+2\mu}{\mu n}.\quad\cdots\cdots\cdots\cdots\cdots(9)$$

Writing

$$\alpha=\frac{\lambda+2\mu}{\mu},\quad\cdots\cdots\cdots\cdots\cdots\cdots\cdots\cdots\cdots(10)$$

and substituting the relations of (9) in (7), we find the general expressions of the spherical problem of elasticity as follows:

$$\left.\begin{aligned} \Delta&=\left(A_{mn}r^n+\frac{A_{mn}}{r^{n+1}}\right)P_n^m(\cos\theta)\begin{matrix}\cos\\ \sin\end{matrix}\Big\}m\phi,\\ u_1=u_1\text{ in }(5)+u_4&=\left[\frac{A_{mn}\{(n+2)-\alpha n\}}{2(2n+3)}\,r^{n+1}\right.\\ &\qquad\left.+\frac{A'_{mn}\{(n-1)-\alpha\,(n+1)\}}{2(2n-1)\,r^n}\right]P_n^m(\cos\theta)\begin{matrix}\cos\\ \sin\end{matrix}\Big\}m\phi,\\ v_1=v_1\text{ in }(5)+v_4&=\left[\frac{A_{mn}\left\{1-\alpha\dfrac{n+3}{n+1}\right\}}{2(2n+3)}\,r^{n+1}\right.\\ &\qquad\left.-\frac{A'_{mn}\left\{1-\alpha\dfrac{n-2}{n}\right\}}{2(2n-1)\,r^n}\right]\frac{dP_n^m(\cos\theta)}{d\theta}\begin{matrix}\cos\\ \sin\end{matrix}\Big\}m\phi,\\ w_1=w_1\text{ in}(5)+w_4&=\left[-\frac{mA_{mn}\left\{1-\alpha\dfrac{n+3}{n+1}\right\}}{2(2n+3)}\,r^{n+1}\right.\\ &\qquad\left.+\frac{mA'_{mn}\left\{1-\alpha\dfrac{n-2}{n}\right\}}{2(2n-1)\,r^n}\right]\frac{P_n^m(\cos\theta)}{\sin\theta}\begin{matrix}\sin\\ -\cos\end{matrix}\Big\}m\phi, \end{aligned}\right\}\quad\cdots\cdots(11)$$

together with the expressions of u_2, v_2, w_2 in (6) and u_3, v_3, w_3 in (8).

Applying in the boundary conditions of stresses or of displacements the values of Δ, u, v, w, in which $u=u_1+u_2+u_3$, $v=v_1+v_2+v_3$, $w=w_1$

$+w_2+w_3$, we can determine various cases of physical problems. Some problems of practical importance, such as the present investigation, the stress-distribution in an elastic solid having cavities or imbedded spheres under certain boundary tractions and like problems, can be solved by means of the foregoing solutions.

2. Spherical Body under Surface Tractions of a Certain Zonal and Azimuthal Distribution.

We shall suppose the body to be strained by the application of the normal forces in the vicinity of a pole and at the antipode, where the forces have a certain zonal and azimuthal distribution. Thus we may put the boundary conditions in the forms:

$$\left.\begin{aligned} \widehat{r\theta}_{r=a} &= \mu\left(\frac{\partial v}{\partial r}-\frac{v}{r}+\frac{1}{r}\frac{\partial u}{\partial \theta}\right)_{r=a}=0, \\ \widehat{r\phi}_{r=a} &= \mu\left(\frac{1}{r\sin\theta}\frac{\partial u}{\partial r}+\frac{\partial v}{\partial \phi}-\frac{v}{r}\right)_{r=a}=0, \\ \widehat{rr}_{r=a} &= \left(\lambda\Delta+2\mu\frac{\partial u}{\partial r}\right)_{r=a}=\sin^2\theta\cos^q\theta\cos m\phi. \end{aligned}\right\} \quad \cdots\cdots\cdots\cdots (12)$$

Disregarding terms which approach to infinity as r tends to zero, we get from the first or the second equation in (12) the following relation:

$$\frac{C_{mn}}{A_{mn}}=\frac{\left\{\left(1-\alpha\frac{n+1}{n+1}\right)(1+n)-\left(1-\alpha\frac{n+3}{n+1}\right)+(n+2)-\alpha n\right\}a^2}{4(1-n)(2n+3)}, \quad \cdots\cdots (13)$$

the terms corresponding (6), which have the arbitrary constants B_{mn}, being omitted as they are not suited for the present case.

It remains now that, when C_{mn} are replaced by A_{mn} by means of (13), we should determine A_{mn} from the condition expressed by the third of the relations in (12). Thus we find the expression of the element $\widehat{rr}$ in the form:

$$A_{mn}\left[\lambda+\frac{(n+2-\alpha n)(n+1)}{2n+3}\mu\right.$$
$$\left.-\frac{n\left\{\left(1-\alpha\frac{n+3}{n+1}\right)(n+1)-\left(1-\alpha\frac{n+3}{n+1}\right)+(n+2)-\alpha\right\}}{2(n+3)}\mu\right]. \quad \cdots\cdots (14)$$

Now we may expand $\sin^2\theta\cos^q\theta\cos m\phi$ in series[1] of harmonic functions as below:

$$\sin^2\theta\cos^q\theta\cos m\phi=\sum_m\sum_n A_n^m a^n P_n^m(\cos\theta)\cos m\phi, \quad \ldots\ldots\ldots (15)$$

where

$$A_n^m=\frac{1}{\pi a^n}\frac{2n+1}{2}\frac{(n-m)!}{(n+m)!}$$
$$\int_{-\pi}^{\pi}\int_0^{\infty}\sin^2\theta\cos^q\theta\cos m\phi\, P_n^m(\cos\theta)\cos m\phi\sin\theta\, d\theta\, d\phi, \quad \ldots\ldots (16)$$

besides

$$A_n^m=A_{mn}\left[\lambda+\frac{(n+2-\alpha n)(n+1)}{2n+3}\mu\right.$$
$$\left.-\frac{n\left\{1-\alpha\frac{n+3}{n+1}\right)(n+1)-\left(1-\alpha\frac{n+3}{n+1}\right)+(n+2)-\alpha n\right\}}{2(2n+3)}\mu\right]\ldots\ldots (17)$$

From (16) and (17), we can determine the values of A_{mn}. Substituting these values of A_{mn} in the expressions of $\widehat{rr}$, $\widehat{\theta\theta}$, $\widehat{\phi\phi}$, $\widehat{r\theta}$, $\widehat{r\phi}$, $\widehat{\theta\phi}$, such that,

$$\left.\begin{aligned}
&\widehat{rr}=\lambda\Delta+2\mu\frac{\partial u}{\partial r}, \qquad \widehat{\theta\theta}=\lambda\Delta+2\mu\left(\frac{1}{r}\frac{\partial v}{\partial\theta}+\frac{u}{r}\right),\\
&\widehat{\phi\phi}=\lambda\Delta+2\mu\left(\frac{v}{r}\cot\theta+\frac{u}{r}+\frac{1}{r\sin\theta}\frac{\partial w}{\partial\phi}\right),\\
&\widehat{r\theta}=\mu\left(\frac{\partial v}{\partial r}-\frac{v}{r}+\frac{1}{r}\frac{\partial u}{\partial\theta}\right), \quad \widehat{r\phi}=\mu\left(\frac{1}{r\sin\theta}\frac{\partial u}{\partial\phi}+\frac{\partial w}{\partial r}-\frac{w}{r}\right),\\
&\widehat{\theta\phi}=\mu\left(\frac{1}{r}\frac{\partial w}{\partial\theta}+\frac{1}{r\sin\theta}\frac{\partial v}{\partial\phi}-\frac{w}{r}\cot\theta\right),
\end{aligned}\right\}\ldots\ldots (18)$$

and taking the case in which $q=8$, $m=2$, we obtain the stress-distributions of all the components of stresses as in the following forms:

$$\widehat{rr}_{r=a}=\sin^2\theta\cos^8\theta\cos 2\phi, \quad \ldots\ldots\ldots (19)$$

$$\widehat{rr}=\sum_{n=2}^{10}\frac{1}{a^n}\frac{2n+1}{2}\frac{(n-2)!}{(n+2)!}\frac{(n+1)\{3+n-n^2)\lambda+(2+n-n^2)\mu\}r^n}{(2n^2+4n+3)\lambda}$$
$$+\frac{+n\{n(n+2)\lambda+(n^2+2n-1)\mu\}a^2r^{n-2}}{+2(n^2+n+1)\mu}$$
$$\times\int_0^{\pi}\sin^3\theta\cos^8\theta P_n^2(\cos\theta)\, d\theta\times P_n^2(\cos\theta)\cos 2\phi, \quad \ldots\ldots\ldots (20)$$

(1) Whittaker, *Modern Analysis*, p. 393.

$$\widehat{\theta\theta}=\sum_{n=2}^{10}\frac{1}{a^n}\frac{2n+1}{2}\frac{(n-2)!}{(n+2)!}\frac{(1-n^2)\{(n+3)\lambda-(n-2)\mu\}r^n}{(1-n)\{(2n^2+4n+3)\lambda}$$
$$\frac{-n\{n(n+2)\lambda+(n^2+2n-1)\mu\}a^2r^{n-2}}{+2(n^2+n+1)\mu\}}$$
$$\times\int_0^\pi\sin^3\theta\cos^8\theta P_n^2(\cos\theta)\,d\theta\times P_n^2(\cos\theta)\cos 2\phi$$
$$+\sum_{n=2}^{10}\frac{1}{a^n}\frac{2n+1}{2}\frac{(n-2)!}{(n+2)!}\frac{(n-1)\{(n+3)\lambda+(n+5)\mu\}r^n}{(1-n)\{(2n^2+4n+3)\lambda}$$
$$\frac{-\{n(n+2)\lambda+(n^2+2n-1)\mu\}a^2r^{n-2}}{+2(n^2+n+1)\mu\}}$$
$$\times\int_0^\pi\sin^3\theta\cos^8\theta P_n^2(\cos\theta)\,d\theta\times\frac{d^2P_n^2(\cos\theta)}{d\theta^2}\cos 2\phi,\ldots\ldots(21)$$

$$\widehat{\phi\phi}=\sum_{n=2}^{10}\frac{1}{a^n}\frac{2n+1}{2}\frac{(n-2)!}{(n+2)!}\frac{(1-n^2)\{(n+3)\lambda-(n-2)\mu\}r^n}{(1-n)\{(2n^2+4n+3)\lambda}$$
$$\frac{-\{n(n+2)\lambda+(n^2+2n-1)\mu\}a^2r^{n-2}}{+2(n^2+n+1)\mu\}}$$
$$\times\int_0^\pi\sin^3\theta\cos^8\theta P_n^2(\cos\theta)\,d\theta\times P_n^2(\cos\theta)\cos 2\phi$$
$$+\sum_{n=2}^{10}\frac{1}{a^n}\frac{(2n+1)}{2}\frac{(n-2)!}{(n+2)!}\frac{(n-1)\{(n+3)\lambda+(n+5)\mu\}r^n}{(1-n)\{(2n^2+4n+3)\lambda}$$
$$\frac{-\{n(n+2)\lambda+(n^2+2n-1)\mu\}a^2r^{n-2}}{+2(n^2+n+1)\mu\}}$$
$$\times\int_0^\pi\sin^3\theta\cos^8\theta P_n^2(\cos\theta)\,d\theta\times\cot\theta\frac{dP_n^2(\cos\theta)}{d\theta}\cos 2\phi$$
$$-4\sum_{n=2}^{10}\frac{1}{a^n}\frac{(2n+1)}{2}\frac{(n-2)!}{(n+2)!}\frac{(n-1)\{(n+3)\lambda+(n+5)\mu\}r^n}{(1-n)\{(2n^2+4n+3)\lambda}$$
$$\frac{-\{n(n+2)\lambda+(n^2+2n-1)\mu\}a^2r^{n-2}}{+2(n^2+n+1)\mu\}}$$
$$\times\int_0^\pi\sin^3\theta\cos^8\theta P_n^2(\cos\theta)\,d\theta\times\frac{P_n^2(\cos\theta)}{\sin^2\theta}\cos 2\phi,\ldots\ldots(22)$$

$$\widehat{r\theta}=\sum_{n=2}^{10}\frac{1}{a^n}\frac{(2n+1)}{2}\frac{(n-2)!}{(n+2)!}\frac{\{n(n+2)\lambda+(n^2+2n-1)\mu\}(a^2r^{n-2}-r^n)}{(2n^2+4n+3)\lambda+2(n^2+n+1)\mu}$$
$$\times\int_0^\pi\sin^3\theta\cos^8\theta P_n^2(\cos\theta)\,d\theta\times\frac{dP_n^2(\cos\theta)}{d\theta}\cos 2\phi,\ldots\ldots(23)$$

$$\widehat{r\phi}=-2\sum_{n=2}^{10}\frac{1}{a^n}\frac{(2n+1)}{2}\frac{(n-2)!}{(n+2)!}\frac{\{n(n+2)\lambda+(n^2+2n-1)\mu\}(a^2r^{n-2}-r^n)}{(2n^2+4n+3)\lambda+2(n^2+n+1)\mu}$$
$$\times\int_0^\pi\sin^3\theta\cos^8\theta P_n^2(\cos\theta)\,d\theta\times\frac{P_n^2(\cos\theta)}{\sin\theta}\sin 2\phi, \quad \cdots\cdots\cdots (24)$$

$$\widehat{\theta\phi}=\sum_{n=2}^{10}\frac{(2n+1)}{a^n}\frac{(n-2)!}{(n+2)!}\frac{(n-1)\{(n+3)\lambda+(n+5)\mu\}r^n}{(1-n)\{(2n^2+4n+3)\lambda}$$
$$\frac{-\{n(n+2)\lambda+(n^2+2n-1)\mu\}a^2r^{n-2}}{+2(n^2+n+1)\mu\}}$$
$$\times\int_0^\pi\sin^3\theta\cos^8\theta P_n^2(\cos\theta)\,d\theta$$
$$\times\left\{\frac{\cos\theta}{\sin^2\theta}P_n^2(\cos\theta)-\frac{1}{\sin\theta}\frac{dP_n^2(\cos\theta)}{d\theta}\right\}\sin 2\phi\cdots\cdots (25)$$

As the above expressions in series are of finite number of terms, we may rewrite them as in the forms below:

$$\widehat{rr}=\left\{\frac{5}{9.11.13}\frac{3\lambda r^2+2(8\lambda+7\mu)a^2}{(19\lambda+14\mu)a^2}P_2^2(\cos\theta)\right.$$
$$+\frac{8}{11.13.15}\frac{4(24\lambda+23\mu)a^2r^2-5(9\lambda+10\mu)r^4}{(51\lambda+42\mu)a^4}P_4^2(\cos\theta)$$
$$+\frac{16}{15.17.33}\frac{6(48\lambda+47\mu)a^2r^4-7(27\lambda+28\mu)r^6}{(99\lambda+86\mu)a^6}P_3^2(\cos\theta)$$
$$+\frac{64}{13.15.19.33}\frac{8(80\lambda+79\mu)a^2r^6-9(53\lambda+54\mu)r^8}{(163\lambda+146\mu)a^8}P_8^2(\cos\theta)$$
$$+\frac{128}{13.15.17.19.33}$$
$$\left.\frac{10(120\lambda+119\mu)a^2r^8-11(87\lambda+88\mu)r^{10}}{(243\lambda+222\mu)a^{10}}P_{10}^2(\cos\theta)\right\}\cos 2\phi, \ldots (20')$$

$$\widehat{\theta\theta}=\left\{\frac{5}{9.11.13}\frac{3.5.\lambda r^2+2(8\lambda+7\mu)a^2}{(19\lambda+14\mu)a^2}P_2^2(\cos\theta)\right.$$
$$+\frac{8}{11.13.15}\frac{15(7\lambda-2\mu)r^4+4(24\lambda+23\mu)a^2r^2}{3(51\lambda+42\mu)a^4}P_4^2(\cos\theta)$$
$$+\frac{16}{15.17.33}\frac{35(9\lambda-4\mu)r^6+6(48\lambda+47\mu)a^2r^4}{5(99\lambda+86\mu)a^6}P_6^2(\cos\theta)$$
$$+\frac{64}{13.15.19.33}\frac{63(11\lambda-6\mu)r^8+8(80\lambda+79\mu)a^2r^6}{7(163\lambda+146\mu)a^8}P_8^2(\cos\theta)$$

$$+\frac{128}{13.15.17.19.33}\frac{99(13\lambda-8\mu)r^{10}+10(120\lambda+119\mu)a^2r^8}{9(243\lambda+222\mu)a^{10}}P_8^2(\cos\theta)\Big\}\cos 2\phi$$

$$+\Big\{\frac{5}{9.11.13}\frac{(8\lambda+7\mu)a^2-(5\lambda+7\mu)r^2}{(19\lambda+14\mu)a^2}\frac{d^2P_2^2(\cos\theta)}{d\theta^2}$$

$$+\frac{8}{11\ 13.15}\frac{(24\lambda+23\mu)a^2r^2-3(7\lambda+9\mu)r^4}{3(51\lambda+42\mu)a^4}\frac{d^2P_4^2(\cos\theta)}{d\theta^2}$$

$$+\frac{16}{15.17.33}\frac{(48\lambda+47\mu)a^2r^4+5(9\lambda+11\mu)r^6}{5(99\lambda+86\mu)a^6}\frac{d^2P_6^2(\cos\theta)}{d\theta^2}$$

$$+\frac{64}{13.15.19.33}\frac{(80\lambda+79\mu)a^2r^6-7(11\lambda+13\mu)r^8}{7(163\lambda+146\mu)a^8}\frac{d^2P_8^2(\cos\theta)}{d\theta^2}$$

$$+\frac{128}{13.15.17.19.33}$$

$$\frac{(120\lambda+119\mu)a^2r^8-9(13\lambda+15\mu)r^{10}}{9(243\lambda+222\mu)a^{10}}\frac{d^2P_{10}^2(\cos\theta)}{d\theta^2}\Big\}\cos 2\phi, \quad \ldots (21')$$

$$\widehat{\phi\phi}=\Big\{\frac{5}{9.11.13}\frac{3.5.\lambda r^2+2(8\lambda+7\mu)a^2}{(19\lambda+14\mu)a^2}P_2^2(\cos\theta)$$

$$+\frac{8}{11.13.15}\frac{15(7\lambda-2\mu)r^4+4(24\lambda+23\mu)a^2r^2}{3(51\lambda+42\mu)a^4}P_4^2(\cos\theta)$$

$$+\frac{16}{15.17.33}\frac{35(9\lambda-4\mu)r^6+6(48\lambda+47\mu)a^2r^4}{5(99\lambda+86\mu)a^6}P_6^2(\cos\theta)$$

$$+\frac{64}{13.15.19.33}\frac{63(11\lambda-6\mu)r^8+8(80\lambda+79\mu)a^2r^6}{7(163\lambda+146\mu)a^8}P_8^2(\cos\theta)$$

$$+\frac{128}{13.15.17.19.33}\frac{99(13\lambda-8\mu)r^{10}+10(120\lambda+119\mu)a^2r^8}{9(243\lambda+222\mu)a^{10}}P_{10}^2(\cos\theta)\Big\}\cos 2\phi$$

$$+\Big\{\frac{5}{9.11.13}\frac{(8\lambda+7\mu)a^2-(5\lambda+7\mu)r^2}{(19\lambda+14\mu)a^2}\Big(\frac{dP_2^2(\cos\theta)}{d\theta}\cot\theta-4\frac{P_2^2(\cos\theta)}{\sin^2\theta}\Big)$$

$$+\frac{8}{11.13.15}\frac{(24\lambda+23\mu)a^2r^2-3(7\lambda+9\mu)r^4}{3(51\lambda+42\mu)a^4}\Big(\frac{dP_4^2(\cos\theta)}{d\theta}\cot\theta-4\frac{P_4^2(\cos\theta)}{\sin^2\theta}\Big)$$

$$+\frac{16}{15.17.33}\frac{(48\lambda+47\mu)a^2r^4-5(9\lambda+11\mu)r^6}{5(99\lambda+86\mu)a^6}\Big(\frac{dP_6^2(\cos\theta)}{d\theta}\cot\theta-4\frac{P_6^2(\cos\theta)}{\sin^2\theta}\Big)$$

$$+\frac{64}{13.15.19.33}\frac{(80\lambda+79\mu)a^2r^6-7(11\lambda+13\mu)r^8}{7(163\lambda+146\mu)a^8}\Big(\frac{dP_8^2(\cos\theta)}{d\theta}\cot\theta$$

$$-4\frac{P_8^2(\cos\theta)}{\sin^2\theta}\Big)$$

$$+\frac{128}{13.15.17.19.33}\frac{(120\lambda+119\mu)a^2r^8-9(13\lambda+15\lambda)r^{10}}{9(243\lambda+222\mu)a^{10}}\left(\frac{dP_{10}^2(\cos\theta)}{d\theta}\cot\theta-4\frac{P_{10}^2(\cos\theta)}{\sin^2\theta}\right)\Big\}\cos 2\phi, \quad \ldots\ldots (22')$$

$$\widehat{r\theta}=\Big\{\frac{5}{9.11.13}\frac{(8\lambda+7\mu)(a^2-r^2)}{(19\lambda+14\mu)a^2}\frac{dP_2^2(\cos\theta)}{d\theta}$$
$$+\frac{8}{11.13.15}\frac{(24\lambda+23\mu)(a^2r^2-r^4)}{(51\lambda+42\mu)a^4}\frac{dP_4^2(\cos\theta)}{d\theta}$$
$$+\frac{16}{15.17.33}\frac{(48\lambda+47\mu)(a^2r^4-r^6)}{(99\lambda+86\mu)a^6}\frac{dP_6^2(\cos\theta)}{d\theta}$$
$$+\frac{64}{13.15.19.33}\frac{(80\lambda+79\mu)(a^2r^6-r^8)}{(163\lambda+146\mu)a^8}\frac{dP_8^2(\cos\theta)}{d\theta}$$
$$+\frac{128}{13.15.17.19.33}\frac{(120\lambda+119\mu)(a^2r^8-r^{10})}{(243\lambda+222\mu)a^{10}}\frac{dP_{10}^2(\cos\theta)}{d\theta}\Big\}\cos 2\phi, \ldots (23')$$

$$\widehat{r\phi}=-2\Big\{\frac{5}{9.11.13}\frac{(8\lambda+7\mu)(a^2-r^2)}{(19\lambda+14\mu)a^2}\frac{P_2^2(\cos\theta)}{\sin\theta}$$
$$+\frac{8}{11.13.15}\frac{(24\lambda+23\mu)(a^2r^2-r^4)}{(51\lambda+42\mu)a^4}\frac{P_4^2(\cos\theta)}{\sin\theta}$$
$$+\frac{16}{15.17.33}\frac{(48\lambda+47\mu)(a^2r^4-r^6)}{(99\lambda+86\mu)a^6}\frac{P_6^2(\cos\theta)}{\sin\theta}$$
$$+\frac{64}{13.15.19.33}\frac{(80\lambda+79\mu)(a^2r^6-r^8)}{(163\lambda+146\mu)a^8}\frac{P_8^2(\cos\theta)}{\sin\theta}$$
$$+\frac{128}{13.15.17.19.33}\frac{(120\lambda+119\mu)(a^2r^8-r^{10})}{(243\lambda+222\mu)a^{10}}\frac{P_{10}^2(\cos\theta)}{\sin\theta}\Big\}\sin 2\phi, \ldots\ldots (24')$$

$$\widehat{\theta\phi}=2\Big\{\frac{5}{9.11.13}\frac{(8\lambda+7\mu)a^2-(5\lambda+7\mu)r^2}{(19\lambda+14\mu)a^2}\frac{1}{\sin\theta}\left(\frac{\cos\theta}{\sin\theta}P_2^2(\cos\theta)-\frac{dP_2^2(\cos\theta)}{d\theta}\right)$$
$$+\frac{8}{11.13.15}\frac{(24\lambda+23\mu)a^2r^2-3(7\lambda+9\mu)r^4}{3(51\lambda+42\mu)a^4}\frac{1}{\sin\theta}\left(\frac{\cos\theta}{\sin\theta}P_4^2(\cos\theta)-\frac{dP_4^2(\cos\theta)}{d\theta}\right)$$
$$+\frac{16}{15.17.33}\frac{(48\lambda+47\mu)a^2r^4-5(9\lambda+11\mu)r^6}{5(99\lambda+86\mu)a^6}\frac{1}{\sin\theta}\left(\frac{\cos\theta}{\sin\theta}P_6^2(\cos\theta)-\frac{dP_6^2(\cos\theta)}{d\theta}\right)$$

$$+\frac{64}{13.15.19.33}\frac{(80\lambda+79\mu)\,a^2r^6-7(11\lambda+13\mu)\,r^8}{7(163\lambda+146\mu)\,a^8}\frac{1}{\sin\theta}\left(\frac{\cos\theta}{\sin\theta}P_8^2(\cos\theta)-\frac{dP_8^2(\cos\theta)}{d\theta}\right)$$

$$+\frac{128}{13.15.17.19.33}\frac{(120\lambda+119\mu)\,a^2r^8-9(13\lambda+15\mu)\,r^{10}}{9(243\lambda+222\mu)\,a^{10}}\frac{1}{\sin\theta}\left(\frac{\cos\theta}{\sin\theta}P_{10}^2(\cos\theta)-\frac{dP_{10}^2(\cos\theta)}{d\theta}\right)\Big\}\sin 2\phi\ldots\ldots(25')$$

Compiling these in the case $\lambda=\mu$, the results are plotted in the annexed drawing.

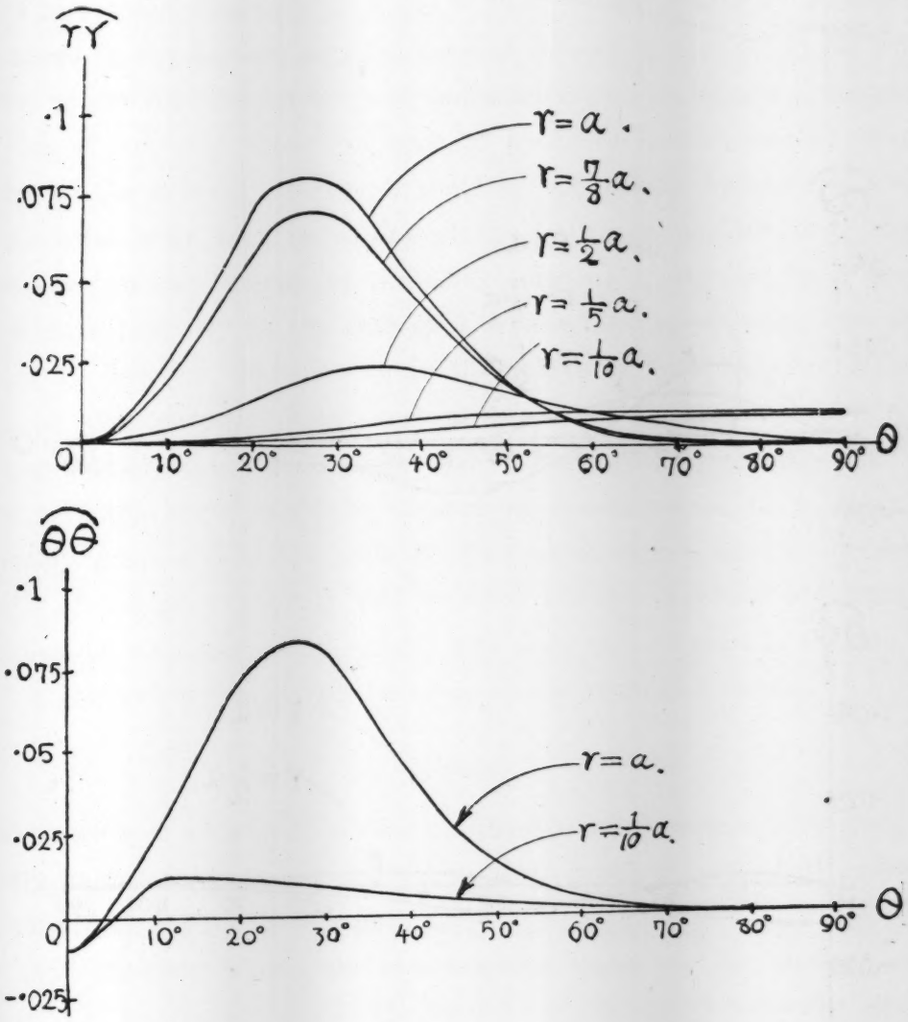

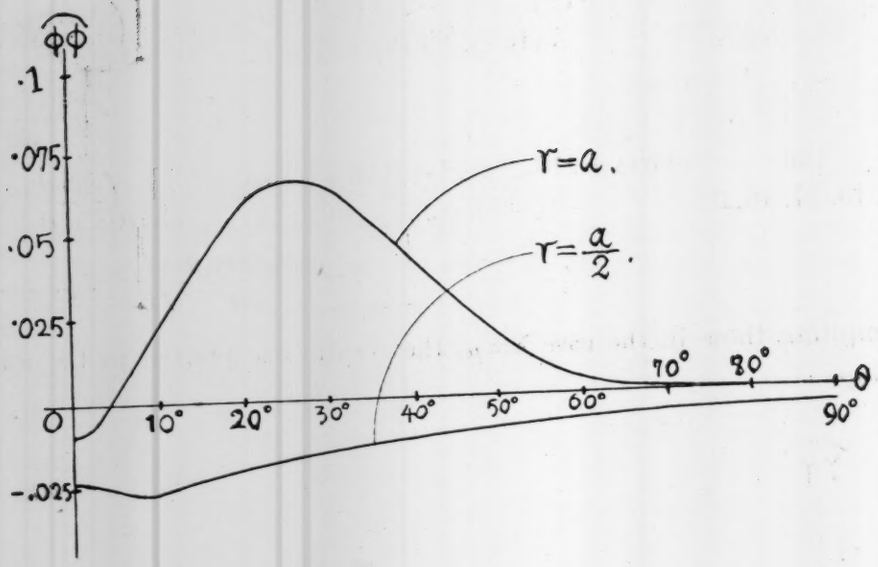
φφ
·1
·075
·05
·025
-·025
r=a.
r=a/2.
0
10°
20°
30°
40°
50°
60°
70°
80°
90°
θ

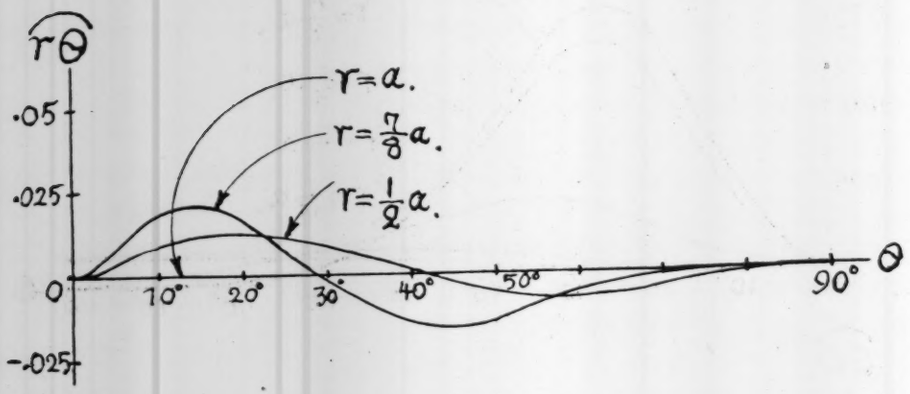
rθ
·05
·025
-·025
r=a.
r=7/8 a.
r=1/2 a.
0
10°
20°
30°
40°
50°
90°
θ

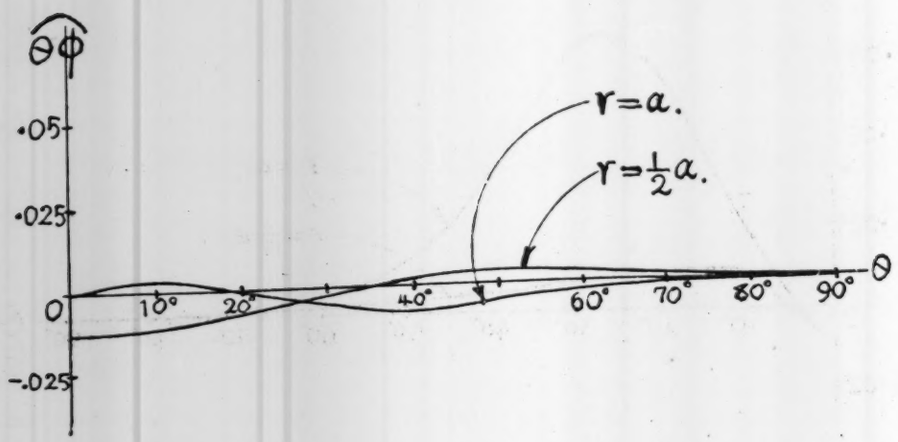
θφ
·05
·025
-·025
r=a.
r=1/2 a.
0
10°
20°
40°
60°
70°
80°
90°
θ

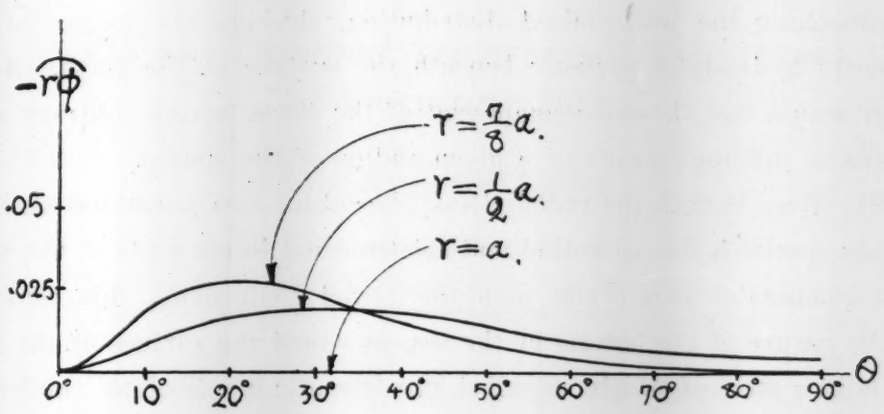

From these diagrams it appears that, however sharply concentrated the stress on the surface may be, the distribution of stresses in the interior of the sphere has the tendency of uniformization; sometimes it occurs that stresses of contrary signs can exist at a certain radius smaller than the radius of the sphere. It reveals that the apparently hydrostatic pressure in the solid body may be explained by the above uniformising property of stresses in the interior of the solid. Again, it will not be difficult to prove such property in the case of a semi-infinite solid body; this special nature is, however, conspicuous in the case of a solid sphere. The fact, that the components of stress, such as $\widehat{\theta\theta}$ and $\widehat{\phi\phi}$ are of comparable magnitude as that of $\widehat{rr}$, has some importance on break-down problem of the earth crust. If the earth could be treated as homogeneous, to a depth considerably greater than the scale of the tracted region on the surface, the results of the present study will be valid for the practical problem. The modification necessitated by gravity and some other causes is nothing more than a correction, which will be made to the principal results.

Résumé.

We have now obtained, by the application of harmonic functions, some results having interests on the geophysical problem, and shall enumerate the principal results as follows:

(1) However sharp the concentrated stress on the surface of the sphere may be, the stresses in the interior of the sphere have the tendency

of approaching the uniformized distribution, showing the nature of the apparently hydrostatic pressure beneath the surface of the earth. Sometimes it occurs that the same component of the stress having contrary signs can exist at different points of a given radius of the sphere.

(2) Even though the radial stress (excepting zero tangential stresses) is merely specified, the azimuthal and colatitudinal components of the stress are of comparable magnitude with the radial component; this conforms with the nature of the bottom of the sea, in which the surface of the solid earth is in a state of nearly so called "hydrostatic equilibrium" under the surface loading.

(3) Besides the problem of tidal loading in the equeous regions of the irregular form on the earth's surface, as in Panama, some portions of the margin lines separating the continental block and the oceanic basin, where the isostatic equilibrium of the crusts cannot hold perfectly and the state of stressed equilibrium is maintained, may be regarded as examples which will be treated of by the present analysis. The problem of apparently isostatic support, which holds for somewhat greater deepth of the earth crust, can be explained by the results of this paper without considering the liquidous basin for such small portions.

In concluding this the authors are indebted to Professor Terada for his kind advice.

October, 1928.

*On the Damped Transversal Vibration of Prismatic Bars.**

By **Kyoji SUYEHIRO,**

Member of the Institute.

壔狀體の減衰振動

所員　末廣恭二

架構の組子や塔や煙突などの如き、梁と見做すべきものの振動を論ずるには、其振動の減衰性を考慮せねば、場合によつては誤つた結論に到達する患がないとも限られぬ、本論文では振動に對する抵抗は、主として固體粘性によるものである、といふ說を基礎として梁の減衰振動を論じ、次の事柄を示してゐる、

（イ）振動の次の高き程急激に減衰性が增加すること、

（ロ）隨て或る一定の次以上の振動は生ずる患なきこと、

（ハ）種々の實例を解析して、減衰性を定むる量 ξ/E（ξ は縱粘性係數、E は「ヤング」率）の値を見出し、煉瓦及「コンクリート」造の梁に對しては此値を 10^{-3} の程度に取れば、實際の減衰性を見出し得ること、

（ニ）煉瓦及「コンクリート」造の梁は、一般に三次或は四次以上の自由振動を爲し得る可能性なきこと。

In the study of the vibration of structures, which is one of the important problems of applied seismology, the resistance against the vibration is very seldom, if ever, considered. Hence, in some cases there is a fear that the conclusion arrived at therefrom is incorrect.

In the present paper the author deals with the free transversal vibration of prismatic bars subjected to resistance. The nature of the free vibration of framed structures, towers, chimneys, etc. can well be inferred from the result of the present investigation.

The resistance against the vibration is, as well known, composed of two sorts, one of them being the air resistance and the other the internal

---

* An outline of this paper was published in Proc. Imp. Aca. 4, 6 (1928).

resistance due to the solid viscosity of the material or to its internal friction. The fact that the former is insignificant compared with the latters was shown by Lord Kelvin[1] and other investigators. Therefore, in the present investigation the air resistance is not taken into consideration.

The solid viscosity was first studied by W. Voigt and recently by K. Honda.[2] According to these investigators the viscosity of solid is similar to that of fluid and may be divided into two kinds:—

the tangential viscosity, $\eta\dfrac{\partial\phi}{\partial t}$,

and the normal viscosity, $\xi\dfrac{\partial e}{\partial t}$,

in which t is the time, and ϕ and e are shearing and tensile strains respectively. Although there is every possibility that the internal resistance does not wholly depend upon the rate of change of strain, but also to stress-amplitude,[3] yet the author takes up these investigators' view, as otherwise the problem is not amenable to mathematics, and as the aim of the present paper is merely to study the general nature of the resisted vibration; the investigation of the exact nature of the internal resistance itself being out of place.

To simplify the problem, let us take that the bar is uniform and straight, and has a longitudinal plane of symmetry, and also that the transversal vibration takes place parallel to this plane. Take the axis of the bar in the position of equilibrium as x, and an axis perpendicular to it and parallel to the plane of symmetry as y.

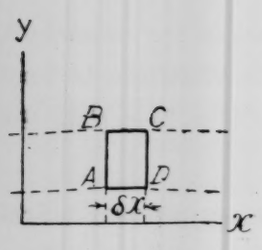

Then the equation of the lateral motion of an elementary slice $ABCD$ taken across the bar and having the thickness δx is

$$\rho A\frac{\partial^2 y}{\partial t^2}\delta x=\frac{\partial F}{\partial x}\delta x+A\eta\frac{\partial^2\phi}{\partial t\,\partial x}\delta x,$$

and as

(1) Lord Kelvin's Mathematical and Physical Papers, **3**.
(2) K. Honda, Phil. Mag. **42** (1921).
(3) Kimball and Lovell, Phys. Rev. **30**, 6 (1927).

$$\phi = \frac{F}{A\mu}, \qquad \ldots\ldots\ldots\ldots\ldots\ldots\ldots\ldots (1)$$

we have

$$\rho A \frac{\partial^2 y}{\partial t^2}\delta x = \frac{\partial F}{\partial x}\delta x + \frac{\eta}{\mu}\frac{\partial^2 F}{\partial x \partial t}\delta x, \qquad \ldots\ldots\ldots\ldots\ldots\ldots (2)$$

in which A is the sectional area of the bar, ρ its density, μ the modulus of rigidity, and F the shearing force at the section.

Again, if we denote the moment of inertia of the cross section about its neutral axis by I, the Young's modulus by E, and the bending moment at the section by M, the equation of the angular motion of the elementary slice is

$$\rho I \frac{\partial^2}{\partial t^2}\left(\frac{\partial y}{\partial x}\right)\delta x = -\frac{\partial M}{\partial x}\delta x + F\delta x - \frac{\partial}{\partial x}\left(\int_A \xi \frac{\partial e}{\partial t}.\, b.\, y'.\, dy'\right)\delta x + A\eta \frac{\partial \phi}{\partial t}\delta x \ldots\ldots\ldots (3)$$

in which y' is the distance of a point on the section from its neutral axis and b the breadth of the section. As

$$e = \frac{M}{E}\frac{y'}{I},$$

we have

$$\int_A \frac{\partial e}{\partial t} by'\, dy' = \frac{1}{EI}\frac{\partial M}{\partial t}\int_A y' by'\, dy = \frac{1}{E}\frac{\partial M}{\partial t}.$$

In virtue of this equality and also of (1), (3) can be written

$$\rho I \frac{\partial^2}{\partial t^2}\left(\frac{\partial y}{\partial x}\right)\delta x = -\frac{\partial M}{\partial x}\delta x + F\delta x - \frac{\xi}{E}\frac{\partial^2 M}{\partial x \partial t}\delta x + \frac{\eta}{\mu}\frac{\partial F}{\partial t}\delta x \ldots\ldots\ldots (4)$$

Taking off δx from (2) and (4), and eliminating F between them, we have

$$\rho A \frac{\partial^2 y}{\partial t^2} = \rho I \frac{\partial^2}{\partial t^2}\left(\frac{\partial^2 y}{\partial x^2}\right) + \frac{\partial^2 M}{\partial x^2} + \frac{\xi}{E}\frac{\partial^3 M}{\partial x^2 \partial t}.$$

Remembering that $M = -EI\frac{\partial^2 y}{\partial x^2}$, we obtain

$$\rho A \frac{\partial^2 y}{\partial t^2} = \rho I \frac{\partial^2}{\partial t^2}\left(\frac{\partial^2 y}{\partial x^2}\right) - EI\frac{\partial^4 y}{\partial x^4} - \xi I \frac{\partial^5 y}{\partial x^4 \partial t}. \qquad \ldots\ldots\ldots\ldots (5)$$

If we suppose that the transverse dimensions of the bar are small compared with its length, and confine our attention to the waves having

the lengths sufficiently larger than the transverse dimensions, the first term of the right-hand member of (5) may be neglected. Then the equation of motion for the resisted vibration of bars takes the form,

$$\rho A \frac{\partial^2 y}{\partial t^2} = -EI \frac{\partial^4 y}{\partial x^4} - \xi I \frac{\partial^5 y}{\partial x^4 \partial t}. \quad \cdots\cdots\cdots\cdots\cdots\cdots (6)$$

As this equation has already been obtained by T. Sezawa,[4] its deduction is not needed to be described. But as he did neither mention the process of obtaining it, nor show the extent of the applicability of the equation (6), the author describes the procedure in detail.

Now it is well known that the motion expressed by an equation as (6) may be analysed into component motions corresponding to the variation of normal co-ordinate. Accordingly put

$$y = u_r \phi_r,$$

in which u_r is a normal function and ϕ_r the corresponding normal co-ordinate. Substituting this into (6), we obtain

$$\frac{d^4 u_r}{dx^4} - m_r^4 u_r = 0,$$

and

$$\frac{d^2 \phi_r}{dt^2} + m_r^4 \frac{\xi}{\rho} \kappa^2 \frac{d\phi_r}{dt} + m_r^4 \frac{E}{\rho} \kappa^2 \phi_r = 0.$$

where $m_r = \frac{n_r}{l}$, n_r being the number characterizing the rth. order of vibration and l the length of the bar, and κ^2 stands for I/A.

From the latter equation we have

$$\phi_r = a\, e^{-\frac{1}{2} m_r^4 \frac{\xi}{\rho} \kappa^2 t} \cos\left(\frac{1}{2} \sqrt{4 m_r^4 \frac{E}{\rho} \kappa^2 - m_r^8 \frac{\xi^2}{\rho^2} \kappa^4}\, t - \alpha \right) \cdots\cdots\cdots (7)$$

This expression tells that the transverse vibration of a bar is impossible unless

$$m_r^8 \frac{\xi^2}{\rho^2} \kappa^4 < 4 m_r^4 \frac{E}{\rho} \kappa^2.$$

or

$$\frac{\pi \xi}{E} < \frac{2\pi}{m_r^2 \kappa} \sqrt{\frac{\rho}{E}}.$$

(4) K. Sezawa, This Bulletin, **3** (1927).

which can be written

$$\frac{\pi\xi}{E} < T_r, \qquad \cdots\cdots\cdots\cdots\cdots\cdots\cdots\cdots (8)$$

T_r being the period of the unresisted vibration of the rth order. This expression gives the upper limit of the frequency of the unresisted vibration and furthermore the upper limit of the order of the vibration. With regard to the same of the actual resisted vibration, it can be shown that the shortest period T_m with which an actual bar can vibrate is given by

$$T_m = \frac{2\pi\xi}{E}, \qquad \cdots\cdots\cdots\cdots\cdots\cdots\cdots\cdots (9)$$

(not quite this value, but the nearest to it). This can be obtained from (7) in finding the maximum value of $\frac{1}{2}\sqrt{4m_r^4\frac{E}{\rho}\kappa^2 - m_r^8\frac{\xi^2}{\rho^2}\kappa^4}$.

For steel $E=2\times10^{12}$, and if we take the vale of ξ given by Honda, namely $\xi=5\times10^8$, we have

$$\frac{\xi}{E}=2.5\times10^{-4}$$

Therefore, from (8) and (9)

$$\frac{\pi\xi}{E} \fallingdotseq 10^{-3}\ \text{sec.} \quad \text{and} \quad T_m \fallingdotseq \frac{1}{500}\ \text{sec.}$$

Thus, if the value of ξ given by Honda is correct, the frequency of the transverse vibration of a steel bar cannot exceed 500 times per sec. whatever scantlings it may have. Evidently our experience cannot justify such a conclusion.

By the way, the values of ξ found by several investigators differ so enormously that even the order of the magnitude cannot be definitely given. As this fact may most likely be attributed to the dissipation of the energy of the vibration of a piece of metal under test through its clamped end, the author experimented with a tuning fork made by a maker having the highest reputation in order to minimize the said effect. The value thus obtained was

$$\xi=5\times10^5$$

Although the author does not pretend that this value is correct, yet the

upper limit of the frequency of the vibration found from this value is not against our daily experience.

Thus even the viscous property of the steel is not quite unravelled, and still more obscure is that of ordinary building materials. Indeed, nobody has ever experimented upon it, and accordingly treatment of the damped vibration of a bar made of a building material is hopeless for the present. The following inference deduced from some seismological experiments may, however, gives us some rough idea about it.

Now the intensity of the resistance against the transversal vibration may be found from the exponential term in (7),

$$e^{-\frac{1}{2}m_r^4\frac{\xi}{\rho}\kappa^2 t}=e^{-\frac{1}{2}\frac{\xi}{E}\frac{4\pi^2}{T_r^2}t}=e^{-\frac{1}{2}kt}$$

in which k stands for $\frac{\xi}{E}\frac{4\pi^2}{T_r^2}$. Therefore, if the logarithmic decrement of the amplitude and the natural period of a vibration are given, we can guess the value of $\frac{\xi}{E}$. By the way, as the coeffcient of damping is inversely proportional to the square of the period of vibration, the higher the order of vibration, the quicker the vibration dies away. For instance, in a cantilever the coefficient of damping of the vibration of the second order is

$$\left(\frac{n_2}{n_1}\right)^4=\left(\frac{4.694}{1.875}\right)^4\fallingdotseq 39$$

times as large as that of the first order.

Now making use of the results of several investigators' experiments on the vibration of pillars, chimneys etc., we obtain the following results:—

(1) Experimenter, F. Omori.[5]

A brick column, 4.95 m. high $\times$ 0.455 m. broad $\times$ 0.225 m. deep.

Period of fundamental vibration = 0.26 sec.

Logarithmic decrement = 0.148

From these data, we obtain

$$\frac{\xi}{E}=1.95\times 10^{-3}$$

Therefore, from (8) and (9)

(5) F. Omori, Bull. Imp. Earthq. Inv. Comm. **2**, 3 (1908).

$$T_r > \frac{1}{160} \text{ sec.} \quad \text{and} \quad T_m \fallingdotseq \frac{1}{80} \text{ sec.}$$

Thus in this case the actual frequency cannot exceed 80 times per sec.

If we assume that the ratio of the frequencies of the vibrations of different orders is the same as that of a uniform prismatic cantilever, the upper limit of the frequency of the unresisted vibration is less than that of the 5th. order. In the remaining examples the upper limit of the frequency is not shown, as its calculation can easily be done. But it is worth especially mentioning that in all cases the vibration of the order higher than, say, the third or fourth cannot actually takes place, so that in dealing with the vibrations of a structure those of high orders should not be taken into consideration.

(2) Experimenter, F. Omori.[6]

A brick chimney, 15.45 m. high × 1.32 m. square.

Period of fundamental vibration = 1.03 sec.

Logarithmic decrement = 0.06

From these data we get

$$\frac{\xi}{E} = 3.13 \times 10^{-3}$$

(3) Experimenter, T. Taniguti.[7]

A reinforced concrete square frame:

Height, 200 cm.

Breadth, 200 cm.

Section, Rectangle, 10 cm. in depth (across the plane of the frame), and 8 cm. in breadth (in the plane of it).

Period of fundamental vibration = 0.14 sec.

Logarithmic decrement = 0.26

From these values we obtain

$$\frac{\xi}{E} = 1.85 \times 10^{-3}$$

---

(6) F. Omori, Pub. Imp. Earthq. Inv. Comm. 12 (1902).

(7) T. Taniguti, Jour. Jap. Soc. Arch. 506 (1928).

(4) Experimenter, T. Tanakadate.[8]

A brick chimney, 5.9 m. high × 1.06 m. square with two flues.

(a) Vibration in the direction of the least moment of inertia of section.

Period of fundamental vibration = 0.333 sec.

Logarithmic decrement = 0.253

Whence we have

$$\frac{\xi}{E} = 4.28 \times 10^{-3}$$

(b) Vibration in the direction of the largest moment of inertia of section.

Period of fundamental vibration = 0.450 sec.

Logarithmic decrement = 0.210

From these data we obtain

$$\frac{\xi}{E} = 4.78 \times 10^{-3}$$

It should be kept in mind that in all cases some portion of the energy of vibration might have dissipated through the fixed end. Therefore, the values of $\frac{\xi}{E}$ given in the above examples may have little value for finding ξ as a physical constant. However, for practical purpose of estimating the resistance against the vibration of an actual structural member the informations given above may be of some value.

(8) A Tanakadate, Rep. Imp. Earthq. Inv. Comm. (in Jap.) 21 (1898).

An Interpretation of the Results of the Repeated Precise Levellings in the Tango District after the Tango Earthquake in 1927.[1]

By **Chûji TSUBOI.**

Earthquake Research Institute.

昭和二年丹後地震後の水準測量成果の一解釋

坪　井　忠　二

昭和二年三月七日丹後地方を襲つた大地震に就ては、各方面に亘つて盛に研究が行はれた爲に地震に關する我々の知識が偉程進歩した樣に見える。其の中で最も著しい業績の一つは陸地測量部の手に依つて行はれた同地方の三角測量と水準測量との改測である。丹後地方には古い水準路線が一本通つて居るが此の他に地震後同地方には新に路線が幾本も設けられて之等の路線に沿つて水準測量が繰返して行はれることになつた。夫等の水準路線は第二圖に點線で示した通りである。水準測量は地震後今日迄に既に三回も繰返されて其の結果は其の都度研究所彙報に發表されて居る。夫等の結果から我々は丹後地方の地殻が地震後次第に變動して行く有樣を知る事が出來るのである。之等の測量の結果は非常に貴重な材料であつて出來るだけ色々な立場から解釋して見る事が必要であらう。既に寺田、宮部兩氏は地震後の三角測量から求めた地殻の水平運動と水準測量から求めた垂直運動との間に密接な關係がある事に注目して此の地方の地震後の運動はアイソスタシーの理論の要求する所と一致して居ると述べられて居る。自分が之等の問題に興味を抱いて居つた時偶々東北帝國大學の田山學士の「丹後但馬地震地域の地體構造と最近地史に就て」(齋藤報恩會學術研究報告第六號)が發行された。同氏の論文中の第一圖には但馬丹後地方の地塊が非常に細く圖示されてある。此の圖を見て居て早速氣が付いた事は此の樣な構造と地震後の地殻の變動との間に何か關係がありはしまいかと云ふ事であつた。それで早速調査を始める事にしたのであるが此の點に就いて田山氏の論文から暗示を得た事に對して謝意を表して置き度い。

それで次の樣な方法に依つて調査を行ふ事にした。第二圖に示した樣に水準路線の中で比較的急に屈曲して居る點にＡＢＣ等の名を付けて夫等の相隣る二つ

---

(1) Preliminary report appeared in Proc. Imp. Acad., 4 (1928), 529.

を直線で結び其の間にある各水準點を此の直線の上に直角に投影した。此の投影を水平軸に採り各水準點の高さの變りを垂直軸に採つて地殻の變動を表して見ると第三圖の樣になる。圖中●は第一回水準測量と第二回との間の變動量を○は第二回と第三回との間の變動量を表したものである。此の圖で著しく氣が付く事は各水準點の變動を表す點が多くの直線分の上に乘つて居る事と夫等の直線分の交點が●と○との二系列に就いても略同一の横軸上にある事とである。之等の事實を說明する爲に此の地方が所謂地塊から成立つて居て夫等が宛も水に浮んで居る木片の集りの樣に個々別々の運動をして居るとも考へられるであらう。特に第三圖で見られる樣に時に依つて傾動の方向を變じて居る地塊もある事は此の考を裏書する樣である。此の樣にして水準測量の結果の方から定めた地塊は第四圖に示した通りである。又一方地質學的方面の材料から定めた新しい斷層や地質學上の弱線は第五圖に示した通りである。第四圖の地塊の境を之等の斷層の位置と比較して見ると二つのものが極めてよく一致して居る事が認められる。卽地質學上の新らしい斷層は今なほ活動して居て夫が水準測量の結果に現れたと考へるのが至當であらう。數年間の觀測で測り得る程の短い間の地殻運動にも地質學上の構造が之程の意味を持つて居ると云ふ事は誠に注目す可き事と云はなければならない。之等の地塊運動と丹後大地震や其の餘震との間の關係に就いて何かはつきりした事を云ふ事は今の所では出來ない。唯注目すべき事實として第三圖bの樣に二つの地塊が始めは共通な傾動をなしてから後に別々の運動を始めた時に其の二つの地塊の境で發生したと考へられる樣な餘震が觀測されなかつた事を擧げて置く。若し地下に何か活動力の源となる樣なものを假定すれば其の影響を受けて一方では或る地方の地塊運動が促進され又他方では其の地方に地震が起こされると考へる事も出來るかも知れない。此の樣に考へると地塊運動と地震と云ふものは互に原因結果の關係で連なつて居るものではなくて共通の原因の二つの違つた現れと解釋す可きであるのかも知れない。

昭和三年十月

---

1. In the country of Japan, from which a world-shaking earthquake originates not rarely, the scope of seismology naturally goes further beyond the study of the propagation of purely elastic seismic waves and is extended to the investigation of those geophysical phenomena that are characteristic to the localities of the earthquake origin. Thorough studies of these phenomena are of prime importance for the earthquake research, as by means of those studies some informations are likely to be obtained concerning the cause and the mechanism of the occurrence of an earthquake. A change in the topographic features often observed in the case of a severe earthquake

in the neighbourhood of its origin, such as the formation of a remarkable fault, the warping of the ground, etc., is one of the most remarkable of these phenomena. Such topographic changes are sometimes too remarkable to be overlooked in passing observations, but they are often only to be detected by a series of delicate instrumental measurements. Thus, for instance, they are revealed by the comparison of the results of triangulations or precise levellings carried out before and after an earthquake over the disturbed area. During the past 40 years, 9 earthquakes have been reported[1] in this country with which some topographic changes were revealed to have accompanied, and it was also the case with the Tango great earthquake of 1927.

2. The Tango earthquake of which 2908 persons fell victims took place on March 7th, 1927, with its epicentral position $\varphi = 135° 1' \text{ E}$, $\lambda = 35° 39' \text{ N}$ as determined by Prof. A. Imamura.[2] In this earthquake,

Fig. 1. Shades....Meizoseismal Area.

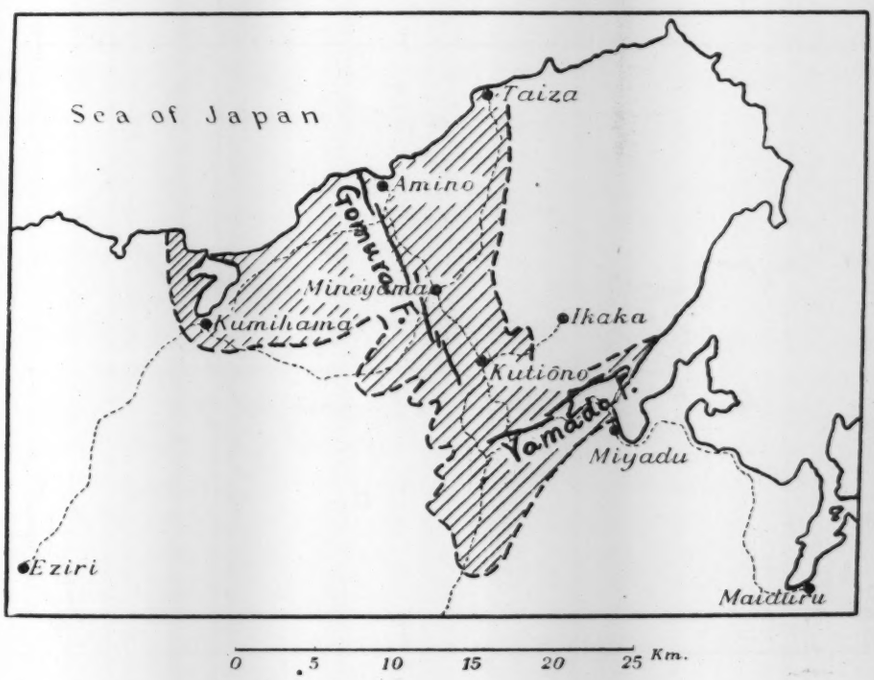

(1) A. Imamura, Proc. Imp. Acad., 4 (1928), 56.
(2) A. Imamura, Bull. Earthq. Res. Inst., 4 (1928), 179.

two remarkable faults were formed in accordance with the old dislocation lines, namely the Gômura fault and the Yamada fault which run nearly perpendicular to each other as shown in Fig. 1.(1)

All the geologists who visited the disturbed area and tried to trace back the history of the geological development of this district agree in saying that this earthquake is nothing but an episode in the course of geological development of this district.

3. Immediately after this earthquake, the Japanese Land Survey Department undertook the revision of triangulations and precise levellings over the disturbed area. One levelling route runs across the meizoseismal area along which precise levellings were once carried out 40 years before the earthquake. In addition to this, a number of bench marks were newly installed after the earthquake along the main roads in this district so that a net of the levelling routes thus laid out covers closely the disturbed area. These levelling routes are shown by dotted lines in Fig. 2.

Fig. 2.

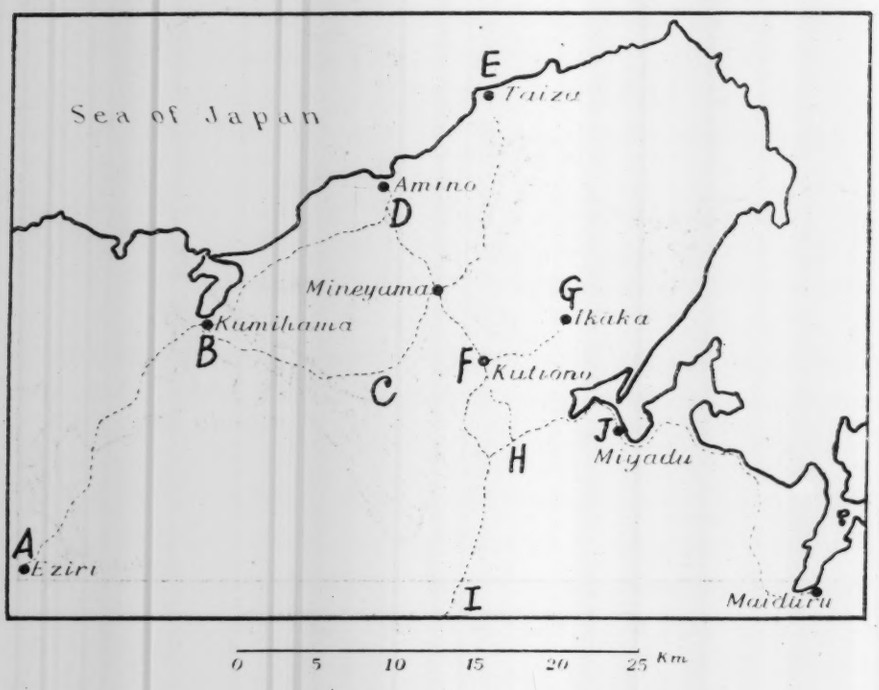

(1) Taken from N. Yamasaki and F. Tada, Proc. Imp. Acad., 3 (1927), 223.

The postseismic levellings were repeatedly carried out along these routes in view of getting, if possible, some informations regarding the mode in which the ground in this district settles after being greatly disturbed by the catastrophe. The first of the postseismic levellings was carried out from April 12 to June 16, 1927, the second from June 1 to July 31, 1927, and the third from March 3 to April 20, 1928. The results of these levellings were already published in the Bulletin of this Institute.[1] These results are extremely interesting and have already been subjected to much discussions.[2]

In the present paper will be given the results of a comparative study made upon the results of the three series of the postseismic precise levellings, by which a very peculiar mode in the settling movements of the crust in this region was found.

4. The vertical displacements of the bench marks in the Tango district in the interval between two successive levellings are given in the following tables. The data in the tables were taken from the series of reports by the Land Survey Department and were rearranged into a form to be conveniently referred to. The geographical positions of the bench marks may be identified by the reference to the map in Fig. 2.

TABLE I.

I....Height in the first levelling.
II....Height in the second levelling.
III....Height in the third levelling.

Bench Mark	II−I	III - II
		mm
1363		−17.4
1364		−18.0
	mm	
1365	+8.5	−17.3
1366	+6.2	−19.1
1367	+5.0	−19.3
1368	+4.9	−15.8

(1) The Land Survey Department, Bull. Earthq. Res. Inst., **3** (1927), 167; **4** (1928), 225; **5** (1928), 165.

(2) T. Terada and N. Miyabe, Proc. Imp. Acad., **4** (1928), 211.

1369	+3.5	−16.1
1370	+2.3	−14.7
1371	+0.3	−15.0
1372	+0.2	−14.2
1373	−1.1	−14.6
1374	−0.5	−15.6
1375	−2.0	−13.0
1376	−1.0	−13.0
1241 (J Miyadu)	−3.5	−11.0
1240	−3.2	− 8.7
1239	−1.2	− 8.7
1238	−2.2	−10.2
1237	−3.6	−15.8
1236	−2.8	−11.1
1235 (H)	−0.1	+ 1.2
1234	−2.7	+ 2.8
1233	−1.4	− 1.3
1232 (F Kutiôno)	0.0	0.0
1231	−5.8	− 2.2
1230	−5.2	− 6.3
1229 (Mineyama)	−3.1	− 2.4
1228	+2.5	+ 7.6
1227	−2.5	+ 5.0
1226 (C)	−8.0	+ 4.6
1225	−9.0	+ 2.8
1224	−7.0	+ 1.0
1223	−2.5	+ 0.5
1222	−5.6	+ 2.5
1221	−7.8	+ 4.3
1220	−6.6	− 4.0
1219	−5.1	− 2.2
1218 (B Kumihama)	−8.5	+ 0.2
1217	−7.1	+ 1.9
1216	−3.6	+ 2.6
1215	−3.5	+ 2.4
1214	−1.1	− 0.4
1213	+0.4	− 7.3
1212	—	−23.5
1211	−3.0	−22.2
1210	−2.4	−16.9
1209	−1.2	−17.7
1208	−1.8	−20.9
1207	−0.2	−22.7
1206 (A Eziri)	−0.1	−22.4

TABLE II.

Bench Mark	II—I	III—II
1256	+3.0	−38.8
10446	+4.7	−38.0
10447	+5.7	−39.3
10448	+9.2	−41.0
10449	+9.2	−37.7
10450	+10.7	−33.7
10451	+5.8	−32.7
10452	+4.4	−33.5
10453	+6.1	−35.8
10454	−2.1	−31.0
10455	−5.2	−25.3
10456	−4.0	−19.7
10457 (I)	+0.8	−17.8
10458	−0.8	−18.1
10459	+0.2	−14.0
10460	−2.4	−11.6
10461	−2.6	−23.8
10462	−3.4	+ 6.8
10463	−1.1	− 5.0
10464	+2.5	+ 6.4
1232 (F Kutiôno)	0.0	0.0
10465	−0.8	− 4.9
10466	−1.4	− 3.3
10467	−2.4	− 4.4
10468 (G Ikaka)	−1.6	− 1.4

TABLE III.

Bench Mark	II - I	III−II
1218 (B Kumihama)	−5.4	+0.2
10489	−6.8	+0.9
10488	−6.8	−0.1
10487	−3.5	−1.6
10486	−2.9	−0.3
10485	−2.2	−1.5
10484	−1.3	−2.6
10483	−1.3	+4.1
10482	+2.7	+6.6
10479 (D Amino)	+5.1	+12.4

TABLE IV.

Bench Mark	II−I	III−II
10481	+3.9	
10480	−0.5	
10479 (D Amino)	+5.1	+12.4
10478	+3.7	+10.0
10477	−2.2	+ 4.7
1229 (Mineyama)	−3.1	− 2.4
10469	−2.7	− 2.5
10470	−2.0	− 3.0
10471	−0.5	− 4.7
10472	+0.1	− 0.1
10473	+2.1	− 1.9
10474	+2.0	− 2.5
10475	+3.8	− 2.8
10476 (E Taiza)	+3.2	− 1.4

5. These results were subjected to an examination in the following manner. Every turning points of the levelling routes with a sharp bent was marked by A. B. C. etc., as is shown in Fig. 2, every adjacent two of which were connected by a segment of straight line. The position of every bench mark between the two points is normally projected upon the segment which connect the two. Taking these projections along the horizontal axis, the vertical displacement of a bench mark is represented by a point with its height from its foot taken proportional to $\triangle h$. A few examples of the diagrams thus obtained are shown in Fig. 3, in which the mark ● corresponds to the displacement of a bench mark during the interval between the first and second levellings while ○ to that between the second and the third.

In making these diagrams, the Kutiôno bench mark (No. 1232) was assumed as fixed in height throughout the three levellings to which the vertical displacements of all the other bench marks were referred. No loss in generality is, of course, introduced by this assumption.

6. Two remarkable features will be recognised in the manner of distribution of the points in the diagrams; the one is that the points lie on a number of segments of straight lines, and the other is that the joints

Fig. 3a.

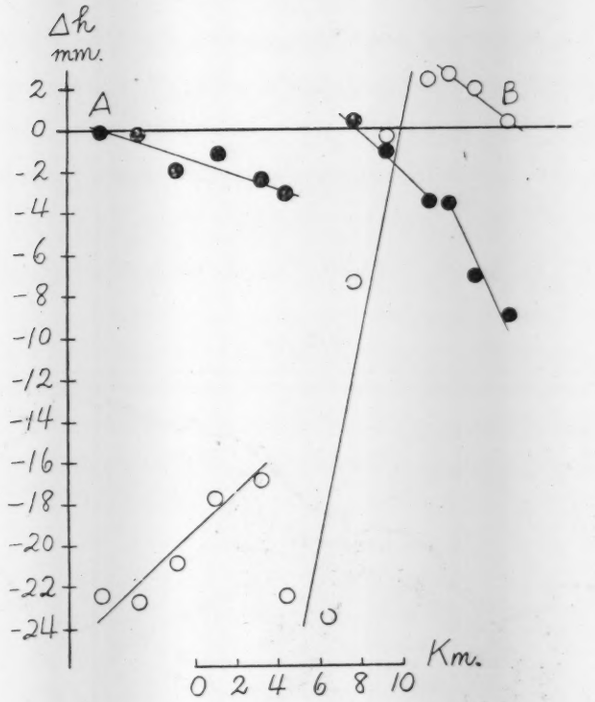

Fig. 3b.

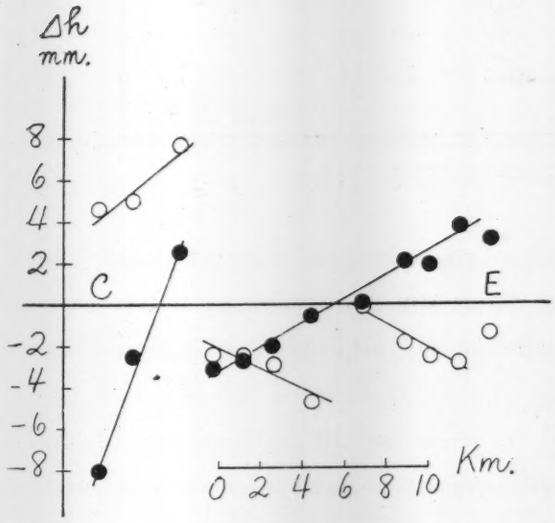

Fig. 3c.

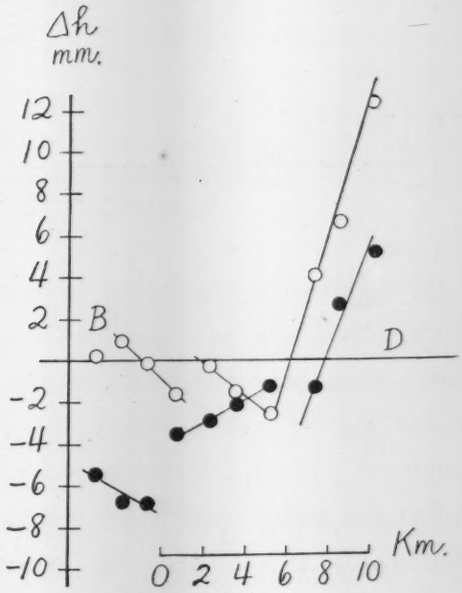

of these segments occur at the same abscissæ for both series of graphs which correspond to different epochs of the levellings. The latter two facts are well elucidated by assuming that the ground in this district is made up of a number of discrete structural units, each of which behaves as a rigid body as a whole, being bordered with its neighbours by boundary lines corresponding to the joints of segments in the above figures.

The positions of the boundaries of these units as revealed by the above analysis are shown by thick lines in Fig. 4, each shaded part between two

Fig. 4.

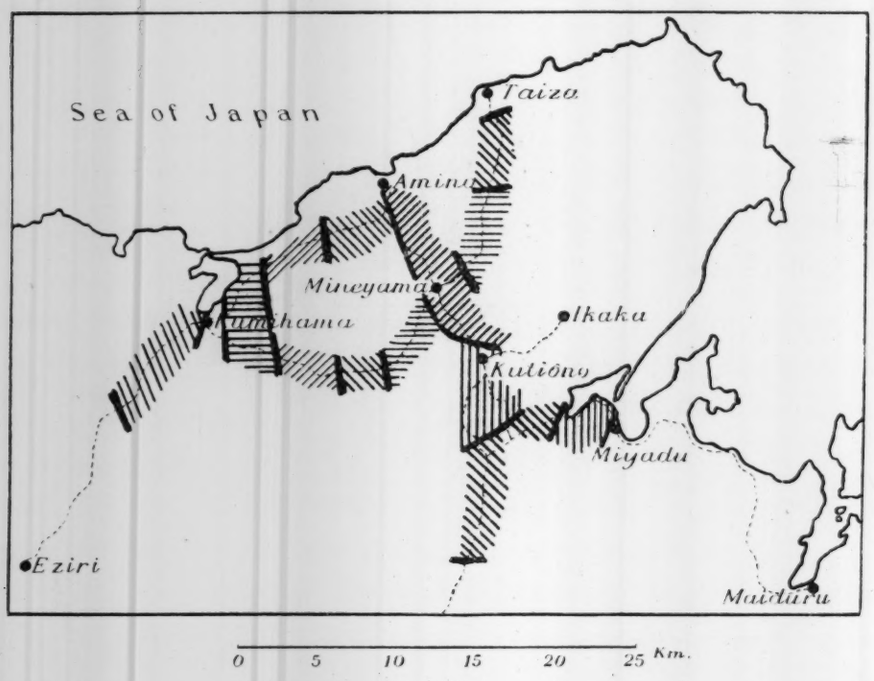

of these lines corresponding to a unit of structure of the ground. The bench marks lying on one and the same unit are rigidly connected to each other, being only subjected to the common tilting, upheaval, depression, etc., of the unit as a whole. In Fig. 3, the inclination of some of the structural units is seen to be inverted in sense for different epochs of the levellings. Each structural unit must have been able to move comparatively easily at least after the great earthquake.

7. After the structure of the Tango earthquake district has been ex-

plored by a *physical* method and a remarkable structural feature has been found, the *geological* data concerning the structure of this district will now be referred to, so as to get, if possible, a geological interpretation of the above feature. The geological structure of this district were investigated by many workers[1] who made visits to the district immediately after the earthquake. Through the efforts of these geologists, a number of young faults as well as geologically weak lines are found to run in different directions as shown in Fig. 5.

Fig. 5.

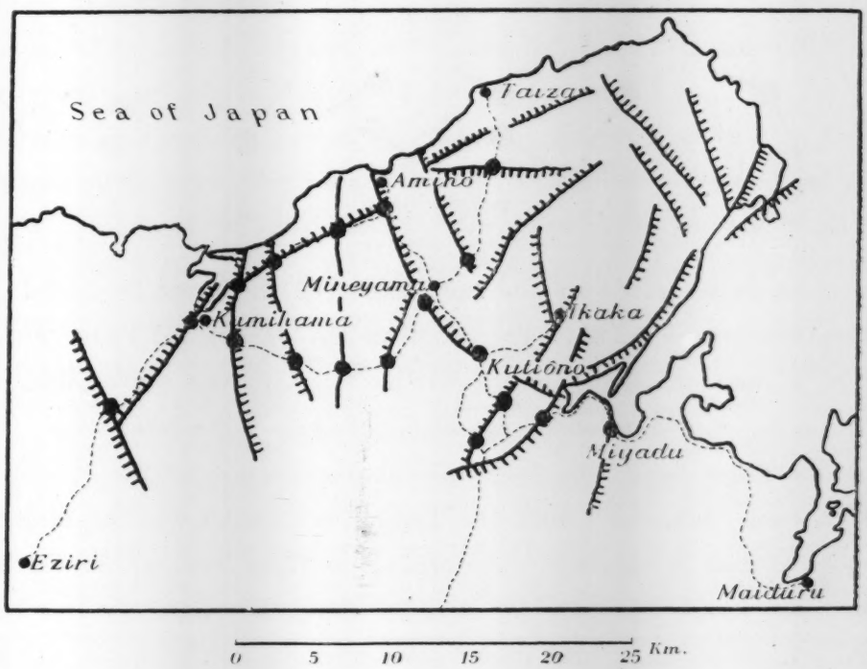

The levelling routes cross with several of these lines at the points marked by black dots as shown in Fig. 5. When the positions of these points are compared with those of boundary lines between the structural units in Fig. 4, a very close coincidence is found to exist between them.

(1) B. Kotô, Journ. Fac. Sci Tok. Imp. Univ., Sec. II, Vol. II, Part 6, (1928).
H. Tsuya, Bull. Earthq. Res. Inst., 4 (1928), 139.
K. Watanabe and H. Satô, Rep. Imp. Geol. Survey, No. 110 (1928).
F. Tada, Bull. Earthq. Res. Inst., 5 (1928), 111, etc.

What is inferred from this fact is that these young faults are still in their phase of activity and the intervening ground between any two of them behaves approximately as a block of rigid body. It is quite a remarkable fact that the tectonic structure of the crust still maintains its significance in such a momentary movement as is here dealt with.

8. The movements of the ground at the boundaries of the structural units may be classified into following types, of which the numbers of the case actually observed in the present study are shown in the second row under the corresponding entries.

Fig. 6.

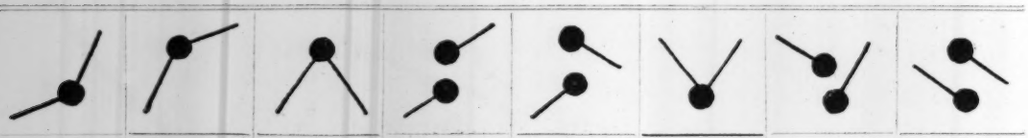

0	1	1	0	1	5	1	5

9. A peculiar mode of the movements of the crust is found in the case illustrated in Fig. 3b. The existing two structural units were subjected to a common tilting in the earlier stage of the movements, before their respective and differential movements began in the later stage.

On the other hand, the geographical distribution of the epicenters of the after-shocks connected with the Tango earthquake was investigated by A. Imamura and N. Nasu.[1] According to their results, *no* earthquake was recorded whose epicentre lay near or along the boundary line between the two structural units now under consideration in the epoch when these two units began their respective movements. This is quite an important fact from which much may be suggested concerning the mechanism of occurence of an earthquake in special connection with the movements of the crust, though it will be premature to draw any definite conclusions out of this single datum.

10. Whether or not the activity of the young faults in the Tango

(1) A. Imamura and N. Nasu, Proc. Imp. Acad., **3** (1927), 227.
N. Nasu, Ibid., **4** (1928), 378.

district has been accelerated by the earthquake is not certain. There are, on the other hand, good many reasons to expect that the earth crust, especially in Japan, is in a state of perpetual movement. The rate of movement is often so rapid as to be well detected by a measurement with delicate instrument in an interval of several ten years.(1) It seems to be not improbable that when some subterranean geophysical agencies, if there are such things at all, once begin their activities in some localities, the block movements in the same localities may be accelerated as one of their results and at the same time an earthquake may occur in the same localities as another of their results. The latter two phenomena are then not causally connected with each other, but rather are the different manifestations of the action of the same subterranean agencies.

Aftr all, a literally *mosaic* structure of the earth crust was found in the Tango earthquake district and the movement of each of its structural elements was traced in some detail. The present writer was thus finally led to believe, with most geologists, that the earth crust with its discrete structural constituents is as ever in a state of perpetual movement and the phenomena of earthquake is nothing but an accidental manifestation of the activity of some subterranean agencies then prevailing in the earthquake district.

In the course of this study, the writer had much occasions to have talks about the present problem with Professors T. Terada, M. Ishimoto, S. Tsuboi, Messrs. F. Tada and H. Tsuya which were very useful for him. The writer wishes to express his best thanks and indebtness to these gentlemen for their kind advices and instructions. Finally he highly appreciates the elaborate works of the Land Survey Department of the Imperial Army which have made so great a contribution to the development of Seismology hardly to be overestimated.

October 1928.

---

(1) A. Imamura, Proc. Imp. Acad., 4 (1928), 56, 109.
N. Yamasaki, Ibid., 4 (1928), 60.

Tilting Motion of the Earth Crust caused by Tidal Loading.

Ryûtarô TAKAHASI,

潮汐の負荷による地殻の傾斜運動

高　橋　龍　太　郎

石本式熔融シリカ製の傾斜計を神奈川三崎の臨海實驗所内に据えてなされた觀測である。觀測は昭和三年七月二十七日から初まつて以來現在まで續いて行はれてゐるが、其の内八月中の分丈けをまとめたものが本論文である。

器械は海岸から二十米程離れた所に据えられてゐるが、其れは油壺灣内の潮汐と全く相應した傾斜運動をする事を示してゐる。即ち海面が一米昇ると約一秒丈け海岸の方に向つて傾く事が判かつた。油壺灣内には時折著しいセイシユが見られるのであるが、此の傾斜計はそれをも記錄するのである。

傾斜計の偏差を起すあらゆる原因について考察されたが、其の結果此の傾斜計の偏差は殆んど全部潮汐の負荷による地殻の彎曲による事が判つた。然し從來ある樣な理論で計算したのでは何うしても實際の傾斜とは方向の違つたものになる。此の現象を說明するには傾斜計から百五十米以上の距離にある海水の負荷の變化は觀測點の傾斜には影響を及ぼさないとせねばならぬ事が判つた。此の油壺灣内のセイシユが傾斜を起す原因となる事實ともよく合致するのである。

又一方潮汐の一日潮の振幅と、其に依つて引起される地殻の傾斜との比は半日潮の振幅と其に依つて引起される地殻の傾斜との比と多少其の値を異にする樣に認められる。更にセイシユの週期振幅と其れに依つて起される傾斜との關係を調べたら尙一更面白い事が現れるであらう。

1. The earth crust which has ever been regarded traditionally as a symbol of eternal firmness is, in fact, subjected not only to secular movements of folding, faulting and warping in great scale but also to local movements of tilting of very short period. The reality of the latter kind of crustal movement was recently revealed by the observation of Professor M. Ishimoto[1] with his newly devised all-silica tiltmeter. He observed

(1) *Bull Earth. Res. Inst.* 4 203 (1928).
Jap. Journ. Astro. Geophys. 6 83 (1928).

some characteristic modes of tilting of the earth crust which take place preceding the outbreak of an earthquake by a few days. On the other hand, precise levellings carried out by the hand of the Land Survey Department immediately after the Great Kwantô Earthquake,(1) the Tango Earthquake,(2) the Sekihara Earthquake,(3) the Simabara Earthquake,(4) the Ômati Earthquake(5) etc. over their respective meizo-seismal area, have revealed a number of interesting and instructive features concerning the deformation of the earth crust caused by an earthquake disturbance. In the case of the Tango Earthquake the results were especially interesting. According to C. Tsuboi's study,(6) some of the land blocks of the Tango Earthquake district changed their senses of inclination in a short time interval less than one year. In these connections, it was considered to be of some special interest to make a continuous observation of the tilting motion of the earth crust at some place in the Miura Peninsula on account of its position relative to the Bay of Sagami in which the origin of the Great Kwantô Earthquake of 1923 was situated. By the kind advice of Professor M. Ishimoto the present author installed a pair of tiltmeters at Misaki, a village at the southern extremity of the Miura Peninsula. After a week's observation, it was found that the tilting of the earth crust caused by the tidal loadings is very conspicuous amounting to about 1″ and follow quite faithfully the phases of tides. The present paper is a summary of the study made on the tilting of the earth crust due to this latter cause. As to the secular or cumulative tilting of the crust which was the initial object of the present observation, nothing can yet be said from the result of observation of so short a duration as at hand.

The tilting of the earth crust caused by tidal loading was already studied by R. Sekiguti.(7) His observations were made at Zinsen (Corea)

(1) *Bull. Earth. Res. Inst.* **1** 65 (1926).
(2) *Bull. Earth. Res. Inst.* **3**, **4**, **5**.
(3) *Pros. Imp. Acad.* **4** No. 2 (1928).
(4) *Bull. Imp. Earthq. Investigation Committee* p. 63 (1928).
(5) *Proc. Imp. Earthq. I. C.* (in Japanese) No. 94.
(6) *Bull. Earth. Res. Inst.* **6** (1928).
(7) *Mem. Imp. Mar. Obs.* **1** 1 (1917).

where the tidal range is the largest in the Far East. The instrument used in his observations was the Omori horizontal pendulum of period 28 sec. with a magnification 150. The instrument is nothing but an ordinary seismograph having no special equipment for the observation of tilting. He calculated the tilting of the earth crust caused by tidal loading from the widening and narrowing of the intervals between the successive lines of the seismogram, and estimated the effective rigidity of the earth crust to be 6×10^{11}c.g.s. The maximum amplitude of tilting was 0″.04, of which 0″.007 was due to the attraction of tides. His observation was limited only to E–W component. As to the daily variations of the inclination of the ground due to the thermal effect of the solar radiation, nothing is touched in his paper. According to M. Ishimoto, however, the daily tilting due to this latter cause generally amount to 1″, even when the temperature of the observing room is kept sensibly constant.(1) D. Nukiyama(2) made another series of similar observation at Mera in the Bôsô Peninsula by using an astronomical spirit level. His observations were so much affected by the atmospheric temperatures, pressures and other meteorological disturbances that any definite relation between tidal loading and tilting of the ground could scarcely be obtained.

On the theoretical side of the present problem, there are many elegant works. A combined work of Lamé and Crapeyron seems to be the first to treat the problem of the distributed pressure on a semi-infinite homogeneous non-gravitating elastic medium, and their solution was afterwards improved by J. Boussinesq. K. Terazawa(3) succeeded in solving the same problem, expanding the load in a form of Fourier-Bessel's series. He treated as one of the special case of his solution the case when a uniform pressure is exerted on a circular area, and discussed the correction to be made on Michelson's observation of the earth tide, applying his results of calculation on the tidal load due to the Atlantic Ocean. H Lamb.(4)

---

(1) M. Ishimoto:—*Bull. Earthq. Res. Inst.* **4** 203 (1928).
(2) *Jap. Journ. Astro. Geophys.* **2** 91 (1928).
(3) *Journ. Coll. Sci. Tokyo* **37** Art. 7 (1916).
(4) *Proc. London Math. Soc.* **24** 276 (1902).

solved also the same problem in a similar manner as that of K. Terazawa. Beside these works, H. Nagaoka[1] solved the case when the load is not uniform, starting from the solution of Boussinesq. The theoretical part of R. Sekiguti's paper is based upon the solution of H. Nagaoka.

The present problem is again closely related to the observation of the earth tide. The earth tide, observed by the variation of the angle between the horizontal plane and the terrestrial surface, is superposed by the effect due to bending of the earth crust by tidal loading and cannot be analysed without a knowledge of the latter. One of the extensive studies made in this line is that of T. Shida,[2] based upon his observation at Kyôto. In his paper it is assumed that the effective rigidity of the earth crust increases linearly with the distance. He made also an estimation of the magnitude of the correction term due to the tidal loading to be applied to the observation of Hecker.[3] He introduced the law of linear increase of the effective rigidity of the earth crust from a reasoning that the greater the distance of the stressed area is, the deeper is the stratum which comes effectively into play. The difficulty of the problem, however, lies in the fact that it is quite beyond our imagination in what manner the successive layers will thereby come into play.

2. The instrument with which the present observation was made was installed in a horizontal cave in the south-east side of a hill in the site of the Marine Biological Station of the Tôkyô Imperial University at Misaki. ($\varphi = 35°10', \lambda = 139°37'$). The Misaki Marine Biological Station is situated at the extremity of a small promontory at Misaki surrounded by the Bay of Sagami, the Bay of Koaziro and the Bay of Aburatubo. The cave faces to the neck of the Aburatubo Bay. About 300 metres apart towards the interior of the Aburatubo Bay there is a tide-gauge station belonging to the Military Land Survey Department. (see Photo. 1 and Fig. 1.). The Miura Peninsula on which the district Misaki lies is covered by a thick layer of tuff which belongs to the Miura Series of the Tertiary Period. The layer

(1) *Proc. Tokyo Math. Phys. Soc.* **6** (1912) 208.
(2) *Mem. Coll. Sci. Kyoto IV* No. 1 (1912).
(3) *Mem. Coll. Sci. Kyoto IV* No. 1 (1912).

Photo 1.

underlying the Miura Series is supposed to be the Mineoka Series of the Mesozoic Era. The cave is bored into the bed of natural tuff and is not lined by any artificial material. The cave and its neighbourhood are covered by a thick growth of weeds and forest of pine trees sheltering them from the direct rays of the solar radiation. The dimensions of the cave are 2 m.× 2 m.×4 m., and the space is imperfectly divided into two chambers. In the inner and northern chamber there is a Γ-shaped pedestal of concrete, the edges of which are parallel to the directions N–S and E–W respectively. A pair of tiltmeters were installed on the platform of the pedestal in the diriections N–S and E–W to record the N–S and E–W component of tilting respectively. On the wall of the southern chamber a wooden door is provided for entrance. The position of the instrument is 8.69 metres high above the mean sea level and 22.6 metres apart from the nearest beach line.

The instrument used in the present observation is a pair of tiltmeters after M. Ishimoto's design. It is a small horizontal pendulum of

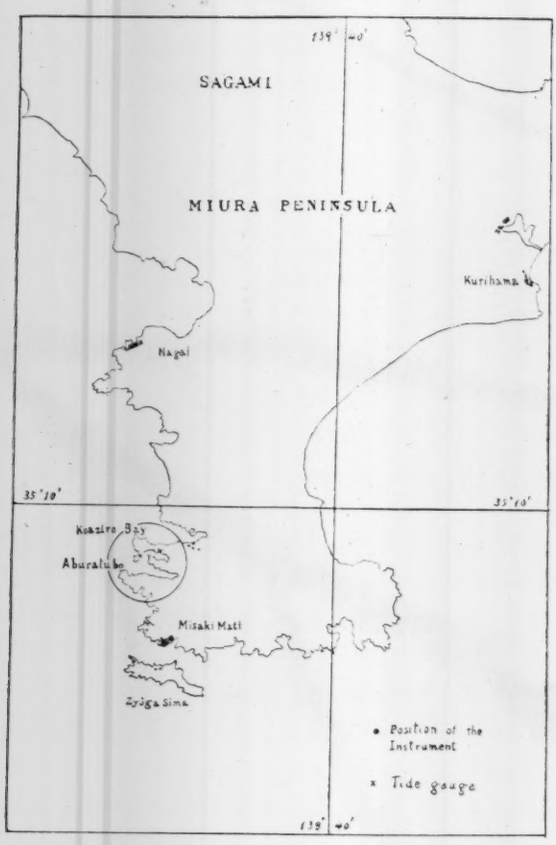

Fig. 1.

Zöllner's suspension type, its frame works, movable horizontal rod, the suspension fibres being all made of vitreous silica. The instrument is, therefore, almost entirely free from errors due to the effect of temperature variation, the elastic after-effect etc. To the movable horizontal rod of the pendulum is attached a small concave mirror which reflect the light from a light source to bromide photographic paper a metre apart from the instrument. The bromide paper is wound around a cylinder which makes one revolution a week by a clock work. The sensibility of the instrument is so adjusted that a deflection of one centimetre on the record correspond to 1″ tilting of the ground. The bromide paper is developed on every Saturday. A Richard recording thermometer is also installed in the cave. The time-mark is automatically made on the record at 6 o'clock in the morning and at 6 o'clock in the evening by extinguishing the light source for a short time.

3. The present series of observation was commenced on 27th of July, 1928. A part of the record of the observation is reproduced for illustration in Fig. 2 and in Fig. 3. The upper curve in Fig. 3 is the record of the tide-gauge in the Aburatubo Bay, the middle curve is that of the E–W

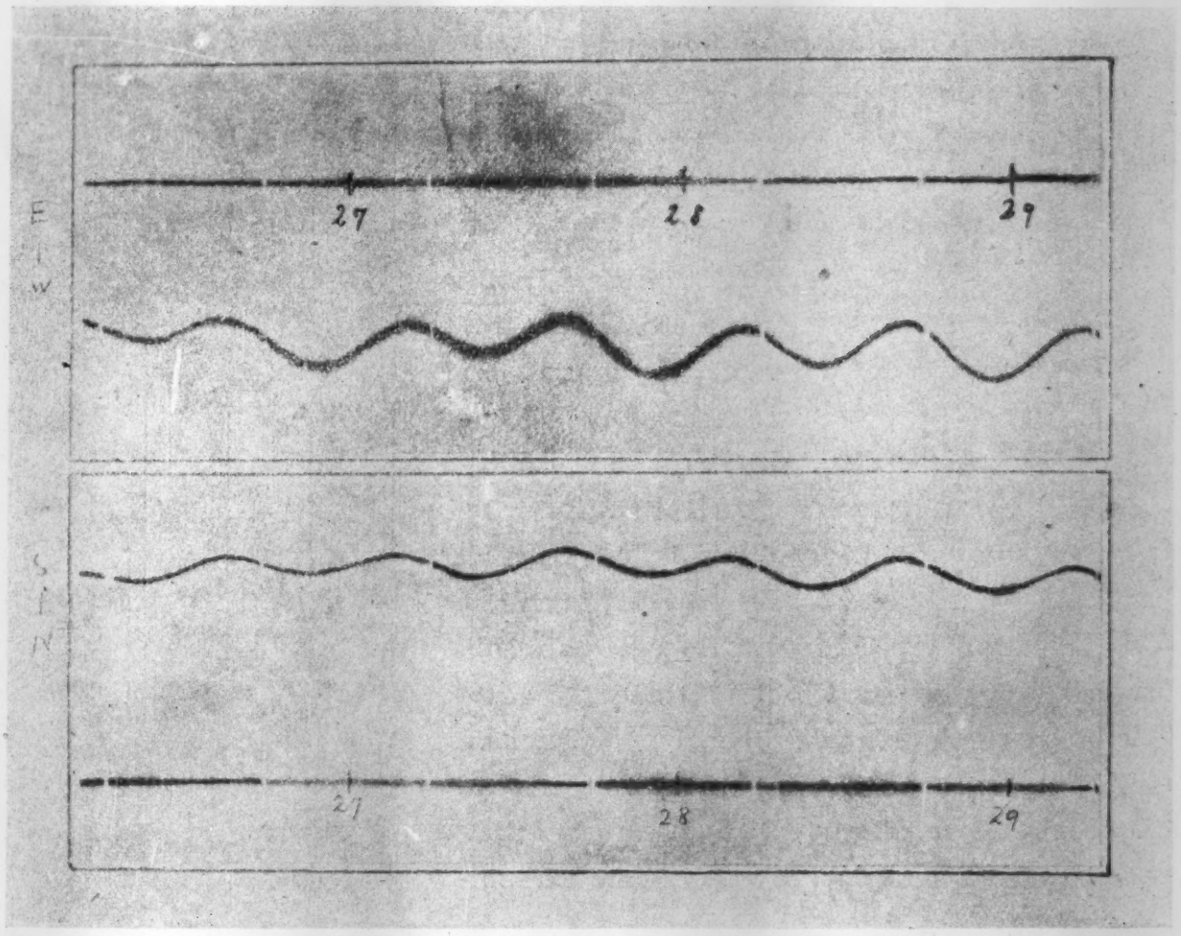

Fig. 2.

component, the lower curve is that of the N–S component of tilting obtained by the tiltmeter. The letters E W S and N in Fig. 3 are given to show the sense in which the ground is tilted *downwards*. As will be seen in Fig. 3, the curves of tilting motion of the earth crust are very similar to the curve of ebb and flood of tides in the Aburatubo Bay. That these three curves in Fig. 3 resemble very closely to each other prove that the daily tilting due to the thermal effects of the earth crust caused by the

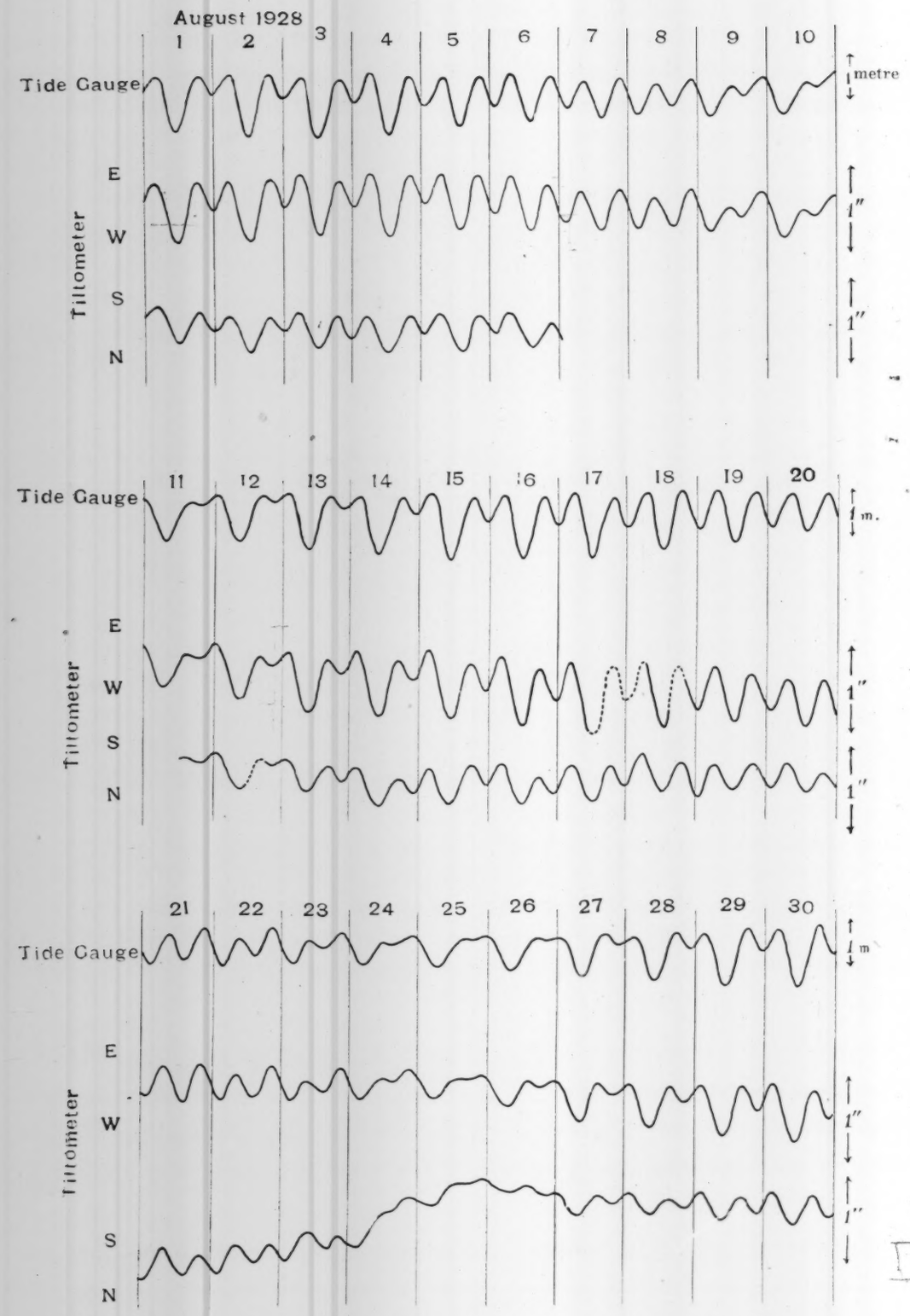
August 1928
1 2 3 4 5 6 7 8 9 10
Tide Gauge
metre
Tiltometer
E
W
S
N
1″
1″
11 12 13 14 15 16 17 18 19 20
Tide Gauge
m.
Tiltometer
E
W
S
N
1″
1″
21 22 23 24 25 26 27 28 29 30
Tide Gauge
m
Tiltometer
E
W
S
N
1″
1″

Fig. 3.

solar radiation is very small. The daily tilting of the crust due to the thermal effect is, as said in the above paragraph, generally amounts to 1″ in such a place as Miyadu, Tôkyô, Tukuba etc. That the daily tilting is exceptionally small at Misaki is probably due to the fact that the observing station is near the sea and the cave and its neighbourhood are overgrown by bushes and forests of pine trees which protect the ground from the direct radiation of the sun. The change of temperature in the observing chamber is so small that no sensible variation can be recorded by the ordinary thermograph. The temperature was 21.0°C on 1st. of August whence it varied gradually and linearly down to 20°.5C in the course of a month.

In the Bay of Aburatubo remarkable seiches with a period of 15 minutes are sometimes observed of which the amplitude amounts to 30 cm. in the case of a storm. The record of the tiltmeter shows, on careful examination, that it is superposed by a minute zig-zag indentatiton of which the average period is 15 minutes. This is in all probability due to the tilting of the ground caused by the seiches of the sea water in the bay. (see Fig. 4).

The resultant of E–W and N–S tiltings is directed towards ESE.,

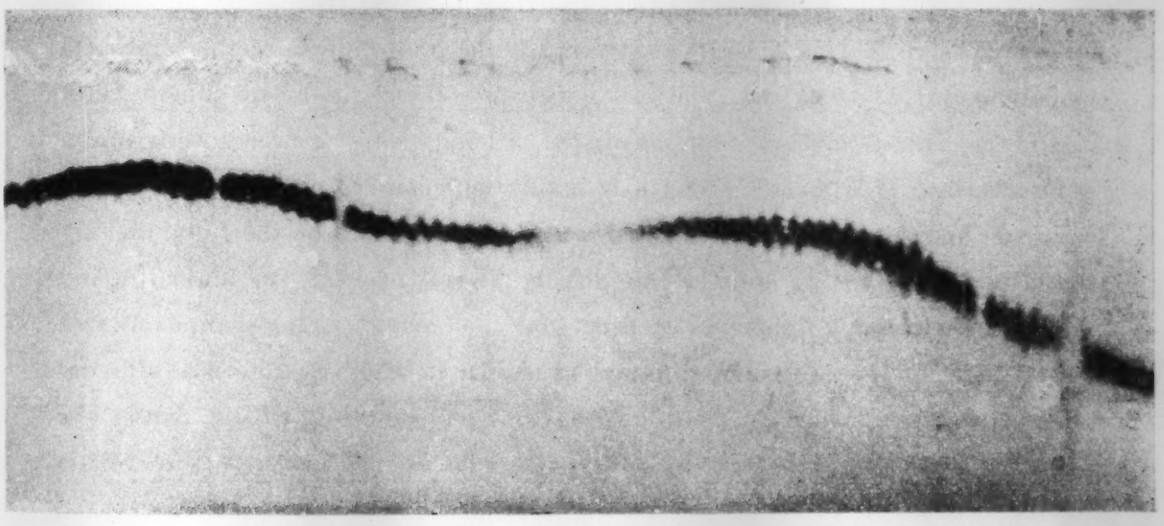

Fig. 4.
Zig-zag tilting caused by the seiches of the sea water in the Aburatubo Bay.
E-W Component.

which is the direction perpendicular to the nearest beach line. The tilting of the ground produced by the rise of the sea surface by 1 metre amounts to 0″.57 in E–W component and to 0″.35 in N–S component. The parallelism between the modes of variation of the tilting and the tides is very conspicuous. The lag or advance between the phases of the tilting and the tides is so small, if any, that they could not be detected by the present instrument. In the present instrument the recording drum makes one revolution a week and one hour corresponds to only 1.65 mm. on the record. The reduction constant or the sensibility of the tiltmeter is a function of the period of free oscillation of the tiltmeter, which is again a function of the angle between the plumb line and the line joining the suspension points of the movable rod of the tiltmeter. A tilting of the ground in the direction E–W will, therefore, produce a variation in the sensibility of N–S component tiltmeter, and vice versa. The variation in the sensibility is, however, smaller than 1% if the tilting of the ground is less than 1″. During the period of the present observation the zero-point displacement of the two components of tilting were less than 2″, thus the reduction constants for both the tiltmeters can be regarded to have remained practically constant in that period.

To study the relations between the tides and the tilting of the ground more closely, the tides were analysed by the well-known method into its component tides and the relations between each of these component tides and the corresponding component of tilting were studied separately. Observations of a month's length is barely sufficient to make studies of the diurnal and semi-diurnal components. Out of the data of the lunar hourly readings of the tilting and the tide during August of 1928, the lunar diurnal and semi-diurnal components of tides and the corresponding components of the tilting of the crust are obtained as shown in Fig. 5. The semi-diurnal curves represent nearly M_2 tide and the corresponding tilting, while the diurnal ones are disturbed by other components. A month's observation is not sufficient to separate this from other components. At Aburatubo the spring range is 1.0 metre and the mean high water interval is 5^h16^m. The half amplitude of M_2 tide will be 34 cm. because the theoretical value of

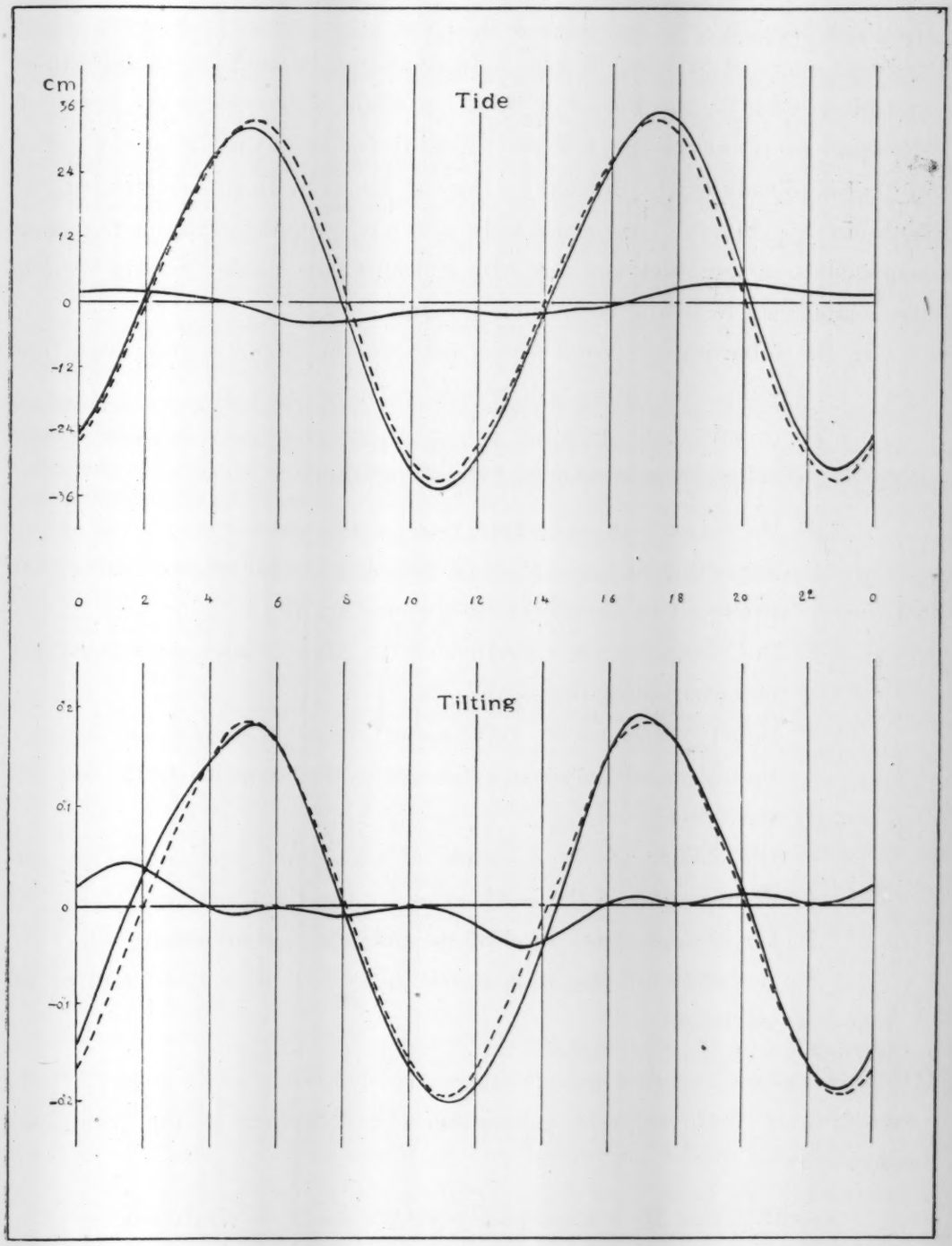

Fig. 5.

The curve shown by full line is the compound curve of the lunar semi-diurnal component (dotted line) and the lunar diurnal component. The lunar diurnal component is shown by the curve of smaller amplitude.

H_s/H_m is equal to 0.465 and $2(H_m+H_s)$ = the spring range = 1.0 metre. The deduced curve of M_2 tide in Fig. 5 fairly coincides both in its amplitude and phase with the theoretical M_2 tide. A slight difference in the forms of the mean curves of the tide and the tilting is due to inequality of the ratios of the amplitude of the diurnal to that of the semi-diurnal component in both curves. Similar treatments were also made for determining the solar components of the tides and the tilting, leading to similar results though the components to tilting show some irregularities.

In the following the correlations between the lunar semi-diurnal tide and the corresponding tilting will be studied in some detail.

4. There are eight possible causes which may produce the lunar periodic deflection of a horizontal pendulum tiltmeter, namely

1 the direct tide-generating force of the moon;
2 the tilting of the surface of the earth as the effect of earth tide produced by the direct tide-generating force;
3 the change of the direction of the plumb line due to the tidal deformation of the earth;
4 the attraction of sea water caused by the oceanic tides;
5 the tilting of the earth crust due to the variation of the load of sea water;
6 the change of the direction of the plumb line caused by the deformation of the earth crust by the tidal loading;
7 the change of the level of the underground water;
8 the effect of the atmospheric tide, both as of load and as of attraction.

Of these causes, the first one produces the deflection of the order 0″.01. According to the results of calculation the deflection of the pendulum amounts to

$$-0''.013 \sin 2t \quad \text{Eastward}, \qquad 0''.007 \cos 2t \quad \text{Westward},$$

at Aburatubo, where t is the local lunar time. These deflections are so small that they are entirely covered by the deflections coming from other causes. The deflection due to the second cause is of the sense opposite to

the first and amounts to the order of 0″.01 if the diminishing factor be taken at 0.7 or so. The deflections due to the third and sixth cause are very difficult to calculate but may be regarded to be negligibly small. Change of level of the underground water, which was enumerated as the seventh cause, may well has some effects on the vertical intensity of gravity but its effect on the horizontal force contributing to the deflection of the tiltmeter will be insignificantly small. The deflection due to the eighth cause is so small that it has no bearing on the present observation. The observed deflection of the tiltmeter, therefore, must be essentially attributed to the remaining fourth and fifth causes. The effect of the attraction of the sea water will be calculated in the next paragraph.

5. In the earlier part of the following calculation of the attraction of the sea water, t is reckoned, for the convenience's sake, from the instant of the high water at Aburatubo, and afterwards is transformed to the local lunar time of Aburatubo. Within a distance of 100 m. from the station the formulae

$$\frac{100\,k\rho}{g\sin 1''}(\sin\theta_1-\sin\theta_2)\left[\left(c+\frac{h}{2}\right)\left(\sinh^{-1}\frac{r_1}{c+\frac{h}{2}}-\sinh^{-1}\frac{r_2}{c+\frac{h}{2}}\right)\right.$$

$$\left.-\left(c-\frac{h}{2}\right)\left(\sinh^{-1}\frac{r_1}{c-\frac{h}{2}}-\sinh^{-1}\frac{r_2}{c-\frac{h}{2}}\right)\right],\qquad \text{Eastward,}$$

$$\frac{100\,k\rho}{g\sin 1''}(\cos\theta_1-\cos\theta_2)\left[\left(c+\frac{h}{2}\right)\left(\sinh^{-1}\frac{r_1}{c+\frac{h}{2}}-\sinh^{-1}\frac{r_2}{c+\frac{h}{2}}\right)\right.$$

$$\left.-\left(c-\frac{h}{2}\right)\left(\sinh^{-1}\frac{r_1}{c-\frac{h}{2}}-\sinh^{-1}\frac{r_2}{c-\frac{h}{2}}\right)\right],\qquad \text{Southward,}$$

were used, where c is the height of the instrument above the mean sea level, r the distance of an elementary water area from the instrument and h the amplitude of the tide, all being measured in metre. Beyond a distance of 100 m. the following formulae were used

$$\frac{100\,k\rho h}{g\sin 1''}(\sin\theta_1-\sin\theta_2)(\log\ r_1-\log_e r_2),\qquad \text{Eastward,}$$

$$\frac{100\,k\rho h}{g\sin 1''}(\cos\theta_1-\cos\theta_2)(\log_e r_1-\log_e r_2), \qquad \text{Southward,}$$

where k=the gravitational constant,

ρ=the density of the sea water,

g=the gravity,

θ=the azimuth of the elementary area measured from East in the counter-clockwise sense.

The amplitude of the deflection of the plumb line due to the attraction of the tide is given in the following table:

	East-Comp.		West-Comp.	
	cos 2t	sin 2t	cos 2t	sin 2t
20 m.–100 m.	0″.001368	0″.000000	0″.000875	0″.000000
100 m.– 1 km.	— 681	0000	387	0000
1 km.– 1 km.	— 2004	0000	— 287	0000
5 km.–100 km.	— 198	0000	1698	0000
100 km.–610 km.	760	663	1141	— 521
Sum	—0″.000765	0″.000663	0″.003805	—0″.000521

where t is reckoned from the high water. As the mean high water interval is 5^h16^m or 76.0° at Aburatubo, the expression of the deflection of the tiltmeter due to M_2 tide within 610 km. will become

$$0''.001013\cos(2t-291.1^\circ) \qquad \text{Eastward,}$$
$$0''.003840\cos(2t-144.2^\circ) \qquad \text{Southward,}$$

in the lunar time of Aburatubo. For the region beyond 610 km. we can use without much errors the values formerly obtained by T. Shida, which refer to the attraction of the tide of the corresponding region for Kyôto. The values obtained by T. Shida for 610 km. to 4400 km. are

East-Comp.		West-Comp.	
cos 2t	sin 2t	cos 2t	sin 2t
0″.000305	0″.001217	0″.000975	0″.000250

This is equivalent to

$0''.001255 \cos(2t - 75.0°)$ Eastward,

$0''.001005 \cos(2t - 194.4°)$ Southward.

The argument t in this expression is, however, in the local time of Kyôto. In the local time of Aburatubo they become

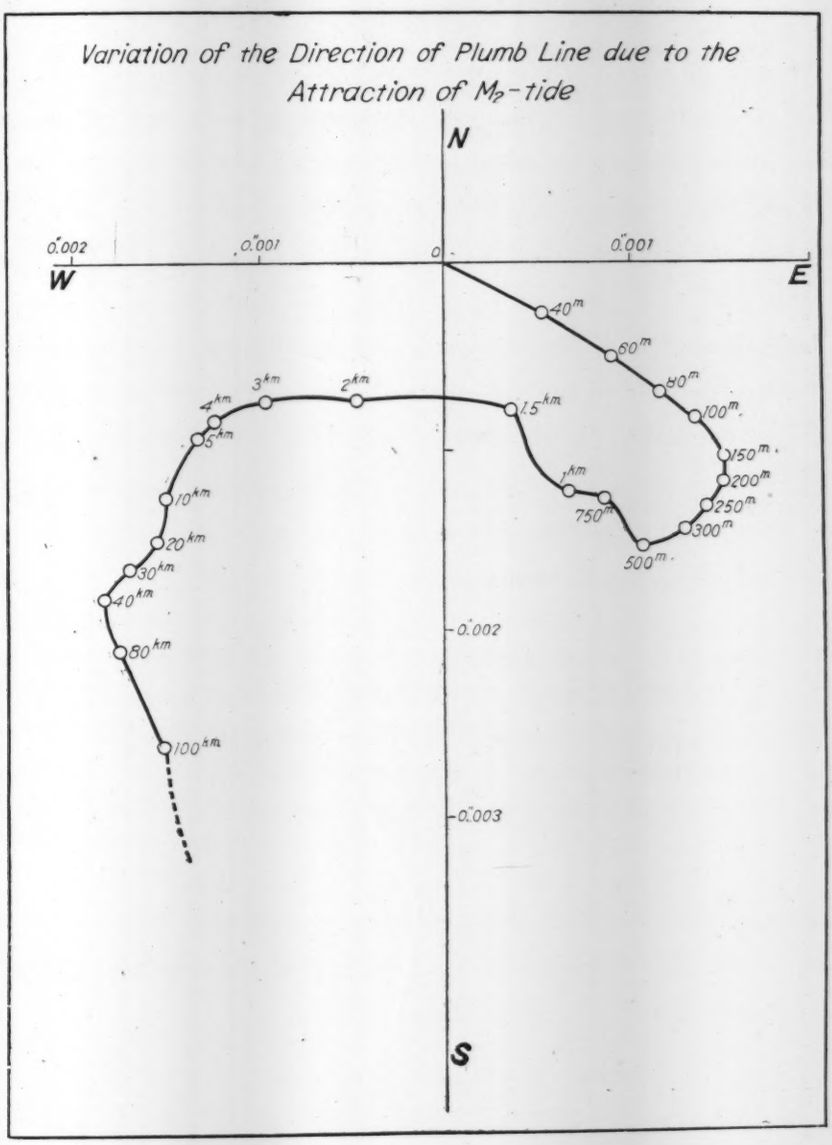

Fig. 6.

The curve is the locus of the head of the vector representing the attraction of M_2 tide when the calculation is extended to successive steps of distance.

$0''.001255 \cos(2t-83.6°)$ Eastward,
$0''.001005 \cos(2t-202.1°)$ Southward.

These values combined with the values corresponding to the region of 20 m.–610 km. become

$0''.000723 \cos(2t-22.0°)$ Eastward,
$0''.00478 \cos(2t-148.6°)$ Southward.

As can be seen in the above expressions the vector head of the deflection caused by the attraction of the tide describes a very flat ellipse with its major axis directed towards South-West-South. After all, the amount of deflection of the tiltmeter due to the attraction of the tide is insignificantly small, though the position of the instrument is very near to the sea.

6. We will now proceed to examine the fifth cause. Almost whole of the deflection of the tiltmeter must be attributed to this single cause, as the deflections due to all the other causes have proved to be small as explained in the above paragraphs. According to Boussinesq's solution the tilting of the earth crust due to the tidal loading occurs in the same direction with the attraction of the tide, no matter how the load may be distributed. Boussinesq's solution is

$$u=-\frac{1}{4\pi\mu}\frac{\partial^2}{\partial x\partial z}\int rdP-\frac{1}{4\pi(\lambda+\mu)}\frac{\partial}{\partial x}\int\log(z+r)\,dP,$$
$$v=-\frac{1}{4\pi\mu}\frac{\partial^2}{\partial y\partial z}\int rdP-\frac{1}{4\pi(\lambda+\mu)}\frac{\partial}{\partial y}\int\log(z+r)\,dP,$$
$$w=-\frac{1}{4\pi\mu}\frac{\partial^2}{\partial z^2}\int rdP+\frac{2\lambda+3\mu}{4\pi\mu(\lambda+\mu)}\int\frac{dP}{r}.$$

Differentiating the vertical displacement w corresponding to $z=0$ with respect to x, we have x-component of tilting of the surface of the elastic medium on which the load is distributed. Thus,

$$\frac{\partial w_0}{\partial x}=\frac{\lambda+2\mu}{4\pi\mu(\lambda+\mu)}g\rho\frac{\partial}{\partial x}\int\frac{hd\sigma}{r},$$

putting

$$dP\doteq g\rho hd\sigma.$$

The deflection of the tiltmeter due to the attraction of tides is given by

$$\frac{k\rho}{g}\frac{\partial}{\partial x}\int\frac{hd\sigma}{r}.$$

Therefore the deflection of the tiltmeter due to the tilting of the earth crust by the tidal loading is equivalent to the deflection of the tiltmeter due to the attraction of the tides multiplied by

$$\frac{\lambda+2\mu}{4\pi\mu(\lambda+\mu)}\frac{g^2}{k}.$$

As already remarked in the above paragraph, the attraction of the tide is directed nearly to South. The tilting of the ground must, therefore, according to the solution of Boussinesq, also be directed to South. The tilting of the ground actually observed at Aburatubo is, however, directed to ESE, revealing the failure of Boussinesq's solution in this case.

The earth crust is by no means of such a simple structure as assumed in the usual mathematical theory of elasticity and it is of no wonder that the solution of Boussinesq does not hold good in this actual case.(1) Moreover, the rocks constituting the surface layers of the earth crust do not obey Hooke's law on which the theory of elasticity is based. Still less can we say about the elastic properties of the substances forming the inner part of the earth. One of the convenient ways of access left for us in this respect is to assume that the rigidity of the crust which is effective in producing the tilting due to a load at a given station is a function both of the distance between the load and the station and of the period of variation of the load. This assumption is equivalent to taking μ in Boussinesq's solution to vary with the distance and the period of variation of the load. The rigidity in such a sense of word, will be called hereafter the *effective* rigidity of the earth crust. The functional form of the effective rigidity thus defined may be regarded as a measure of the states and properties of the earth crust. The functional form of this effective rigidity is

(1) The surface of the earth crust near the observing station can by no means be regarded as a plane because the distance of the station from the nearest beach line is only 20 m., while the Bay of Aburatubo is 3-4 m. deep and the station is 8.7 m. high above the mean sea level. The pressure acting on the surface of the crust cannot consequently be regarded as pure vertical one, some portion of it being exerted horizontally. Notwithstanding these circumstances Boussinesq's solution was applied only as the first step to the solution of the present problem.

quite arbitrary being subjected only to two conditions that firstly it must give for $r=0$ the rigidity μ_0 of the rock in the neighbourhood of the station and secondly for $r=\infty$ the rigidity μ_∞ of the earth as a whole. T. Shida assumed the reciprocal of the effective rigidity to be of a hyperbolic form with respect to r, and R. Sekiguti obtained for the effective rigidity of the earth crust corresponding to the distance of a few kilometres the value 6×10^{11}. The functional form of the effective rigidity suitable for the present case will be studied in the following.

Tilting of the ground from its mean position can be represented by a vector directed towards the positive sense of tilting with a length proportional to the amount of tilting. The vector head representing the theoretical tilting due to the tidal loading will describe the dotted curve in Fig. 7, when the calculation is extended to the successive steps of distance. The calculation is made by taking the rigidity in Boussinesq's solution to be 1.4×10^{10}c.g.s., i.e. the value of the rigidity of the tuff in the neighbourhood of the station. The dotted curve in Fig. 7, being calculated by Boussinesq's solution, is entirely similar to the curve in Fig. 6 corresponding to the attraction of the tide.

As will be seen in the figure, the direction of the calculated tilting under the assumption of uniform rigidity of the earth crust deviates from that of the actually observed tilting as soon as the load distributed on the area beyond 150 m. from the station is taken into account. The load acting on the area beyond 150 m. from the station does, it appears therefore, not take part in producing the tilting at the station, in other words, the effective rigidity of the crust for a load distributed beyond the distance of 150 m. must be very large compared with that for the load distributed within 150 m. The effective rigidity of the crust must undergo a very rapid increase at or near the distance of 150 m. if any jump of the effective rigidity is not involved. Other assumptions, such as that of linear increase of effective rigidity from μ_0 to μ_∞ in the range 20 m.–150 m., cannot explain the actual amount of tilting, though they give the same direction of tilting with the actually observed one. Assuming the effective rigidity to be of the form

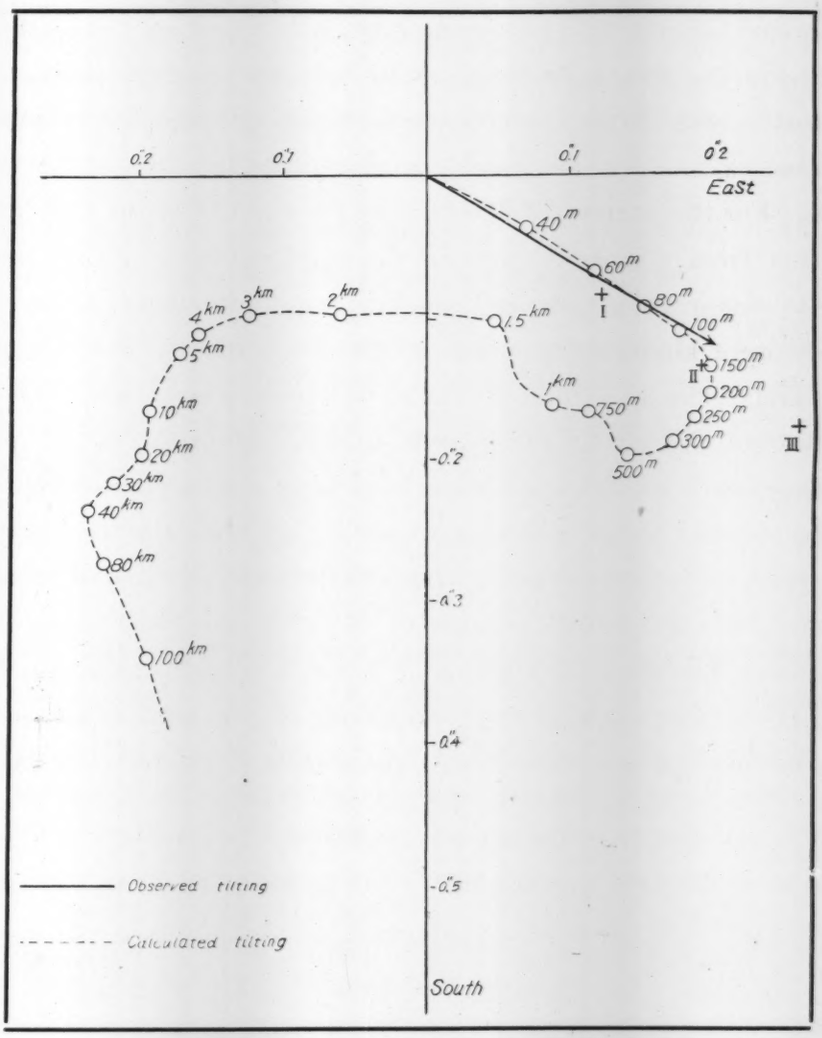

Fig. 7.
Tilting of the Earth Crust caused by M_2-tide.

$$\frac{1}{\mu_e}=\frac{1}{\mu_\infty}+\frac{1}{\dfrac{\mu_0\mu_\infty}{\mu_\infty-\mu_0}+ar^n},$$

we will determine the value of n for which the effective rigidity in the present actual case can be expressed most suitably in the first approximation.

7. Before entering into the discussion of the form of the rigidity function, we must consider the values of rigidity corresponding to $r=0$ and $r=\infty$.

For the rigidity of the earth crust corresponding to $r=0$ that of tuff covering the Miura Peninsula is to be taken, for the position of the instrument is only 20 m. apart from the beach line and the bottom of the Aburatubo Bay (3–5 m. in depth) is also probably covered by the same material. For the purpose of determining the rigidity of the tuff, specimens were taken from a mass of rock in the neighbourhood of the cave, with which the compression tests and bending tests were made. The compression tests were kindly carried out by the hand of Dr. M. Matsumura in the Research Office of Public Works of the Home Department. The bending tests were effected by the present author. According to the late Professor Kusakabe's investigation rocks have in general a characteristic elastic property, showing sensible hysterisis effect. It was also the case in the present tests. The stress-strain curve was different in cases of loading and unloading, leaving a small permanent set after the removal of the load. In both cases, however, the rigidity or Young's modulus increases with the stress. The author adopted for the rigidity of the tuff the mean value of rigidity for loading and unloading. The results of the tests are as follows:

E (c.g.s.)	μ (c.g.s.)	Stress	
5.7×10^{10}	2.3×10^{10}	11 kg/cm²	Compression
4.0	1.6	5.6	test
3.5	1.4	4.0	Bending
2.1	0.8	1.0	test

μ is deduced from the value of E under the assumption that $\sigma=\frac{1}{4}$.

Though it is difficult to know what state of strain may prevail in the actual bed of the tuff, we may take, without much errors in any case, the middle value of the above results

$$\mu_0 = 1.4\times10^{10} \text{c.g.s.}$$

as the rigidity of the tuff.

The rigidity corresponding to $r=\infty$, which may be assumed to be the rigidity of the earth as a whole, has been determined by many authors by different methods under different assumptions. This value of rigidity has

not, however, any important bearing on the further development of the present discussion, so that we will adopt for it, for a while, the value obttained by T. Shida by the observation of the earth tide. The value is

$$\mu_\infty = 12.0 \times 10^{11} \text{c.g.s.}$$

8. To determine the coefficient a in the expression of the rigidity assumed in the above paragraph, one more assumption is necessary. We will assume that the rigidity takes the value $\frac{\mu_0+\mu_\infty}{2}$ at $r=150$ m. This assumption may be justified because the rigidity function must increase very rapidly in the neighbourhood of $r=150$ m., as is seen in Fig. 7. Assuming simply the form

$$\frac{1}{\mu_e} = \frac{1}{\mu_\infty} + \frac{1}{\frac{\mu_0\mu_\infty}{\mu_\infty-\mu_0} + ar^n} \fallingdotseq \frac{1}{\mu_0+ar^n} + \frac{1}{\mu_\infty}$$

for the rigidity function we will notice that the larger the index n in the above expression is, the more satisfactory result can be obtained by the expression. The general features of the matter will not be altered whatever form for the rigidity function we may assume. This is nothing but to introduce a discontinuity or a jump in the effective rigidity of the earth crust at the distance of 150 m. from the station. That is to say, the load acting at the distance greater than 150 m. has little effect upon the tilting of the observing point. Such phenomena are always observed in experiments with some granular substances such as sand, soil and rocks. Prof. T. Terada and N. Miyabe[1] have made a series of interesting experiments with a layer of sand. The experiments consist in pushing down vertically a rectangular block of brass into a horizontal layer of sand. According to their results, the part of the sand layer distant from the load seems to behave as if it was perfectly rigid, though the part of the surface layer of sand near the load was seen to be tilted and disturbed. If the pressure acting on the sand layer had been small, the disturbed layer of sand would have recovered to their original states when the load was taken off. The tuff covering the Miura Peninsula is very rough and resembles to the

(1) not yet published.

closely packed sand. The fact here observed that the stresses extent far apart are not effective in producing the tilting of the observing point is quite natural if the rock material forming the substratum of the observing station has such a property as is said above. Moreover, the province of Miura has been subjected to upheavals and subsidences many times even in historical ages and there exist many apparent faults and fissures of small scale in the neighbourhood of Aburatubo. If the dicrete portions of rock mass divided by these small fissures may be regarded to play the rôle of particles of sand in the experiments of T. Terada and N. Miyabe, such a discontinuity of the effective rigidity as is assumed above may be realized to some degree of approximation.(1)

Taking successively as the effective rigidity of the earth crust within the distance of 150 m. the values 1.1×10^{10}c.g.s., 1.4×10^{10}c.g.s. and $2.3\times^{10}$c.g.s., we have the points I, II and III in Fig. 7 as the vector head of the calculated amount and direction of tilting. The observed tilting is shown by the full line in the figure. As can be seen in the figure we can thus completely explain the phenomena of tilting assuming the effective rigidity of the crust within 150 m. to be 1.4×10^{10}c.g.s. and introducing a jump of the effective rigidity at some 150 m. from the station. The effective rigidity in the outer region beyond the discontinuity may obey the law of linear increase as was assumed by T. Shida or may obey other laws such as of quadratic increase. It cannot, however, be determined by the present observation alone. At any rate, for the region within 150 m. neither the law of Shida nor any law of continuous form holds good, but we must introduce a discontinuity of the effective rigidity of the earth crust at a distance of some 150 m. from the observing station.

There may be proposed many other ways of explaining the outlines of the phenomena described in this paper. For instance, the entire geological unit or land block on which Misaki lies may undergo a tilting as a whole by the tidal load. The author does not think, however, that the force of

(1) The discontinuity of the effective rigidity of the crust may again take place if there is a layer of hard rocks under the bed of the tuff. At Misaki the layer just beneath the Miura Series is supposed to be the Mineoka Series of the Mesozoic Era consisting of rocks much harder than the tuff.

so short a period as 12 hours will be able to give a sensible motion to the large mass of a land block. Moreover, the fact that conspicuous tiltings are also produced by the seiches of the local sea water in the Aburatubo Bay seems to exclude such an idea.

Another way of explanation is to assume the existence of a fault in the sea basin cutting off the elastic connection of the land block on which the observing station lies from the outer region beyond the fault, so that the stresses in the latter do not affect the tilting of the former. There exist indeed many remarkable faults in the neighbourhood of Misaki so that a hidden fault may exist in the sea bed off the Aburatubo Bay. It is also another alternative to assume the limited extent of the tuff formation, or to assume that the land block of Misaki ends at 150 m. off the sea shore. These assumptions are, however, quite arbitrary having no positive support. It will be rather plausible to introduce a sharp increase of the effective rigidity of the earth crust at a distance of 150 m. The properties of the rock, the existence of fissures in the earth crust and the stratification of the earth crust may conspire as the causes of such a rapid increase of the rigidity of the earth crust.

9. These discussions are, however, derived from the results of only a single month's observation; to come to any final and decisive results observations must of course be made for a longer period and at different places. For this purpose, the present observation has been continued and will be continued further.

The author is intending to make another series of observations concerning the tilting caused by the seiches of the sea water in the Aburatubo Bay. These observations, if combined with those of tilting caused by the diurnal and semi-diurnal tides, promise to give us some interesting informations regarding the elastic properties of the earth crust. Again it will be very interesting to make a series of observations at different districts at different distances from the sea shore. The knowledg of the mode of variation in the amount of tilting caused by the tides with the distance from the sea will give some clue to a further elucidation of the elastic properties of the crust as well as of the subterranean materials.

10. What has been said in the above paragraphs may be summarised as follows:

1) The tilting of the earth crust near a sea shore follows quite faithfully the ebb and flood of the oceanic tides. At Aburatubo a rise of sea water by 34 cm. produces a tilting of 0″22 at a point 23 metres apart from the beach line.

2) Almost whole of the observed amount of tilting may be explained by the effect of the tidal loading. The deflections of the tiltmeter from the other possible causes are all less than the order of 0″.01.

3) Even the small secondary undulations of tides or the seiches in the Aburatubo Bay produce a sensible tilting of the ground.

4) Neither Boussinesq's solution nor any other known is not fitted for the present case. Shida's postulate of increase of the effective rigidity of the earth crust with distances does not hold good in this case.

5) The most plausible way of explaining the tilting phenomena seems to be of assuming a sudden jump in the value of the effective rigidity of the crust at a distance of about 150 metres from the observing station, taking for the rigidity of the earth crust within the distance of the discontinuity that of the rock underlying the observing station and for the effective rigidity of the crust beyond the discontinuity one of the order of 10^{11}c.g.s.

In conclusion, the writer wishes to express his most cordial thanks to Professors T. Terada, M. Ishimoto and C. Tsuboi for their invaluable advices and encouragements and to the Authorities of the Land Survey Department and the Hydrographic Department who kindly allowed the writer to avail many facilities for the study of the present problem.

His best thanks are also due to Messrs. S. Kozima and R. Takei who kept and are keeping the tiltmeter in its best conditions.

October, 1927.

The Earthquake Research Institute.

Experimental Investigations of the Deformation of Sand Mass by Lateral Pressure.

(With an Appendix.)

By **Torahiko TERADA** and **Naomi MIYABE.**

砂層の崩壊に關する實驗(第二報)

所員　寺田寅彦
同　宮部直巳

前回の實驗では砂層の横壁を後退させて崖崩れに類する崩壊を生じるといふのであつたが、今度の實驗では、其横壁を前進させ、卽ち砂層を壓しつけ、其れによつて生ずる變形を調べたのである。此場合も、前と同樣に、横壁の連續的な進行につれ、辷り面或は斷層が不連續な段階的に發生する。此の辷り面の變化の過程を稍詳しく記載して其の機巧に就て概略の說明を試みた。

又横壁を週期的に前進後退する時に生ずる變形をも調べた。壁の週期的運動によつて砂の變形が唯一方にのみ進行する點に特別の興味があるであらう。

地震の問題に、上記の結果が應用され得べき若干の要項を擧げておいた。

附錄として第一報の實驗に關する若干の考察を述べてある。

In a previous paper,[1] some experiments were described in which a horizontal pile of sand contained in a rectangular vessel was made to form a kind of step-faults by receding one of the end walls of the vessel and it was shown that the formation of the periodic faults is determined by the existence of the upper and lower limits of the inclination of the slip-surface. The following is the results of further experiments carried out with the same apparatus,[2] but this time by pushing on the end wall instead

(1) T. Terada and N. Miyabe, *Bull. Earthq. Res. Inst.*, **4** (1928), 33; the paper is written in Japanese, with an English Abstract in which the references are made to the text figures and Tables so that the foreign readers may follow the essential points there reported. Another abstract has also been given in *Proc. Imp. Acad.*, **3** (1927), 655, in which allusion is already made to an experiment of pressing the end wall.

(2) A photogram of the apparatus is reproduced in Fig. 2, Pl. IV of the paper cited; the movable side wall is 20×20 cm.^{2}

of receding it. Later on, some experiments were also made in which the movable end wall was subjected to an alternate periodic motion of a given amplitude.

I. Formation of Periodic Thrust-Faults by Lateral Pressure.

The movable vertical end-wall of the rectangular vessel in which a horizontal layer of sand is deposited, is pressed on horizontally with a nearly uniform small velocity and the successive stages of deformation were photographed in five series. The first series consists of the photograms taken when the displacements, d, of the movable wall are respectively 0–0.2, 1.0–1.2, 2.0–2.2.... cm., the second series corresponds to $d=0.2$–0.4, 1.2–1.4,.... cm. and so on. For different series, the sand layer was deposited afresh, so that the five series do not represent a continuous motion-picture of a single layer of sand. We were compelled to take this procedure, as it was desirable to take photographs without stopping the moving wall, and with an ordinary photographic apparatus the time required for changing the photographic plate could not be made so short as to allow a series with a shorter step of d than 1 cm.

As before, the exposure was made for an interval of time corresponding to 2 mm. displacement[1] of the end wall such that the traces of moving particles of sand could be clearly defined and the boundary between the moving and stationary masses could be sharply discerned. Horizontal lines of white sands were also used for indicating the deformation of the internal mass. The white sand was applied only near the glass side-wall, such that it cannot affect the property of the sand mass as a whole.

For the present experiments two kinds of sand were used, one finer and the other coarser. The coarser one is the same as employed in the previous experiment cited and consists of grains which passed a sieve of 1 mm.^{2} mesh and was retained by another with 0.25 mm.^{2} mesh. The finer one was obtained by washing out very fine powder from that portion which passed 0.25 mm.^{2} sieve. The sand was well dried before using for the ex-

(1) The velocity of motion of the pressing wall was about 0.02 cm./sec.

periment. The white index sand was also chosen such as to match the average grain size of the main mass.

Some of the photograms obtained are reproduced in Pl. I–III.

It will be seen that, also in the present case, the slip surfaces are produced in discrete steps, while the motion of the pressing wall is continuous.

(A) Fine sand, closely packed (Pl. I and III).

For the explanation of the process by which the successive slip surfaces are developed we will first take the case of the finer sand in closely packed state,[1] as in this case the phenomena take place in most typical and regular form.

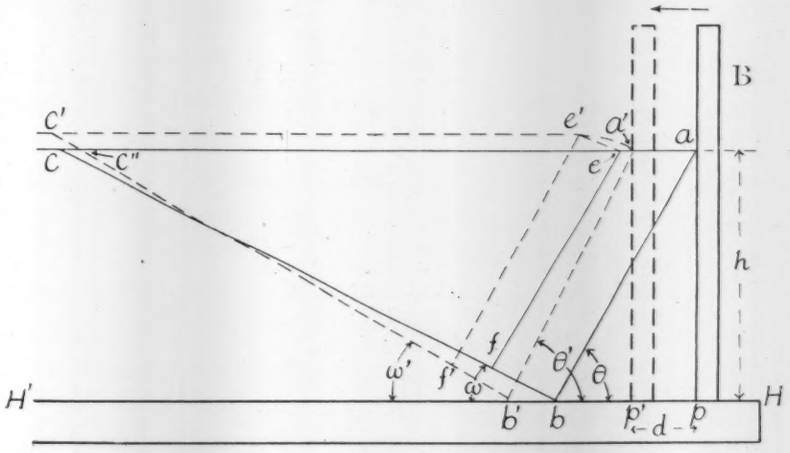

Fig. 1.

Referring to Fig. 1, *HH'* represents the fixed bed plate of the containing vessel, *B* the movable end-wall which is driven in the direction of the arrow, and *ac* is the initial horizontal surface of the sand layer. When the wall *B* is pushed in a slip surface *bc* is formed immediately. The sand mass on the right side of *bc* is set in general motion, while the mass on its left side remains quite unaffected. When the end-wall advances for a small finite distance the angle of inclination, ω, of the slip line generally increases. In the meantime, the angle of inclination, θ, of the line *ab* is also increased so that the motion of the point *b* does not keep pace with

(1) In the present experiments, the closely packed state was obtained by depositing successively layers of small thickness which were pressed by a horizontal plate from above before laying a further layer.

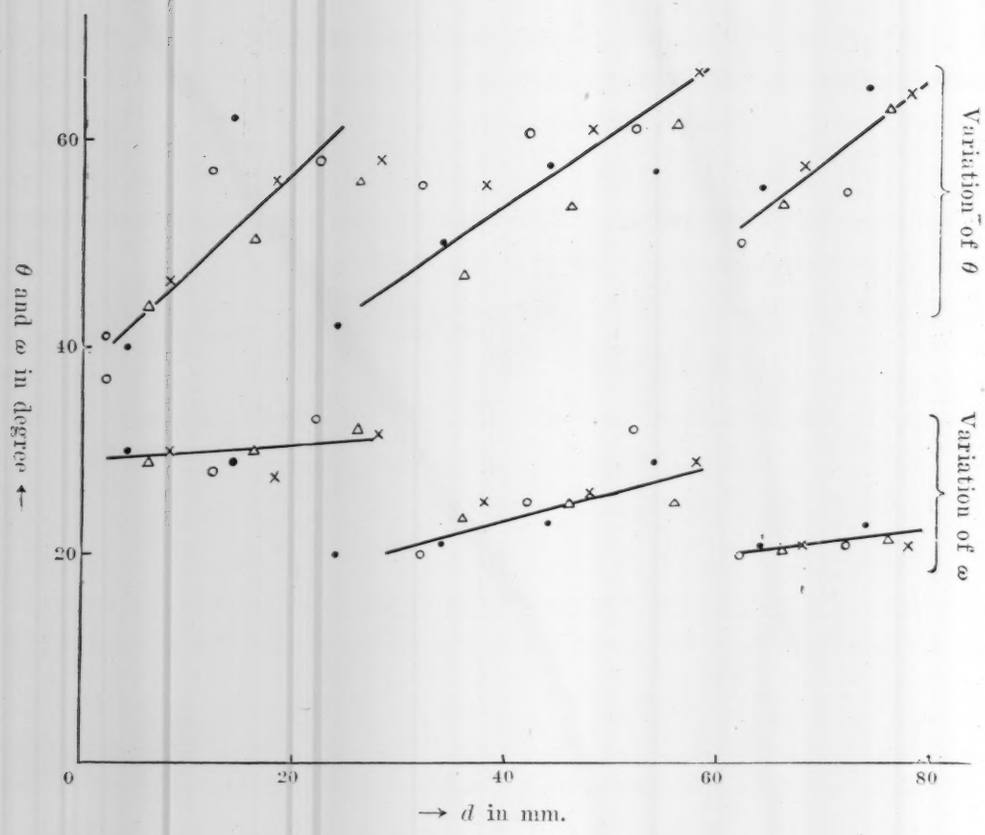

Fig. 2.

that of the wall B. Fig. 2 shows the modes of variation of θ and ω, taking the displacement, d, of the wall B as abscissa. The diagram in full line is drawn schematically from the mean values for the five sets of experiment, as the fluctuation of the data among different series is considerable and the curve for each separate set cannot give any exact quantitative information except for the order of magnitude.

As may be judged from the photographic traces of sand particles, the portion of the sand mass contained within the triangular prism $a'p'b'$ (Fig. 1) is moving horizontally as if it were a rigid body fixed to the moving wall, and sliding on the bed plate HH' against the friction upon it, thus consuming a part of the work done by the moving wall.

As already mentioned, the foot of the slip line, b', is gradually overtook by the wall B, on account of the change in the angle θ. Thus, corresponding to the displacement of the wall, $pp'=d$, the displacement of b is

$$bb' = pp' + b'p' - bp$$
$$= d + h\,(\cot\theta' - \cot\theta),$$

where $h = ap$, and the change in h is neglected. The second term is always negative as θ' increase with d. Similarly, cc'', the displacement of the point at which the slip line meets the free surface is

$$c''c = bb' + h\,(\cot\omega' - \cot\omega)$$
$$= d + h\,(\cot\theta' - \cot\theta + \cot\omega' - \cot\omega).$$

As ω also increases with d, cc'' is still smaller than bb'. As a matter of fact, cc'' is generally negative, i.e. the point c'', and also the slip line as a whole, recedes as B advances. This may be clearly seen on examining the series of photograms from the mode of the change of position of the slip line relative to the mass at rest. Fig. 3 will illustrate the successive

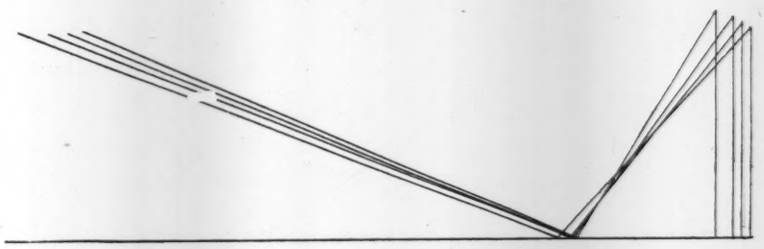

Fig. 3.

positions of the slip lines in an actual experiment. This receding motion of the slip line is, however, generally small and, for a rough approximation, we may say that a portion of sand mass initially contained in a prismatic boundary efc, where ef is an ideal plane, is pushed up along a fixed plane fc to a final position $e'f'c'$, meanwhile the entire prism behaves approximately as a rigid body. On the other hand, the mass initially contained in $ab''bfe$ (ab'' is to be drawn parallel to $a'b'$ to meet the bed at b'') is deformed into a new shape $a'b'f'e'$.

When the deformation is advanced for a certain extent, the sand on the sloping surface $e'a'$ will glide down and result in raising the point a' above the initial level so that we must replace in the above expression h' (cot θ'—h cot θ) for h (cot θ'—cot θ) where $h' = a'p'$ is also a function of d, which could be calculated approximately if wanted.

Thus, a sensible deformation of sand mass is chiefly confined within the region $a'b'f'e'$ which is behaving like a plastic mass, while a thin layer along the slip line plays apparently a rôle of viscous lubricant, as far as a kinematical analogy is concerned.

When the motion of B is still continued and accordingly the angles θ and ω are continually increasing as shown in Fig. 2 a critical stage is attained when further increases of the above angles are prohibited. At this stage a new set of the slip surfaces is started suddenly as shown in Fig. 4, in which $b'c'$ represents the slip line formerly active

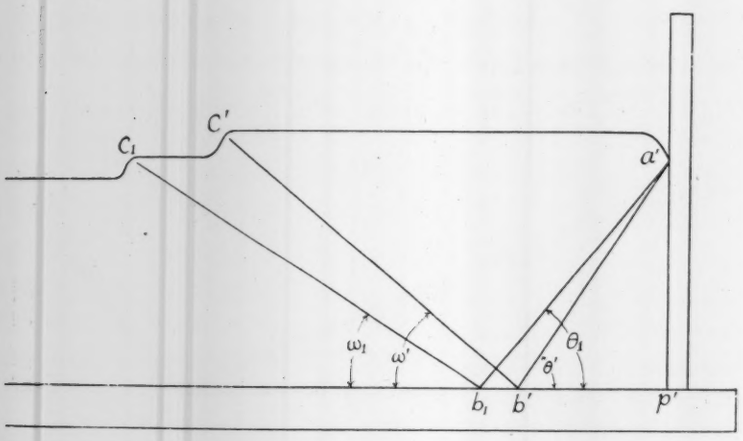

Fig. 4.

and b_1c_1 the new one. The subsequent course of deformation is essentially a repetition of what was described above. Thus, the angles θ_1 and ω_1 which now play the parts of θ and ω, gradually increase with d. That a wedge-shaped portion gliding up along the nearly stationary line b_1c_1 is practically rigid may be seen from the fact that the conspicuous bend of the white index line marking the trace of the former slip line $b'c'$ is neatly preserved during the second step of deformation.

When the wall B is further advanced a second critical stage is attained and then a third slip line b_2c_2 suddenly appears and so on.

Referring to Fig. 2, it may be remarked that the upper and lower limits of θ increase successively for the successive steps of formation of the new slip line. On the other hand, the corresponding limits for the angle ω gradually

decrease for the successive steps, contrary to the corresponding variation of θ. This will suggest already that the two angles are related with each other in a complementary manner and the simultaneous variation is due to the change in a certain common factor determining the inclinations of slip planes relative to the horizontal.

It will be seen that the length between the upper ends of the second and third slip line, $c'c_1$ (Fig. 4), is determined firstly by the possible range of variation of θ and secondly by the amount of increase of h' during the second step. The latter factor is in its turn governed by the first factor. Hence, when the range of θ is small, the successive steps will occur in a rapid succession and the sets of slip lines will be closely spaced, as will be seen later in the case of coarser sand.

In some experiments with the same fine sand it occurs accidentally that, while the gliding is still going on along the slip line $b'c'$ (Fig. 5), some dis-

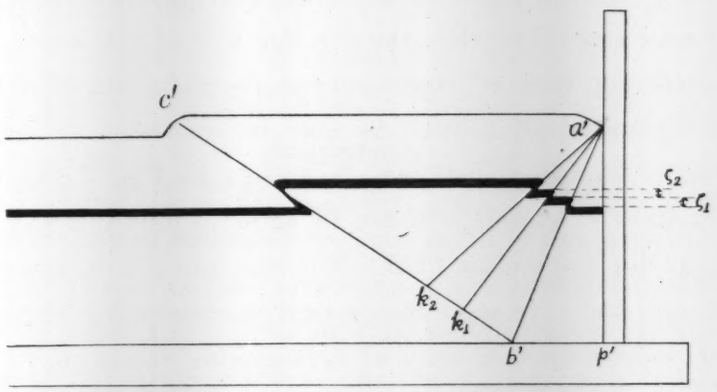

Fig. 5.

continuous deformation appears in front of the moving wall. It has been already mentioned that the mass between $a'b'$ and $e'f'$ (Fig. 1) is subjected to a general shearing, but in most cases the shearing is chiefly localized near the line $a'b'$ so that a sharp bend of the white index line may be observed along $a'b'$, which thus forms also a kind of slip line. Referring to Fig. 6, let $a'p'$ and $a''p''$ be two successive positions of the moving wall. Assuming b' as approximately stationary and drawing $a'b''$ parallel to $a''b'$, it follows that the sand formerly contained in the prism $ab'b''$ has been deformed into the new prism $a''b'k$, such that the areas of the two triangles are equal

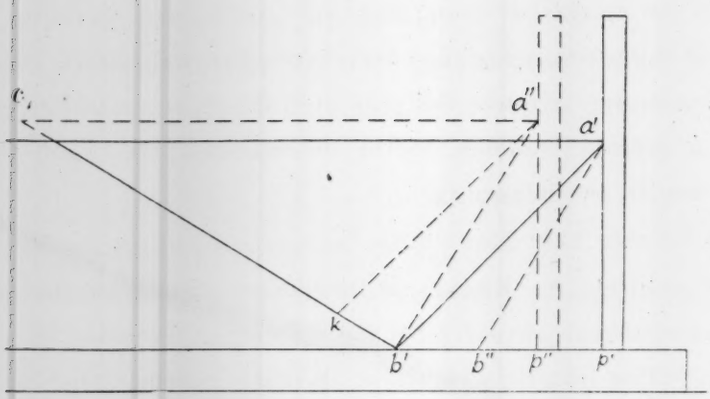

Fig. 6.

to each other. The slip line must have been displaced, in the meantime, relative to the sand mass from a position near $a''k$ to $a''b'$.(1) When such a transition of the slip line relative to sand takes place gradually we obtain a smooth bend of the index line as shown in Photo. 356, 361, etc. It happens, however, in some cases that while the slip line $a''b'$ is still active an auxiliary slip plane shoot out from a'' somewhere in the direction of $a''k$, i.e. in the position of the initial slip line. As may be confirmed by measuring the increases of the two step distances ζ_1 and ζ_2 in Fig. 5, we observe that the two slip lines $a''b'$ and $a''k$ are in action simultaneously, or at least alternately, during the motion of B. The slip line $a''k$ is, however, not able to break through $b'c'$. In some case, a third auxiliary slip line $a''k_2$ (Fig. 5) may appear, before the first step of deformation comes to an end. What causes such a variety is not quite clear, but it may be brought forth by different circumstances such as a heterogeneity in sand and an accidental fluctuation in the magnitude and direction of pressure from the moving wall. The latter fluctuation is unavoidable, since with the increase of the pressure, the iron rod pressing on the wall may sensibly yield to an accidental bending moment.

On account of the shearing motion, which deforms the prism $a'b'b''$ into $a''kb'$, the pressure transmitted from B through the sand mass will be

(1) It may be easily seen that $a''k$ as above defined is approximately coincident with the original position of $a'b'$ relative to sand.

weakened in magnitude and deviated in direction, as we go further in front. This effect will be of importance in determining the inclination of the slip plane as will be referred to later.

After the foregoing explanations, we may now attempt to discuss the mechanical process by which the sequence of the phenomena is brought about, though anything like a handy theory is at present difficult to propound and may better be reserved until more quantitative experimental data have been accumulated.

In the first outset of the motion of the pressing wall, when the trace of slip surface begins to appear, the active pressure on the slip surface will be the resultant of the component due to the weight of the overlying mass and the component due to the pressing wall. The latter will at first be small, so that the resultant pressure on the slip plane ab will be nearly vertical, and still more so on the surface bc. On this assumption we will expect that

$$\theta=\omega=\phi,$$

where ϕ is the angle of natural repose as given by

$$\tan\phi=\mu,$$

μ being the coefficient of friction. Unfortunately, it is difficult to determine the truely initial values of θ and ω with the present method of experiment. As far as may be judged from the photogram obtained, however, the above expectation is fulfilled in some measure by the fact that the difference of the initial values of the two angles, estimated from Fig. 2 by extrapolation, is small and falls within a few degrees which is of the order of magnitude of the experimental error.

As the moving wall is advanced the pressure on it will rapidly increase and tend to outweigh the effect of gravity. In the extreme case when the pressure becomes predominant the resultant pressure on the surface $a'b'$ will become nearly horizontal. The statical relation in this case will be

$$\cot\theta=\mu=\tan\phi.$$

On the other hand, the pressure upon the slip plane $b'c'$ remote from the pressing wall could not undergo the same variation as in the case of $a'b'$, because, as already mentioned, the pressure transmitted from the wall will

be weakened and at the same time deflected due to the yielding of the intermediate mass. Hence, the increase of ω with the displacement of the wall will take place with much slower rate than that of θ. This is actually observed in most cases. Another result to be expected is that near the end of each step, that is just before the start of the next discontinuous fault, the sum $\theta+\omega$ will be roughly equal but fall short a little of 90°. This is indeed the case, as may be seen from the second column of the annexed Table in which the values of $180°-(\theta+\omega)$ for different cases with different sizes of grains and different states of packing are given for comparison.

Sand	Fine Grain		Coarse Grain	
Packing / No. of Slip. Surf.	Loose	Close	Loose	Close
I	102	98	94	97
II	104	99	94	96
III	105	101	96	93
IV	—	—	100	96

The fact that the angle $180°-(\theta+\omega)$ generally increases with the number of steps corresponds to the fact that the gradual increase of the average of limiting values of θ with the successive steps outweighs the corresponding decrease of ω. As may be seen from Fig. 2 the limiting values of θ actually increases with the number of steps more rapidly than the corresponding value of ω decreases. The meaning of such a variation with the number of step may partly be sought in the change in the value of μ and partly also in the change in the mode of transmission of the active pressure on the wall B due to the change in the boundary condition effected by the upheaval of conspicuous mound. A detailed discussion in this respect is at present difficult to be made.

When the slip line $a'b'$ has been brought to its extreme position as determined by the relation $\theta=\cot^{-1}\mu$, a further adjustment of the slip surface by its relative displacement through the sand mass is no more possible and the slip line becomes as it were clutched, so that a further movement is only possible by starting a fresh slip surface from the top of the

wall. By a sudden start of the new slip, the active pressure upon it will be momentarily released to some extent, so that the conditions tend to fall back to the initial state, resulting in sudden decreases of θ and ω.

(B) Fine sand, loosely packed (Pl. III).

The results for the case when the same fine sand as employed in the above experiment is in loosely packed state are qualitatively similar to the above case with close packing. For the loose mass, however, the angle θ is generally larger than for the closely packed sand. This may at least partly be explained by a difference in the coefficient of friction of which the dynamical value may depend on the initial state of packing more strikingly than in the case of the statical coefficient. On the other hand, the difference of ω for the two states of packing is not so marked as in the case of θ. As far as may be judged from the present results, it seems that the limiting value of ω at the final stage of each discontinuous stage, i.e. before starting a new slip line, is generally a little greater in the case of loose packing than in the case of close packing. The cause of the difference may probably be sought chiefly in the difference of the mode of transmission of the applied pressure, though sufficient experimental data are wanting at present to enable us to enter into a detailed discussion on this point.

Generally speaking, the modes of deformation is much more irregular in the case of loose packing, as may be illustrated by irregular forms of the white index lines (for example, Pl. III, Photo. 419). The irregularity is due to the fact that the active slip line is subjected occasionally to an accidental abrupt change of position relative to the sand mass.

Another characteristics of loose mass is that the shearing deformation in front of the slip line $a'b'$ is not confined to a well defined quadratic prism as in the case of closely packed one, but is extended onwards such that it is generally difficult to mark off sharply a wedge-formed portion which is behaving apparently as a rigid body.

(C) Coarser sand, closely packed (Pl. II).

Compared with the finer sand in closely packed state, the value of θ is not sensibly different in the closely packed coarser sand as far as may be judged from the present data. This is plausible, as μ is chiefly deter-

mined by the material of the particles, but not so much by the grain size. On the other hand, the angle ω is generally greater for the coarser sand than for the finer. The factor considered in (*A*) regarding the transmission of pressure is probably here effective. It will be interesting to observe that the general mode of variation of ω for the closely packed coarser sand is nearly similar to that of loosely packed finer sand.

The most striking characteristics of the coarser sand is that the successive slip planes are more closely spaced than in the case of the finer sand. This may be explained at least partly by the difference in the rate of increase of pressure with the displacement of wall, i.e. a quantity corresponding to Young's modulus of an elastic body. A systematic experimental investigation of the relations between this factor and the grain size as well as the state of packing is necessary for a further discussion in this line.

(D) Coarser sand, loosely packed (Pl. III).

In the case of the loosely packed coarser sand, the characteristics of the coarser sand mentioned above in comparison with the finer sand, with respect to the case of close packing, is much more enhanced. The discontinuous steps in faulting take place in rapid succession such that each step is mostly difficult to be sharply discerned. The result is that instead of a regular step of white line with a number of horizontal segments (for example Photo. 376) we have a curved line disturbed with minute ripples of irregular zigzag indentations (Photo. 238). Even in this case, however, we may discern a small wedge-shaped portion at the top of the raised mass, which still preserves its initial configuration as a rigid mass. Hence, it will be interesting to regard the extended *portion* of sand with the inclined trends of the index line as taking up here the rôle played by the sharply defined slip *planes* in the case of fine sand.

Taken as a whole it will be remarked that the difference between the fine sand in closely packed state and the coarse sand in loosely packed state is somewhat similar to the difference between a *brittle* material and a *plastic* one, as far as the geometrical, and perhaps also the kinematical, relation of deformation is concerned. This point may throw some light on the problems of plastic deformation of ordinary substance.

II. Deformation caused by Reciprocating Motion of Movable Wall.

In the next series of experiment, the movable wall B was subjected to a reciprocating motion with a range of motion of 0.6 cm. The velocity of motion was kept nearly constant at 0.02 cm./sec. as before. Pl. IV (a), (b), (c), (d), (e) show the typical modes of deformation produced in a fine sand layer by this treatment. (a) represents the state at the end of the first progressive motion of the wall B, where we may clearly discern the principal system of characteristic lines, corresponding to $a'b'$, $b'c'$ and $e'f'$ of Fig. 1. (b) was obtained after the end of the first retrograde motion of B, during which a wedge-shaped portion aps has slipped down along a slip plane running aslant from the foot of the wall, just as was shown in our previous report. Next, the reciprocating motion of B was repeated ten times of cycles and then (c) was obtained. It will be seen that the quasi-rigid portion on the right side of the left slip plane has been considerably raised on account of the purely periodic motion of B. In the meantime, the sand just in front of the wall B has been successively lowered in its level, as this portion is nearly fixed to B during the progressive motion and slides down by every retrograde motion. In (c) we may observe that a double step-fault is already developed in front of B. Besides, it will be noticed that the slanting free surface of sand on the right side of the photogram is nearly parallel to the slip line bc marking the boundary of the mass at rest.[1] Next, the wall B was moved in alternate directions for another ten times, after which the entire mass has been deformed in a form as shown by (d) of the Plate.

Referring to the photogram (d), it will be seen that the slip line bc has become completely inactive and a new set of slip lines, $a\beta$ and $\beta\gamma$, has appeared which now plays the rôle formerly played by ab and bc. Here, the relation is apparently somewhat similar to an ideal case in which the line bc is replaced by a fixed bed plate and a moving piston or wall at ab

(1) This means $\omega=\phi$, showing that the pressure transmitted from B is small in the region of this slip line.

is pushed in a direction parallel to the line bc, meanwhile the direction of gravity is nearly parallel to ab. According to the considerations above made on the relative direction of the slip line and the resultant pressure, it will be seen that, in the present case, the applied pressure of the wall is deflected upwards more or less parallel to the slanting free surface. Referring to the photogram, it will be interesting to observe that, in the region within the prism $ab\beta$, the white index line which has previously been everywhere horizontal, appears here nearly vertical. A comparison with (c) will show that this is the trace of a former slip line pushed inwards by the reciprocating motion.

On repeating the reciprocating motion for further ten times, the photogram (e) is obtained. Here, the slip lines $a\beta$ and $\beta\gamma$ are already stopped and a second set, $\alpha_1\beta_1$ and $\beta_1\gamma_1$ has been developed.

It is well known that there is a class of mechanism by which a progressive motion of a certain working part of it is produced by a purely reciprocating motion of another. The present case will afford another interesting example which promises to find an important application to some geophysical problem, as will be presently seen. The essential point of the mechanism consists in the existence of the two distinct slip planes which are called into play alternately by the alternate motion of the wall which is the prime mover.

III. Applications to Geophysical Problems.

Different experiments have been made by geologists to imitate the deformations of the earth crust subjected to horizontal thrust. They are, however, mostly based on a tacit assumption that the crust behaves as a sort of an ordinary plastic body in small scale. It is, however, well known that in the problem of elastic deformation the effect of gravity, which is usually neglected in the cases of bodies of laboratory scale, gradually increase in its importance with the increase of the size of the body. On the other hand, the effective elastic strength of the earth crust as a whole will probably of a quite different order of magnitude compared with that of a small defectless test piece handled in laboratory, as the superficial crust is

run across by numerous joints and fissures. Such a crust will, of course, behave as a more or less perfect elastic bodies towards a disturbance such as earthquake waves propagating through it. When, however, a deformation of vast scale and of lasting nature such as indicated by geological structures is concerned, the matter will be quite different and the crust will resemble in some measure an aggregate of discrete units, blocks or grains as the case may be. Each unit may be supposed practically rigid, while the connection between the consecutive units is elastically weak and held chiefly by a sort of friction. In other words, the crust will resemble a layer of sand in some respect, if the above supposition be justifiable.

We have seen from the results of our experiments that a sand mass may behave sometimes like a brittle solid body and sometimes as a plastic material, according to circumstances. At any rate, therefore, the use of sand as the material for experiments will include a wider possibility than experimenting with ordinary plastic mass. Thus, H. M. Cadell[1] succeeded early in imitating a characteristic geological structure in Scotland by the use of sand layer, which is difficult to obtain with an ordinary plastic material.

In view of these considerations, it will not be without interest to attempt here to apply the present results of experiment for explaining some geological or geophysical phenomena, of course with much reserve and precaution.

(*a*) We have seen that when the movable end-wall is receded or pushed on continuously a fault line is formed which remains active for a definite interval of time and then stops to make way for a second active fault which suddenly appears at a certain distance from the first. It is probable that some of the actual groups of parallel fault lines might have been formed by a similar process.

(*b*) When the end-wall of the experimental apparatus is moved to and fro alternately, two different fault lines become alternately active. It occurs in an earthquake district that two distinct epicentral zones alternately

(1) H. M. Cadell, *Trans. Roy. Soc., Edinburgh*, **35** (1888).

reveal their activity, with a period equal to some of the meteorological periods. The two phenomena may have some feature in common with respect to their mechanisms.

(c) Mechanisms by which a periodic horizontal stress in the earth crust may produce a progressive upheaval or depression have sometimes been discussed among geophysists. We have seen above a rather striking example of such mechanisms, in which a reciprocating motion with a range of 6 mm. resulted in heaving up a mound of more than 20 mm. height. Though our case is not adequate[1] for an immediate application, the above will serve as a demonstration of possibility in this line.

(d) In the present experiment, the bed plate is fixed and practically rigid and thus introduces a boundary condition that cannot be realized in the case of the earth crust. The above experimental condition may, however, correspond to a geological case when a superficial layer of small elastic strength lying upon a more rigid bed is subjected to a lateral thrust. For imitating the entire crust, however, it is desirable to experiment with a sand layer floating upon a more plastic bed. We are now preparing for a next series of experiment in which a layer of "miduame" will form a yielding substratum.

Apart from these and other possible geophysical applications, the above results seems also to suggest many points which may throw some new light on the problems connected with the fracture of solid and plastic materials in general. A way is suggested of bringing the brittle, plastic and fluidous materials on a continuous scale of some property which may conveniently be expressed in terms of some definite factors corresponding to those factors essential in the case of our sand model. Before approaching this side of the problem we must wait long until sufficient experimental data have been accumulated under widely varied conditions.[2] Especially, the effect of cohesion between the sand particles is one of the most important factor to

(1) Especially because here the friction against the bed plate is considerable which may be absent or small in the case of a "floating" crust.

(2) In the case of plastic deformation, there is, of course, no factor corresponding to gravity in the present case, but the mode of variation of stress with the progress of strain by yielding may in many respect be analogous to the present case.

be investigated; it may affect the modes of deformation in a profound manner.

Recently, we were enabled to begin a cinematographical investigation of the deformation of sand mass by which means a considerable saving in time is obtained. In the next report, we hope we will be able to give some account of the results obtained. As the above series of experiments with ordinary photographic camera has now come to an end, it was considered convenient to give here a provisional summary of the result thus far obtained. The discussions here made regarding the mechanical explanation of the phenomena is still of a tentative character which may want a considerable modification in the course of further investigations. The chief aim of these discussions was to suggest different theoretical as well as experimental problems which may be raised regarding the matter in question.

APPENDIX.

A Further Note on the Mechanism of Formation of Step-Faults Produced by Receding the Wall.

In the previous paper, we have seen that the formation of step-faults by receding the end wall of the containing vessel is determined by the existence of upper and lower limits of the angle of inclination of the slip plane. The variation of the angle of inclination was expressed in terms of the variation in the apparent coefficient of friction of sand in motion. It is, indeed, undeniable that the true coefficient of friction may differ sensibly in the case as is here concerned from the statical case when only the initial infinitesimal slip is in question. As will be seen from the considerations mentioned above in connection with the discussion of the results of the present experiments, there is, however, another important factor determining the angle of inclination of the slip plane, i.e. the variation in the effective pressure on the wall B brought about by the motion of it.

According to the statical theory of earth pressure on retaining wall, the angle of inclination of the slip plane, θ_1, will be given by

$$\tan\theta_1=\frac{\sin\phi+\sin 45^\circ}{\cos\phi},$$

where ϕ is the angle of natural slope, and the coefficient of friction μ' on the wall is assumed to be equal to the coefficient μ on the sand.

If, however, $\mu'=0$, the inclination is given by

$$\tan\theta_2=\frac{\sin\phi+1}{\cos\phi}.$$

On the other hand, if the pressure on the wall is annulled, the sand mass will glide freely on the slip plane so that the inclination will be given by

$$\tan\theta_3=\tan\phi=\mu.$$

In the actual case with the sand in motion, the limiting angle θ_3 can never be attained, as long as the motion of the receding wall is slow and uniform. When, however, the wedge-shaped mass in front of the wall is in continuous motion we may compare the case with the statical one by saying that the effective friction against the wall is diminished, as in the layer immediately in front of the wall the horizontal pressure is being partly released and thence the total friction against the wall is reduced. This will tend to make the angle of inclination approach the value θ_2.

In the actual examples, we have ϕ approximately equal to 30°, whence

$$\theta_1=64^\circ 20',\qquad \theta_2=60^\circ.$$

The actual range of variation seems to concide roughly with that given by the above. Besides, the fact that the slip surface is generally curved and the inclination of its tangent decreases with the depth of the point along the slip line, may also be explained by considering that the lower layer is undergoing a relatively larger horizontal extension than the upper[1] and thence approaches more to the case of free fall.

We hope we will return to the discussion of these points when more sufficient data have been accumulated.

---

(1) Previous paper, *loc. cit.* p. 52–53, Table I and II.

Photo. No. 341

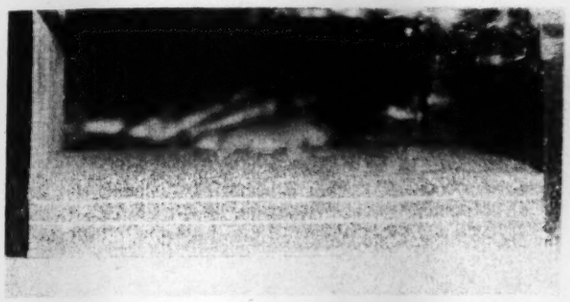

346

351

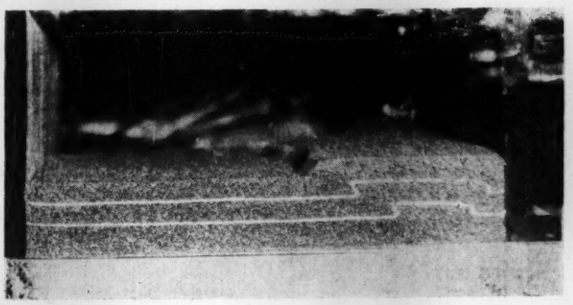

356

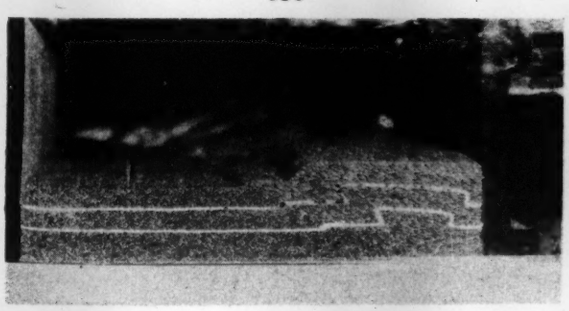

Photo. No. 361

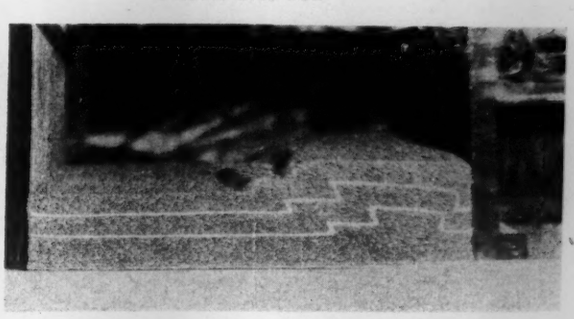

376

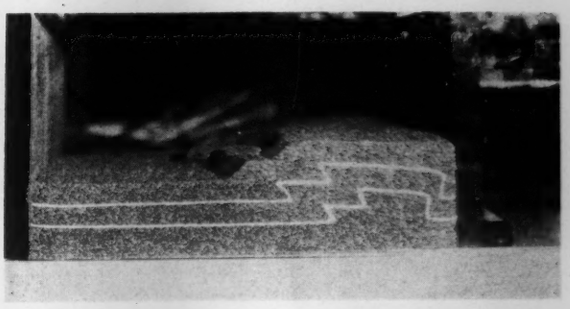

366

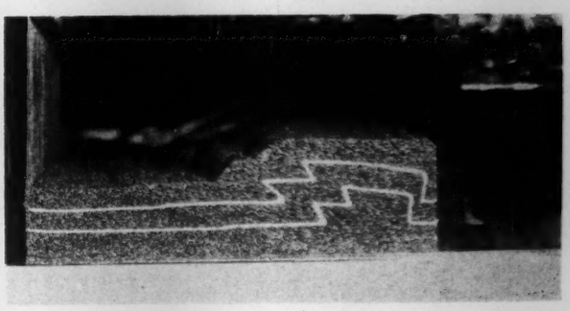

371

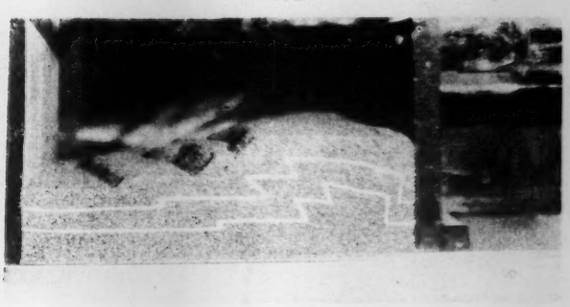

Finer Sand, Closely Packed.

Photo. No. 245

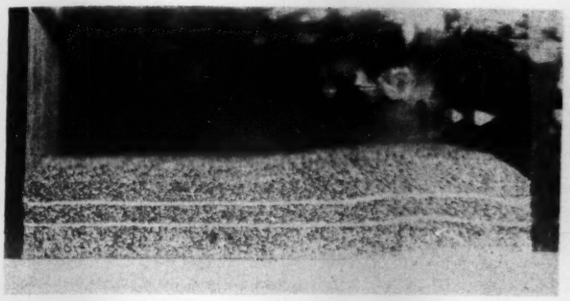

Photo. No. 255

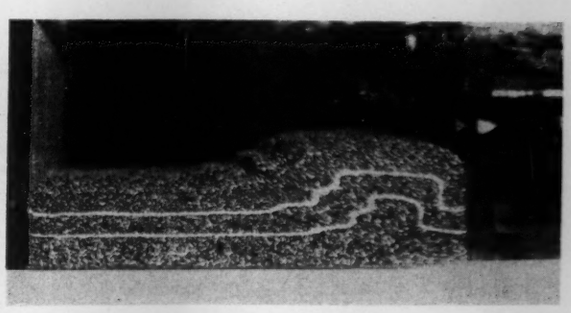

250

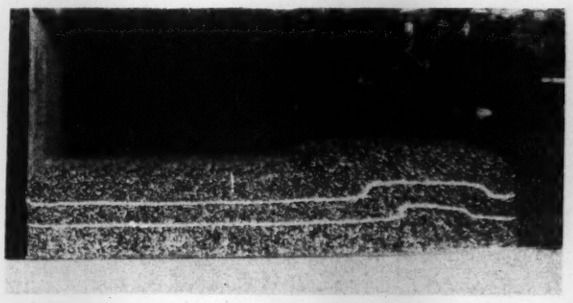

270

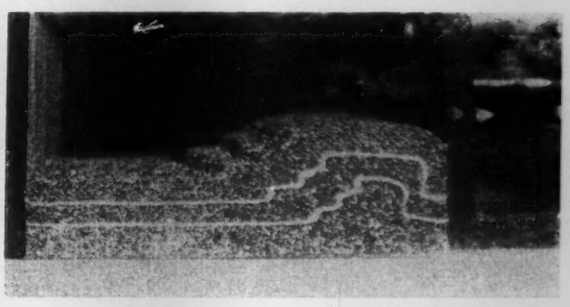

260

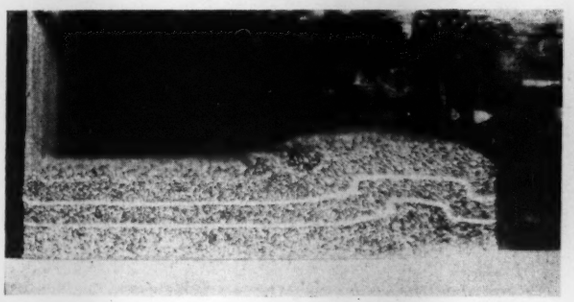

275

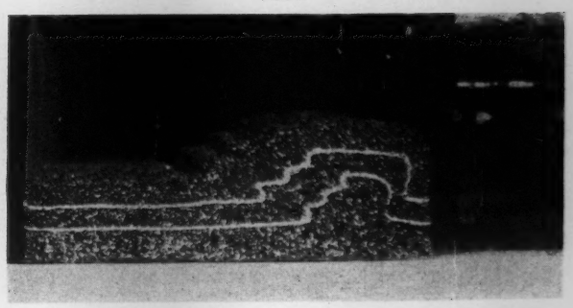

265

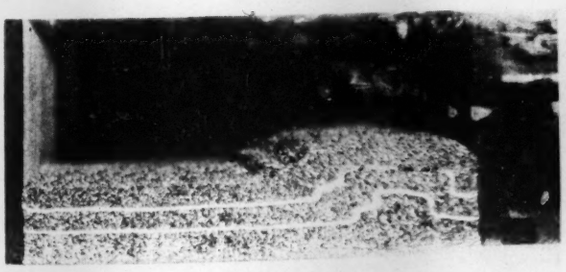

280

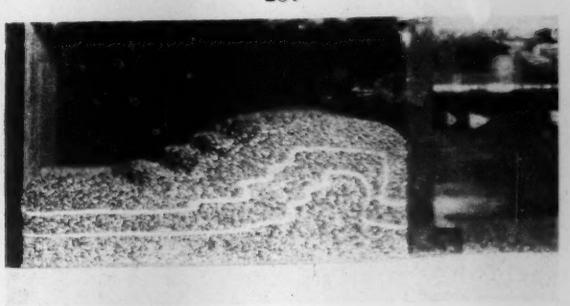

Coarser Sand, Closely Packed.

（震研彙報、第六號、圖版、寺田、宮部）

Photo. No. 368

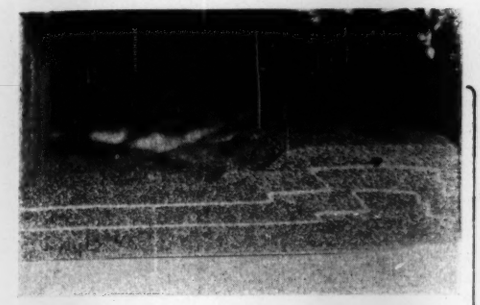

380

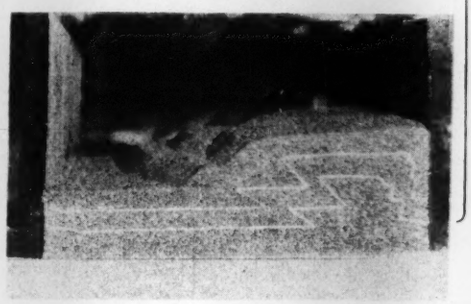

Finer Sand, Closely Packed.

419

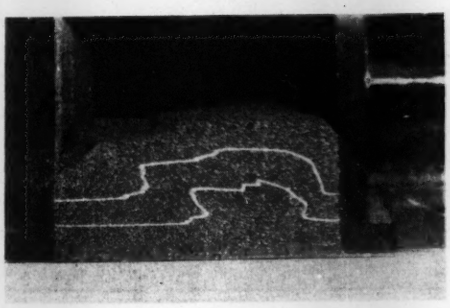

420

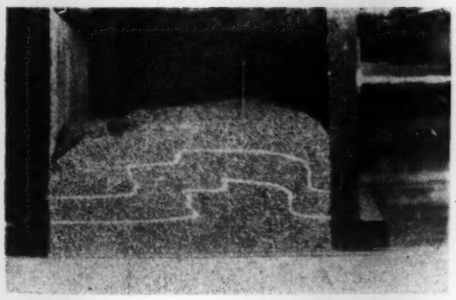

Finer Sand, Loosely Packed.

Photo. No. 208

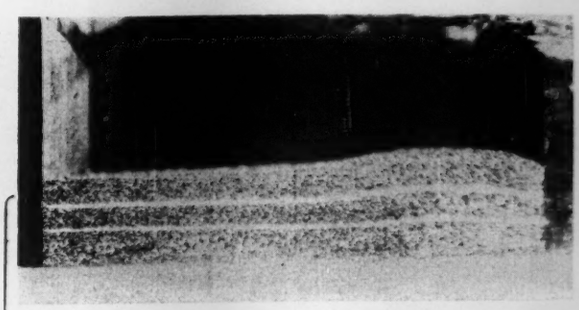

218

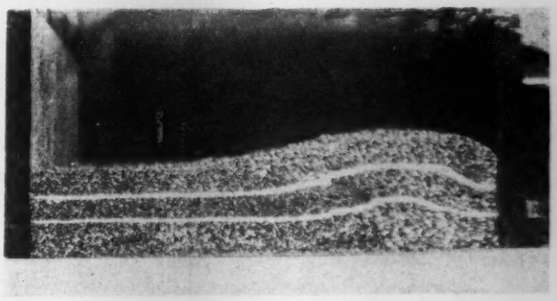

228

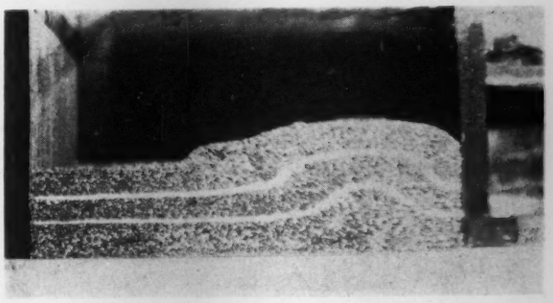

238

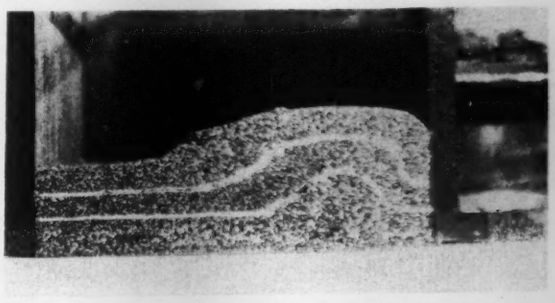

Coarser Sand, Loosely Packed.

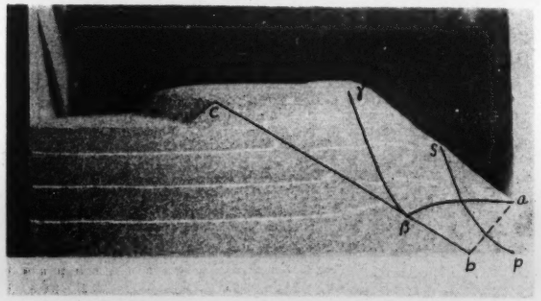

(*d*)

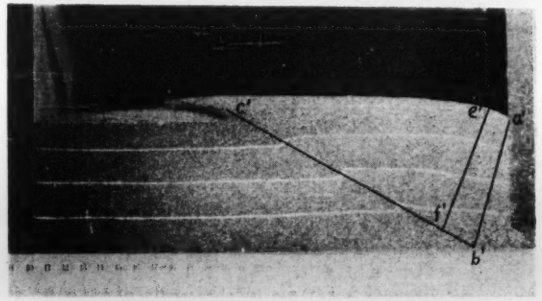

(*a*)

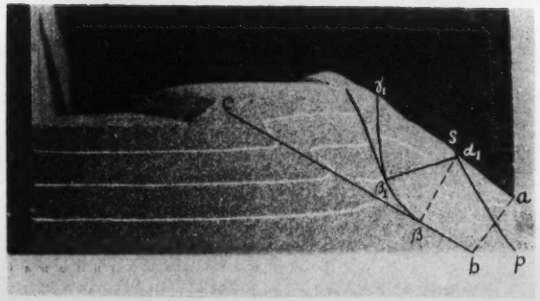

(*e*)

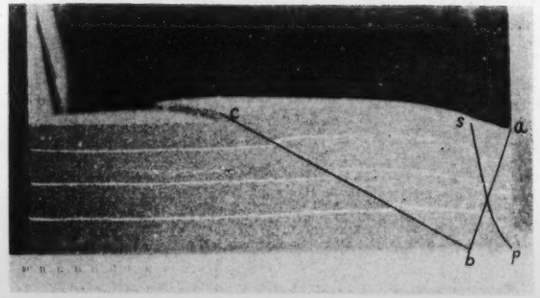

(*b*)

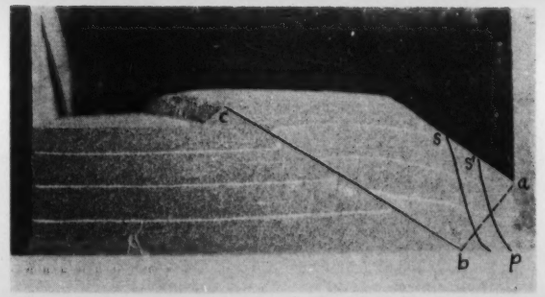

(*c*)

(*a*) First positive motion.
(*b*) First negative motion.
(*c*) After (*b*), 10 reciprocating motion.
(*d*) After (*c*) ,, ,,
(*e*) After (*d*) ,, ,,

（震研彙報、第六號、圖版、寺田、宮部）

地震發生の機巧に就いて

所員　石本巳四雄

1. 緒言
2. 地塊の存在と其の運動
3. 地震發生と氣壓勾配
4. 岩漿の性質
5. 彈性波發生の機巧
6. 地震及び此れに附隨する諸現象の解釋
7. 結語

Sur le mécanisme de la production des ondes sismiques

(extrait)

Par **Mishio ISHIMOTO,**

Il est certain qu'un grand tremblement de terre se produit avec accompagnement de changements topographiques: les changements ont été particulièrement remarquables lors des trois derniers grands tremblements de terre survenus au Japon. Les études nous ont conduit à considérer que le changement topographique n'est pas celui qui correspond à des ondes sismiques rayonnant dans toutes les directions.

Nous pouvons maintenant mettre en évidence l'existence de blocs et leurs mouvements, en utilisant des mesures faites par le nivellement de précision. Les mesures ont ainsi montré que les mouvements de blocs sont tellement libres qu'il n'existe presque aucune corrélation entre ceux-ci et nous pouvons en déduire l'existence d'une couche malléable sous le groupement des blocs.

Le fait que le gradient de pression atmosphérique joue un rôle important sur l'apparition du tremblement de terre nous suggère l'existence d'une couche malléable dans laquelle la matière visqeuse se déplace aisément sous l'action de la différence de pression atmosphérique.

Les études sur les propriétés du magma, telles que le phénomène de différentiation, la vitesse de l'intrusion magmatique, etc., nous permettent de considérer l'origine de la production des ondes sismiques comme le résultat du choc provoqué par le changement brusque du moment cinétique de l'intrusif.

Dans le cas d'un faible tremblement de terre, il n'y aura que le choc donné par l'intrusion; mais dans celui d'un grand tremblement de terre, il pourra même se former des fissures dans la croûte terrestre à la suite de choc énorme produit.

Nous avons, en effet, de nombreuses répliques juste après le grand tremblement de terre, lesquelles s'expliquent par des injections de magma dans les fissures formées par le premier grand choc. Nous pouvons alors déduire des changements topographiques comme le résultat de movements d'après l'équilibre isostatique du bloc.

Les ondes sismiques s'amortissent quand elles passent une faille: la faille, soit la produite, soit la tectonique. Nous observons donc une anomalie de l'intensité sismique au passage des failles situées perpendiculairement à la direction de la propagation des ondes sismiques.

En introduisant l'effet du magma, nous pouvons aussi mieux expliquer d'autres phénomènes accompagnant le tremblement de terre.

---

1. 緒　　言

地震發生の機巧に關しては種々の議論が爲されてあるが、其の中において豫め注意を要するものは、所謂地震と地形變動との問題であろう。震央附近においては地形變動が出現する場合が屢ゝであり、此の附近における地震動は極めて複雜のものであるから、遠地觀測により得たる結果を其の儘用ひても、多くは其の實相に觸れて居ない樣に感ぜられる。震央附近における地變が地震動と關係して如何なる性質のものであるか、又遠距離にも到達する地震波動が如何にして發生し傳播するかと云ふ問題に關しては、大地震の研究に俟つものが多い。關東大地震以來、但馬丹後兩度の大地震に相遇した吾々は、多くの事實を知る樣になつた。その中地形變動に關するものが最も重要な位置を占めて居ると云へるであろう。著者は此等の事實を基礎として判斷を進めて行つた所、地震發生に關して從來の考へ方と多少異つた議論に到達したのであつて、地震波動の發生及び地形變動の根元を地下岩漿の存在を以て說明せんとするものである。

2. 地塊の存在と其の運動

地塊の存在する事は、地質學上の事實より首肯し得る事であつて、長年月に亘つて一地區が一塊をなして運動を爲した形跡は、歷然たるものがあるのである。勿論運動

と稱しても吾々の容易に認知し得るものは、實にその傾動であつて、其の運動の大なる場合には相當大なる山脈を成生するのである。

現在において地塊傾動の存在を驗するに當つては、水準測量の援助を得るが最も適當であり、又一地點における傾動の時間的變化を觀測するには、傾斜計を使用する事によつて達せられる。而して此れらの器械を用ひて觀測された地塊傾動の事實は、最近において可成りの多數に上つて居る。

關東大地震と殆ど同時に相模灣沿岸及び房州一帶に及んで、土地隆起が發現したのであるが、陸地測量部において施行せられたる測量を本として攻究せられたる結果[1]によれば地塊の存在と其の傾動の事實とは明かに證明されたのである。地塊は 7 km, 14 km の徑を有し、傾動は多種多樣の方向においてゞある。此れらの傾動の値は、地震時の前後において施行せられた測量結果の差であるから、運動全部が地震と同時に發生したものとは直ちには考へられない。然し乍ら、何れも地震に關係して生じた運動であつて、地震と前後して大部分出現したものである事は疑ひ無いものであらう。

地震とは全く關係なく施行せられた水準測量の結果の中、昨年（昭和二年）越後沿岸地方における結果[2]は最も適當な例として擧げる事が出來るのである。此の場合においても地塊の存在は明かであつて、一地塊の徑は 50 km を算し極めて緩徐なる傾動を示して居るのが明かになつたのである。而して地塊は外觀上、河川溪谷の存在位置を以て境として居るのであるから、此の運動は最近に開始せられたものに非ずして、相當長年月に亘つて運動を續行して居たかの如く思はれる。卽ち地震とは全く關係無い場所においても、かゝる運動が存在すると云ふ一つの證據が得られたのである。

なほ此の測量直後、三島郡關原村附近に於いて强震の發生があり、直ちに此の部分のみの再測量の結果、强震程度の地震に於いても地變として測量し得べき變動の生ずる事實[3]が發見されたのは、偶然とは云へ非常の收獲であつたと云はねばならない。

去年（昭和二年）三月七日に發現した丹後大地震においては、前後數回に亘つて水準測量[4]が繰返へされ、大地震と同時に出現した地塊運動の外、時の經過と共に如何に其の運動が進行するかゞ實測されたのである。坪井(忠)氏の攻究[5]によれば、地震

(1) 熱海景良、武藤勝彥：昭和三年四月地震研究所談話會にて發表（未刊行）。
(2) 山崎直方：帝國學士院記事　第四卷　第二號。
　　今村明恒：　同　上。
(3) 今村明恒：帝國學士院記事　第四卷　第三號。
(4) 陸地測量部：地震研究所彙報　第三號、第四號、第五號。
(5) 坪井忠二：地震研究所彙報　第六號

後地塊の運動は極めて自由なものがあり、種々の形式において各地塊が個々の運動をなす事が認められたのである。此の場合地塊の徑は 5km 乃至 10km の間にある。なほ此れと同時に三角測量が數回行はれ、地塊の水平移動の測定が爲されたのであつて、傾動と關係して水平移動の存在する事が證明されたのである。然し乍ら觀測點が少數である爲め、各地塊を云々する程度には行つて居ない。

要するに輓近水準測量によつて到着したる結果は以上の如きものであつて、全く地塊及び其の傾動の存在が明かにされたと云へるのである。以上の事實が發見されたる上は、各點の相對的位置を論ずるに當つて解析的方法を用ふる事は實際の現象を取扱ふ上に適當でない様に感ずるのである。即ち斷層附近においても、已に地殻の彎曲現象が認められないのであつて、各地塊の運動を代表すべき平面の連續を以て、地形變化が表はされなければならない様に思はれる。

以上の事實を約言するならば、地塊運動は地震の有無に拘らず繼續されて居るが、大地震後における地塊の特長は、其の運動が極めて活潑である事と、其の形狀の小である事とであつて、恐らく大地震と同時に大地塊が小地塊に分裂し運動を開始したものでは無いかと想像される。但しかゝる現象は未だ同一地區において經驗されたもので無いから、充分立證されたものと云はれない。然し乍ら兎も角も大地震後の地塊運動は特に活潑であり、各地塊の關係も極めて自由であると云ふ事は少くとも云へるのである。

一地塊の運動を時間的に研究するには傾斜計を使用して連續的に傾斜變化を記錄する方法が便利である。傾斜計による觀測は未だ日が淺く、これにより得た結果は極めて多數であるとは云へないが丹後地震後宮津及び河邊村において觀測せる結果(1)によれば、地塊運動と餘震發生との間には密接の關係が存在する事が分つたのである。器械は一地點に据付けて其の點の傾斜變化を觀測して居るのであるから、其の記錄は勿論一地點における傾斜變化には相違ない。然し乍ら地塊の存在と其の運動とが立證されてある今日においては、一地點の傾斜變化は其の存在する地塊の傾斜變化を代表するものと認めて差支へ無いのである。但し溫度變化の影響は多少傾斜變化を隱蔽する傾向があるからこれは相當顧慮する必要があるのである。

宮津、河邊における傾斜觀測結果によれば、相當大なる餘震數日前に變化を生じ、地震直時においては寧ろ著しい變化が認められず、地震と共に傾斜變化が終結を告げ

---

(1) 石本巳四雄： 地震研究所彙報 第四號。

て居るのである。此の最も代表的のものとして、昭和二年七月七日の餘震前後における傾斜變化を轉載する。

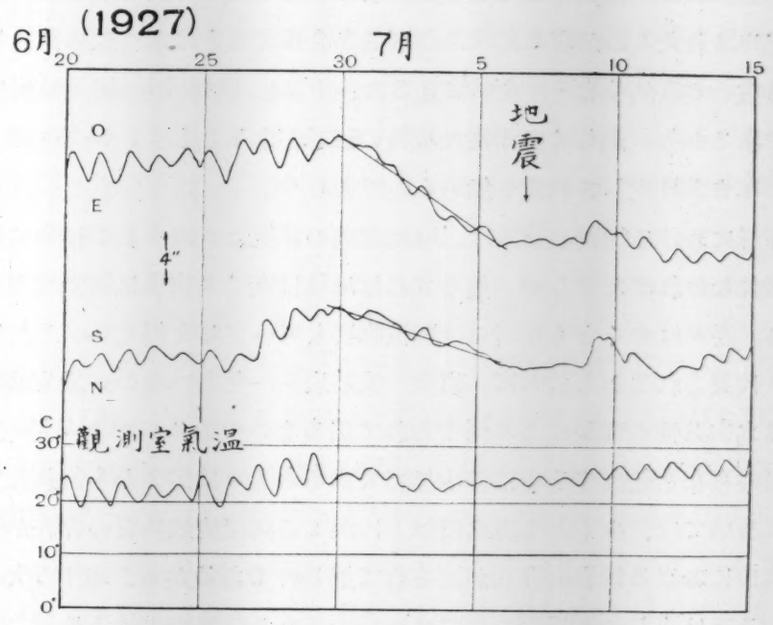

第一圖　宮津における觀測

那須氏(1)は一つの餘震に換ふるに餘震群を以て此の現象の說明を試みて居られるが、結局最後に比較的大なる餘震を以て終結を告げて居るのであるから、此の最後の餘震を以て此れ等の傾斜を生じたる原因の代表と見る事が出來るのである。即ち地震前に地塊の傾動があり、結局餘震を誘導するものであつて、地震時及び其れ以後においては傾斜變化を生じて居ない。勿論この餘震は宮津地塊附近に發生したものでは無いから、宮津地塊の運動そのものを以て地震發生に關して云々する事は多少の誹謗を免れないものであるかも知れない。然し乍ら河邊觀測においても同樣の事實が明かにされて居るのであつて、然も此の場合震央は河邊地塊に極めて接近して居のである。要するに餘震前において地塊運動が烈しく、地震後においては平穩に復歸すると云ふ現象は認めて差支へ無いものと信ずる。なほ關東地方に發生する弱震程度のものにおいてても、東京三鷹等の觀測において此れと同樣の現象は認められて居るのである。

以上の事實は地塊運動の極めて自由であり、且つ地震現象に密接な關係を持つと云ふ證據であるが、其の原因に就いては地塊の厚さ及び此れ等の地塊下に橫はる物質に

(1)　那須信治：　地震研究所彙報　第六號。

論及しなければならない。地塊の厚さに關しては充分の智識は無いとしても地震波研究により 50 km 附近に不連續面の存在を認めて居る外、最近に至り我が國においても 15 km 乃至 20 km 附近にも不連續面のある事が立證[1]されて居るのである。地震波により見出されたものが直ちに地塊の厚さと合致するとは考へないが、丹後地震後發生した餘震の垂直的分布[2]に就いて見るに、15 km 及び 7 km附近に震原が密集して居るのであるから、恐らく此の邊に地塊の限界があるらしく、15 km 乃至 7 km を以て地塊の厚さと推定して差支へ無いものであらう。

地塊の下層における物質の狀態は、地塊運動の狀況より察すれば極めて流動性に富むものと云はなければならない。然らざれば地塊は斯くも自由に運動する事は出來ない筈である。吾々は少くとも此所に流動性物質を考へざるを得ない。これは如何なる物質により代表されるかと云へば、岩漿—液狀岩漿—を考へるのが最も適當であり、其の存在は火山其他の現象により信ぜられて居るものである。地下 7 km 附近に於いて已に岩漿の存在を是認する事は多少無理であると人々は云ふかも知れない。然し乍ら火山帶においては、少くとも海水面以上にかゝる高溫液狀物質の存在が可能である事、即ち火山における熔岩の存在が許されて居るのであるから、地下 7 km 附近に岩漿の存在する事は決して不思議の事では無いのである。又此の地下岩漿の存在は一局部即ち地震災害地方に限られてあると考へられるが、一方時間的に云ふならば、其の一局部においても常には大して流動性を帶びては居ないが、時あつてか流動狀態に變ずるとも考へられる。此れは大地震及び此れに引續いて地塊運動が特に烈しいと云ふ事實と、地震發現の無い地方においては地殼が比較的安定であると云ふ事實から想像されるものである。火山が時に液狀岩漿を噴火口に湛える事もあり、又或る時には全く休眠狀態に陷る事もあるのと類似の現象が地下にもあると考へられる。

要するに地塊運動は其の下層部に存在する岩漿の狀態により惹起されるものらしく、若し一つの地塊が單獨に存在する場合には最も安定の平衡を保つ方向に運動するものとなるであらう。地塊相互において水平方向に如何なる力が作用して居るかは不明であるが、三角測量の結果は水平移動が垂直移動に比較して同程度であると云ふ事實を示して居るのであるから、相當これも問題とすべきであり、此所に水平力即ち横壓力に關しても議論が爲されなければならない。兎もあれ、地塊下における岩漿の存在は何れの場合においても必要とするのである。

---

(1) 松澤武雄： 地震研究所彙報 第五號。
(2) 那須信治： 同 上 第六號。

なほ日本における地下熱上昇の割合を見るに、此れは比較的大であつて、20 m にて 1° 上昇する場合を普通とするのである。此の割合を以て進むとしても、7 km にては 350°. 15 km にては 750° にて岩石熔融の溫度には成らないのである。然し乍ら、前述の如く火山地帶においては地表迄も岩漿の上昇する事は敢て不可能の事では無いから、或る地域を限つて地下に岩漿溜の存在を想像しても差支へ無いものと信ずる。

要するに地變を生ずべきものは結局地下岩漿の作用に起因するものであつて、大地震により涸渇せる溫泉の更生、或ひは新溫泉の噴出の如きは、地變を生ずる岩漿運動の熱的作用に起因するものであらう。

3. 地震發生と氣壓勾配

地下流動岩漿の存在を更に確かむる現象として氣壓勾配が地震發生に密接の關係を有する事實を擧げ度い。一地點における氣壓の高低が其の地方における地震發生に關係を有する事實[1]を詳細に研究されたのは故大森教授であらう。教授は全國に亘つて一日中の地震回數分布は其の地方における氣壓の一日變化に關係ある事を確められたのである。又日本全國に亘つて地震發生回數の季節により異る事實[2]は、氣壓配置に起因するものとして說明された。寺田教授[3]は氣壓の絕對値を採用する替りに其の勾配が地震頻度と關係を有つ事を指摘され、其後此の方面の研究は極めて多數に上つて居る。而して何れの研究も氣壓勾配が地震發生に與つて力ある事を立證して居るのである。寺田教授は 100 km に對して 2 mm 乃至 3 mm の氣壓差が地震發生を左右すると云ふ事實は極めて不思議な現象として述べられて居るが、地震發生の機巧も此の事實から考へ直さなければならないのである。

中村(左)教授[4]は關東大地震の餘震について其の關係を研究されたが、小田原附近に震央を有する餘震は殊に著しく氣壓勾配の影響により發生して居る現象を見出した。又長谷川氏[5]は濃尾斷層附近に發生した小地震に就いて研究された結果、氣壓勾配の方向が斷層に直角である場合地震が發生すると云ふ事實が確められたのである。此の研究は地下に想像し得べき斷層に對して氣壓勾配が如何なる方向をとるかと云ふ極めて興味ある研究に相違ない。然し乍ら、今一步地震發生の機巧に迄も立入つて此

---

(5) 大森房吉：震災豫防調査會報告　第二號。
(1) 大森房吉：震災豫防調査會報告　第三〇號。
(2) 寺田寅彦：氣象集誌　第二八年　第一號。
(3) 中村左衞門太郎：天文地球物理學輯報　第三卷　第二號。
(4) 長谷川謙二：氣象集誌　三二年　第一一號。

の現象は說明さるべきものではあるまいか。

丹後地震の餘震に就いては著者(1)も多少の研究を試みたのである。氣壓勾配としては毎日午前六時における京都、神戸、境、福井等の氣壓値と宮津における同時刻のものとの差を求めて圖に表はして見た。然し乍ら京都—宮津、神戸—宮津の氣壓差は類似の曲線であり、又此れが最もよく餘震の發生と關係を有つ事が判明したのである。即ち京都、神戸方面において數日に亘つて次第に氣壓差が增加する場合には、結局丹後地方に餘震が發生するのである。此の場合氣壓勾配の方向（氣壓の減ずる方向）は西北であつて、地震と同時に出現した主な斷層—郷村斷層—に對しては並行であると云はねばならない。なほ此れ迄の研究においては多く地震當時における氣壓勾配を論じて居るものが多いのであるが。著者は寧ろ氣壓勾配の變化する道程に着目し度いのである。如何となれば、宮津、河邊における地表傾斜變化は數日間に亘る變化を示して居るからである。即ち氣壓勾配そのものが直接地震發生を促すものに非ずして氣壓勾配の時間的變化が地塊の運動を促し、結局地震發生に終ると見なければ成らないのである。石川氏(2)も氣壓勾配の變化と地震及び火山噴火との間に關係ある事を指摘され、多くの例證が擧げられて居るが、又最近井上氏(3)の研究によれば、關東地方に發生する地震は比較的長周期に變化する氣壓勾配に關係を有すると云はれて居る。

なほ玆に一言附加し度き事は、傾斜觀測による地塊運動は時間的に働く力を考へに入れても、なほ說明し難いものがあるのである。其れは京都—宮津間にて求めたる氣壓勾配が次第に大となるものに對してのみ地塊の運動が開始されると云ふ事實であつて、京都—宮津間における氣壓差よりも、今一層廣い面積に亘る氣壓配置が寧ろ其の原因となつて地塊運動を生ぜしむるかの如く見受けられる。此れは要するに吾々の氣壓勾配に對する、或ひは地塊運動に對する智識が不充分である結果に過ぎないのであつて、將來の研究問題として殘されるものである。

以上の事實の說明に關しては、著者は地塊運動の場合と同じく地下岩漿の存在を以て解決を試みんとするものである。今假りに廣い面積に亘り液狀岩漿層が極めて自由に運動し得る地塊下に存在するものと考へやう。かゝる假想地殼に氣壓差が生ずれば如何なる現象が起るのであらうか。此の問題は大洋における氣壓配置の問題と比較されるものとなる。若し海水面(4)の昇降が氣壓を全部補償するものと爲すならば、驗潮

(1)　石本巳四雄：　地震研究所彙報　第四號。
(2)　石川高見：　氣象集誌　第二輯　第三卷　第二號。
(3)　井上宇胤：　地震研究所彙報　第五號。
(4)　潮汐による海水面の昇降は此の場合考へない事とする。

儀により求められた異常潮位は少くとも太洋全部に關する氣壓配置に追從するものとなるべきであつて、結局その地點の絶對氣壓に關係を持つと考へて大差ない。此の現象を假想地殻の問題に當て嵌めるならば、岩漿流動はその地點の氣壓値に追從するものと云へるであらう。此れは大森教授の云はれた氣壓絶對値に關係する地震發生に相當する說明ではあるまいか。然るに實際において、かゝる假想地殻は天體の引力に起因する潮汐の觀測上甚だしく實在性の乏しいものであつて、岩漿層の存在は相當限界されたる部分にあるらしく、其の部分において岩漿運動を考へる時には兩端における氣壓差に注意する方が至當であると云ふ事になる。

岩漿の存在を是認する事によつて尙有利となる事は、氣壓差が靜水壓として傳達される結果、二點間の距離に關係しないで其のまゝの力が働くと云ふ事である。例を以て云ふならば第二圖の如き U 字管に水を滿たし一方に壓力を加へるとする。加へら

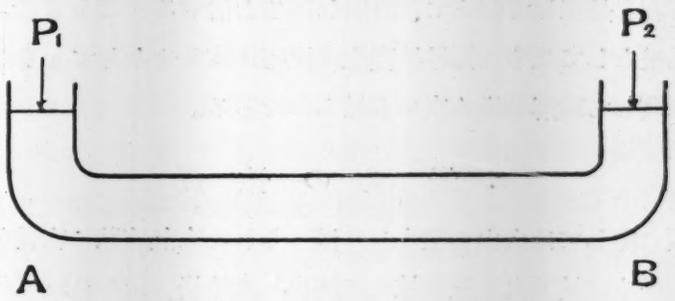

第　二　圖

れた力は其のまゝ管の水に傳へられるが、水が自由に運動する場合には一方の水面の上昇により釣合ふのである。此の場合管の長さには無關係である。若し此れと類似の現象が地下に行はれて居るならば、氣壓勾配よりも、氣壓差が寧ろ問題となるべきであらう。100 km にて 2 mm 乃至 3 mm の水銀柱の差は勾配としては相當小なるものであるが、力として傳達されるものは此の差に相當するのである。但し地表においては地塊の存在がある事、又液狀岩漿も多少の粘性を有する爲か或ひは他の原因により一時的の力に對しては相當の抵抗をするものらしく、數日間同じ力が同一方向から働く場合には壓力が傳達され岩漿流動が行はれるものと見られる。此の事實は丹後大地震發生の場合に明かに見出されたものである。氣壓の變化のみならず潮位の差が地震發生に關係を指つ事[1]も事實らしいが、此の影響は氣壓程著しいもので無い樣である。

以上の說明は地震發生に關する岩漿流動を單に物理的現象として見たものである

(1)　中村左衞門太郎：　前揭。

が、此所に化學的變化迄も顧慮する場合には多少の改竄を必要とするものである。即ち岩漿の分漿作用と蒸氣壓に關する現象が當然問題とならなければならない。此等の事實は岩漿流動現象の說明には極めて都合よきものであり、又此の化學的變化は地震を發生せしむべき本體であると考へて差支無いものであるかも知れない。恐らくそれが事實であらう。然し乍ら此の中には將來の研究に俟つべきものが多々あるのであるから、著者は敢て此の問題に深入りせず單に分漿作用により極めて大なる蒸氣壓を發生し得べき機巧[1]のある事を指摘し、岩漿流動の極めて容易に行はれる事實を擧げるに止めて置き度い。

斯様に岩漿の流動と地塊運動とは同一現象であつて、切放して考へる事の出來ない問題であり乍ら、吾々の觀測し得るものは單に地塊運動のみであつて、此の結果として地震が發生すると云ふ現象しか見て居ないのである。然し乍ら、地塊運動の現象は塊下に岩漿の存在を是認して初めて、說明し得ると信ずるのである。かくて著者は此の地塊運動の結果として生ずる彈性波發生の機巧に論及せんとするのであるが、先づ岩漿の性狀に關して理解を進め度いと思ふのである。

4. 岩 漿 の 性 質

岩漿の諸性質に關しては火山の噴火口に湛へられた高熱液狀の物質を直接研究するものもあるが、多くは且て火口壁を越えて流出した熔岩、或ひは地質學上深成岩として發見される岩石に就いて攻究を進めたものが其の主なるものであらう。

火山において研究される高熱の熔岩は地下における岩漿其のものでは無く、寧ろ本體である原始岩漿は尙ほ深所に存在し、其れより誘導されたものが多いと考へられて居る。なほ深成岩に於いても同じく誘導岩漿の地殼內空隙を滿したものと考へられて居るから、其の間には密接な關係がある事が云はれて居る。即ち何れの場合においても、極めて深所に存在する原始岩漿の分漿作用により生成されたものとして稍淺い場所に來り、なほ分漿作用を續けつゝ岩漿溜を作ると想像されて居る。此の分漿現象は岩漿の化學的研究に俟つ外は無いのであるが、其の樣式は多種多樣であつて一般に未だ不明の點が多い樣である。然し乍ら其の中二三の事實、例へば花崗岩の岩漿は極めて稀薄なる溶液となつて遠方に到達し、狹い小脈をも充塡すると云はれて居る。即ち或る岩漿の粘度は極めて小なるものがあつて、壓力變化に伴つて流動が生ずると考へられて居る。然るに此の流動も單に器械的壓力の增減のみにより行はれるものとして

(1) G. W. Morey: Journ. Wash. Accad. Sci. 12 (1922) 219.

說明をするのは困難であつて、氣壓差による力が直ちに岩漿流動を支配するとは考へられない。岩漿溜においては分漿作用が行はれて居り、溫度變化に從つて成分の平衡が次第に變化して行くが吾々の問題とする物理的變化特に其の蒸氣壓の變化には著しいものがあるのである。溫度の低下に從つて岩漿の蒸氣壓は增加し、(1) 遂に外壓以上に及ぶ場合に於いては爆發か或ひは岩漿の流動が惹起されなければならない。氣壓勾配による壓力も外力の一つであるから、若し岩漿の蒸氣壓が極めて外壓に接近して居る場合に於いては、氣壓の消長は岩漿流動を助長する上に當然の原因であつて差支へない。即ち氣壓及び氣壓勾配の影響は直接岩漿を流動せしめる役を演ずると云ふよりも、寧ろ此等の壓力が蒸氣壓を通じて猛烈なる流動を惹起すと考ふる方が適當であろう。

岩漿の流動する速度は同一間隙においては岩漿の粘度と其れに加へられたる壓力とにより決定されるものである。相當狹い間隙を通じて岩漿の流動する場合には、其の速度が問題となる。即ち目下存在する岩脈が果して幾何の時間を以て充塡されたかを明瞭にし度いのである。貫入當時においては少くとも液狀を呈して居たのであるから、其の溫度は 1000°C 附近であると推定出來る。又地質學上接觸變成岩成生の事實は、周圍の岩石と岩漿との間には可なりの溫度差の存在を意味するものであり、岩漿溜は相當遠距離にある事が自ら必要となるものである。即ち貫入岩の中には高溫の液狀物質が相當溫度差のある物體の中に充塡されたるものがあると見られ、此の事實に從つて考察を進めるのである。而して先づ高溫の液體岩漿が間隙中にて如何なる速度を以て冷却し行くか考へ度いのである。

二次限の空間において幅員 2 cm を有する無限大の距離に達する間隙を想像し、高熱の岩漿も周圍の岩石も何れも等しい比熱 (c) 傳熱度 (k) 及び比重 (ρ) を有するとする。時刻 $T=0$ において間隙が充塡され、時と共に冷却する有樣を百分率に表はしたものは第三圖である。但し常數はすべて花崗岩の値が用ひられてある。 ($c=0.13$, $k=5.3\times10^{-3}$, $\rho=2.5$, $a=\sqrt{\frac{kc}{\rho}}=0.105$ c.g.s.)

第三圖の示す如く僅か 100 秒時後には岩漿の溫度差は 1/2 となるのである。液狀岩漿の溫度 (1000°) が半減されたる場合 (500°) においては、岩漿は全く固體化すると考へて差支へないのであろう。岩漿の貫入距離は幾程であるか明瞭には分つて居ないとしても、接觸變成岩の成生される程度の溫度差を持つものであるから、岩漿溜か

(1) 杉健一: 地質學雜誌 第四二三號。

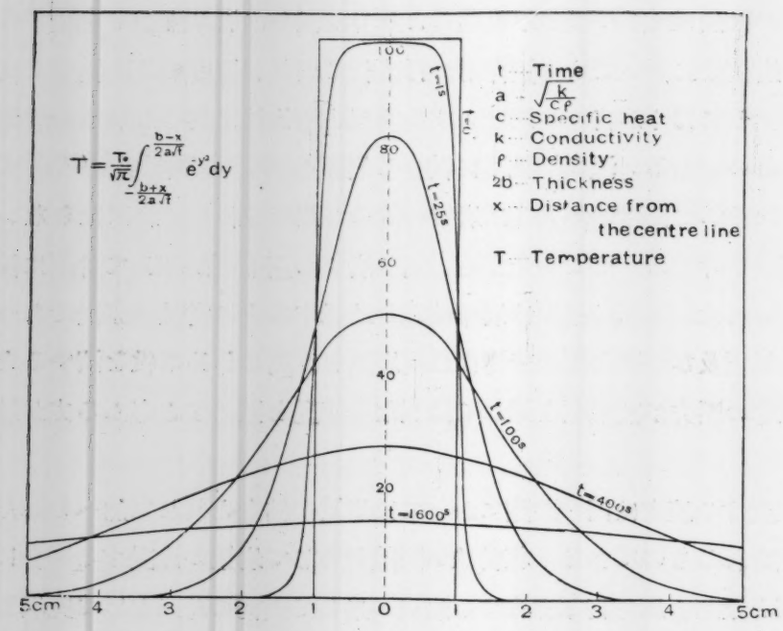

第 三 圖

らは相當遠距離にあるものと見ざるを得ない。先づ數百米より數粁に亘ると假定して差支へ無いものであろう。此の距離を 100 秒にて到達すると爲すならば、其の速度は極めて早いものと云はねばならない。實際に於いては岩脈の幅員は數ミリメートル程度のものも存在するのであるから、その速度も極めて早いものがあると想像される。勿論速度が大である關係上多少の粘性のために熱の發生する事も考へ得べき事ではあるが、岩漿の粘性に關する吾々の智識は不充分であるため論議を進める事は困難に陷る。即ち粘性は極めて小であると云ふ假定の下に論を進めて居るに過ぎない。なほ幅員の大なる岩脈において、其の單位面積に加へらるべき壓力が等しい場合においては、其の速度は益々大なるものとなるであろう。何となれば此の速度を阻害するものは岩漿の粘性效果によるものであつて幅員の增加に伴つて此の影響は著しく輕減されるものであるからである。

以上は岩脈に就いての議論であるが、深成岩中に底盤 (Batholith) 餅盤 (Laccolith) の如きものがあつて、此等の成生が岩脈と同じ貫入作用によつて成生されたものとすれば、極めて迅速の運動を以て空隙が充塡されたであらう。又假令その岩漿の運動は速かで無くとも運動量は極めて大であると想像出來るのである。著者は地震の勢力が極めて大であるのは斯樣の現象が地下において行はれ、地震波動が發生するものと說明を試みるものであるが、同じく貫入岩の成生は極めて單時間であると云ふ說明をし

て居る地質學者は多いのである。而してその結果として火山爆發と同様の現象を生ずると論じて居る例(1)もある。

> These considerations show that the extend dike intrusions resemble volcanic eruptions in that both take place in an intermittent and paraxysmal manner.....

斯様の考を以てすれば、火山現象も液狀岩漿上昇により說明されるが、火山においては噴火口存在のために現在に於いては大規模の底盤成全の如きものは發生しないのを普通とするであらう。一般火山爆發において小地震を伴ふは、地表附近における岩脈成生に原因するものらしく、ヴェスヴィオ火山火口において、或ひは富士寶永山火口において岩脈の存在する事は有名の事に屬する。即ち火山地震と稱せられるものは極めて表面的のものと見られ、大地震後に發生する餘震に比べ得べきものにて、單に小規模の岩漿貫入が行はれるに過ぎないものであらう。

小川教授(2)は地質學の立場より地震發生の本體は岩漿運動にありとせられ、種々の例證を擧げて說明を試みられたるは敬服に値するものであるが、地震動發生の機巧に就いては詳しく論ぜられて居ない。石川氏(3)は異常震域の研究に附隨して日本海地震が火山性地層と密接なる關係ある事を指摘せられ、地震發生が岩漿の作用によるものと主張されて居る，著者は勿論此れ等論者と同意見ではあるが，岩漿運動を以て急激なる運動即ち地震波發生の機巧をも說明せんとするものである。

5. 彈性波發生の機巧

此れ迄述べ來つた現象から地震波動即ち彈性波が如何なる作用によつて發生されるかを考察して見たいのである。著者は地塊の存在及び其の運動が極めて自由である事實より地塊下には流動性物質を想像し、此れが恰も氣壓勾配に促進されて移動する事を述べたのである。而して地震發生と地塊運動との關係に就いては、地震前に傾斜變化を生じ地震發生と共に終結を告げて居る事實を述べたのである。即ち地塊運動は岩漿移動の表面的發現であつて、彈性波發生は結局岩漿運動の急激に停止する際に生ぜられた衝撃と考へるのである。即ち岩漿は流動する事によつて極めて大なる運動量を持つと考へられ，此れが一時に停止する時において其の運動量は衝撃となり，此所に彈

(1) J. Barrell: Prof. Paper No. 57, (1907) 157–159.

(2) 小川琢治: 地球 第一卷 第三號。

(3) 石川高見: 氣象集誌 第二輯 第六卷 第三號。

性波が發生し四方に傳播されるものと考へられる。又分漿作用も合せ考ふる時には、地下に於いて已に外壓に對抗すべき蒸氣壓が發生したる場合には、上層に位する地塊は全く不安定の狀態となり動搖を開始するであらう。而して或る方向に傾斜する事により空隙が生じ、此の空間に岩漿の貫入する事によつて蒸氣壓も減じ地塊も安定すると見られる。勿論小地震或ひは深層地震の如きは地塊の不安定を惹起せざるべく、地塊の動搖に關しては無關係のものとして存在するであらう。

大地震の場合においては地下に行はるべき岩漿の運動量ば極めて大であり、從つて此の大衝撃の爲めに地殻に裂罅の生ずる事も想像される。即ち物質破壞の極限以上の振幅を有する彈性波の存在は不可能となるからである。此の意味において震源においては物質破壞限度だけの彈性波が發生するのであつて、恰も裂罅成生により地震波が放射されたかの如き現象を呈する。而して此の波動が比較的强度の小なる彈性體に突入する場合には、此所にも亦破壞が生じ得べく、從つて勢力の減衰も行はれるであろう。即ち言葉を替えて云ふならば、裂罅は地震を發生するものに非ずして反つて地震波を減衰する役を演ずるものと考へられる。

地震動の原因が全く岩漿運動の衝撃による結果であると云ふ現象に關聯して地表における衝撃の結果が記象上何等差別の無い地震動を發生した例を擧げたい。Galizin[1] は Pamir 地方において 2 km³ 乃至 3 km³ の容積を有する岩石が 300 m 乃至 600 m 落下して災害を生じた事實を研究した結果、同日 Pulkovo にて記錄せられた地震の原動力は落下による衝撃により發生せられたものであると云ふ結論を得たのである。即ち此の程度の衝撃においても遠距離迄も到達する振動を與へ得る大地震が發生したのである。地下における衝撃においても此れ以上の勢力を有するものは極めて多かるべく、適當の假說の下にその勢力を計算する事も可能であると思ふ。

大地震後の地塊の狀態は其の大いさの小である事と、其の運動が極めて自由であると云ふ事である。此の爲めに地塊下の物質は液狀を呈すると云ふ論斷を下したのであるが、其の形狀の小であると云ふ事は大地震の際生じたる波動のストレスに堪える事なく小分裂を生じたのであるかも知れない。其れも本來の弱線である構造線に沿ふて發生したものと見られるのである。斯樣にして地塊は極めて自由になつたのであるから、地塊下の岩漿流動に從つて最も安定なる平衡に達する運動、或ひは水平力の存在がありとすれば其の力に從つて地塊の移動が生ずるであろう。かくて此れらの地塊

(1) B. Galizin: C. R. 160 (1915) 810–813.

運動が烈しい場合においては地表に所謂斷層の發現を見るのであつて、斷層の出現を以て地震の本體であるとは考へられない。

大地震の場合においては衝撃が極めて猛烈である爲めに地塊に裂罅を生ぜしめ、或ひは小地塊に分裂せしめるであらうが、小地震、或ひは餘震の場合には斯様の現象は無く地塊間隙又は裂罅を求めて岩漿の貫入があり、單なる岩漿衝撃の結果が地震波動を放射するのであろう。即ち大地震は底盤或ひは餅盤の成生に例へられるが、餘震程度の地震は單なる岩脈成生と考へられる。

6. 地震及び此れに附隨する諸現象の解釋

以上論じ來りたる事を地震及び此れに關係する諸現象に對照して其說明を試み度いのである。

震原の深さに就いては種々研究の結果が報告されてあるが、大地震後の餘震には餘り深い震原はなく、丹後地震の場合には 7 km 及び 15 km 附近に密集して居り、30 km を越へるものは殆ど無いと云ふ狀態である。地震の原因に就いては已に岩漿の蒸氣壓を問題として居るのであるから、此等の深さに相當して其所の壓力以上の蒸氣壓の存在が想像出來るのである。關東地方等に發生する地震においては 40 km 程度のものも多數あるが、和達技師[1]の研究による深層地震においては 300 km—500 km に及ぶ深さを有するものがある。此の地震の原因は岩漿自體の中に生じた變化であるが、其の機巧は同じく分漿作用による蒸氣壓の變化を以て說明さるべきものと信ずる。斯様な深い所に於いて發せられる地震は極めて其の勢力が大であるにも拘らず餘震を伴ふ事が全く無いのは要するに此の部分における物質の狀態に異るものがあるのであつて、地表に近いものとは異つて大衝撃によりても裂罅の生ぜざる物質である事の證據ではあるまいか。

地震發生の機巧として地震計に記錄された初動方向から、地下に發生した斷層が想像されて居るが此れは必ずしも地震の本源が斷層であると云ふ說明にはならない。岩漿の衝撃の方向により震原において發せられる震動は、其の方向に從つた彈性波である事も又地塊それ自身にある振動方向を持つて居て、此れが四方に放射されると考へるならば、裂罅の發生は敢えて問題とはならぬであろう。

火山地震における記象と一般構造地震と稱せらるゝ記象との間には區別がある様に

---

(1) 和達清夫：氣象集誌　第二輯　第五卷　第六號。

云はれて居る。然るに丹後大地震後發生した餘震の記象においては、全く火山地震の其れと區別出來ぬものが大部分であつた様である。(1) 此れは餘震の震原が比較的淺かつた事及び地震波の通路が比較的簡單であつた事に起因するものと解釋される。即ち此の事實は火山地震及び構造地震は勢力の大小こそはあれ、その發生の機巧において差異の無いものであると云ふ事實を示すものであつて、同じく岩漿運動の結果に外ならないと思はれる。

大地震の際に生じたる地變に就いて多少の考察を爲すならば、濃尾地震において根尾谷斷層を第一に注意して見たい。地變としては此斷層が最も鮮かに發現したのである。然るに最も災害の激烈を極めた地域は此の斷層附近と云ふよりも、岐阜大垣の中間を經て名古屋の西方に至る方面であつたのである。此の地震後此の地方に施行せられた水準測量の結果によれば、此の最激震地方に相當して土地の隆起沈降が發見されたのである。大森教授は此所に地下斷層を想像され、(2) 被害大のであつた事を說明して居られるが、假令此所の地下に斷層が生じたとするも、其の大いさにおいては根尾谷斷層に比敵すべきものでは無いのである。なほ教授は此地區において何物か地下より急激に突上げたるものゝ存在がある様であると述べられて居るが、此の意味は此の地區において最も烈しく衝撃を感じたものと解釋しては如何なものであらうか。而してこの衝撃により地塊が分裂せられ自由に運動を開始した爲め所謂斷層が發生したのであると著者は解釋をし度いのである。斯様な判斷を下す事によつて此の斷層の出現が地震後であつた事、然かも急激に非ずしてヅルヅルと段違ひを生じたと云ふ事が充分に納得出來ると思ふ。

地震波—彈性波—のストレスが地殼の有する强度以上に達する場合には破壞が生ずるのであるが、地殼に弱い部分が存在して居る時には、進行して來た地な波は此所に破壞を發生せしめ地塊の運動に從つて所謂斷層と認められるものが成生されるのである。前述の如く根尾谷斷層はかくして出現したと思はれるが、假令破壞はあつても一般には所謂斷層を成生するとは限らぬ様である。又地震波が比較的弱い部分即ち地塊の境界等を通過する場合、その勢力の一部分は反射され、一部分は減衰され、殘部は通過して行くのであるから、斷層線に沿ふて震度の異常が認められる事を常とする。根尾川下流においては地震と共に所謂斷層の出現は認められなかつたが、此の谷の兩側

(1) 今村明恒：地震研究所彙報　第四號　一九五頁。
(2) 大森房吉：地震學講話　三四〇頁。

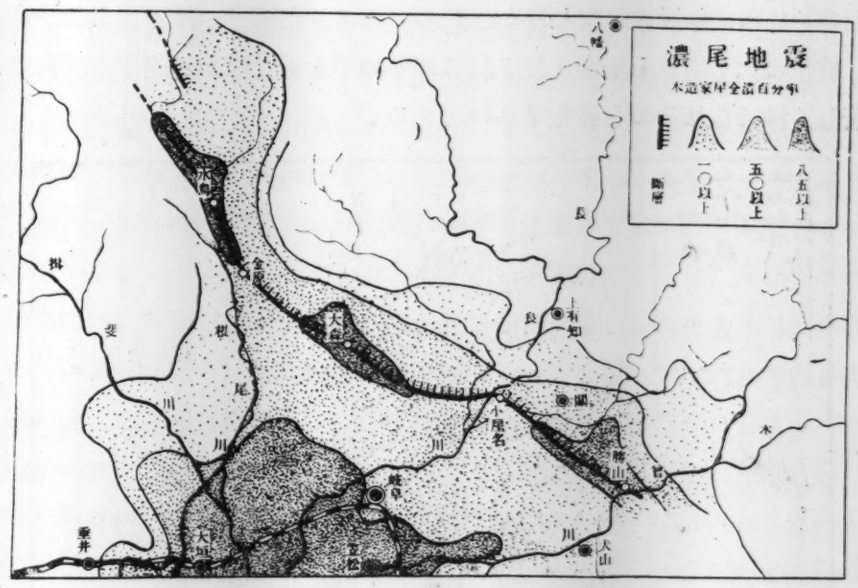

第　四　圖

において著しく震度の異る事實が存在するのである(第四圖)。[1] 即ち根尾川の震央側において 60%-70% の被害率は此の川を越える事によつて約 25% に激減して居るのである。此れと類似の現象は他の大震の場合にも明かに認められる事であるが、一種の異常震域として將來研究せられなければならない。

關東大地震においては著しい斷層が地表に出現しなかつたのである。此の事實は頗る意外として海底に斷層の存在を考へる論者もあるが、著者は必ずしも斷層の存在を必要とはしないのである。相模灣底における斷層の有無は兎も角、地表における災害程度を檢する時は隆起部分と著しく合致する事が見出せるのである。此れは岩漿運動の結果斯様の地變を出現し、又此の地域下より地震波が發生したと見られるのである。即ち此の考を以てすれば相模海底における陷沒地帶も岩漿運動に伴ふ結果として自ら明かなものであつて、彼の櫻島噴火に際し噴火口附近即ち島の中央においては土地隆起を生じ、島の周圍においては反つて沈降を示した類似現象[2]として考へられるものである。

關東大地震の場合には地震に先立つて地變は發生しなかつた様である。大地震の衝撃により地塊は分裂し、運動を開始したのであらうが、各地塊の相互的運動が烈しく

(1)　岐岐測候所濃尾大震報告により製作。
(2)　大森房吉：　震災豫防調査會歐文報告　第八卷　第二號。

無かつた爲めに所謂斷層は出現しなかつたのである。なほ此の地震による被害狀況を見るに、前述の如く構造上斷層と目されて居る地帶を地震波が通過する時には、其の勢力が著しく減ぜられるのを發見するのである。

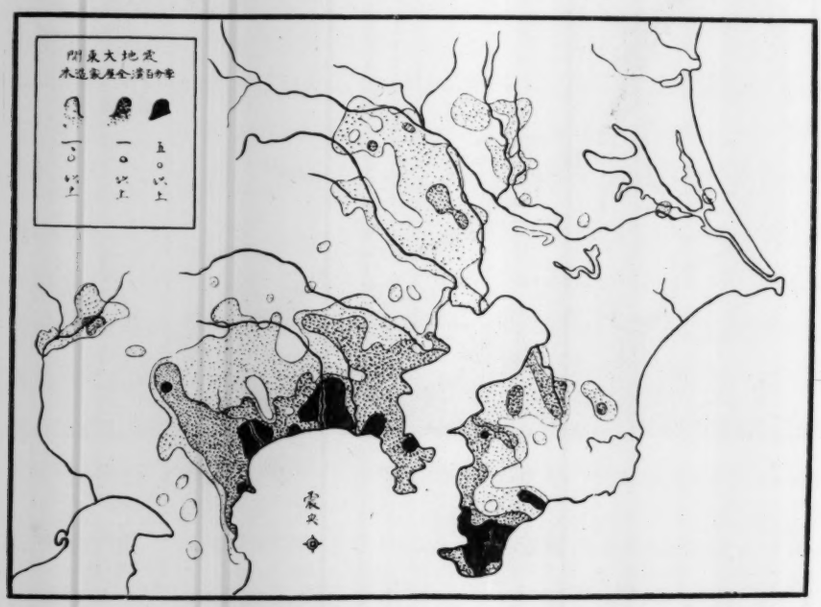

第五圖（松澤氏による）

地震動の進行に對して直角の位置にある構造線は震動を減衰するに反し、平行なるものは無關係であるのは當然の事であるが、第五圖(1)において見る如く多摩川下流における被害分布は兩岸において明かに異る例を示して居るのである。なほ江戸川流域、小貝川流域においても斯樣の例が見出される、勿論地質的關係の存在により、此れ等の現象は往々地盤の影響として取扱はれて居るが、單に其れのみにて說明し得るものでは無く、寧ろ斷層の兩側において其の震度の明かに異る事實を擧げて、斷層において地震波の反射、減衰の現象のある事を指摘したいのである。なほ房總半島における震度の分布が、同じく構造線の片側に沿ふて發現して居る事も注意する事が出來るのである。

彈性波が地震と同時に生じた所謂斷層により阻害された事實は但馬、丹後の二大地震において其の例が見られるのである。但馬地震の場合其の震央(2)は津久井灣附近と推定されて居り、陸上田結附近に斷層(3)が出現したのである。而して此の地震による

(1) 松澤武雄：震災豫防調査會報告　第百號(甲)。
(2) 今村明恒：同　上　第百一號。
(3) 山崎直方：同　上　同　。

被害狀況を見るに田結斷層の陰に當る久美濱附近は、此れと等距離の點に比較して災害が極めて輕微であつたのである。丹後地震においては地震と殆ど同時に二大斷層が發生し、此の附近が最も災害が甚しかつたのである。然し乍ら被害分布狀況を詳しく注意する時は、斷層の兩側において其の程度の著しく異るのを發見するであろう。此の事實は實際に家屋破壞調査をされた谷口氏(1)も注意して居られる事であるが、口大野附近において僅か 3 km の距離なれども甚だしく被害の異る事、或ひは此れと同じ現象が山田斷層において岩瀧附近に見出されるのである。此れは要するに震原にて發せられたる地震波は此の二大斷層に相當する構造線に於いて各地塊の運動を自由にすると同時に自ら反射減衰を惹起し、斯様の震度分布を發生したものと見られる。

丹後地震において震央より相當距りたる大阪附近において震動の比較的烈しかつた事は明白であるが、雜誌「地球」に發表された被害分布圖(2)においても正に其の現象が指摘されてある。此の現象は强ち大阪附近の地盤が軟弱であると云ふ理由のみで說明さるべきものでは無いと思ふ。前述の如く地震波が構造線面を通過する場合に著しくその勢力が減衰されるのは事實である。從つて構造線と平行して進行した波は大阪附近迄も相當の勢力を保持して居たと云ふ見解の下にも說明出來ると信ずる。然し乍ら此の場合には地表には推定する構造線以上に地下に特別の構造があつて地震波を導くと同時に氣壓勾配による力を傳達し得るのではあるまいか。

今村教授は日本海沿岸に出現した數回の大地震を調査された結果(3)海岸における土地隆起は多くは地震に先立つ事數時間であつたと述べられて居る。此の現象は地變と地震とが明かに別種のものである事を示すものであつて、先づ地表に認め得べき地塊運動があり、而して後岩漿衝擊が誘導されて震動を發したものと思はれる。丹後地震の場合にも海岸地方に於ける土地隆起があり、其後の衝擊の結果として二大斷層が出現した様である。

大地震後發生する餘震數は大森教授(4)により研究せられ、其の頻度は双曲線を以て次第に減少すると云はれて居る。日下部教授(5)は歪の次第に消滅恢復するにより、其の双曲線となる事實を證明されたが、著者は餘震減少の事實を熱的現象と考へ度いのである。即ち大地震の際生じた岩漿衝擊は數多の裂罅を地殼に與へたであらうし、或

(1) 谷口忠：地震研究所　第三號。
(2) 本間不二男：地球　第九卷　第五號。
(3) 今村明恒：地震研究所彙報　第四號。
(4) 大森房吉：震災豫防調査會報告　第二號。
(5) 日下部四郎太：震災豫防調査會歐文報告　一七號。

は從前より存在して居た裂罅もあつたであらう。而して此れらの裂罅は勿論岩漿內に存在する空隙をも充塡する爲めに岩漿の流動が行はれると見られる。岩漿流動は要するに溫度の函數であり、岩漿溜の冷却と共に餘震の減少する事は察するに難くない事である。即ち物體冷却の定理に從へば、溫度は對數曲線をなして低下するのであり、大森教授の出された實驗式と極めて類似のものとなるのである。

地震に附隨する現象としては鳴動を擧げる事が出來る。此の音色は太鼓の如しとも、遠雷の如しとも、大砲の如しとも云はれて居る。即ち何れにしても何物か地下において打突けた結果發生する如き音色である。此れらの音響は地震と共に發したものと考へられるから、地震發生の機巧も自ら衝撃により誘導されたものと考へるのが適當であらう。不幸にして著者は未だ多くの鳴動を體驗して居ないので其の現象に充分の判斷を下す事の出來ないのは至極殘念に思ふものである。

なほ岩漿流動により地震が發生するとすれば、地殼變動のみならず重力變化も必然的に惹き起さるゝと考へられるから、此の現象に就いて觀測研究の進捗する事を期して止まない次第である。

7. 結　　語

地塊運動と地震とが同一根源、即ち岩漿の存在により生ずる事は以上の說明で充分であると思ふが、地質學的になほ詳細の考察を必要とするものである。土地隆起沈降に關する議論は地塊物質と次下層物質との物理的差異の結着に歸せられ、造山運動の瞬間的現象を今日見て居ると考へられる。

現在構成されて居る山岳は相當新しい地質を其の山頂に持たぬものは少ないであらうが、其の基部において深成岩の基礎を持たぬものは殆ど無いと云へるのである。深成岩は且て岩漿より誘導され固化したものであり、土地隆起の結果として地表に現はれたものと考へられる。而して現在においても尙地塊下における岩漿が時と共に分漿作用を續行して居るならば、玆に地震が發生するのである。關東地方において筑波山下に絶えず小地震の發生があるが、これは深成岩下において未だ流動岩漿の存在する事を暗示する現象なるべく、傾斜計觀測によれば此の山が氣壓の影響を受けて東西に動搖する事實[1]は益々岩漿の存在を考へしむるものである。

要するに地震發生は造山運動の副產物であるに過ぎないのであつて、火山活動と相

(1) 石本巳四雄：天文地球物理學研輯報　第四卷　第二號　一〇〇頁。

俟つて地殻の動搖性を示す現象と見られるのである。從つてこの原動力である岩漿の性質特に物理化學的研究を益々進捗せしめる事により、地震學の一目的は大半達し得るものと信ずる。

擱筆に臨み此の論文を草するに當つて充分の援助を賜つた高橋理學士に、又挿圖に關しては非常の努力を惜まれ無かつた大塚君に謝意を表する。

昭和三年十月

東京帝國大學地震研究所

On the Mechanism of the Great Sagami Bay Earthquake on September 1, 1923.

By **Sakuhei FUJIWHARA** and **Takeo TAKAYAMA,**

大正十二年相模灘大地震の機巧に就いて

所員　藤原咲平
助手　高山威雄

摘　要

相模灘大地震卽關東大地震の原因に就ては諸說紛々たり、著者等は先づ是等諸說を列擧し、次に批判の材料となるべき事實を擧げ、自說の概要を述べて、之を事實に徵し、其毫も事實と矛盾するなきのみならず、土地の渦動的水平移動等は本說に依りてのみ說明し得る所以を明にしたり。次に進んで自說の根據となるべき諸項目を吟味し、又他諸家の說との比較に於て根本的相違なきを確めたり。次に更に事實の確實性の吟味をなし、相模灣方面に於ける渦卷的水平移動の實在せるを確かめ、之に依つて又房州瀧山斷層の主貌を推論し、之を事實に徵して推論の如くなるを確かめたり。かくて

關東大地震は北太平洋方面よりの一般的地流に原因を有し、相模灣及附近に於ける渦卷的逆地流の爲に蓄積せられたる勢力の發露なるを推定したり。

CONTENTS

1. Introduction.
2. Sketch of the former theories.
3. Facts to be explained.
4. Outline of the proposed theory.
5. Explanation of the Facts from the proposed theory.
6. Discussions on the proposed theory.
7. Comparison with other theories.
8. Discussions on the recognized facts.

SYNOPSIS

A theory of the earth vortical formation is proposed for the explanation of the mechanism of the great Sagami Bay Earthquake, 1923, based on the observed facts and results of survey, making use of model experiments.

Introduction.

§1. In August of 1925 one of the present authors summarised many theories published in Japan on the cause of the great Sagami Bay earthquake on September 1, 1923, giving at the same time his own theory from the vortical point of view.[1] Since this was written in Japanese, Professor B. Koto persuaded him to translate it in English. Three years have since elapsed without doing so during which the triangulation over the shaken area was made by the Land Survey Department of the Japanese Army and now two maps (Reproduced and put together in Fig. 1.) have been completed showing the relative horizontal and vertical displacement of trianguration stations in the area concerned. The results of this survey stand in a good accordance with the inferred motion from the vortical theory. Hence in this opportunity it will be of some interest to recapiturate the former theory in more universal language and in fuller scope.

Sketch of the Former Theories.

§2. *Theories already proposed.* There are many theories and hypotheses proposed by many seismologists, geologists and geophysisists in Japan on the cause of that earthquake. These are tabulated as follows:—

	Theory	Author	Reference
No. 1.	Upthrust	T. Kato	Rep. Imp. Earthq. Inv. Comm. 100, B (1925) p. 9.
2.	Block movement	N. Yamasaki	ditto p. 51.
3.	Submarine fault	A. Imamura	ditto A, p. 54.
4.	Underground fault	Saem. Nakamura	ditto p. 118–119.
5.	T-shape fissure	T. Shida	The next paper by T. Ogawa
6.	Plutonic origin	T. Ogawa	Chikyu (The Globe) Vol. 1, (1924) No. 1–5.

(1) S. Fujiwhara, On the mechanism of Sagami Bay earthquake, Kensin Ziho, (Japanese seismological magazine, issued from the Central Meteorological Observatory) **1**, p. 161–170.

7.	Linear rebound	M. Matsuyama	Conceil Intern. Rech., Soc. Seismology, Bureau Centr. Seism. Strasbourg, Travaux Scientifique. Fasc. 2 (1925) p. 23.
8.	Local horizontal folding due to emigration of continent	T. Terada	Rep. Imp. Earthq. Inv. Comm. 100, B, (1925) p. 66–72. Proc. Imp. Acad. Vol. 4, (1928) p. 55.
9.	Vortical rebound	K. Suda.	Memoirs Imp. Marine Obs. Kobe, Vol. 1, (1924) pp. 200–205.
10.	Sudden yield to stress of vortical nature	S. Fujiwhara	Journ. Met. Soc. Japan, (1924) p. 32–36.
11.	Vortical recoil due to the Pacific movement	S. Fujiwhara	Kensin Ziho, Vol. 1 (1925) p. 165–170.

Very recently Professor H. Nagaoka has proposed a hypothesis based on a magma theory, but it is not yet in press.(1)

At first sight these theories seem to contradict to each other, but by careful studies they are found to be in harmony to some degree. We shall come later on this point.

§3. *Historical note,* No. 10 in the above table, which was issued three months after the great earthquake, gives only a suggestion that the earthquake might be caused by an elastic release of stress accumulated by a *torsional* or *vortical strain* of the earth's crust in the vicinity, of Sagami Bay. He has pointed out that by giving shear to a flexible plate or to a sheet of paper, an elevation of horse-shoe shape and depression in side it can easily be produced, resembling the form of uplifted and subsided area actually occurred on the occasion of the great earthquake. This theory was seconded by K. Suda in his big paper—No. 9. in the above table—on the same subject.

From the analysis of Japanese volcanic ranges by using the law of échelon cracks, Fujiwhara has proved that Japanese Islands are subject to

(1) H. Nagaoka, Lectures delivered at the meeting of the Earthq. Res. Inst. Feb. 21, Mar. 20, April 24, May 28, June 19, 1928.

a compressional shearing stress acting from NE to SW along the north-eastern coast facing to Pacific Ocean.(1)

This gives another support to the above theory, so that in the note No. 11 in the above table the shearing force which caused the vortical strain is considered to originate from the general Pacific movement, being impeded by Volcanoes such as Osima, Amagisan, Hakone and Huzi (Fuji).

FACTS TO BE EXPLAINED.

§4. *Four main facts.* In order to criticize the raised theories, the facts must first be grasped exactly. The facts of primary importance are:—

(1) An earthquake of first-class intensity occurred over Sagami Bay and its surrounding districts at 11h 58 m., Sept. 1, 1923.(2)

(2) The coast of the Bay from Manazuru to the southern end of Bosyu was suddenly uplifted by the amount at least from one to two meters as shown in Fig. 1. Along the west coast of the Bay the elevation was rather small, at Atami it was 0.1 to 0.7 m. and at Hasima it was 0.9 m., while the level of Osima remained without change.(3)

(3) The bottom of Sagami Bay subsided by the amount up to 210 m. during years from 1912 to 1923. Surrounding the subsided area there is uplifted area in a horse-shoe shape opening to SE.(4)

(4) A *tsunami*—earthquake sea bore—took place and was observed along the whole coast of the Bay.(5)

---

(1) S. Fujiwhara, 地理學評論 Geographical Review of Japan. **1** (1925) p. 735. Also see Gerland Beitr. Bd. 16. p. 1–14.

(2) K. Suda, On the great Japanese Earthquake on Sept. 1, 1923. Mem. Imp. Mar. Obs. **1**, p. 139. Jan. 1924. Saem. Nakamura, Report on the great Kwanto earthquake (Japanese) issued from the Centr. Met. Obs. Sept. 1924. A. Imamura,, The great Kwanto earthquake on Sept. 1, 1923. Rep. Imp. Earthq. Inv. Comm. No. 100-A (1925), p. 21.

(3) The fact was first observed on the level mark on beach by all authorities in the field. Later it was accurately measured by the leveling by the Land Survey Department. Rep. Imp. Earthq. Im. Comm. No. 100, B. p. 55. Also See Seiji Nakamura, ditto p. 73.

(4) Result of the sounding by the Fishery Institute and more acculately by the Hydrographic Department of the Navy. Bull. Hydro. Depart. **5**, Pl. 11. Also see Rep. Imp. Earthq. Inv. Comm. No. 100, B, p. 61.

(5) Reports of K. Suda, A. Imamura, Saem. Nakamura and others loc cit. Especially T. Terada and S. Yamaguti, on Tsunami etc. (Japanese) Rep. Earthq. Inv. Comm. No. 100, B. p. 113.

(5) The regions round Sagami Bay were subject to a vortical displacement during years between 1884 and 1924. In Fig. 1 the motion relative to Teruisiyama as origin and to the initial direction connecting this with Tukubasan is represented by arrows.(1)

§5. *Subordinate facts.* Beside these facts of primary importance, there were also a number of facts of primary importance, but accompanying some ambiguity, and those of secondary importance. They are:—

(6) From the record of tide gauge at Aburatubo in Miura Peninsula, it was likely that the land at this place was continuously sinking these 20 years since the gauge was first installed in 1900. The sinking amounted to 10 cm. relative to the mean sea level. The inhabitants of the district noticed the fact on the gradual landward retrogradation of beach line. (2)

(7) The coast round Sagami Bay especially the part from Boso Peninsula to Odawara has been subject to upheaval as well in geological as historical ages.(3)

(8) A tiltometer installed by the Late Prof. F. Omori at Tokyo is said to have recorded 1″.7 of integrated tilting of the earth towards west from July 30th to Aug. 17th, 1923, which is free from temperature effect.(4)

(9) Four small faults and one big crack system were formed, as shown in Fig. 2(5)

(10) The isoseismic curves were very irregular on this occasion, having long

---

(1) Land Survey Department, Provisory Map showing the Horizontal Displacement of the Primary Triangulation Points in Kwanto Districts, observed after the Great Earthquake of Sept. 1, 1923. Bull. Earthq. Res. Inst. **4**, Pl. 65.

(2) N. Kawakami, On the Secular Upheaval and Subsidence of Land in Some Districts of Japan. Memoirs Imp. Marine Obs. Kobe, **2**, No. 1, p. 71. The fact was first noticed by F. Omori, then later by St. Nakamura, K. Suda, H. Nagaoka, A. Imamura, H. Tanakadate, etc.

(3) D. Kikuchi, 1891, J. Milne, Seismology p. 3. H. Tujimura, Text book of Geomorphology (地形學) p. 456, 1923. A Imamura Rep. Imp. Earthq. Inv. Comm. No. 100, B, p. 91. H. Tanakadate, Rising and sinking of the Coast in connection with the great Kwanto Earthquake (Japanese). Journal of Geogr. Soc. Japan, 38 year No. 445, 446, 448, and 449. The last is most elaborate.

(4) A. Imamura, Proc. Imp. Acad. Japan. **4**, No. 4, p. 149.

(5) T. Kato, Rep. Imp. Earthq. Inv. Comm. No. 100, B, p. 1. N. Yamasaki, Ditto p. 11.

Fig. 2.
Directions of Shocks judged from fallen or dislocated Bodies.

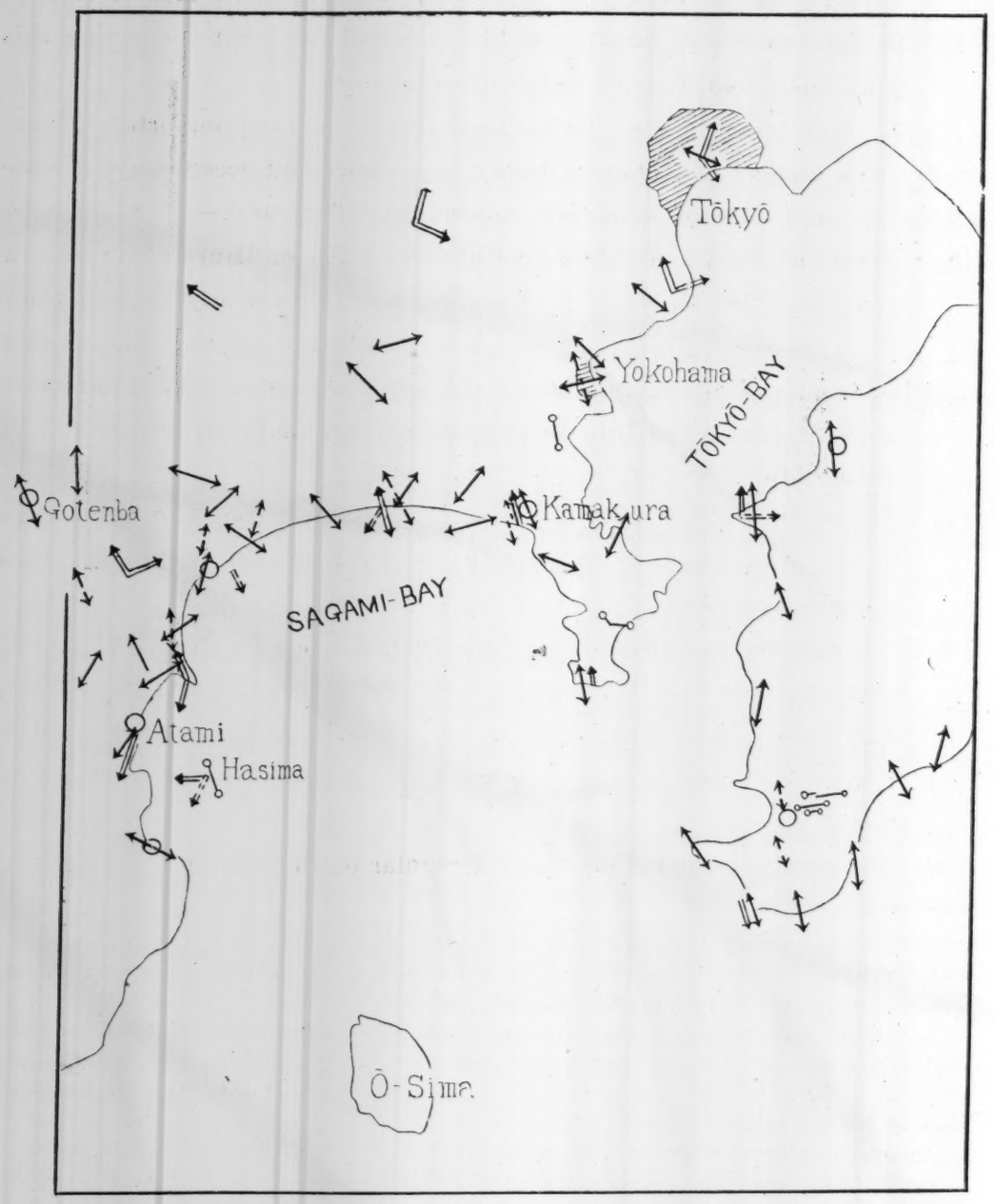

extension towards NW. This is most clearly seen from the percentage distribution of wooden houses which were crushed by the earthquake.(1) The form of isoseisms are not zonal but radiant.

(11) The distribution of the direction of the earthquake motion judged from the direction of the fallen stone monuments, crushed or displaced houses etc. was irregular, but rather vortical. See Fig. 2.(2)

(12) Submarine telegraphic cables were snapped by the earthquake at the mouths of Sagami Bay and Tokyo Bay.(3) See Fig. 1.

(13) On the 2nd Sept. 1923, deep sea fishes are said to have been found floating dead at the mouth of Sagami Bay.(4)

(14) Landslips are most intense on the mountain slopes along the west coast of the Bay. Then next in the mountainous region to NW of the Bay.(5) A curious fact is that in Hakone volcanic region land slided more remarkably on the base or middle slopes than on the upper part.(6)

(15) Change in the temperature, amount of issue, colour, mineral contents etc. of hot or mineral springs and also the changes of levels of lakes and wells are said to have occurred before and after the great earthquake.(7)

(16) The distribution of after shocks are not uniform as pointed out by K. Suda,(8) K. Shiratori,(9) T. Hirano(10) and A. Imamura.(11) After shocks were repeated having their epicenters in two or three district zones. Some intermittent activity between these zones was observed.(12)

(17) The law of exponential decrement of the frequency of aftershocks was

---

(1) T. Matuzawa, Rep. Imp. Eartthq. Inv. Comm. No. 100, A, p. 163.
(2) S. Fujiwhara, Kensin Ziho, **1** p. 165.
(3) loc. cit. Bull Hydro. Depart., **5**, Pl. 11.
(4) K. Suda, loc. cit. also see Bull. Hydro. Depart., **5**, Pl. 11.
(5) Saem. Nakamura, loc. cit. p. 32. T. Matuzawa, A. Imamura, etc. Rep. Earthq. Inv. Comm. No. 100, B, p. 81, 85. K. Suda, loc. cit. p. 159.
(6) Eye observation of the present author.
(7) Saem. Nakamura, loc. cit. p. 18–23, etc. K. Suda, loc. cit. p. 171.
(8) K. Suda, loc. cit. p. 186.
(9) K. Shiratori, Jap. Journ. Astr. Geophys. **2**, No. 4, (1925) p. 173.
(10) T. Hirano, Journ. Met. Soc. Jap. 2nd Ser. **2**, (1924) No. 3. p. 77.
(11) A. Imamura, Rep. Imp. Earthq. Inv. Comm. No. 100, A. p. 58.
(12) T. Hirano, loc. cit. p. 78.

not simple and unique in this case as pointed out by K. Suda, who gave general warning on the residual seismic activity still stored up in dangerous degree in the crust of these districts,[1] which was answered by the heavy shock on the morning of Jan. 15, 1924 with much damage.

(18) Any definite point could not be determined as the exact position of the epicenter by analysing seismographic records obtained at more than 10 stations within 150 km. of distance from Sagami Bay. So many authorities proposed so many positions and at last K. Suda and T. Hirano[2] arrived at the conception of the 'seismic domain' or the epicentral region in order to avoid the infinite velocity of propagation of seismic waves as existed.

(19) The distribution of the initial motions recorded by seismographs at many stations near by also led seismologists to some confusion. Seam. Nakamura[3] concluded that the first motion was emitted from a point near Hadano on the north west coast of the Bay at the depth of about 60 km, where a fault plane with inclination of 77° from the vertical plane to west[4] was formed and along this plane, its east part slides upward and west part down. There is, however, still some anbiguity on the way of reasoning. Very recently S. Kunitomi attacked the same phenomena with fuller data than those of Nakamura taking the earth's discontinuity and phases of P, $\overline{P}$ etc. into consideration. He concluded that the first motion must have started from a point near Atuki at the depth of 28 km. The plane of invisible slip was inclined 47° toward W 16° S from the vertical plane and western lower part of the crust has slided up and eastern upper part down. Epicenters by Nakamura and Kunitomi are entered in Fig. 5. Those by Matuzawa and Matuyama also converge to this vicinity. Hence the epicenter of the first motion of this great earthquake is safely concluded to have been on land between Hadano and Atuki.

---

(1) K. Suda, loc. cit. p. 181–185.

(2) T. Hirano, Journ. Met. Soc. Japan, 43 y. (1924) p. 16. K. Suda, loc. cit.

(3) Saem. Nakamura, loc. cit. pp. 44, 45.

(4) S. Kunitomi, Read before the monthly meeting of Met. Soc. Japan, Nov. , 1928. but not yet printed.

The Outline of the Proposed Theory.

§6. *The vortical formation at the earth-discontinuity.* The vortical displacement is explained as the effect of the rotational motion caused by the shearing stress at the line of discontinuity, i.e. the intersect of the surface of discontinuity in the earth's crust with the earth's surface. The most important discontinuity in the vicinity of Japan is one marking the boundary of the northwest Pacific Ocean and well known as one part of Circum Pacific zone of orogenic and seismic activities. As proved elsewhere[1] this part of the crust is making southwesterly shift in general and the relative motion at the boundary is SW-ly on the ocean side and NE-ly on the land side. Under such circumstances shearing stress must be accumulated with consequent shear. As the result, a rotational or vortical displacement of the crust must take place along the line of discontinuity or the line of shear, so far as the material is rather safe against shearing stress but weak against compressional, and most weak against tensile stress ——the earth and rock materials have such nature——, the material has tendency to break in crossed echelons along the line of shear and consequently presents a block structure. The effect of the elementary rotation of each block can produce a big vortical deformation in the general aspect. Such a mechanism of the earth vortices was explained already from actual facts as well as from model experiments.[2]

§7. *Volcanic hindrance.* Heiskanen,[3] on the basis of gravitational survey of M. Matsuyama and others,,[4] has shown that in this part of Japan the isostatic compensation is not yet complete. Consequently, the vertical motion of land masses and horizontal flow of magma must be going on in the present days. Indeed the volcanic ranges seem to be the result of the excess of compressive force as inferred in the author's former paper.[5]

(1) S. Fujiwhara, Gerland Beiträge f. Geophys. **16** (1926) S. 1–14. Also see Jap. Journ. Astro. Geophys. **3**, p. 113.

(2) S. Fujiwhara, Journ. Met. Soc. Japan, year 43, p. 32–36.

(3) Heiskanen, Zeitschrift f. Geophys. III (1927) H. 5.

(4) M. Matsuyama, T. Yamamoto, S. Hirayama, K. Sotome, T. Matukawa, etc. Rep. Imp. Jap. Geod. Comm. Vol. 1–5.

(5) S. Fujiwhara, loc. cit. Gerland Beitr. f. Geophys. Bd. 16 (1926) p. 4.

No excess of compression can exist without a local support or resistance against the general pressure, hence we must conceive some resisting action, whatever its original mechanism may be, existing in the neighbourhood of volcanoes against the general flow of magma and accompanying crust movement. Thus it may now be admitted that a volcano can be looked upon as a visible mark on the earth's surface of invisible resistance against the underground slow but steady flow.

§8. *Formation of an earth vortex by the back current behind Osima Volcano.* Let us now suppose that Osima with other companion volcanoes exerts resistance against the general Pacific movement of the crust towards W or SW, which perhaps is associated with magma flow underneath. Then the general movement must change its direction towards SSW or S by Osima and in the area to north of the volcano, there must exist a back current of the earth-motion in clockwise sense of rotation as usually seen on the flow of water by a hindrance at any bank of river. Though this back current flows very slowly in the earth crust, it will be sufficient to make up a vortical formation in the lapse of sufficiently long time.

§9. *Horse-shoe distribution of stress.* As already explained, such vortical formation accompanies elevation and depression of horse-shoe shape, which fact is also shown by an experiment in the next paragraph. From this view Sagami Bay corresponds to the central depression of the horse-shoe, and has been formed throughout the present and past geological ages and the process is still going on. Professor Terada has already pointed out this fact from the observation of radial and concentric semicircular tectonic lines round the bay.(1) To accomplish this formation the stress distribution in the earth's crust must also be of the horse-shoe type.

§10. *Sudden yield of crust.* The crustal movement may be continuous to some extent so far as its rigidity gradually yields to stress. But in the case when there is some hindrance choking the general motion locally, then the stress must accumulate and indeed up to the critical stage. Prof. Naga-

---

(1) T. Terada, Romazi Sekai, (1924).

oka[1] got success to give solution to the equation for asymmetric free vibration

$$\frac{d^2\xi}{dt^2} = -f\xi + g\xi^2.$$

So far as $f > g\xi$, the motion is stable, while when $f < g\xi$, ξ tends to ∞, that means the break down of the material.

In the actual case there act some external forces, and also from the boundary condition the matter becomes complicate. But, at any rate, the state of unstable motion must taken into consideration.

Hence we can divide three stages of yielding.

1. $f > g\xi$ the yielding is slow and oscilatory
2. $f < g\xi$ the yielding becomes somewhat rapid and astatic, but still continuous
3. $\xi = \infty$ the break down or discontinuity

Applying this to the actual case we can also imagine that the so called bradyseisms[2] correspond to the stage 1. The period, during which some symptoms are occuring corresponds to the stage 2 and the earthquake or the final rupture corresponds to the stage 3.

Thus in the region of Sagami Bay the motion of and stress in the crust and the increase and decrease of pressure in magma underneath must have been distributed in horse-shoe shape all through ages and the stress in this sense had been as ever accumulated since the last release of stress or in the other words the last great earthquakes in 1853 and 1854. This belongs to stage 1. Then comes a period of symptoms, the stage 2, and at last the time came for the stage 3, when the crust made a discontinuous yielding again on Sept. 1, 1923, as to pace one more step on its destined course or as to repeate its cycles of about 70 years interval. It was effected in a sudden bending (warping) in horse-shoe shape, by which action the land and the water were tossed so violently that brought such a huge disaster as ever recorded.

---

(1) H. Nagaoka, Asymmetric vibration of finite amplitude Proc. Imp. Acad. Japan. **3**, No. 2. p. 61.

(2) The thought that the slow motion of the earth's crust is the cause or antecident of the sudden motion was initiated by Milne (Seismology p. 33, 34) and cultivated by Omori, Kusakabe, etc.

EXPLANATION OF FACTS FROM THE PROPOSED THEORY.

§11. *The scheme of explanation.* The fact (1) in §3, i.e. the time and place of the present earthquake could be explained as above. As to the exact time of occurence, we can only do it when the earthquake-forecast will have become possible and it belongs to some future.

As already remarked, there are so many theories on the cause of this earthquake,[1] but only one which can explain the fact (5), i.e. the vortical displacement of land, is the theory of vortical formation due to the general crustal movement in the Pacific region. Therefore, if the remaining facts be explicable from this theory or at least be not in contradiction with it, then the theory must be admitted for the time being.

§12. *The explanation of the main facts from model experiments.* The fact (2) and (3) i.e. the upheaval and depression of the land and sea bottom are very clearly shown by a model experiment with vortical displacement as shown in Fig. 3 and 4.

The first experiment (Fig. 3.) was made with a circular rubber plate of 10 cm. radius, 1.5 mm. thickness laid horizontally on a bed of cotton wool of uniform thickness of about 2 cm., and nailed at two points on a wooden desk underlying the cotton bed. On the surface of the plate a rough chart of Sagami Bay and its vicinity was drawn. One of the nails passed just through the position of Osima Volcano and the other just south of it. This second nail was used only for nothing but to hinder the rotation of the plate slidingly round the first nail. On the points corresponding Amagi, Hakone and Fuji Volcanoes three metal pieces were mounted in order to exert some pressure on these points.[2] A piece of wooden plate was attached on the part of eastern ocean. All these are shown in Fig. 3. a. With a string attached at the southern end of the wooden piece, this was pulled toward south and distorsion, upheaval and depression of the surface of the rubber plate were produced, whose aspect is shown in Fig. 3. b.

(1) Some one calls this as Kwanto-Earthquake and some other as Japan-Earthquake, all the same as the great Sagami-Bay Earthquake of 1923.

(2) These are proved imperfect. These volcanoes must have been fixed more firmly.

White arcs in the Figure show the rotational displacement, which is of nearly the same nature with the actual one as shown in Fig. 1. Only difference is that the rubber plate wants plasticity, while the earth's crust has it, and as its consequence the rotational or better the vortical motion relative to Teruisiyama, the actual case as shown in Fig. 1, is conspicuous only round Sagami Bay and not remarkable in the northern part of the map, while in Fig. 3. b, the fixed point or reference point is selected at Osima and nearly the same rotation is imposed over the northern part.

Dark shadowy part in Fig. 3, b is the part sloping against light which came from the north of the map at the time of photographing it. The white part is the slope facing north and hence the boundary of white and dark parts is either depressed valley—south white, north dark—or uplifted ridge—north white, south dark. Thus as shown in this figure the bottom of Sagami Bay is depressed as in the experiment as in the actual case, and the arcuate part along the north coast of Sagami Bay is uplifted equally well in the fact and in the experiment. In Fig. 3. c the contour lines on the face of the rubber plate in Fig. 3. b is shown in remarkable coincidence with actual contours.(1) A few number of nearly the same experiment, were done which gave the same results. It is noteworthy that in the experiment with the rubber plate the sense to rise or to sink is indeterminate and just reversed figure can be produced. Even a very slight depression (or elevation) existing before the experiment at the part to be deformed can serve to lead the further deformation to depression (or to elevation). But the general aspect cannot be altered by such initial slight deformations.

§13. *Explanation of faults formation by the model experiment.* Next we improved the experiment by covering the surface of the rubber plate with paste—mixture of powder of zink oxide and wheat, half amount each —with uniform thickness of about 2 mm. We attached one more string at the top of the wooden piece, and pulled along this during the experi-

(1) Figures entered indicate elevation as positive and depression as negative. The measurement of depth from a given standard plane, was made twice, before and after the experiment and the differences are reckoned as the bearing of elevation and depression.

ment in order to keep these part without E-W displacement. The result of the experiment is shown in Fig. 4. a, b and c, in which a is the state before the displacement, b the state of successive displacement and c the final state. The light comes from SW direction and hence the slope facing NE is shown dark. The general feature of the depression and elevation was nearly the same as the former experiments. Th rotational displacement appeared but very little in this case being checked by the upper string.(1) The most remarkable feature in Fig. 4. c is that surface cracks are formed across Bôsô and Miura Peninsulae just as was in the actual case shown in Fig. 2. We see some cracks between Hudi (Fuji) and Hakone Volcanoes in the experiment but not in the actual case. This perhaps due to that, the volcanoes were more immovable in the actual case than in the imitated experiment. Any how the fact 9—the formation of faults—turns out to be a good support of the theory.

§14. *Explanation of tsunami, snapped cables and dead deep sea fishes.* So far as the experiments show, the orographic change must be most intense from the mouth to the central part of Sagami Bay, which servves to explain the fact (4), (12) and (13) in §. i.e. tsunami or seismic bore, break of submarine cables and dead deep sea fishes.

§15. *Explanation of bradyseisms.* The pressure and traction from Pacific side upon Kwanto and Sagami Bay districts are supposed to be ever continuous since at least young geological ages with some fractuations —the cyclic nature of vortex—in intensity, so that the repeated upheavals of coastal districts round Sagami Bay were brought in geological as well as in historical ages. Thus the fact (7) can also stand in a good harmony with the proposed theory.

§16. *Explanation of the tilting of the earth and changes in under ground water.* The fact(8), the tilting of earth before the great earthquake and the fact (15), changes of under ground water or hot springs before and after the earthquake depend on the nature of the superficial

(1) If we can use some material more plastic than a rubber plate, then the rotational displacement round Sagami Bay will be exhibited satisfactory with the same process as above.

crust in the vicinity. Acted by the partial pressure and traction from the ocean side and by the reaction from the volcanic masses on the west, the crust in this site may yield, first very slowly then rather quickly but still continuously as explained after Nagaoka's theory. In its second stage the tilting must have started first and then the chang in the underground water. Hence these two facts also present no discordance with the proposed theory.

§17. *The explanation of the aftershocks-anomaly.* Among the remaining facts, (16) and (17), the anomaly of aftershocks in space and in time, are of local character giving suggestions on the structure and on the stress distribution in the earthcrust under the Kwanto district. The zonal character may be compared to the wave formation marging a vortex area as is usually observable with cloud or water vortices. The experimental result of T. Terada and N. Miyabe is also very suggestive on this point, in which zonal activity is very clearly observable.

If the general stress of fractuating nature superpose with the local stress round the newly broken area, where gradient of the local stress is still very steep, such phenomenon as intermittent zonal activity can take place. We shall however, left this problem to other places.[2]

In all respects these facts are also favourably explained in the view of the present theory.

§18. *Explanation of the irregular isoseisms.* The fact (10) that is the irregular distribution of crushed wooden houses can not be explained by the linear dislocation theory so good as by the vortical theory. There are 5 points to be considered, they are:—

1). The distance from Sagami Bay, nearer to it, greater the number.

2). The softness of soil and hardness of rocks.

3). The block structure of the crust. Along the boundaries of blocks the damage must be great.

4). The existence of the third and forth arms of discontinuity.

---

(1) T. Terada and N. Miyabe, This report Vol.

(2) A lecture on this point was already given by the present author at the colloquium of the Eartthq. Research Inst. July 3, 1928, but not yet printed.

5). Asymmetry of vortex in its developing stage.

Those vortices taking rise at discontinuity have normally two principal arms of discontinuity. The third arm is also very common with earth vortices, for example, the third arm of Celebes vortex extends north to Philippin Islands. As is clearly seen, the zone of damage extends very far toward NW covering Kôhu, Matumoto and Nagano districts, while no damage was reported from Titibu district in nearer position to Sagami Bay. West shadow of Huzi volcano, southern part of Idu province are also districts of less damage. Osima in the very proximity also experienced rather small damage. The NW extension must be due to a conspicuous geotectonic line which was noticed by K. Suda[1] and also by H. Yabe and R. Aoki,[2] and corresponds to the third arm of Sagami Bay vortex in our sense. Asymmetry of the vortex is always remarkable in such cases, so that the less damage in Osima and Idu and great damage in Tanzawa district is explained. This fact is thus in favour of the theory.

§19. *Explanation of the abundant landslips on the W and NW sides of the Bay.* The fact (14) may be explained as that, if the volcanic range between Hakone and Amagi volcanoes is comparatively immovable, then the zone of superficial fracture shown in Fig. 4. c must bend southward along the eastern slope of the range. Then naturally land slides more abundantly in these regions. Hence this fact can also stands in accordance with our theory.

§20. *Explanation of the diffused epicenters.* The fact (18) may be understood as such that the earthquake occurred in virtue of a horse-shoe deformation of the crust over a great area. Hence it is naturally difficult to determine the so called epicenter as a point.

§21. *Explanation of long range subsidence of the shore at Aburatubo.* The fact (6) may be explained in various ways:—

1). During the first stage of the continuous yielding of the crust in horse-shoe shape as explained before, the depression of the sea bottom may

---

(1) K. Suda, loc. cit. Pl. IV, Fig. 4. Kofu-Matsumoto line.

(2) H. Yabe and R. Aoki, Relation between Kwanto earthquake and geological structure etc. Saito-Ho-on-Kwai, Nenpo, No. 1 (1925).

be easier than the upheaval of land. The great difference in the character of the crust of the ocean and continent was noticed by Knot, Wegener, Gutenberg, Joly, and many others. T. Terada[1] in his recent researches attributes much plasticity to the bed crust of the ocean and also to that of Sagami Bay, which deeper than 3000 m. and is believed to have more oceanic character than the continental shelf. Hence the easier deformation of the Sagami Bay bottom is not groundless. If so, then the shore land at Aburatubo must have depressed by 10 cm. during 20 years subsiding with the Bay bed. In the second stage of yielding, however, the choking agency against the land motion would gradually be taken away and uplifting set in for two years before the great earthquake.[2] At the third stage in Nagaoka's sense, the sudden rupture might have brought the upheaval of 100 to 200 cm. to the effect. This is nearly the same as to consider the sudden elevation of the coastal land as the effect of rebound.

2). We may also suppose that after the former rupture in 1854, the superficial part of the crust was kept in a state of continuous down settling independent of underlying increase of uplifting stress.

3). A small hindrance against the general flow of magma or westward shift of the crust existed somewhere east of Sagami Bay before the earthquake and by the motion outside of this hindrance, the material under the bottom of the Bay was sacked gradually out through the mouth part of the Bay during these 70 years since the great earthquake in 1854. Shortly before the resent earthquake, the hindrance was gradually taken away and then gradual upheaval of the coast started so that sufficient compression was stored up under the land mass until the great rupture had taken place effecting the upheaval of the coast land.

4). Fractuating flooding in magma flow.

5). The amount 10 cm. is comparatively small and can be explained

---

(1) T. Terada and N. Miyabe, Proc. Imp. Acad. 4 (1928) p. 55.

(2) There must be a number of corresponding second stages as the scales of the phenomena concerned. During the third stage of the phenomenon of the greater scale there may be conceived first and second stages of the phenomena of the smaller scale forming members of the family of the greater phonomenon.

otherwise, for example by some meteorological effect on tide.(1) In no way, however, this fact is not against our theory.

§22. *Explanation of the distribution of the first motion of the great earthquake.* As explained in Fig. 4. c the part of land around Hadano or Atuki correspond to the zone of fracture, hence, the first break may started one of such places.

The surface of dislocasion shown by Nakamura or Kunitomi was invisible on the earth surface, hence, if true, this must have been a trigger dislocation, but not the main. Hence the fact (19), does not contradict with the proposed theory.(2)

§23. *A conclusion.* Thus by the proposed theory five main facts (1)–(5), and seven subordinate ones (7), (9), (10), (11), (12), (13) and (14) were explained and the facts (8), (15), (16) and (18) stand rather in favour of the theory, while the remaining facts (6), (17) and (19) do not contradict with the theory.

Hence the proposed theory may be admitted for the present.

DISCUSSION ON THE PROPOSED THEORY.

§24. *Shearing stress and vortical formation.* In the proposed theory in §4, the shearing stress at the eartth discontinuity is assumed. On such shearing stress Kosmat had clear idea and used it in his theory of Alps.(3) A. Wegener also noticed the vortical form in the vicinity of Celebes etc. in his famous researches on the emigration of continents.(4) Hence the idea of vortical formation in the earthcrust or on the earth's surface is by no means extravagant. On the discontinuity in the vicinity of Japan,

---

(1) T. Terada and S. Yamaguti, Jap. Journ. of Astro. and Geoph. **4**, 1, p. 35.

(2) According to Nakamura the fault is overthrust and hence the region of Hadano must be compressional. After Kunitomi the fault is a normal fault and hence the region of Atuki must be under tensile stress. Both are the case as shown in Fig. 5, so that we cannot discriminate these two inferences from this. But Kunitomi's inference taking Mohorovičić wave into consideration is fuller and this may be looked uppon as standard for the present.

(3) F. Kosmat, Die Beziehung des Sudosteuropäischen Gebirgsbanes zur Alpentektonik. Geolog. Rundschau, Bd. 15 H. 3, S. 275.

(4) A. Wegener, Die Entstehung der Kontinente und Ozeane, SS. 46, 97, etc.

there are very many researches, among which Gutenberg's work,[1] pointing out the discontinuity in the physical nature between the earth crusts of Eurasian Continent and Pacific bed is worth mentioning.

§25. *Block structure.* On the block structure of the earthcrust in the vicinity of Kwanto, Yamasaki's investigation is most important.[2] He has pointed out the block structure of the earth on the northern coast of Sagami Bay and in Bôso peninsula, and it was newly proved that each of them is making its own tilting, after the survey by the Landsurvey Department.[3]

The vortical formation in the blocked area is not yet investigated. But if we use a model as illustrated in Hobbs's book,[4] only enlarging the area, and make up a big vortex underneath the floating blocks which are now of uniform thickness, then. So far as the vortex is young, or asymmetrical, the blocks may present horse-shoe elevation and depression; after becoming symmetrical, then they will present a circular central depression.

At all events, the blocked earthcrust will exhibit the similar effect as increasing plasticity of the earth material, because elastic reaction is slacked at the boundary of blocks. Hence the vortical formation will be easier by the block structure than by a uniform elastic sheet.

§26. *Stress acting on Japanese arc.* As to the general shift of North Western Pacific earthmass, the readers are referred to the author's former paper,[5] in which the evidences of the anticlockwise rotation of the area are pointed out.

There is a famous theory of Suess on the stress acting on the crust

---

(1) B. Gutenberg, Dispersion und Extinktion von seismischen Oberflächenwellen und der Aufban der obersten Erdschichten. Pys. Zeitscher. 25 J. 1924, S. 377–381.

(2) N. Yamasaki, Physiographical Studies of the Great Earthquake of the Kwanto District, 1923, Journ. Faculty of Science, Tokyo University, **2**, Part 2.

(3) This fact was reported by K. Muto at the meeting of the Earthq. Res. Inst. on May 22, 1928, but is not yet in print.

(4) Hobbs, Seismology Pl. III.

(5) S. Fujiwhara, On the Echélon Structure of Japanese Volcanic Ranges etc. Gerland Beiträge, Bd. 16. S. 1–14. Also the same author Torsional form on the Face of Earth. Nagaoka anniversary Vol. p. 333, also Jap. Journ. Astro. Geoph. **3**, p. 103.

of Japanese region. In this theory the origine of compression is supposed due to the side pressure directed outwardly caused by the gravitational action on the Asiatic continental mass. But this idea evidently contradicts with the theory of isostacy. Under isostatic balance such a side pressure cannot be exist. Moreover Japan Sea which lies between Japan and the Continent is sufficiently deep, and if such side pressure actually existed, it must have exhibited more markedly along the inner margin i.e. the coast of China, Korea and Siberia than in Japan. But in actual case, the seismic and volcanic activity is much stronger in Japan, than in the continental coast. Hence the above theory is quite groundless. Moreover, if Wegener's theory of the west drift of continents is true, then the stress in this site must be traction from the continental side instead of pressure. After Richthofen, the sense of traction is from Oceanic side.(1) The present author, however, does not know which one of these theories is true.

Be what it may be, but the fact is an east-west compression—in rough sense—is acting along the Japanese arc. This can be proved from various points. S. Kunitomi's recent research on the anisotropic propagation of seismic waves(2) give certain bearing upon this point. K. Suda's analysis of the sense of stresses in Japan from the distribution of the first motion also reveals the similar fact.(3) The present author also has proved the fact from the analysis of the échelon faults formed on the occasions of some great earthquakes.(4)

§27. *Sense of horizontal stress.* As to the sense of horizontal stress acting in the earthcrust, no perfect determination is yet established. It is well known that Hobbs(5) considered the landward compression from the Ocean side, against the theory of continental creep of Suess. In the case

(1) Richthofen, Geomorphologische Studien aus Astasien. 1903.

(2) S. Kunitomi, Propagation of Seismic waves in Japan etc. (Japanese) Journ. Met. Soc. Japan. **3**, Nos. 3, 7, 11, **4**, Nos. 5, 9, **6**, No. 3. Also see Gerland Beitr. Bd. 17, S. 36.

(3) K. Suda, Umito Sora, **5**, p. 85.

(4) Read before the annual meeting of Physico-mathematical Soc. of Japan on April 3rd 1928, but not yet printed.

(5) W. H. Hobbs, Mechanics of Formation or Arcuate Mountains. Journ. Geol. **22**, 1914.

of elastic deformation there is no difference if pushed from land or from Ocean, only actor is the compressional stress in both cases. But in the case of plastic deformation and especially when there exist some local hindrances against the general push, we can determine the sense of push. Very recently T. Terada and N. Miyabe[1] made experiments with sandy material and found the asymmetrical deformation caused on the sand surface. MacCarthy's experiments in underthrusting show also nearly the same fact.[2] These will serve to determine the sense of push or pull in the actual case in future.

§28. *Origine of stress.* As to the origine of the horizontal stress there are many theories.

W. Inoue proposed a hypothesis that a very slow cylindrical rotation in the earth about an axis penetrating Africa to Pacific was and is going on.[3]

In the well known theory by J. Joly based on the radio activity of rocks the compensational exchange of material between continent and ocean is assumed[4] as usually done in harmony with the theory of isostacy.[5]

A. Daly proposed a theory of horizontal slide of the crust in its full thickness due to chilled tension.[6]

J. W. Evans pointed out the E-W contraction in the equatorial zone of the earth, taking into consideration the effect of cooling and the change of the rotation-period of the earth after the calculation of Stoneley. Evans noticed in this respect the region of compression around Pacific Ocean. On this point, perhaps nearly all geophysists may have their own theories and the current thought of the day seems to recognize the horizontal shift

---

(1) T. Terada and N. Miyabe, this Bul. **4**, p. 33 (1928); **6**, p. 109 (1929).

(2) G. R. MacCarthy, Amer. Journ. Sci., **16**, 51, (1928).

(3) W. Inoue, Gerland Beitr. **19**, s. 231 (1928).

(4) J. Joly, The surface history of the earth 1924 and other papers appearing later.

(5) The works of Hayford, Helmelt, Hicker etc. discribed in any text book, e.g. Jeffreys: The earth.

(6) A. Daly, Relation of Mountain-Building to igneous action. Proc. Amer. Phil. Soc. **64**, No. 2, 1925, p. 296.

(7) J. W. Evans, Regions of Compression, Nature, 1927, Jan. p. 15–17, etc.

and accompanying compression at the boundary of the ocean and continent.

It is note worthy here that, as Saemont. Nakamura[1] has already noticed, Hawaiian volcano, situating at the central part of North Pacific, had experienced a sudden subsidence of the lava surface on the occasion of the concerning Japanese earthquake.[2] This might be explained as chance, but the simultaneous occurrence of a great earthquare with the eruption of a distant volcano is by no means seldom, and hence wants future investigation.

§29. *Reaction of Volcanoes.* One of important assumptions in our theory is the impedance of volcanoes against the general crustal or magma movement. As reported by Prof. Seiji Nakamura[3] and also by the Land Survey Department.[4] Osima actually did not rise nor sink. Volcano Huzi (Fuji) got no effect from the earthquake in a remarkable contrast with Kohu (Kofu) which, situating in a greater distance from Sagami Bay than Mt. Huzi, was shaken very violently and rents and cracks were formed abanduntly in the vicinity.[5] If the immovability of volcanoes be true, its reason is not yet very clear. Tentatively it may be that the volcanic rocks, newly solidified, are very strong and volcanic neck or tube which already consolidated exerts resistance against the general motion as if a nail or pin prevents a board or sheet paper to remove.

§30. *Horse-shoe bending.* To solve the horse-shoe bending mathematically is very difficult. But the possibility of it can be imagined from the analogy of St. Venent's problem. In the vortex of water or air the horse-shoe shape happens most commonly.[6] A characteristic feature is

---

(1) There are Many S. Nakamuras in Japan. Seidan Nakamura=Kiyoo Nakamura, Academician, Meteorologist, former director of the Central Meteorological Obs.
Seiji Nakamura, Dean of the Faculty of Science, Tokyo Imperial Univresity, Physisist with some researches on Oceanology and Volcanology.
Saemontaro Nakamura, Prof. of Geophysics, Tôhoku Imperial University, Seismologist.
Sintaro Nakamura, Prof. of Geology, Kyoto Imperial University, Geologist.

(2) Jugger, Volcanological Bulletin, 1923.

(3) Seiji Nakamura, Rep. Imp. Earthq. Inv. Comm. No. 100, B. p. 73.

(4) loc. cit.

(5) H. Obata, Rep. Imp. Earthq. Inv. Comm. No. 100, A p. 141.

(6) S. Fujiwhara, The natural tendency towards symmetry of motion etc., Quart. Journ. Roy. Met. Soc. **47**, p. 387, 1921.

that the vortical horse-shoe is usually not symmetrical with its axis. We can see this character also in Fig. 1. in which the elevation to the west of Osima is very thin, while that covering northern and eastern regions of Sagami Bay is very eminent, resembling the rain area of Bjerknes's cyclone.(1)

Comparison with other Theories.

§31. *Theories of Suda and Fujiwhara.* Among theories summarised in §2, No. 9 by Mr. K. Suda is nearly the same as the present one, though he touched rather slightly on the vortical nature. In No. 11 by the present author, the sudden upheaval of the coastal region is considered due to vortical rebound. But since this point cannot be proved exactly from the fact, the vortical displacement and consequent bending are only treated in the present note.

§32. *Terada's Theory.* The theory No. 8 of Prof. Terada is very suggestive one. A model which recoils in the direction of stress—ordinary one recoils oppositly—and another model of floating continent on viscous solid are offered. His final conclusion is the local horizontal fold and this is nearly the same as our horse-shoe bending. There is no contradiction between his and our present one.

§33. *Linear rebound* was actually proved on the occasion of San Fransisco Earthquake in 1906.(2) The slow horizontal displacement on the east and west sides of the great San Andrews fault was northwesterly before the great earthquake and the sudden displacement on the occasion of the earthquake was still NWly on the west side, while SEly on the east side. This is the most evident proof of the linear rebound. In our case, however, no such relation was observed. Only fact supporting the rebound hypothesis is the fact (6) in §3, which alone is not sufficient to prove either vortical nor lenear rebound.

§34. *Lenear dislocation.* The most remarkable feature of the lenear

(1) J. Bjerknes, On the structure of moving cyclones. Geophysik Publicationer, **1**, No. 1, 1919.

(2) A. C. Lawson and others No. 1, H. F. Reid No. 2, Publ. No. 87, Carn. Inst. Washington.

dislocation i.e. fault formation in straight line is the zonal distribution of the inner isoseismic lines as was the case in the San Francisco earthquake or in the Tango earthquake. In the case of Sagami Bay earthquake this condition was not fulfilled as proved by a very accurate method by T. Matsuzawa[1] and also by others.[2] There is no rigorous proof for the linear dislocation at the bottom of Sagami Bay. The investigation by T. Terada and N. Miyabe stands in favour of the vortical theory,[3] because the curves of equal displacement plotted by them are round but not zonal. The investigation of A. Imamura and F. Kishinouye contributes as well to the theory of the horse-shoe bending as to that of the lenear dislocasion.[4] Indeed the axis of our horse-shoe coincide with the supposed line of dislocasion by others, and these two theories come together to the same insistence that the horizontal motion of the NE side of Sagami Bay relative to its SW side was SE-ward. Hence those theories No. 1, 2, 3, 4 and 7 are all correct so far as the first approximation is concerned. Of course, in our theory too, some subordinate fissurs in the slope and bottom of Sagami Bay may be admitted.

§35. *Plutonic Theory.* As to the theory No. 6 in §2 i.e. a plutonic hypothesis stands also in accordance with our theory so far as the slow magma motion is concerned. It is more natural to suppose the yield of crust to the accumulated pressure both in lithoral and in magma layer than to imagine a sudden removal of such great amount of magma through considerable distance and over tremendous area as Sagami Bay and its environment in such a short duration as a few minutes during which the upheaval of two or three meters of the Sagami Bay coast was perfected. Hence plutonic hypothesis is not true in this case so far as insisting the sudden magma motion as the direct cause of the great earthquake. But

---

(1) T. Matuzawa, Rep. Earthq. Inv. Comp. No. 100, A, plate facing to p. 260.

(2) Saem. Nakamura, K. Suda etc. loc cit.

(3) T. Terada and N. Miyabe, On the Horizontal Displacements of etc. Proc. Imp. Acad. **4**, (1928) p. 49.

(4) A. Imamura and F. Kishinouye, On the horizontal shift etc. Bul. Earthq. Research Inst. **5**, (1928), p. 40.

slow magma motion is necessary in the course of the isostatic compensation, which supposed true in the vortical theory.

Thus by close investigations, all theories based on the same facts turn out to be only different expressions of neary the same thing.

Discussions on the recognized Facts.

§36. *Vertical displacement of the Sagami Bay bed.* The two most important facts upon which our theory rests are the upheaval and subsidence of land and sea bottom and the horizontal displacement in the shaken area. The enormous subsidence of the bottom of Sagami Bay was the subject most doubted. By an elaborate investigation by T. Terada,[1] it was, however, proved to be correct, at least, as far as the main figures concerned. T. Ogawa pointed out that the horizontal motion of mad is very easy at the bottom of Sea when tossed by violent shocks. This is quite true, and by this action mady material originally was on the submarine hill or in the upper slope must settle down and occupie the lowest part of the bottom. By closer examination of the original chart of Fig. 1 we find that the parts marked 1, 2, 6, 7, 18, 19, 20, 22, 23 and 25 in Fig. 1. were surely elevated in spite of their original higher positions, and the parts 3, 15 and 30 originally of maximum depths were subsided. The parts 5, 4, 17 etc. might be due to the land slips according to Ogawa's principle. This fact that even deepest part has subsided is a powerful support to the present theory.

The question that whether the subsidence and the horizontal displacement were performed whether gradually or suddenly is one not yet answered. But it is very probable, as Prof. T. Terada and others also remarked, that some fractions of these displacements were due to the momentary motion. The horizontal displacement of the land area is also subject to similar question. Very recently Land Survey Department published the result of the measurement of the base line in Mitakamura in shaken area and

---

(1) T. Terada, On the Vertical Displacement of the Sea Bottom etc. Proc. Imp. Acad. IV (1928) No. 2, p. 45.

(2) T. Ogawa, chikyu, the Globe, **1**, p. 405, (1924).

the result is that the base line elongated suddenly at the time of the great earthquake and recontracted a little after the quake. Then again it continue the elongation in a greater rate than before the earthquake. This is a favourable fact to our theory.

§37. *Convergence and Vorticity.* On the vorticity apparently shown by the horizontal displacement, suspection was also casted, because such idea as vortical motion in the earth's crust is quite new and was hardly accepted by, excepting a very few geophysicists. First of all, it was doubted that this might be the result of the choice of the reference point at Teruisiyama. To make clear of this question the author calculated the specific convergence C and specific rotation R of each area in squares as shown in Fig. 5. The formulæ are

$$KC=\frac{1}{l^2}\int_s V_n ds=\frac{1}{l^2}\int(vdl_1-vdl_3+udl_4-udl_2)$$
$$=\frac{1}{l}(\bar{v}_1-\bar{v}_3+\bar{u}_4-\bar{u}_2),$$
$$KR=\frac{1}{l^2}\int_l V_t dl=\frac{1}{l^2}\int(udl_1-udl_3+vdl_2-vdl_4)$$
$$=\frac{1}{l}(\bar{u}_1-\bar{u}_3+\bar{v}_2-\bar{v}_4),$$

where K is the magnification factor of the linear scale, l the length of the side, ds the side element, V_n and V_t the normal and tangential component displacements on the side, dl_1, dl_2, dl_3, dl_4 are elements of respective 4 sides round the square in the sense of anticlockwise rotation as positive, $\bar{u}_1$, $\bar{u}_2$, $\bar{u}_3$ and $\bar{u}_4$ are the average component displacements on the respective 4 sides, parallel to dl_1, $\bar{v}_1$, $\bar{v}_2$, $\bar{v}_3$ and $\bar{v}_4$ are the average component displacements on the respective 4 sides perpendicular to dl_1, or parallel to dl_2. The squares are taken proper in order that $\bar{u}$ and $\bar{v}$ are calculable by inter- or exterpolation within the least amount of errors. Though this choice of squares is somewhat arbitrary, it is certain that the main feature obtained is not altered by another plausible choice.

In the next table are shown the values of mean components displacements along and normal to four sides of twelve squares thus chosen.

These mean values are determined by interpolation or exterporation, and owing to the want of sufficient number of measurements, they are relyable only to the first figures.

TABLE I.

Components displacements along and normal to the sides of 12 squares.

Components / No. of Squares	$\bar{u}_1$	$\bar{v}_1$	$\bar{u}_2$	$\bar{v}_2$	$\bar{u}_3$	$\bar{v}_3$	$\bar{u}_4$	$\bar{v}_4$	L	KC	KR
									c.m.		
1	53	272	99	−106	199	− 78	80	194	10	31	− 46
2	70	− 25	80	0	145	−180	112	−150	5	37	15
3	78	− 27	34	2	44	7	85	− 55	6	3	15
4	145	−180	85	− 55	76	− 37	140	−170	5	− 19	37
5	91	243	115	100	120	140	119	177	6	18	− 18
6	118	150	148	58	96	29	122	193	7	12	− 19
7	123	38	120	78	130	85	127	115	5	− 8	− 9
8	106	− 4	50	10	36	19	120	78	7	7	0
9	240	0	124	− 58	106	− 4	148	58	6	5	0
10	193	−184	140	−170	104	− 63	150	− 94	4	− 28	3
11	127	− 70	63	− 63	67	− 50	100	− 58	2	8	28
12	92	− 46	− 4	20	27	0	60	− 31	7	2	16

Substituting these values into the above formulae for KR and KC we get the values of KC and KR, which are entered in Fig. 5. They are correct at least to the first figures. The curves of equal rotation and equal contraction are drawn. These curves are now free from the choice of the reference point at Teruisiyama and can be looked upon as indicating bare fact.

We can see on this chart that Sagami Bay was subject to the greatest rotation in the clockwise sense, while there exists a zone of the counter rotation round the area of the primary vortex. Such is one of the characteristics of natural vortices in air or in water.

The area of greatest contraction, situating a little east of the primary

vortex, just as already shown by T. Terada by different method,[1] indicates that the phenomenon is not the simple result of lenear dislocation.

As the small Takikawa faults near Hozyo—Fig. 2— are formed in the area of contraction i.e. of compressive stress and anticlockwise rotation or negative shear, the sense of echelon must be negative.[2] This is satisfactory the case as evidently shown in Fig. 12, p. 112 of Yamasaki's reports.[3] The sense of rotation also coinsides well with fact exhibited by the same faults as illustrated in Fig. 13, Plate 27 in the same report.[4]

Such coinsidences of the theory with facts strongly indicate the validity of the theory of vortical formation on the face of the earth and the vortical generation of some of earthquakes.

Oct. 6th, 1928.

In The Earthquake Research Institute, Tokyo.

---

(1) T. Terada and N. Miyabe, loc. cit. Proc. Imp. Acad. **4**, (1928) pp. 49–52.

(2) See S. Fujiwhara, Gerland Beitr. Bd. 16. S. 2.

(3) N. Yamasaki, loc. cit. Journ. Fac. Sci. Imp. Univ. Tokyo, Sect. 2, **2**, part 2.

(4) As to the Sinkawa and Sitaura faults there is no description on the echélon aspect.

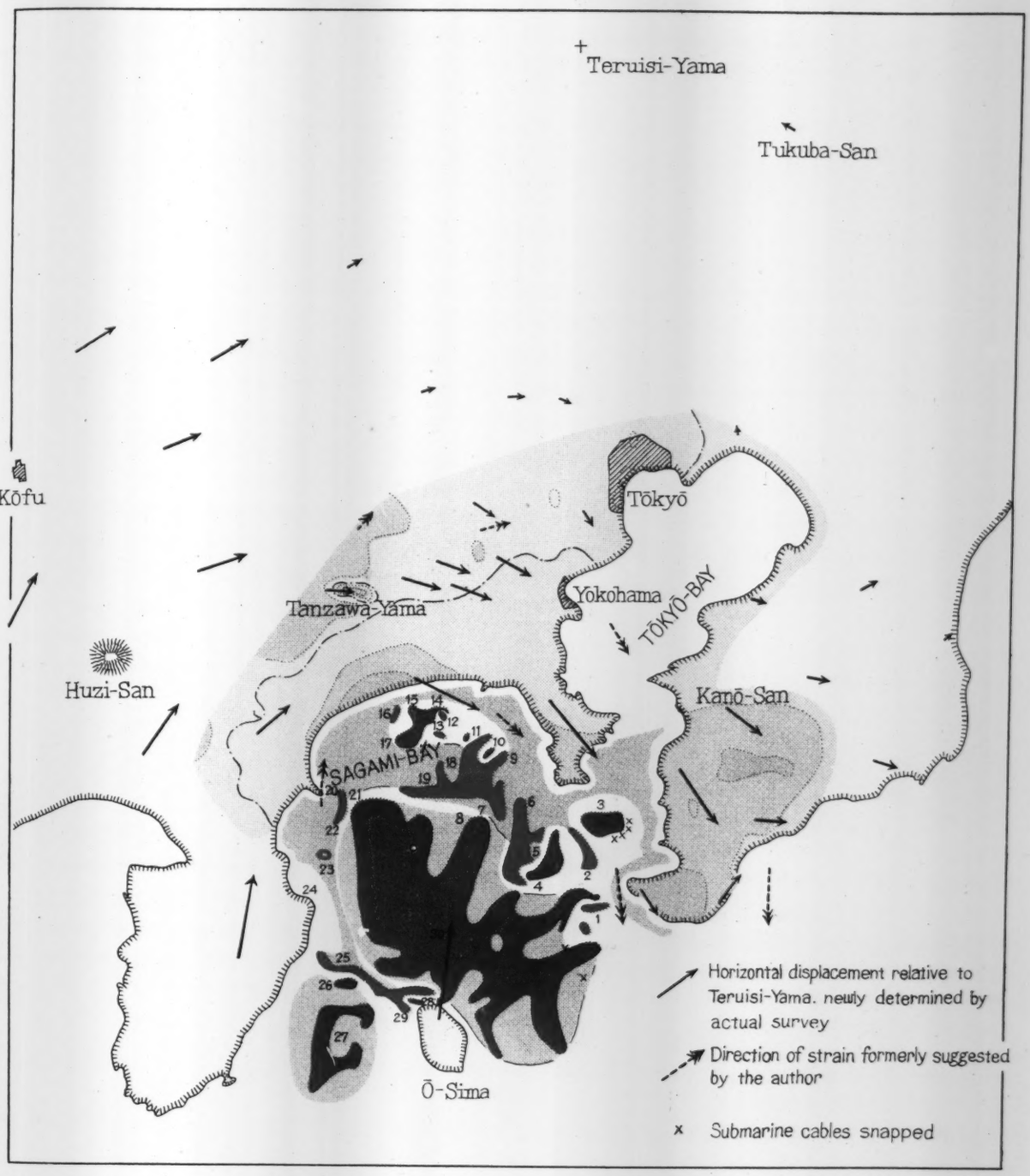

（震研彙報、第六號、圖版、藤原、高山）

Fig. 1.
Horizontal and Vertical Displacement, as revealed by Actual Survey.

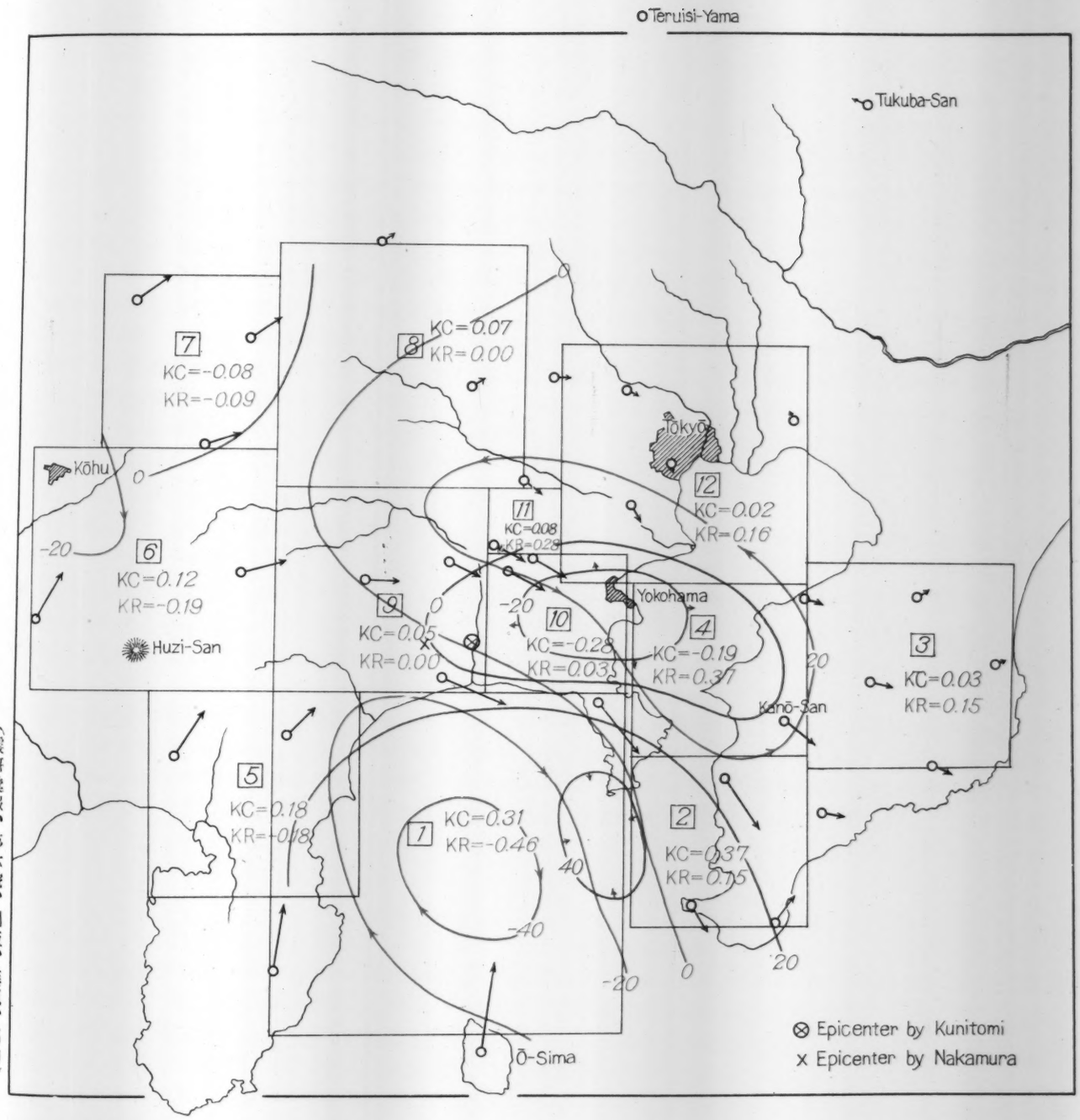

Fig. 5.
Convergence (in blue) and Rotation (in red) in the Shaken Area.

（震研彙報、第六號、圖版、藤原、高山）

Fig. 3 a.

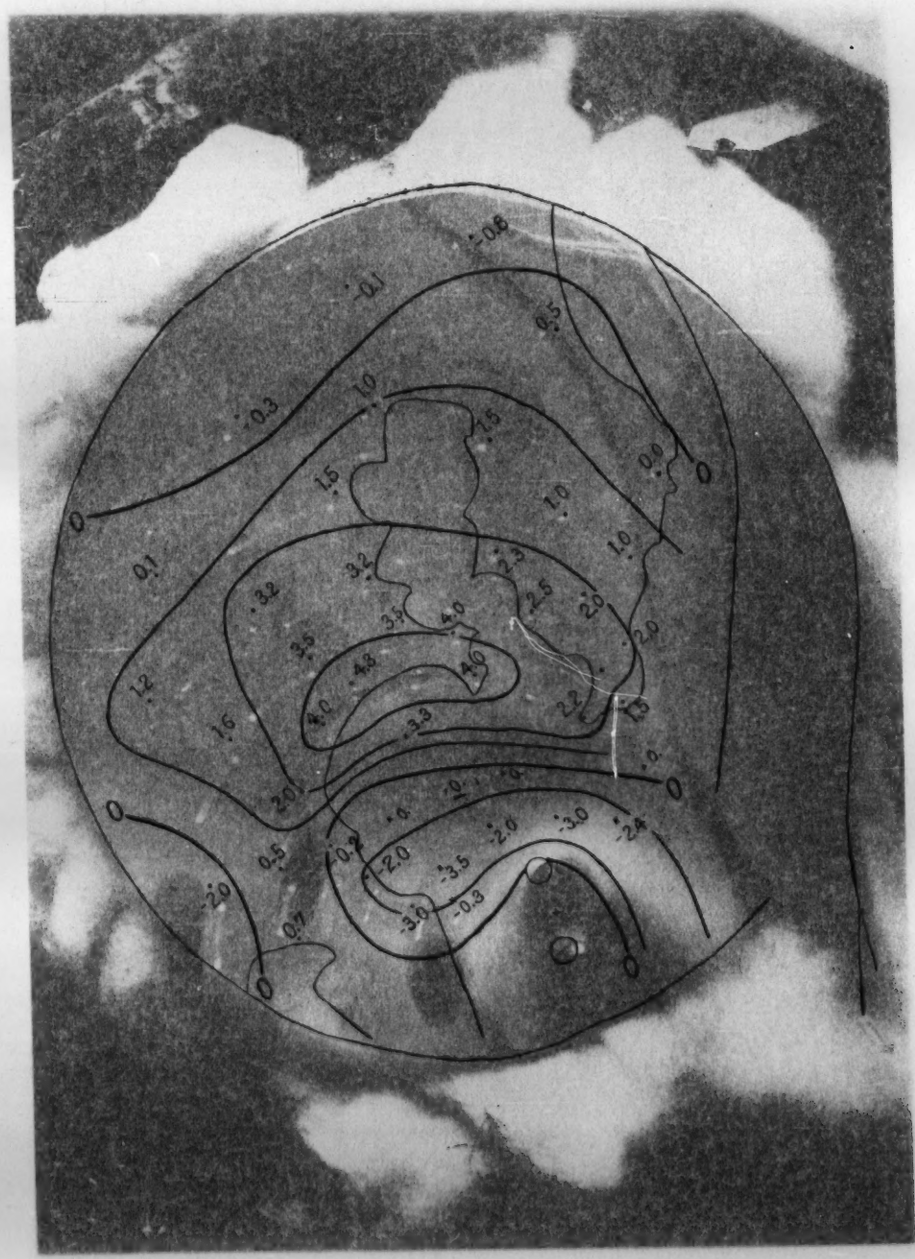

Fig. 3 b.

（震研彙報、第六號、圖版、藤原、高山）

Fig. 3 a.

Fig. 3 b.

（震研彙報、第六號、圖版、藤原、高山）

Fig. 4 c.

Fig. 4 b.

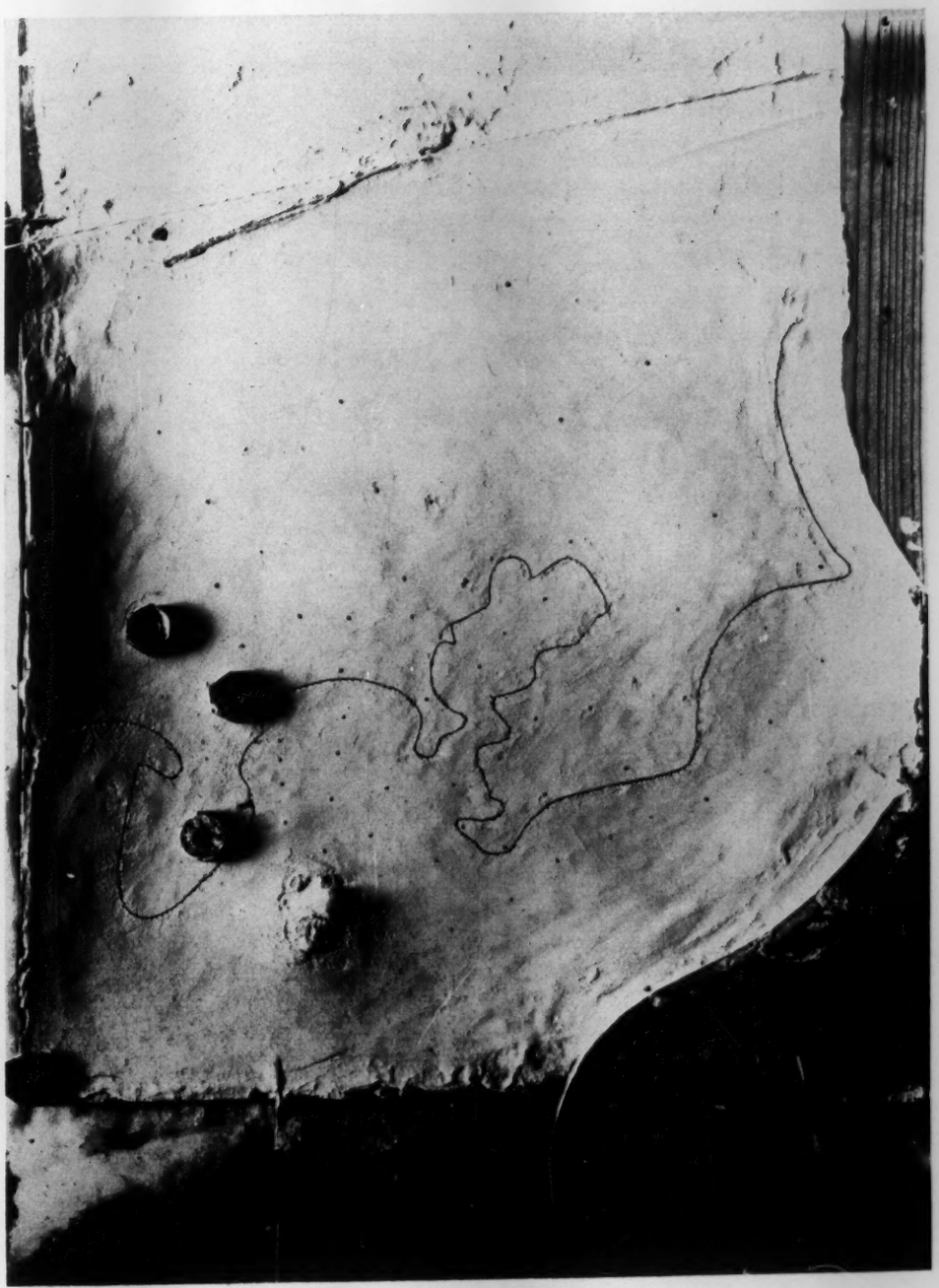

Fig. 4 a.

Observation of some Recent Earthquakes and their Time-distance Curves.

(Part II).

By **Takeɔ MATUZAWA,**

Nukigaki (abstract in Japanese.)

(1) Distortion no Nami ni oitemo Dilatation no Nami no Baai to dôyô ni S, S* oyobi $\bar{S}$ no mitôri no Nami ga zissai ni kwansoku sareru kotowo tasikameta.

(2) Onoono Nami no araware-yasui Zyôken wo osihakari Zisin no Karada ni kanziru Kuiki no Mondai nimo hureta.

(3) Sore ni kwankeisite Syoki-Bidô-Keizoku-Zikan to Singen-Kyori tono 1-zi Siki no Keisû no iroiro na Atae no Imi wo gironsita.

I. Introduction.

In part I, the author investigated the mode of propagation of seismic waves of dilatational character, and showed that even in such an island area as Japan three phases of movements, P, P* and $\bar{P}$ can be observed if conditions are favourable.

As a natural consequence of this, a similar investigation with regard to the propagation of seismic waves of distortional character becomes necessary. It forms the main subject of this paper.

II. Review of Some Recent Earthquakes.

As the distortional movements are superposed on the dilatational movements, determination of incidence of each phase is in general less accurate than that of the P phase. By selecting favourable cases and by means of suitable interpretation, however, the author has been able to determine a set of time-distance curves corresponding to each phase, which turned out fairly useful for practical purpose.

The Etigo earthquake of Oct. 27, 1927.

This example is the same as that investigated in part I, and utilising the same data in Table I, part I, a set of time-distance curves is constructed as shown in Fig. I.

Time-Distance Curve of Etigo Earthquake
of Oct. 27, 1927.

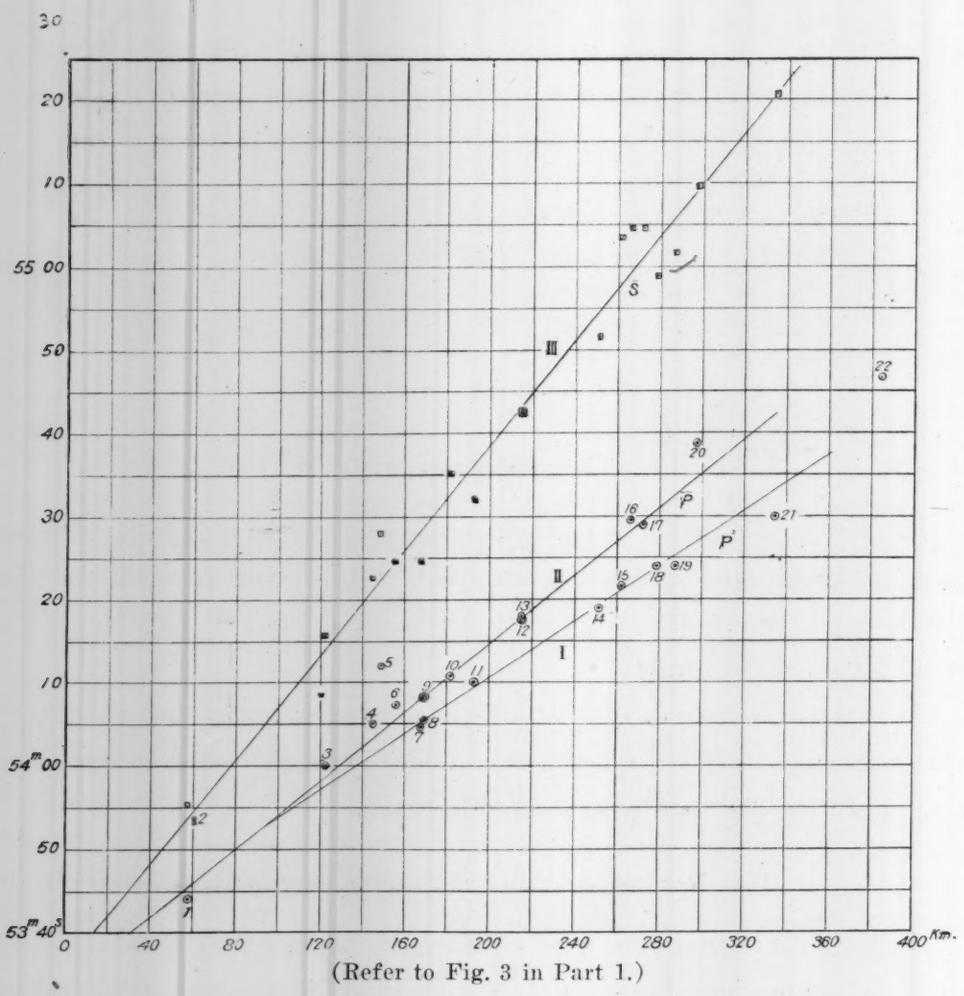

(Refer to Fig. 3 in Part 1.)

Fig. 1.

The points belonging to curve III were plotted in such a manner that the reported duration of the preliminary tremor is represented as the time measured from the corresponding point on curve I or II, according as the

reported time of commencement belong either to curve I, or to curve II. Curve III is characterised by $\frac{\partial \Delta}{\partial T}=3.16$ km/sec. The observed value at Hongô (shown by double square in Fig. 1) is quite in accord with that curve. If this value of velocity is interpreted as that of the $\overline{S}$ phase, it seems somewhat too small compared with the current value 3.3 km/sec. On the other hand, Dr. N. Nasu[1] investigated the proportional constants of the linear equation between the hypocentral distance and the duration of the preliminary tremor ($y=kt$) in the case of after-shocks of the great Tango earthquake of March 7, 1927, hypocentres of which were mainly distributed within a depth of some fifteen kilometres, and obtained the value 8.4 km/sec. It will very naturally be inferred that this value corresponds to that due to the $\overline{P}$ and the $\overline{S}$ waves in the uppermost layer. Adopting 5.0 km/sec. as the velocity of propagation of the $\overline{P}$ waves which was obtained in part I, that of the $\overline{S}$ phase can be calculated as 3.13 km/sec., which is well in accord, within the limit of errors, with the value obtained above. Thus, curve III may very naturally be interpreted as that of the $\overline{S}$ movement.

In this case, the S^* movement seems to have been difficult to identify, due perhaps to a similar reason as discussed in part I. Indeed, closer examination of the seismogram recorded at Titibu (Pl. II. Fig. 2 in part I) will show the existence of the S^* and S phases. Other examples of identification of the S^* phase will be shown later.

The Earthquake of Feb. 4, 1926.

This earthquake occurred far off the coast of Erimo-saki, Hokkaidô, and was feebly felt by our unaided senses even at Tôkyô, some 670 km. distant from the seismic origin. It has been the subject of close study by Dr. S. I. Kunitomi[2] but as my views differ from his in certain respects, the subject is dealt with in the following paragraphs.

In this case, the distribution of the duration of preliminary tremor exhibited a peculiar manner as was shown in Fig. 3 of Mr. Kunitomi's paper,

---

(1) N. Nasu, Proc. Imp. Acad. 4 (1928) No. 7, 379.
(2) S. I. Kunitomi, Journ. Meteor. Soc. Jap. [ii] 4 (1926) No. 9.

thus furnishing a favourable example for investigating the propagation of the distortional movements. The present author assumed $\varphi = 41° 22'$ N and $\lambda = 142° 25'$ E as the geographic coordinates of its epicentre, which seem to be in favourable accord with observed values of time of commencement and duration of the preliminary tremor. Relevant data were taken from "Kisyô Yôran" and Mr. Kunitomi's paper,[1] and tabulated in Table I.

TABLE I.

Earthquake, Feb. 4, 1926. (Assumed origin; $\varphi = 41° 22'$ N, $\lambda = 142° 25'$ E.)

No.	Station	Latitude Longitude	Δkm.	Time of Commencement	Duration of Preliminary Tremor	Remarks
				h m s	s	
1	Hakodate	41° 47′N 140° 43′E	146	15 44 34.5	12.5	
2	Muroran	42 20 140 57	159	39.0	14.0	s 14.3 by Kunitomi.
3	Miyako	39 38 141 59	200	46.0	18.0	
4	Sapporo	43 4 141 21	209	35.4	13.8	23.5 „ „
5	Morioka	39 42 141 10	215	47.2		29.7 „ „
6	Kusiro	42 59 144 24	239	30.0	28.0	29.7 „ „
7	Akita	39 41 140 6	271	50.0	34.0	32.4 „ „
8	Mizusawa	39 8 141 8	271	52.0	26.0	
9	Asahigawa	43 47 142 23	270.2	42.0	43.4	
10	Isinomaki	38 26 141 19	337	54.0	47.0	48.6 „ „
11	Nemuro	43 20 145 35	337	45 07.1	35.4	36.5 „ „
12	Haboro	44 23 141 42	341	44 58.1	57.3	
13	Yamagata	38 15 140 21	387	35.0	40.4	55.0 „ „
14	Niigata	37 55 139 3	482	45 18.5	60.5	65.2 „ „
15	Onahama	36 56 140 54	509	25.0	75.2	67.5 „ „
16	Utunomiya	36 34 139 53	576	27.7	75.2	
17	Mito	36 23 140 28	579	28.0	76.9	74.9 „ „
18	Takada	37 6 138 15	593	30.6	59.7	
19	Tukuba	36 13 140 06	605	10.9	58.0	

(to be continued.)

(1) l.c. p. 179.

(Continued.)

No.	Station	Latitude Longitude	Δ km.	Time of Commencement	Duration of Preliminary Tremor	Remarks
20	Maebasi	36 24 139 4	622	15 45 38.5	76.7	
21	Kumagai	36 9 139 23	635	33.8	83.8	
22	Nagano	36 40 138 12	637	30.0	99.0	89.0 by Kunitomi.
23	Tyôsi	35 44 140 51	640	34.7	97.5	88.4 „ „
24	Hongô	35 43 139 46	675	41.0	68.3 101.3	P-S by the present author. P-S*
24′	Tôkyô					94.0 by Kunitomi.
25	Husiki	36 47 137 3	687	46 13.4	42.3	91.0 „ „ Reported T.C. may be that of the P wave. 91.0 may be P-S.*
26	Matumoto	36 14 137 59	687	45 40.0	64.0	90.0 by Kunitomi.
27	Yokohama	35 27 139 39	700	43.3	100.0	
28	Kôhu	35 38 138 34	719	48.0		100.1 „ „
29	Mera	34 55 139 50	750	45.1	105.5	103.8 „ „
30	Iida	35 31 137 50	761	45.6	99.6	
31	Numazu	35 6 138 51	761	58.4	97.7	105.5 „ „
32	Hukui	36 3 136 16	795	38.0	80.0	
33	Gihu	35 24 136 46	824	58.7	79.8	99.6 by Kunitomi. 79.8 may be P-S duration.
34	Nagoya	35 10 136 58	835	46 11.0	80.0	
35	Tu	34 44 136 31	900	45 11.5	63.3	T.C. may be 46^m instead of 45^s.
36	Kyôto	35 01 135 44	914	46 8.9	98.4	
37	Toyooka	35 32 134 49	924	6.1	90.3	
38	Oosaka	34 39 135 26	963	19.2	117.3	
39	Kôbe	34 41 135 11	975	14.4	98.7	
40	Sakai	35 33 133 14	1002.5	29.3		
41	Sumoto	34 21 134 53	1021	16.3	105.4	
42	Kure	34 14 132 33	1165	15.8	117.6	

Using these values a time-distance diagram is constructed as shown in Fig. 2.

Time-Distance Curve of Earthquake on Feb. 4, 1926
(φ=41° 22′ N, (λ=142° 25′ E)

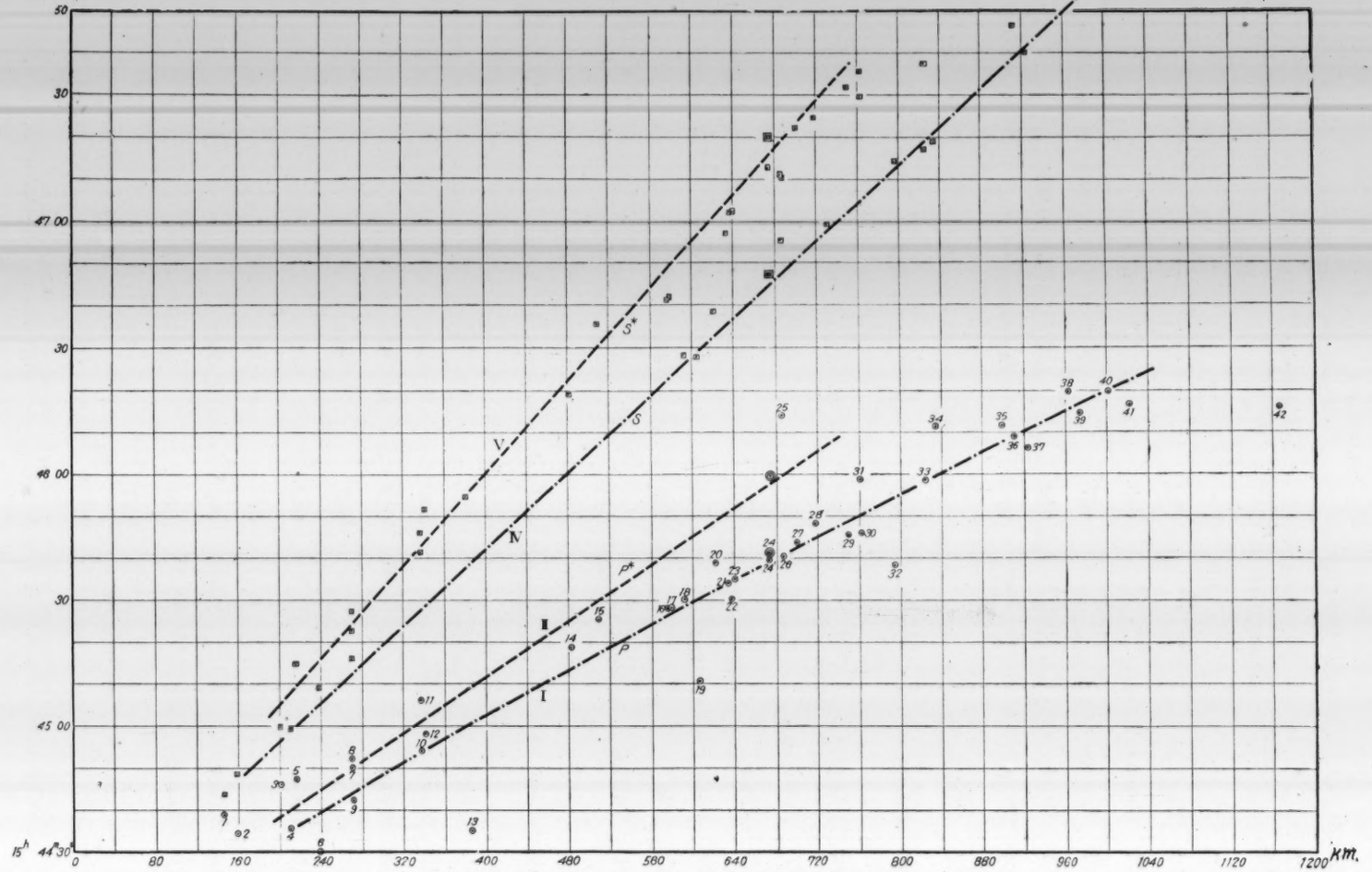

(Numbers are to be referred to Table I.)

Fig. 2.

The P and the P* curves are drawn so that they are reconcilable to those obtained in part I. Points corresponding to distortional movements are plotted so that the reported duration of the preliminary tremor is represented as the time reckoned from the corresponding point on the P or P* curves, according to whichever of their branches the observed time of commencement may seem to belong. As can be seen from the figure, the distributed points belonging to the distortional movements can be separated into two branches of curves (IV and V), in an especially clear manner for remote stations, and which are characterised by $\frac{\partial \Delta}{\partial T}=4.40$ km/sec. and 3.62 km/sec. respectively. Thus the curves IV and V can be interpreted as belonging to the S movement and the S* respectively. It seems that at certain stations the commencement of the S phase was measured as being that of the principal phase, while at others that of the S*phase was so interpreted. In support of this conjecture a study of seismograms obtained at Hongô will be sufficient. (Pl. X. Fig. 3 and Pl. XI. Fig. 4). We find indeed that four phases, P, P*, S and S*, can be identified at just the same positions (within, of course, the limit of unmistakable identification) as expected from the curves in Fig. 2. In Fig. 2, values observed at Hongô are plotted by double circles and double squares. It must be remarked that quick movements are for the most part superposed on the S movements, as clearly seen in Fig. 4. This point will be taken up later.

At all events, the irregular appearance of the distribution of the iso-P-S line seems to be only apparent and due to difficulty in the identification of each phase. As far as the effect of the superficial strata alone of the earth's crust is concerned, it is quite naturally conjectured from the knowledge of trajectory of waves that the greater the epicentral distance the more clearly can the S phase be observed.

The Earthquake of July 13, 1927.

This earthquake occurred far off the coast of Kusiro, Hokkaidô, and was feebly felt without instrumental aid at Tôkyô about 900 km. distant from the epicentre. The geographic coordinates of its epicentre, $\varphi=42°$ 36′ N and $\lambda=145°$ 35′ E, accord favourably with the observed data. The

data taken from "Kisyô Yôran" (except Hongô) are tabulated below. (Table II.)

TABLE II.

Earthquake of July 13, 1927. ($\varphi = 42° 36'$ N, $\lambda = 145° 35'$ E.)

No.	Station	Latitude Longitude	Δ km.	Time of Commencement h m s	Duration of Preliminary Tremor s	Remark
1	Nemuro	43° 20′N 145° 35′E	81.5	6 9 15.9	3.2	T.C. is too late by one minute.
2	Kusiro	42 59 144 24	102	8 21.9		
3	Obihiro	42 55 143 12	196	33.0		
4	Asahigawa	43 47 142 23	290.5	49.0	25.0	
5	Muroran	42 20 140 57	378	9 5.0	47.0	
6	Hakodate	41 47 140 43	409	9.3	46.5	
7	Miyako	39 38 141 59	446	6.0	52.0	
8	Aomori	40 50 140 45	446	6.0	51.0	
9	Morioka	39 42 141 10	490	19.7	57.5	
10	Oodomari	49 39 142 46	501	53.0	45.0	T.C. is somewhat inconsistent.
11	Mizusawa	39 8 141 8	535	26.0	65.0	
12	Akita	39 41 140 6	559	24.0	66.9	
13	Isinomaki	38 26 141 19	586	29.0	65.7	
14	Yamagata	38 15 140 21	653	39.6	77.1	
15	Hukusima	37 45 140 24	694	10 8.0	78.0	?
16	Aizu	37 34 140 7	727	32.0	87.4	?
17	Onahama	35 56 140 54	744	9 31.0	78.2	?
18	Sikka	39 14 143 7	761	10 15.0		?
19	Niigata	37 55 139 3	769	9 59.0	73.2	
20	Mito	36 23 140 28	817	57.0	87.0	
21	Utunomiya	36 34 139 53	827	44.3	95.6	?
22	Kakioka	36 14 140 11	844	10 1.6	95.2	
23	Tukuba	36 13 140 6	850	2.5	30.0	

(to be continued.)

(Continued.)

No.	Station	Latitude Longitude	Δ km.	Time of Commencement	Duration of Preliminary Tremor	Remark
24	Tyôsi	35 44 140 51	862	10 9.5	95.3	
25	Takada	37 6 138 15	873	8.6	93.3	
26	Maebasi	36 24 139 4	886	8.8	94.6	
27	Kumagai	36 9 139 23	892	8.0	91.8	
28	Hongô	35 43 139 46	912	12.0	98.9	
29	Nagano	36 40 138 12	912	15.7	97.0	
30	Tôkyô	35 41 139 46	917	12.0	100.5	
31	Yokohama	35 27 139 39	948	30.0	92.0	?
32	Matumoto	36 14 137 59	960	4.0	161.0	?
33	Kôhu	35 38 138 34	981	25.0		
34	Mera	34 55 139 50	986	19.6	106.3	
35	Takayama	36 9 137 15	1011	9 43.5	107.4	?
36	Numazu	35 6 138 51	1018	10 26.6	100.7	
37	Hukui	36 3 136 16	1180	11 26.0		T.C. is too late by one minute.
38	Gihu	35 24 136 46	1091	10 34.6	116.9	
39	Nagoya	35 10 136 58	1110	11 5.9	109.6	
40	Ibukiyama	35 25 136 24	1122	10 34.8	64.3	
41	Hikone	35 16 136 15	1143	34.8	118.8	
42	Tu	34 44 136 31	1172	43.0	121.0	
43	Kyôto	35 1 135 44	1197	42.7		
44	Toyooka	35 32 134 49	1212	44.0		
45	Oosaka	34 39 135 26	1243	52.7	124.2	
46	Kôbe	34 41 135 11	1258	55.2	150.4	
47	Wakayama	34 14 135 9	1299	57.0		
48	Sumoto	34 21 134 53	1301	55.9	268.1	
49	Sakai	35 33 133 14	1320	9 57.1		T.C. is too early by one minute.
50	Hamada	34 54 132 4	1448	11 16.6	149.7	

(to be continued.)

(Continued.)

No.	Station	Latitude Longitude	Δ km.	Time of Commencement	Duration of Preliminary Tremor	Remark
51	Kôti	33 33 133 32	1452	6 11 13.2	159.2	
52	Oöita	33 14 131 37	1600	30.0	182.5	
	Hukuoka	33 35 130 25	1656	37.7	182.2	
	Kumamoto	32 49 130 42	1695	12 54.0		T.C. is too late by one minutes.
	Miyazaki	31 55 131 26	1720	11 59.0	185.4	
	Titizima	27 5 142 11	1750	54.4		
	Kagosima	31 34 130 33	1803	58.3		T.C. is too early by one minute.
	Nagasaki	32 44 129 52	1758	14 49.0	137.0	T.C. is too late by three minute.

Using these values a time-distance diagram is constructed in a similar manner as described in the foregoing case. (Pl. XII. XIII. Fig. 5).

The S curve is of course characterised by $\frac{\partial \Delta}{\partial T}=4.4$ km/sec. In this case it is remarkable that the distribution of points representing the observed values can be grouped into somewhat well defined P and S curves only. This may be due to the fact that the origin of this earthquake was perhaps too deepseated to produce the P^*, $\overline{P}$, S^* and $\overline{S}$ phases. This may therefore be a suitable example for observation of the S phase even at near stations.

Seismograms obtained at Hongô, Tôkyô, will be shown in Pl. XIV. Fig. 6. It may be seen that slow motions predominate from the commencement, superposed by quick motions. In this case also, in the S phase (not in S^* or $\overline{S}$), quick movements predominate. This is generally observed in the case of earthquakes occurring off the Pacific coast of Hokkaidô as well as in the case of deepseated earthquakes. Thus a governing factor common to both cases is that the length of the trajectory of waves in the superficial layer is not long and the angle of incidence at the boundary of stratification not great. Dissipation of quick vibrations in the superficial layer, geologically much disturbed, will far exceed that in the lower layers. A smaller part of energy moreover will be refracted into the upper layer if the angle of incidence is greater. Perhaps in the cases cited above, quick vibrations

generated at a seismic origin will be observed without much loss through dissipation even at a considerable distance.(1) The present author's opinion on the apparent abnormal distribution of locality where seismic shocks are felt by our unaided senses is in line with Dr. K. Wadati's view(2) that this phenomenon depends mainly on the geological structure of the region.(3)

The Great Tango Earthquake of March 7, 1927.

In the above three examples, existence of the S, S* and $\overline{S}$ movements is confirmed while approximate positions of time-distance curves corresponding to them have been determined.

This earthquake was investigated in part I, but the investigation with regard to the distortional movements was reserved for a future occasion. Using the same data, a time-distance diagram is constructed as shown in Fig. 7.

Here attention will be confined to the distortional movements only. As is apparent from the figure, the upper boundary of the distributed points is coincident with a line characterised by $\frac{\partial \Delta}{\partial T}=3.16$ km/sec. Small values of difference of time between $\overline{S}$ and $\overline{P}$ at $\Delta=0$ (though not very exact) showed that the origin of fracture was no deeper than twenty kilometres or so, which is quite in accord with results obtained from other points of view. A line drawn through the approximate mean position of the densely distributed points is characterised by $\frac{\partial \Delta}{\partial T}=3.62$ km/sec. Thus it can be surmised that at most stations the commencement of the S* phase was interpreted as being that of the principal portion. In fact, in seismograms

(1) Mr. T. Isikawa's explanation of this observed fact is that certain kinds of secondary oscillations near an observing station are excited by the incidence of seismic waves (Journ. Meteor. Soc. Japan [ii] **6** (1928) No. 3), although the existence of many exceptional cases somewhat impairs this theory. Dr. S. I. Kunitomi's explanation (Journ. Meteor. Soc. Japan [ii] **6** (1928) No. 4) is that local earthquakes are excited by the incidence of seismic waves, a theory which may require closer statistical study.

(2) K. Wadati, Journ. Meteor. Soc. Japan [ii] **5** (1927) 137.

(3) After all, this may not differ essentially from Mr. T. Isikawa's opinion, but if I understand him correctly, his idea seems to imply that, whatever the incident waves may be, a certain kind of secondary undulations is excited. In short, the essential difference in the two opinions hinges on which factor the stress is laid, whether on the resonator, or on the exciter.

Time-Distance Curve of Tango Earthquake on March 7, 1927.

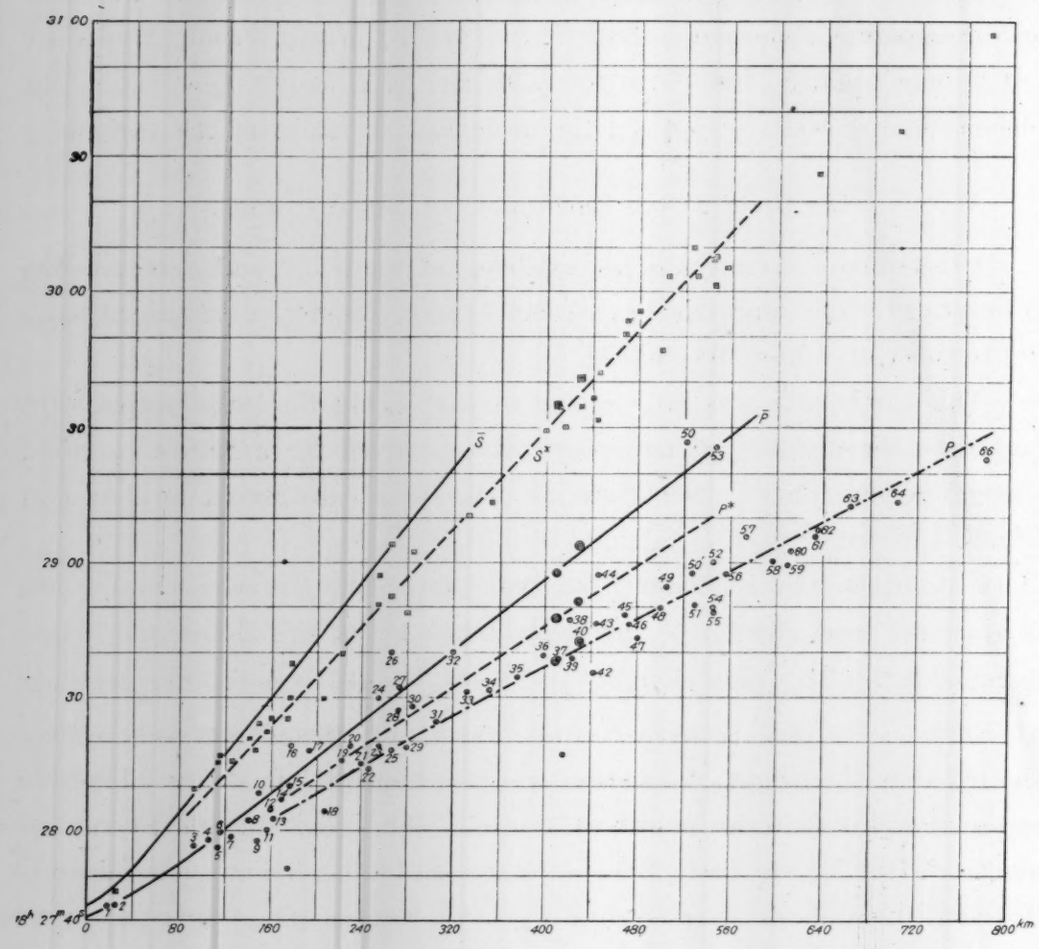

(Refer to Pl. V. Fig. 6 in Part I.)

Fig. 7.

obtained at Hongô (Pl. III, Fig. 4 in part I) and at Kamakura (Pl. IV, Fig. 5 in part I), commencement of the S* phase could be very clearly distinguished. Identification of other phases in the distortional waves may be difficult without referring to the time-distance curves.

The same remark may be applied to the case of the Tazima earthquake, May 23, 1925 (Pl. VI, Fig. 7 in part I) and the Tango earthquake, April 1, 1927 (Pl. VII, Fig. 9 in part I).

In these two cases also it is remarkable that the S* phase could be identified without any difficulty.

This fact may perhaps be due to the small depth of the seismic origin. Another point to be noted is that quick vibrations, like those in the case of the Hokkaidô earthquakes, were not superposed. It may be that strong motion seismographs fail to record small, quick vibrations, but even in Pl. VII, Fig. 9 in part I, which was recorded by Prof. Imamura's tromometer,(1) which is very sensitive to quick motions, such motions are not shown. Even in the two other cases above mentioned, inspection of the seismograms obtained by more sensitive instruments, failed to show such motions. In these cases, the origins whence came the quick vibrations accompanied with local crustal fracture were in all probability too shallow to transmit them to a remote distance. Movements of wider portions of crust to produce the P movements, as discussed in part I, would not produce very quick motions.

The Earthquake of Aug. 3, 1926.

This earthquake occurred off the coast of Haneda (Tôkyô Bay) and was strongly felt at Tôkyô. Its seismometrical aspects were studied and the results published by Professor Imamura and Mr. Ch. Yasuda(2) and also by K. Sagisaka(3) and H. Satô, so that only the mode of propagation of disturbance will be described and discussed here. The position of its epicentre was determined as $\varphi = 35° 33' \text{ N}$ and $\lambda = 139° 48' \text{ E}$. Data concerning this earthquake taken from "Kisyô Yoran" (except those obtained at Hongô) are tabulated in Table III.

---

(1) A. Imamura, Bull. Eqk. Res. Inst. **1** (1926) 7–25.
(2) A. Imamura and Ch. Yasuda, Bull. Eqk. Res. Inst. **3** (1927) 115.
(3) K. Sagisaka and H. Satô, Journ. Meteor. Soc. Japan [ii] **4** (1926) No. 12.

TABLE III.

Earthquake of Aug. 3, 1926. ($\varphi = 25° 33'$ N, $\lambda = 139° 48'$ E)

No.	Station	Latitude (N)	Longitude (E)	Δ km.	Time of Commencement	Dur. of P. T.
					h m s	s
1	Hongô			16.1	18 26 22.0	7.6
2	Tôkyô			,,	23.9	5.7
3	Yokohama			17.7	21.5	5.0
4	Yokosuka			32.2	22.0	
5	Mera	34° 55′	139° 50′	67.7	26.6	
6	Kumagai			76.8	30.4	11.1
7	Kakioka	36 14	140 11	83.8	28.3	11.5
8	Tyôsi			95.8	31.9	12.5
9	Numazu			100.5	31.0	12.0
10	Kôhu			112.7	26.0	18.0
11	Mito			112.7	31.0	10.0
12	Maebasi			116.0	30.8	21.4
13	Matumoto	36 14	137 59	179.5	40.0	18.0
14	Iida	35 31	137 50	180	41.3	21.8
15	Onahama	36 56	140 54	185	37.0	17.3
16	Nagano	36 40	138 12	190.5	41.7	25.4
17	Hamamatu	34 43	137 43	212	52.0	25.0
18	Takada	37 6	138 15	222	46.8	28.5
18′	Aidu	37 34	140 7	228	52.0	25.1
19	Takayama	36 9	137 15	237	50.8	32.2
20	Nagoya	35 10	136 58	259	51.0	34.0
21	Niigata	37 55	139 3	274	50.5	43.8
22	Gihu	35 24	136 46	274	53.3	29.4
23	Husiki	36 47	137 3	281	56.3	41.9
24	Yamagata	38 15	140 21	303	51.9	37.0
25	Hikone	35 16	136 15	324	27 7.3	37.5

(to be continued.)

(Continued.)

No.	Station	Latitude (N)	Longitude (E)	Δ km.	Time of Commencement	Dur. of P. T.
26	Hukui	36 3	136 16	326	18 26 46.9	34.5
27	Isinomaki	38 26	141 19	341	27 6.2	29.5
28	Kyôto	35 1	135 44	372	3.5	49.5
29	Oosaka	34 39	135 26	409	7.9	60.2
30	Miyazu	35 32	135 12	415	9.3	50.9
31	Mizusawa	39 8	141 8	416	11.0	44.0
32	Kôbe	34 41	135 11	430	13.0	56.6
33	Siomisaki	33 27	135 46	437	4.2	52.5
34	Wakayama	34 14	135 9	446	15.0	54.0
35	Akita	39 41	140 6	459	19.0	74.0
36	Sumoto	34 21	134 53	467	14.8	65.6
37	Miyako	39 38	141 59	494	18.0	50.0
38	Tokusima	34 4	134 33	507	16.0	80.0
39	Okayama	34 40	133 54	546	36.0	70.0
40	Matuyama	33 50	132 45	671	59.0	99.1
41	Hakodate	41 47	140 43	697	51.0	99.0

From these data a time-distance diagram has been constructed as shown in Fig. 8.

The P and P* curves are so drawn that they will be in accord with those obtained in part I. With regard to the distortional movements, points are almost confined between the S and S* curves, though $\frac{\partial \Delta}{\partial T}=4{,}49$ for the S and 3.73 for the S* phase. Therefore, they are somewhat greater than former values. This may perhaps be due to the circumstance that the stations were clustered more or less near the epicentre while the origin of the earthquake was somewhat deep. This can be understood from the fact that at most stations the P or P* and the S or S* phases were observed and not the $\overline{\mathrm{P}}$ or the $\overline{\mathrm{S}}$ phase. The time-difference between the commencement of the S* and that of the P* at $\Delta=0$ can be estimated as 5.2 sec. or so. If

Time-Distance Curve Earthquake on Aug. 3, 1926
($\varphi = 35°\ 33'$ N, $\lambda = 139°\ 48'$ E)

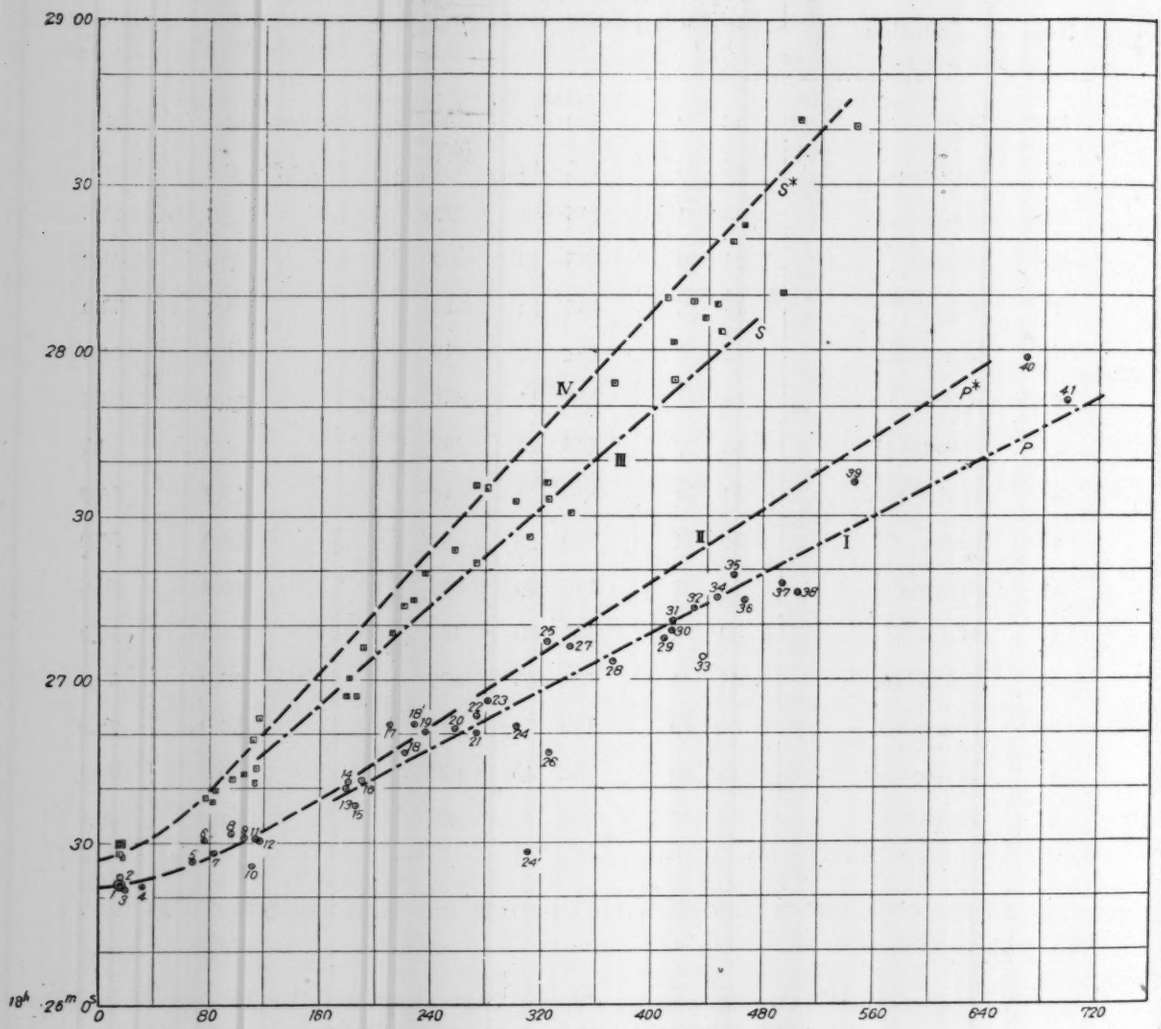

(Numbers are to be referred to Table III.)

Fig. 8.

the thickness of the uppermost stratum is taken as 20 km, the depth of the origin is estimated as 45 km. or thereabouts, which would harmonise with the fact that the P, P*, S and S* phases were observed to the exclusion of the P and $\overline{S}$ phases.

The Earthquake of June 5, 1926.

One more example of a south-western earthquake will be added, since

it is necessary to verify if there is a difference of propagation or not between the south-western and the north-eastern earthquakes.

Earthquakes of sufficient energy for this purpose have been rare in the South-western Japan, and yet this instance will show that the velocity of propagation is not essentially different in the two cases. The author assumes the position of its epicentre as $\varphi = 30°\ 36'$N and $\lambda = 130°\ 40'$E, for by taking this position the distribution of intensity and results of instrumental observation are in fair agreement. The stations are distributed over a narrow band forming the Japanese Islands, and in this case the origin was situated nearly at its end. Therefore, errors of position of epicentre do not seriously affect the slope of the time-distance curves, which becomes a measure of the velocity of propagation. Data were taken from "Kisyô Yôran" and are tabulated in Table IV.

TABLE IV.

Earthquake of June 5, 1926. ($\varphi = 30°\ 36'$ N, $\lambda = 130°\ 40'$ E)

No.	Station	Latitude (N)	Longitude (E)	Δ km.	Time of Com.	Dur. of P. T.	Remark
					h m s	s	
1	Kagosima	31° 34′	130° 33′	107.7	18 10 5.9	18.0	
2	Miyazaki	31 55	131 26	164.7	11.4	22.0	
3	Nagasaki	32 44	129 52	248	11.0	25.0	
4	Kumamoto	32 49	130 42	250	16.4	25.4	
5	Saga	33 12	130 18	292	11 0	29.5	
6	Ooita	33 14	131 37	305	10 21.5	31.	
7	Hukuoka	33 35	130 25	333	18.7	30.0	
8	Simonoseki	33 57	130 56	374	16.0	34.0	
9	Matuyama	33 50	132 45	394	7.9	31.6	
10	Kôti	33 33	133 32	424	36.5	40.0	
11	Hamada	34 54	132 4	496	11 2.0	26.0	$\bar{P}$—S?
12	Tadotu	34 17	133 46	501	10 19.0	46.0	
13	Tokusima	34 4	134 33	530	59.0	53.0	
14	Sumoto	34 21	134 53	576	56.1	56.8	

(to be continued.)

(Continued.)

No.	Station	Latitude (N)	Longitude (E)	Δ km.	Time of Com.	Dur. of P. T.	Remark
15	Wakayama	34 14	135 9	583	18 10 50.1	57.5	
16	Kôbe	34 41	135 11	620	11 0	61.2	
17	Oosaka	34 39	135 26	633	3.5	64.0	
18	Kyôto	35 1	135 44	681	10 36.4	66.0	T.C. may be incorrect.
19	Hikone	35 16	136 15	735	11 16.8	71.7	
20	Nagoya	35 10	136 58	776	10 28.0	77.0	T.C. may be too early by one minute.
21	Gihu	35 24	136 46	781	11 20.2	74.7	
22	Hamamatu	34 43	137 43	802	23.0	55.0	?
23	Takayama	36 9	137 15	869	56.1		
24	Husiki	36 47	137 3	904	32.5	109.6	
25	Numazu	35 6	138 51	912	34.4	115.0	
26	Matumoto	36 14	137 59	922	8.0		
27	Zinsen	37 29	126 37	940	23.0	52.0	?
28	Nagano	36 40	138 12	968	42.6	14.9	?
29	Mera	34 55	139 50	981	56.9		
30	Kôhu	35 38	138 34	990	10 11.0	84.0	T.C. may be too early by 2 min.
31	Yokohama	35 27	139 39	993	12 21.9	85.0	T.C. is somewhat too late.
32	Takada	37 6	138 15	1011	11 46.6	14.0	?
33	Maebasi	36 24	139 4	1009	12 9.2	81.6	T.C. is too late.
34	Tôkyô	35 41	139 46	1016	11 59.7	106.7	
35	Hongô				52.4	110.3	By the present author.
36	Kumagai	36 9	139 23	1018	10 49.9	102.7	T.C. is too early by one minute.
37	Utunomiya	36 34	139 53	1079	11 52.6		
38	Kakioka	36 14	140 11	1080	12 2.9	126.0	
39	Mito	36 23	140 28	1110	4.0	112.0	
40	Niigata	37 55	139 3	1120	11 56.3	166.9	

By plotting these values and in the same way as done in the preceding cases time-distance relations are obtained as shown in Fig. 9.

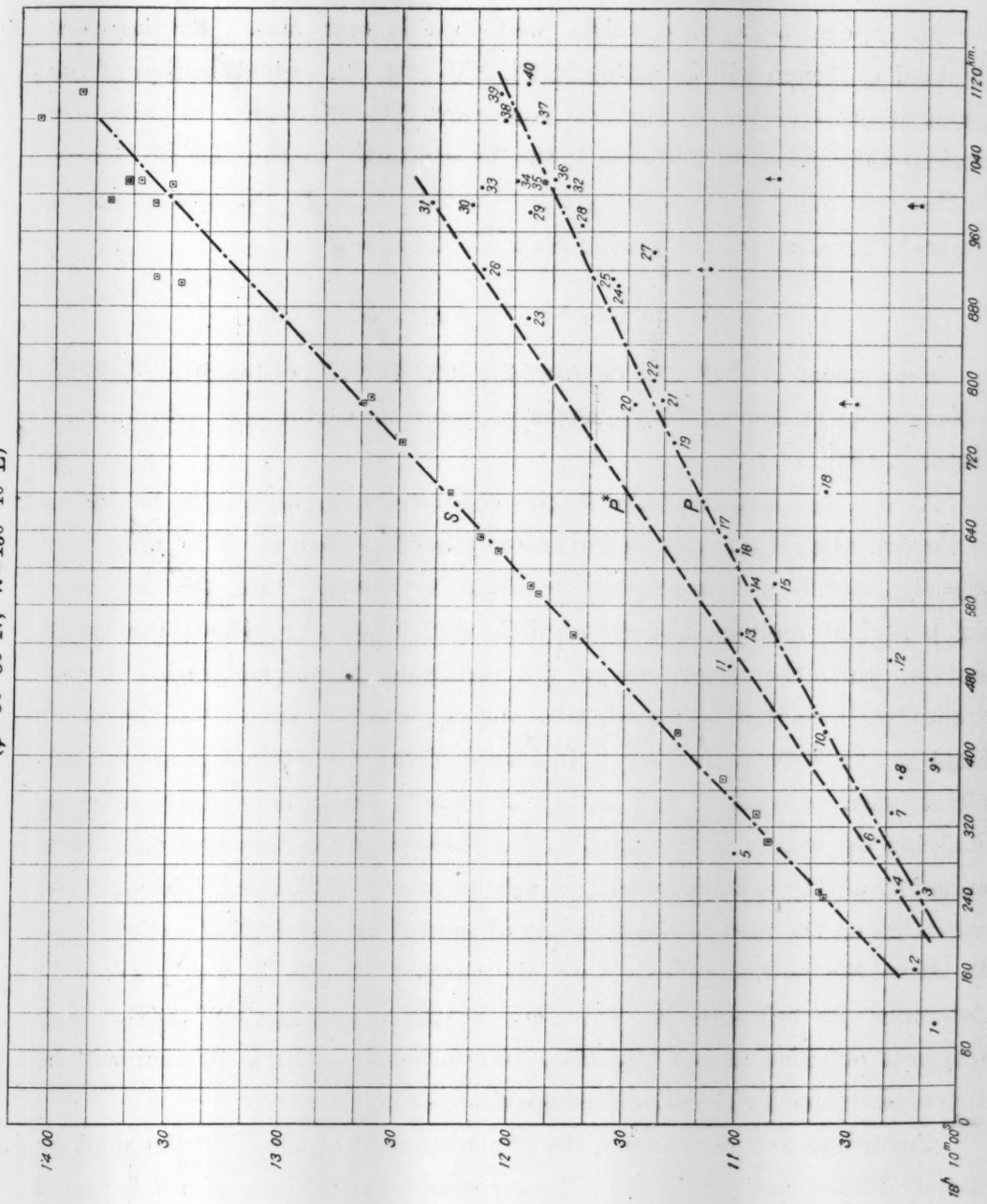

(Numbers are to be referred to Table IV.)

Fig. 9.

From the figure it may be seen that the time-distance curves obtained previously can be applied fairly well to this case also. Seismograms obtained at Hongô will be added in Pl. XV. Fig. 10. Identification of the commencement of the P phase is somewhat difficult, owing to pulsatory motions then going on although it can be measured without serious errors. In this case quick motions are not so conspicuous as in the case of earthquakes originating off the Pacific coast of Hokkaidô.

III. Application to an Ambiguous Case.

From about $17^h\ 56^m\ 43^s.5$ on Aug. 24, 1927 (L.M.T. of longitude 135°E) seismographs at Hongô, Tôkyô, began to record an earthquake with unusual features. (Fig. 11.)

As can be seen from the figure, commencement of phases belonging to the distortional movements can scarcely be identified, or, if so, only very vaguely, that is as concerns these particular seismograms. In this case, the period of motions underwent little fluctuation throughout the whole motion, while the magnitude of the amplitude of motion varied almost gradually,[1] so that to classify the motions was not easy. On the other hand, accurate determination of incidence of the distortional phase, especially in such an unusual case as this one ought not to be without value in studying the nature of the earth's crust. For this purpose, accurate determination of the seismic epicentre are extremely desirable. Through the courtesies on the part of the directors of several meteorological stations, and to whom the author records here his warmest thanks, it was possible to determine its epicentre as being $\varphi = 36°\ 26'\text{N}$ and $\lambda = 142°\ 30'\text{E}$. Seismograms obtained at the Mizusawa International Latitude Station will be reproduced here for the sake of comparison. (Fig. 12).

According to these records, the commencement of the distortional phase is well defined, and yet in the NS component slow motions with $9^s.5$ period can be seen. In this component of motion, the commencement of the distortional phase is less defined.

(1) These were not due to instrumental errors, since the proper period of the seismographs used was far greater than those of the incident movements.

Earthquake of Aug. 24, 1927.
(φ=36° 26′ N, λ=142° 30′ E)
(Observed at Hongô)

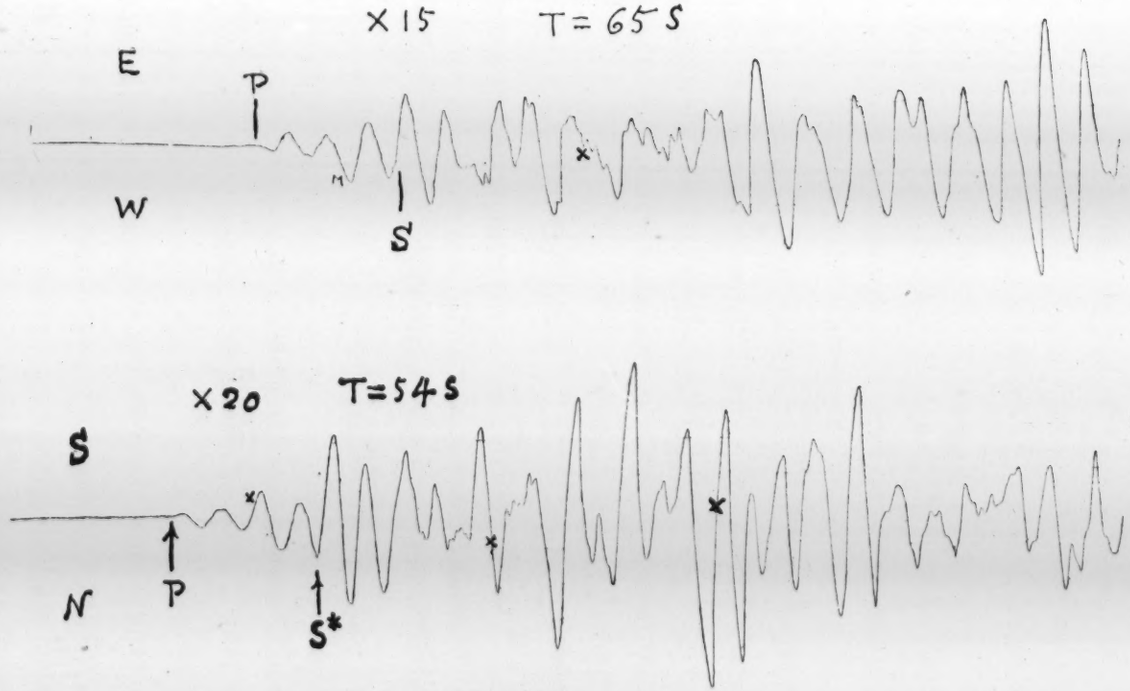

× Miuute mark.
(For S in the EW comp. read S*.)
Fig. 11.

Earthquake of Aug. 24, 1927.
(φ=36° 26′ N, λ=142° 30′ E)
(Observed at Mizusawa)

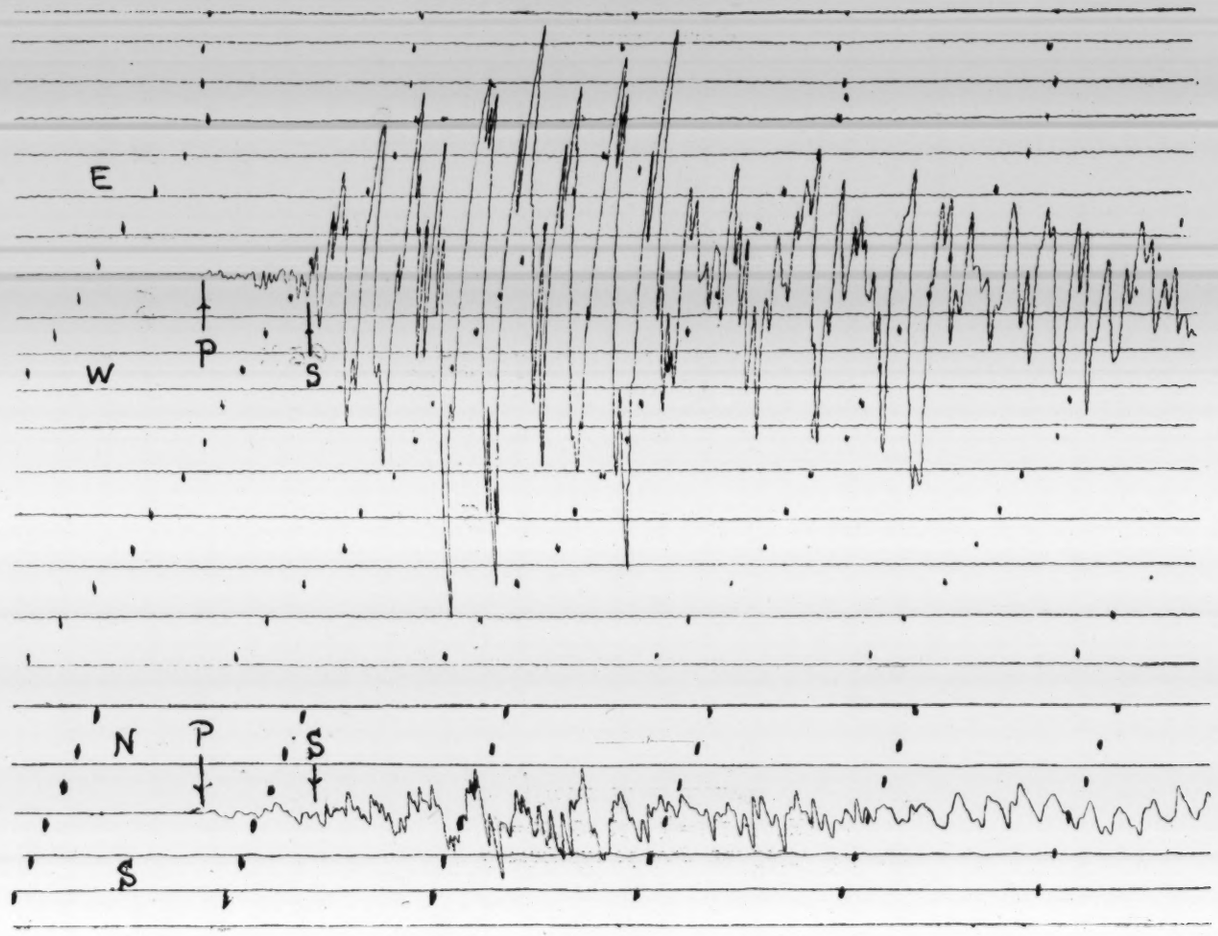

Fig. 12.

Returning to the case of Hongô, if the position of the epicentre is assumed as above, its epicentral distance will be about 250 km. For such a distance, the P-S and P-S* differences may be expected to be about 27 sec. and 37 sec. respectively. In Fig. 11 the S* can be found though not distinctly, at the expected position as a somewhat sudden increase of magnitude of motion. Thus the essential characteristic of this earthquake observed at Hongô is the long period of motions even in the dilatational movements. The epicentre was situated in the deep sea bed of the Pacific more than 3000 metres deep, and it will be included in th class of "Deep sea earthquakes" as proposed by Mr. K. Wadati.(1)

Comparison of seismograms at Hongô and at Mizusawa will show that the orientation of stations relative to the epicentre plays an important rôle in connection with the character of motions observed, which again will mainly be due to the mechanism associated with the particular earthquakes.(2)

IV. Concluding Remarks.

The foregoing examples leave no room for doubt as to the existence of three phases in the two movements, distortional as well as dilatational. The difference in their appearances, needless to say, depends on the depth of the seismic origin, and on the epicentral distance, and also on the mechanism of earthquake occurrence.

The presence of proofs that superficial crustal stratification may be expected even in such an unstable island area as Japan, goes a long way to show how persistent is the stratifying process, notwithstanding the remarkable geological disturbances the islands have been subjected to.

According to Wegener's hypothesis, the mode of stratification of land areas is not the same as what obtains in the bottom of the Pacific Ocean. A definite answer on this point is not deducible from the foregoing investigations of near earthquakes, for the reason that in every case investigated, the seismic wave traversed a considerable portion of terrestrial as well as suboceanic region. This point however willl be discussed in part IV.

(1) K. Wadati, Jorn. Meteor. Soc. Jap. [ii] **6** (1928) No. 1.
(2) T. Matuzawa, Jap. Journ. Astr. Geophys., **4** (1926) No. 1.

We shalll now offer a few remarks on the coefficient of a linear equation connecting the epicentral distance, (not very large, say, less than 1000 km.), and the duration of the preliminary tremor. In the equation $y=kt$, the valué of k was determined by F. Omori as $k=7.42$ (km/sec). This value of k has been usefull and convenient for determination of epicentres of earthquakes in Japan, especially for the case of earthquakes with epicentral distance of only a few hundreds of kilometres.

Roughly speaking, the physical meaning of k is that $k=\frac{v_P v_S}{v_P - v_S}$ where v_P is the velocity of propagation of the first phase and v_S is that of the second phase. Now that three phases in each of the dilatational and the distortional phase are identified, this point needs to be examined thoroughly.

Velocity of propagation of each phase is well expressed by

$v_P=7.5$ km/sec.(1) $v_P{}^*=6.1$ km/sec. $v_{\bar{P}}=5.0$ km/sec.

$v_S=4.5$,, $v_S{}^*=3.7$,, $v_{\bar{S}}=3.15$,,

In ordinary cases the first phase observed is the P. On the other hand, the second phase observed is frequently the S* in cases of ordinary inland earthquakes, an example of which is the Tango earthquake observed at Tôkyô. If such is the case, then the value of k will be 7.3 (km/sec) which is in accord with Omori's value.

In such cases as when the depth of origin of the earthquake is great, or when the epicentral distance is not small, the second phase observed will be the S. In such a case Omori's value cannot be applied, as was seen in the case of the earthquake of July 13, 1927, observed at Hongô, Tôkyô. The value of k will be expected to be 11.25(2) (km/sec.)

When an earthquake whose origin is not deep-seated is observed at a small distance, the first phase observed corresponds to the $\overline{P}$ and the second will be the S. In such a case k is calculated as 8.51 (km/sec.) which is not very different from experience.

---

(1) This value will be discussed in part III.

(2) After this paper was written, the author came across a paper by Mr. M. Simizu (Journ. Meteor. Soc. Japan [ii] **6** (1928) 261–263) in which exactly the same value was given from direct determination of k, using earthquakes of moderate distance. His cases seem to have been very favourable for observation of the P and the S phase respectively.

In the above discussions, if the effects of each layer traversed by a trajectory of waves are taken into account, the problem will naturally be complicated. At any rate, a suitable interpretation of observed waves is of paramount importance in applying the linear equation.

July 4, 1928.

Supplement to Section II; Earthquake of July 7, 1928.

After the close of the preceding paper, data of the earthquake on July 7, 1928 became available. This was a strong earthquake which occurred in the approximate middle part of the Kii-Suidô, its geographic coordinates were $\varphi = 34°\ 00'$N and $\lambda = 134°\ 52'$E approximately. Localities where the shock was felt with our unaided senses were distributed somewhat wide. For example, at Kure about 200 km. distant from the epicentre it was felt slightly. Data were taken from "Kisyô Yôran" and tabulated below.

TABLE IV.

No.	Station	φ (N)	λ (E)	Δ (km.)	Time of Comm.	P.T.
					h m s	s
1	Tokusima	34° 4′	134° 33′	30.2	17 39 38.5	6.0
2	Wakayama	34 14	135 9	36.8	43.0	8.5
3	Kôbe	34 41	135 11	79.5	47.0	11.1
4	Siomisaki	33 27	135 46	96.3	44.4	11.6
5	Muroto	33 15	135 11	105.4	47.4	10.0
6	Tadotu	34 17	133 46	109.1	47.0	13.0
7	Yagi	34 31	135 48	109.1	48.8	12.6
8	Oosaka	34 39	135 26	109.9	44.6	15.2
9	Kôti	33 33	133 32	134.9	51.1	13.6
10	Kyôto	35 1	135 44	138.6	53.4	16.8
11	Toyooka	35 32	134 49	170.1	59.2	20.9
12	Tu	34 44	136 31	173.8	59.3	15.2

(to be continued.)

(Continued.)

No.	Station	φ (N)	λ (E)	Δ (km.)	Time of Comm.	P. T.
13	Matuyama	33 50	132 45	199.7	17 39 54.0	15.7 ?
14	Hikone	35 16	136 15	192.3	59.0	21.2
15	Hirosima	34 23	132 27	229.3	40 2.4	23.4
16	Nagoya	35 10	136 58	231.1	6.6	24.8 PS 27.6 PL
17	Gihu	35 24	136 46	234.8	7.9	25.0
18	Hukui	36 3	136 16	262.5	13.5	23.0
19	Hamada	34 54	132 4	275.5	9.6	25.5
20	Ooita	33 14	131 37	314.3	17.7	48.8
21	Takayama	36 9	137 15	323.5	15.4	14.7 ?
22	Matumoto	36 14	137 59	375.3	19.0	24.0 ?
23	Kôhu	35 38	138 34	384.6	26.8	37.9
24	Numazu	35 6	138 51	384.6	29.5	59.0
25	Miyazaki	31 55	131 26	395.6	24.5	37.3
26	Kumamoto	32 49	130 42	408.6	27.2	
27	Hukuoka	33 35	130 25	414.2	26.8	65.9
28	Oiwake	36 20	138 33	422.8	34.2	42.5
29	Nagano	36 40	138 12	425.3	39.3	51.3
30	Unzendake	32 44	130 15	451.1	31.6	20.8
31	Yokosuka	35 17	139 40	462.2	47.6	56.8
32	Yokohama	35 27	139 39	465.9	43.4	60.0
33	Maebasi	36 24	139 4	465.9	48.1	37.9
34	Nagasaki	32 44	129 52	484.4	35.6	
35	Tôkyô	35 41	139 46	484.4	47.0	65.0
36	Kagosima	31 34	130 33	484.4	48.9	
37	Kumagai	36 9	139 23	493.7	38.6	49.1
38	Sakai	35 33	133 14	229.2	{23.9 S ?	{18.0 S* ?
39	Hongô	35 43	139 46	484.2	42.9	38.9 S 60.8 S*

Using these data the time-distance diagram has been constructed as shown in Fig. 13.

Earthquake on July 7, 1928.
($\varphi = 34°\ 00'$ N, $\lambda = 134°\ 52'$ E)

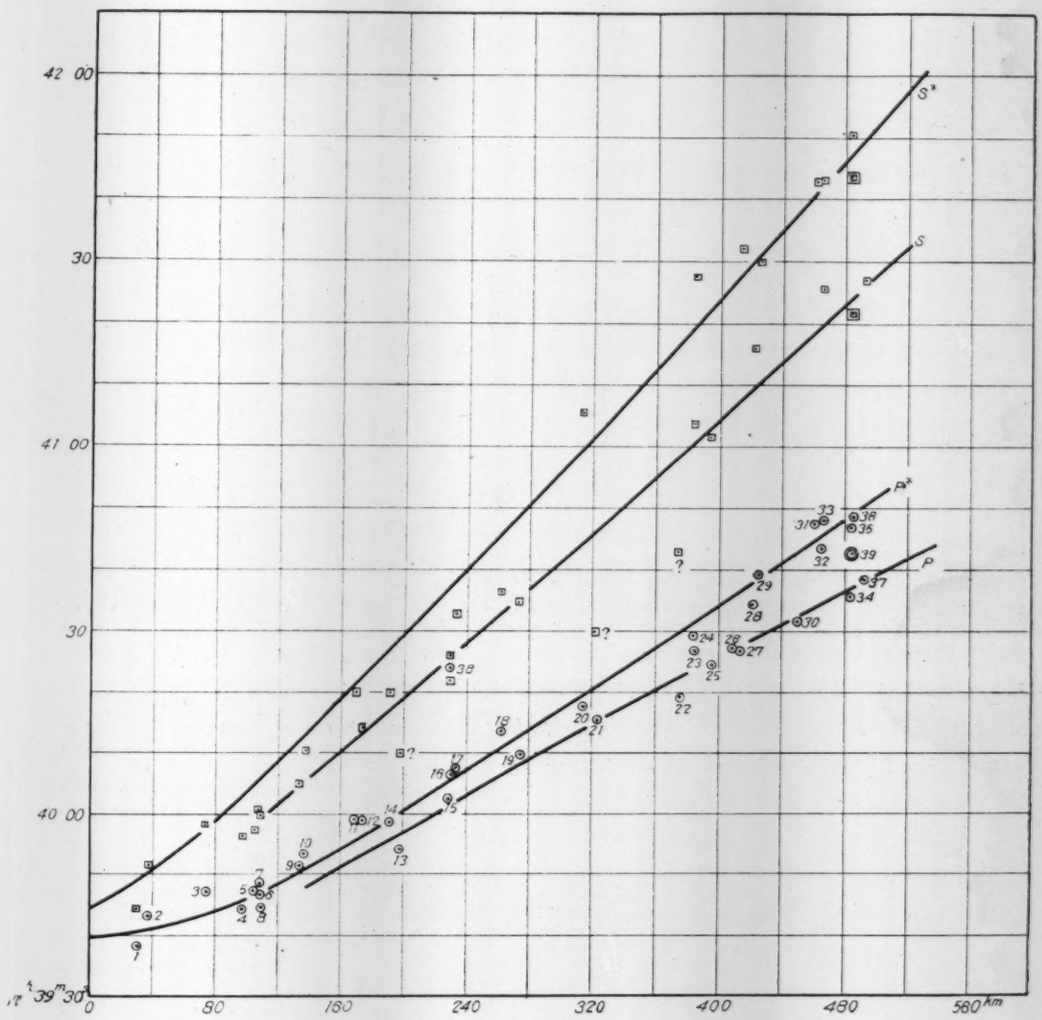

Fig. 13.

In the figure, the double circle and the double square were plotted using the data determined by the present author. With regard to the dilatational phase, the reported time of commencement was confined mainly between the P and the P* curves. Even at Hongô, the commencement of the P phase was very small in magnitude and moreover too disturbed by pulsatory motions to be determined accurately. Consequently a certain point between the P and the P* was judged as the commencement. The time of com-

mencement reported by the Central Meteorological Station was quite in accord with that of the P*. The reported time of commencement of the principal portion is grouped fairly well into that belonging to the S and to the S*. At Hongô, the S and the S* were well defined, though the magnitude of the former was very small compared with that of the latter. The general appearance of the time-distance diagram in this case is quite similar to that of the earthquake on Aug. 3, 1926 off the coast of Haneda (see Fig. 8). Therefore, remarks similar to those stated in that case will be applied in this case. Thus, this will be a good example showing that the mode of propagation in the case of earthquakes in the western Japan is not essentially different from that in the case of earthquakes in the eastern Japan.

Sept. 28, 1928.

When this paper was in the press, Dr. H. Jeffreys kindly send me his paper "On two British Earthquakes" (Monthly Notice of R. A. S. Geophys. Suppl. **1** (1927) No. 9) in which three phases in the distortional waves were also clearly shown. Dr. V. Conrad, who has remarked the existence of the P* phase for the first time, was also kind enough to send me "Das Schwadorfer Beben vom 8 Obtober 1927" (Gerl. Beitr. z. Geophys. **20** (1928) Ht. 3/4) in which similar subjects were shown.

ERRATA TO PART I.

Page 5, line 21. For 18.2 read 20.6
„ „ 125 „ 147×2.

Earthquake of Feb. 4, 1926.
($\lambda = 41° 22'$ N, $\varphi = 142° 25'$ E)

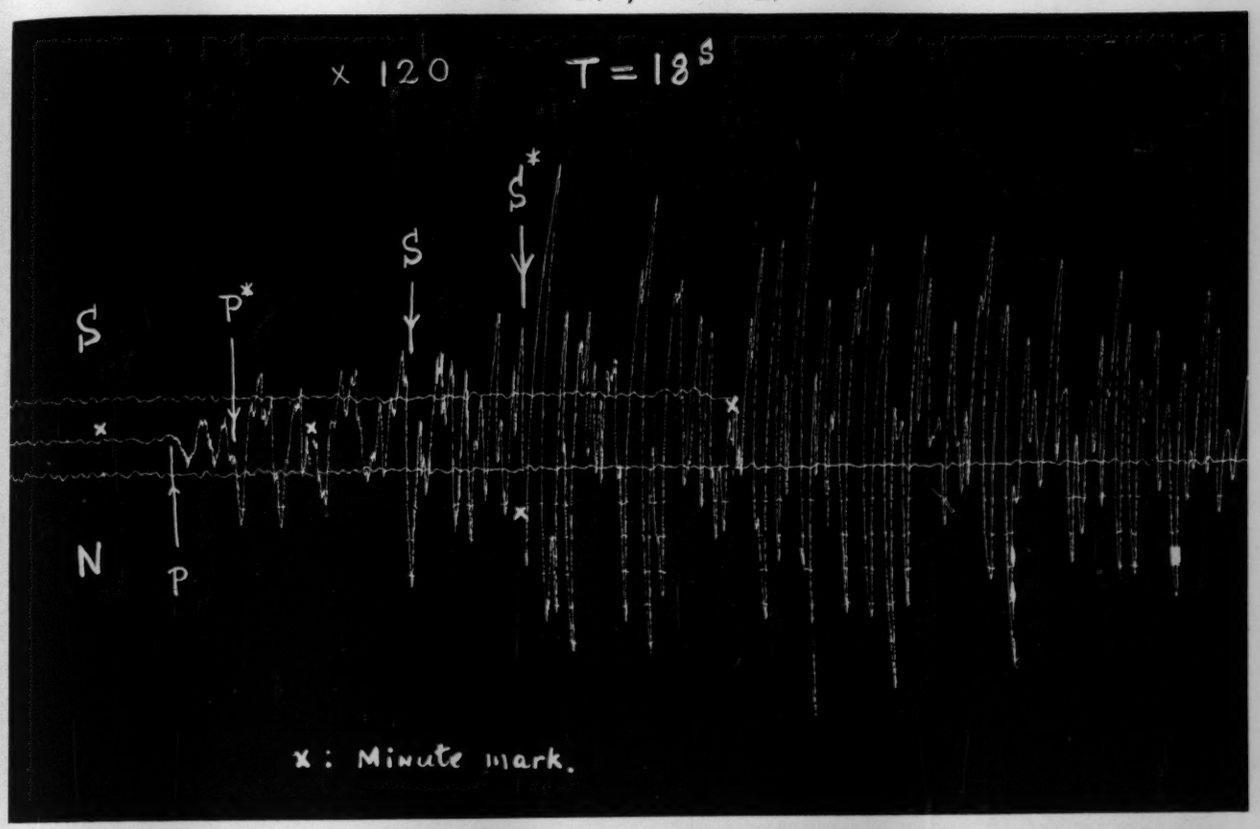

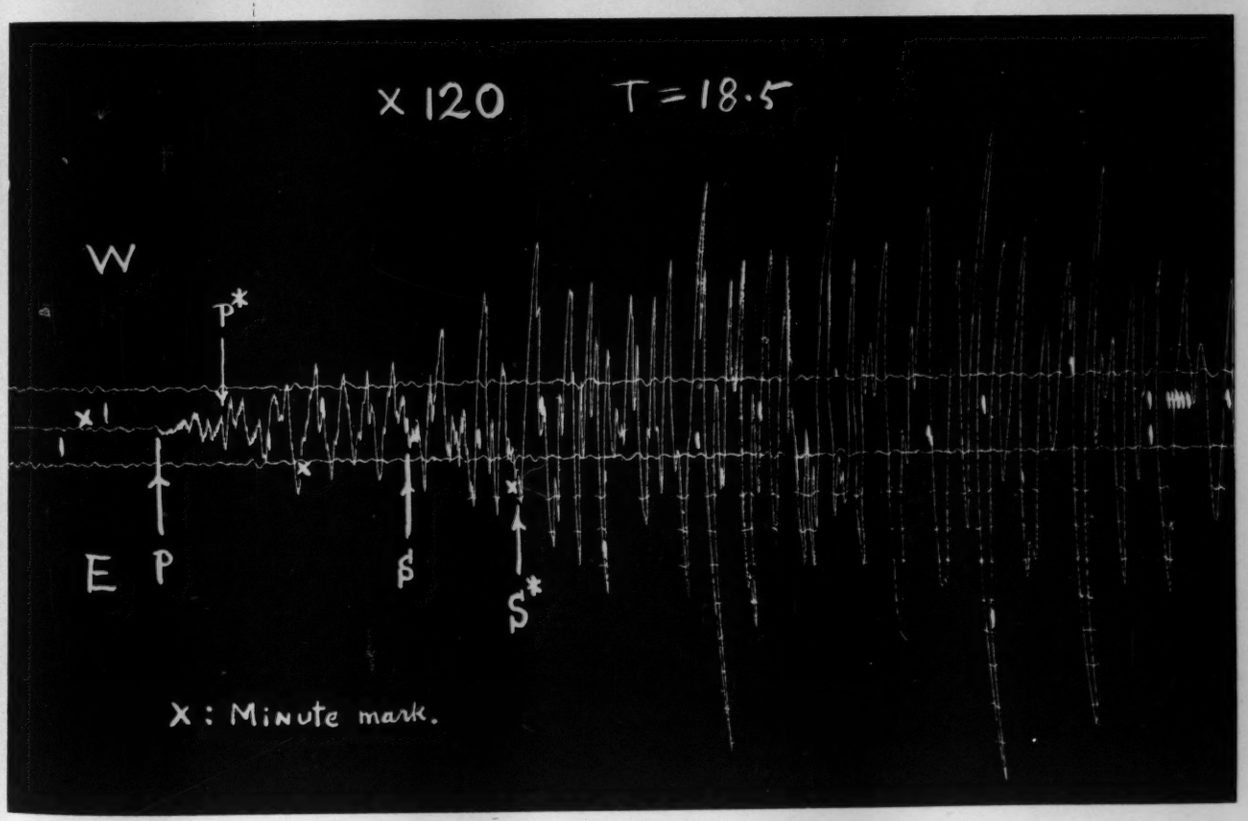

Fig. 3.

（震研彙報、第六號、圖版、松澤）

Earthquake of Feb. 4, 1926.
(φ=41° 22′ N, λ=142° 25′ E)

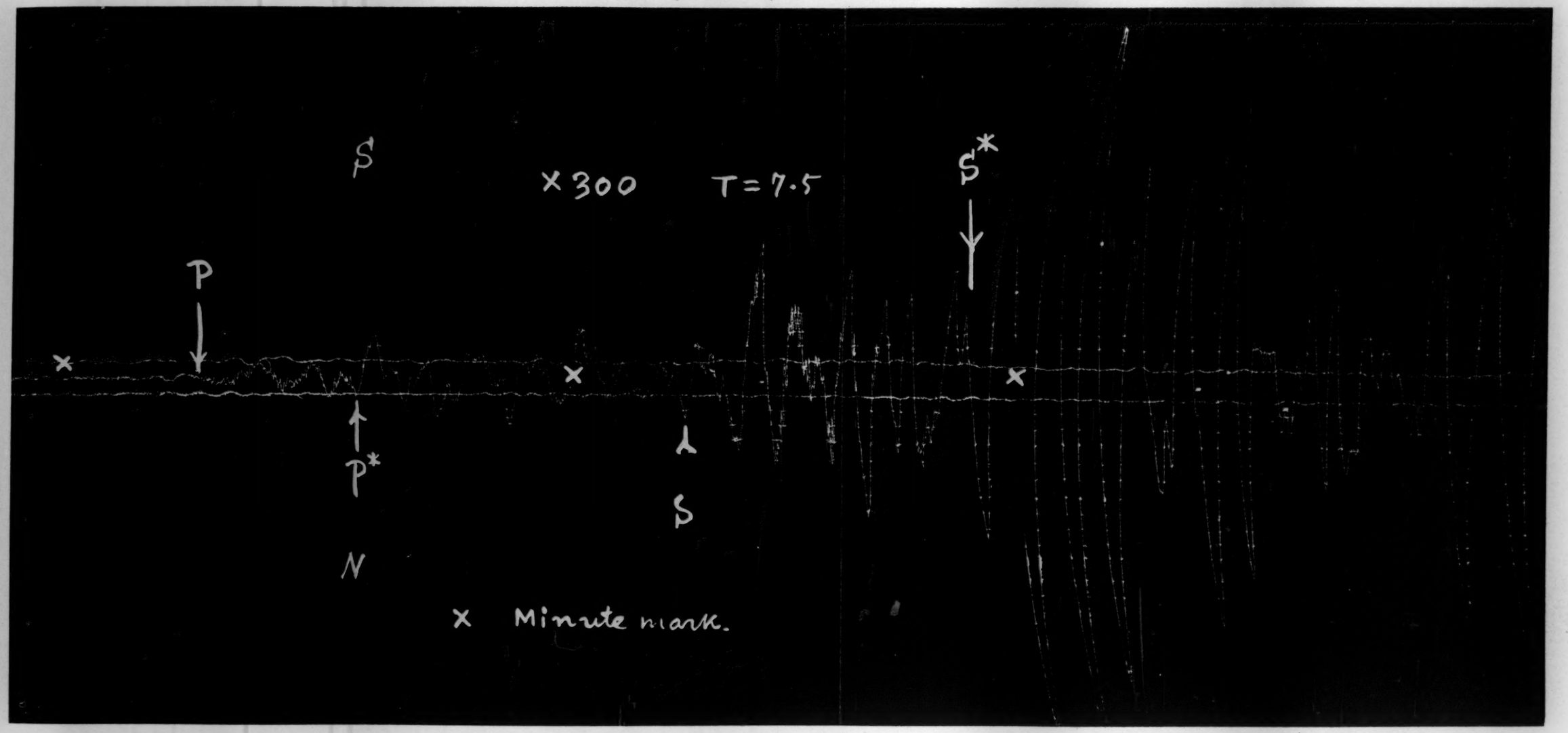

Fig. 4.

（震研彙報、第六號、圖版、松澤）

Time-Distance Curve of Earthquake on July 13, 1927

($\varphi = 42°\ 36'$ N, $\lambda = 145°\ 35'$ E)

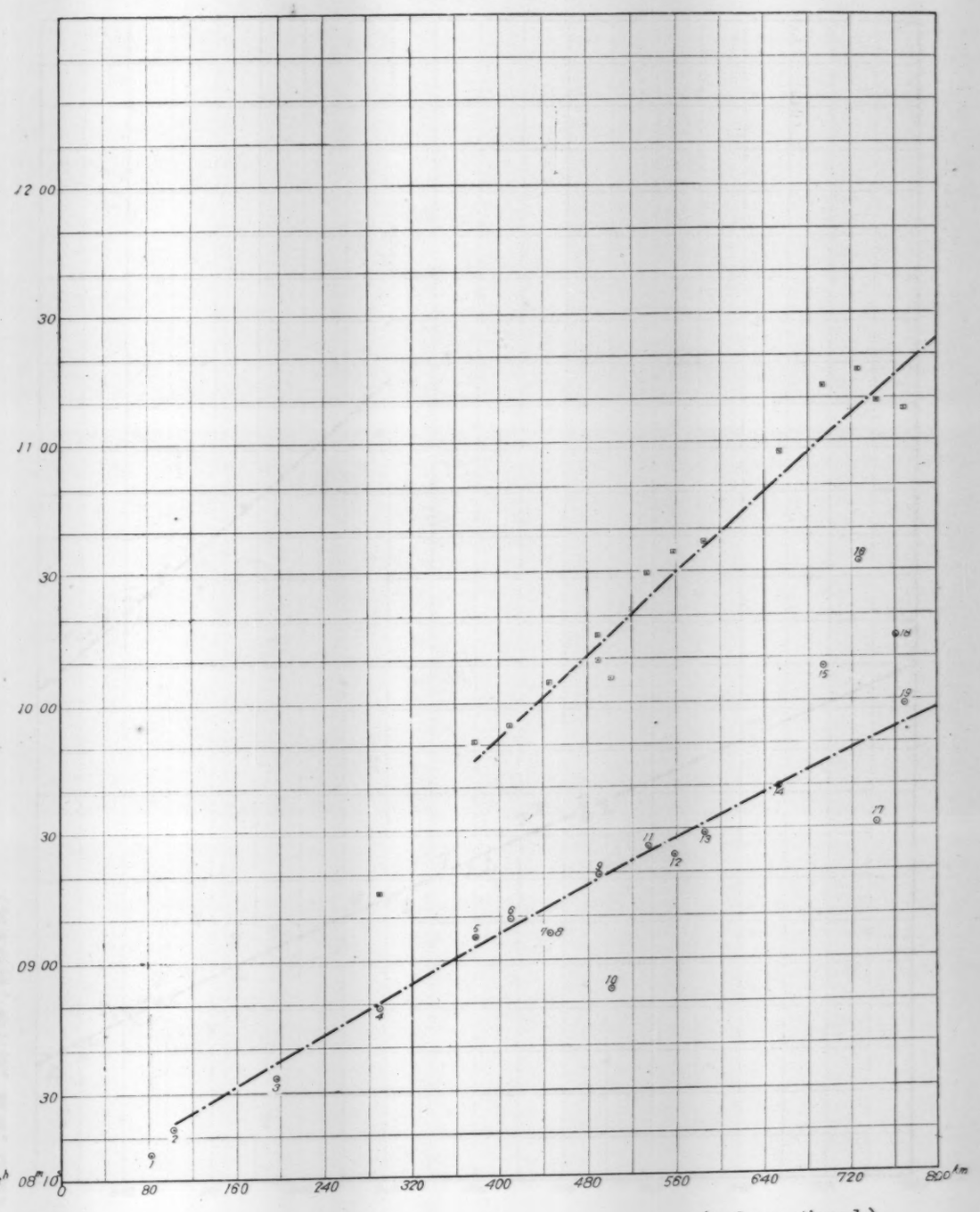

(to be continued.)

(Numbers are to be referred to Table II.)

Fig. 5.

（震研彙報、六號、圖版、松澤）

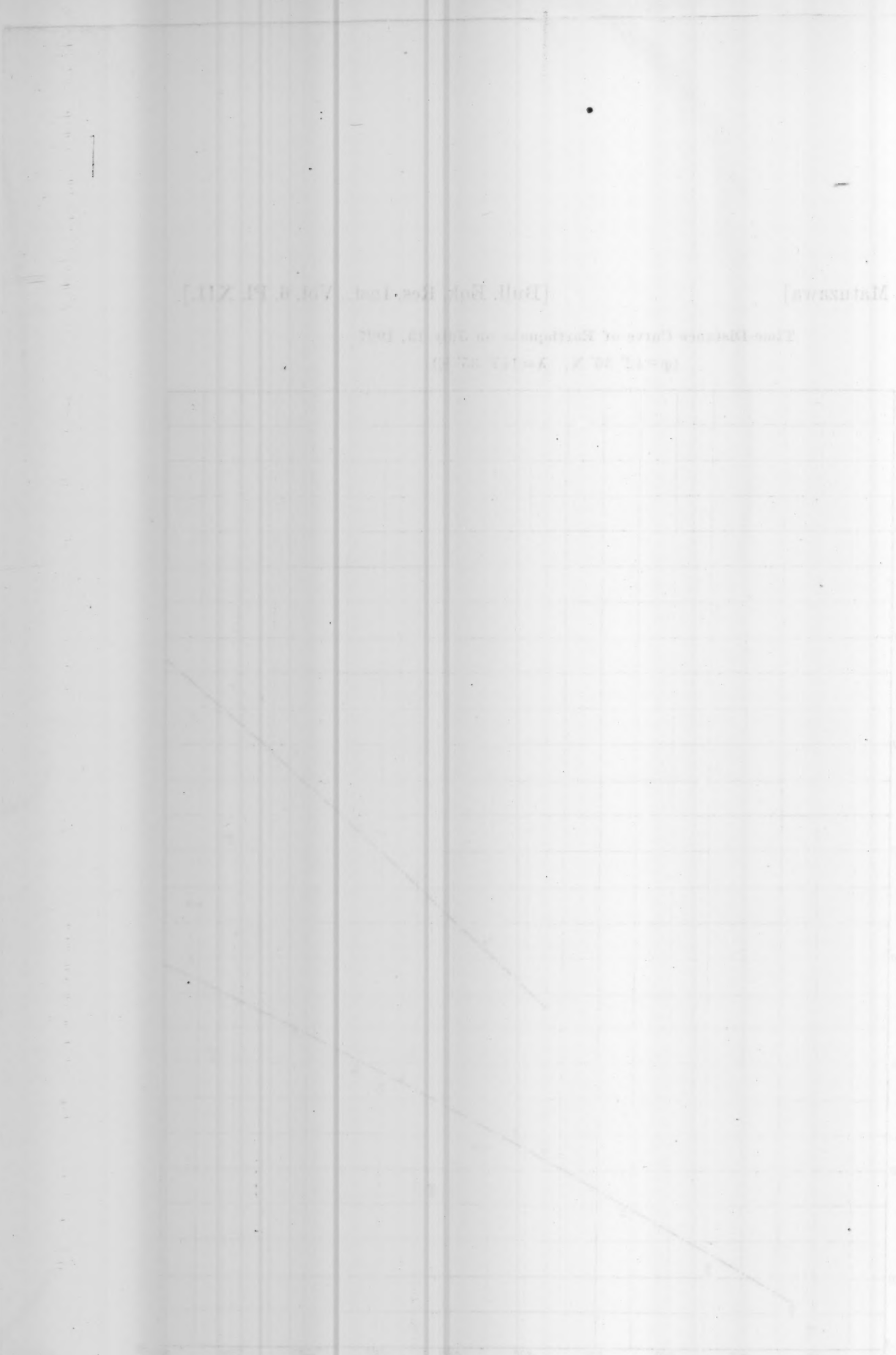

(Continued.)

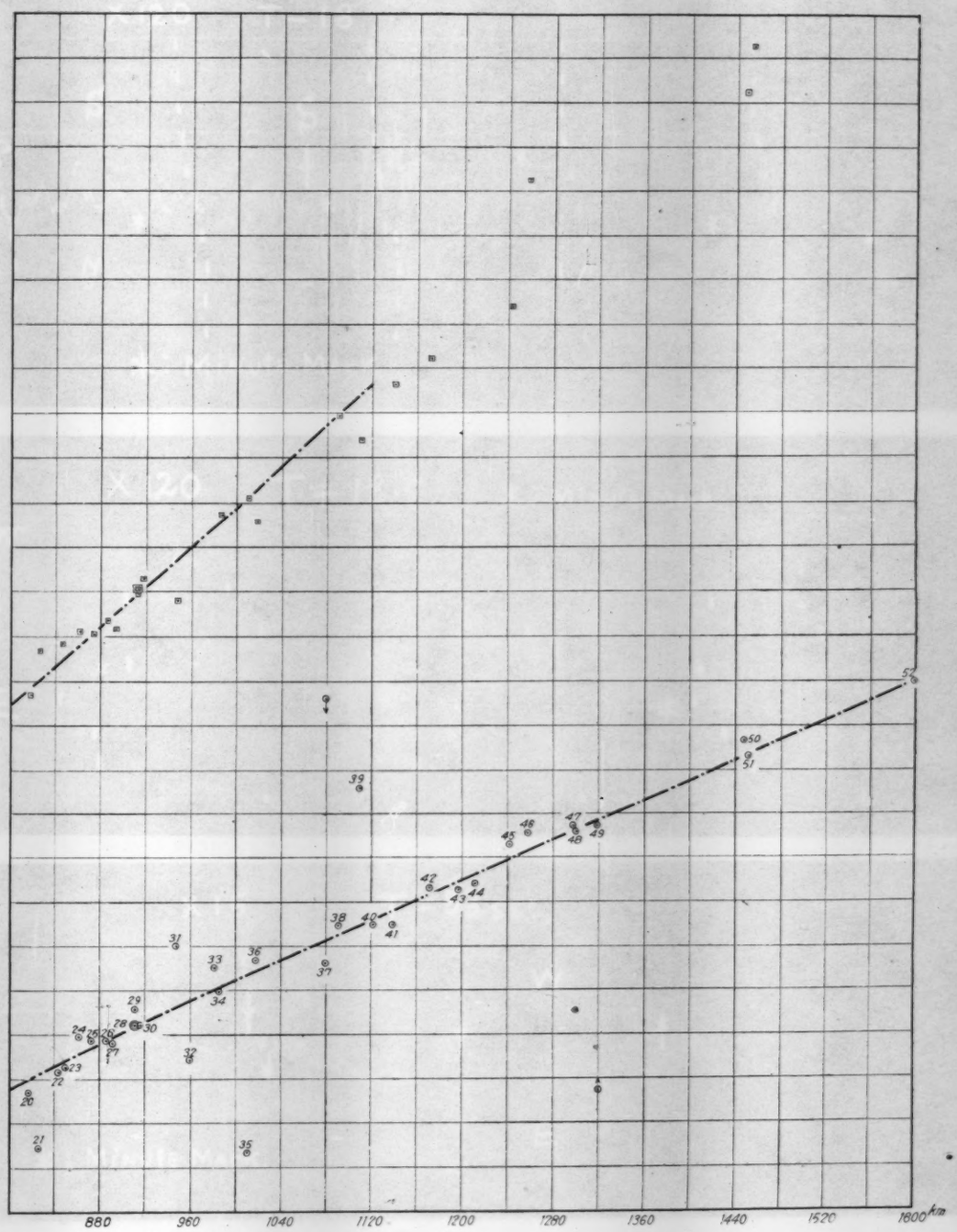

Fig. 5.

(震研彙報、第六號、圖版、松澤)

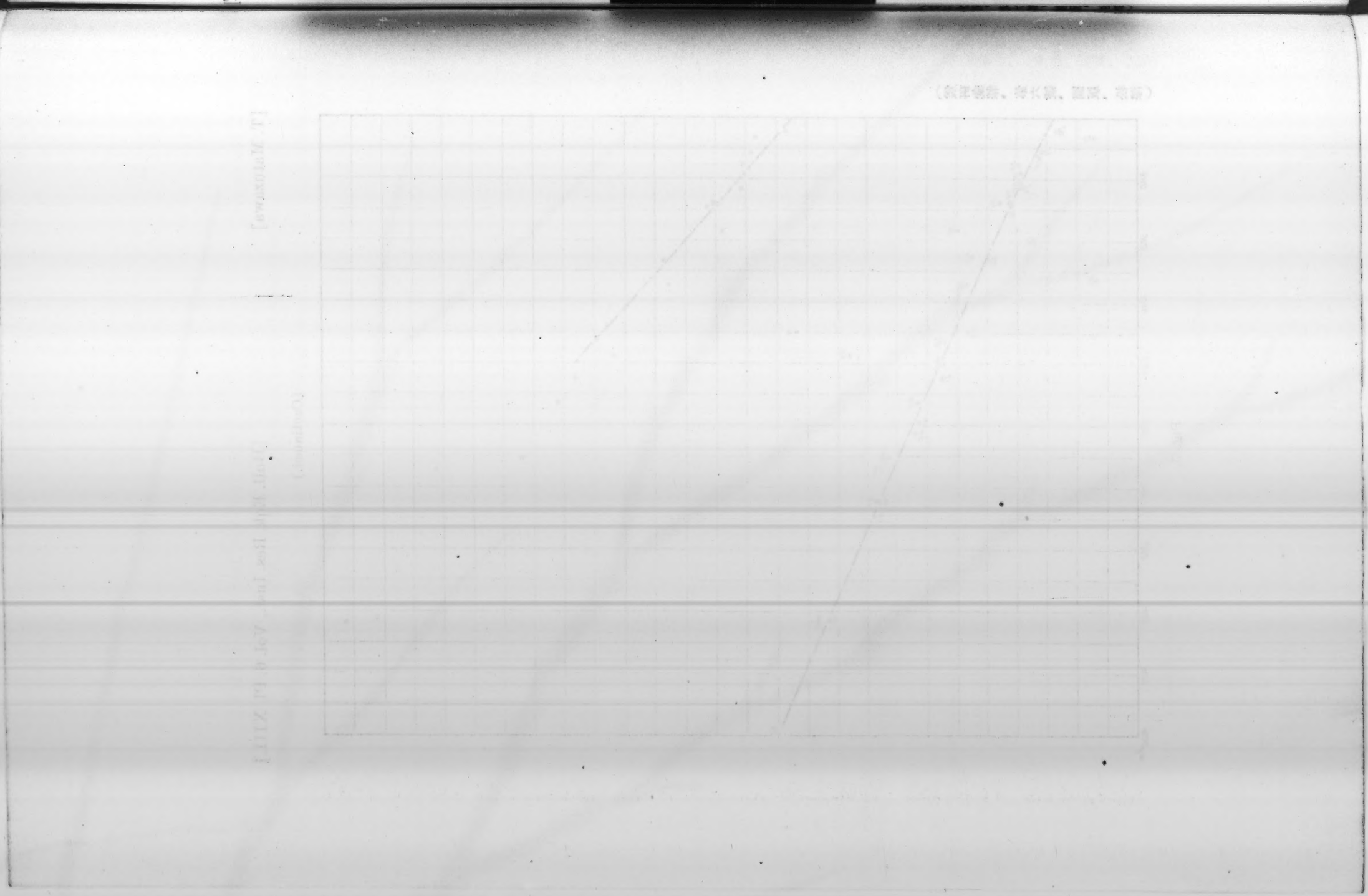

Earthquake of June 5, 1026.
($\varphi = 42°\ 36'$ N, $\lambda = 145°\ 35'$ E)

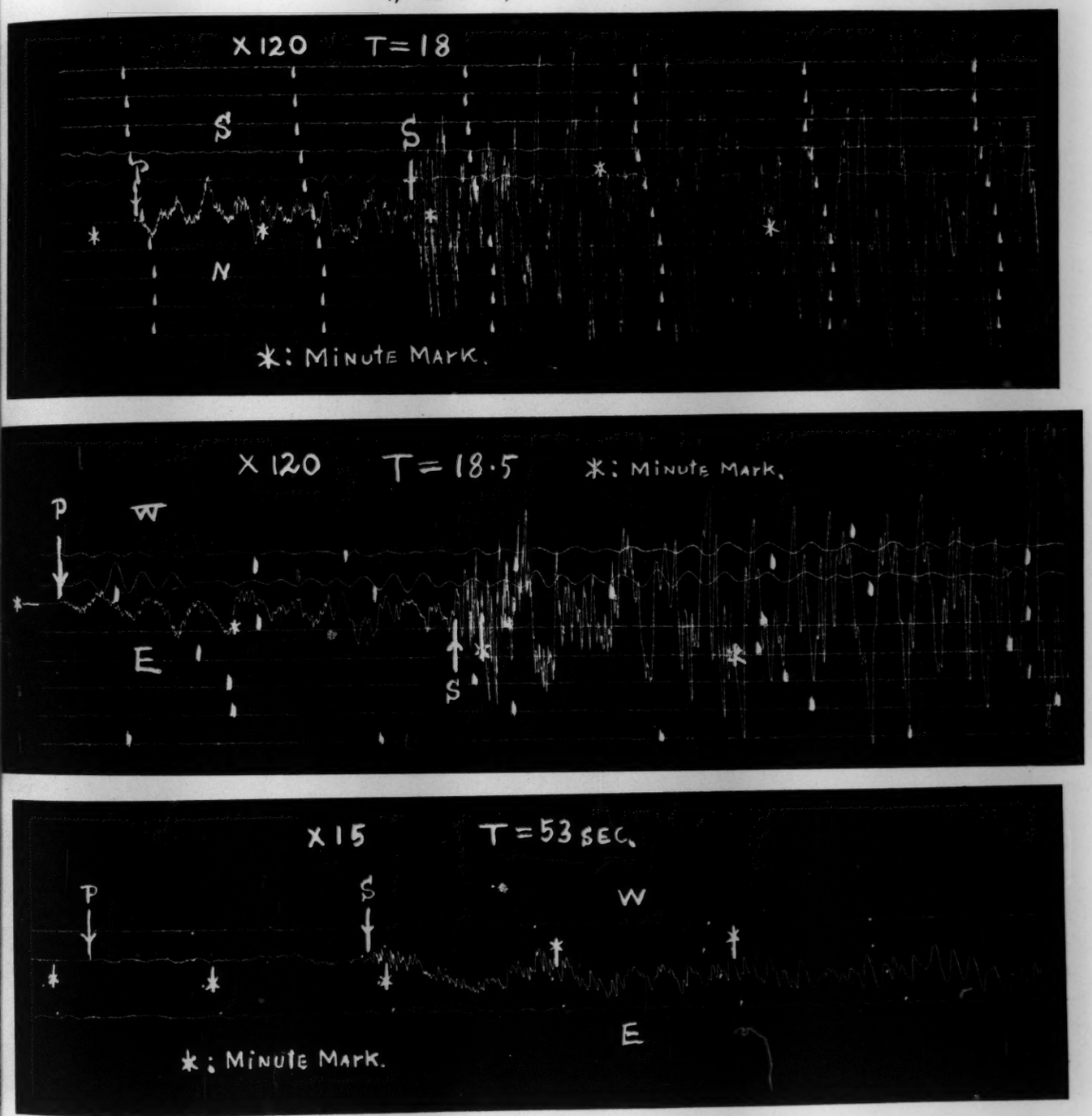

Fig. 6.

Earthquake of July 13, 1927.
($\varphi = 30°\ 26'$ N, $\lambda - 130°\ 40'$ E)

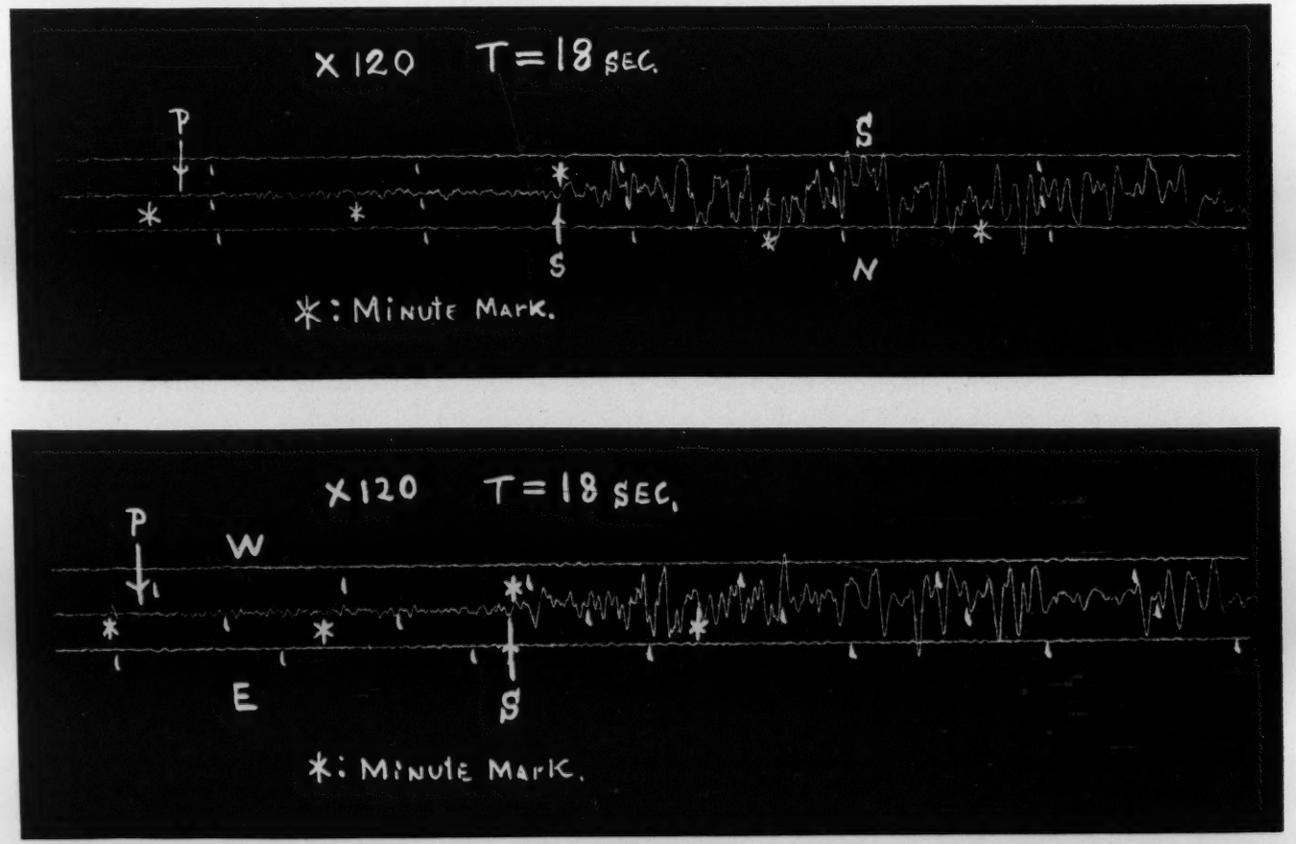

Fig. 10.

（震研彙報、第六號、圖版、松澤）

Observation of Some Recent Earthquakes and Their Time-distance Curves.

(Part III.)

By **Takeo MATUZAWA,**

Nukigaki (abstract in Japanese.)

(1) Sono I de motometa P Nami no Sôzi-Kyokusen no Kaiseki wo kokoromita. Hyômen ni tikai hutatuno Sô no Eikyô wo kangaete sono sita no Sô ni okeru mono wo keisan sita.

(2) Hyômen kara 120 km. gurai no Tokoro de Nami no Hayasa no Masikata no niwakani kawaru Tokoro ga aru yôni mieru.

I. INTRODUCTION.

It has turned out that the time-distance curve obtained in part I can well be applied for near stations, except, however, for extremely near places (say less than 500 km. or so), where the effect of the focal depth and the areal extent of the focal region affects considerably the slope of the curve. At present, the author is not aware of any method of reduction of the source of waves to a point for reasons stated in part I.[1] Therefore, the result of analysis of the curve may not be free from objections from the standpoint of mathematical rigorousness, although any attempts at such investigation from different view points will not be a mere waste of time.

II. ANALYSIS OF THE TIME-DISTANCE CURVE OF THE P PHASE.

As regards the time-distance curve of the P phase within short distances, that of the Tango earthquake will be considered since the effects due to the dimension of the epicentral region seem to be smaller than that of the Kwantô earthquake. At a greater distance, the curves for both earth-

(1) T. Matuzawa, this Bull. 5 (1928) 25.

quakes approach[1] each other and eventually coincide.

The depth of the origin of the P movements will tentatively be assumed to lie in the middle part of the second layer, that is, at a depth of 35 km.[2] The velocity of propagation in the first and the second layer is assumed as constant and to be 5.0 km/sec. and 6.1 km/sec., while the thickness of each of them is assumed to be 20 km. and 30 km. respectively. Thus the problem becomes one of the distribution of velocity in the lower layer below 50 km.

The reduction of the observed time-distance curve to the focal depth can be applied at the same time by means of the reduction with regard to the superficial stratifications.

At first it is necessary to construct the T-Δ diagram reduced to the lower layer. Corrections which must be applied are as follows (refer to Fig. 1).

$\Delta_1 = d_1 \tan i_0$, reduction to the distance in the first layer

$\Delta_2 = \frac{3}{2} d_2 \tan i_1$, " " " " " " second layer

$t_1 = \frac{d_1}{v_1 \cos i_0}$, " " " time " " first layer

$t_2 = \frac{3}{2} \frac{d_2}{v_2 \cos i_1}$, " " " " " " second layer

where $\sin i_0 = v_1 \frac{\partial T}{\partial \Delta}$ and $\sin i_1 = \frac{v_2}{v_1} \sin i_0$.

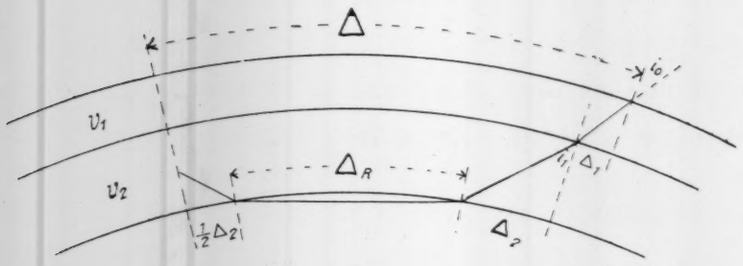

Fig. 1.

(1) This would seem paradoxical if the medium were homogeneous, but as the observed P phase is a refracted wave with an initial downward trend, the effect of the horizontal area of the source will gradually become obscure at a distance.

(2) The observed distance, 120 km. in round numbers, of the first appearance of the P phase is in accord with this assumption.

Therefore, from the T-Δ curve at the surface, the $T_R - \Delta_R$ curve will be obtained. The values are tabulated in table I.

TABLE I.

Δ_R km.	0.0	92.0	314	525	732	935	1138	1339
T_R sec.	−3.9	10.0	40.9	69.25	95.6	119.6	143.6	167.6

1542	1745	1949	2151	2354	2557	2759.5	2860
191.8	214.7	236.4	256.6	277.3	298.1	317.7	327.2

The T-Δ curve by these values is partly shown in Fig. 2.

The negative value of t at the origin can be considered as being due to the effect of areal extent of the focal region. Therefore, a curve so drawn from the origin as to be asymptotic to the curve at some 550 km. or so will be very near to that reduced to a point source.

In the next place, the reduced curve will be analysed. The formula for its analysis is

$$\log_{10} r_m = \log_{10} R - \frac{\log_{10} e}{\pi R} \int_0^{\Delta} x d\Delta$$

where r_m is the minimum distance from the centre of the earth to which a trajectory of waves emerging at a distance Δ attains, R is the radius of the earth and $x = \cosh^{-1} \frac{\sin(i_0)}{\sin(i_0)_{\Delta}}$ in which $(i_0)_{\Delta}$ is the angle of incidence at the station considered, and (i_0) is that at a certain intermediate station. This equation can favourably be applied in this case, for it corresponds to that in which there are no longer any layers of discontinuity and the starting point of the waves is situated at the surface. In this case, reducing the thickness of superficial layers, 50 km., from the mean radius of the earth, $R = 6317$ km. The equation then becomes

$$\log_{10} r_m = 3.80051 - 0.00002188 \int_0^{\Delta} x d\Delta \text{ in km.}$$

The velocity of propagation at r_m can easily be calculated by

$$v = v_0 \frac{r_m}{R \sin i_0} .$$

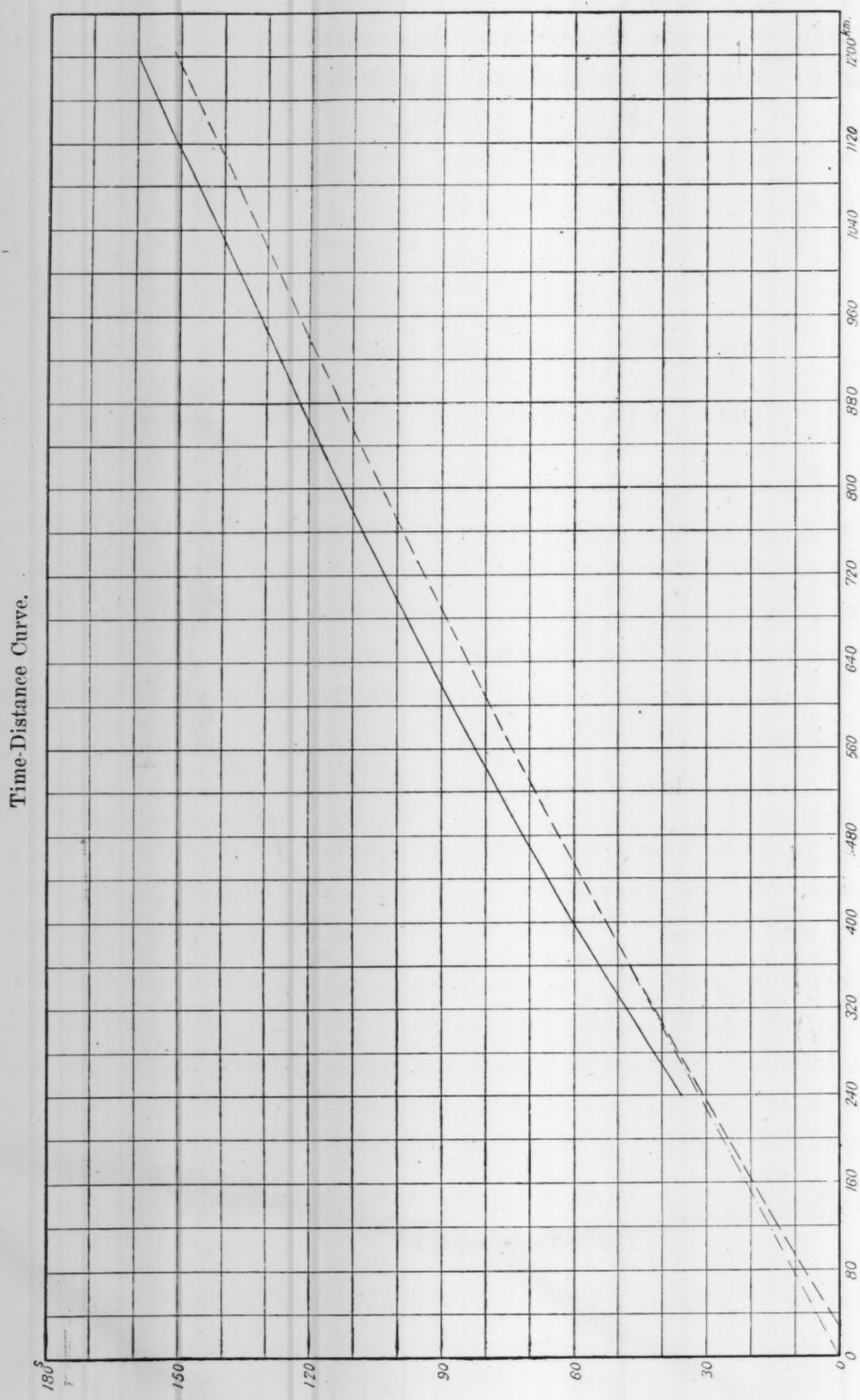

(Full curve: That of the Kwantô Earthquake on Sept. 1, 1923).

Fig. 2.

At first, the curve without artificial treatment with regard to the effect of focal area will be examined. The $\Delta - \sin i_0$ values are tabulated in Table II.

TABLE II.

Δ km.	0.00	200	400	600	800	1000	1200	1400
$\sin i_0$	1.00	0.977	0.935	0.883	0.845	0.825	0.806	0.790

1600	1800	2000	2200	2400	2600	2800
0.773	0.750	0.727	0.706	0.687	0.668	0.652

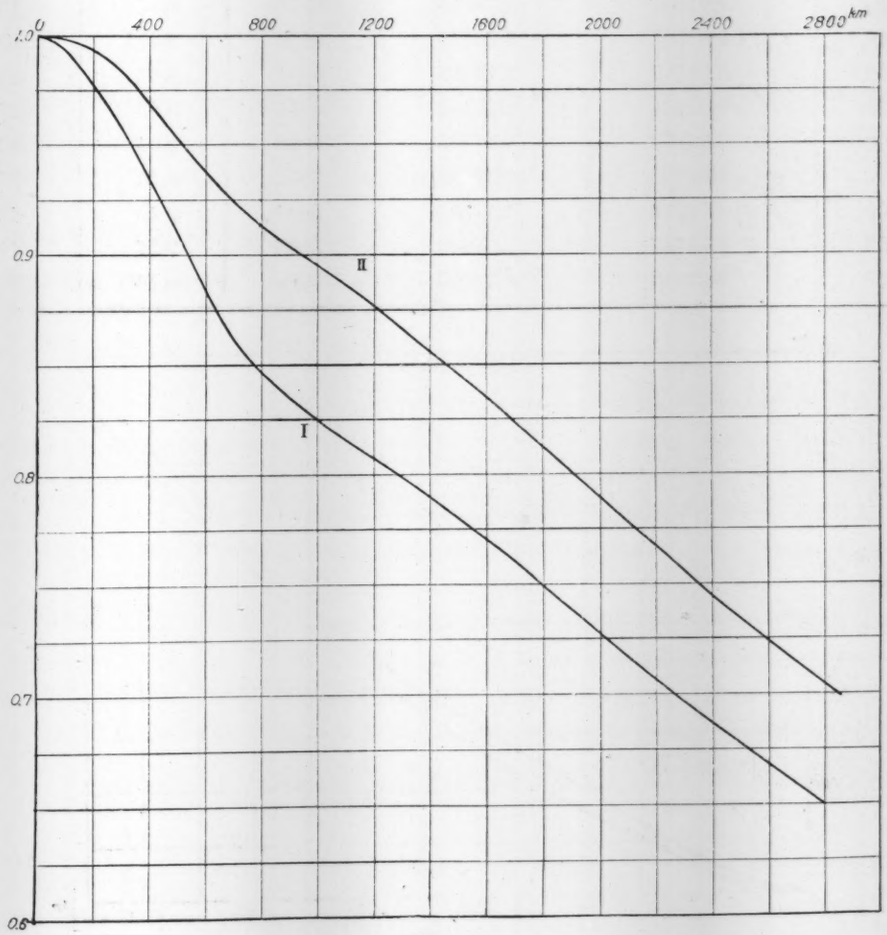

Fig. 3.

The relation is shown by curve I in Fig. 3.

From this relation of Δ and $\sin i_0$, a set of $\Delta - x$ curves can be obtained. Therefore, the integration can easily be evaluated mechanically. Accordingly, $\Delta - r_m - v$ relations can be obtained as tabulated in Table III.

TABLE III.

Δ km.	$0.00002188\int_0^{\Delta} x d\Delta$	$\log_{10} rm$	rm	v	$R-rm$
200	0.00065	3.79986	6308	7.07	9
400	0.00231	3.79820	6283	7.36	34
600	0.00486	3.79565	6247	7.75	70
800	0.00717	3.79334	6214	8.055	103
1000	0.00880	3.79171	6190	8.22	127
1200	0.01107	3.78944	6158	8.37	159
1400	0.01334	3.78717	6126	8.495	191
1600	0.01563	3.78488	6094	8.64	223
1800	0.01918	3.78133	6044	8.83	273
2000	0.02236	3.77815	6000	9.04	317
2200	0.02660	3.77391	5942	9.22	375
2400	0.03006	3.77045	5895	9.40	422
2600	0.03447	3.76604	5835	9.57	482
2800	0.03715	3.76336	5799	9.74	518

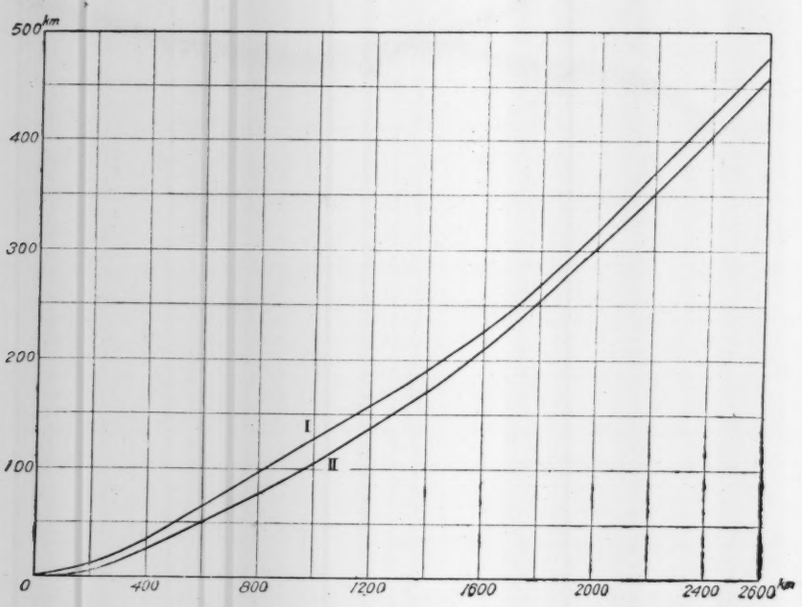

Fig. 4.

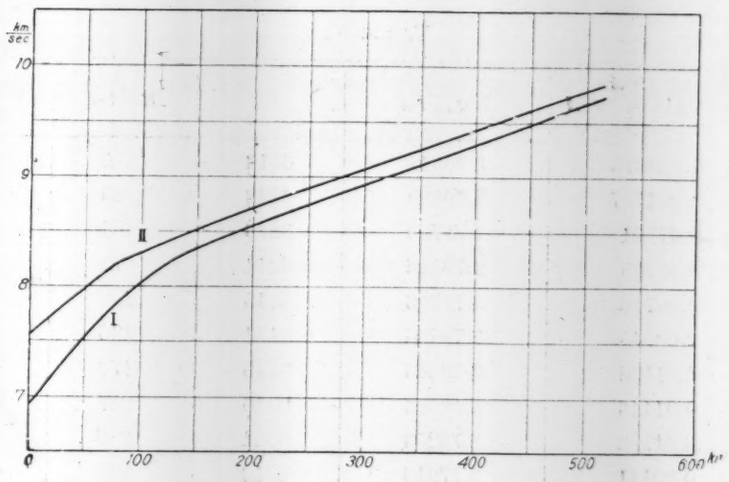

Fig. 5.

The curve I in Fig. 4 shows the Δ—$(R-r_m)$ relation and the Curve I in Fig. 5 shows the relation between the depth $(R-r_m)$ and the velocity of propagation.

In a process similar to the above, the curve with tentative reduction to a point source as stated before will be examined. The $\Delta-\sin i_0$ relation is tabulated in Table IV and shown in Fig. 3 (curve II).

TABLE IV.

Δ km.	0.00	200	400	600	800	1000	1200	1400
$\sin i_0$	1.00	0.995	0.970	0.938	0.913	0.897	0.876	0.855

1600	1800	2000	2200	2400	2600	2800
0.836	0.813	0.790	0.769	0.748	0.725	0.705

(Remark; v_0 becomes 7.55 km/sec. from $\left(\frac{\partial T}{\partial \Delta}\right)$ at $\Delta=0$).

The $\Delta-r_m-v$ values can be seen in Table V, while the Δ—$(R-r_m)$ relation and the v—$(R-r_m)$ relation can be seen in Fig. 4 (curve II) and in Fig. 5 (curve II) respectively.

TABLE V.

Δ km.	$0.00002188\int_0^{\Delta} x d\Delta$	$\log_{10} rm$	rm	$R-rm$	$v=\frac{7.55}{6317}\times\frac{rm}{\sin i_0}$
200	0.000375	3.80014	6312	5	7.58
400	0.001707	3.79880	6292	25	7.75
600	0.00351	3.79700	6266	51	7.98
800	0.00505	3.79546	6244	73	8.17
1000	0.00708	3.79343	6215	102	8.28
1200	0.00945	3.79106	6181	136	8.43
1400	0.01196	3.78855	6145	172	8.59
1600	0.01448	3.78603	6110	207	8.735
1800	0.01798	3.78253	6061	256	8.91
2000	0.02141	3.77910	6013	304	9.10
2200	0.02483	3.77568	5966	351	9.27
2400	0.02849	3.77202	5916	401	9.45
2600	0.03286	3.76765	5857	460	9.655
2800	0.03699	3.76352	5801	516	9.835

The value of velocity, 7.55 km/sec., obtained from the corrected curve is not far different from that by Mohorovičič, 7.6 km/sec. As will be seen from Fig. 5, the rate of change of velocity seems to undergo a sudden change at the depth of 70 km. or so from the lower discontinuity, that is, about 120 km. from the surface of the Earth. This value seems to coincide with that of the depth of isostatic compensation obtained by Helmert and Hayford. Whether or no this apparent coincidence is due to an accidental error of observation, will no doubt be solved in the course of time.

One more remark will be added. If the original time-distance curve of earthquakes is determined only from the data of stations at considerable epicentral distance, and a part of the curve near the origin is constructed by producing the part of the curve at a distance, then a curve corresponding to that of Fig. 5 will be such that a sudden change of direction cannot be found, and the velocity at the origin will be estimated as 8.0 km/sec. or so. This value seems to be nearly the same as that obtained by B. Gutenberg.

July 4, 1928.

Observation of Some Recent Earthquakes and their Time-Distance Curves.

(Part IV.)

By **Takeo MATUZAWA,**

Nukigaki (abstract in Japanese.)

(1) Zissai no Zisin no Baai ni *Rayleigh* oyobi *Love* no tonaeru yôna Hyômen ni tutawaru Nami no Kwansoku sareru koto wo tokiakasita.

(2) Korera no Nami wa aru *Dispersion* wo simesu. Sosite sono Zyôkyô wa Tairiku wo tutawaru mono to Taiheiyô wo tutawaru mono tode medatta Tigai ga aru.

(3) *Dispersion* no Seisitu wa Hyômen no sôzyô no Kôzô wo katei suru Koto ni yotte daitai setumei dekiru.

(4) Onoono Sô ni okeru *Distortion* no Nami no Hayasa wa sono-2 ni oite motometa mono to muzyun sinai.

(5) Sita no Bubun ni okeru Nami no Hayasa ga sidai ni kawaru Baai no Eikyô wo giron sita.

I. Introduction.

In the preceding papers attention was mainly confined to the dilatational and the distortional waves observed at stations within small epicentral distances. In this paper, problems relating to surface waves will mainly be treated. For this purpose study of remote earthquakes is necessary, for in cases of near earthquakes, separation of the surface waves from the distortional waves is not sufficient to admit of any definite conclusions being drawn.

The inference that the velocity of propagation of seismic waves may differ according to whether their path lies under the oceanic area or under the continental land dates back, as far as the present author is aware, to

1909, when the late Professor F. Omori[1] investigated the propagation of disturbance due to the Guatemala earthquake of April 19, 1902, and that of the Kangra (India) earthquake of April 4, 1905. His method of reduction was, however, somewhat different from that employed by modern seismology.

Recently many valuable papers in this direction have appeared from authors, such as E. Tams,[2] G. Angenheister,[3] S. W. Wisser,[4] B. Gutenberg,[5] W. Hiller[6] et. al. Results found by these authorities are not in all cases in agreement with each other. Some of them show almost no difference of velocity of propagation of surface waves along the continent from that along the oceanic area, whilst others show much difference, even as much as twenty percent. Such discrepancies seem to come from many apparent factors. Above all, the practical difficulty of identification of the waves seems to constitute the main ground for divergence of opinion.

The geographical position of Japan is very favourable for observation of purely trans-pacific seismic waves. The distance from Tôkyô to regions of great seismicity, as far as the Pacific Coast of South America, extends from zero to almost 18000 km. The only spot from whence seismic disturbances do not come, or seldom come, is in a small segment (about 20°) covering a part of Polynesia. Under these circumstances, typical examples of trans-pacific seismic waves have been obtained in the long series of observations made at the Seismological Institute, Imperial University of Tôkyô, especially by long period seismographs with proper period of 50 sec. or more. The data treated in this paper will accordingly not be confined to recent earthquakes.

II. Real Existence of two Kinds of Surface Waves.

From the theoretical point of view, Rayleigh wave can be propagated along a surface of a certain medium. In addition to this, waves of Love's

(1) F. Omori, Bull. Imp. Earthq. Invest. Comm. **3** (1909) 61–68.
(2) E. Tams, Zentral Bl. f. Mineralogie usw. (1921).
(3) G. Angenheister, Nach. d. Kgl. Ges. d. Wissensch. Göttingen (1921) 113.
(4) S. W. Wisser, Kon. Magnet en Met. Obs. et Batavia (1921) 7.
(5) B. Gutenberg, Zeits. f. Geophys. **1** (1925) 94; Phys. Zeits. **25** (1924) 377 etc.
(6) W. Hiller, Beitr. z. Geophys. **17** (1927) 3.

type can also be propagated if the medium is stratified under the boundary surface. Whether or no such waves are really existent is a problem which can easily be solved by seismometry. And yet some physicists are often sceptical of the real existence of surface waves, perhaps from difficulty of accurate identification of waves. On the other hand, even among seismologists, there is a diversity of opinion on the separate existence of two kinds of surface waves, i.e. the Love's type and the Rayleigh's type owing to the lack of typical examples free from any ambiguity. Therefore, some typical seismograms will be reproduced here. (Figs. 1, 2 and 3)

Atacama Earthquake, 1922 Nov. 11, $4^h\,32^m$.
(Upper 3 lines: $\frac{E}{W}$ comp. Lower 3 lines: $\frac{S}{N}$ comp.)

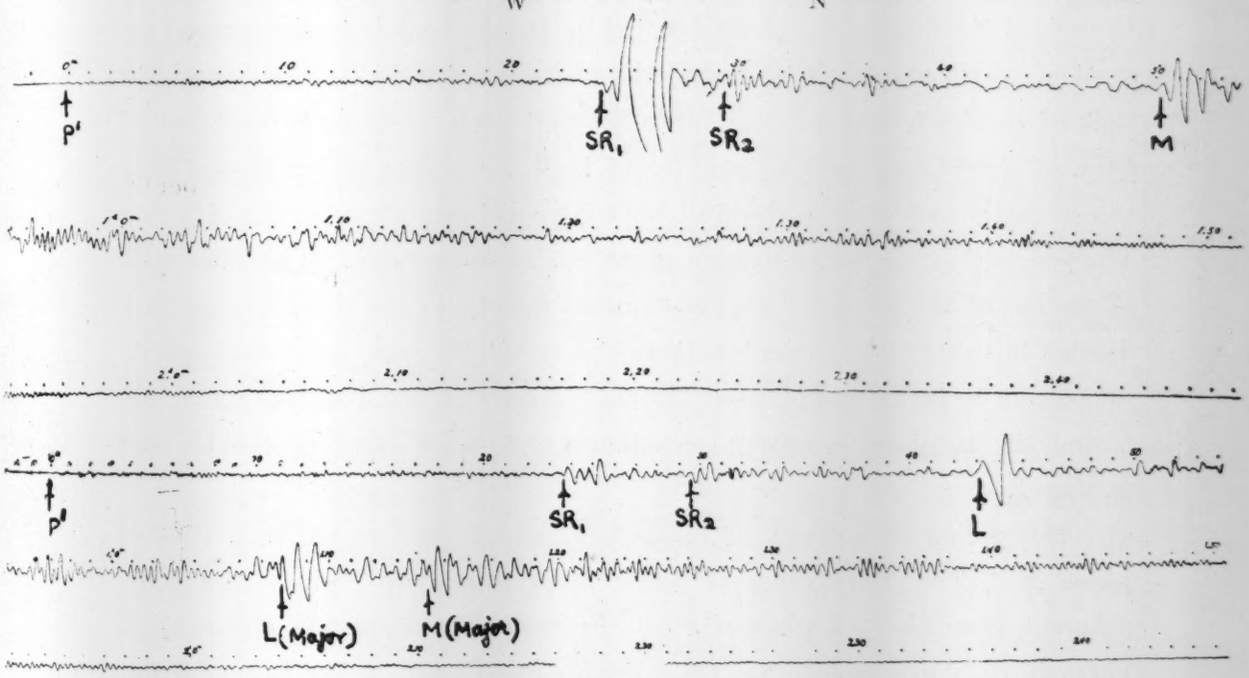

Fig. 1.

Earthquake, 1926 Oct. 26.
($\varphi = 2°$ S, $\lambda = 138°$ E)

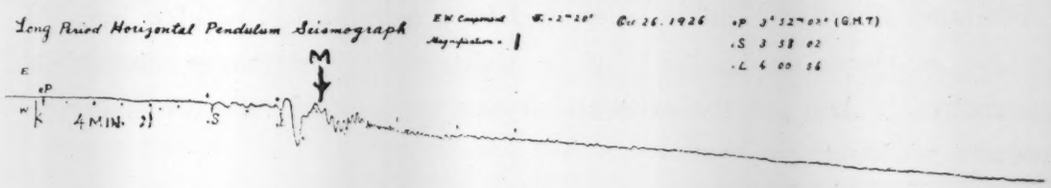

Fig. 2.

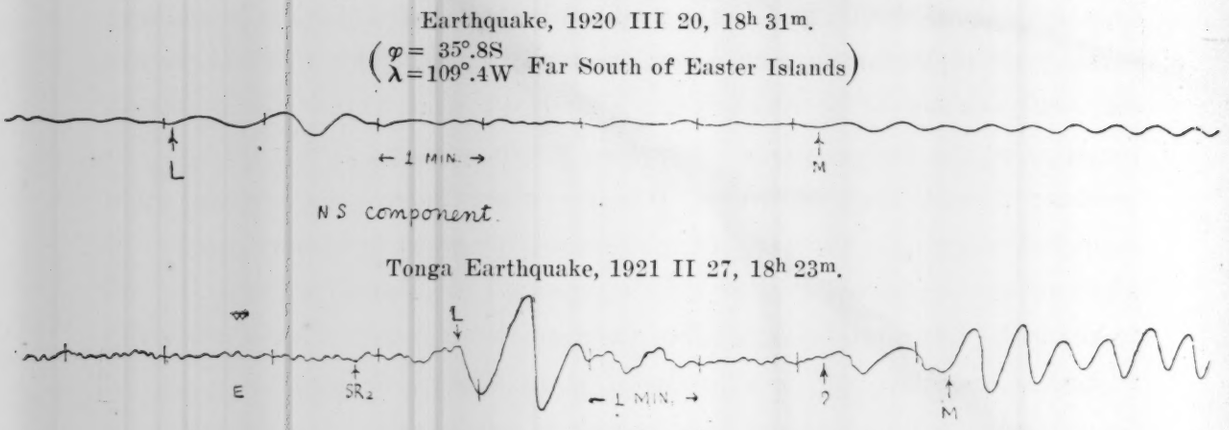

Fig. 3.

In each of the figures the phase denoted by L corresponds to the commencement of waves of Love's type, and the phase denoted by M corresponds to that of Rayleigh waves. The inference that each of these two phases of train of waves may belong to different kind of surface waves respectively can be easily seen from a study of their time-distance curves. (Fig. 4)
The polarisation of waves in each phase is also remarkable. The amplitude of motion of the L phase is predominant, mainly in the direction perpendicular to that of the epicentre, though it is not the case, rigorously speaking, owing to many complicated factors. Moreover, the polarisation of the L and the M phase is nearly perpendicular to each other as can be seen in Fig. 1.

The period of motions of phase L is usually far longer than that of phase M. The wave form of phase M is somewhat regular and more coherent than that of phase L. In the case of transpacific waves, such characteristics are usually distinct. On the other hand, in the case of transcontinental waves, separation of the L and the M phase does not seem to be so distinct as in the former case. The L phase commences with gradually increasing amplitude and is superposed by a more or less regular, large M phase, as shown in fig. 25(1) of B. Galitzin's "Vorlesungen über Seismometrie." And yet the existence of two kinds of surface waves hardly admits of doubt.

(1) B. Galitzin, Vorlesungen über Seismometrie, (1914) 110.

III. Data of Earthquakes.

One good way of studying the mode of propagation of seismic waves is to compare seismograms of one and the same earthquake observed at different places. And yet to study many different cases in such a way is not an easy matter to put into practice. Because of this reason my seismometric study will be confined to that of seismograms obtained in our Institute, while reports from other stations will be referred to as a supplement. In the following list, the position of the epicentre and the time of occurrence of earthquakes are adopted from the International Seismological Summary, B. A. Seism. Reports and B. A. Seism. Circular, unless special remarks to the contrary are not added.

Table I-a.

(Transpacific)

Epicentre.	Δ km.	Time of Occur. at the Epicentre.	Phase L			Phase M			Remark.
			Time of Comm.	Vel. km/sec.	Period Sec.	Time of Comm.	Vel. km/sec.	Period Sec.	
46.0° N 154.0 E	1650	1922 May 4 9h 12m 48s				20m 11s	3.70	17.5s	
48.0 N 157.0 E	1970	1921 May 21 22 25 42				35 23	3.39	12	
24° 33′ N 122 25 E	2060	1922 Sept. 1 19 15 53	25m 16h	3.73	50	27 45	2.89	8	By the author.
24.8 N 122.4 E	2060	1910 Sept. 1 14 21 04				35 43	2.35	14	,,
52.5 N 157.5 E	2200	1922 March 4 13 7 34	16 51	4.02	32				
23.0 N 121.7 E	2240	1919 Dec. 19 20 37 24	46 31	4.08	40				
22.8 N 121.7 E	2260	1910 Sept. 1 0 44 45				59 07	2.62	14	
24.0 N 116.5 E	2586	1918 Feb. 13 6 7 10	17 50	4.03	55~40	20 21	3.27	20	
11.5 N 144.0 E	2730	1917 May 9 15 54 59	05 34	4.17		06 23	3.88	30	

(to be continued)

(continued)

Epicentre.	Δ km.	Time of Occur. at the Epicentre.	Phase L			Phase M			Remark.
			Time of Comm.	Vel. km/sec.	Period Sec.	Time of Comm.	Vel. km/sec.	Period Sec.	
8.0 N 128.0 E	3305	1921 Nov. 11 18 36 06	50 02	3.95	35	52 03	3.45	29	
Off the S coast of Mindanao	3500	1924 April 14 16 20 19	34 30	4.11	12~13	35 33	3.83	30	By the author.
49.5 N 178.0 W	3720	1913 March 31 3 40 48	56 55	3.85					
45.0 N 170.0 W	3950	1910 Sept. 9 1 13 00	29 28	4.00	16	32 39	3.35		
3.0 N 122.0 E	4070	1913 Jan. 11 13 17 02	33 25	4.14	15.6	35 31	3.67	24	
Off the NW coast of Celebes	4550	1917 Aug. 30		4.22	37		3.49	54	By the author.
5.0 S 154.0 E	4760	1913 May 30 11 46 46	12h 04 47 (06 42	4.40 4.12	38 17)	08 30	3.68	24	( ), 2nd group.
54.5 N 160.0 W	4990	1917 May 31 8 47 20	9h 07 42	4.07		09 28	3.76		
8.5 S 144.0 E	5100	1920 May 7 21 31 13	52 38	3.97	40	55 26	3.66	15	
10.0 S 156.0 E	5210	1926 Mar. 27 10 48 27	11h 08 56	4.29	15	13 16	3.54	14 18	By the author.
Alaska	5300	1912 July 7 7 56 48	17 33	4.25	40				,,
11.0 S 161.0 E	5650	1926 April 12 8 32 15	54 10	4.30	35	57 33	3.72	20	
Simalur, Nias.	5860	1907 Jan. 4 14 28 or so.		3.78	45		3.56	32	O is not certain exactly.
4.2 S 102.0 E	5930	1914 June 25 19 7 15	30 12	4.32	30	33 33	3.76	30	From data of Batavia.
11.4 S 111.5 E	6023	1921 Sept. 11 4 01 25	28 02	3.77	35	38 04	2.74	18	By the author.
13.5 S 167.0 E	6180	1920 May 20 7 25 46	49 53	4.27	37	52 31	3.85	18	
15.0 S 165.0 E	6330	1919 Aug. 31 17 20 34	44 54	4.33	28	47 10	3.97	30	
12.0 S 164.0 E	6780	1913 Oct. 14 7 53 14	8h 34 07	4.42	50				By the author.

(to be continued)

(continued)

Epicentre.	Δ km.	Time of Occur. at the Epicentre.	Phase L			Phase M			Remark.
			Time of Comm.	Vel. km/sec.	Period Sec.	Time of Comm.	Vel. km/sec.	Period Sec.	
20.6 S 168.8 E	6970	1920 Sept. 20 14 38 50				15h 10 12	3.70	21	
Tonga	7750	1917 June 26 5 49 29				6h 20 57	3.84		By the author.
72.0 N 8.5 W	7790	1922 April 8 20 42 12	21h 12 35	4.27	17	21 17	3.32	14	
22.5 S 173.5 W	8130	1913 June 26 4 57 01	5h 26 39 (27 21	4.56 4.47	45 30)				
Kermadec	8400	1919 April 17 11 22 09	54 14	4.36	30	56 23	4.09	35	By the author.
40.15 N 117.10 W	8500	1915 Oct. 3 6 52 49	7h 26 35	4.25	27	7h 31 10	3.76	24	
29.2 S 177.0 W	8540	1917 May 1 18 26 46	58 25	4.50		19h 05 01	3.72	19	
34° 39′N 135 26 E	8580	1906 April 18		4.43	32		4.02	35	San Francisco.
40.9 S 177.1 E	9340	1917 Aug. 5 15 50 01	25 58	4.33	35~42	29 55	3.90	35	By E.F. Pigot S.J.
58.0 S 159.0 E	10500	1924 June 26 1 37 10	17 22	4.35	60	22 24	3.87		By the author.
18.0 N 100.0 W	11340	1907 April 15 6 5 42		4.63	30		3.51 (3.29 (3.19	30 29) 24)	From catalogo de los temblores en Mexico (1909) 440.
17.0 N 100.0 W	11410	1911 Dec. 16 19 14 38	20h 01 51	4.03	33				By the author.
14.5 N 91.0 W	12300	1917 June 8 0 51 28				1h 48 21	3.61	23	
13° 46′N 90 50 W	12360	1915 Sept. 7 (1) 1 20 17	07 21	4.37		14 21	3.81		By the author.
19.0 N 80.0 W	12630	1917 Feb. 20 19 29 32	17 16	4.42	30	21 26 (27 40	4.07 3.63	24 20)	
14.5 N 86.0 W	12650	1921 March 28 7 49 20	37 54	4.35	60	44 34	3.82	30	
35.8 S 109.4 W	13920	1920 March 20 18 31 15	22 30	4.48	41~34	28 40	4.04	29	See Fig. 3.

(to be continued)

(continued)

Epicentre.	Δ km.	Time of Occur. at the Epicentre.	Phase L			Phase M			Remark.
			Time of Comm.	Vel. km/sec.	Period Sec.	Time of Comm.	Vel. km/sec.	Period Sec.	
10° 30′N 66 54 W	14160	1900 Oct. 29 10 10 30	12h 00 41	4.55		12h 25 21	3.15		By F. Omori.(2)
3° 12′ S 82 50 W	14320	1922 Jan. 17(3) 3 50 24	4h 41 33	4.65					
14.0 S 75.5 W	15790	1916 Oett 3 1 26 13	2h 24 13	4.54		32 13	3.95		
18.0 S 73.0 W	16240	1913 Aug. 6 22 14 14				23h 22 08	3.99	23	
16° 28′ S 71 30 W	16260	1922 Oct. 11 14 49 55	15h 50 45	4.45	38	16h 04 32	3.79	17	From data of La Paz.
26.5 S 70.5 W	16970	1918 Dec. 4 11 47 44	12h 51 04	4.47	45～50	58 50	3.97	40～50	
28° 20′ S 71 0 W	17000	1922 Nov. 11 4 32 55	5h 35 56	4.55	55	5h 42 28	4.07	45	By Sieberg and Gutenberg.
23.0 S 66.0 W	17160	1916 Aug. 25 9 43 57	10h 46 56	4.54	35～50	56 32	4.03	27	

(1) Seismograms of this earthquake are quite similar to those of the earthquake of Sept. 23, 1902. See F. Omori, Publ. Imp. Eqke. Invest. Comm. **21** (1905) 52.

(2) F. Omori, ibid. **13** (1903) 137.

(3) According to P. Byerly, Bull. Seism. Stations (Berkley) Vol. 2, No. 3, this earthquake consisted of three simultaneous earthquakes at Brasil ($\varphi=4°35'.2S$, $\lambda=63°56'.3W$), Venezuela ($\varphi=5°11'.5N$, $\lambda=66°45'.2W$) and Ecuador ($\varphi=3°12'.1S$, $\lambda=82°50'.2W$). Observed values at Tôkyô are consistent with Ecuador as the origin.

TABLE I-b.

(Transcontinental earthquakes)

Epicentre.	Δ km.	Time of Occur. at the Epicentre.	Phase L			Phase M			Remark.
			Time of Comm.	Vel. km/sec.	Period Sec.	Time of Comm.	Vel. km/sec.	Period Sec.	
35.61 N 105.40 E	3090	1920 Dec. 16 12 05 50	20 09	3.60	27				By Y. Dammann.(1)
31.5 N 100.8 E	3560	1924 March 24 12 41 04	56 34	3.83	50	59 46	3.17	22	By the author.

(to be continued)

(continued)

Epicentre.	Δ km.	Time of Occur. at the Epicentre.	Phase L			Phase M			Remark.
			Time of Comm.	Vel. km/sec.	Period Sec.	Time of Comm.	Vel. km/sec.	Period Sec.	
26.0 N 100.0 E	3920	1925 March 16 14 41 54	59 14	3.77	38	15^h 02 29	3.18	14.5	By the author.
Maldive Islands	4570	1912 May 23 2 23 52	41 56	4.22	43	45 14 (47 09	3.59 3.27	21 13)	Along margin of Asia
42.75 N 77.10 E	5330	1911 Jan. 3 23 25 30	47 52	3.97	57				By the author.
31° 49′N 77 00 E	5720	1905 April 4 0 49 48		3.67	54		3.11	30	From F. Omori.(2)
38° 16′N 73 34 E	5760	1911 Feb. 18 18 40 59	19^h 07 05	3.68	38	12 59	3.00	22	
39° 40′N 67 30 E	6230	1907 Oct. 21 4 23 550		3.71	42		3.41		By the author.
39.6 N 41.5 E	8130	1924 Sept. 13 14 33 54	15^h 07 29	4.03	60	11 29	3.51	34	
44.0 N 25.0 E	8980	1913 June 14 9 23 21	10^h 08 28	4:15		17 05	3.42	22	
40.0 N 26.4 E	9190	1912 Aug. 9 1 28 551	06 03 (08 10	4.12 3.90	20 40)?	15 02	3.32	20	By the author.
38° 7½′N 18 35 E	10000	1908 Dec. 28 4 20 27		3.83	26		3.46 3.04	23 25	T.C. at Messina.

(1) Y. Dammann, le tremblement de terre du Kan-sou au 16 Dec. 1920. Publ. du Bureau Central Seismologique international, (1925).

(2) F. Omori, Publ. Eqke. Invest. Comm. **24** (1907) 6.

(3) This earthquake was discussed by H. Jeffreys, the Earth (1924) 170, as caused by a land slip at Pamir.

In preparing this table, identification of each phase was sometimes quite doubtful, as will be appreciated from the nature of seismograms. And yet for greater distances, say more than 8000 km., each phase of waves is resolved clearly without superposition of one another, as stated in the foregoing section. Another difficulty is the identification of the L phase at a locality of small epicentral distance and is due to the fact that the time of arrival of the SR phases (distortional waves reflected at the surface of the Earth) is not much different from that of the L phase. Thus, strictly

speaking, the commencement of the L phase is quite liable to be mistaken. The time-distance relation of the SR phases, however, is tolerably definite owing to the small effect of dispersion, and the magnitude of amplitude of reflected waves, especially reflected more than twice, is usually small. Therefore, their identification is not always impossible, if the epicentre, the time of occurrence at the epicentre etc., of an earthquake can be determined from other data.

IV. TIME-DISTANCE RELATIONS.

As is apparent from Fig. 4, the lower boundary of the points representing the time-distance relation of the L phase is a straight line which is characterised by $\frac{\partial \Delta}{\partial T}=4.45$ km/sec. It must be remarked that this value is the same as that of the velocity of propagation of the S phase as obtained in part II of this paper. A similar phenomenon can be seen with regard to the M phase, especially for greater distances, and the straight line bordering the lower limit is characterised by $\frac{\partial \Delta}{\partial T}=3.9$ km/sec. The fact that the time-distance curves of these phases can be represented by straight lines shows that these phases can be interpreted as surface waves.

V. DISPERSION OF WAVES.

Dispersion of surface waves of Love's type, especially from the practical point of view, has been fully discussed by B. Gutenberg.[1] If the writer's understanding is correct, he has used many trains of waves in an earthquake from the consideration that such separation of train of waves might be due to dispersion. In the present paper, however, attention will be focussed on the commencement of each phase, for it is not certain that any train of waves appearing later is excited simultaneously at the origin of an earthquake. With these considerations in view, the velocity-period diagram has been constructed as shown in Fig. 5-a and 5-b.

---

(1) B. Gutenberg, Phys. Zeits. **25** (1924) 377; **27** (1926) 111–114; Zeits. f. Geophys. **1** (1924–25) 94.

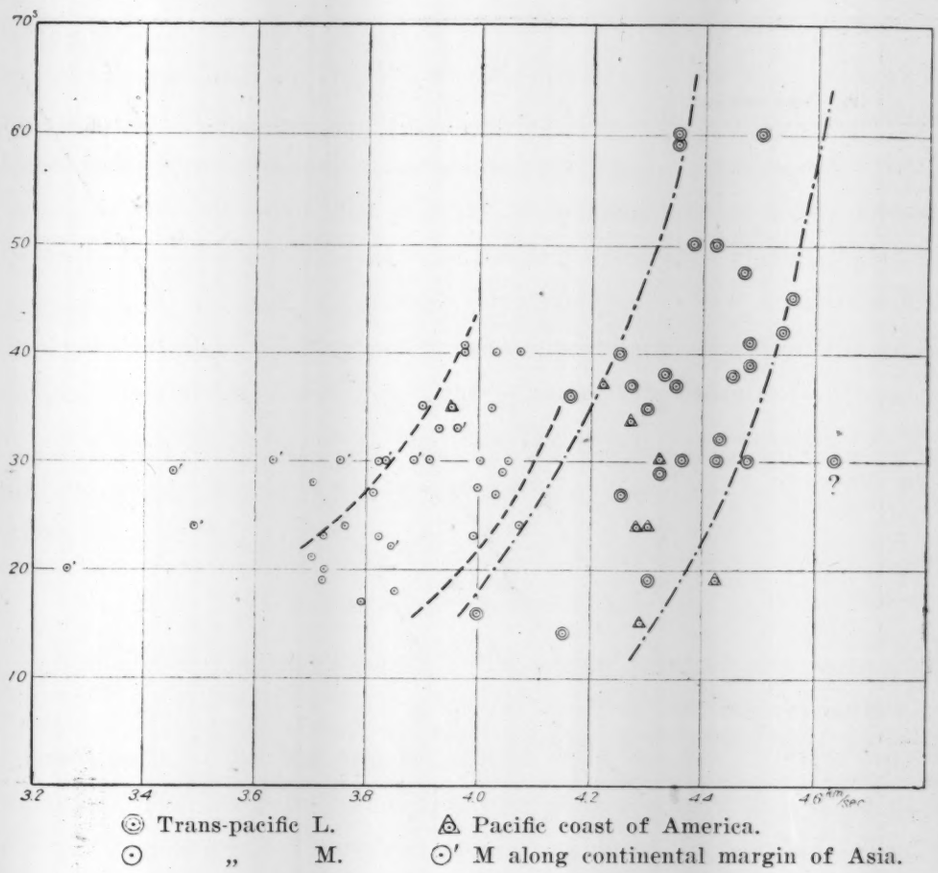

Fig. 5-a.

In Fig. 5-a, that of transpacific waves is shown, and in Fig. 5-b that of trans-continental waves is plotted. In both cases, dispersion of waves can be seen, though not very sharply, which is inevitable from the difficulty of accurate identification of waves. Moreover, it is almost certain that the mode of dispersion in the case of trans-pacific waves is quite different, quantitatively, from that of the trans-continental waves. For the same period of motion, trans-pacific waves are propagated much faster than the trans-continental waves. The same characteristic can be seen in the case of the M phase.

For example, for the M phase movements with period of about 15 sec., the velocity of the trans-continental waves is 3.1 km/sec. or so, and that of the transpacific waves is nearly 3.6 km/sec. These values are not in-

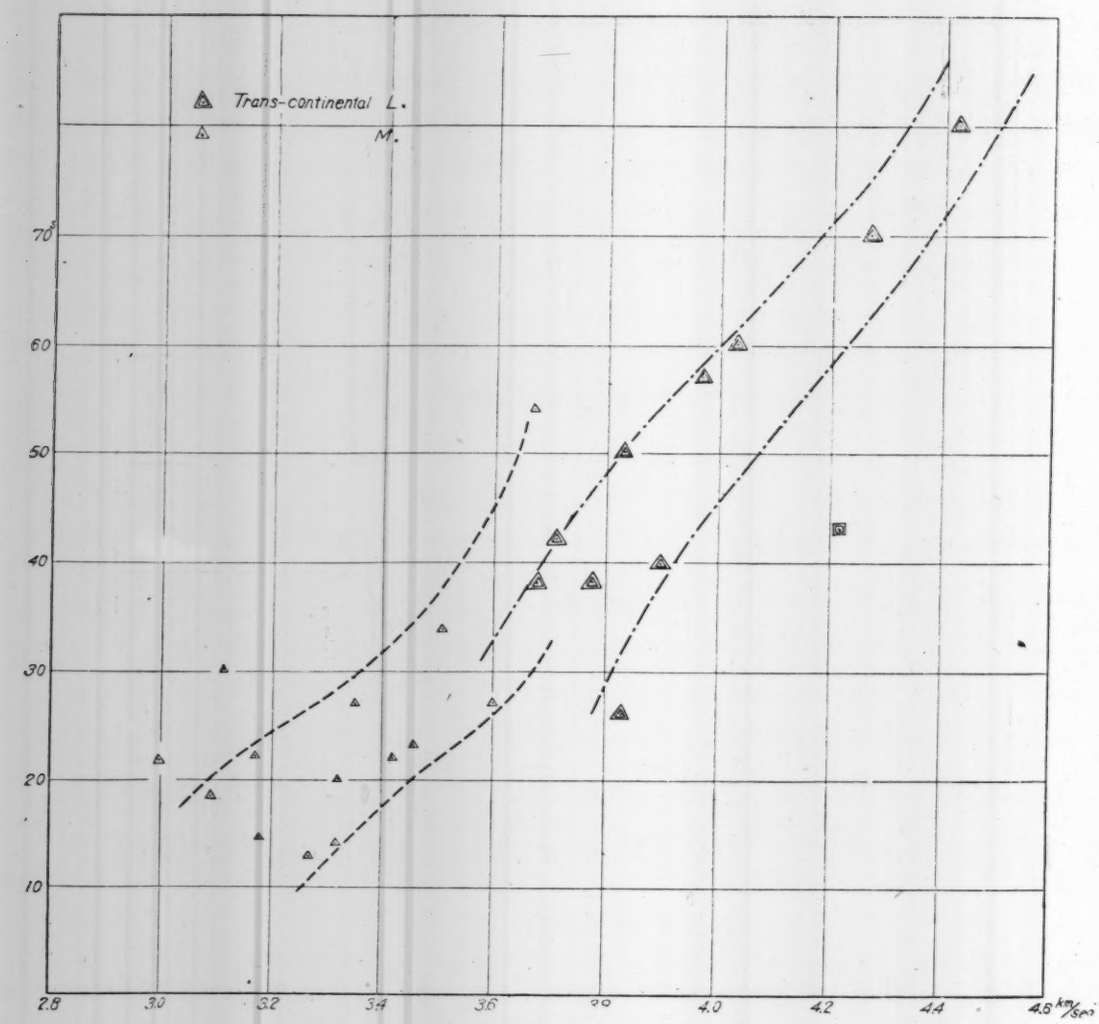

Fig. 5-b.

consistent with the result in connection with waves of Rayleigh's type (R–Wellen by his notation) obtained by W. Hiller.[2] It must be remarked that the word "Trans-continental" here used must not be interpreted literally, because Japan is bounded on all sides by sea.

VI. Discussion of the Results.

The facts observed with regard to the dispersion of surface waves stated above must now be examined in the light of the theory of elasticity.

(2) W. Hiller, Beitr. z. Geophys. **17** (1927) 3.

Mathematical calculations covering several cases[1] have already been published in Proceedings of the Physico-Mathematical Society of Japan, 3rd Ser. Vol. 10 (1928) No. 3, though numerical values taken as examples differed from those obtained in this investigation. It can be seen that the observed relation between the velocity of propagation and the period of movements is explained, at least, qualitatively, from the elastic theory even in taking into account the double stratification. The author will not examine the effect of group velocity, since in this investigation the velocity of propogation of wave front is what is under consideration. Thus, it is quite untenable in this case to compare the result here obtained with the theoretical group velocity which is a formal consequence of wave superposition.

Effect of gradual change of medium.

In the above mentioned paper[2] the author treated only cases of dispersion in stratified layers, each of which is of an uniform structure. In part I and part II, the first and the second layer can very well be regarded as uniform. The lower layer must, however, be regarded as having undergone gradual changes. Therefore, this effect must be verified. Verification will only be confined to the case of single stratification, for the object is to examine how the gradual change of medium affects the character of the period-velocity relation.

The equation of motion of love's type in a heterogeneous medium[3] is given by, using customary notations, and assuming heterogenuity in the z direction only,

$$\rho \frac{\partial^2 v}{\partial t^2} = \mu \nabla^2 v + \frac{\partial \mu}{\partial z} \frac{\partial v}{\partial z}, \qquad u = 0 \quad \text{and} \quad w = 0.$$

---

(1) The author came across a paper by Stoneley and others, published almost about the same time, in which similar subjects were discussed. (Geophys. Suppl. Month. Not. Astr. Soc. London **1** (1928) 521.)

(2) T. Matuzawa, Proc. Physic Mathm. Soc. Japan [ii] **10** (1928) No. 3.

(3) A similar case without stratification was already discussed by the late Prof. K. Aichi (Proc. Physic. Mathm. Soc. Japan [iii] **4** (1922) 137–142.) In his paper the last term of the equation of motion was unduly neglected.

By putting $v=v(z)\cos(fx+pt)$, where f and p are constants,

$$\mu\frac{d^2v}{dz^2}+(\rho p^2-\mu f^2)v+\frac{d\mu}{dz}\frac{dv}{dz}=0.$$

Again, by $v=\dfrac{V}{\sqrt{\mu}}$

$$\frac{d^2V}{dz^2}+IV=0, \quad \text{where} \quad I=b+\frac{1}{4}\frac{1}{\mu^2}\left(\frac{d\mu}{dz}\right)^2-\frac{1}{2\mu}\frac{d^2\mu}{dz^2}$$

by putting

$$b=\frac{\rho p^2}{\mu}-f^2.$$

Taking the z axis vertically upward and a point on the boundary surface of discontinuity as the origin and assuming linear relations such as $\mu=\mu_2-\beta z$ and $\sqrt{\dfrac{\mu}{\rho}}=v_0-\beta_1 z$, for discussion of small range of z the following approximation is permissible;

$$I=A+Bz, \quad \text{where} \quad A=\frac{p^2}{v_0^2}+\frac{\beta^2}{4\mu^2}-f^2 \quad \text{and} \quad B=2\left(\frac{p^2\beta_1}{v_0^3}+\frac{\beta^2}{2\mu_2}\right).$$

Thus,

$$\frac{d^2V}{dz^2}+(A+Bz)V=0.$$

Substituting $t=A+Bz$

$$\frac{d^2V}{dt^2}+\frac{t}{B^2}V=0.$$

In the present case treating of surface waves, the case of negative value of t may be important. Thus the solution of the equation is given by

$$V=\sqrt{t}\left\{\mathfrak{a}H^{(1)}_{\frac{1}{3}}\left(\frac{2}{3B}t^{\frac{3}{2}}\right)+\mathfrak{b}H^{(2)}_{\frac{1}{3}}\left(\frac{2}{3B}t^{\frac{3}{2}}\right)\right\},$$

Accordingly

$$v=\frac{\sqrt{t}}{\sqrt{\mu_2+\beta\dfrac{A}{B}-\dfrac{\beta}{B}t}}\left\{\mathfrak{a}H^{(1)}_{\frac{1}{3}}+\mathfrak{b}H^{(2)}_{\frac{1}{3}}\right\},$$

where $\mathfrak{a}$ and $\mathfrak{b}$ are arbitrary constants.

For large absolute value of t, v must vanish. Thus, $\mathfrak{b}=0$.

$$\frac{dv}{dt}=\mathfrak{a}\left[\frac{1}{2}t^{-\frac{1}{2}}\left(\mu_2+\beta\frac{A}{B}-\frac{B}{B}t\right)^{-\frac{1}{2}}\left\{1+\frac{\beta}{B}t\left(\mu_2+\beta\frac{A}{B}-\frac{\beta}{B}t\right)^{-1}\right\}H^{(1)}_{\frac{1}{3}}\right.$$

$$\left.+\frac{t}{B}\left(\mu_2+\beta\frac{A}{B}-\frac{\beta}{B}t\right)^{-\frac{1}{2}}\frac{dH^{(1)}_{\frac{1}{3}}(x)}{dx}\right), \quad \text{where} \quad x=\frac{2}{3B}t^{\frac{3}{2}}.$$

In the next place, boundary conditions must be considered. As the xy plane is taken along the lower boundary of the uniform superficial layer, the value of z is positive in this domain. Quantities in this layer will be denoted by adding suffix (1) and those in the lower medium by suffix (2). The thickness of the layer will be noted by H.

In the superficial layer

$$v_1=(A_1\cos s_1 z+B_1\sin s_1 z)\cos(pt+fx).$$

Boundary conditions are as usual

$$\frac{\partial v_1}{\partial z}=0 \quad \text{at} \quad z=H$$

$$\left.\begin{aligned} v_1&=v_2 \\ \mu_1\frac{\partial v_1}{\partial z}&=\mu_2\frac{\partial v^2}{\partial z}\end{aligned}\right\} \quad \text{at} \quad z=0.$$

Taking into account that

$$\frac{dv_2}{dz}=B\frac{dv_2}{dl} \quad \text{and} \quad \frac{dH^{(1)}_{\frac{1}{3}}(x)}{dx}=\frac{1}{2}\left(H^{(1)}_{\frac{1}{3}-1}(x)-H^{(1)}_{\frac{1}{3}+1}(x)\right),$$

these conditions are

$$-A_1\sin s_1 H+B_1\cos s_1 H=0,$$

$$A_1=\sqrt{\frac{A}{\mu_2}}\left\{\mathfrak{a}\,H^{(1)}_{\frac{1}{3}}\left(\frac{2}{3B}A^{\frac{3}{2}}\right)\right\},$$

and

$$B_1=\frac{\mu_2 B}{\mu_1 s_1}\frac{\mathfrak{a}}{2}\left\{\frac{1}{\sqrt{\mu_2 A}}\left(1+\frac{\beta}{B}\frac{A}{\mu_2}\right)H^{(1)}_{\frac{1}{3}}+\frac{A}{B\sqrt{\mu_2}}\left(H^{(1)}_{-\frac{2}{3}}-H^{(1)}_{\frac{4}{3}}\right)\right\}.$$

Eliminating A_1, B_1 and $\mathfrak{a}$

$$\tan s_1 H=\left\{\frac{1}{2}\frac{\mu_2 B}{\mu_1 s_1}\frac{1}{A}\left(1+\frac{\beta}{B}\frac{A}{\mu_2}\right)+\frac{1}{2}\frac{\mu_2\sqrt{A}}{\mu_1 s_1}H^{(1)}_{-\frac{2}{3}}-H^{(1)}_{\frac{4}{3}}\right)\Big/H^{(1)}_{\frac{1}{3}}\right\}$$

in which the argument of function H is $\frac{2}{3B}A^{\frac{3}{2}}$.

In the case of a large absolute value of this argument, an asymptotic expansion of function H, that is $H^{(1)}_n(x)\approx\sqrt{\frac{2}{\pi x}}\,e^{i\frac{2n+1}{4}\pi}e^{ix}$ may be utilised.

Thus, $\left(H^{(1)}_{-\frac{2}{3}}-H^{(1)}_{\frac{4}{3}}\right)\Big/H^{(1)}_{\frac{1}{3}}=-2i.$

Putting $\quad A=\frac{p^2}{v_0{}^2}+\frac{\beta^2}{2\mu_2{}^2}-f^2=-s_2{}^2 \quad$ and $\quad B=2\left(\frac{p^2\beta_1}{v_0{}^3}+\frac{\beta^3}{4\mu_2{}^3}\right)$

$$\tan s_1 H=\frac{\mu_2 s_2}{\mu_1 s_1}-\frac{1}{2}\frac{\mu_2 B}{\mu_1 s_1}+\frac{1}{2}\frac{\beta}{\mu_1 s_1}.$$

If the last two terms are neglected, the equation degenerates to that with regard to the uniform medium.

A numerical example will be given to show the order of magnitude of the effect.

Assuming that $H=50$ km., $v_1=3.7$ km/sec., $v_2=4.5$ km/sec., $\mu_1=41.07$ (km. g. s.), $\mu_2=68.85$ (km. g. s.), $\beta=0.01$ (km. g. s.) and $\beta_1=0.005$ (km. g. s.) the period-velocity relation can be determined. The coefficients β and β_1 are assumed, taking into account the result obtanied in the discussion of the P phase in part III. As the Poison's ratio in the earth's crust does not seem to undergo much change, such an assumption will not be purposeless in order to obtain an idea of the order of magnitude of the effect. In Fig. 6, the full curve denotes the relation in the case of the uniform layer. The crosses represent the relation when the underlying layer assumes a gradual change.

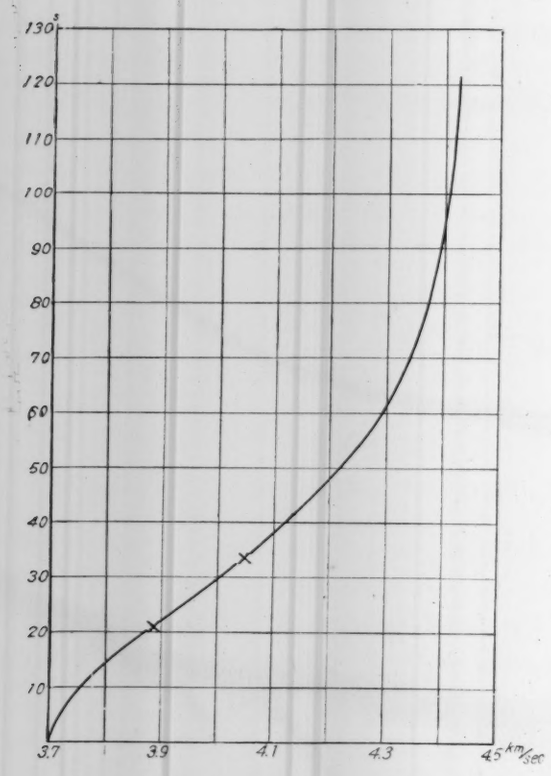

Fig. 6.

It may be seen from the figure that the effect of the gradual change of the medium is not so great, at least, when the wave length of the disturbance is not to great compared with the thickness of the layer. When the wave length becomes large, the argument of the Hankel's function $\frac{2}{3B}A^{\frac{3}{2}}$ becomes so small that the asymptotic expansion of it cannot be applied. In such cases, tables of $H^{(1)}_{\frac{1}{3}}$, $H^{(1)}_{\frac{4}{3}}$ and $H^{(1)}_{-\frac{2}{3}}$ are necessary for calculation, but no such tables being accessible, numerical calculation for such a case will not be attempted here.

VII. Conclusion.

In this paper the real existence of two kinds of surface waves, that is, Rayleigh waves and waves of Love's type, has been affirmed from the seismometrical point of view. Especially in the case of trans-pacific waves from a remote origin, they can be distinctly identified. They both undergo dispersion of a certain character wich is to be expected from the theory of elasticity, qualitatively, at least. From the dispersion of waves across the Pacific it would seem justifiable to assume that the superficial earth's crust under the Pacific also is stratified.

Velocities of propagation of the S, S^* and $\bar{S}$ waves determined in part II are quite consistent with the mode of dispersion of the waves of Love's type here obtained. Under the Pacific, however, it seems that the layer in which the velocity of propagation of the distortional movement is 3.15 km/sec. may be absent. Comparison of Fig. 5-a with Fig. 6 will show that the thickness of the upper layer may be much less than 50 km. As the density of each layer is not known for certain, the author will not attempt to find, by arbitrarily adjusting the constants, a value for the thickness by means of which the observed dispersion might be explained in a plausible manner.

It is also remarkable to note that the dispersion of trans-pacific waves is different, quantitatively, from that of trans-continental waves, which difference would furnish plausible evidence for the existence of a different crustal stratification in both region, as has been suggested by some european writers.

Before concluding this paper the author takes the opportunity to express his cordial thanks to Professor A. Imamura for his kind advices and valuable suggestions.

July 17, 1928.

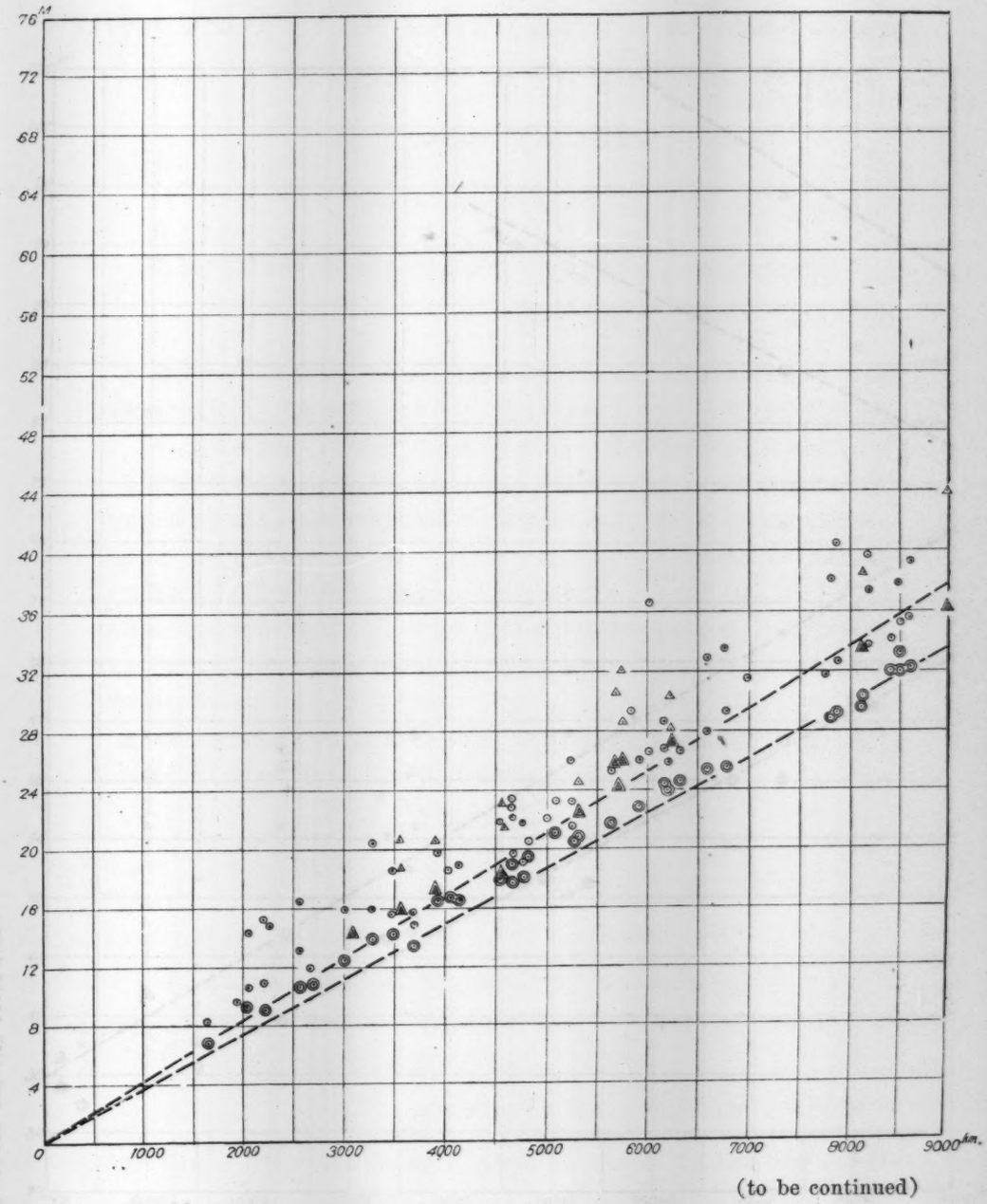

(to be continued)

◎ Trans-pacific L. △ Trans-continental L.
⊙ „ M. △ „ M.

Fig. 4-a.

(震研彙報、第六號、圖版、松澤)

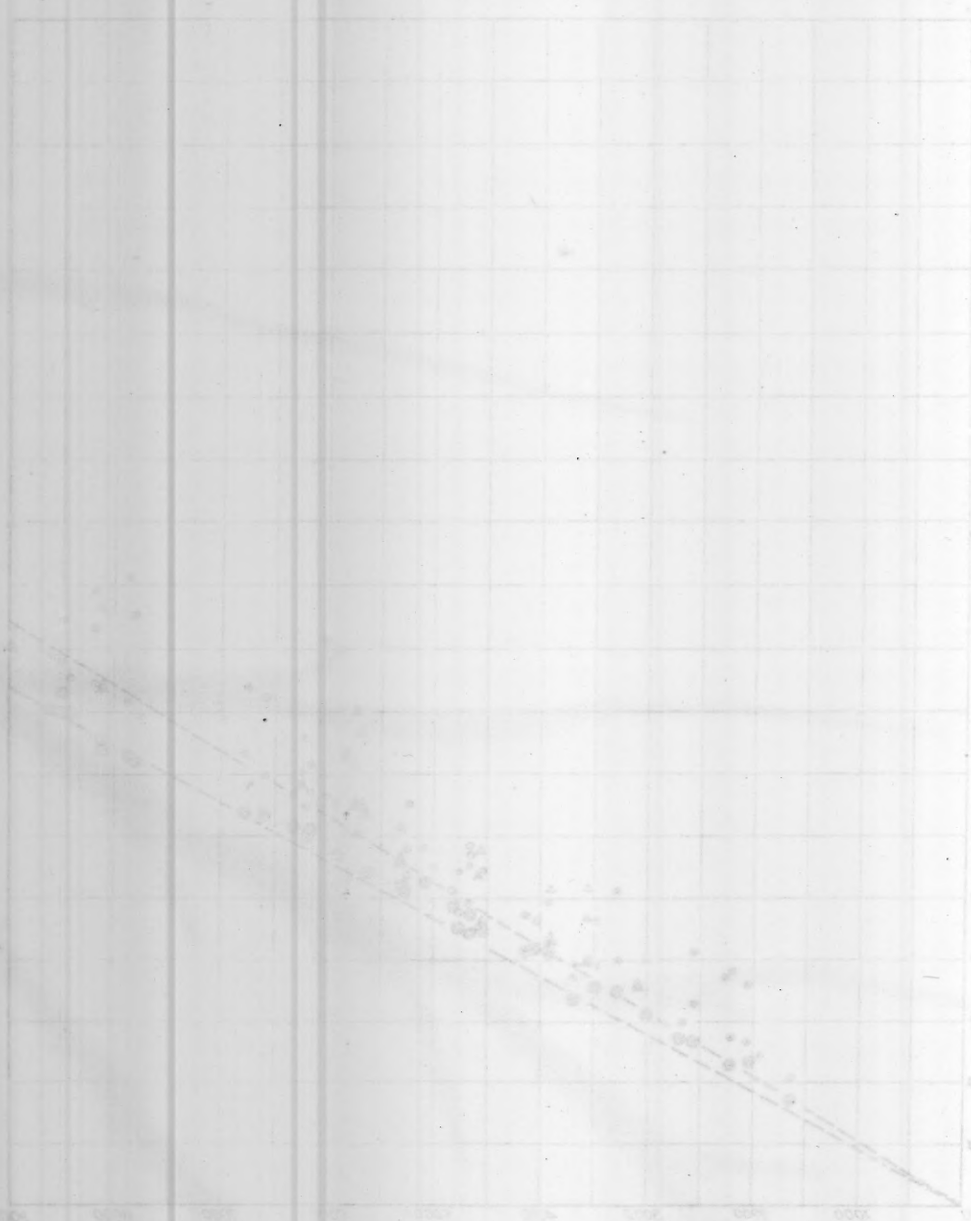

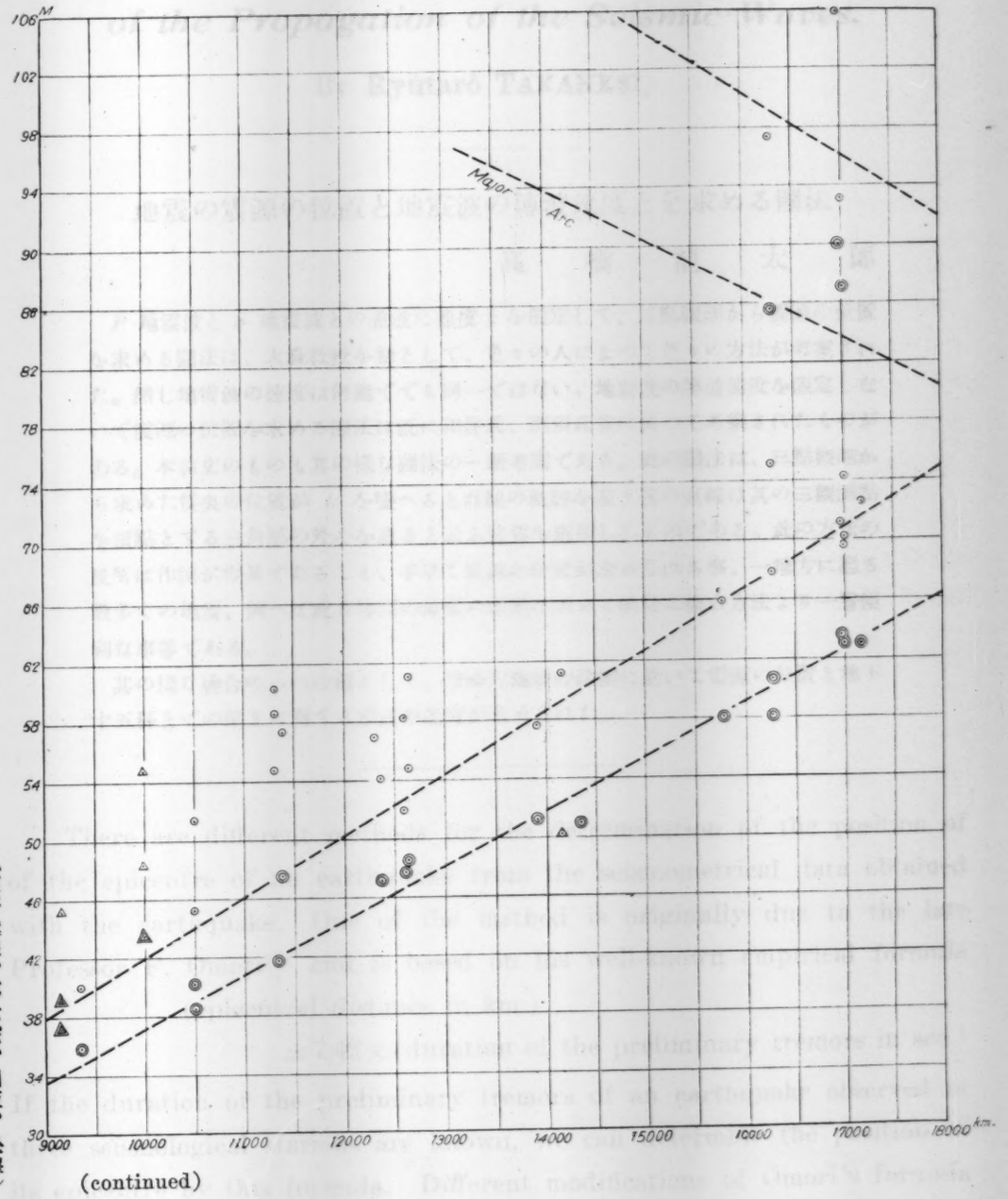

(震研彙報、第六號、圖版、松澤)

(continued)

Fig. 4-b.

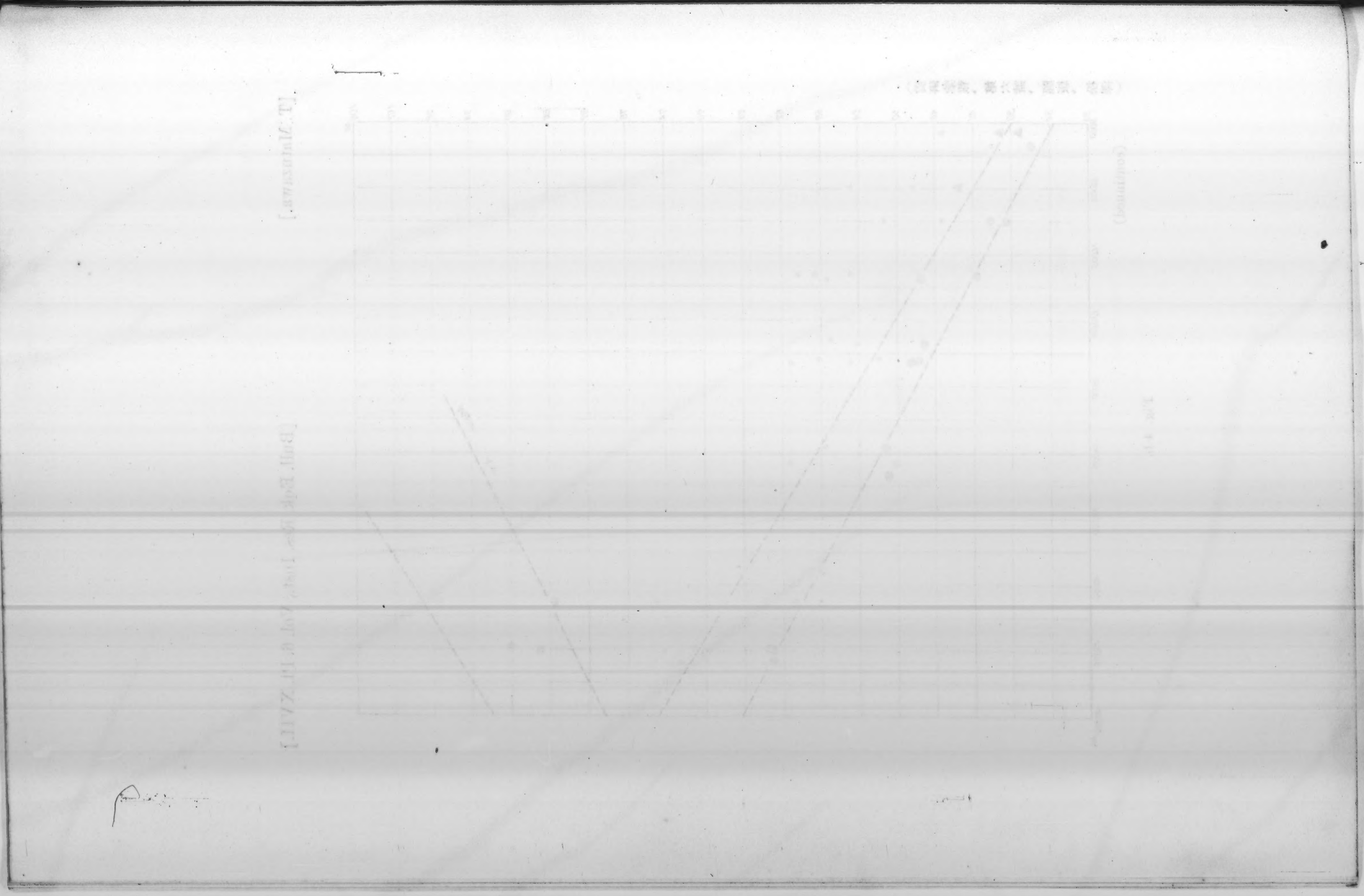

A Graphical Determination of the Position of the Hypocentre of an Earthquake and the Velocity of the Propagation of the Seismic Waves.

By **Ryûtarô TAKAHKSI,**

地震の震源の位置と地震波の傳波速度とを求める圖法

高　橋　龍　太　郎

P 地震波と *S* 地震波との差波に速度 *k* を假定して、三點觀測から震源の位置を求める圖法は、大森教授を初として、色々の人によつて色々の方法が考案された。然し地震波の速度は何處でても同一ではない、地震波の傳波速度を假定しないで震源の位置を求める圖法は既に和達氏、那須氏等に依つて考案されたものがある。本論文のものも其の樣な圖法の一新考案である。此の圖法は、三點觀測から求めた震央の位置が *k* を變へると直線の軌跡を畫き其の直線は其の三觀測點を頂點とする三角形の外心を通ると云ふ性質を應用したものである。此の方法の長所は作圖が容易であること、手早く震源の位置が求められる事、一地方に起る數多くの地震、例へば或る地震の餘震の震源を求める場合に他の方法より一層便利な事等である。

其の樣な場合の一つの例として、丹後大地震の餘震に就いて震源の位置と地下十五粁までの深さに對する震波の速度が求められた。

There are different methods for the determination of the position of of the epicentre of an earthquake from the seismometrical data obtained with the earthquake. One of the method is originally due to the late Professor F. Omori[1] and is based on his well-known empirical formula

(epicentral distance in km.)
$= 7.42 \times$ (duration of the preliminary tremors in sec.)

If the duration of the preliminary tremors of an earthquake observed at three seismological stations are known, we can determine the position of its epicentre by this formula. Different modifications of Omori's formula

(1) Journ. Coll. Sci. Tokio XI 147 (1899).

have hitherto been suggested by many, of whom we may specially mention the names of S. Kusakabe, Seam. Nakamura, K. Hasegawa, K. Wadati, etc. In all of these methods, however, it has been necessary to assume the difference of the velocities of the compressional P and the distorsional S seismic waves, what is the same thing to assume the velocity of the differential P-S wave.

With the gradual increase of the number of seismological stations in this country, we are enabled to observe often an earthquake of a small intensity of which the seismometrical data from more than three stations are available. It becomes thus possible to determine the position of the hypocentre of the earthquake out of these data without any assumption concerning the velocity of the P-S wave as was formerly necessary. So far as the author is aware of, there have been devised two methods to effect this. One of these methods is that based upon the geometrical theorem due to Appolonius that the locus of the point whose distances from two given points remain in a given constant ratio is a sphere whose centre lies on the straight line joining the two given points. This method was adopted by K. Wadati[2] in his investigation of "deep earthquakes." Essentially the same method was also used by the present author for finding the coefficient in so-called Omori's formula which fits well for the earthquakes occuring in the Kwantô district. This method has, however, several disadvantages in its practice, especially when the duration of the preliminary tremors observed at any two stations happens to be nearly equal. In such a case, the sphere of constant ratio becomes very large in its diameter and tends to a plane, thus the sphere becomes practically difficult to be drawn. Moreover, the duration of the preliminary tremors measured on seismograms being limited in its accuracy to the order of 0.1 sec., large errors are unavoidable in the determination of the epicentre in the above case.

The other method consists in finding a coefficient k in Omori's formula for which two epicentres obtained with different combinations of three stations may fall as closely as possible. The method was adopted by

(2) Geophys. Mag. I 162 (1928).

N. Nasu[3] in his determination of the coefficient of Omori's formula for the after-shocks of the Great Tango Earthquake of 1927. This method is of a tentative nature and seems to be rather troublesome in its procedure though it has its own merit in that the errors in the determination of the epicentre is comparatively small.

The method which the present author is going to suggest in this paper owes, indeed, its origine to Nasu's method and is so devised as to be effected in a possibly short time without any tentative assignment of the value of k as was necessary in the case of Nasu's method.

Let $A\,B\,C$ be three seismological stations at which the observed durations of preliminary tremors are t_1 t_2 and t_3 respectively. (Fig. 1). Draw three circles of radii kt_1 kt_2 and kt_3 with their centres at A, B, C respectively. Join the intersections of the circles A and B, B and C. The intersection D of these two straight lines gives the position of the epicentre of the earthquake. When the constant k is varied successively and continuously the point D will describe a path of straight line. The proof of this theorem is as follows:—

Let E be the intersection of $\overline{AB}$ with the line which joins the intersections of the two circles A and B. Then we have

$$\overline{AE}^2-\overline{BE}^2=k^2(t_1^2-t_2^2),$$
$$\overline{AE}+\overline{BE}=\overline{AB}=a,$$

where a is the distance between A and B.

$$\overline{AE}-\overline{BE}=k^2\left(\frac{t_1^2-t_2^2}{a}\right),$$

$$\overline{AE}=k^2\left(\frac{t_1^2-t_2^2}{2a}\right)+\frac{a}{2}=Mk^2+N, \quad \ldots\ldots\ldots\ldots\ldots\ldots (1)$$

where M and N are constants for a given earthquake. Similarly, we have

$$\overline{BF}=k^2\left(\frac{t_2^2-t_3^3}{2b}\right)+\frac{b}{2}=M'k^2+N', \quad \ldots\ldots\ldots\ldots\ldots\ldots (2)$$

where F is the foot of the perpendicular from D to $\overline{BC}$, b the distance between B and C and M' and N' are constants.

(3) Proc. Imp. Acad. IV 378 (1928).

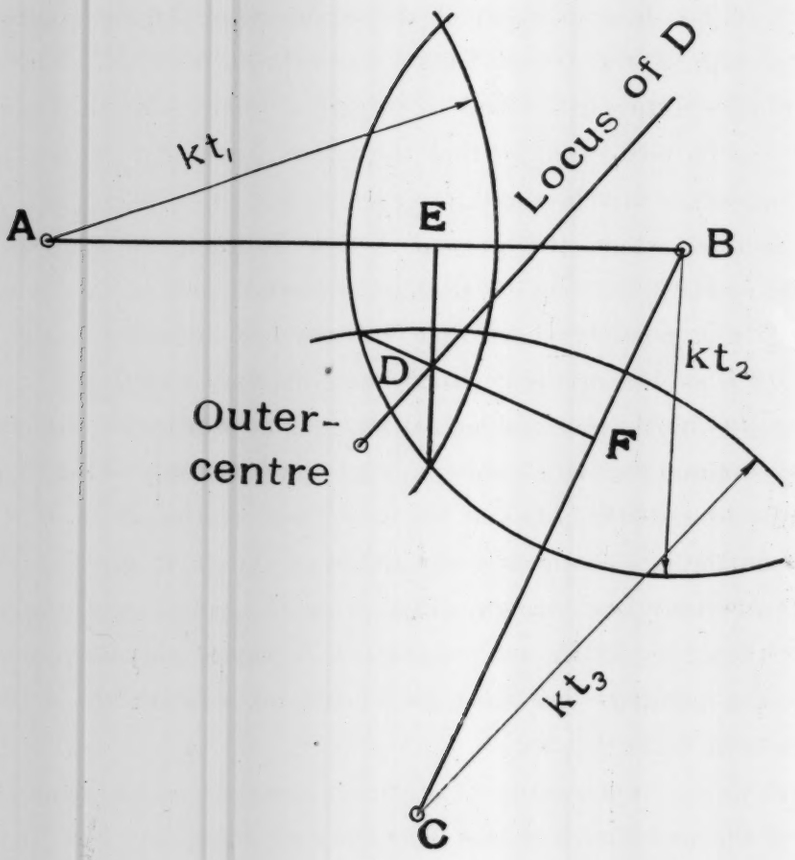

Fig. 1.

As can readily be seen from (1) and (2), the differential coefficient $\frac{d\overline{AE}}{d\overline{AF}}$ is a constant, so that the locus of D is a straight line. If $k=0$, then $\overline{AB}=a/2$ and $\overline{BF}=b/2$, so that it is seen that this straight line passes through the outer-centre of the triangle ABC.

This geometrical property can readily be utilised in the determination of the epicentre of an earthquake in the following manner. Take two different combinations of three seismological stations out of the four given stations and find the points D's in both combinations for an arbitrary value of k, say $k=8$. Join the points D's thus obtained to the corresponding outer-centres of the triangles. The intersection of these two straight lines gives the position of the epicentre. That the two lines will really intersect under the ground can easily be seen if we notice that

the two of the four stations are common in both combinations. The value of the parameter k which correspond to this intersection can be readily obtained because the distance of a point on the locus of D from the outer-centre of the triangle is proportional to k^2 as is seen in (1), and the distance of the point corresponding to $k=8$ from the outer-centre of the triangle is known. The focal depth can be obtained without difficulty from the distance of the epicentre from any one of the stations and the coefficient k obtained above.

From an example illustrated in Fig. 2, the practice of the method may be understood. The earthquake taken in the example in one of the aftershocks of the Great Tango Earthquake of 1927. The data of the preliminary tremors of the earthquake is as follows:

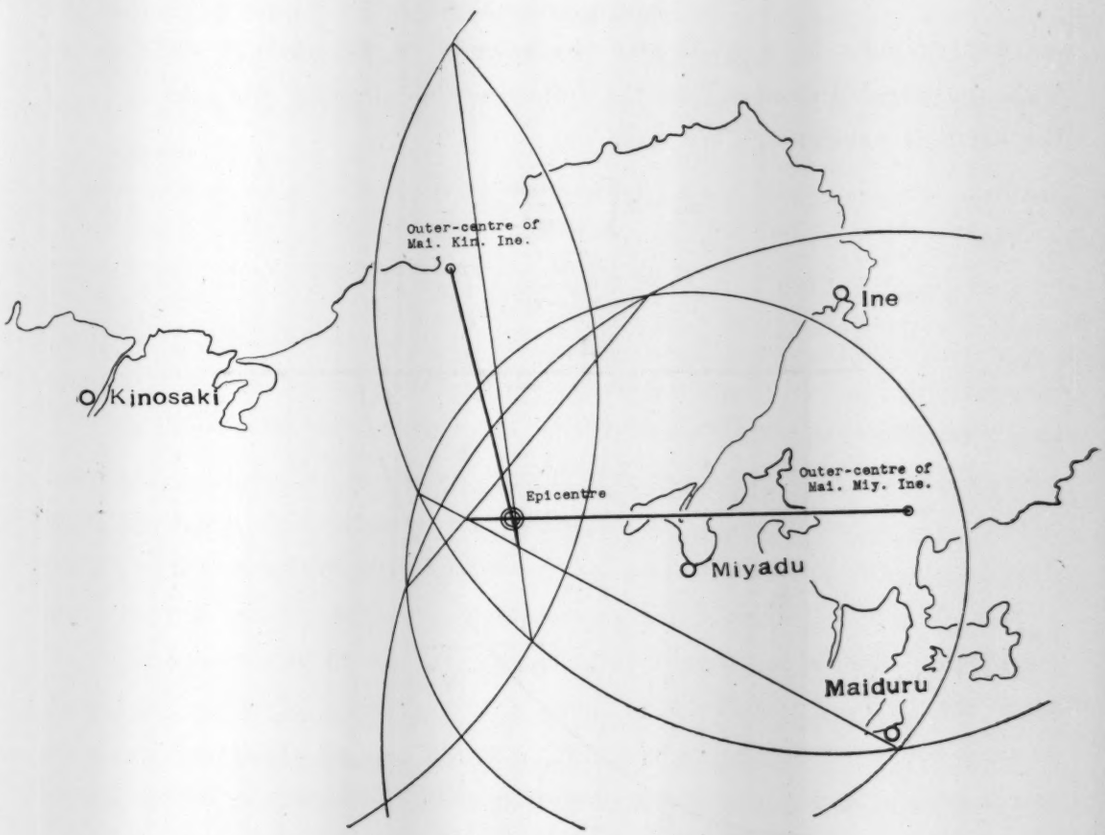

Fig. 2.

Date				Preliminary tremors observed at			
				Maiduru	Kinosaki	Ine	Miyadu
III	19	5h	17m	3.6s	3.6s	3.3s	2.0s

In the method proposed in the above, the velolcity of propagation of seismic waves has been assumed to be invariable with depth, which is of course an undue assumption. Consider a virtual ray of seismic waves which travels from the focus to a seismological station in a straight line with a uniform velocity and let its velocity be such that it starts the focus and arrives at the station simultaneously with the real wave. Assuming the velocity of the real wave to be a function of the depth only, expressed by the equation

$$\frac{1}{v}=n=a+bh,$$

we will examine in what degree the velocity of the virtual wave varies with epicentral distances. In the following calculations, the curvature of the earth is neglected. We have

$$\Delta_h=\alpha\int_0^h\frac{dh}{\sqrt{n^2-\alpha^2}},$$

$$T_h=\frac{n^2dh}{\sqrt{n^2-\alpha^2}},$$

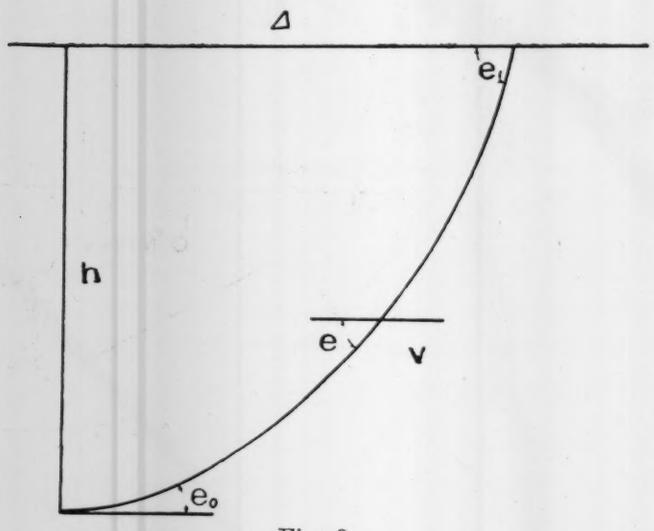

Fig. 3.

where Δ_h is the distance of the epicentre from a station,

T_h is the time of travel of the wave from the focus to the station,

$\alpha = n \cos e =$ a constant for a definite ray,

$n = \dfrac{1}{v}$

e is the angle which the ray of the wave makes with the horizontal plane at the depth h,

e_0 is the value of e at the focus.

After the integration we have

$$\Delta_h = \frac{\alpha}{b} \frac{1}{0.4343} \log_{10} \frac{\sqrt{n^2-\alpha^2}+n}{\sqrt{a^2-\alpha^2}+a},$$

$$T_h = \frac{n}{2b}\sqrt{n^2-a^2} + \frac{\alpha\Delta}{2} - \frac{a}{2b}\sqrt{a^2-a^2}.$$

The velocity of the virtual wave which is equal to $\dfrac{\sqrt{\Delta_h^2+h^2}}{T_h}$ is given in the following table. In the table it was taken

$$a=0.154, \qquad b=0.002, \qquad h=20 \text{ km.}$$

(which gives for $h=0$, $v=6.49$; for $h=20$, $v=8.77$; a rather remarkable change)

e_0	0°	15°	30°	45°	60°	75°	90°
Δ	—	33.43	22.81	15.42	9.51	4.56	0
T	—	5.16	4.05	3.37	2.96	2.74	2.68
Velocity of virtual ray	—	7.56	7.54	7.50	7.48	7.47	7.46

As is seen in the above table, the velocity of the virtual wave does not vary much so far as the epicentral distance is not very large compared with the depth of the focus. Therefore, we are justified to use the straight path and the mean velocity of the virtual wave instead of the curved path and varying velocity without introducing sensible errors.

The hypocentre of an earthquake is of course not a mere geometrical point, but must be a domain with some wide extension. The true form of the hypocentral region, however, remains in obscurity in our present knowledge of earthquake. It is only convention that we give the nearest point of the hypocentral region from a station the name of hypocentre.

In the course of the present study the writer has met with some earthquakes for which no definite focus can be obtained by the present method. This may sometimes be due to the broad extension of the hypocentral region and sometimes due to the mis-recording of the duration of preliminary tremors or more probably due to the fact that in the meizo-seismal region a bodily movement of the earth-crust is superposed on the ordinary seismic waves.

According to the results of the calculations the errors involved in the determination of the hypocentre by the present method becomes large when the epicentre lies outside of the network of the seismological stations. Therefore, we must select the stations in such a way that the epicentre of an earthquake falls inside of the network of the stations.

The present method may be adopted with special advantage when we want to determine the hypocentres of a number of earthquakes occuring in a definite earthquakes district. As an example of the practice of this method in such a case, the results of the study made upon the after-shocks of the Great Tango Earthquake are given in the following table. The earthquake taken in the present study are those observed during the period from 13th. March to 31st. August of 1927, with their amplitude greater than 100μ. The data of the duration of the preliminary tremors were placed at the writer's disposal through the kindness of N. Nasu and K. Wadati. In the last two columns of the table are given the depth of focus and the coefficient k as obtained by the present method.

Date				Preliminary tremors observed at					k	Depth
		h	m	Maiduru	Kinosaki	Ine	Miyadu	Toyooka		
				s	s	s	s	s		km.
3	12	15	28	3.0	4.1		1.8	3.6	7.6	10.3
3	13	10	20	5.4	3.4	4.2		3.4		
		13	37	3.7	3.3	2.9	2.4	2.6	8.5	15.5
		16	06	3.2	3.6		1.8	3.0	7.6	5.7
		20	34	6.7	3.1	4.7		3.2		
3	14	12	49	4.1	3.1	3.4	2.4	2.6	7.6	10.5
3	15	13	34	3.4	3.4	3.3	2.0	2.4	8.2	12.2
3	18	21	47	3.1	4.3	3.7	3.1	3.8	11.4	32.0

(to be continued)

(continued)

Date				Preliminary tremors observed at					k	Depth
		h	m	Maiduru	Kinosaki	Ine	Miyadu	Toyooka		
				s	s	s	s	s		km.
3	19	05	17	3.6	3.6	3.3	2.0	2.9	7.6	10.8
		15	50	7.4	3.8	5.7	6.1	4.6		
3	20	10	54	4.2	3.4	2.8		3.7	7.6	6.3
3	22	03	16	6.5	3.3	4.8		2.2		
		12	57	3.7	3.3	3.2	2.5	3.2	8.9	18.4
3	23	22	50	3.7	3.5	2.8	2.4	3.2	8.7	16.5
3	24	08	41	3.5	3.8	3.2	3.1	3.4	12.1	36.6
3	25	00	34		2.9	4.2	3.1	3.4	6.6	7.8
		19	13	4.4	2.7	3.4	2.6	3.0	7.7	6.5
3	29	05	06	5.1	2.6	3.9	2.4	2.7	6.9	5.7
3	30	22	30	3.0	5.3	3.1	3.4	3.4		
4	01	06	07	2.6	4.8	3.6		3.8		
		09	49	2.5	4.5	3.6		4.2		
		11	42	4.2	2.7	4.2		2.2	7.7	6.8
		18	23	2.3	4.9	2.9	1.7	3.9	8.1	13.4
4	03	02	07	2.2	5.1	3.7	1.4	4.2	7.1	6.0
4	12	09	33	5.0	2.2	4.1	3.3	2.6	7.9	11.7
4	15	10	49	5.0	2.3	4.3		3.0		
4	16	22	34	4.5	2.8	4.2	3.1	2.6	8.2	17.5
4	17	15	44	3.7	4.2	3.5	1.4		6.4	1.7
4	20	05	49	2.1			1.5	3.9		
4	28	08	37	7.5	4.0	5.3	6.0	4.2		
5	03	11	48	4.5	2.4	4.3		3.7		
5	23	01	30	4.7	3.2	3.4				
5	24	21	08	6.0	3.2	4.7	3.7	3.4	6.1	9.4
5	29	01	30	6.1	1.1	5.0	2.3	2.9		
		04	32	5.9	1.1	5.6	3.6	1.6		
6	06	09	12	6.0	2.6	5.0	2.6	3.9		
6	11	03	35	5.0	3.4	4.3		3.5	9.0	27.2
6	17	18	30	3.4	3.6	3.1	1.4	3.2	7.2	2.7
6	19	18	33	2.9	4.5	3.6	1.3	3.6	6.7	3.4
6	24	19	42	6.0	2.9	3.8	4.2		8.1	4.6
7	07	05	24	5.1	2.7	4.1	3.8	3.1	9.6	23.0
8	05	11	44	4.3	3.0	3.3	2.4	2.9	7.3	7.9
		21	40	5.1	2.6	4.4	4.6	3.1		
8	07	00	20	3.4	3.3	3.4	2.2	2.4	8.7	15.0
8	16	23	25	8.5	9.1	11.0		8.1		
8	19	12	45	5.4	2.7	4.6	5.0	3.6		
8	30	23	03	4.0	3.2	3.7		3.7		

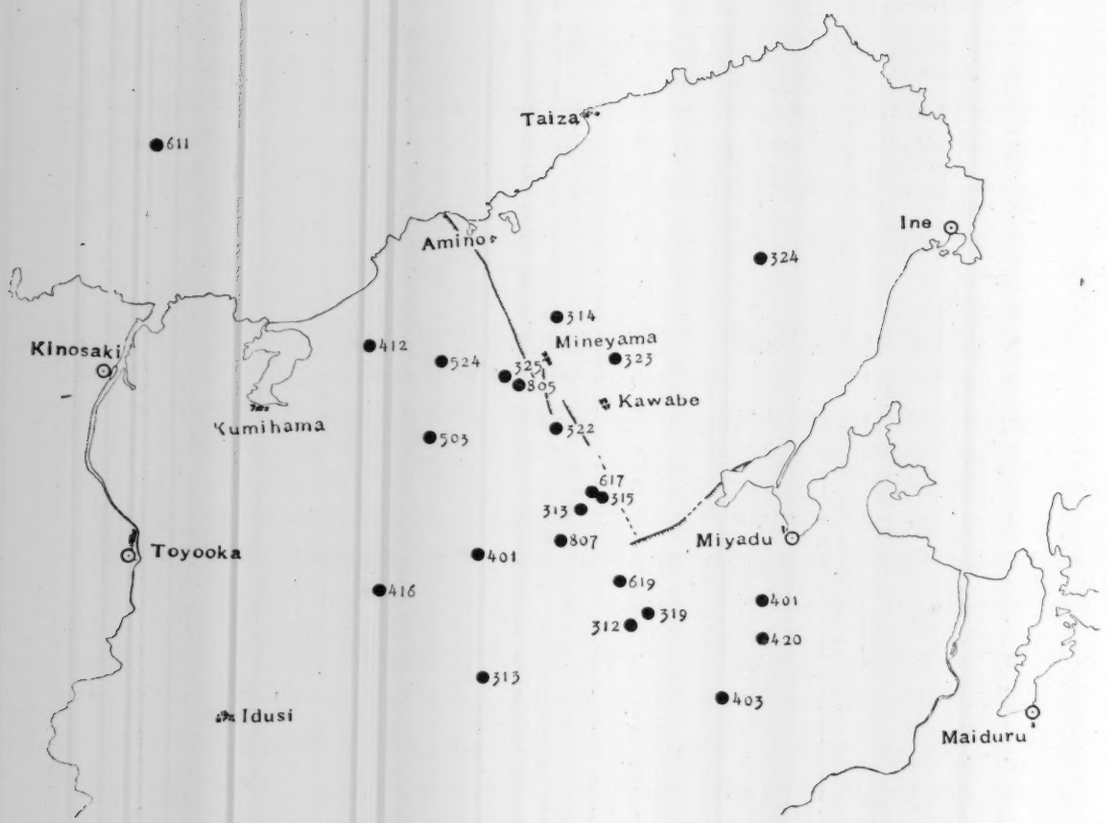

Fig. 4.

The geographical distribution of the epicentres found by the present method is shown in Fig. 4. The epicentres are distributed rather densely in two regions, the one in the west side of the Gomura fault and the other in the south side of the Yamada fault, diverging westward and southward respectively. In the Tango Peninsula proper which is distinctly separated from the main land by these two faults, only three epicentres are to be seen. This may be accounted for by assuming that the land block composing the mass of the Tango Peninsula is very rigid and stable in itself, while its adjacent blocks are movable and deformable, frequently giving rise to after-shocks in their contact planes or in the interior of themselves. With this connection, Professor Ishimoto's[4] observation of the tilting of the ground of the Tango District may be referred to. According to his

(4) Bull. Eqk. R. I. IV 203 (1928).

results, the tilting motion of the ground preceding an after-shock is often observed at Miyadu which lies on one of the movable blocks, while at Kawabe which lies on the stable mass of the Tango Peninsula no such tilting is observed. All of these facts seems to be in good accordance with each other.

In Fig. 5, is given the relation between the coefficient k and the depth

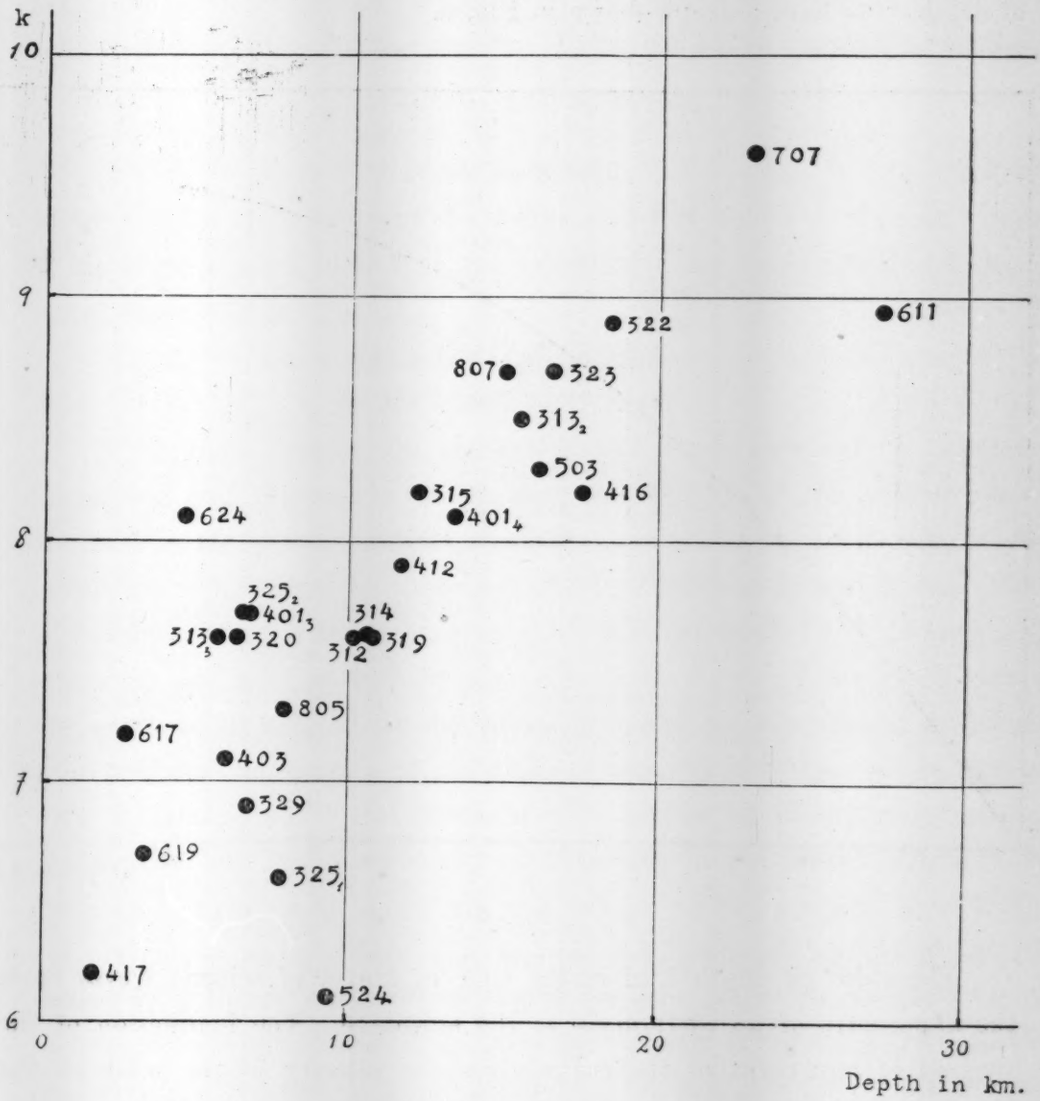

Fig. 5.

The numbers 315, 807 show that the earthquakes corresponding to those points ocurred on the 15th, of the third month of 1927 and on the 7th of the eighth month.

of the focus. A remarkable increase of k with depth may be seen. Generally speaking, errors introduced in this method is of the sense to make k increase with depth. For all that the fact that the values of k found from independent earthquakes has a tendency to lie on a rapidly ascending straight line seems to be due to something real.

Protting the depth of the hypocentres against the corresponding value of depth/k we have a graph shown in Fig. 6.

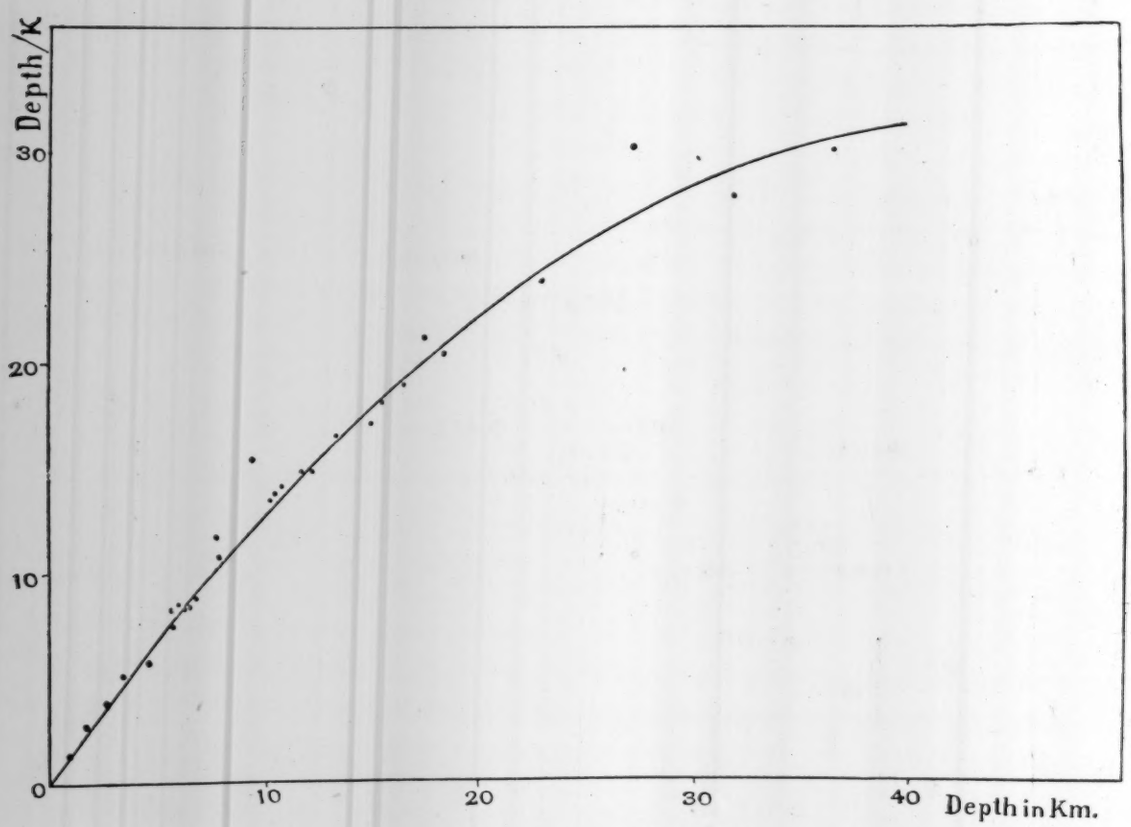

Fig. 6.

The value of depth/k gives the time of travel of seismic waves from the hypocentre of an earthquake to the epicentre. The inclination of the tangent at any point of the curve gives the velocity of the wave at the corresponding depth. Assuming the curve to be expressed by a form

$$\text{depth}/k = t = Ax + Bx^2,$$

where x being the depth in km., the constants A and B were determined

by the method of least squares out of the data amounting to 28 in number. The result is

$$t=0.1437x-0.001628x^2.$$

For the determination of the coefficient of the terms of the order higher than two the number of data is not sufficiently large. Moreover, for the depth more than about 15 or 20 km. the above expression for t cannot be very much relied upon, as the points to determine the coefficient is too rare and scattered widely in that region. From the above expression, we have

$$\frac{dt}{dx}=\frac{1}{v}=0.144-0.00326\,x,$$

$$v=6.95(1+0.0226\,x),$$

where v gives the velocity of the differential P-S wave. If Poisson's ratio of the crust is taken to be 0.27, the velocities of the longitudinal and transversal wave will be

$$v_p=6.06\,(1+0.0226\,x),$$

$$v_s=3.40\,(1+0.0226\,x).$$

When these results are compared with those obtained by Wiehert, Gutenberg and others, we notice that the velocity of the seismic waves obtained in the present study increases so rapidly with depth that it surpasses the values given by them at a depth of between 15 and 20 km. This is, however, of no wonder because the values obtained by Gutenberg and others do not hold so well for the superficial layers of the earth within the depth of 50 km., while the values obtained by the present author is valid only for the layers within a depth of some 15 or 20 km. If we assume with T. Matsuzawa,[5] the existence of a surface of discontinuity at the depth of 15 km. and the velocity of the wave in the deeper layers to be given by the results of Gutenberg and others, we can connect, if we want, our present values to theirs. But we need not make such unnatural connections. It is rather a wonder to obtain the same value for the velocity of the seismic waves in the surface layer for entirely different districts whose geological constructions are very different from each other, even though they may be the same in the deeper layers.

(5) Bull. Eqk. R. I. V 1 (1928).

In conclusion, the present writer wishes to express his most cordial thanks to Professors M. Isimoto and T. Terada and to Dr. C. Tsuboi for their valuable advices and encouragements. His best thanks are also due to Drs. N. Nasu and K. Wadati who kindly placed the valuable data concerning the after-shocks of the Tango Great Earthquake at the author's disposal.

October, 1928.

Earthquake Research Institute.

丹後地震の餘震觀測調査報告

(第一報)

囑託　那須信治

On the Aftershocks of the Tango Earthquake.

By **Nobuji NASU,**

Introduction.—The destructive Tango earthquake, which occurred in the coast of the Sea of Japan on March 7, 1927, at 18h 27m was the most appalling catastrophe experienced in this country since the great Kwanto earthquake of 1923. It caused much greater loss of lives and property than in the case of the Tazima earthquake, which took place on May 23, 1925, at the place about 18 kms. to the west of the recent one.

Soon after the catastrophe, I in cooperation with Prof. A. Imamura instituted in the seismic area a network of seismological stations for the purpose of studying aftershocks, while Dr. M. Ishimoto, a member of the Earthquake Research Institute, started his clinographic observation at Miyadu and Kobemura. (See M. Ishimoto: Observations sur les variations de l'inclinaison de la surface terrestre à Miyadu-mati et Kawabémura après le grand tremblement de terre de Tango. Vol. 4, this Bulletin.) The results of our works have briefly been reported by Prof. Imamura in the paper entitled "On the Destructive Tango Earthquakes on March 7, 1927," (Vol. 4 of this Bulletin).

1) Instruments.

The instruments used for the present purpose were ones designed by Prof. Imamura (see this Bulletin Vol. 1, p. 7.), the instrumental constants having been as follows:

Instrument	Free Vibration Period in sec.	Pointer Magnification	Registrable Amplitude	Time Scale mm./min.
25th year type	7	25–50	0.001–1 mm.	60–120
Impreved Omori type	4	50–120	Do.	40–70

Memits of these instruments lies, first, in the fairness of registra-

tion even for the seismic motion as small as one micron, and secondly, in the rapidness of driving rate of the record-reciever which can be driven as fast as 120 mm. per minute.

The network of stations was framed as follows (see Fig. 2.):—

First period. (From March 11 to December 22, 1927)

Station	Instrument	Distance (in km.) from	
		Kinosaki	Inemura
Maiduru	25th year type	50.4	25.5
Kinosaki	Do.	0	43.5
Inemura	Improved Omori type	43.5	0

Second period. (From January 21, 1928 up to precent.)

Station	Instrument	Distance (in km.) from		
		Kinosaki	Kobemura	Taiza
Maiduru	25th year type	50.4	27.0	38.3
Kinosaki	Do.	0	25.6	28.0
Kobemura	Improved Omori type	27.0	0	14.8
Taiza	Do.	28.0	14.8	0

2) Formula adopted for the computation of focal distance d by means of the duration of preliminary tremors t.

The formula first adopted for this purpose was the well-known one of the late Prof. Omori, viz:—

$$d = 7.42\,t\,,$$

but as it was found to be unsatisfactory for the present district, we changed our policy and amended the network by adding one more station as shown in the second network, such that we can work out not only the position of seismic focus, but also the constant factor which is to be used instead of 7.42 in Omori's formula, provided the observations at the four stations are perfect. From observations carried out since January of this year, I have found that the formula,

$$d = 8.4\,t$$

to be satisfactory for the shocks originated in this district. (See Table 2–3.) Strictly speaking, the factor in this formula is by no means constant, but varies slightly with the focal depth such that when the focus

is seated in a layer shallower than 10 km., it takes a value lying between 7.8 and 9.3, though on the average it works out as 8.4, whilst it approaches this mean value in the subterranean layer lying between the depths of 10 and 20 km. This irregular variation of the factor may be due to the complex arrangement of the various geological formations in those layers, especially in the upper ones.

It must be remarked that most of the aftershocks originated in the layers shallower than 30 km.

3) Classification of the aftershocks.

The seismograms of aftershocks furnished us with the means of classifying them according to their different characters.

a) According to the type of seismogram: A-type and B-type.

A-type: The initial phase $\overline{P}$ is comparatively large. The principal portion consists of an isolated wave of a period of about 0.5 second, a series of waves of quick period (about 0.12 sec.) being superposed on it. Surface waves of about 2.5–3.0 sec. are accompanied in the initial half of the whole course of earthquake motion. (See Fig. 1.)

B-tyype: The initial phase $\overline{P}$ is comparatively small. The principal portion consists of waves of quick period as in type A. Surface waves do not appear so clearly as in the case of A-type.

Such a distinction might be caused by the difference of directions of the seismogenic forces as welll as the difference of the focal depths. It is to be remarked that the character of A-type is found in that of an eruptive volcanic earthquake, while that of B-type exists in that of non-eruptive one.

b) According to the distribution of directions of the initial earth's movement: similar and non-similar to that of the first earthquake.

Adopting the method of imagining the mechanism of earthquake occurrence by means of the distribution of directions of the initial earthquake motion at the seismological stations in surrounding regions, it may be inferred that almost all the aftershocks were similar in their characters to the great Tango earthquake. There were only a few exceptional cases.

4) Distribution of the aftershocks on a horizontal plane: distribution of epicentres.

The different group of aftershocks changed their seats from time to time within a limit not so far from the new faults—the Gomura and the

Yamada faults. But the more active zones were in the west of the Gomura fault and the south of the Yamada fault. One of the interesting facts is that the eastern part of the former fault, i.e. the Oku-Tango peninsula, shows a rare distribution of aftershocks. This may suggest that the peninsula made a bodily dislocation towards the NNW during the outbreaks of the great earthquake and its aftershocks.

Fig. 2 shows the distribution of aftershocks, which took place during March 12–August 31, 1927, and of which the epicentres could be determined by means of our seismic triangulation.

Fig. 3–8. Ditto, each corresponding to the period mentioned there.

In the figures the epicentre of the strongest aftershocks of April 1, is indicated by the largest dot and those of the shocks in which the miximum amplitude at any of our station exceeded 100 microns by dots of next size. Figures attached to each dot correspond to those in the column of epicentre in the table at the end of this report.

5) Distribution of the aftershocks on vartical plane.

As to be understood from the distribution of the faults (see Fig. 2), the land mass in the seismic area can be divided into a number of fragmental blocks with those faults as their boundaries. Let us now draw a vertical plane normal to one of the faults—say, the Gomura fault—and project on it the foci of aftershocks contained in a block adjacent to that fault—say the block 3, (the same Fig.), arranging the aftershocks into two classes according to the times of their occurrences, (see Fig. 9).

It will be noticed that some of the points thus projected can be grouped together into a number of systems of finite lines (foci depending on a common line being generally successive occurrences), of which those belonging to a common system are essentially parallel to each other and make an echelon arrangement by themselves. This suggests that the aftershocks originated in a parallel row, or rows, of planes, that is to say, in a number of cracks which are likely to have been produced in the blocks as the result of shearing stresses applied to it.

It must be remarked that in taking the vertical plane of projection parallel to the Gomura fault, a similar result is obtained again for the foci contained in the same block (see Fig. 11).

Fig. 12–19 show similar figures relating to each of the other six blocks.

The cracks or faults thus worked out are, for the most part, hidden under the earth's surface, the most conspicuous ones being as follows:

W. of the Gomura faullt		S. of the Yamada fault	
Direction	Dip	Direction	Dip
WSW	75°	NNW	50°–60°
„	45°	SE	45°
ENE	70°	NE	45°
		SW	50°
NNW	45°	„	80°
SSE	45°		

Actually the Gomura fault was found near Takahasi and Nimbari dipping at 60°–80° towards SW; this is in tolerably good accordance with the data given above at the top of two columns in the lefthand side.

6) Frequency of the aftershocks.

a) Daily frequency. (See Fig. 20.)

It was found that the daily number of the aftershocks during the period from March 7 to 30 may be calculated approximately by the formula,

$$y=\frac{218}{x+0\,7}$$

where x is date reckoned from the time of occurrence of the first big earthquake, i.e. March 7, 18h 27m, and y number of shocks in the corresponding date. But as the strongest aftershocks which took place on April 1, accompanied its own aftershocks in addition, it became necessary to change the formula thenceforth available as follows:

$$y=\frac{218}{x+0.7}+\frac{34}{x-25+0.16}$$

b) Hourly frequency during 54 hours after the great earthquake. (See Fig. 21.)

In Fig. 21,

Curve—a shows the hourly frequency with max, M_1, M_2....M_8 each of which took place at 7 or 8 hours before or after the next one.

Curve—b shows that of aftershocks felt with our unaided senses.

Curve—c that of aftershocks not felt with our unaided senses.

By means of these curves, we can imagine how the tectonic adjustment was going on after the great earthquake. The sensible, comparatively large, aftershocks were brought about by the formation of new

cracks, while the insensible ones were chiefly caused by the growth of secondary small cracks. It may be said that the larger cracks were produced one after another very actively during 30 hours following the outbreak of the first big shock, though in general the activity decreased with time. On the other hand, it seems that the minor secondary cracks grew one after another near the principal faults. These facts are suggested by the curves -b and -c, the former shows the decrease in the activity of the sensible shocks and the latter the gradual increase in number of the insensible ones during the above-mentioned period.

c) Frequency in other districts. (See Fig. 22).

The Mino-Owari district once experienced a great earthquake on Oct. 28, 1891, and thence minor shocks have been occuring there one after another. It will be understood from Fig. 22 that an abrupt increase in frequency was experienced soon after the Tango earthquake.

The district of Wakayama did not show any evidence of such a sympathetic occurrence, though both districts are at about equal distances from the origin of the Tango earthquake.

7) Emigration of the active centre. (See Fig. 23, Nos. 1, 2, 3).

On tracing the position of the foci of comparatively conspicuous aftershocks, which took place soon after the great earthquake up to the beginning of March of this year, it was found to be convenient for statistical study to divide them into 17 groups according to the period of their occurrences. In Fig. 23 aftershocks belonging to one group are indicated with large figures corresponding to the number of that group, together with small suffix corresponding to the earthquake numbers in that group.

One of the noteworthy results is that the active centre changed its position from place to place in an oscillatory manner.

8) Relation between the activities of the different earthquake groups and the preseismic tiltings of the earth.

It is well known that the tiltings of the earth take place as a preseismic phenomenon. Naturally, there must be some relation between such tiltings and the seats of the corresponding earthquake groups.

Prof. Ishimoto, who has been carrying on the clinographic observations at Miyadu and Kôbemura, obtained a very interesting result that the earth shows a characteristic tilting for a few days before the occurrence of earthquake when it is of a moderate size. On comparing Ishimoto's result concerning such a tilting with the active centre indicated by the seat of the corresponding earthquake group, it was found

that the tilting dips towards the active centre when the centre is seated in a region where subsidence took place at the time of the great earthquake or later than it, while, on the contrary, when the centre is seated in an upheaved region, the sense of the tilting is opposite to one in the above case. Examples showing the above relation are as follows: (See Figs. 24–28.)

Tilting			Active centre		
	Duration	Direction (downwards towards)		Region of	Direction (from Miyadu)
a	Mar. 15–20	SE	A	Upheaval	NW or SE
b	20–23	—	B	Do.	NW
c	23–25	NW	C	Subsidence	NW
d	25–30	SE	D	Upheaval (?)	W or NW
e	30–Apr. 1	NW	E	Do.	SE or S
f	15–22	W?	F	Subsidence (?)	NW or S
g	22–23	E?	G	Upheaval	SW
h	23–25	NW	H	Do.	SE or SW
i	25–May 7	NE	I	?	NW
j	8–15	NW	J	Subsidence	NW
k	15–17	E	K	Upheaval	NW
l	15–June 10	—	L	—	NW
m	10–15	S?	M	Upheaval	NW
n	15–17	N?	N	Upheaval (?)	W
o	25–30	S	O	Upheaval	NW
p	30–July 7	NE	P	Do.	NW
q	9–12	NE	Q	Subsidence	N
r	25–Aug. 5	NE	R	Upheaval	NW
s	5–Sept. 1	NE	S	Do.	NW

Again according to Prof. Ishimoto, the clinograph at Miyadu showed sudden change of the earth tilting in the NE direction repeated four times during the period from June 30 to the end of August. It may suggest that the Oku-Tango peninsula was displaced, as a whole, downwards towards the NNW at those four steps. The tectonic change which may correspond to such displacement has been discovered as the result of the second post-seismic precise levelling carried out by the Military Land Survey Department over the diffrent routes in the seismic area. (See Vol. 4 of this Bulletin.)

緒言

昭和二年三月七日丹後烈震後、東京帝國大學地震研究所に於て各所員の專門的分擔調査が開始された。自分は今村教授の擔當せられた餘震の觀測に就いて其の實施、並に驗測調査に從事した。爾來、今日に至る迄猶ほ繼續中である。

餘震調査の結果は先に帝國學士院紀事、第三卷第四號及地震研究所彙報第四號に其の一部を報告されたが此等の報告に更に其後に於ける調査の結果を綜合して茲に記載する次第である。

先づ今回の烈震の程度を觀るに、本報最近に於て關東大震に次ぐ大災厄であつて、人命財產の損失は大正十四年五月二十三日の但馬地震の場合に於けるものの數倍に達し又地形地物の變動に於ても今回は稍々廣範圍に亘つて著しく現はれた。此等の點より觀るに、前年但馬を襲つた大地震よりは遙かに大規模のものである。

丹後烈震後、同地方に於ては頻々と餘震が發生して居つた。この際に於て稍々統一されたる餘震の觀測が望ましい事であつた。又該地方に於て實地に觀測に從事する者としては野外觀測の最も好い經驗を得べき時であつた。

これより前、地震學教室に於て地震計測整備が專ら今村教授に依つて行はれた。其際新しく造られたる携帶用微動計數個及此等の附屬品が平常準備されてあつたので此回は此等の內三臺を選んで震災地に設置することにした。即ち大正十四年式携帶用微動計二箇及此と同一考案に依つて改良せられたる大森式簡單微動計一箇である。此等の器械は餘震中の微小なるものをも觀測するに適當であつた。

此等の器械が有する常數は次表の通りである。

第一表 (TABLE 1)

型式	自己振動週期	倍率	記錄し得る振幅	記錄速度
大正十四年式（今村式）	7 sec.	50	.001-1.0 mm.	60-120 mm./min.
改良大森式（大森、今村式）	4 sec.	50-120	.001-1.0 mm.	50-70 mm./min.

此等の微動計の準備を整へ地震學教室の脇元雇員外二名の觀測者と共に三月十日に出發し大地震數日後震災地に於て觀測網が完成せられたので觀測した餘震の數も比較的多數に上つてゐる。

器械の取扱に關しては絶えず細心の注意を以て行ひ、殊に損じ易い部分、例へば微動計の重錘を支ふる上下の自由尖端、描針の廻轉軸の尖端等は隨時之を取換へ又記錄裝置も整調に廻轉し得る樣に手入を度々行つた。

今回の如き微小なる餘震を十分に記錄し得たのは使用された器械が目的に適してゐた事によるが、また一面觀測者が以上の如き取扱上に於ける細心の注意を拂つた賜に外ならないと思ふ。

尙ほ計測の正確を期するため、最初の十數日は各微動計の記錄速度を其の最大限にして用ふることにした。それは餘震の初期微動繼續時間が比較的に短く、僅かに三秒或は四秒程度のものが多かつたので平常觀測の場合の約二倍の記錄速度とする方が便利であつた爲である。

觀測點は出發前に大略、舞鶴町、城崎町及殘りの一點は丹後半島の日本海沿岸附近に設置する豫定であつた。併し現場に臨んで見ると前記の二箇所は幸ひ好都合であつたが、丹後半島內に設置することは當時交通杜絶のため不可能であつた。僅かに半島東部にある伊根村に達する汽船の便があつたので、他の一箇所は此處に設置することにした。以上の三點ならば震源の深さを顧慮しても適當であり又事務上からは日々の觀測結果の報告にも便利であつたのである。

そこで十四年式微動計は舞鶴、城崎に夫々一臺宛、改良型大森式簡單微動計は伊根村に据付け、舞鶴町は三月十一日午後九時四十分頃より、城崎町は同十二日午後二時三十分頃より、伊根村は同日午後二時四十分頃より何れも觀測を開始した。此等の三觀測點の相互距離は伊根村舞鶴間二五・五粁、舞鶴城崎間五〇・四粁、城崎伊根村間四三・五粁である。

三月七日午前六時二十七分の大地震の概要

先づ餘震の調査に際して豫備的智識として本烈震の概略を知つておく必要がある。殊に烈震後に於ける活動區域の進展する有樣を調べ又は餘震の性質が本震と同一性質のものか否かといふ點に就いて判定を下す際には最も必要である。幸ひ本大地震に關しては今村教授が詳細に調査され、その報告が地震研究所彙報第四號に揭載されてあり、又中央氣象臺の國富技師も同時に氣象集誌、昭和二年四月號に調査の結果を發表して居られる。この二つは本烈震の驗震學的の考察として最も有益な資料である。今此等の論文の內より數項目を引用してこゝに本烈震の概要として記して見よう。

第一水平斷層的發震力が著しかつた事である。此は各地の測候所に於て觀測せられ

たる地震動の初動の方向を綜合して判斷された結果である。これは地殼を等質一樣な彈性體と假定し、今この內部に假想的水平斷層運動を起すとこの運動によにて射出された縱波の初動は力の作用線及力の作用點に於て之れに直角なる直線によつて限られたる四つの象限內では夫々相異る方向を示すのである。

即ち今回鄕村斷層附近に行はれた地殼の相對的水平斷層運動を考へ各地の測候所に於て觀測せられた初動の方向を觀るに可なり一致して上述の假想的の彈性體內の初動の方向に依つて說明される。此回の丹後地震の如く比較的判然と初動の方向が各象限內で分類される例は稀らしい現象である。此の事實によつても水平的剪斷作用が可なり顯著であつた事が想像される。

次に震央は淺茂川附近であつて震原の深さは比較的淺い。國富技師の調査されたのでは約十四粁の深さであつた。同氏の震原の深さの決定の方法は P 及 $\overline{P}$ 波の走時曲線を利用するのであるが此の餘震の三點觀測によつても爾後の餘震は大體上述の深さに發生するものが多いやうである。また大地震の震央であつた附近では此の觀測が開始されてから後は比較的餘震が少い。それは烈震後數日の中に餘震の活動區域が移動したのに起因すると思はれる。

震原位置推定に用ひたる公式

丹後地方の如き比較的狹い範圍內では震原の推定には從來一般に行はれてゐる如く初期微動の繼續時間に依る方法を用ひて相當に正確に結果を求め得るであらう。併し從來の公式を其儘用ひて差支なきか否かは實際の觀測値と照合せて見る必要がある。

そこで最初の間は大森公式の

$$d=7.42\,t$$

を使用して震原距離を求めてゐたが該公式の適、不適を定めるには今一箇所觀測點の增加が必要である。試みに幾何學的に說明すれば震原（發震點）を一點 (X, Y, Z) とし四つの觀測點が同一平面上に位置してゐると假定す。即各觀測點の座標を夫々 $(0, 0, 0)$, $(x_1\,0, 0)$, $(x_2, y_2, 0)$, $(x_3, y_3, 0)$ とすれば發震點と觀測點との距離の間に次の關係がある。

$$(X-x_n)^2+(Y-y_n)^2+Z^2=k^2t_n^2$$

$n=0, \ldots .3$. 但し $(x_0, y_0, y_1$ は共に 0 とす), t_n は觀測點 $(x_n, y_n, 0)$ に就いて計測されたる初期微動繼續時間（秒）、k は係數である。

上述の式を四觀測點に就いて求め、それより震原の座標 (X, Y, Z) 及 k を求めるのであるが k に就いては次式を得る。

$$k=\sqrt{\frac{d_1^2(x_3y_2-x_2y_3)-(d_3^2y_2-d_2^2y_3)\,d_1}{\tau_1(x_3y_2-x_2y_3)+(y_3\tau_2-y_2\tau_3)\,d_1}}$$

こゝに d_1, d_2, d_3 は觀測點 $(x_1, 0, 0)$, $(x_2, y_2, 0)$, $(x_3, y_3, 0)$ と基準觀測點 $(0, 0, 0)$, との相互距離（粁）であつて實際の場合は $(0, 0, 0)$ を舞鶴に選び $(x_1, 0, 0), \ldots$ を城崎町、河邊村、間人町とすれば $d_1=50.4$ 粁、$d_2=27.0$ 粁、$d_3=38.3$ 粁

$$\begin{cases} x_1=d_1=50.4 \text{ 粁} \\ \end{cases} \quad \begin{cases} x_2=260. \text{ 粁} \\ y_2=\ 7.7 \text{ 粁} \end{cases} \quad \begin{cases} x_3=31.7 \\ y_3=21.4 \end{cases}$$

である。

$$\tau_1=t_1^2-t_0^2,\ \tau_2=t_2^2-t_0^2,\ \tau_3=t_3^2-t_0^2$$

先づ此の方法によつて二三正確なる觀測の結果より該地方に於ける餘震に適する常數 k を求めてみると大體 8.2 乃至 8.7 を得たのである。併し實際の場合には以上の方法は便利なものではない。多數の餘震を取扱ふ上にはどうしても作圖法に依るより外はない。これには比例配分を用ふるのが便利である（方法の說明は略す）。併しこゝでは比例を用ふる方法を用ひないで多少面倒ではあるが常數を上式で定めた後その値に應じて震原距離を各觀測點に就いて算出しその距離を半徑、各觀測點を中心として夫々圓周を描き、二圓の共通弦を引きそれ等が交はる交點を震央と定めたのである。計算上甚だしい常數の差異を示してゐる餘震でもその震原に多少大きさを與へるときは以上述べた 8.4 附近の常數値で十分滿足される例もあると思はれる。これは震原を幾何學的の點と考へないでこれに或る大きさを認めなければならぬことを暗示してゐるのであらう。即ち單位地塊ともいふべきものが震原となつた場合である。

これは後に述べる樣に丹後地方に存在する地下裂罅によつて地殼は多數の部分的地塊に切り刻まれてゐる。その內には數立方粁位のものもあるやうである。斯る地塊が一つの震原となり得る事も考へられる。

前述の理由により本年一月より更に間人町に新觀測點を設置し四點觀測により震原の位置並に公式中の常數をも同時に決定することにした。尙ほ餘震の活動が平靜になり、比較的微小な餘震のみが發生してゐたので從來の觀測網では廣大に過ぎるので新觀測點の設置に先立つて觀測網の縮少を行つた。即ち舞鶴、城崎、河邊村の三箇所と

して昨年十二月末日から觀測を續けてゐた。それに本年一月から前述の間人町の觀測點が新に加へられたのである。

常數決定並震原の位置推定に就いて少しく附記しておく事がある。一般に丹後地方に發する餘震は比較的初動が明瞭に現はれるものが多い。前に報告した際に述べた様に A 型のものは勿論, B 型の餘震に於ても相當判然として最初の波動を見定めることが出來る。そのために初期微動の繼續時間を計測するには非常に好都合であつた。唯記錄圓筒の不規則な廻轉に起因して起る誤差を見出すことがあるがそれも極めて稀である。この不規則な廻轉に依る誤差と認めた場合には之に補正を加へた。その補正の數値も ±0.5 秒以下である。

前述の通り震原が稍々廣大な範圍に擴がつてゐる場合その形狀を判然と決定することは困難である。それ故こゝでは震原の形狀に關しては觸れてゐない。而し前にも述べた如く從來の公式中の常數を變更したものを用ひて四箇所に於て震原を推定すると可なり狹い場所に發震點があると思はれる例が多い。此の事から微弱な餘震の震原は多くは小區域內にある様にも思はれる。そこで發震點が比較的狹い範圍に在りと看做し得るものを選んで初期微動繼續時間 t と震原距離 d との關係は次の公式に依ると四箇所の觀測がよく一致する様に思はれる。即ち

$$d=8.4\,t$$

の公式である。

第 二 表 (TABLE 2)

日 時 (Date)	初期微動繼續時間 (Duration of preliminary tremors)				公式中の常數 (Factor in the formula)	震原の深さ (Focal depth)
	Maiduru	Kinosaki	Taiza	Kobemura		
h m						km.
II 18, 18 49	5.2	2.6	2.4	2.3	8.2	7.8
I 30, 18 41	5.1	2.8	1.7	2.3	8.6	9.7
II 19, 5 27	3.8	3.3	2.0	1.2	8.7	10.4
II 14, 20 39	4.0	2.8	2.8	1.7	8.2	11.7
II 12, 21 27	5.0	3.0	1.6	2.2	8.3	12.0
III 1, 22 34	5.5	2.0	2.9	2.7	8.3	14.3
II 29, 10 38	3.2	3.6	3.3	2.0	8.6	14.8

平均 8.43 (mean)

この公式の決定に用ひた餘震中最も正確なものを選んで常數の値及その餘震の起つた日時及震原の深さを記すれば第二表の様である。

尙又以上の外昨年九月一日より十二月末日に至る四ケ月の期間中に起つた餘震の宮津、豐岡の兩測候所の觀測の結果と當觀測所に於て求めたるものとを合せて常數の決定を行つた。その內比較的よく震原を推定し得たものを記すれば次表の通りである。

第　三　表　(TABLE 3)

日　時 (Date)	公式中の常數 (Factor in the formula)	震原の深さ (Depth of focus)
h m		km.
XI 16, 20 20	8.2	0
XII 4, 9 56	8.3	0
XII 30, 13 52	8.5	0
XI 11, 9 24	8.8	7.0
IX 23, 5 11	8.2	7.2
XII 4, 18 28	9.3	7.6
X 24, 7 57	8.3	8.0
X 28, 0 24	7.8	10.5
XII 28, 12 35	8.5	13.0
XII 8, 2 14	8.2	13.5
XI 26, 20 10	8.1	15.6
XI 10, 11 43	8.3	18.0
X 22, 5 57	8.3	18.7
XII 8, 2 14	8.2	19.8
X 3, 8 29	8.2	24.6
	8.39 (mean)	

以上の結果から觀ると地下十粁附近に至るまでは 7.8-9.3 迄の間に常數の値があるが十粁より二十粁內外の深さに發した餘震に對しては大體似たやうな數値を示してゐる。即地表近くでは雜複なる地質構造による影響が地震波の傳播に及ぼされるため上

層部に發した餘震で求められた常數は前述の如くやゝ不規則な價を取るのであつて十粁以上二十粁附近に至る深さに起つたものから求めた常數は左程變化はない。此はこれらの複雜な地質分布による影響が比較的少いとも考へられる。

餘震の分布を見るに大體十粁附近を境として上部と下部に分たれる。即上部の層内には餘震の分布は稀であるが下方の層には餘震の大部分が分布されてゐる。これ等は嚴密に層をなしてゐると斷言は出來ないが或はその様な配列が地下に行はれてゐるとも思はれる。

以上述べた層の事は公式決定とは直接關係のある事ではないが公式決定に際して得た結果の一部である。

餘震の種類

餘震の種類を記象の型から區別して A 型、B 型の二つあることは前の報告にも記されてゐる。この區別は分類の便宜上用ひたのである。

即ち餘震の發生する大略の位置及深さを知るに便利である（今村博士報告：地震研所彙報第四號究一九四頁參照）。

即 A 型と稱するものは初動 $\overline{P}$ は比較的大きく表はれ、主要動 $\overline{S}$ の $\overline{P}$ に對する比は一・五乃至四・〇位であることが報告されたが其後に於て更に此の比が 0.7 程度のものが起つてゐるのを見出した。主要動は週期凡そ〇・五秒の一箇の波動から成立ち、之に〇・一二秒程度の短い週期の波動が重なつて數秒間續いてゐる。又今一つ特徴とするところは稍々緩漫なる波動（週期二・五秒乃至三・〇秒）が全地震動の全般を占めてゐることである。

B 型は初動 $\overline{P}$ が比較的に小さく、主要動 $\overline{S}$ の $\overline{P}$ に對する比は一〇乃至三〇に達す主要動は A 型と同樣に稍々急激な週期の波動から成立つてゐるが A 型にある様な比較的緩漫な波動が表はれてゐない。

A 型、B 型の實例の寫眞は前にも揭示されてあるから茲には省略する（地研彙報同上）。

その後に起つた餘震の内で A 型に屬するもので初動が極端に大きく現はれたものを第一圖に示して置く。この二つの餘震は四月一日の强震後十四時四十九分頃に起つたのと七月二十二日十二時三十七分頃に起つたものとである。これ等の二つの型式を見るに舞鶴に於けるものは通常地震の形とは全然異なるものであつて火山の爆發に伴ふ地震の型式とよく似た點がある。

試に $\overline{S}$ と $\overline{P}$ の水平動振幅の比を求めて見ると前者の餘震の場合には 0.7 程度であり後者の場合も同様 0.7 程度である。これ等には上下動の分變位を計算に入れてないが主要動と稱する $\overline{S}$ 相が常規を脫して小さく現はれた事は疑ない。舞鶴の記象に於ては以上の結果であるがこれを他の觀測點に於ける記象に就いて見るに必ずしも $\overline{S}$ が $\overline{P}$ より大きく現はれてゐない。そこで從來屢〻論じられたる如く $\overline{S}$ と $\overline{P}$ の大いさの比は震原に於て作用する發震力の方向と之に對する各觀測點の位置的關係に依るものであらうと考へられる。この問題に就いては松澤武雄—學術研究會議天文地球物理學輯報第四卷第一號及須田皖次氏—海と空第五卷第十號、第十一號に夫々論文がある。

此の二論文によつて此等の餘震の震原に於ける發震力の方向が如何様であつたかが想像される。勿論理論上に於て求められた結論が直ちに實際上に適應されるや否や—そこには多少一致しないこともあるが大體の傾向だけは理論的の研究によつて十分云ひ表はされてゐる。此二餘震の震原と各觀測點との位置的關係と $\overline{S}$ と $\overline{P}$ の比を求める時には上下動の振幅も加算しなければならないがこれには射出角を想定して $\overline{S}$ 及 $\overline{P}$ の全振幅を求めることが必要であるがこゝでは水平動の實測値に就いてのべる。尙ほこゝに附言しておくことは此等の特別な二餘震の起つた場所の附近には多數の他の餘震が發生してゐる。それ等の餘震の記象の型式は普通の地震のものと同じであ° それ故にこの異常的な初動の大きな型式は地震波の經路の差異によるとは考へられない。そこで以上三觀測點に於ける波動の型式の異なる所以を考へるに、先づ須田氏の $\overline{P}$, $\overline{S}$ の大いさを求める式を引用して次の關係式を以て表はすことにする。

$$\frac{\overline{S}}{\overline{P}}=m=\frac{1+K_{\overline{S}}}{1+K_{\overline{P}}}\frac{\lambda+2\mu}{\mu}\tan\theta$$

或は

$$=\frac{1+K_{\overline{S}}}{1+K_{\overline{P}}}\left(\frac{a}{b}\right)^2\tan\theta$$

こゝに λ, μ は地殻を構成する物質のラーメの係數、a 及 b は $\overline{P}$ 波及 $\overline{S}$ 波の傳播速度、θ は震原と觀測點とを結ぶ線と地震力の作用線とがなす角、$K_{\overline{P}}$, 及 $K_{\overline{S}}$ は常數である。

$K_{\overline{P}}$, $K_{\overline{S}}$ の近距離の場合の値を求めるには多數の觀測點が必要であるからこゝでは判きりと定めることが出來ないが須田氏の結果に依ると五十粁內外では何れも0.03程度のものであるから $(1+K_{\overline{S}})/(1+K_{\overline{P}})$ は1に近いものであるとのことである。a^2/b^2

も先づ大略3位であるから全體としてはこれらの變化はさ程影響はない。觀測點の位置的關係即ち最後の項の $\tan\theta$ が最も有力なものである。

即發震力が觀測點と震原とを結ぶ線に沿つて作用するときは $\tan\theta=0$ なるために $\overline{P}$ は $\overline{S}$ に比して非常に大きく、計算上では無限大の比を與へるが併し實際の地震に就いて見るに先づ以上の二餘震の例に於ける $\overline{P}, \overline{S}$ の比即(0.7)が最小程度であらう。

そこでこの二例の場合の發震力は丁度震原と觀測點とを結ぶ線の方向に作用したのであらう。今假りに最初の大地震に於ける發震力の方向と略々同じ方向の發震力が後者の七月二十二日の餘震の場合に働き前者の四月一日强震後の餘震の場合はこの强度の發震力とは直角な方向のものが作用したとすれば此の二餘震の場合に於ける發震力の方向と舞鶴に於ける $\overline{P}$ の異常な大きさとの關係が多少判然となる樣に見える。七月二十二日の餘震は鄕村斷層の西部に發生したもので發震力の方向を想像するに藤原博士、高山威雄氏の丹後地震の地割の實驗（驗震時報第三卷第一號）に依て求められたる如く鄕村斷層帶に約三十度西北の方向として餘震の震央を通じ此方向に一直線を引くと丁度舞鶴を通過するのである。

即此の餘震の發震力は全く最初の大地震と同じ方向のものであらう。

四月一日の餘震は宮津の南方約七粁に震央を有し同日の强震の震原附近に起つたものである。併し發震力は舊斷層線に直角に作用したとすれば此の場合も丁度舞鶴の方向に一致するのである。そして舊斷層線に沿つては同日の强震が發しこの餘震は謂はゞ二次的な裂罅が舊斷層線に直角に生じたに起因すると考へられる。此等の裂罅の配列の有樣は改めて後に述べることにする。

さて $\overline{P}, \overline{S}$ の大いさを水平動のみに就いて實測した結果を次に記して置く。尙ほこれらに前述の $\overline{P}$ 及 $\overline{S}$ の射出角を想定してその大いさの比を求めると舞鶴では $\overline{P}/\overline{S}$ が 0.5 乃至 0.6 位にもなり得ることを附言しておく。

第 四 表 (TABLE 4)

Station	April 1, 14h 49m		July 22, 12h 27m	
	θ	(Horiz. comp.) $\overline{P}/\overline{S}$	θ	(Horiz. comp.) P/S
Maiduru	0°	0.7	0°	0.72
Kinosaki	15°	16.0	23°	10.0
Inemura	80°	13.3	50°	11.3

A型、B型の差異は以上の如く震原に於て作用する發震力の方向と觀測點の關係的位置によつて生ずるが緩漫な波動がA型にあるのは震原が比較的淺いために表面波が優れて現はれたのであらう。

次に餘震に鳴動を伴ふものと然らざるものがある。此の區別は當時地方人士も氣附く程明瞭であつた。但し鳴動の來る方面及地震動と何づれを先きに感じたかを地方人に聞いて見てもその答は區々でめる。そこで出張中鳴動を伴ふ餘震の日時を記して置いて後其の餘震の位置を推定して見ると三月十日頃から二十二日頃迄は概ね郷村斷層の西南部にあるものが多く加悦谷の附近にも少しはあつたやうである。宮津測候所の調査によると四月一日宮津附近の强震の際にも大なる砲聲の如き音響を伴ひ其後約十分間は續々と起る餘震の度毎に鳴動が聞えたさうである。今回の鳴動を伴ふ餘震が上記の郷村斷層西南部及加悦谷に限られて起つてゐたことは地下に於ける岩石構造が此の地方に限つて特異なものであつたとも考へられる。

初動の方向に依る餘震の種類

初動の方向を各觀測點で求めてその分布狀態に依つて地震の機構を推察し得ることは前にも述べたが其後の餘震に就いて同じ事を行つて見ると大抵の場合は三月七日の大地震の場合か或は四月一日の强震の場合に一致する樣に見える。

即ち剪斷性のものである。國富技師の報告によると本震直後の十八時四十四分の大なる餘震は本震とは全く反對向きの性質のものであつたと云ふことである。此の例に屬する餘震もあるが極めて少數である。その餘震の起つた日時を記すと三月二十日十四時二十分、同二十三日二十二時五十分、同三十一日十九時十三分、四月十六日二十時五十七分、同二十五日十九時二十七分、五月三日十一時四十八分、七月七日五時三十四分等である。

此等の餘震の起つた日時を稍々詳細に調べて見ると石本教授の宮津に於ける地表傾斜變化の觀測の結果（同氏論文地震研究所彙報第四號）と多少關係があるやうに思はれる。

即傾斜が或る方向から他の方向に轉ぜんとしつゝある時或は變化後比較的短時日內に此等の餘震が起つてゐる。即ち地表傾斜變化によつて表はされた某地の地殼變動の變換期にかゝる逆の方向の發震力が作用した結果であらうと想像されるが今少しく研究しなければ判然とした事は云へない。

餘震の震央の分布

此の觀測を開始して以來八月三十一日に至る迄の餘震の內震央を決定し得たもののみを總べて記入したのが第二圖である。同圖には觀測點、觀測網、新斷層、舊斷層、地塊の境界線（後に述べる）等をも合せて記入してある。此圖に依つて觀ると奥丹後半島內即ち郷村斷層以東の地域には僅かに數回の餘震が起つたに過ぎないが郷村斷層の西方及山田斷層の南方には極めて多數の餘震が頻發した事が判る。

第二圖　震域圖、餘震觀測網、新舊斷層線、地塊境界線、餘震の震央を示す

Fig. 2. Map showing the seismic area with the networks of stations, the faults, the boundaries of blocks, and the epicentres of aftershocks.

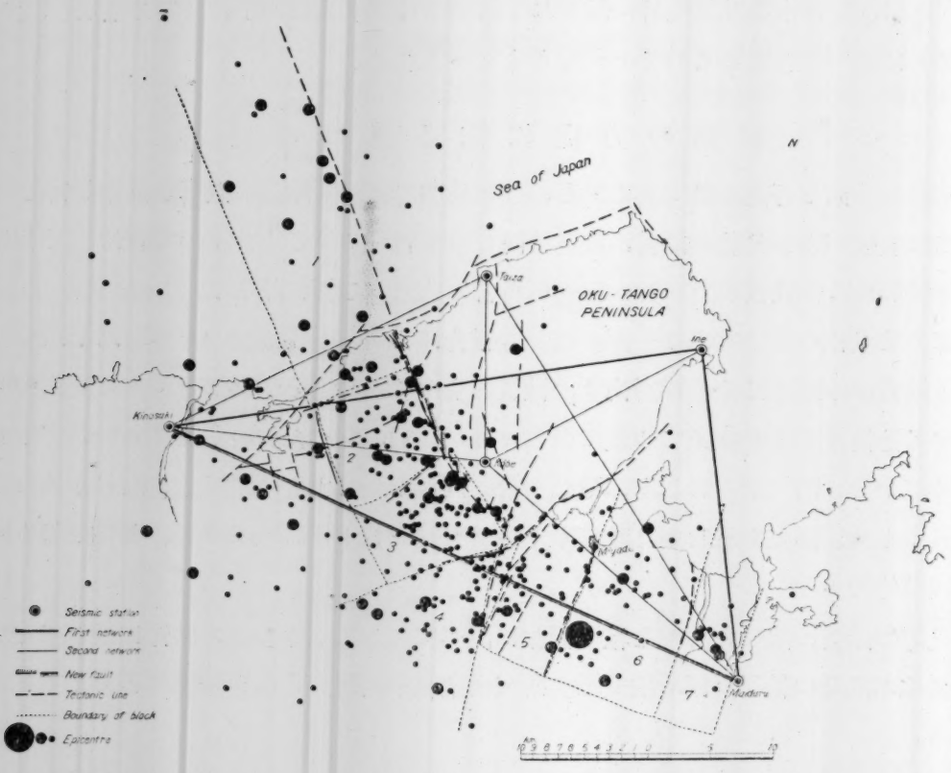

斯る稠密な餘震の分布は斷層の裂罅面が單一ならず多數地下に存在して居ることによるのである。尙ほ日本海の側には郷村斷層の系統に屬する裂罅が發生したために其處に起つたと考へられる餘震が多數ある。又山田斷層に於ては東北及西南の兩方向に裂罅面が地下に延長して存在してゐることを認め得る。

此に依つて郷村斷層の全長は約四十五粁、山田斷層は約三十粁程度であつて地表に

表はれたる部分の約二倍半乃至三倍にも達するのである。

前述の通り奥丹後半島内には極めて少數の餘震が起つたに過ぎない事は半島自身が一塊となつて北々西に移動したためであつて比較的安定な地塊であることを示し興味ある現象であつて今回の觀測に依つて得たる重要な結果の一つである。

第二圖餘震の震央を示す圓中最大なるものは四月一日の强震。其の次の大さのものは餘震中比較的大なる餘震の震央である。その程度は少くも我々の一觀測點に於て最大全振幅100ミクロンを示すものである。其他の小點はそれ以下のもので最大動儘かに數ミクロンにしか達しないものもある。以下少しく短時日に分割して震央の分布を示す。即ち

第三圖は三月十二日より同二十日迄
第四圖は同二十一日より同三十一日迄
第五圖は四月一日より同十一日正午迄
第六圖は四月十一日正午より同三十日迄

第三圖　震央分布圖（三月十二日—同二十日）

Fig. 3.　Map showing the distribution of aftershocks for March 12–20.

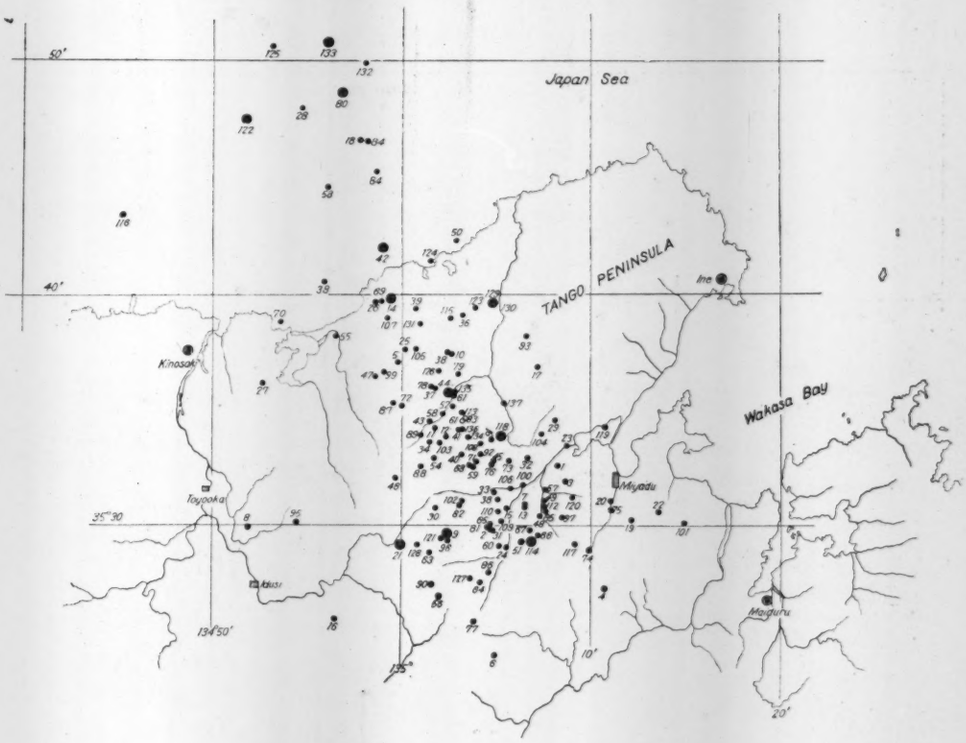

第七圖は五月一日より同三十日迄

第八圖は六月一日より八月三十一日迄

各點に附してある番號は此の報告の最後に附してある觀測附表中の震央欄の番號に相當する。震央の內、圖の範圍外に出でたるもの及多少疑問のあるものは圖には記入してない。

此等に依つて示されたる震央の分布狀態に變化があることは認められるがこれに就いては後の項に詳しく述べる。

舊斷層線と餘震との關係に就いて少しく述べて見やう。此回の餘震の分布中舊斷層線の附近に起つたものは例へば城崎附近、久美濱灣附近、佐野附近、四月一日の强震の起つた宮津附近のものである。

第四圖　震央分布圖（三月二十日－同三十一日）

Fig. 4.　Map showing the distribution of aftershocks for March 20–31.

第五圖　震央分布圖（四月一日－同十一日）

Fig. 5.　Map showing the distribution of aftershocks for April 1–11.

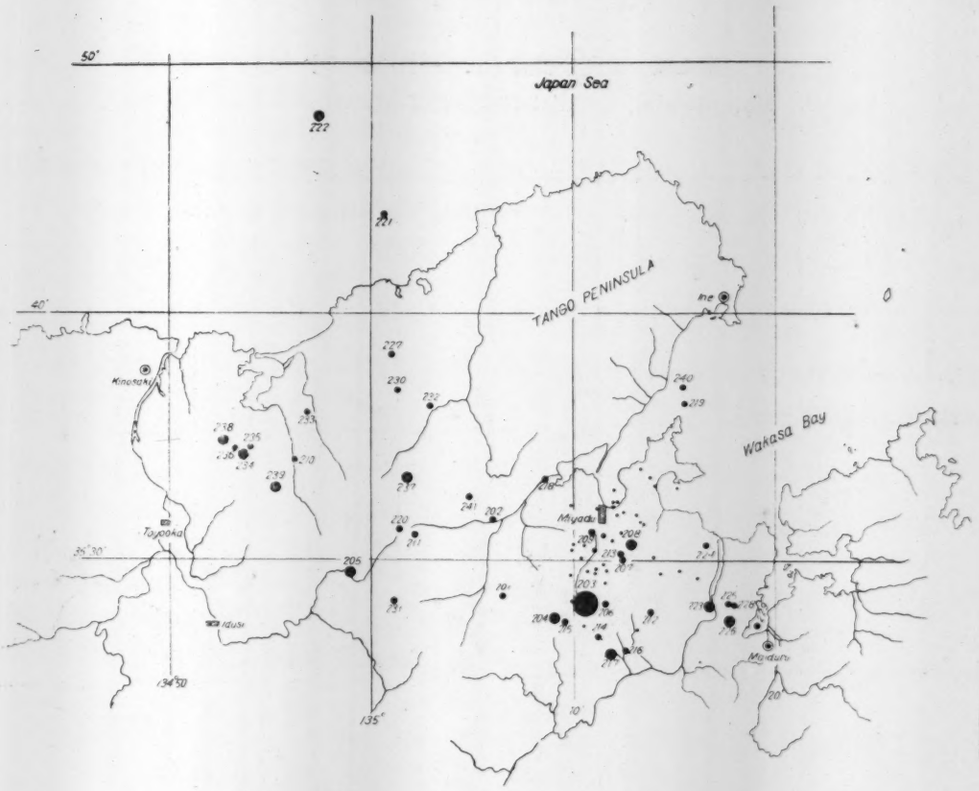

第六圖　震央分布圖（四月十一日－同三十日）

Fig. 6.　Map showing the distribution of aftershocks for April 11–30.

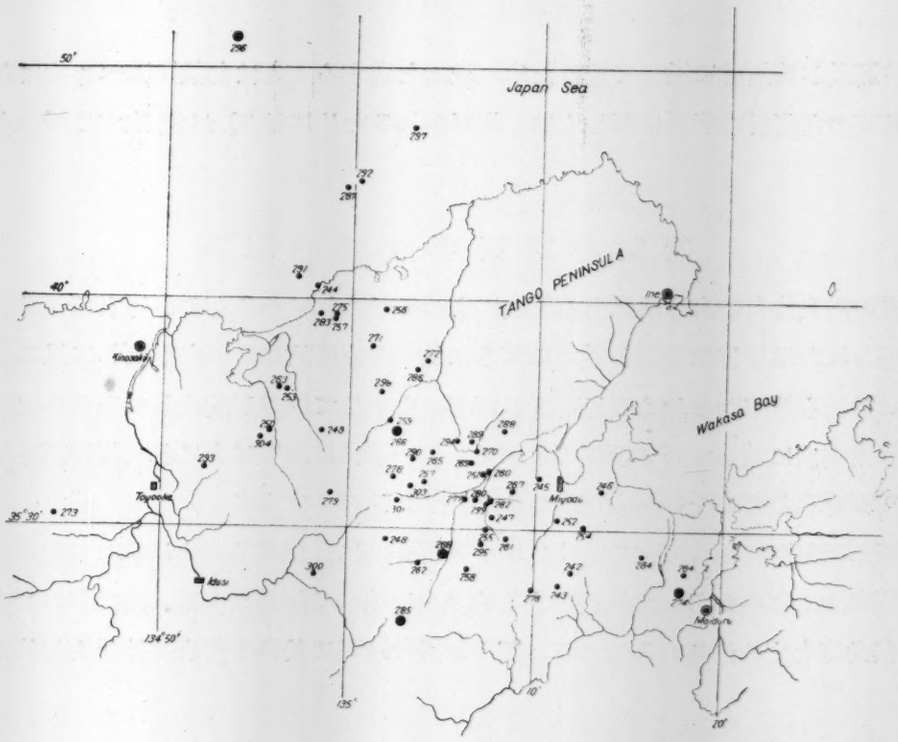

第七圖 震央分布圖（五月一日—同三十一日）

Fig. 7. Map showing the distribution of aftershocks for May 1–31.

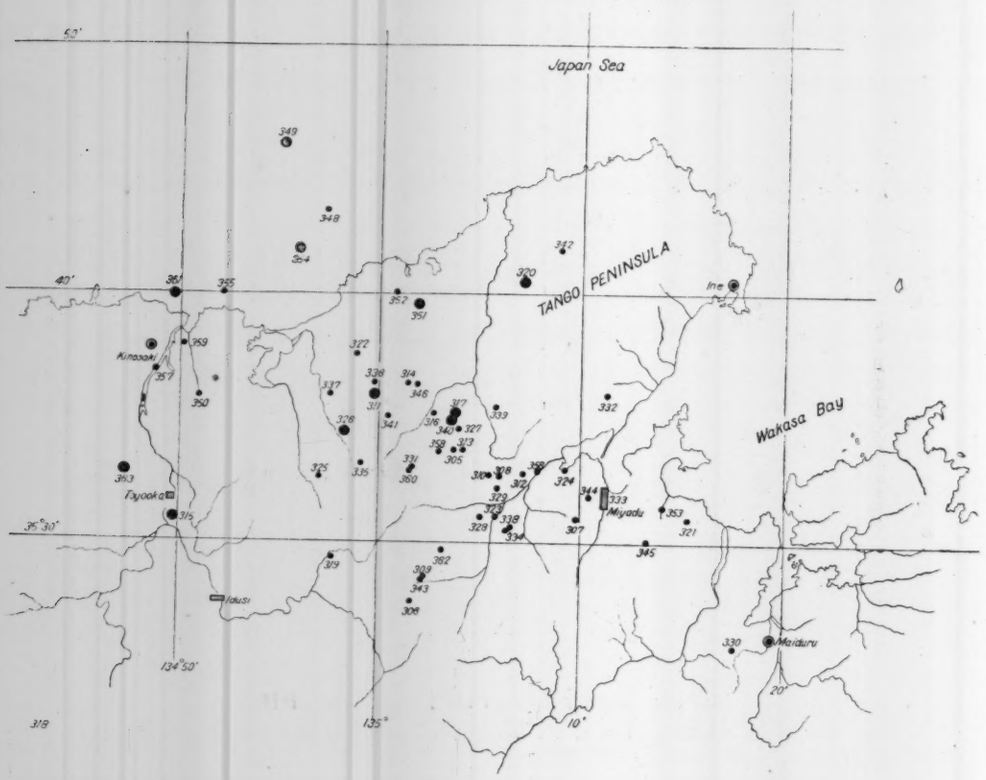

地塊運動が舊斷層に沿つて起るために地震を發することは勿論疑ふべきではないが更に此等の舊斷層の附近に新しく地下斷層が起るために地震が發生する場合もあらう。

餘震の震原の立體的配列

餘震の震央分布の有様は以上の數圖によつて示されてあるがこれ等を舊斷層線によつて限られた地塊毎に分割し震原の深さに依つて立體的に震原を配列して見る必要がある。前にも述べたる如く鄕村斷層の西側に主として餘震が發生してゐるのは該斷層面が西南方向に傾いてゐる關係でもあるが、一面には地表に表はれた斷層以外に箇數の裂罅が存在してゐたのか或は新に生じたかに依るのである。

餘震が斷層面に沿つて起るか或は地下列罅が新に發生することに依つて起るとすれば驗震學上の立場からして餘震の立體的分布に依つて斷層面の數、及此等の有する大體の伏角等を定め得るのみである。卽ち斷層の地表に於ける調査の結果と相俟つて重

第八圖　震央分布圖（六月一日－八月三十一日）
（黒丸は六月中に起りたる餘震の震央）
（白丸は七月中　同　上　）
（三角は八月中　同　上　）

Fig. 8. Map showing the distribution of aftershocks for June 1–August 31.
Black circle relates to the aftershocks occurred in June.
Blank circle .....in July.
Triangle .....in August.

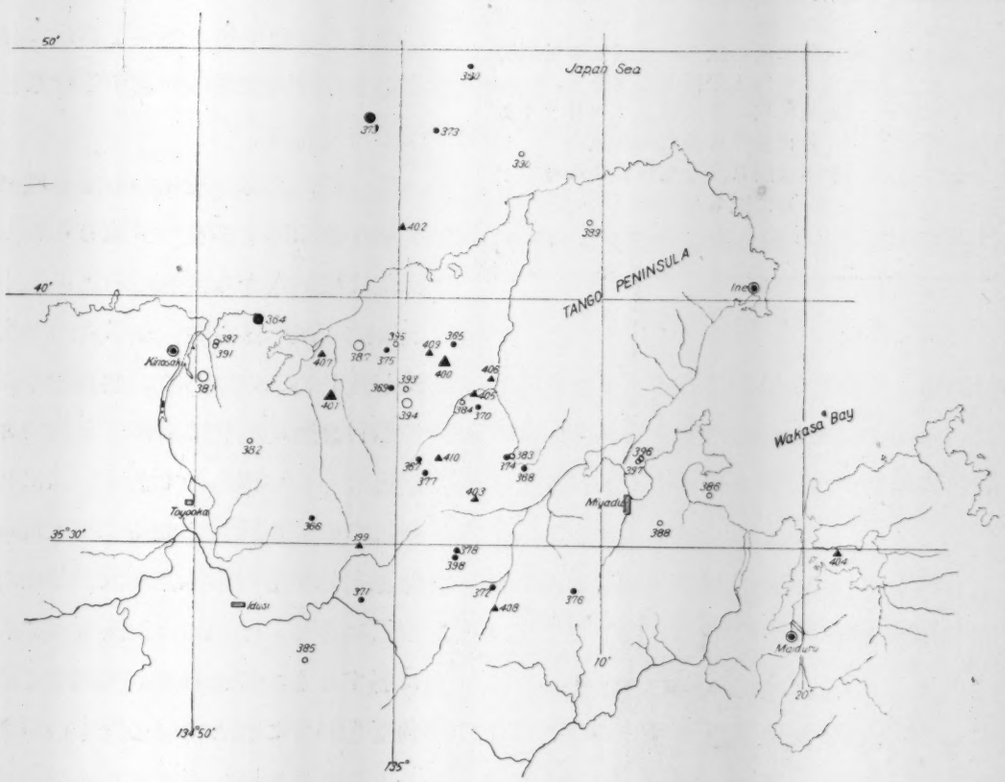

要な調査方法となり得る。また他方では從來餘震の發生に關してやゝ不明であつた事項も多少說明される樣にもなる事と思はれるので地震學の應用方面として興味ある事であつて著者は將來も研究を續けて行きたい希望を有してゐる。

此回の如き比較的小區域內に多數の震原を決定し得た事は何より斯る研究には好都合であつた。

先づ餘震の立體的分布を述べる前に今回の兩斷層、主として鄕村斷層の地上配列の模樣に就いて考察する必要がある。これには今村博士の調査報告或は山崎博士、多田所員の共同調査報告及藤原博士、高山威雄氏の丹後地震の地割れの實驗（前記）等が有益な資料である。

今回の鄉村斷層の地表に於ける斷層片の配列を觀るに其の北部に於けるものは雁行狀態はさ程明瞭でないが南部に位置するものは互に離り合つて雁行的配列が顯著である。これは今村博士の說の通り該斷層帶の北部と南部に於て地震力の方向が多少異つた結果であらう。卽北部に於ては該斷層帶に直角に面した方向に、南部に於ては略ぼ之と平行な方向に作用したと考へられる。それ等の關係から北部と南部の地塊內では地下に於ても斷層面の配列の模樣が異るであらうと想像される。

第九圖　第三地塊內の餘震の震原を鄉村斷層線に直角なる平面上に投影す。
黑丸は三月十二日より四月二十九日に於ける餘震の震原
十字は四月二十九日より八月三十一日に至る

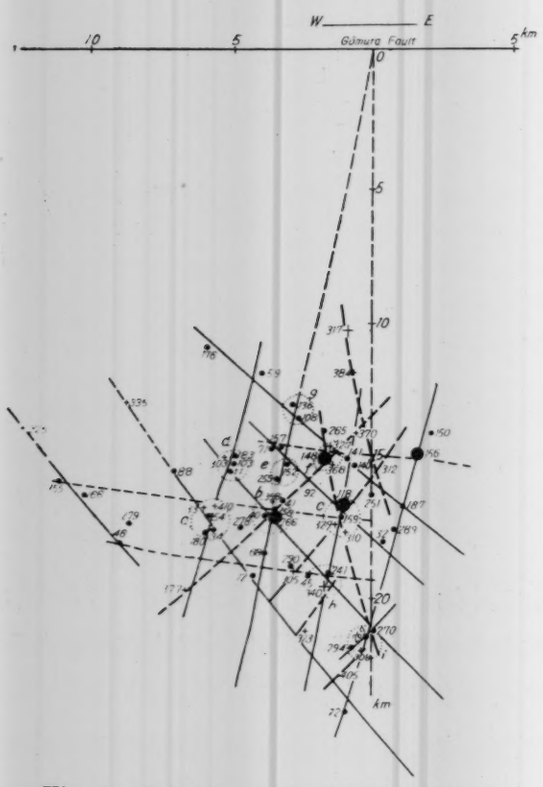

Fig. 9. Seismic foci in the block No. 3 projected on the vertical plane normal to the Gomura fault.
Circle relates to the aftershocks occurred during the period March 12–April 29.
Cross ....April 29–August 31.

此等の各地塊毎の配列を調べて見ると全く此の想像に一致する樣な結果を得て居る。

又一般に裂罅の發生の有樣を觀察するに靡原博士が嘗つて論じられた樣に比較的大きな裂罅の附近に此と對稱的（例へば直角）な二次的の裂罅が生じ得るのである。然らば今回の鄉村斷層に對して略ぼ之と直角な斷層も存在し得るのである。試に丹後地方の舊斷層線を觀るに丁度此の關係を示すものが木津附近、菱山峠附近にある。今回の山田斷層もこれに屬するものであらう。又同じく直角なものでこれとは違つたものがある。假りに地表に現はれた斷層の面が鉛直に地下にあるとすればこれに直角ではあるが水平に近い伏角で橫はる斷層もあらう。これ等の多くは地下に隱されてゐて現はれないのであるが、この水平に近い斷層に沿つて地塊が運動するとすれば地表に於ける水平移動に於て一米乃至二・三米のものが起るのは當然である。

此回の餘震の立體的分布を調べる

ために丹後地方を便宜上舊斷層線を境界として七箇の地塊に別けた（第二圖參照）。こゝで云ふ地塊は本來の意味に於けるものとは多少異るかも知れないが適當な語が無いため以下假りにこの語を用ふることにする。

先づ地塊毎に基準となる構造線（Tectonic）を選ぶ。例へば鄕村斷層線を選ぶ。此れに直角（垂直）な平面を假定し、其面上に地塊內に起つた餘震の震原を投影する。この場合を（A）とする。他方、基準線を含み垂直な平面上にも投影する。これを(B)とする。

震央の分布に依つて震原から此等の投影面までの垂直距離が推定されるからその距離を横軸上に取り、深さを縱軸下方に取れば良い。

以下各地塊毎に投影した結果に就いて述べる。

（I）　便宜上第三地塊から述べる。　この地塊は東は鄕村斷層、南は山田斷層又は其延長に依つて境されてゐる。

（A）　の場合（第九圖參照）。

鄕村斷層から各餘震の震央までの距離及び深さは夫々粁を以て示してある。原點○は地表面に於ける該斷層の位置であつて圖の右はそれより東部、左は西部に相當する。斯くして投影された餘震の一般の分布狀態を見るに地下十粁より深い所では略ぼ等間隔に二乃至三粁の深さで分布されてゐる事が認められる。

卽同圖中の細い點線で示してあるのがそれである。卽十二粁、十五粁、十七粁、二十一粁にあるものである。他の地塊では多少深さがこれとは違つてゐるが等間隔にあることは同じである。

これ等の餘震は或は地下に略ぼ等間隔をなしてゐる或る面上に發生したのであらうと考へる。然し同一の略ぼ水平と思はれる此等の假定的の面上に於ける配列を見るに又一つの規則に從つてゐる樣に見える。且又これ等の面と面との間にも震原が數箇分布されてゐる。

これ等の略ぼ水平な面上並に其中間にあるものを觀察すると又一箇の面上にあるのである。以上の事からしてこれ等の面が斷層面であらうと考へられる。而して餘震が此等の斷層面に沿つて順次に起つてゐる場合が多い。

圖中の震央の番號に依つて見得られる事であるが餘震が或る一線に沿つて位置するときは地下に於て裂罅がその線で示される方向に進んで行くのであらうと思ふ。これには圖の面に垂直な方向への擴がりもあるが要するに此の方法ではその裂罅面の投影を示してゐるのである。

第十圖　鄉村斷層線以西に於ける餘震の震央の配列を示す（同一線上の餘震は略ぼ同じ深さに起りたるもの）

$a, b, c, a' b' c'$ 線上の餘震は深さ……約十七粁
d, e, d', e', f' …… 十五粁
g …… 十三粁
h …… 十九粁
i ……二十一粁

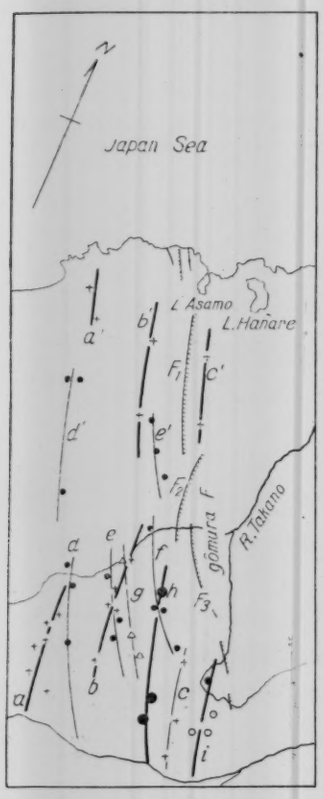

Fig. 10. Seismic foci situated in the west of the Gomura fault projected on a horizontal plane. (Foci of nearly equal depth are grouped thus: 17 km. to a, b, c, a', b', c'; 15 km. to d, e, d', e', f; 13 km. to g; 19 km. to h; 21 km. to i.)

同圖中先に述べた等間隔で略々水平と假定した面上に餘震が所々に集團して發生してゐる內十七粁附近のものが三の群に別たれる。

これを a, b, c 集團と名付けておく。其他十五粁附近には d, e, f 集團、十三粁附近には g 集團がある。尙ほこれ等よりは深い十九粁附近に h, 二十一粁附近には i 集團がある。

a より i に至る集團が夫々水平的には如何樣に配列されてゐるかを觀るに d, e, f, g に屬する震原は大體地表に現はれた斷層線に略ぼ平行な線上に位置してゐる（第十圖參照）。

然し a, b, c, h, i 等の下層部にある震原の配列は鄉村斷層の中部或は北部のものに平行に近い（斷層片の F_2 に平行）（第十圖參照）。

南部と北部の比較のために同圖中には北部に位置する第二地塊に於けるものも記入してある。a', b', c' は深さ十七粁、d', e' は十五粁のものである。此圖によつて想像されることは北部の地塊に於ては比較的規則正しく a'……e' が地表に現はれた斷層片に平行であるが南部では深さによつてさうではない。これには地震力の方向が上層と下層とで違つてゐたのであつて今村博士の說の如く南北兩地塊で違つてゐたとすればそれは十五粁より淺い所でさうであつたと云ひ得られる。

再ひ第九圖の震原の配列を見るに前述の各集團及その中間に位する者も大體數系統の伏角を有する裂罅面上にあるやうである。著しい裂罅を擧げると伏角七十度乃至八十度西南西のもの及これに略ぼ直角な系統のもの及四十五度の角度で此等に交る系統のものがある。最後者は前二系統の五に略ぼ直角な裂罅によつて切り下げられた局部的の地塊が次には二つの對角線に近い方向に更に分

割されたために現はれたとも想像される。

一般に裂罅の發生する狀態から考へると之等の對角線に近いものは基準たる二系統の裂罅が出來た後に現はれるとする方が至當である。又こゝで基準となる二系統の裂罅の內何れの伏角のものが先に生じたかは疑問であるが、今回の鄕村斷層の場合は先づ伏角七十度程度の裂罅が第一に出來然る後に之に直角及四十五度の裂罅が順次に出來たのであらう。

而してこの方法に依つて推定された鄕村斷層の伏角の內西南西へ平均七十五度のものは多田所員の實地踏査の結果、高橋、新治隆起の伏角西南六十度乃至八十度のものと丁度一致してゐる。

以上の基準二系統の裂罅の生じた原因に就いて少しく考察して見やう。藤原博士の說に依ると一般に壓縮、展張の二種の裂罅が生じ、之等の內何れかが材料の如何に依つて優れて現はれる。然し大概の場合は兩者が共存する。又時間的の關係では展張裂罅を生じて然る後に壓縮裂罅を生ずる場合が多い。

此の觀測の結果早期と末期に於て餘震が發生した各々の裂罅は多少伏角等を異にすることも知り得たのである。爾後早期末期の二期に大別して配列の模樣を圖示することゝする。そこで第三地塊で裂罅の何れの系統が展張、壓縮の性質であるかを定めるには地塊內に作用して歪力を想像せなければならぬ。

此等の裂罅群を作る歪力としては鄕村斷層の東西兩側に於て作用する垂直な歪力と他は同斷層に直角な水平歪力である。而して前者の歪力が斯る雁行的の裂罅群を生ぜしめるに最も有力に

第十一圖　第三、第四、第五地塊內（鄕村斷層線以西）に於ける餘震の震原を鄕村斷層線を含み垂直なる平面上に投影せしものを示す。

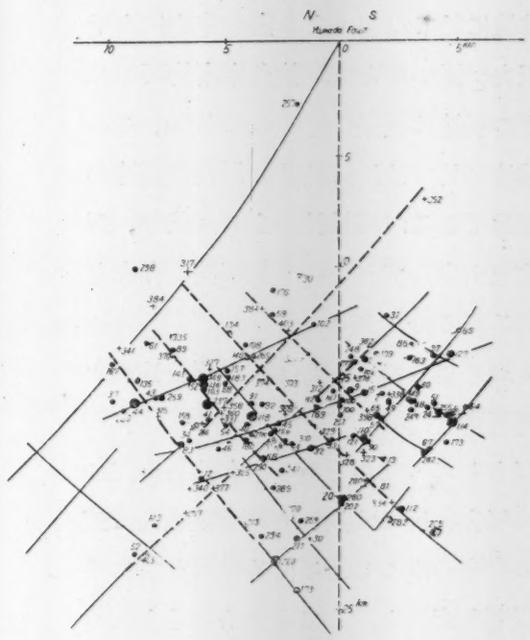

Fig. 11. Seismic foci in the blocks No. 3, No. 4, No. 5 (foci situated in the west of the Gomura fault) projected on the vertical plane passing through to the Gomura fault.

作用し得るのである。

即該斷層帶の東側地域の沈降と西側地域の隆起とを引き起すやうな歪力によつて生ずる展張裂罅は伏角西南七十五度の裂罅に相當し、壓縮裂罅は之に直角なものに相當する。

(B) の場合　即ち鄉村斷層を含み垂直な平面に投影した場合(第十一圖)。

第三の地塊內に於ける此の場合は多少複雜な有樣を示してゐる。然し第一、第二の地塊の (B) の場合 (第十三、十五圖) から推して考へると矢張りこれ等地塊內と同配列されてゐる樣にやうである。但し伏角等は (A) の場合とは違つてゐる。これ等の裂罅面は鄉村斷層に沿つて水平に作用する歪力によつて生じ得るものである。

第十二圖　第二地塊內の餘震の震原を鄉村斷層線に直角なる平面上に投影せしものを示す

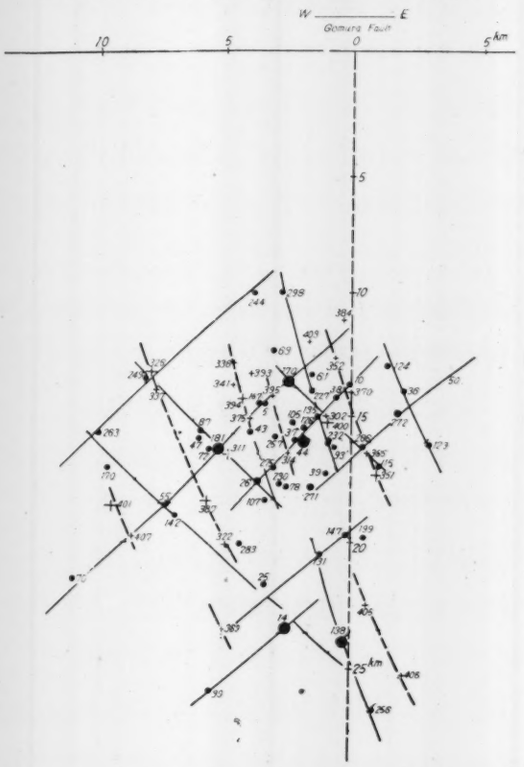

Fig. 12. Seismic foci in the block No. 2 projected on the vertical plane normal to the Gomura fault.

今陸地測量部の測量の結果からこの地塊に於ては北方より南の方向に水平歪力が働いたとす。伏角東南約四十五度の裂罅は展張性のものである。この地塊に於ては比較的此の性質の裂罅が優勢であるが壓縮性のもの (伏角、西北三十度乃至五十度) も明瞭に存在を認め得るのである。

即ち以上の (A), (B) の場合は夫々鄉村斷層に對して想像される三方向の歪力を考へたのである。勿論この二つの場合に於ては局部的に小區域內で歪の分布の違つてゐるために局部的に不規則な配列を示してゐるものもあらうが、併し以上は大體の形勢を示したに過ぎないのである。

以下各地塊に於ける震原の位置を示すに黑點を用ひたのは三月十二日より四月二十九日頃までの早期に起つた餘震に、十字はそれ以後八月下旬迄の末期に起つたものに

關係してゐる。此の期日の區別に依つて裂罅の配列の變遷が比較的判然と指示されるやうである。

(II)　第二の地塊內の震原の立體的分布

(A) の場合（第十二圖）。

此の地塊は東に鄕村斷層、西に久美濱灣東部を南北に縱走する斷層、南に菱山峠の斷層、北に木津の斷層があつて、地表では略々正方形に區劃された地塊である。配列の有樣は西南西四十五度の斷層面及これに直角なもの、末期に至つて此等とは多少異なる伏角を有する裂罅があるのが見得られる。

第十三圖　第二地塊內に於ける餘震の震原を鄕村斷層線を含み且つ垂直なる平面上に投影せるものを示す

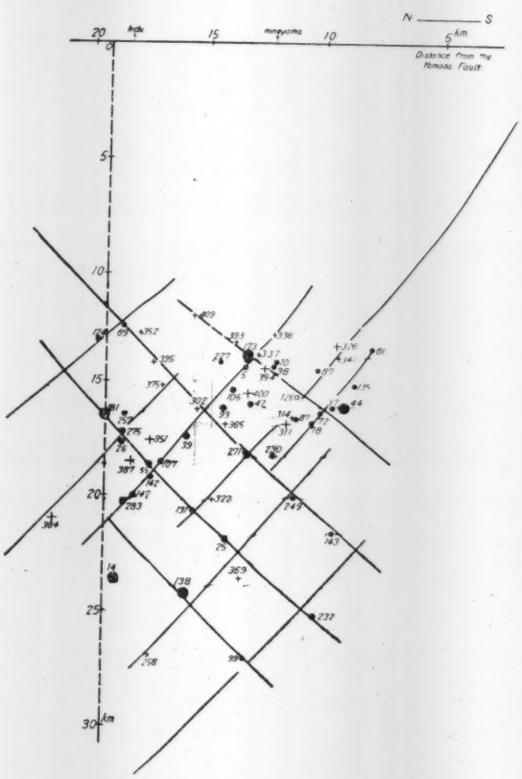

Fig. 13. Seismic foci in the block No. 2 projected on the vertical plane passing through the Gomura fault.

而して斷層面と想像される面が約數粁の間隔に深さの方向に重疊してゐる有樣等は第三地塊の場合と同樣である。斷層の伏角は西南四十五度、(早期に著し) 東北七十度（末期に著し）と定められる。

(B) の場合（第十三圖）

此圖は第二の地塊內の震原を鄕村斷層を含む垂直平面上に投影したものである。

伏角北西六十度、東南四十五度の裂罅が著しく現はれてゐる。もし之等のものが今回地表に現はれて出たとすれば鄕村斷層に直角な斷層線が新しく見出されたであらう。

今回の鄕村斷層帶も舊斷層帶上に現はれたのであつて往古に於てこの舊斷層帶及木津、菱山峠の舊斷層も或は今回の地變と同樣の地變の際生じたのであらう。又新舊兩山田斷層上でも度々地變が繰返されたのでは無からうかといふ想像が震原の配列を見ると配列を見ると起つて來るのである。

以上の例に依つて斷層の地下の狀態を考察するに地表に於ける斷層面の斜面が稍〻深い所まで同樣に存在し得るものと考へられる。又斷層面の或る數組が水平的のみならず深さの方向にも分布されてゐて水平、垂直の兩方向に於ても雁行狀を示すのである。今回の鄕村斷層の如き水平雁行は主として水平の歪力に依つて生じ、垂直の雁行は水平歪力に依つても生ずるが同時に垂直歪力に依つて生ずるのが最も優勢である。平易に以上の事柄を述べるために百葉箱の如き扉の例を引用する。

この扉が數個立て〻列べてあるとする。その形が地下に於ける斷層の一部と同じである。

而して一箇々々の扉を形造るものは主として垂直の歪力に依るが數箇の扉を立て〻列べるには水平歪力が主たるものである。この水平の歪力が尙ほ進んで作用し扉の面上に或る方向（例へば四十五度）に皺割れを作る場合がある。

これが以上（B）の場合の裂罅に相當するのである。これは卑近な例であるが斷層の成生に關して最も適當な說明と思ふ。

(III) 第一地塊內に於ける震原の立體的分布

此の地塊は日本海中に存在するものであつて內部では鄕村斷層の延長上と思はれる場所に餘震が度々起つてゐる。今此等の餘震の震原の配列からこの地塊內の斷層の模樣を想定した結果を次に述べる。

（A）の場合（第十四圖）

此の場合で最も著しい事は鄕村斷層の傾斜面の延長上に數箇の餘震の震原が配列されてゐることである。而して假りに此等の震原の位置が正しいものと假定すれば該斷層の傾斜面は略垂直に近く十數粁の深さにまで達してゐると云つて差支ない。

其他此の斷層の傾斜面とは或る角度をなして存在するものもあるやうである。

（B）の場合（第十五圖）

此の場合は第二地塊の（B）の場合と相關連して裂罅の有樣を想定したのである。

著しい結果としては略直角に交る二系統の平面上に餘震の震原が存在することである。

而して此等の平面の或るものは第二地塊の內部にまで延長し或は反對に第二地塊內部から第一地塊內部にまで延長されたものである。

以上三箇の地塊內の餘震の震原の配列から鄕村斷層の地下に於ける有樣が想像されたこと〻思ふ。以下山田斷層以南に就て述べる。

第十四圖　第一地塊內の餘震の震原を鄕村斷層線に垂直なる平面上に投影したるものを示す

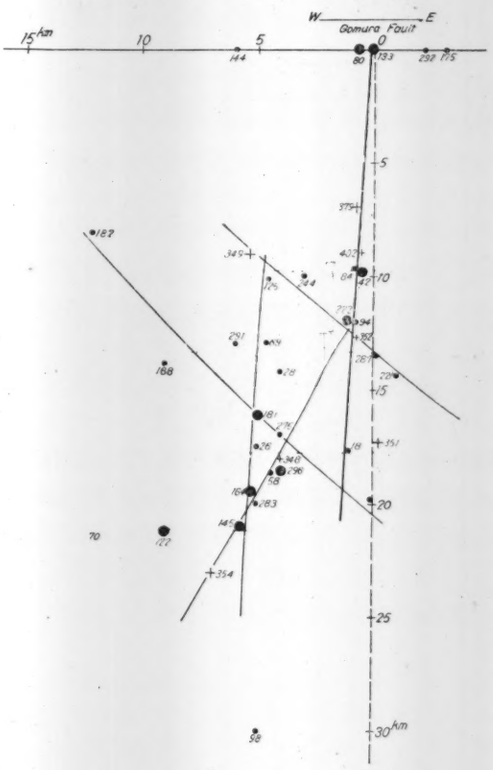

Fig. 14. Seismic foci in the block No. 1 projected on the vertical plane normal to the Gomura fault.

第十五圖　第一地塊內の餘震の震原を鄕村斷層を含み垂直なる平面上に投影せしものを示す

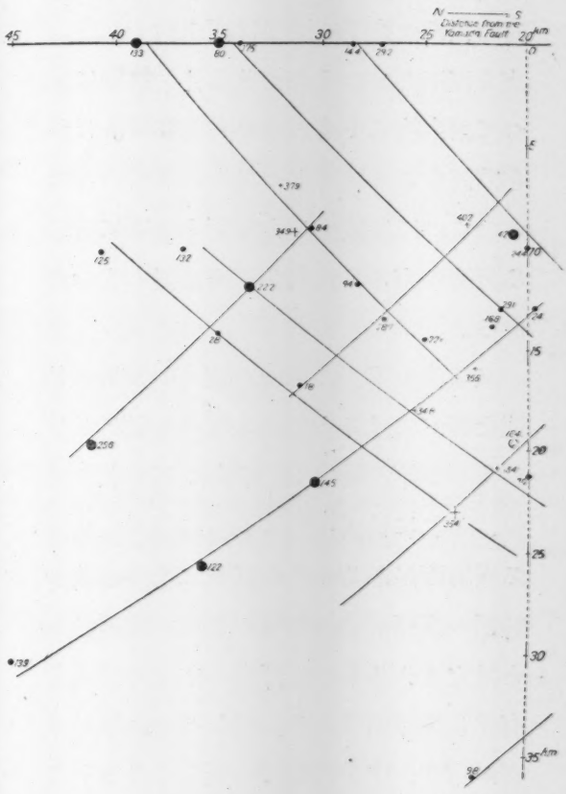

Fig. 15. Seismic foci in the block No. 1 projected on the vertical plane passing through the Gomura fault.

(IV)　第四地塊に就いて。此の地塊は北は山田斷層の延長、東は加悅町附近の舊斷層に依つて境されてゐる三角形の地塊である。

今四辻附近が丁度三角形の一頂點になるのであるから、これを原點（○）と定める。そして前記の二境界線のなす角の二等分線を假定すると、その線は四辻から西南の方向に床ノ尾山の東約七・五粁の地點を通過する。この二等分線を含む垂直平面を投影面と假定してこの地塊內の震原を投影すると第十六圖の様になる。横軸の數字は四辻からこの二等分線上を西南の方向へ測つた距離（粁）である。

尙ほこの圖の原點は第九圖の横軸の1附近に相當する。

全般の分布を見ると前數例と同様略々數粁を置いて上下に重疊する面上に限られてゐる。

斷層の分布は早期及末期（此の區別は前同様）を通じ大體系三統に別たれる。斜面の伏角は初期に於ては西南四十五度、東北四十五度のものが著しく、後期に至つて西南約八十度のものが著しい。これを前回の第九圖即この地塊の北隣の地塊内のものに比較すると早期と後期に於ける裂罅の有する伏角が丁度反對のものがある。

第十六圖　第四地塊内の餘震の震原を該地塊の表面に於て東及北の境界を構成せる二斷層線の交角の二等分線を含み且つ垂直なる平面上に投影せしものを示す

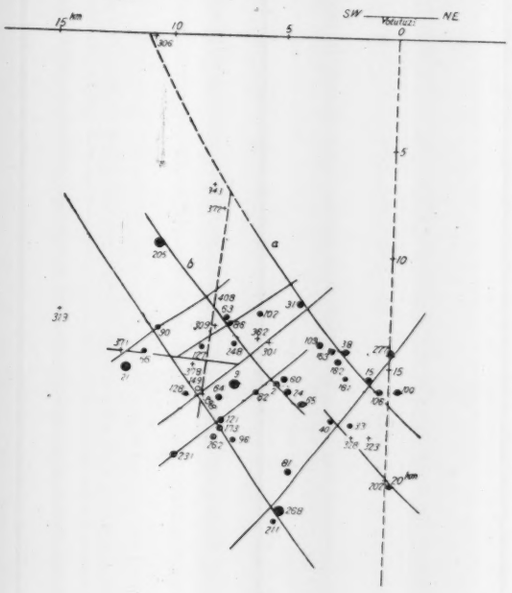

Fig. 16. Seismic foci in the block No. 4 projected on the vertical plane bisecting the angle between the northern and eastern boundaries of the upper surface of the block.

又第四及第三の地塊の箇々の裂罅の位置を調べて見ると第四地塊の早期に於けるものが第三地塊で末期に現はれたもの、これには西南四十五度の伏角を有する裂罅面があるが此の反對に第三地塊の前期の裂罅が第四地塊の後期に現はれたと推定されるものは西南八十度の伏角を有する裂罅面である。而してそれ等の或面が第九、第十六圖で一致して位置を占めてゐる關係から第三地塊の早期に現はれた裂罅が末期に至つて第四地塊内に延長し、反對に第四地塊の前期の裂罅は第三地塊に延長した様に想像される。斯の如く地塊内で相互に裂罅の延長發生を交換するやうな事は誠に興味ある現象である。此の地塊内の餘震の一部を鄉村斷層の延長線を含む垂直面に投影した場合は既に第十一圖に示してある。

(V)　第五地塊内の斷層

千丈ケ岳より北東の方向に天ノ橋立附近に至る加悦谷東部の地塊に就いて述べる。此の地塊は多田所員の説に從へば宮津附近にある東北より西南に走る略々平行な斷層線で兩側が境されてゐる。

前の第一、第二、第三の地塊の場合と反對に以後投影の際斷層線を含み且つ垂直なる平面上に震原を投影した場合を（A），之に直角な平面上に投影した場合を（B）とする。兩者の場合原點は加悦町南方約三粁與謝を選んだ。即 A の場合の横軸の數字

は斷層線上を原點から東北の方向に測つた距離であつて、(B) の場合は原點を通じて斷層線に直角な方向、即ち東南の方向に進むものとす。

(A) の場合（第十七圖）

この場合の原點○は第十六圖の横軸の 6 附近に相當する。

一般の震原分布は二系統の面上に配列してゐると想像される。

裂罅面では前述の第四地塊の內部に存在せしものの延長と見られるものがある。即 a', b' 等であつて第四地塊內の a, b 裂罅の延長であらう。（第十六圖參照）

(B) の場合（第十八圖）

第十八圖は第五、第六、第七の地塊を通じて、それ等の (B) の場合を示したのである。

第十七圖　第五地塊內の餘震の震原を同地塊の西北の境界を構成する斷層線を含み垂直なる平面上に投影せしものを示す

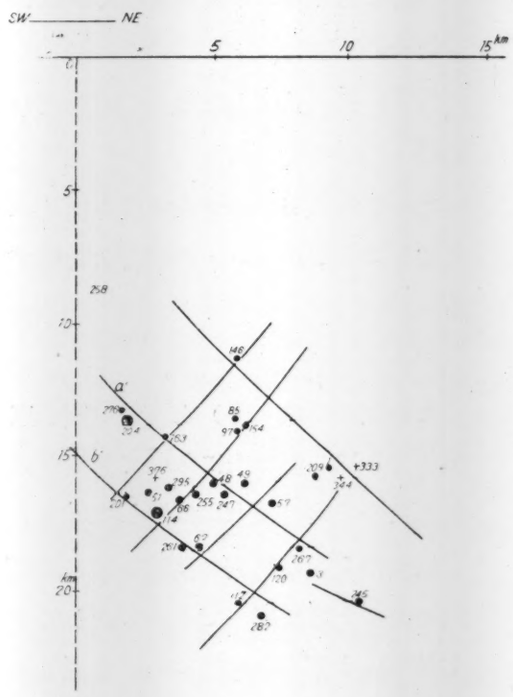

Fig. 17. Seismic foci in the block No. 5, projected on the vertical plane, passing through the fault line which forms the north-western boundary of the block.

第十八圖　第五、第六、第七地塊內の餘震の震原を斷層線に直角なる垂直平面上に投影せしものを示す

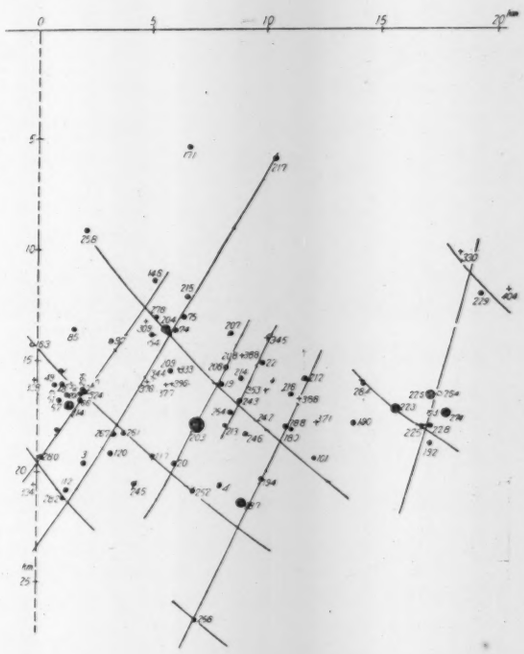

Fig. 18. Seismic foci in the blocks Nos. 5, 6, 7, projected on the vertical plane normal to the faults.

此の圖に依つて便宜上以上三箇の地塊の（B）の場合を合せて說明す。

此等の地塊は主として四月一日の强震後に起れる數多の餘震の震原を含むものであつて、地塊內部に於ける裂罅の分布狀態は稍複雜なものの樣に想像されるがしかし實際此の投影方法に依つて裂罅の有樣を推定すると前述の數箇の地塊內に於ける有樣と同樣規則的に分布されてゐるような結果を示してゐる。即ち該强震後震原附近に比較的正しく裂罅が發生したのであらう。これ等の間隔等も略ぼ五粁內外である。もし該强震後に於ける餘震の震原を逐一追跡し得る程度に十分の觀測資料を得て居つたなら勿更に之等裂罅の複雜な發生狀態を知ることが出來た事と思ふ。相憎、伊根村、城崎の觀測に故障があつたので是等の目的に添ひ兼ねるのは遺憾な事である。而し比較的規則正しい配列の摸樣を推定し得た事に滿足する次第である。列罅は西北に約六十度、東南に約四十五度の伏角を有する二系統が著しく現はれてゐる。

第十九圖　第六、第七地塊に於ける餘震の震原を斷層線（東北より西南に走行す）を含み且垂直なる平面上に投影せしものを示す

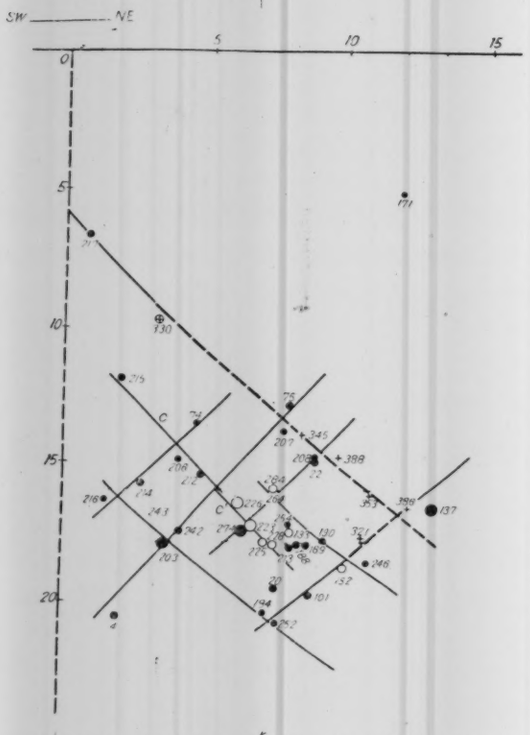

Fig. 19. Seismic foci in the blocks No. 6 and No. 7 projected on the vertical plane passing through the fault which passes through Miyadu with the trend of NE—SW
Block circle and cross relate to the block No. 6.
Blank circle and cross-circle relate to the block No. 7.

（VI）第六及第七地塊內の斷層面の配列

これ等の（B）の場合は以上に述べた通りであるが（A）の場合を說明する。

（A）の場合（第十九圖）

この圖の原點（○）と第十七圖の原點(○)とは一直線上にあつて舊斷層線に直角の方向の線上に位置してゐる。

餘震の大體の配列の模樣は第五地塊內のものと略ぼ同一である。而して第七地塊內と第六地塊內に於ける裂罅の配列で特に記すべき差違がないが c' を以て示された第七地塊內の裂罅は第六地裂內の c 裂罅の延長である事等は判

然と表はれてゐる。

其他第六地塊內では末期に餘震の起つた裂罅が著しく目立つてゐる。

一般の裂罅の伏角を觀るに大體東北に約四十五度の系統のものと西南に約四十五度程度のものと二系統である。

以上各地塊に就いて述べた餘震の震原の立體的配列の結論として一般に云ひ得られることは餘震は大地震後に於て地下裂罅に沿つて起る現象である。且餘震の發生する狀態は時間と共に多少變化する樣模が認められる。

今一つは餘震の分布から斷層面は伏角によつて數系統に別たれることである。

即今回現はれたる斷層及其附近のものの伏角を大體推定すれば次表の通りである。

鄕村斷層及其西部		山田斷層及其南部	
方　向	伏　角	方　向	伏　角
WSW	75°	NNW, NW	50-60°
〃	45°	SE	45°
NEE	70°	NE	45°
SSE	45°	SW	50°
NNW	45°		80°

尙ほ斷層に關して考察されることは裂罅が順次に生ずるまでには相當時間を要することである。即斷層が地下に生じて地表に表はれる迄には相當の時間を經てから後であらうと思ふ。又地表に出現するに地下のものがその儘延長して表はれることもあるが又階段的に順次に裂罅を生じて行く事もあらう。それ故假りに大地震が地下の大なる裂罅に依つて起つたとしても斷層が地表に現はれるには地震動よりは多少遲れて來ることがある。明治二十三年の濃尾大地震の斷層の出現（地震動を感じた後に）を實見した話、及今回山田斷層線に接近して建てられてあつた家屋が大地震の地動のために破壞されずに斷層出現に際して土地の起伏のため倒れた事實は此の現象を物語るものである。此點は如何なるものであらうか、こゝでは斷定を下し兼ねるのである。

以上述べ來つた餘震の立體的配列の結論として今少し詳細に渉つて觀察を試みやう。

先づ現在の地震計に依つて計測されたる初期微動の繼續時間が如何程まで正確であるかを考へなければならぬ。即ち記錄裝置の廻轉の速度の一樣なるや否やは直ちに該計測値に影響するわけである。

今回用るたる地震計の記錄裝置の回轉速度は此の報告の最初に揭げたる機械常數表中に示された通りである。此の速度即一秒一粍乃至二粍の割合を以て地震動を記錄するのであるから從來使用されたる一秒僅に〇・五粍或はそれ以下の記錄速度を有する地震計に依つて計測されたもものよりは遙に確實である。

且又回轉の模樣を見るに數回の例外はあるが所要の短時間內に於て著しく不規則であることを見出さない。それ故に誤差が記象紙上に於ける讀算誤差のみとして震原推定上に生ずる誤差に就いて以下述べやうと思ふ。

先づ記象紙上に於ける讀算誤差の程度に就いて豫め述る必要がある。

一秒一粍の割合（普通）のものならば一粍の十分の一迄は讀み得るのであるから十分の一秒までは正確であるとしてよい。

なほ前にも述べた如く一層正確な計測値を得るために今回は餘震の回數の頻繁であつた頃には更に記錄速度をこの二倍とし一秒二粍程度とした。これは誤差を十分の一秒程度より少くするためである。これによれば誤差は百分の五秒程度になり得る。

今此等の誤差が初期微動繼續時間の計測値に含まれてゐるとして震原の位置推定上に來すべき誤差の概算を試みる。

先づ幾何學的に求めるとして x 軸を舞鶴から城崎の方向（西北）に y 軸を之に直角（東北）に z 軸を下方に取り、簡單に三觀測點が同一水準面（$Z=0$ 平面）上にあるとし舞鶴を座標の原點 $(0,0,0)$、城崎を $(x_1,0,0)$、伊根村を $(x_2,y_2,0)$ の點とする。

震原の座標を (X,Y,Z) としこれより各觀測點に至る距離（粁）が夫々 kt_0, kt_1, kt_2 とす。玆に t_0,t_1,t_2 は各觀測點に就いて計測された初期微動の繼續時間（秒）である。k は前述の公式中の常數 8.4 である。

然るときは各觀測點に就いて次式が成立する。

$$X^2+Y^2+Z^2=\overline{kt_0}^2$$
$$(X-x_1)^2+Y^2+Z^2=\overline{kt_1}^2$$
$$(X-x_2)^2+(Y-y_2)^2+Z^2=\overline{kt_2}^2$$

此方程式を X, Y, Z に就いて解き震央及震原の深さを表はす式を求むれば次の通りである。

震央

$$\begin{cases} X=\dfrac{d_1^2+\overline{kt_0^2}-\overline{kt_1^2}}{2d_1} \\ Y=\dfrac{1}{2y_2}\left\{(d_2^2+\overline{kt_0^2}-\overline{kt_2^2})-\dfrac{x_2}{d_1}(d_1^2+\overline{kt_0^2}-\overline{kt_1^2})\right\} \end{cases}$$

震原の深さ

$$Z=\left[\overline{kt_0^2}-\frac{1}{4}\left\{\frac{(d_1^2+\overline{kt_0^2}-\overline{kt_1^2})^2}{d_1^2}\left(1+\frac{x_2^2}{y_2^2}\right)\right.\right.$$

$$\left.\left.-2\frac{x_2}{d_1 y_2^2}(d_1^2+\overline{kt_0^2}-\overline{kt_1^2})\,(d_2^2+\overline{kt_0^2}-\overline{kt_2^2})+\frac{(d_2^2+\overline{kt_0^2}-\overline{kt_2^2})^2}{y_2^2}\right]^{\frac{1}{2}}\right.$$

玆に d_1, d_2 は舞鶴より城崎及伊根村に至る夫々の距離（粁）にある。

$$d_1=x_1=50.4\ \text{km.}$$

$$d_2=\sqrt{x_2+y_2}=25.5\ \text{km.}$$

$$\begin{pmatrix} x_2=13.0\ \text{km.} \\ y_2=22.0\ \text{km.} \end{pmatrix}$$

以下簡單ならしめるために

$$d_1^2+\overline{kt_0^2}-\overline{kt_1^2}=m$$

$$d_2^2+\overline{kt_0^2}-\overline{kt_2^2}=n$$

なる記號を用ふ。

然る時は

震央;

$$\begin{cases} X=\dfrac{m}{2d_1} \\ Y=\dfrac{1}{2y_2}\left\{n-\dfrac{x_2}{d_1}m\right\} \end{cases}$$

震原の深さ;

$$Z=\sqrt{\overline{kt_0^2}-\frac{1}{4}\left[\frac{m^2}{d_1^2}\left(1+\frac{x_2^2}{y_2^2}\right)-2\frac{x_2}{d_1 y_2^2}mn+\frac{n^2}{y_2^2}\right]}$$

誤差の計算のために X, Y, Z の各々の t_0, t_1, t_2 に就いての偏微分係數を求める。

X に就いて、

$$\frac{\partial X}{\partial t_0}=\frac{k^2}{d_1}t_0.$$

$$\frac{\partial X}{\partial t_1}=-\frac{k^2}{d_1}t_1.$$

$$\frac{\partial X}{\partial t_2}=0.$$

$$\therefore\quad \delta X\fallingdotseq\left(\frac{\partial X}{\partial t_0}+\frac{\partial X}{\partial t_1}\right)\delta t\fallingdotseq\frac{k^2}{d_1}(t_0-t_1)\,\delta t.\qquad [t_0, t_1, t_2 \text{ の誤差同じとす}]$$

Y に就いて

$$\frac{\partial Y}{\partial t_0}=\frac{k^2}{y_2}\left(1-\frac{x_2}{d_1}\right)t_0.$$

$$\frac{\partial Y}{\partial t_1}=\frac{k^2}{y_2}\left(1-\frac{x_2}{d_1}\right)t_1.$$

$$\frac{\partial Y}{\partial t_2}=-\frac{k^2}{y_2}t_2.$$

$$\therefore\quad \delta Y\fallingdotseq\left(\frac{\partial Y}{\partial t_0}+\frac{\partial Y}{\partial t_1}+\frac{\partial Y}{\partial t_2}\right)\delta t\fallingdotseq\frac{k^2}{y_2}\left\{(t_0-t_1)-\frac{x_2}{d_1}(t_0-t_1)\right\}\delta t.$$

Z に就いて

$$\frac{\partial Z}{\partial t_0}=\frac{1}{Z}\,k_2\,t_0\left\{\left(1-\frac{m}{2{d_1}^2}\right)-\frac{1}{2{y_2}^2}\left(n-\frac{x_2}{d_1}m\right)\left(1-\frac{x_2}{d_1}\right)\right\}$$

$$\frac{\partial Z}{\partial t_1}=\frac{1}{2Z}\cdot\frac{k^2\,t_0}{d_1}\left\{\frac{m}{d_1}-\frac{x_2}{{y_2}^2}\left(n-\frac{x_2}{d_1}m\right)\right\}$$

$$\frac{\partial Z}{\partial t_2}=\frac{1}{2Z}\,\frac{k^2\,t_2}{{y_2}^2}\left(n-\frac{x_2}{d_1}m\right)$$

$$\therefore\quad \delta Z=\left(\frac{\partial Z}{\partial t_0}+\frac{\partial Z}{\partial t_1}+\frac{\partial Z}{\partial t_2}\right)\delta t=\frac{k_2}{Z}\left[\left\{\left(1-\frac{m}{2{d_1}^2}\right)-\frac{1}{2{y_2}^2}\left(n-\frac{x_2}{d_1}m\right)\left(1-\frac{x_2}{d_1}\right)\right\}t_0\right.$$

$$\left.+\frac{1}{2d_1}\left\{\frac{m}{d_1}-\frac{x_2}{{y_2}^2}\left(n-\frac{x_2}{d_1}m\right)\right\}t_1+\frac{1}{2{y_2}^2}\left(n-\frac{x_2}{d_1}m\right)t_2\right]\delta t$$

故に震央及震原の深さの誤差は初期微動繼續時間 t_0, t_1, t_2 及 $\delta t_0, \delta t_1, \delta t_2$ が誤差として取る値（符號も考ふる必要あり）に依つて違つて來るが一々論することは出來ないから特別な場合に就いて述べる。

(I)　$\left.\begin{array}{l} t_1=t_2=t_3=t \\ \delta t=\pm 0.1\ \text{sec.}\end{array}\right\}$ なる場合

即ち三觀測點に於ける初期微動繼續時間が同じであつた場合に各觀測點に於て該繼

續時間を 0.1 sec. 多く或は少く誤算したるときに於ける震原の位置は如何様に變ずるかを求めるのである。

此の場合震央の位置は $X=25.2$ 粁、$Y=0$

$$\frac{\partial X}{\partial t_0}+\frac{\partial X}{\partial t_1}=0$$

$$\frac{\partial Y}{\partial t_0}+\frac{\partial Y}{\partial t_1}+\frac{\partial Y}{\partial t_2}=0$$

$$\frac{\partial Z}{\partial t_0}+\frac{\partial Z}{\partial t_1}+\frac{\partial Z}{\partial t_2}=\frac{k^2}{Z}t$$

震原の深さ

$$Z=\sqrt{kt_0{}^2-\frac{d_1{}^2}{4}-\frac{1}{4y_2{}^2}(d_2{}^2-x_2\,d_1)^2}$$

尙ほ觀測網の形を見ると三觀測點は略直角三角形であつて直角の頂點が伊根村に相當することから

$$d_2{}^2=x_2\,d_1$$

なる關係を實際上用ひて差支ないから Z の平方根内の最後の項は零になる。

故に

$$Z=\sqrt{kt^2-\frac{d_1{}^2}{4}}$$

となる。

而して $t_0=t_1=t_2=t$ なる假定のもとに我々の各觀測點を中心とし半徑 kt なる三つの半球が一點に交るためには t は 3 秒以上でなければならない。それ故に次の二つの場合に就きて述べておく。

(a)　$t_0=t_1=t_2=4$ sec. の場合

$$\frac{\partial Z}{\partial t_0}+\frac{\partial Z}{\partial t_1}+\frac{\partial Z}{\partial t_2}=\frac{k^2}{Z}t$$

$$=13$$

こゝに $Z=22$ km. である（k 及 d_1 の値は前に述べてある）。

故に　$\delta t_0=\delta t_1=\delta t_2=\pm 0.1$ sec.　とすれば震原の深さに於ては約一・三粁の增加或は減少となる。

(b)　$t_0=t_1=t_2=5$ sec. の場合

$$\delta Z=\left(\frac{\partial Z}{\partial t_0}=\frac{\partial Z}{\partial t_1}+\frac{\partial Z}{\partial t_2}\right)\delta t=10.4\,\delta t$$

この場合 $Z=34$ km. となる。

而して、$\delta t_0=\delta t_1=\delta t_2=\pm 0.1$ sec. とすれば深さに於ては約一粁の増減が誤差となるわけである。

(II) $t_0\neq t_1\neq t_2$ なる一般の場合に就きて述べる。この場合は t_0, t_1, t_2 の色々の値の組合せによつて誤差の色々の値を得るもすべての場合に就いて計算することは到底出來ないから最も多く計測された値に近い場合の二例に依つて計算する。

(a) $\left.\begin{aligned} t_0&=4\text{ sec.}\\ t_1&=3\text{ sec.}\\ t_2&=3\text{ sec.}\end{aligned}\right\}$ の場合

震央の座標; $X=30$ km.　$Y=8.4$ km.

震央の誤差;

$$\delta X=\left(\frac{\partial X}{\partial t_0}+\frac{\partial X}{\partial t_1}\right)\delta t=\frac{k^2}{d_1}(t_0-t_1)\,\delta t=0.14$$

$$\delta Y=\left(\frac{\partial Y}{\partial t_0}+\frac{\partial Y}{\partial t_1}+\frac{\partial Y}{\partial t_2}\right)\delta t=\frac{k^2}{y_2}\left\{(t_0-t_1)-\frac{x_2}{d_1}(t_0-t_2)\right\}\delta t=0.24$$

故に $\delta t_0=\delta t_1=\delta t_2=\pm 0.1$ sec. の場合には震央の X の誤差は〇・一四粁、Y の誤差は〇・一四粁で極めて僅かである。

次に震原の深さ;

$$Z=12.8\text{ km.}$$

深さの誤差;

$$\delta Z=\left(\frac{\partial Z}{\partial t_0}+\frac{\partial Z}{\partial t_1}+\frac{\partial Z}{\partial t_2}\right)\delta t=\frac{k_2}{Z}(0.12\,t_0+0.5\,t+0.38\,t_2)\times 0.1=1.7\text{ km.}$$

δt_0, δt_1, δt_2 が前同様 ± 0.1 sec. であるとすれば Z の誤差は一・七粁の増減である。

この誤差は δt_0, δt_1, δt_2 が同符號の場合に取るべき値であつて此等の何れかが異符號の場合にはこれより小さな値を取る。言を換へて云へば三觀測點のすべてで十分の一秒の誤差を含んで初期微動の繼續時間を計測した場合の震原の深さの誤差であるから Z の最大誤差と見做してよい。

但し X, Y の誤差は $\delta t_0, \delta t_1, \delta t_2$ の異符號の場合には前に示した値よりは異る値を取る。例へば $\delta t_0=+0.1$ sec. $\delta t_1=-0.1$ sec. $\delta t_2=-0.1$ sec. の場合、t_0, t_1, t_2 を (II), (a) の値として計算すると X の誤差は一粁の増加となり Y の誤差は一・七粁の増加

となる。深さに於ては一粁減となる。

以上示した例は實際の場合は鄕村斷層線に接近して起る餘震の一例である。

(b) $t_0=2$ sec.
$t_1=5$ sec.
$t_2=3$ sec.
} なる場合

$$\delta t_0=\delta t_1=\delta t_2=\pm 0.1 \text{ sec.}$$

此の場合の震央は

$$X=10 \text{ km.}$$
$$Y=1 \text{ km.}$$

震原の深さは

$$Z=13.5 \text{ km.}$$

$$\frac{\partial X}{\partial t_0}+\frac{\partial X}{\partial t_1}=5.2$$

$$\frac{\partial Y}{\partial t_0}+\frac{\partial Y}{\partial t_1}+\frac{\partial Y}{\partial t_2}=8.8$$

$$\frac{\partial Z}{\partial t_0}+\frac{\partial Z}{\partial t_1}+\frac{\partial Z}{\partial t_2}=\frac{k_2}{Z}(0.8\,t_0+0.09\,t_1+0.04\,t_2)$$
$$=10.5$$

故に震央の座標 X の誤差は〇・五粁、Y の誤差は 〇・九粁、震原の深さの誤差は約一粁である。

前例に從つて誤差が觀則點毎に異符號をとる場合を述べる。

$\delta t_0=+0.1$ sec. $\delta t_1=-0.1$ sec. $\delta t_2=-0.1$ sec. とすれば

$$\delta X=\left(\frac{\partial X}{\partial t_0}+\frac{\partial X}{\partial t_1}\right)\delta t=1.$$

$$\delta Y=\left(\frac{\partial Y}{\partial t_0}+\frac{\partial Y}{\partial t_1}+\frac{\partial Y}{\partial t_2}\right)\delta t=1.2$$

$$\delta Z=\left(\frac{\partial Z}{\partial t_0}+\frac{\partial Z}{\partial t_1}+\frac{\partial Z}{\partial t_2}\right)\delta t=0.5$$

故に震央の座標 X の誤差は一・〇粁、Y の誤差は一・二粁、震原の深さの誤差は〇・五粁として差支ない。

(b) の例は實地上に於ては宮津附近に發したる餘震に就いて適應し得るのである。

以上述べ來りたる如く誤差の範圍も震原の配別上から考へると看過し得る程度に小さいとは云ひ得ない。が觀測の比較的狹小なること、震原の深さの比較的淺いために大なる震原位置の誤差はないものと認め得、勿論計測學が今日以上に發達した曉には尙ほ一層正確な觀察を下し得ると信ず。

餘震の回數に關する統計的調査

從來餘震の回數の統計的調査は多方面に涉つて行はれてゐる。其の例に從つて今回の丹後地方の餘震に就いて一・二種類調査を行つた。尙ほ統計的方面で氣壓勾配と今回の餘震の發生に關するものは石本教授に依つてなされ、同氏の論文中にあることを附記しておく。

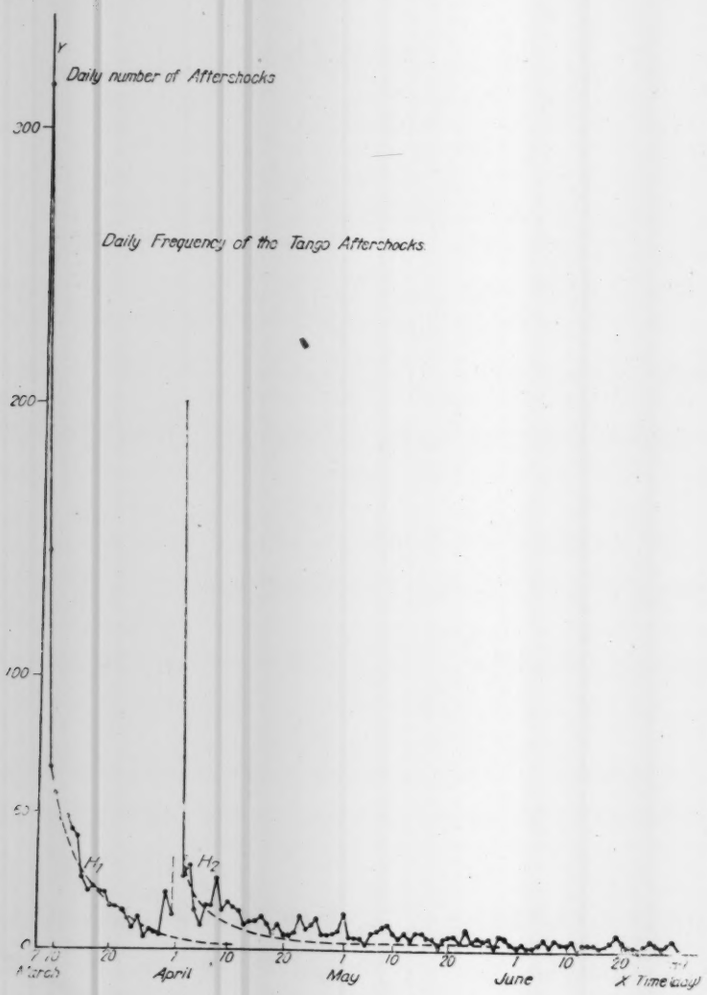

第二十圖　丹後餘震の日々回數

(a) 餘震の日々の變化 —— 大地震後より日々回數の變化を示したのが第十八圖である。

便宜上最初の十數日は大地震後毎一晝夜に於けるものを示してある。即第一日は三月七日午後六時二十七分より翌八日午後六時三十分に至る迄を示す。稍々回數の少くなつた頃便宜上その日の午前零時から午後十二時に至る二十四時間を區切としてゐる。その關係上三月二十日午前零時から午後六時に至る間に於て起つた餘震の回數は圖では三月十九、二十日の兩日に重複して計算されて示されてある。

最初より三月三十日頃に至る間は比較的規則正しく次式を以て大略日々の回數を計算し得る樣に減少してゐる。

$$y=\frac{218}{x+0.7}$$

茲に x は三月七日から計られた日數であつて、その日の日々回數が y である。

四月一日の强震後この强震自身の餘震が伴つて起つたので日々回數は再び增加を示してゐる。それ故四月一日以後に於ては前式のものに更に一式を加へたものが日々回數を示すのである。即ち次の式を用ふるのである。

$$y=\frac{218}{x+0.7}+\frac{34}{x-25+0.16}$$

これに依れば約半歲の後と雖も一日中に一・二回の餘震の起るわけになる。

尙ほ此の調査中大地震後數日中に起つた餘震の回數は中央氣象臺の調査の結果を以て補足したのである。

(b) 大地震直後五十四時間內に於ける毎時間の餘震回數の變化 —— 之には主として中央氣象臺で調査された回數を用ひた。

餘震の程度を有感覺、無感覺と大別し此等の餘震の時間毎の回數變化及此等の區別をなさずに同じく毎時間の回數の變化を調べた結果を第十九圖に示す。

a 曲線は有感、無感覺の餘震を通じて毎時間の回數の變化を示し、b 曲線は有感覺のものゝみ、c 曲線は無感覺のものゝみに就いて同上の調査を試みた結果である。

即 a 曲線は餘震の全般的の活動狀態を知る上に必要である。この曲線で目立つて見得る現象は $M_1,\ldots M_8$ に至る回數增加を示す點が大地震直後七乃至八時間の間隔を置いて表はれてゐることである。これは間歇的な地變の結果と想像される。

b 曲線を見ると大地震直後に於ては主として比較的大なる餘震のみが起つた事が判る。

第二十一圖　大地震後五十四時間に至る毎時間の餘震回數

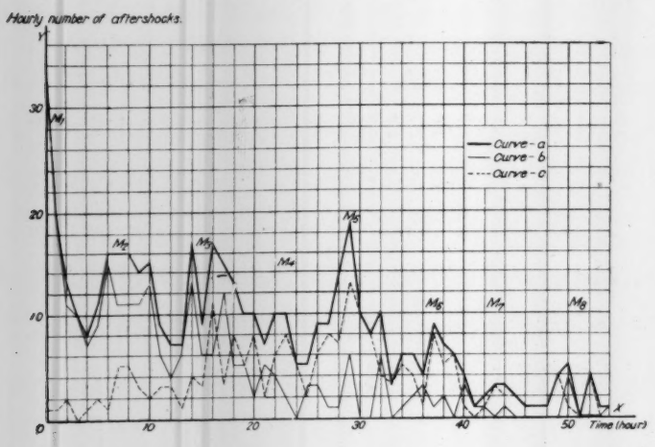

Fig. 21. Hourly frequency of aftershocks during the 54 hours following the great Tango earthquake.

c 曲線は大地震直後より次第に增加し最大回數に達するまでには約三十時間を經過してゐる。

有感、無感地震の區別は人身感覺を主としてのもので勿論物理的意味に於ける區別ではなく單に地震發生の規模及距離の大小等を概略知る便宜上のものである。而し裂罅が地下に於て生ずる際に餘震が發するとすれば裂罅の性質殊に其の大小を以て上述の有感、無感の餘震の區別はなし得られると思ふ。以上に示されたる曲線により大地震直後に於ては比較的大る裂罅を生じ從つて有感覺餘震に於ても本震の十分の一程度の震動區域を有するものが起り得るのである。此等の大なる裂罅の周圍に二次的の微細な裂罅が次期に於て次第に增加する。卽圖中の c 曲線が大地震直後より順次に增加を示してゐるのは恐らくこの現象が地下に於て行はれた結果と想像するのである。

(c)　誘發的の關係に於いて地震回數の增加したる一例 —— 今回の丹後大地震を丹後半島附近に起つた地變と考へれば單に東部半島の移動に歸することも出來るが稍々大なる構造線に沿つて起つたと考へる。卽ち山崎博士の說の琵琶湖、伊勢灣を通ずる線或は今村博士の濃尾大地震の際の斷層帶等に沿つて地變が起つたとすれば其の大なる構造線附近に於ても之と同時或は多少の時間を置いて地震を發し得るのである。それ故に某地に此の大地震が起つた後に地震の回數が增加した結果誘發されて起つたかの如き觀を呈するが實は今も述べる如き大構造線上の地變が主震域以外に起つた結果であらう。此點に於て多少誘發なる文句は適當とは考へないが從來使用されてゐる例に從つて之を用ひて置く。

此回の地震後直ちに地震回數を增加した地方は岐阜、名古屋附近である。尙琵琶湖の東岸にも地震が發してゐる。中央氣象臺で調査された各地の地震の時刻を見るとこの地方の著しい回數增加は丹後大地震の突發した直後から始まつてゐる。

第二十圖には和歌山附近とこの地方とを比較するために昭和二年二月から二月末日迄の日々回數を擧げてある。和歌山地方は格別回數の增加を示さないのは前述の構造線に關係が少いためであらうと考へる。

第二十二圖　和歌山及濃尾（岐阜）地方に於ける昭和二年二月及三月中の地震日々回數（濃尾地方に於て丹後大地震後回數增加ありたるを示す）

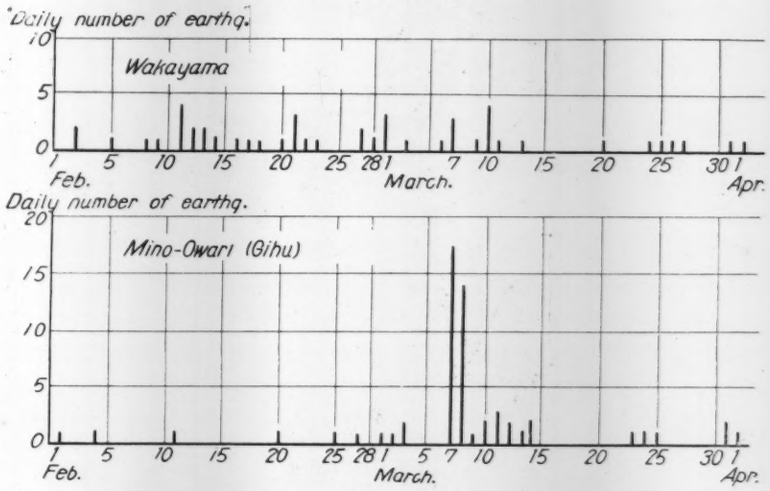

Fig. 22. Daily frequency of earthquakes in the districts of Wakayama and Mino-Owari during February and March, 1927.

餘震の主活動區域の移動——餘震が丹後地方一帶に分布されてゐる有樣は前述の通りであるが餘震の震央を順次に追跡して見ると或る日數の間は略々定つた場所にあり、其後何日か經過後はこれとは違つた場所にあることが判る。こゝでは餘震中の比較的大きなものを選んで其れ等の位置する大體の區域を假りに餘震の主活動區域と稱へることにする。これ等の移動を示すために丹後大地震後より約一年間即今年の三月上旬に至る間に於ける主たる餘震を起つた順に大體十七期に別けることが便利である。

第二十三圖（其の一、其の二、其の三）に之等の主活動區域の移動の有樣を示してある。餘震群を示すために同一期間に起つた餘震の震央は同じ數字を以て表はし同數字の下方の小數字を以て更に同一期間に起つた餘震を相互に區別してある。別紙の表

第二十三圖 比較的著しき餘震の群生せしを示す

其一 三月七日（昭和二）より五月二十九日に至る間

其二 六月六日より十二月四日に至る間

其三 十二月四日より二月二十九日（昭和三）に至る間

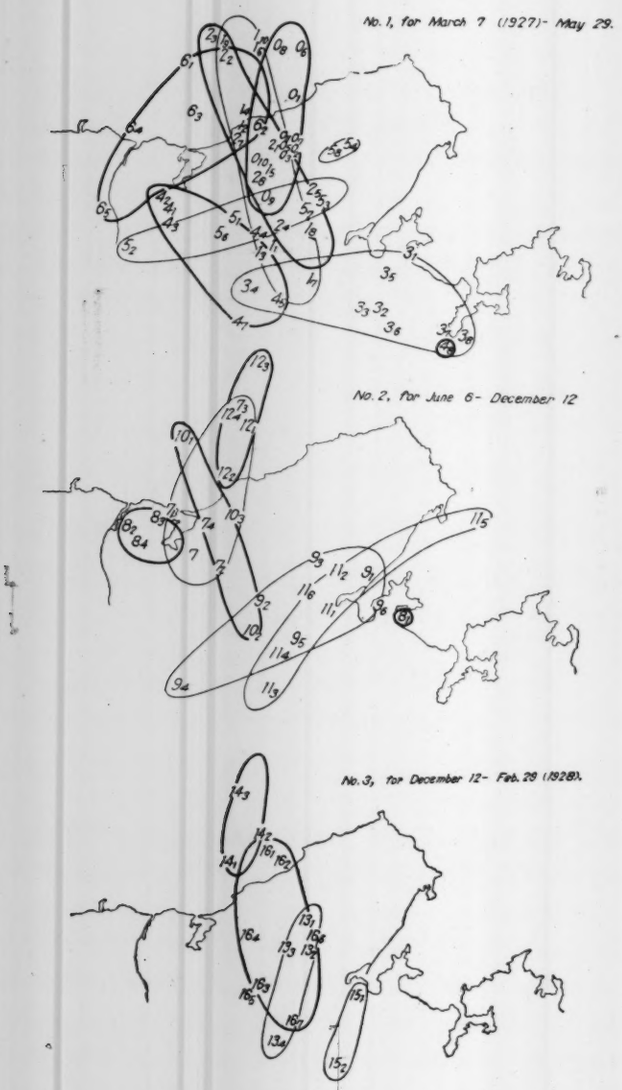

Fig. 23. Map showing the seats of the groups of the comparatively conspicuous aftershocks.

Group	Earthq. No.	Time	Group	Earthq. No.	Time
		h m			h m
0	1	March 7, 18 28	6	1	May 20, 16 52
	2	14 44		2	23, 01 36
	3	19 46		3	24, 23 01
	4	22 24		4	29, 01 30
	5	8, 00 36		5	04 32
	6	00 48	7	1	June 6, 05 07
	7	09 13		2	17, 18 30
	8	23 43		3	24, 19 42
	9	9, 20 44		4	July 7, 05 34
	10	11, 07 35		5	Aug. 5, 11 44
	11	09 50		6	21 40
1	1	March 13, 06 30	8	1	Sept. 1, 04 58
	2	10 20		2	04 59
	3	13 37		3	5, 22 58
	4	14, 10 34		4	7, 06 07
	5	12 49	9	1	Sept. 14, 14 14
	6	16, 16 04		2	18, 07 17
	7	18, 21 47		3	23, 05 11
	8	19, 05 17		4	25, 06 09
	9	15 50		5	27, 07 56
	10	20, 14 14		6	08 29
2	1	March 21, 00 11	10	1	Oct. 3, 08 29
	2	22, 02 17		2	14, 12 37
	3	05 16		3	22, 05 57
	4	12 57	11	1	Oct. 24, 07 57
	5	23, 22 50		2	28, 00 24
	6	25, 19 13		3	02 53
	7	29, 05 06		4	Nov. 10, 11 47
3	1	March 30, 22 30		5	12, 00 44
	2	April 1, 06 07		6	09 24
	3	08 49	12	1	Nov. 16, 20 29
	4	11 42		2	26, 20 10
	5	14 49		3	Dec. 4, 09 56
	6	18 23		4	12 34
	7	8, 17 42	13	1	Dec. 4, 18 28
	8	22 05		2	8, 01 17
4	1	April 10, 19 26		3	02 14
	2	11, 01 32		4	17, 14 28
	3	02 59	14	1	Dec. 22, 20 42
	4	16, 20 57		2	28, 11 35
	5	22 34		3	30, 13 52
	6	20, 05 49			(1928)
	7	25, 19 27	15	1	Jan. 10, 12 32
5	1	May 3, 11 48		2	30, 05 01
	2	5, 07 04	16	1	Jan. 30, 18 14
	3	6, 17 19		2	Feb. 12, 21 30
	4	7, 08 54		3	15, 20 39
	5	8, 09 07		4	18, 18 49
	6	13, 17 43		5	18 49
	7	14, 19 24		6	19, 05 27
				7	29, 10 38

によつてそれ等が示されてある。

0 餘震群は大地震直後から十一日に至る間のもので氣象要覽に記載されたものを以て補足したのである。此の餘震群の各々は比較的大規模のものばかりであつて後々の餘震とは當然大いさの點に於て格段の相變である。

先づ大地震の八分の一以下十數分の一程度である。此の餘震群の位置は大體淺茂川附近にあつて大地震の發震地に近くあることが見られる。

其後に於ては3の餘震群が移動した有様は極めて明瞭である。卽前にも數回述べたる四月一日の强震に先立つて三月三十日頃より急に餘震が宮津の附近に表はれた。そして强震を發し、それ以後數日間はこゝに主として餘震を發してゐたのである。

以後（4 以下8に至る餘震群）は全くこれまでの移動とは反對の向きに卽ち北西の方向に主活動區域が位置を轉じた有様が見られる。

8 以下 16 に至る餘震群の移動の模様は圖によつて示されてあるから、こゝでは說明を略す。此等の結果を綜合するに餘震群の占むる位置卽ちこれに依つて示されたる地下變動の主活動區域は略ぼ鄉村斷層帶の西部に位し、南は海岸線より約三〇粁附近まで、北は日本海中約四〇粁まで、西は園山川流域に至る迄の地塊內部に限られてゐる。これは餘震活動區域の重要な結論の一つである。又大地震直後より約半歲を經過して再び主活動區域が元の位置の附近に歸つて來た事及活動區域の移動の有様は南北に恰も振動體の如き形式に依つて移轉しつゝ全體としては或る方向に進むこと、これ等の事柄は興味あるものである。

從來考へられてゐる様に歪の集積が起るとすれば其集積の有様も以上の主活動區域の移動の形式から想像されることである。更に餘震の活動區域の移動に關して詳細に研究せんがため地表傾斜變化との關係に就きて次に述ぶる如き方法によつて調べた。

地表傾斜變化と餘震群の位置によりて示されたる地震活動區域の移動との關係 —— 餘震群の移動の狀態は以上述べた様であるが之を更に短時日の期間に分割して其の震央を追跡し見ると今回石本敎授に依つて觀測された地表傾斜變化と密接な關係があるやうに見える。同氏は餘震中の比較的著しいものに就いて其等の起る前の地表傾斜變化との關係を詳細に調査し既に其報告を當彙報第四號（二〇三頁）に發表せられた。

以下述べるものは同氏の觀測結果を基準として此の餘震觀測の結果から推定される事項である。

先づ傾斜變化に就きて考ふるに某地に於ける地殼內の變動の如何に依つて地表傾斜は或は其の方向を轉じ或は著しく表はれる場合或は然らざる場合もあらう。言を換へ

れば甲地に餘震群の密生してゐる期間内の地表傾斜變化と乙地に密生してゐる期間内の者とは違つた方向で示されることもあり又傾斜變化の緩急もあらう。

又同一地點に地震が起るとするも、其の地點の隆起、沈降の場合とでは傾斜變化の方向が全然反對であることも想像される。

此等は丹後地方の如く大地震後地殻内の構造が甚だしく不安定の狀態になつてゐるのであるから地表傾斜の變化を起し得る程度に或る力が作用する場合は地塊内部に於て餘震の發生を促し得ると想像した結果である。

第　六　表　(TABLE 6)

Tiliting			Active Centre		
Duration		Direction (downwards towards)	Region of		Direction (from Miyadu)
a	Mar. 15–20	SE	*A*	Upheaval	NW or SW
b	20–23	—	*B*	Do.	NW
c	23–25	NW	*C*	Subsidence	NW
d	25–30	SE	*D*	Upheaval	W or NW
e	30–Apr. 1	NW	*E*	Do.	SE or S
f	Apr. 15–22	W?	*F*	New Subsidence (?)	NW or S
g	22–23	E?	*G*	New Upheaval	SW
h	23–25	NW	*H*	Do.	SE or SW
i	25–May 7	NE	*I*	?	NW
j	8–15	NW	*J*	Subsidence	NW
k	15–17	E	*K*	Upheaval	NW
l	15–June 10	—	*L*	—	NW
m	10–15	S?	*M*	Upheaval	NW
n	15–17	N?	*N*	Upheaval (?)	W
o	25–30	S	*O*	Upheaval	NW
p	30–July 7	NE	*P*	Do.	NW
q	9–12	NE	*Q*	Subsidence	N
r	25–Aug. 5	NE	*R*	Upheaval (?)	NW
s	5–Sept. 1	NE	*S*	Do.	NW

そこで宮津に於ける或る向きの傾斜變化が起りつゝある期間に起つた餘震群の位置、卽ち之に依つて推定される地殻變動の活動區域の位置と傾斜の向きとを比較したのである。

此の目的には石本氏論文第一圖及附圖第一に依つて傾斜變化を $a,\ldots.s$ の傾斜群に別ちそれに相當して餘震群を $A\ldots.S$ に區別したのである。此等の餘震群は餘震中今回の觀測で震原を決定し得たものを全部用ひて區別したのである。

第二十四圖——第二十八圖　は餘震群の位置及宮津に於ける傾斜の向きとの關係を示す（表と對照）

第二十四圖　宮津町に於ける地表傾斜變化の繼續期間中に於ける餘震の主活動區域を示す
（宮津町に附したる矢は傾斜方向を示す）

其一、三月十五日より四月一日に至る間

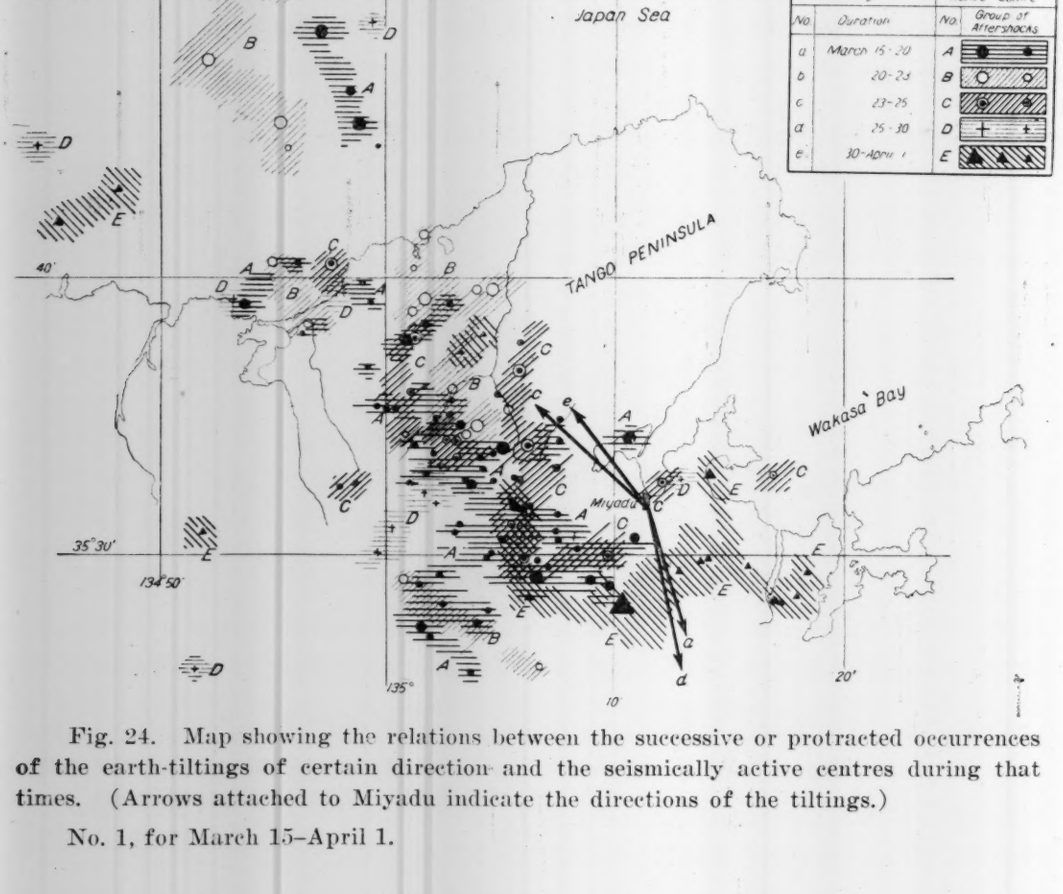

Fig. 24. Map showing the relations between the successive or protracted occurrences of the earth-tiltings of certain direction and the seismically active centres during that times. (Arrows attached to Miyadu indicate the directions of the tiltings.)

No. 1, for March 15–April 1.

一例を擧げると三月十五日より二十日に至る間の宮津の地表傾斜の方向は A の矢を以て東南に示されてあり、餘震群の位置は横に太い線影を以て示されてある。

一般の結論を述べると餘震群の位置と傾斜變化との關係は大略次の三種類に別たれる。

（一）餘震群が稍々遠距離に位置してゐるときは傾斜變化は著しく現はれない。B 及 L 餘震群の場合がそれである。

（二）傾斜の俯きが丁度餘震群の占むる位置の方へ向ふ場合。

（三）此れとは反對に餘震群の位置と反する場合。

第二十五圖　宮津町に於ける地表傾斜變化の繼續期間中の餘震の活動區域を示す
（宮津町に附したる矢は傾斜の方向を示す）

其の二、四月十五日より同三十日に至る間

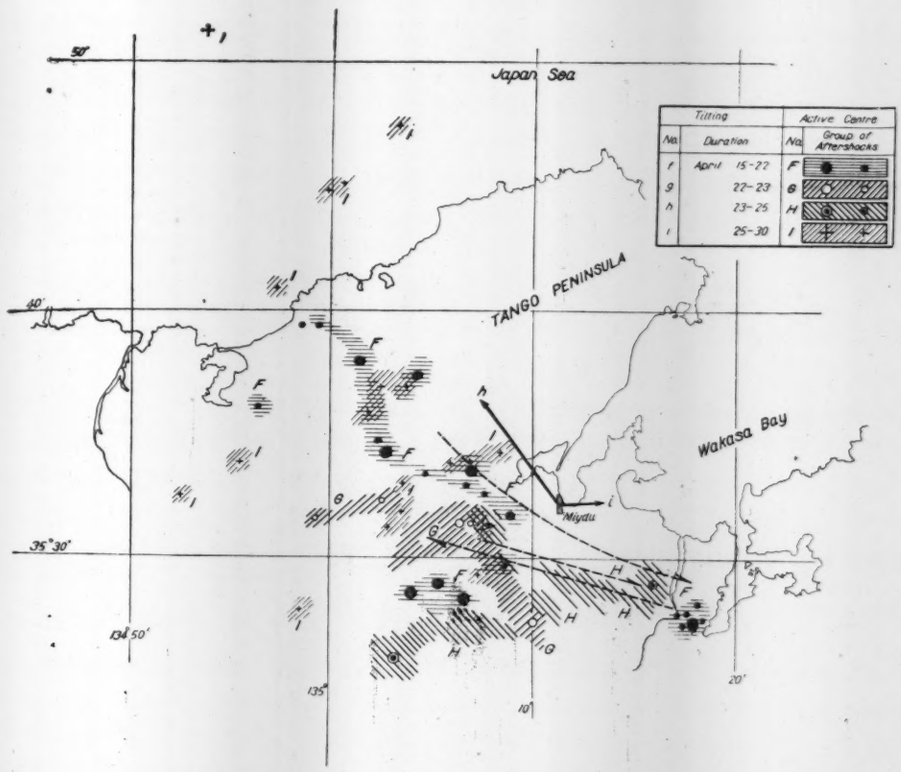

Fig. 25. Map showing the relations between the successive or protected occurrences of the earth-tiltings of certain direction and the seismically active centres during that times. (Arrows attached to Miyadu indicate the directions of the tiltings.)

No. 2, for April 15–30.

何れの場合でも餘震群の移動と傾斜方向の轉ずることは密接なる關係があつて時間的の關係では比較的接近して兩現象が現はれる。

上の（二）の場合に屬する餘震群は C, F, J, O, Q 等であつて、此等の群に屬する餘震の震點を調べて見ると大地震の際の地形變動が主として沈降地帶であつた場所に起つてゐる。卽 C が鄕村斷層の東側に位置する例及 J の山田斷層南側に位置する例等は著しく此の關係を示してゐる。F は多少これとは趣を異にしてゐる。F の位置から考ふれば鄕村斷層帶附近が一時沈降の現象を呈したのではなからうかと思はれる。何れにせよ此の場合は傾斜變化の向きと餘震群の位置の關係は（二）の場合として說明し得られる。

第二十六圖　宮津町に於ける地表傾斜變化の繼續期間中に於ける餘震の主活動區域を示す
（宮津市に附したる矢は傾斜の方向を示す）

第三、五月一日より六月十日に至る間

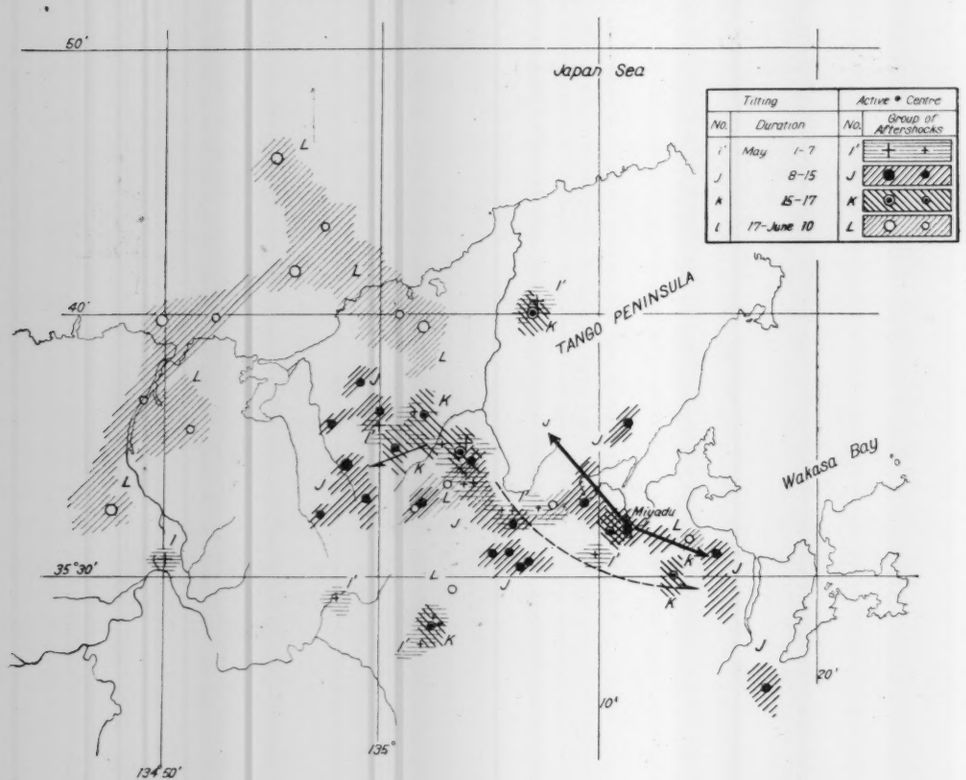

Fig. 26. Map showing the relations between the successive or protracted occurrences of the earth-tiltings of certain direction and the seismically active centres during that times. (Arrows attached to Miyadu indicate the directions of the tiltings.)

No. 3, for May 1–June 10.

第二十七圖　宮津町に於ける地表傾斜變化の繼續期間中に於ける餘震の主活動區域を示す
（宮津町に附したる矢は傾斜の方向を示す）

其四、六月十日より七月七日に至る間

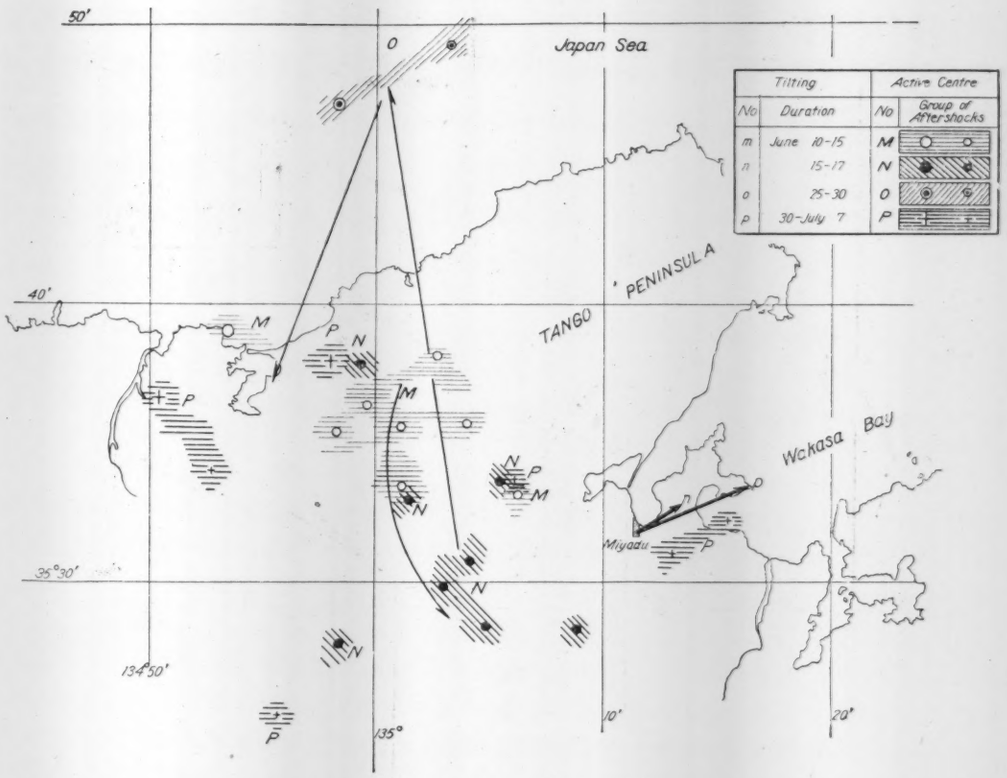

Fig. 27. Map showing the relations between the successive or protracted occurrences of the earth-tiltings of certain direction and the seismically active centres during that times. (Arrows attached to Miyadu indicate the directions of the tiltings.)

No. 4, for June 10–July 7.

（三）の場合は $A, D, E, G, H, I, K, M, N, P, R, S$ である。此等の各群の占むる位置を見るに一般に隆起地帶が多い。勿論宮津の觀測地點に對して相對的の關係に於ける意味の隆起地帶も含まれてゐる。例へば E 餘震群の如き場合である。この E 餘震群の表はれた期間に於て地表傾斜變化は著しく西北に向ひ、一兩日後四月一日の强震に至つたのである。

尙ほ此等の餘震群 P, Q, R, S 及此に關係ある傾斜群中で p, q, r, s は陸地測量部の震災後第二回の一二等三角點移動檢測の成果（地震研究所彙報第四號）に於て示された移動と直接關係があると考へる。

第二十八圖　宮津町に於ける地表傾斜變化の繼續期間中に於ける餘震の主活動區域を示す
（宮津町に附したる矢は傾斜の方向を示す）

其五、七月九日より九月一日に至る間

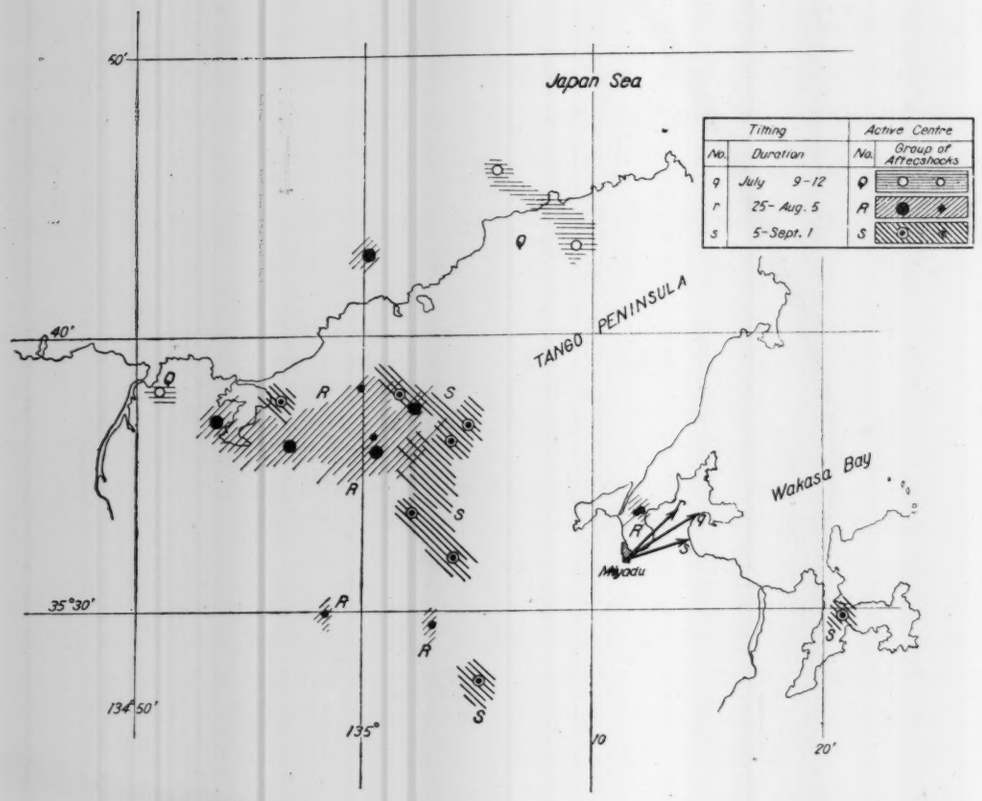

Fig. 28. Map showing the relations between the successive or protracted occurrences of the earth-tilting of certain direction and the seismically active centres during that times. (Arrows attached to Miyadu indicate the direction of the tiltings.)

即第二回目の丹後地方の一二等三角點の移動の有様を見るに大地震の際の變動の方向の如何に關せず西北の方向に各點の移動が起つてゐる。そして移動量は此處に大體城崎、舞鶴附近を通じて西北から東南に向ふ一線を考へるとその線に至る距離の大小に比例する様である。此れは或は此の假想的の線に沿つて丹後地方の廻轉的變位が行はれたのであらうと想像される。同時に大地震の際に於て隆起したる方面は更に隆起し奥丹後半島の如き沈降地帶は更に沈降を伴つたのではなからうか。

此等の事柄を想像すると前述の p, q, r, s の傾斜が稍々急激に現はれた四期間に於て右の地變を生じたのであらうと推定する。

本報告の擱筆に當つて調査に關して多大の援助を惜まれなかつた末廣所長に深く謝意を表したい。又研究調査の當初より今村教授の懇篤なる教示を受けたことに對しては切に感銘する次第である。

尙又直接觀測に從事せられたる地震學教室の脇元、高橋、和田、新井、加藤の諸氏舞鶴桂林寺の兒玉至玄氏、伊根村小學校の林田信丸氏、城崎赤石屋旅館主坂本誠一氏河邊村助役吉岡利一郎氏、間人町小學校增井梅吉氏の諸氏には永々御盡力下された事を厚く御禮申述べる。

最後に地表傾斜變化其他に關して有益なる資料を與へ又調査中不斷指示を受けた石本教授に對して感謝の意を表する次第である。

（昭・三・六・三〇）

第 七 表　(TABLE 7)

丹後地震の餘震觀測表（昭和二年自三月十一日至八月三十一日）

List of the Aftershocks of the Tango Earthquake (For March 11–August 31, 1927)

初微 (Pre. tr.) = 初期微動繼續時間 (Duration of Preliminary Tremor)
初動 (Init. Mot.) = (Initial Motion)
最大動 (Max. 2A) = 最大全振幅 Maximum Double Amplitude)
E.W. = 東西動 (East West Component): (+) 東へ (towards E.)
　　－ 西へ (towards W.)
N.S. = 南北動 (North South Component): (+) 北へ (towards N.)
　　－ 南へ (towards S.)

日時 Time of Occurrence		舞鶴 (Maiduru)					城崎 (Kinosaki)					伊根 (Ine)					震央 Epi-centre	震原の深さ Focal Depth	摘要 Remark
		初微 Prel. tr.	初動 Init. E.W.	初動 Init. N.S.	最大動 Max. 2A E.W.	最大動 Max. 2A N.S.	初微 Prel. tr.	初動 Init. E.W.	初動 Init. N.S.	最大動 Max. 2A E.W.	最大動 Max. 2A N.S.	初微 Prel. tr.	初動 Init. E.W.	初動 Init. N.S.	最大動 Max. 2A E.W.	最大動 Max. 2A N.S.			
		s	μ	μ	π	μ	s	μ	μ	μ	μ	s	μ	μ	μ	μ		km	
March 11 (1927)	22 12	3.2	—	—	2	2	—	—	—	—	—	—	—	—	—	—	—	—	
	25	5.4	—	—	2	2	—	—	—	—	—	—	—	—	—	—	—	—	
	37	5.3	—	—	3	2	—	—	—	—	—	—	—	—	—	—	—	—	
	46	4.9	—	—	2	2	—	—	—	—	—	—	—	—	—	—	—	—	
	55	3.8	—	—	2	1	—	—	—	—	—	—	—	—	—	—	—	—	
	23 21	4 2	—	—	4	3	—	—	—	—	—	—	—	—	—	—	—	—	
	22	5.4	—	—	3	2	—	—	—	—	—	—	—	—	—	—	—	—	
	43	3.8	−5	—	53	—	—	—	—	—	—	—	—	—	—	—	—	—	
	54	4.2	—	—	2	—	—	—	—	—	—	—	—	—	—	—	—	—	
12	0 13	4.2	—	—	3	3	—	—	—	—	—	—	—	—	—	—	—	—	
	40	3.9	—	—	6	6	—	—	—	—	—	—	—	—	—	—	—	—	
	1 24	4.0	—	—	4	4	—	—	—	—	—	—	—	—	—	—	—	—	
	57	4.2	—	—	14	12	—	—	—	—	—	—	—	—	—	—	—	—	
	2 19	—	—	—	2	2	—	—	—	—	—	—	—	—	—	—	—	—	
	3 39	3.3	—	—	3	3	—	—	—	—	—	—	—	—	—	—	—	—	
	47	4.3	—	—	10	8	—	—	—	—	—	—	—	—	—	—	—	—	
	52	4.0	—	—	3	2	—	—	—	—	—	—	—	—	—	—	—	—	
	53	—	—	—	—	—	—	—	—	—	—	—	—	—	—	—	—	—	
	59	3.9	—	—	2	1	—	—	—	—	—	—	—	—	—	—	—	—	
	5 30	5.0	−59	+32	122	68	—	—	—	—	—	—	—	—	—	—	—	—	
	33	—	—	—	3	3	—	—	—	—	—	—	—	—	—	—	—	—	
	7 44	—	—	—	—	—	—	—	—	—	—	—	—	—	—	—	—	—	
	9 04	3.0	− 5	—	12	—	—	—	—	—	—	—	—	—	—	—	—	—	
	08	5.3	—	—	5	—	—	—	—	—	—	—	—	—	—	—	—	—	
	18	4.6	—	—	3	—	—	—	—	—	—	—	—	—	—	—	—	—	
	25	4.1	—	—	7	—	—	—	—	—	—	—	—	—	—	—	—	—	
	31	5.8	—	—	7	—	—	—	—	—	—	—	—	—	—	—	—	—	
	38	3.6	− 2	—	13	—	—	—	—	—	—	—	—	—	—	—	—	—	
	10 30	—	—	—	—	—	—	—	—	—	—	—	—	—	—	—	—	—	
	11 03	—	—	—	—	—	—	—	—	—	—	—	—	—	—	—	—	—	
	22	—	—	—	—	—	—	—	—	—	—	—	—	—	—	—	—	—	
	23	—	—	—	—	—	—	—	—	—	—	—	—	—	—	—	—	—	
	30	—	—	—	—	—	—	—	—	—	—	—	—	—	—	—	—	—	
	44	—	—	—	—	—	—	—	—	—	—	—	—	—	—	—	—	—	
	12 19	—	—	—	—	—	—	—	—	—	—	—	—	—	—	—	—	—	

12 20	—	—	—	—	—	—	—	—	—	—	—	—	—	—	—	—	—
21	—	—	—	—	—	—	—	—	—	—	—	—	—	—	—	—	—
14 06	—	—	—	—	—	—	—	—	—	—	—	—	—	—	—	—	—
27	—	—	—	—	—	—	—	—	—	—	—	—	—	—	—	—	—
41	—	—	—	—	—	—	—	—	—	—	—	—	—	—	—	—	—
56	—	—	—	—	—	3.4	—	—	—	12	—	—	—	—	—	—	—
15 28	3.0	−26	+16	82	52	4.1	86	−47	278	147	3.0	−20	−15	50	40	1	15.5
42	3.3	−12	3	32	26	3.8	—	—	16	18	3.7	—	—	10	12	2	15.7
16 44	—	—	—	3	3	3.8	—	—	10	12	—	—	—	—	—	—	—
17 14	3.5	− 4	2	8	8	3.7	—	—	23	—	—	—	—	—	—	—	—
15	—	—	—	3	3	4.3	—	—	11	—	—	—	—	—	—	—	—
25	3.0	—	—	3	2	4.5	—	—	11	—	—	—	—	—	—	—	—
28	4.0	—	—	5	3	3.3	—	—	22	—	—	—	—	—	—	—	—
31	3.8	—	—	3	2	4.4	—	—	15	—	—	—	—	—	—	—	—
37	7.2	—	—	6	6	—	—	—	—	—	—	—	—	—	—	—	—
51	3.2	− 5	5	20	13	4.4	—	—	33	17	3.4	—	—	22	28	3	19.6
18 21	2.9	—	—	10	7	5.1	—	—	42	—	4.0	—	—	16	10	4	20.6
41	4.5	—	—	5	5	2.6	—	—	49	23	3.6	—	—	1	1	5	14.3
20 03	3.0	—	—	5	5	4.3	—	—	40	28	4.4	—	—	8	10	6	11.8
04	3.0	—	—	3	3	4.3	—	—	18	22	4.4	—	—	5	7	—	11.8
35	3.3	—	—	5	5	4.1	—	—	10	8	3.6	—	—	4	7	5	18.6
21 43	5.2	—	− 1	3	3	2.2	—	—	41	29	5.3	—	—	8	6	8	12.2
54	4.3	—	—	3	3	2.9	—	—	10	8	—	—	—	—	—	—	—
0 23	4.5	—	—	2	2	—	—	—	—	—	—	—	—	2	2	—	—
1 34	4.5	—	—	3	3	—	—	—	—	—	5.4	—	—	3	2	—	—
2 05	3.6	− 2	3	5	4	—	—	—	—	—	4.2	—	—	4	4	—	—
10	4.0	− 3	2	5	4	—	—	—	—	—	3.6	—	—	5	6	—	—
13	3.4	—	—	4	3	—	—	—	—	—	4.3	—	—	3	2	—	—
40	3.2	—	—	8	4	—	—	—	—	—	2.9	—	—	2	1	—	—
4 10	4.3	—	—	4	4	—	—	—	—	—	4.2	—	—	5	7	—	—
43	4.0	—	—	3	3	—	—	—	—	—	5.0	—	—	3	2	—	—
6 30	3.6	− 2	2	49	24	3.5	—	—	92	140	4.0	− 7	− 5	12	20	9	15.8
45	—	—	—	2	1	—	—	—	—	—	—	—	—	—	—	—	—
58	—	—	—	3	3	—	—	—	—	—	4.3	—	—	2	2	—	—
7 44	4.1	—	—	4	2	3.0	3	—	12	15	3.1	—	—	3	4	10	14.0
53	4.0	—	—	5	3	3.0	—	—	10	5	3.6	—	—	2	2	11	15.5
55	4.1	− 2	2	28	16	3.4	—	—	34	21	3.8	− 2	− 2	8	6	12	19.3
8 28	3.3	—	—	4	3	4.1	—	—	12	7	3.6	—	—	4	2	13	18.6
54	2.5	—	—	3	2	—	—	—	—	—	3.0	—	—	4	6	—	—
9 13	—	—	—	2	1	—	—	—	—	—	—	—	—	2	1	—	—
10 20	5.4	—	—	8	5	3.4	—	—	185	84	4.2	− 7	2	20	26	14	23.4
11 09	3.2	—	—	20	14	3.8	—	—	16	13	3.5	—	—	5	10	15	15.6

日時 Time of Accurrence		舞鶴 (Maiduru)					城崎 (Kinosaki)					伊根 (Ine)					震央 Epi-centre	震原の深さ Focal Depth	摘要 Remark
		初微	初動 Init. Mot.		最大動 Max. 2A		初微	初動 Init. Mot.		最大動 Max. 2A		初微	初動 Init. Mot.		最大動 Max. 2A				
		Pre tr.	E.W.	N.S.	E.W.	N.S.	Pre tr.	E.W.	N.S.	E.W.	N.S.	Pre tr.	E.W.	N.S.	E.W.	N.S.			
	h m	s	μ	μ	μ	μ	s	μ	μ	μ	μ	s	μ	μ	μ			Km	
March	25	4.3	—	—	4	3	3.1	—	—	22	20	5.1	—	—	6	4	16	10.7	
	40	4.0	—	—	2	2	4.1	—	—	10	11	3.2	—	—	5	4	17	21.3	
	12 47	6.2	—	—	2	2	3.3	—	—	10	10	4.2	—	—	4	2	18	16.7	
	52	2.4	− 2	1	9	11	4.8	—	—	10	15	2.5	—	—	8	5	19	16.0	
	13 02	2.9	—		10	5	4.8	—	—	10	14	3.3	—	—	6	5	20	19.6	
	37	4.0	− 6	5	17	12	3.2	25	15	217	225	4.4	—	—	30	38	21	15.3	
	42	2.2	—		2	2	5.0	—	—	2	2	2.9	—	—	2	2	22	15.0	
	47	3.4	—		2	2	—	—	—	4	4	—	—	—	2	2	—	—	
	15 26	3.2	—		2	2	4.2	—	—	5	3	3.0	—	—	2	4	23	17.5	
	34	3.2	—		9	6	4.0	—	—	28	25	3.8	—	—	3	4	24	16.2	
	49	4.4	—		4	3	3.0	—	—	12	6	—	—	—	—	—	—	—	
	56	—	—		—	—	3.5	—	—	15	21	—	—	—	—	—	—	—	
	16 06	3.2	− 3	4	24	42	3.6	+ 8	−12	125	185	—	—	—	—	—	—	—	
	19	3.9			5	2	3.4	—	—	12	11	—	—	—	—	—	—	—	
	18 20	4.9			2	2	3.3	—	—	24	17	4.0	—	—	2	2	25	21.6	
	32	5.1	− 1	1	8	5	2.8	—	—	11	15	3.9	—	—	12	—	26	12.5	
	20 23	6.4	—		5	5	3.7	—	—	47	25	5.8	—	—	12	—	27	30.6	
	31	6.1	—		5	3	—	—	—	—	—	6.0	—	—	3	—	—	—	
	34	6.7	—		10	7	3.1	—	—	77	46	4.7	4	− 1	23	35	28	14.2	
	22 27	3.0	—		3	3	—	—	—	—	—	3.6	—	—	4	3	—	—	
	23 12	—	—		2	2	—	—	—	—	—	—	—	—	—	—	—	—	
	24	3.8	—		3	2	—	—	—	—	—	—	—	—	—	—	—	—	
	27	3.4	− 2	2	10	6	4.1	—	—	10	15	3.0	—	—	5	5	29	18.1	
	33	3.6	—	—	4	3	—	—	—	—	—	—	—	—	—	—	—	—	
14	0 11	—	—	—	3	1	3.3	—	—	7	4	—	—	—	—	—	—	—	
	30	3.2	—	—	2	1	—	—	—	4	4	—	—	—	—	—	—	—	
	47	3.5	—	—	3	2	3.7	—	—	4	4	3.7	—	—	4	4	30	10.4	
	1 11	—	—	—	3	3	3.0	—	—	17	20	3.4	—	—	2	1	—	—	
	18	3.8	—	—	2	2	—	—	—	—	—	3.5	—	—	2	2	—	—	
	58	3.1	—	—	3	3	3.7	—	—	17	14	3.6	—	—	4	3	31	12.3	
	2 06	3.4	—	—	4	3	4.0	—	—	5	4	3.3	—	—	3	2	32	18.1	
	14	3.5	—	—	2	1	3.8	—	—	17	11	3.6	—	—	5	3	33	17.6	
	3 22	—	—	—	2	2	3.8	—	—	5	5	—	—	—	2	2	—	—	
	53	4.1	—	—	3	3	3.2	—	—	10	10	3.8	—	—	3	3	34	17.6	
	57	3.4	—	—	6	4	3.8	—	—	18	14	3.6	—	—	5	3	35	17.0	

	5 57	4.3	− 2	− 1	8	4	3.1	—	—	15	26	3.0	—	—	11	17	36	14.0
	39	4.2	—	—	3	2	3.0	—	—	6	6	3.5	—	—	4	4	37	15.9
	6 46	4.2	− 5	3	6	6	3.0	10	− 6	27	30	3.2	—	—	21	16	38	14.2
	58	4.8	—	—	2	2	3.0	—	—	36	17	3.6	—	—	2	2	39	17.3
	7 35	—	—	—	3	2	3.2	—	—	8	7	3.5	—	—	2	2	—	—
	51	3.8	—	—	3	3	3.4	—	—	10	11	3.6	—	—	2	3	40	17.0
	53	3.9	—	—	4	3	3.3	—	—	18	16	3.5	—	—	3	3	41	16.6
	8 35	—	—	—	—	—	—	—	—	—	—	3.6	—	—	3	5	—	—
	10 34	—	—	—	—	—	3.1	—	—	19	30	4.1	—	—	1	2	—	—
	44	5.1	—	—	25	24	3.3	—	—	76	110	4.1	− 6	− 2	12	29	42	10.0
	11 20	4.1	—	—	5	5	3.0	—	—	9	18	3.6	—	—	5	3	43	15.6
	12 30	—	—	—	—	—	2.6	—	—	22	23	4.3	—	—	3	2	—	—
	49	4.1	−15	5	33	37	3.1	25	−20	610	455	3.4	0	15	48	127	44	16.0
	13 21	4.7	—	—	7	4	3.7	—	—	30	21	3.6	—	—	11	10	45	19.2
	14 02	4.3	—	—	3	4	3.1	—	—	5	5	4.2	—	—	3	2	46	18.0
	16	4.7	—	—	10	5	2.6	—	—	25	37	3.9	—	—	26	17	47	15.9
	18 42	3.0	− 1	1	4	3	4.1	—	—	12	11	3.4	—	—	2	1	48	16.0
	19 13	3.0	—	—	8	5	4.1	—	—	19	16	3.3	—	—	3	3	49	16.0
	33	4.8	− 3	2	6	4	3.2	—	—	10	7	3.0	—	—	3	3	50	13.3
	54	3.1	− 3	2	4	3	4.1	—	—	12	11	3.7	—	—	6	8	51	16.4
	20 12	4.4	− 2	− 1	10	5	3.7	—	—	10	7	3.9	—	—	4	6	52	22.5
	22 13	4.1	—	—	3	3	3.2	—	—	12	10	3.6	—	—	5	5	53	17.3
	13	—	—	—	5	5	—	—	—	—	—	3.7	—	—	12	18	—	—
	29	3.2	—	—	2	2	—	—	—	—	—	3.4	—	—	3	2	—	—
	30	—	—	—	2	2	—	—	—	—	—	—	—	—	—	—	—	—
	23 08	—	—	—	2	1	—	—	—	—	—	5.5	2	2	17	7	—	—
	25	—	—	—	3	3	—	—	—	—	—	—	—	—	2	2	—	—
	25	3.5	—	—	7	5	—	—	—	—	—	3.8	—	—	3	4	—	—
15	3 02	—	—	—	2	1	3.2	—	—	6	5	3.0	—	—	3	3	—	—
	08	4.0	—	—	3	2	3.2	—	—	12	10	3.8	—	—	7	4	54	17.0
	37	—	—	—	6	4	3.3	—	—	20	13	—	—	—	—	—	—	—
	4 28	4.2	—	—	2	2	3.2	—	—	7	5	4.0	—	—	3	2	—	—
	34	5.3	—	—	3	2	2.6	—	—	15	12	4.3	—	—	4	2	55	18.4
	6 52	—	—	—	2	2	4.0	—	—	11	7	4.2	—	—	2	1	—	—
	55	—	—	—	6	5	3.3	—	—	27	—	3.7	—	—	4	3	—	—
	7 08	3.6	—	—	6	6	3.7	—	—	25	18	4.4	—	—	2	5	56	14.6
	10 23	3.1	− 2	2	9	7	4.1	—	—	7	10	3.3	—	—	4	12	57	16.8
	12 05	6.1	—	—	3	3	3.0	—	—	18	17	4.2	—	—	6	7	53	18.2
	13 04	3.7	—	—	2	2	—	—	—	—	—	3.8	—	—	2	3	—	—
	13 40	3.4	− 4	2	22	20	3.4	7	− 5	82	20	3.3	—	—	13	30	59	12.0
	46	3.2	—	—	8	6	3.9	—	—	13	11	3.8	—	—	6	7	60	15.5
	142 4	3.9	—	—	8	6	3.0	—	—	14	21	3.2	—	—	12	22	61	13.4

日時 Time of Accurrence		舞鶴 (Maiduru)					城崎 (Kinosaki)					伊根 (Ine)					震央 Epi-centre	震原の深さ Depth Focal	摘要 Remark
		初微	初動 Init.		最大動 Max. 2A		初微	初動 Init.		最大動 Max. 2A		初微	初動 Init.		最大動 Max. 2A				
		Pre tr.	E.W.	N.S.	E.W.	N.S.	Pre. tr.	E.W.	N.S.	E.W.	N.S.	Pre. tr.	E.W.	N.S.	E.W.	N.S.			
	h m	s	s	μ	μ	μ	s	μ	μ	μ	μ	s	μ	μ	μ	μ		km	
	25	—	—	—	3	2	—	—	—	—	—	—	—	—	3	2	—	—	
	16 12	3.8	—	—	4	3	3.2	—	—	20	37	3.3	—	—	3	3	62	15.0	
	20	3.6	—	—	10	8	3.3	—	—	18	15	4.1	—	—	7	8	63	12.8	
	20	3.4	—	—	5	5	4.0	—	—	28	10	4.2	—	—	17	15	64	16.5	
	39	3.4	—	—	7	5	3.8	—	—	24	11	3.8	—	—	10	15	65	16.7	
	44	3.0	− 2	2	6	6	4.2	—	—	18	15	3.6	—	—	8	8	66	16.6	
	55	3.2	—	—	2	2	4.2	—	—	7	5	3.7	—	—	4	7	67	18.2	
	20 34	3.8	—	—	6	5	3.6	—	—	13	12	3.7	—	—	3	2	68	18.5	
	21 20	4.9	—	—	3	3	2.4	—	—	22	15	3.6	—	—	10	6	69	12.5	
	22 49	4.0	—	—	5	4	—	—	—	7	15	3.8	—	—	10	8	—	—	
	23 32	5.9	—	—	3	2	2.7	—	—	7	12	4.9	—	—	7	7	70	21.3	
16	2 24	—	—	—	1	1	—	—	—	5	4	3.8	—	—	3	2	—	—	
	3 22	3.5	—	—	9	6	3.4	—	—	7	4	3.4	—	—	5	3	71	14.5	
	4 34	—	—	—	3	2	—	—	—	7	5	3.5	—	—	4	2	—	—	
	6 36	4.4	—	—	3	2	2.8	—	—	31	18	3.8	—	—	5	5	72	16.2	
	8 57	3.8	—	—	4	2	3.3	—	—	10	8	—	—	—	—	—	—	—	
	9 31	3.5	—	—	3	2	3.8	—	—	13	13	3.4	—	—	5	5	73	17.7	
	10 36	4.0	—	—	4	3	—	—	—	5	5	—	—	—	—	—	—	—	
	51	2.4	−13	3	39	60	4.5	8	4	41	48	3.3	—	—	37	40	74	13.6	
	11 05	2.3	− 6	5	22	25	4.6	—	—	12	20	2.9	—	—	18	15	75	13.0	
	21	3.6	− 1	2	3	3	3.7	—	—	10	12	3.5	—	—	2	5	76	17.7	
	12 01	3.2	—	—	13	8	4.0	—	—	11	13	4.3	—	—	5	6	77	12.9	
	31	4.3	—	—	5	5	3.1	—	—	—	11	3.6	—	—	3	3	78	17.7	
	13 39	4.2	—	—	4	4	3.3	—	—	6	5	3.4	—	—	3	3	79	16.6	
	16 04	6.3	1	− 2	5	5	2.9	—	—	103	55	4.0	—	—	12	10	80	0	
	51	3.6	—	—	—	—	4.0	—	—	5	5	4.0	—	—	6	6	81	19.7	
	17 05	3.6	—	—	11	9	3.5	—	—	15	19	3.8	—	—	10	10	82	16.0	
	12	3.8	− 5	2	36	16	3.2	—	—	28	28	3.3	− 5	4	12	12	83	15.0	
	36	3.6	—	—	—	—	—	—	—	8	8	3.2	—	—	7	10	—	—	
	55	5.9	− 5	2	6	4	2.9	—	—	34	25	3.8	− 3	1	20	59	84	9.5	
	21 25	—	—	—	—	—	3.3	—	—	11	8	4.3	—	—	2	3	—	—	
	23 55	2.8	—	—	3	2	4.0	—	—	12	15	3.6	—	—	3	4	85	13.6	
17	0 09	—	—	—	3	3	—	—	—	—	—	2.8	—	—	3	8	—	—	
	1 29	3.1	− 2	2	10	8	3.8	—	—	10	20	3.9	—	—	5	7	86	13.0	
	2 05	4.4	—	—	2	2	2.7	—	—	3	4	3.8	—	—	2	1	87	15.5	

		32	4.0	—	—	4	3	3.0	—	—	21	12	3.8	—	—	12	20	88	15.1
	3	27	4.0	—	—	2	1	2.8	—	—	3	3	3.6	—	—	2	2	89	13.7
	4	15	4.4	—	—	5	5	3.2	—	—	32	35	4.3	—	—	4	12	90	13.2
	5	53	3.6	−2	1	93	39	3.5	+16	−6	72	50	3.3	−11	−7	20	15	91	16.0
	6	18	3.6	—	—	5	5	3.5	—	—	7	7	3.4	—	—	2	3	92	16.1
		37	—	—	—	2	2	—	—	—	5	6	3.2	—	—	2	2	—	—
		51	6.3	—	—	2	2	6.2	—	—	5	4	5.6	—	—	7	3	93	44.0
		52	4.5	—	—	5	6	3.0	—	—	22	15	3.4	—	—	12	5	93′	16.0
	7	40	5.7	−2	—	5	6	2.9	—	—	46	90	3.7	—	—	7	28	94	11.9
		40	4.9	—	—	3	3	2.6	—	—	45	70	5.0	—	—	2	3	95	15.5
	8	38	—	—	—	2	2	—	—	—	—	—	4.5	—	—	3	3	—	—
	14	14	3.8	−2	2	7	5	3.7	—	—	5	12	4.2	—	—	8	12	96	18.3
		39	2.7	—	—	10	9	4.2	—	—	9	11	3.2	—	—	3	5	97	14.1
	17	01	3.5	—	—	10	5	—	—	—	—	—	—	—	—	—	—	—	—
		21	6.7	—	—	2	2	4.5	—	—	12	5	5.7	—	—	2	2	98	36.0
		22	—	—	—	2	1	3.2	—	—	7	4	5.4	—	—	8	5	—	—
		23	5.3	—	—	3	2	3.7	—	—	17	11	5.3	—	—	6	4	99	26.9
		52	3.2	−2	2	10	10	3.9	—	—	8	8	3.3	—	—	9	12	100	16.0
	20	06	5.3	—	—	3	2	—	—	—	—	—	—	—	—	3	3	—	—
	21	45	2.6	—	—	6	3	5.5	—	—	4	3	3.3	—	—	2	2	101	19.8
	22	40	3.4	—	—	10	4	3.3	—	—	12	12	3.6	—	—	8	5	102	12.6
	23	41	3.9	−2	1	10	5	3.1	—	—	14	16	3.6	—	—	5	6	103	15.3
18	0	08	3 3	—	—	3	3	3.9	—	—	18	12	3.0	—	—	5	7	104	16.1
	2	42	4.5	−6	2	40	26	2.8	14	−6	42	37	3.5	−9	−7	29	23	105	15.2
	3	06	3.3	−5	2	29	19	3.8	4	−1	14	12	3.4	—	—	11	20	106	16.2
		44	5.0	—	—	2	2	2.9	—	—	9	9	3.9	—	—	3	5	107	18.3
		50	3.5	—	—	3	2	3.3	—	—	8	6	3.2	—	—	3	3	108	13.5
	4	52	3.1	−2	1	2	2	3.8	—	—	9	21	3.7	—	—	5	6	109	14.0
	6	16	3.4	—	—	10	10	3.9	—	—	10	15	3.1	—	—	3	2	110	17.5
		34	—	—	—	5	5	—	—	—	10	8	3.4	—	—	5	7	—	—
	9	29	3.1	−2	2	13	14	3.7	—	—	3	4	3.5	—	—	5	7	111	13.3
		47	2.6	—	—	3	3	—	—	—	—	—	6.0	—	—	10	5	—	—
	13	35	3.4	—	—	4	3	4.4	—	—	6	5	4.0	—	—	12	15	112	20.8
	14	40	3.9	—	—	5	3	3.4	—	—	6	6	3.7	—	—	16	16	113	17.8
	15	13	4.0	−5	−3	9	9	—	—	—	—	—	3.5	—	—	10	8	—	—
		17	3.8	—	—	2	2	—	—	—	—	—	3.6	—	—	3	2	—	—
		50	2.9	—	—	4	4	—	—	—	—	—	3.2	—	—	2	1	—	—
	17	29	4.0	−3	−2	5	5	—	—	—	—	—	5.0	—	—	4	2	—	—
	18	42	3.8	−1	—	10	7	—	—	—	—	—	3.6	—	—	9	3	—	—
	21	45	2.8	−1	—	3	2	—	—	—	3	3	3.4	—	—	3	2	—	—
		47	3.1	−39	13	395	27?	4.2	+79	−33	370	430	3.7	—	—	390	420	114	17.0
	22	32	—	—	—	3	2	3.0	—	—	5	6	—	—	—	2	1	—	—

日時 Time of Accurrence		舞鶴 (Maiduru)					城崎 (Kinosaki)					伊根 (Ine)					震央 Epi-centre	震原の深さ Focal Depth	摘要 Remark
		初	初動 Init.		最大動 Max. 2A		初微	初動 Init.		最大動 Max. 2A		初微	初動 Init.		最大動 Max. 2A				
		Pre. tr.	E.W.	N.S.	E.W.	N.S.	Pre. tr.	E.W.	N.S.	E.W.	N.S.	Pre. tr.	E.W.	N.S.	E.W.	N.S.			
	h m	s	s	μ	μ	μ	s	μ	μ	μ	μ	s	μ	μ	μ	μ		km	
	55	—	—	—	—	—	—	—	—	4	4	3.0	—	—	2	2	—	—	
	23 43	4.5	—	—	4	3	3.2	—	19	—	—	3.3	—	—	12	11	115	17.0	
19	1 51	—	—	—	2	2	—	—	—	—	—	3.2	—	—	3	2	—	—	
	2 12	4.2	—	—	2	2	—	—	—	—	—	3.7	—	—	2	2	—	—	
	3 55	—	—	—	3	2	—	—	—	—	—	—	—	—	3	3	—	—	
	4 .00	8.0	—	—	5	4	2.0	—	—	13	—	6.3	—	—	6	4	116	0	
	35	3.0	—	—	5	3	4.7	—	—	48	—	3.7	—	—	2	3	117	19.4	
	5 17	3.6	− 5	− 2	31	36	3.6	− 8	—	108	—	3.3	− 7	3	12	17	118	16.7	
	6 08	2.8	—	—	5	4	—	—	—	—	—	3.0	—	—	2	2	—	—	
	28	3.2	—	—	95	123	4.6	—	—	30	—	2.9	− 3	2	34	67	119	19.2	
	30	—	—	—	3	3	—	—	—	—	—	—	—	—	—	—	—	—	
	34	—	—	—	2	2	4.0	—	—	5	—	4.4	—	—	5	7	—	—	
	8 10	3.1	—	—	24	15	4.5	—	—	7	11	3.4	—	—	10	12	120	19.2	
	12 51	3.8	—	—	3	2	3.6	—	—	29	20	4.2	—	—	13	22	121	17.5	
	15 50	7.4	− 2	2	11	9	3.8	—	—	105	60	5.7	—	—	12	10	122	25.5	
	18 09	—	—	—	7	5	—	—	—	—	—	—	—	—	—	—	—	—	
	22	—	—	—	3	3	—	—	—	—	—	—	—	—	—	—	—	—	
	19 00	4.4	—	—	7	5	3.4	—	—	35	33	3.1	—	—	9	13	123	16.8	
	54	4.8	− 2	1	11	7	2.9	—	—	17	32	3.2	—	—	25	12	124	13.0	
	55	7.2	—	—	5	3	3.3	—	—	23	27	5.0	—	—	16	9	125	10.2	
	22 24	—	—	—	3	3	—	—	—	—	—	—	—	—	2	2	—	—	
20	2 36	4.2	− 3	1	4	3	3.0	—	—	21	16	3.4	—	—	7	15	126	15.5	
	3 20	3.3	—	—	5	4	3.8	—	—	16	12	4.1	—	—	3	5	127	14.2	
	4 46	—	—	—	2	2	—	—	—	4	3	3.3	—	—	2	2	—	—	
	9 52	3.9	− 2	1	5	3	3.4	5	− 2	17	30	4.3	—	—	10	13	128	16.2	
	10 54	4.2	—	—	8	7	3.4	16	−15	100	41	2.8	—	—	123	25	129	14.6	
	54	4.2	—	—	4	3	3.4	—	—	—	—	2.8	—	—	5	3	130	14.6	
	11 27	4.9	—	—	3	3	3.3	—	—	52	53	3.8	—	—	10	10	131	20.5	
	13 45	6.6	—	—	3	3	3.6	—	—	10	6	4.2	—	—	5	3	132	10.0	
	14 12	6.8	− 2	3	32	62	3.3	− 4	− 5	500	370	4.4	− 9	2	97	205	133	0	
	15 03	3.7	− 2	1	11	10	3.7	—	—	8	6	3.8	—	—	—	—	134	13.0	
	22 45	4.0	− 3	2	13	8	3.1	—	—	46	47	3.3	—	—	8	17	135	15.0	
	45	3.8	—	—	10	8	3.2	—	—	14	21	3.4	—	—	8	13	136	15.2	
	47	3.7	− 3	2	17	10	3.6	7	− 2	12	29	3.1	—	—	15	20	137	16.6	
	23 41	4.0	—	—	5	3	—	—	—	—	—	—	—	—	—	—	—	—	

21	0 11	5.1	—	—	11	5	3.7	4	0	48	103	4.0	—	—	3	2	138	24.0
	1 52	2.6	—	—	4	4	4.5	—	—	5	3	—	—	—	—	—	—	—
	2 16	3.2	−1	1	4	3	3.9	—	—	10	12	—	—	—	2	2	—	—
	2 42	8.3	—	—	21	15	5.0	—	—	17	50	6.3	—	—	11	18	139	30.0
	54	3.5	—	—	3	2	3.5	—	—	12	18	3.1	—	—	6	7	140	15.0
	3 54	4.0	—	—	3	2	3.2	—	—	12	7	—	—	—	—	—	—	—
	11 06	3.5	—	—	3	3	—	—	—	—	—	—	—	—	—	—	—	—
	49	3.7	−2	1	6	4	3.4	6	−3	7	8	3.0	—	—	12	14	141	14.8
	14 12	3.7	−2	1	4	3	—	—	—	—	—	—	—	—	—	—	—	—
	16 37	—	—	—	3	2	—	—	—	—	—	—	—	—	—	—	—	—
	39	3.2	—	—	6	5	—	—	—	—	—	—	—	—	—	—	—	—
	17 45	3.4	—	—	4	5	—	—	—	—	—	—	—	—	—	—	—	—
	18 00	2.6	—	—	2	2	—	—	—	—	—	—	—	—	—	—	—	—
	19 01	—	—	—	4	3	2.6	—	—	16	10	—	—	—	—	—	—	—
	22 21	5.3	—	—	2	2	2.7	—	—	25	8	4.3	—	—	7	3	142	18.9
22	0 46	4.5	—	—	3	3	3.4	—	—	15	7	4.1	—	—	3	5	143	21.4
	2 17	6.7	—	—	3	2	2.0	—	—	11	24	4.9	—	—	3	6	144	0
	3 16	6.5	—	—	5	6	3.3	—	—	83	203	4.8	—	—	11	18	145	21.2
	5 16	2.3	—	—	8	8	4.3	—	—	7	14	3.0	—	—	10	13	146	11.4
	6 54	5.0	—	—	3	3	3.3	—	—	40	12	3.7	—	—	5	4	147	19,8
	8 18	2.9	—	—	9	4	—	—	—	—	—	3.3	—	—	4	3	—	—
	12 57	3.7	−26	9	94	63	3.3	55	−28	240	115	3.2	−10	−3	93	188	148	15.0
	57	3.7	—	—	27	27	—	—	—	—	—	—	—	—	—	—	—	—
	15 18	3.6	—	2	11	9	3.7	8	−4	12	12	4.2	—	—	7	7	149	16.0
	16 58	3.5	—	—	7	4	3.8	—	—	10	11	3.5	—	—	3	3	—	—
	18 10	—	—	—	6	4	—	—	—	8	7	—	—	—	—	—	—	—
	19 27	—	—	—	5	2	—	—	—	—	—	3.6	—	—	5	7	—	—
	20 55	3.7	—	—	3	3	3.5	—	—	8	6	2.7	—	—	3	5	150	14.0
	23 13	—	—	—	5	4	3.3	—	—	—	—	3.5	—	—	3	2	—	—
23	1 29	2.3	—	—	10	5	3.8	—	—	6	8	3.7	—	—	7	7	151	0
	4 48	3.8	—	—	10	7	3.2	—	—	12	15	3.4	—	—	5	10	152	15.2
	5 55	5.3	—	—	3	2	3.0	—	—	—	—	4.9	—	—	2	2	153	22.0
	12 30	4.9	—	—	9	11	—	—	—	—	—	—	—	—	—	—	—	—
	18 19	2.5	—	—	3	2	—	—	—	—	—	2.8	—	—	5	7	—	—
	52	—	—	—	3	2	—	—	—	—	—	2.8	—	—	2	2	—	—
	52	2.5	—	—	23	38	4.4	—	—	60	60	3.1	—	—	12	7	154	13.9
	19 03	3.7	—	—	11	9	—	—	—	—	—	3.5	—	—	8	7	—	—
	20 44	3.8	—	—	2	2	—	—	—	—	—	—	—	—	—	—	—	—
	21 58	4.1	−3	2	7	5	2.7	—	—	18	20	4.3	—	—	10	13	155	15.8
	22 50	3.7	5	−2	40	50	3.5	8	2	27	35	2.8	−17	−12	70	117	156	14.6
24	1 56	3.2	−3	1	12	11	3.7	—	—	10	12	3.4	—	—	7	10	157	14.6
	6 40	4.0	—	—	2	2	3.2	—	—	10	10	3.6	—	—	3	2	158	16.8

日時 Time of Accurrence		舞鶴 (Maiduru)					城崎 (Kinosaki)					伊根 (Ine)					震央 Epi-centre	震源の深さ Focal Depth	摘要 Remark
		初微	初動 Init.		最大動 Max. 2A		初微	初動 Init.		最大動 Max. 2A		初微	初動 Init.		最大動 Max. 2A				
		Pre. tr.	E.W.	N.S.	E.W.	N.S.	Pre. tr.	E.W.	N.S.	E.W.	N.S.	Pre. tr.	E.W.	N.S.	E.W.	N.S.			
	h m	s	μ	μ	μ	μ	μ	μ	μ	μ	μ	s	μ	μ	μ	μ		km	
	8 41	3.5	−10	5	140	47	3.8	—	—	29	21	3.2	—	—	30	57	159	17.3	
	56	2.2	—	—	8	11	5.7	—	—	12	20	2.8	—	—	4	3	160	14.7	
	10 18	3.3	− 2	1	24	11	3.7	—	—	10	12	3.4	—	—	5	7	161	15.4	
	33	3.2	—	—	7	5	3.7	—	—	7	5	3.4	—	—	10	8	162	14.5	
	17 39	3.0	− 2	2	5	5	3.9	—	—	10	30	3.5	—	—	5	3	163	14.3	
25	0 08	—	—	—	—		3.8	—	—	3	5	4.0	—	—	2	2	—	—	
	34	5.5	—	—	30	25	2.9	21	5	65	150	4.2	−15	3	52	90	164	19.5	
	4 14	3.9	—	—	5	3	3.6	—	—	10	5	3.0	—	—	10	12	165	17.0	
	9 17	4.4	—	—	3	2	2.8	—	—	8	7	4.2	—	—	2	2	166	16.2	
	10 39	3.7	—	—	5	3	—	—	—	—	—	3.2	—	—	5	5	—	—	
	13 36	4.2	—	—	13	7	2.8	—	—	22	15	3.5	—	—	5	5	167	14.3	
	14 16	5.6	—	—	3	2	2.1	—	—	7	5	4.3	—	—	11	7	168	13.9	
	17 40	3.2	− 2	1	19	16	4.0	5	− 2	13	11	3.1	—	—	14	11	169	16.3	
	19 13	4.4	—	—	35	31	2.7	35	−15	365	110	3.4	6	0	133	82	170	13.7	
	41	8.4	—	—	3	3	3.9	—	—	24	11	6.1	—	—	3	2	171	5.0	
	43	4.0	—	—	4	3	4.3	—	—	27	13	3.9	—	—	3	4	172	24.3	
	23 33	3.5	—	—	10	4	4.0	—	—	8	5	4.3	—	—	3	3	173	17.8	
26	7 56	3.0	—	—	3	2	—	—	—	—	—	3.2	—	—	2	2	—	—	
	13 00	3.0	—	—	3	3	4.2	—	—	11	7	3.3	—	—	6	6	174	16.7	
	18 41	3.2	—	—	5	5	—	—	—	—	—	—	—	—	—	—	—	—	
	23 16	3.9	—	—	5	5	—	—	—	—	—	3.4	—	—	2	2	—	—	
27	0 24	—	—	—	3	3	—	—	—	—	—	3.2	—	—	3	4	—	—	
	1 21	6.1	—	—	3	2	3.2	—	—	15	10	3.6	—	—	5	8	175	0	
	3 21	4.0	—	—	2	1	3.0	—	—	26	20	3.5	—	—	7	10	176	11.0	
	4 03	2.9	—	—	5	6	4.9	—	—	15	12	3.0	—	—	4	5	177	19.0	
	7 41	—	—	—	11	9	—	—	—	—	—	3.2	—	—	5	8	—	—	
	19 54	4.1	—	—	2	2	3.2	—	—	9	5	4.2	—	—	2	2	179	17.3	
	22 56	—	—	—	2	2	—	—	—	—	—	—	—	—	—	—	—	—	
28	7 07	3.6	—	—	2	2	—	—	—	—	—	3.8	—	—	2	2	—	—	
	8 53	7.5	—	—	3	2	2.0	—	—	12	14	6.0	—	—	8	9	178	7.8	
	12 00	3.4	—	—	4	3	3.6	—	—	17	25	—	—	—	—	—	—	—	
	13 42	7.0	—	—	2	2	—	—	—	—	—	—	—	—	—	—	—	—	
	14 02	2.9	− 2	2	7	7	—	—	—	—	—	3.5	—	—	5	9	—	—	
29	0 52	4.0	− 2	+ 1	13	10	3.3	5	3	9	17	3.9	—	—	7	17	180	17.8	
	5 06	5.1	—	—	17	7	2.6	42	15	95	200	3.9	− 9	2	—	—	181	16.2	

	8 15	—	—	—	2	1	—	—	—	—	—	—	—	—	—	—	—	—	
	13 21	—	—	—	—	—	1.5	—	—	14	10	4.4	—	—	2	3	182	8.0	
	22 02	3.8	—	—	5	3	3.1	—	—	37	34	3.6	—	—	2	3	183	14.9	
30	2 18	5.3	—	—	3	3	3.3	—	—	17	10	3.8	—	—	2	3	184	19.6	
	4 23	5.1	—	—	4	3	2.8	—	—	11	27	5.7	—	—	3	5	185	10.4	
	11 06	—	—	—	2	1	2.3	—	—	10	15	—	—	—	—	—	—	—	
	36	—	—	—	8	6	2.4	—	—	7	12	—	—	—	—	—	—	—	
	16 23	4.2	—	—	5	3	3.3	—	—	12	12	4.4	—	—	6	11	186	18.2	
	22 30	3.0	−11	3	186	155	5.3	40	−17	210	275	3.1	18	16	232	150	187	21.3	
	39	2.4	—	—	3	3	5.3	—	—	3	3	3.2	—	—	—	—	188	18.0	
	39	2.4	—	—	5	5	5.3	—	—	3	2	3.2	—	—	—	—	189	18.0	
	41	2.3	−5	3	7	10	5.8	—	—	5	3	3.2	—	—	3	2	190	18.8	
	45	2.4	—	—	2	2	—	—	—	—	—	—	—	—	—	—	—	—	
	50	2.4	—	—	3	3	—	—	—	—	—	—	—	—	—	—	—	—	
	52	1.8	−1	1	3	3	—	—	—	—	—	—	—	—	—	—	191	—	
	57	2.3	−12	3	34	58	6.0	8	−4	17	15	3.3	2	2	20	12	192	18.9	(Epicentre: Maiduru)
	23 01	2.2	—	—	2	2	—	—	—	—	—	—	—	—	—	—	—	—	
	18	2.1	−1	1	3	5	6.0	—	—	5	3	3.3	—	—	3	2	193	17.4	
	47	2.4	−2	2	3	3		—	—	—	—	—	—	—	—	—	—	—	
	48	2.7	—	—	2	2		—	—	—	—	—	—	—	—	—	—	—	
	48	2.8	—	—	5	5	—	—	—	—	—	3.4	—	—	5	5	—	—	
	49	2.2	−1	1	5	4	—	—	—	—	—	—	—	—	—	—	—	—	
	52	2.4	−5	2	5	3	—	—	—	—	—	—	—	—	—	—	—	—	
	58	—	—	—	2	1	—	—	—	—	—	—	—	—	—	—	—	—	
31	0 53	2.7	—	—	10	3	5.3	—	—	3	3	3.6	—	—	6	7	194	20.4	
	1 00	3.3	—	—	3	2	—	—	—	—	—	—	—	—	—	—	—	—	
	1 16	3.0	—	—	1	1	—	—	—	—	—	—	—	—	—	—	—	—	
	3 35	5.3	−4	1	14	13	2.3	8	2	43	74	5.2	—	—	28	22	195	14.7	
	7 12	2.5	−2	1	5	3	—	—	—	—	—	—	—	—	—	—	—	—	
	33	3.0	−2	1	7	5	—	—	—	—	—	—	—	—	—	—	—	—	
	9 09	4.5	−2	1	6	3	3.8	—	—	18	15	3.5	—	—	7	15	196	21.8	
	13	7.5	—	—	4	4	2.8	—	—	12	22	6.3	—	—	10	—	197	22.6	
	11 44	7.7	—	—	6	6	4.0	—	—	47	23	6.5	—	—	5	6	198	31.8	
	12 14	4.4	—	—	5	3	3.5	—	—	10	21	3.5	—	—	5	5	199	19.9	
	14 53	—	—	—	2	2	—	—	—	—	—	—	—	—	—	—	—	—	
	16 35	—	—	—	1	1	—	—	—	—	—	—	—	—	—	—	—	—	
	19 13	3.4	4	−2	5	4	3.8	—	—	3	4	3.8	—	—	2	2	200	16.7	Strongest after-shock. First S motion threw the pointers out of the smoked paper.
April 1	2 56	3.1	—	—	12	3	4.2	—	—	4	15	3.8	—	—	5	3	201	16.6	
	4 40	3.6	—	—	6	5	4.1	—	—	10	8	3.7	—	—	3	4	202	20.4	
	6 07	2.6	−15	6	>100	>100	4.8	32	−20	>1000	>1000	3.6	12	27	>1000	>1000	203	17.9	
	10	2.0	—	—	25	—	5.2	—	—	—	—	—	—	—	—	5	—	—	
	10	1.8	—	—	16	—	—	—	—	—	—	—	—	—	—	5	—	—	

日時 Time of Occurrence		舞鶴 (Maiduru)					城崎 (Kinosaki)					伊根 (Ine)					震央 Epi-centre	震原の深さ Focal Depth	摘要 Remark
		初微	初動 Init. Mot.		最大動 Max. 2A		初微	初動 Init. Mot.		最大動 Max. 2A		初微	初動 Init. Mot.		最大動 Max. 2A				
		Pre. tr.	E.W.	N.S.	E.W.	N.S.	Pre. tr.	E.W.	N.S.	E.W.	N.S.	Pre. tr.	E.W.	N.S.	E.W.	N.S.			
	h m	s	μ	μ	μ	μ	s	μ	μ	μ	μ	s	μ	μ	μ	μ		km	
April	10	—	—	—	2	3	—	—	—	—	—	—	—	—	—	—	—	—	
	11	2.0	—	—	10	7	—	—	—	—	—	—	—	—	—	—	—	—	
	12	1.4	—	—	20	22	—	—	—	—	—	—	—	—	—	—	—	—	
	12	—	—	—	35	21	5.9	—	—	21	18	3.6	—	—	—	7	—	—	
	13	2.3	− 6	2	15	12	—	—	—	8	10	—	—	—	—	3	—	—	
	13	2.0	—	—	5	5	—	—	—	—	—	—	—	—	—	—	—	—	
	14	2.4	− 6	4	25	20	—	—	—	—	—	—	—	—	—	—	—	—	
	16	2.0	—	—	4	—	—	—	—	—	—	—	—	—	—	—	—	—	
	16	1.8	—	—	4	—	—	—	—	—	—	—	—	—	—	—	—	—	
	17	2.2	—	—	4	3	—	—	—	—	—	—	—	—	—	—	—	—	
	18	2.0	—	—	7	5	—	—	—	—	—	—	—	—	—	—	—	—	
	18	1.8	—	—	4	3	—	—	—	—	—	—	—	—	—	—	—	—	
	20	2.2	—	—	8	3	—	—	—	—	—	—	—	—	—	—	—	—	
	21	2.0	—	—	2	1	—	—	—	—	—	—	—	—	—	—	—	—	
	21	—	—	—	?	?	—	—	—	—	—	—	—	—	—	—	—	—	
	22	2.5	− 5	4	16	16	—	—	—	—	—	3.0	—	—	—	10	—	—	
	23	2.5	—	—	7	5	—	—	—	—	—	—	—	—	—	—	—	—	
	25	2.4	—	3	15	16	—	—	—	—	—	—	—	—	—	—	—	—	
	29	2.6	− 3	2	12	14	—	—	—	—	—	3.2	—	—	—	6	—	—	
	29	2.7	−10	4	19	28	—	—	—	—	—	3.0	—	—	—	7	—	—	
	29	2.3	—	—	2	1	—	—	—	—	—	—	—	—	—	—	—	—	
	31	2.4	− 5	2	18	12	—	—	—	—	—	3.2	—	—	—	11	—	—	
	31	2.3	—	—	6	4	—	—	—	—	—	—	—	—	—	—	—	—	
	34	2.4	—	—	6	5	—	—	—	—	—	—	—	—	—	—	—	—	
	35	2.3	—	—	3	3	—	—	—	—	—	—	—	—	—	—	—	—	
	36	2.3	—	—	7	6	—	—	—	—	—	—	—	—	—	—	—	—	
	40	2.5	—	—	—	—	—	—	—	—	—	—	—	—	—	—	—	—	
	43	2.4	—	—	2	2	—	—	—	—	—	—	—	—	—	—	—	—	
	44	—	—	—	2	2	—	—	—	—	—	—	—	—	—	—	—	—	
	45	—	—	—	3	3	—	—	—	—	—	—	—	—	—	—	—	—	
	46	—	—	—	3	3	—	—	—	—	—	—	—	—	—	—	—	—	
	47	2.8	—	—	2	2	—	—	—	—	—	—	—	—	—	—	—	—	
	48	2.4	− 3	—	8	5	—	—	—	—	—	—	—	—	—	—	—	—	
	53	2.4	− 5	3	7	5	—	—	—	—	—	—	—	—	—	—	—	—	
	54	2.5	− 2	1	3	3	—	—	—	—	—	—	—	—	—	—	—	—	

55	—	—	—	2	2	—	—	—	—	—	—	—	—	—	—	—	—
56	2.4	—	—	2	2	—	—	—	—	—	—	—	—	—	—	—	—
57	2.5	−4	1	7	5	—	—	—	—	—	—	—	—	—	—	—	—
58	2.4	—	—	2	2	—	—	—	—	—	—	—	—	—	—	—	—
58	—	—	—	2	2	—	—	—	—	—	—	—	—	—	—	—	—
7 01	2.5	—	—	2	2	—	—	—	—	—	—	—	—	—	—	—	—
02	2.6	—	—	4	6	—	—	—	—	—	—	—	—	—	—	—	—
05	2.4	—	—	5	5	—	—	—	—	—	—	—	—	—	—	—	—
05	2.3	—	—	4	4	—	—	—	—	—	—	—	—	—	—	—	—
06	2.2	—	—	3	3	—	—	—	—	—	—	—	—	—	—	—	—
11	2.4	—	—	6	6	—	—	—	—	—	2.9	—	—	—	3	—	—
11	2.5	—	—	6	6	—	—	—	—	—	2.9	—	—	—	5	—	—
13	2.6	−7	5	15	15	—	—	—	—	—	3.2	—	—	—	6	—	—
13	3.0	—	—	3	2	—	—	—	—	—	—	—	—	—	—	—	—
15	2.4	—	—	4	4	—	—	—	—	—	—	—	—	—	—	—	—
16	2.5	—	—	5	3	—	—	—	—	—	—	—	—	—	—	—	—
23	2.5	−3	2	4	3	—	—	—	—	—	—	—	—	—	—	—	—
23	—	—	—	2	1	—	—	—	—	—	—	—	—	—	—	—	—
24	2.4	−5	3	5	5	—	—	—	—	—	3.2	—	—	—	10	—	—
25	—	—	—	5	3	—	—	—	—	—	—	—	—	—	—	—	—
28	2.3	—	—	—	—	—	—	—	—	—	—	—	—	—	—	—	—
29	2.0	—	—	3	—	—	—	—	—	—	—	—	—	—	—	—	—
31	2.5	—	—	3	2	—	—	—	—	—	—	—	—	—	—	—	—
32	2.5	−3	3	24	10	—	—	—	—	—	3.4	—	—	—	10	—	—
39	2.4	—	—	4	4	—	—	—	—	—	—	—	—	—	—	—	—
40	—	—	—	3	2	—	—	—	—	—	—	—	—	—	—	—	—
40	—	—	—	3	2	—	—	—	—	—	—	—	—	—	—	—	—
41	2.4	−9	5	17	16	—	—	—	—	—	3.3	—	—	—	7	—	—
41	2.3	−8	5	17	15	—	—	—	—	—	—	—	—	—	—	—	—
41	2.4	—	—	3	2	—	—	—	—	—	—	—	—	—	—	—	—
47	2.2	−2	2	4	3	—	—	—	—	—	—	—	—	—	—	—	—
48	2.2	—	—	5	5	—	—	—	—	—	—	—	—	—	—	—	—
49	2.0	—	—	3	3	—	—	—	—	—	—	—	—	—	—	—	—
52	2.4	−7	3	28	15	—	—	—	—	—	—	—	—	—	—	—	—
53	—	—	—	2	2	—	—	—	—	—	—	—	—	—	—	—	—
55	2.4	—	—	6	4	—	—	—	—	—	—	—	—	—	—	—	—
8 01	?	—	—	—	—	—	—	—	—	—	—	—	—	—	—	—	—
04	?	—	—	—	—	—	—	—	—	—	—	—	—	—	—	—	—
06	2.4	—	—	2	2	—	—	—	—	—	—	—	—	—	—	—	—
11	2.4	−2	2	3	4	—	—	—	—	—	—	—	—	—	—	—	—
12	2.4	—	—	3	2	—	—	—	—	—	3.6	—	—	—	2	—	—
14	?	—	—	3	3	—	—	—	—	—	—	—	—	—	—	—	—

日時 Time of Occurrence		舞鶴 (Maiduru)					城崎 (Kinosaki)					伊根 (Ine)					震央 Epi-centre	震原の深さ Focal Depth	摘要 Remark
		初動	初微 Init. Mot.		最大動 Max. 2A		初微	初動 Init. Mot.		最大動 Max. 2A		初微	初動 Init. Mot.		最大動 Max. 2A				
		Pre. tr.	E.W.	N.S.	E.W.	N.S.	Pre. tr.	E.W.	N.S.	E.W.	N.S.	Pre. tr.	E.W.	N.S.	E.W.	N.S.			
	h m	s	μ	μ	μ	μ	s	μ	μ	μ	μ	s	μ	μ	μ	μ		km	
April	14	—	—	—	2	1	—	—	—	—	—	—	—	—	—	—	—	—	
	17	2.5	—	—	3	3	—	—	—	—	—	—	—	—	—	—	—	—	
	23	2.2	− 2	—	15	17	4.8	—	—	7	5	—	—	—	—	—	—	—	
	27	2.5	− 4	—	5	5	—	—	—	—	—	—	—	—	—	—	—	—	
	32	2·5	—	—	2	2	—	—	—	—	—	—	—	—	—	—	—	—	
	32	—	—	—	2	2	—	—	—	—	—	—	—	—	—	—	—	—	
	40	2.3	—	—	2	3	—	—	—	—	—	—	—	—	—	—	—	—	
	41	2.4	—	—	2	2	—	—	—	—	—	—	—	—	—	—	—	—	
	43	?	—	—		—	—	—	—	—	—	—	—	—	—	—	—	—	
	47	—	—	—	2	—	—	—	—	—	—	—	—	—	—	—	—	—	
	49	2.5	—	—	2	1	—	—	—	—	—	—	—	—	—	—	—	—	
	55	?	—	—	—	—	—	—	—	—	—	—	—	—	—	—	—	—	
	59	2.3	—	—	3	2	—	—	—	—	—	—	—	—	—	—	—	—	
	9 02	—	—	—	—	2	—	—	—	—	—	—	—	—	—	—	—	—	
	12	2.4	—	—	—	2	—	—	—	—	—	—	—	—	—	—	—	—	
	21	—	—	—	2	1	—	—	—	—	—	—	—	—	—	—	—	—	
	27	2.4	—	—	3	2	—	—	—	—	—	—	—	—	—	—	—	—	
	28	—	—	—	2	2	—	—	—	—	—	—	—	—	—	—	—	—	
	9 33	1.5	—	—	3	2	—	—	—	—	—	—	—	—	—	—	—	—	
	40	—	—	—	1	1	—	—	—	—	—	—	—	—	—	—	—	—	
	40	2.4	—	—	2	2	—	—	—	—	—	—	—	—	—	—	—	—	
	42	2.0	—	—	3	3	—	—	—	—	—	—	—	—	—	—	—	—	
	43	—	—	—	1	1	—	—	—	—	—	—	—	—	—	—	—	—	
	48	2.5	—	—	3	2	—	—	—	—	—	—	—	—	—	—	—	—	
	49	2.5	− 4	8	225	222	4.5	—	—	37	36	3.6	—	2	—	37	204	13.6	
	50	2.3	—	—	5	6	—	—	—	—	—	—	—	—	—	—	—	—	
	51	—	—	—	1	1	—	—	—	—	—	—	—	—	—	—	—	—	
	54	2.5	− 2	—	2	2	—	—	—	—	—	—	—	—	—	—	—	—	
	55	—	—	—	1	1	—	—	—	—	—	—	—	—	—	—	—	—	
	57	2.5	—	—	3	3	—	—	—	—	—	—	—	—	—	—	—	—	
	10 07	2.0	—	—	23	31	4.9	—	—	12	5	—	—	—	—	—	—	—	
	13	2.5	—	—	2	2	—	—	—	—	—	—	—	—	—	—	—	—	
	16	2.4	− 2	—	4	4	—	—	—	—	—	—	—	—	—	—	—	—	
	24	2.2	− 4	3	7	6	—	—	—	—	—	—	—	—	—	—	—	—	
	26	—	—	—	1	1	—	—	—	—	—	—	—	—	—	—	—	—	

	27	—	—	—	2	2	—	—	—	—	—	—	—	—	—	—	—	—	
	28	2.2	− 2	2	3	3	—	—	—	—	—	—	—	—	—	—	—	—	
	30	2.0	− 2	3	13	5	—	—	—	—	—	—	—	—	—	—	—	—	
	31	—	—	—	2	2	—	—	—	—	—	—	—	—	—	—	—	—	
	35	2.5	—	—	2	2	—	—	—	—	—	—	—	—	—	—	—	—	
	39	2.2	—	—	3	3	—	—	—	—	—	—	—	—	—	—	—	—	
	40	2.0	—	—	3	3	—	—	—	—	—	—	—	—	—	—	—	—	
	41	2.3	− 3	3	4	4	—	—	—	—	—	—	—	—	—	—	—	—	
	45	2.2	—	—	3	3	—	—	—	—	—	—	—	—	—	—	—	—	
	47	2.3	—	—	3	2	—	—	—	—	—	—	—	—	—	—	—	—	
	51	2.4	− 2	2	3	3	—	—	—	—	—	—	—	—	—	—	—	—	
	55	2.3	—	—	3	3	—	—	—	—	—	—	—	—	—	—	—	—	
	58	—	—	—	1	1	—	—	—	—	—	—	—	—	—	—	—	—	
11	02	2.2	—	—	3	2	—	—	—	—	—	—	—	—	—	—	—	—	
	17	1.6	− 5	5	8	5	4.9	—	—	12	2	—	—	—	—	—	—	—	
	20	—	—	—	2	1	—	—	—	—	—	—	—	—	—	—	—	—	
	25	2.3	—	—	1	1	—	—	—	—	—	—	—	—	—	—	—	—	
	26	—	—	—	1	1	—	—	—	—	—	—	—	—	—	—	—	—	
	38	2.5	—	—	8	11	4.2	—	—	5	5	—	—	—	—	—	—	—	
	40	2.4	—	—	2	2	—	—	—	—	—	—	—	—	—	—	—	—	
	40	2.5	—	—	2	2	—	—	—	—	—	—	—	—	—	—	—	—	
	42	3.9	− 5	2	48	29	2.9	14	− 9	219	165	4.2	—	− 9	—	42	205	9.1	
	43	2.6	—	—	3	2	—	—	—	—	—	—	—	—	—	—	—	—	
	53	2.5	—	—	4	3	—	—	—	—	—	—	—	—	—	—	—	—	
	55	2.3	—	—	3	2	—	—	—	—	—	—	—	—	—	—	—	—	
	57	2.5	− 2	3	4	4	—	—	—	—	—	—	—	—	—	—	—	—	
12	09	2.4	− 4	4	5	6	—	—	—	—	—	—	—	—	—	—	—	—	
	20	2.3	—	—	2	2	—	—	—	—	—	—	—	—	—	—	—	—	
	22	2.4	—	—	2	1	—	—	—	—	—	—	—	—	—	—	—	—	
13	27	2.3	—	—	2	2	—	—	—	—	—	—	—	—	—	—	—	—	
	47	2.3	− 3	2	3	3	—	—	—	—	—	—	—	—	—	—	—	—	
	47	1.8	—	—	6	4	—	—	—	—	—	—	—	—	—	—	—	—	
	48	2.3	—	—	2	2	—	—	—	—	—	—	—	—	—	—	—	—	
	48	2.3	− 3	2	4	4	—	—	—	—	—	—	—	—	—	—	—	—	
	49	2.3	+2	+ 2	12	8	—	—	—	—	—	—	—	—	—	—	—	—	
	50	—	−5	+ 2	13	10	—	—	—	—	—	—	—	—	—	—	—	—	
14	27	2.6	− 5	3	5	4	—	—	—	—	—	—	—	—	—	—	—	—	
	30	2.2	—	—	3	3	—	—	—	—	—	—	—	—	—	—	—	—	
	49	2.3	−50	30	38	25	4.9	4	− 3	60	58	3.4	3	5	25	28	206	15.0	
	50	2.3	− 3	3	3	3	—	—	—	—	—	—	—	—	—	—	—	—	
	56	2.1	—	—	2	1	—	—	—	—	—	—	—	—	—	—	—	—	
	58	2.4	− 2	2	3	3	—	—	—	—	—	—	—	—	—	—	—	—	

日時 Time of Occurrence		舞鶴 (Maiduru)					城崎 (Kinosski)					伊根 (Ine)					震央 Epi-centre	震原の深さ Focal Depth	摘要 Remark
		初微	初動 Init. Mot.		最大動 Max. 2A		初微	初動 Init. Mot.		最大動 Max. 2A		初微	初動 Init. Mot.		最大動 Max. 2A				
		Pre. tr.	E.W.	N.S.	E.W.	N.S.	Pre. tr.	E.W.	N.S.	E.W.	N.S.	Pre. tr.	E.W.	N.S.	E.W.	N.S.			
	h m	s	μ	μ	μ	μ	s	μ	μ	μ	μ	s	μ	μ	μ	μ		km	
	15 09	2.5	—	—	3	3	—	—	—	—	9	—	—	—	—	—	—	—	
	14	3.0	—	—	3	3	3.2	—	—	11	—	—	—	—	—	—	—	—	
	24	2.3	—	—	2	2	—	—	—	—	—	—	—	—	—	—	—	—	
	31	?	—	—	—	—	—	—	—	—	—	—	—	—	—	—	—	—	
	34	2.2	—	—	3	2	—	—	—	—	—	—	—	—	—	—	—	—	
	35	?	—	—	—	—	—	—	—	—	—	—	—	—	—	—	—	—	
	35	?	—	—	—	—	—	—	—	—	—	—	—	—	—	—	—	—	
	16 06	2.3	− 4	2	9	7	—	—	—	—	—	—	—	—	—	—	—	—	
	09	2.4	—	—	3	2	—	—	—	—	—	—	—	—	—	—	—	—	
	15	2.1	—	—	4	4	—	—	—	—	—	—	—	—	—	—	—	—	
	16	2.4	—	—	2	2	—	—	—	—	—	—	—	—	—	—	—	—	
	17	2.0	—	—	4	3	—	—	—	—	—	—	—	—	—	—	—	—	
	20	3.6	—	—	1	2	—	—	—	—	—	—	—	—	—	—	—	—	
	26	2.2	− 4	3	38	57	4.8	—	—	7	5	2.9	—	—	9	12	207	13.7	
	30	2.4	—	—	3	2	—	—	—	—	—	—	—	—	—	—	—	—	
	53	3.8	− 2	2	5	4	—	—	—	—	—	—	—	—	—	—	—	—	
	58	2.8	—	—	4	4	—	—	—	—	—	—	—	—	—	—	—	—	
	17 02	2.4	—	—	3	3	—	—	—	—	—	—	—	—	—	—	—	—	
	18 23	2.3	−152	81	229	250	4.9	86	−42	528	410	2.9	5	8	257	120	208	14.9	
	46	—	—	—	2	1	—	—	—	—	—	—	—	—	—	—	—	—	
	19 06	—	—	—	1	1	—	—	—	—	—	—	—	—	—	—	—	—	
	10	2.5	—	—	3	2	—	—	—	—	—	—	—	—	—	—	—	—	
	24	2.6	− 4	3	10	10	4.6	—	—	9	8	3.0	—	—	7	7	209	15.8	
	33	—	—	—	1	1	—	—	—	—	—	—	—	—	—	—	—	—	
	35	2.4	—	—	1	1	—	—	—	—	—	—	—	—	—	—	—	—	
	53	2.2	− 1	—	7	7	—	—	—	—	—	3.5	—	—	12	10	—	—	
	20 12	2.2	− 2	—	4	3	—	—	—	—	—	—	—	—	—	—	—	—	
	28	5.0	− 2	2	6	7	2.7	—	—	12	28	4.6	—	—	5	4	210	19.0	
	58	2.3	—	—	5	4	—	—	—	—	—	—	—	—	—	—	—	—	
	21 01	2.4	—	—	2	2	—	—	—	—	—	—	—	—	—	—	—	—	
	34	2.5	—	—	2	2	—	—	—	—	—	—	—	—	—	—	—	—	
	38	2.5	− 2	1	5	3	—	—	—	—	—	—	—	—	—	—	—	—	
	47	2.4	—	—	2	2	—	—	—	—	—	—	—	—	—	—	—	—	
	22 33	2.4	− 1	1	5	5	—	—	—	—	—	—	—	—	—	—	—	—	
	23 04	2.4	− 2	2	7	4	—	—	—	—	—	—	—	—	—	—	—	—	

2	1 58	2.3	—	—	6	6	4.8	—	—	4	4	—	—	—	—	—	—	—	
	2 39	2.3	—	—	3	3	—	—	—	—	—	—	—	—	—	—	—	—	
	45	1.9	—	—	4	5	—	—	—	—	—	—	—	—	—	—	—	—	
	5 06	6.8	—	—	3	3	—	—	—	—	—	7.0	—	—	3	4	—	—	
	38	2.0	—	—	4	3	—	—	—	—	—	—	—	—	—	—	—	—	
	6 01	3.7	—	—	2	2	—	—	—	—	—	—	—	—	—	—	—	—	
	28	4.2	—	—	8	7	3.8	—	—	53	35	4.3	—	—	12	7	216	22.0	
	54	2.4	—	—	2	2	—	—	—	—	—	—	—	—	—	—	—	—	
	707	2.1	—	—	3	3	—	—	—	—	—	—	—	—	—	—	—	—	
	18	—	—	—	2	2	—	—	—	—	—	—	—	—	—	—	—	—	
	40	3.8	—	—	2	2	—	—	—	—	—	—	—	—	—	—	—	—	
	10 29	2.1	—	—	12	8	5.3	—	—	4	6	3.4	—	—	7	10	217	15·5	
	11 35	2.6	-3	2	33	10	5.0	7	-4	7	15	3.3	—	—	12	10	218	18.1	
	42	2.4	—	—	2	2	—	—	—	—	—	—	—	—	—	—	—	—	
	14 58	2.4	-2	3	12	6	—	—	—	—	—	—	—	—	—	—	—	—	
	15 24	2.0	—	—	3	3	—	—	—	—	—	—	—	—	—	—	—	—	
	17 21	3.0	—	—	2	0	—	—	—	—	—	—	—	—	—	—	—	—	
	20 58	2.2	—	2	9	8	—	—	—	—	—	—	—	—	—	—	—	—	
	21 22	2.5	-2	2	3	4	—	—	—	—	—	—	—	—	—	—	—	—	
	45	2.8	-1	2	11	6	—	—	—	—	—	—	—	—	—	—	—	—	
	22 32	—	—	—	1	1	—	—	—	—	—	—	—	—	—	—	—	—	
	32	—	—	—	1	1	—	—	—	—	—	—	—	—	—	—	—	—	
	38	—	—	—	?	?	—	—	—	—	—	—	—	—	—	—	—	—	
	40	—	—	—	2	3	—	—	—	—	—	—	—	—	—	—	—	—	
	41	—	—	—	?	?	—	—	—	—	—	—	—	—	—	—	—	—	
	23 18	2.2	-8	4	35	23	4.9	3	-3	13	18	3.6	—	—	16	10	214	15·7	
	37	2.2	—	—	5	5	—	—	—	—	—	—	—	—	—	—	—	—	
3	0 05	2.3	-5	2	11	11	4.7	—	—	5	5	3.5	—	—	5	3	215	1.20	
	48	—	—	—	2	2	—	—	—	—	—	—	—	—	—	—	—	—	
	1 07	2.2	—	—	1	2	—	—	—	—	—	—	—	—	—	—	—	—	
	34	2.3	-5	4	49	46	5.3	4	-2	19	24	3.8	—	—	22	20	216	1.64	
	2 07	2.2	-12	4	159	198	5.1	7	-4	33	38	3.7	—	—	23	25	217	6.8	
	08	2.2	—	—	4	3	—	—	—	—	—	—	—	—	—	—	—	—	
	10	—	—	—	2	1	—	—	—	—	—	—	—	—	—	—	—	—	
	10	—	—	—	2	2	—	—	—	—	—	—	—	—	—	—	—	—	
	28	2.2	2	2	9	6	—	—	—	—	—	—	—	—	—	—	—	—	
	58	—	—	—	3	3	—	—	—	—	—	—	—	—	—	—	—	—	
	3 54	—	—	—	1	1	—	—	—	—	—	—	—	—	—	—	—	—	
	5 46	—	—	—	1	1	—	—	—	—	—	—	—	—	—	—	—	—	
	6 50	2.3	—	—	2	1	—	—	—	—	—	—	—	—	—	—	—	—	
	7 52	2.4	—	—	2	2	—	—	—	—	—	—	—	—	—	—	—	—	
	8 54	—	—	—	1	1	—	—	—	—	—	—	—	—	—	—	—	—	

日時 Time of Accurrence		舞鶴 (Maiduru)					城崎 (Kinosaki)					伊根 (Ine)					震央 Epi-centre	震原の深さ Focal Depth	摘要 Remark
		初微	初動 Init.	Mot.	最大動 Max. 2A		初微	初動 Init.	Mot.	最大動 Max. 2A		初微	初動 Init.	Mot.	最大動 Max. 2A				
		Pre. tr.	E.W.	N.S.	E.W.	N.S.	Pre. tr.	E.W.	N.S.	E.W.	N.S.	Pre. tr.	E.W.	N.S.	E.W.	N.S.			
	h m	s	μ	μ	μ	μ	s	μ	μ	μ	μ	s	μ	μ	μ	μ		km	
	56	—	—	—	1	1	—	—	—	—	—	—	—	—	—	—	—	—	
	9 39	2.8	—	—	5	5	—	—	—	—	—	3.9	—	—	5	5	—	—	
	52	—	—	—	2	2	—	—	—	—	—	—	—	—	—	—	—	—	
	10 13	2.2	—	—	3	2	—	—	—	—	—	—	—	—	—	—	—	—	
	21	2.2	—	—	3	2	—	—	—	—	—	—	—	—	—	—	—	—	
	11 26	—	—	—	2	2	—	—	—	—	—	—	—	—	—	—	—	—	
	12 19	2.2	—	—	2	1	—	—	—	—	—	—	—	—	—	—	—	—	
	24	—	—	—	2	2	—	—	—	—	—	—	—	—	—	—	—	—	
	35	3.5	− 2	2	11	8	5.0	—	—	—	—	—	—	—	—	—	—	—	
	44	2.2	—	—	1	1	—	—	—	—	—	—	—	—	—	—	—	—	
	14 32	—	—	—	—	2	—	—	—	—	—	—	—	—	—	—	—	—	
	17 25	2.2	—	—	2	2	—	—	—	—	—	—	—	—	—	—	—	—	
	20 41	2.2	—	—	1	1	—	—	—	—	—	—	—	—	—	—	—	—	
	21 11	2.8	− 2	1	15	13	—	—	—	—	—	—	—	—	—	—	—	—	
	18	6.2	− 2	2	8	9	—	—	—	—	—	—	—	—	—	—	—	—	
	20	2.2	—	—	3	2	—	—	—	—	—	—	—	—	—	—	—	—	
4	0 59	1.8	—	—	3	2	—	—	—	—	—	—	—	—	—	—	—	—	
	3 14	2.3	− 1	1	2	3	—	—	—	—	—	—	—	—	—	—	—	—	
	4 27	—	—	—	1	1	—	—	—	—	—	—	—	—	—	—	—	—	
	49	2.8	—	—	11	10	—	—	—	—	—	—	—	—	—	—	—	—	
	6 20	2.4	—	—	4	3	—	—	—	—	—	—	—	—	—	—	—	—	
	8 25	—	—	—	?	—	—	—	—	—	—	—	—	—	—	—	—	—	
	11 10	2.3	—	—	2	3	—	—	—	—	—	—	—	—	—	—	—	—	
	13 47	2.3	—	—	2	2	—	—	—	—	—	—	—	—	—	—	—	—	
	14 47	2.3	—	—	2	2	—	—	—	—	—	—	—	—	—	—	—	—	
	15 11	—	—	—	2	1	—	—	—	—	—	—	—	—	—	—	—	—	
	21 12	4.8	− 2	1	3	2	—	—	—	—	—	—	—	—	—	—	—	—	
	23 11	2.3	—	—	1	—	—	—	—	—	—	—	—	—	—	—	—	—	
	30	—	—	—	2	2	—	—	—	—	—	—	—	—	—	—	—	—	
	2 05	2.3	—	—	3	4	—	—	—	—	—	—	—	—	—	—	—	—	
	3 16	2.2	—	—	8	3	—	—	—	5	5	—	—	—	—	—	—	—	
	47	2.6	—	—	8	6	—	—	—	—	—	—	—	—	—	—	—	—	
	5 04	3.1	− 4	2	6	4	4.2	—	—	5	5	—	—	—	—	—	—	—	
	9 41	1.9	—	—	10	3	—	—	—	—	—	—	—	—	—	—	—	—	
	11 29	2.3	—	—	3	2	—	—	—	—	—	—	—	—	—	—	—	—	

		53	—	—	—	1	1	—	—	—	—	—	—	—	—	—	—	—	—
	10	06	2.2	—	—	2	2	—	—	—	—	—	—	—	—	—	—	—	—
6	0	51	2.1	—	—	2	1	—	—	—	—	—	—	—	—	—	—	—	—
	2	14	2.2	—	—	1	1	—	—	—	—	—	—	—	—	—	—	—	—
		58	2.2	−5	3	16	15	4.8	2	−1	12	12	—	—	—	—	—	—	—
	3	10	2.0	—	—	3	1	—	—	—	—	—	—	—	—	—	—	—	—
	4	51	3.6	—	—	2	2	4.7	2	−2	11	12	—	—	—	—	—	—	—
	11	21	2.3	—	—	1	1	—	—	—	—	—	—	—	—	—	—	—	—
		23	2.2	—	—	2	1	—	—	—	—	—	—	—	—	—	—	—	—
		50	2.0	—	—	2	2	—	—	—	—	—	—	—	—	—	—	—	—
	15	54	—	—	—	—	—	—	—	—	—	—	—	—	—	—	—	—	—
	17	30	2.4	—	—	—	—	—	—	—	—	—	—	—	—	—	—	—	—
		32	2.5	—	—	2	1	—	—	—	—	—	—	—	—	—	—	—	—
	18	27	2.4	—	—	3	2	—	—	—	—	—	—	—	—	—	—	—	—
	19	07	—	—	—	2	2	—	—	—	—	—	—	—	—	—	—	—	—
		08	—	—	—	2	2	—	—	—	—	—	—	—	—	—	—	—	—
	20	26	2.3	—	—	2	2	—	—	—	—	—	—	—	—	—	—	—	—
	21	33	2.2	—	—	1	2	—	—	—	—	—	—	—	—	—	—	—	—
7	0	12	2.4	—	—	2	2	—	—	—	—	—	—	—	—	—	—	—	—
	3	46	—	—	—	2	3	—	—	—	—	—	—	—	—	—	—	—	—
	4	10	—	—	—	1	1	—	—	—	—	—	—	—	—	—	—	—	—
		47	4.4	−5	3	18	8	3.8	6	−3	28	31	4.5	—	—	20	15	220	23.6
	5	37	5.4	—	—	5	4	3.1	8	6	33	22	3.6	—	—	5	7	221	14.4
	6	37	2.7	−1	1	4	4	—	—	—	—	—	—	—	—	—	—	—	—
	7	27	3.5	—	—	1	2	—	—	—	—	—	—	—	—	—	—	—	—
	9	45	—	—	—	2	2	—	—	—	—	—	—	—	—	—	—	—	—
	10	19	2.2	—	—	1	1	—	—	—	—	—	—	—	—	—	—	—	—
	13	14	—	—	—	1	1	—	—	—	—	—	—	—	—	—	—	—	—
	16	59	2.4	—	—	1	1	—	—	—	—	—	—	—	—	—	—	—	—
	19	28	2.3	−2	1	5	7	5.5	—	—	10	7	—	—	—	—	—	—	—
		33	3.0	—	—	2	3	—	—	—	—	—	—	—	—	—	—	—	—
		37	4.5	—	—	2	2	—	—	—	—	—	—	—	—	—	—	—	—
	23	46	1.9	—	—	3	4	—	—	—	—	—	—	—	—	—	—	—	—
		57	2.1	—	—	4	4	—	—	—	—	—	—	—	—	—	—	—	—
8	0	54	—	—	—	1	1	—	—	—	—	—	—	—	—	—	—	—	—
	5	17	2.2	—	—	2	2	—	—	—	—	—	—	—	—	—	—	—	—
	7	12	5.7	—	—	4	4	—	—	—	—	—	—	—	—	—	—	—	—
		24	4.2	—	—	4	3	—	—	—	—	—	—	—	—	—	—	—	—
	8	51	1.9	—	—	4	4	—	—	—	—	—	—	—	—	—	—	—	—
	9	24	—	—	—	1	—	—	—	—	—	—	—	—	—	—	—	—	—
	10	22	2.2	—	—	3	3	—	—	—	—	—	—	—	—	—	—	—	—
		27	3.2	—	—	3	2	—	—	—	—	—	—	—	—	—	—	—	—

日時 Time of Occurrence		舞鶴 (Maiduru)					城崎 (Kinosaki)					伊根 (Ine)					震央 Epi-centre	震原の深さ Focal Depth	摘要 Remark
		初微	初動 Init. Mot.		最大動 Max. 2A		初微	初動 Init. Mot.		最大動 Max. 2A		初微	初動 Init. Mot.		最大動 Max. 2A				
		Pre-tr.	E.W.	N.S.	E.W.	N.S.	Pre-tr.	E.W.	N.S.	E.W.	N.S.	Pre-tr.	E.W.	N.S.	E.W.	N.S.			
	h m	s	μ	μ	μ	μ	s	μ	μ	μ	μ	s	μ	μ	μ	μ		km	
	12 00	—	—	—	2	2	—	—	—	—	—	—	—	—	—	—	—	—	
	42	—	—	—	?	?	—	—	—	—	—	—	—	—	—	—	—	—	
	13 26	6.3	−2	3	9	6	3.2	−5	− 6	134	157	4.2	—	—	10	15	222	12.0	
	15 55	4.9	—	—	4	3	3.8	—	—	27	69	—	—	—	—	—	—	—	
	17 42	2.1	−60	42	157	243	5.8	41	−18	257	124	3.4	−10	−20	90	78	223	17.2	
	19 27	2.3	—	—	2	2	—	—	—	—	—	—	—	—	—	—	—	—	
	20 17	2.1	−3	4	12	13	5.5	3	− 2	10	8	—	—	—	—	—	224	—	Epicentres Nos. 221-240 determined by means of prel. tr. and initial motions at Maiduru and Kinosaki.
	17	2.1	−8	3	18	14	5.9	3	− 2	14	11	—	—	—	—	—	225	18.0	
	25	—	—	—	2	2	—	—	—	—	—	—	—	—	—	—	—	—	
	22 05	2.0	110	42	810	970	5.9	119	−57	1336	872	—	—	—	—	—	226	16.5	
	11	—	—	—	4	4	—	—	—	—	—	—	—	—	—	—	—	—	
	15	2.0	—	—	2	1	—	—	—	—	—	—	—	—	—	—	—	—	
	16	3.0	—	—	2	2	—	—	—	—	—	—	—	—	—	—	—	—	
	18	2.0	—	—	3	5	—	—	—	—	—	—	—	—	—	—	—	—	
	23 16	—	−2	—	?	?	—	—	—	—	—	—	—	—	—	—	—	—	
	31	4.5	−2	2	4	5	2.8	−10	0	58	92	—	—	—	—	—	227	14.0	
	37	2.3	−2	2	4	5	6.1	—	—	7	5	—	—	—	—	—	228	18.0	
	46	2.1	−2	2	17	13	6.6	—	—	7	7	—	—	—	—	—	—	—	
9	0 12	1.5	—	1	4	5	6.3	—	—	4	3	—	—	—	—	—	229	12.0	
	18	1.7	—	2	3	4	6.2	—	—	4	4	—	—	—	—	—	—	—	
	1 26	—	—	—	2	2	—	—	—	—	—	—	—	—	—	—	—	—	
	4 08	—	—	—	1	1	—	—	—	—	—	—	—	—	—	—	—	—	
	11	2.0	—	—	4	4	—	—	—	—	—	—	—	—	—	—	—	—	
	8 02	4.5	−3	—	10	6	3.1	15	− 3	59	50	—	—	—	—	—	230	18.0	
	18	2.0	—	2	2	3	—	—	—	—	—	—	—	—	—	—	—	—	
	10 33	—	—	—	1	1	—	—	—	—	—	—	—	—	—	—	—	—	
	11 06	2.3	—	—	3	4	5.9	—	—	11	10	—	—	—	—	—	—	—	
	12 04	2.0	—	—	2	3	—	—	—	—	—	—	—	—	—	—	—	—	
	14 52	4.0	—	—	6	5	3.7	8	− 8	10	8	—	—	—	—	—	231	19.0	
	18 35	4.7	−2	2	4	5	3.9	8	− 2	33	11	—	—	—	—	—	232	25.0	
	20 01	2.3	−2	3	6	4	—	—	—	—	—	—	—	—	—	—	—	—	
	21 26	2.2	—	—	2	2	—	—	—	—	—	—	—	—	—	—	—	—	
10	0 06	2.1	—	—	5	5	—	—	—	—	—	—	—	—	—	—	—	—	
	10	2.0	—	—	3	2	—	—	—	—	—	—	—	—	—	—	—	—	
	19	2.0	—	—	5	4	—	—	—	—	—	—	—	—	—	—	—	—	

		37	2.2	—	—	2	1	—	—	—	—	—	—	—	—	—	—	—	—
	1	10	2.3	—	—	1	2	—	—	—	—	—	—	—	—	—	—	—	—
	2	31	—	—	—	1	1	—	—	—	—	—	—	—	—	—	—	—	—
	5	00	5.0	—	—	2	2	2.8	5	0	—	47	—	—	—	—	—	233	—
	6	02	2.2	—	—	1	1	—	—	—	—	—	—	—	—	—	—	—	—
	10	35	2.8	—	—	2	2	—	—	—	—	—	—	—	—	—	—	—	—
	12	49	7.4	—	—	2	2	—	—	—	—	—	—	—	—	—	—	—	—
	14	23	—	—	—	2	2	—	—	—	—	—	—	—	—	—	—	—	—
	15	37	2.4	—	—	4	4	—	—	—	—	—	—	—	—	—	—	—	—
	18	00	2.5	—	—	2	3	—	—	—	—	—	—	—	—	—	—	—	—
	19	36	6.0	−3	2	5	5	3.6	8	−5	128	45	—	—	—	—	—	234	—
	19	36	6.2	—	—	4	4	3.4	10	−10	31	43	—	—	—	—	—	235	—
		37	—	—	—	5	7	3.3	—	—	84	53	—	—	—	—	—	236	—
		37	—	—	—	5	5	2.7	—	—	151	64	—	—	—	—	—	—	—
11	0	55	4.0	−21	8	34	25	3.1	29	−8	197	385	—	—	—	—	—	237	16.0
	1	32	5.6	−5	3	26	10	2.3	6	−5	482	185	—	—	—	—	—	238	19.0
	2	59	5.2	−2	2	15	11	2.9	5	−7	108	62	—	—	—	—	—	239	—
	5	19	3.2	—	—	4	4	—	—	—	—	—	—	—	—	—	—	—	—
		30	2.6	—	—	6	5	—	—	—	—	—	—	—	—	—	—	—	—
		56	1	—	—	?	?	—	—	—	—	—	—	—	—	—	—	—	—
	7	09	7.2	—	—	2	3	—	—	—	—	—	—	—	—	—	—	—	—
		45	3.2	—	—	9	6	—	—	—	—	—	—	—	—	—	—	—	—
		46	—	—	—	3	3	—	—	—	—	—	—	—	—	—	—	—	—
	8	09	—	—	—	2	2	—	—	—	—	—	—	—	—	—	—	—	—
	11	03	2.5	—	—	4	5	4.9	—	—	5	5	—	—	—	—	—	—	—
		23	2.5	−5	2	5	4	5.7	—	8	8	10	—	—	—	—	—	—	—
	12	46	2.8	−1	3	6	5	5.6	5	−2	15	21	—	—	—	—	—	240	—
	18	54	3.7	−3	2	6	5	3.8	—	—	18	18	3.6	—	—	5	6	241	19.0
	20	50	5.6	−3	2	5	6	—	—	—	—	—	—	—	—	—	—	—	—
12	4	19	2.5	−7	3	8	6	5.1	—	—	12	10	3.6	—	—	6	6	242	17.5
		30	3.0	—	—	3	3	—	—	—	—	—	—	—	—	—	—	—	—
	5	06	2.5	—	—	2	2	5.0	—	—	3	3	3.7	—	—	3	5	243	16.8
	8	59	3.2	—	—	1	2	—	—	—	—	—	—	—	—	—	—	—	—
	9	33	5.0	—	—	27	9	2.2	6	0	48	74	3.6	—	—	23	20	244	10.0
	10	44	—	—	—	2	2	—	—	—	—	—	—	—	—	—	—	—	—
	21	21	—	—	—	1	2	—	—	—	—	—	—	—	—	—	—	—	—
		58	3.2	−3	1	12	11	4.7	—	—	22	10	3.3	—	—	3	4	245	20.5
	22	19	2.7	—	—	2	2	5.1	—	—	2	2	3.0	—	—	2	1	246	18.6
		30	2.8	—	—	2	1	—	—	—	—	—	—	—	—	—	—	—	—
		57	3.0	—	—	5	5	4.2	—	—	11	10	3.4	—	—	3	3	247	16.4
	23	08	—	—	—	2	2	—	—	—	—	—	—	—	—	—	—	—	—
		12	2.3	−3	1	11	4	—	—	—	—	—	—	—	—	—	—	—	—

日時 Time of Occurrence		舞鶴 (Maiduru)					城崎 (Kinosaki)					伊根 (Ine)					震央 Epi-centre	震原の深さ Focal Depth	摘要 Remark
		初微	初動 Init. Mot.		最大動 Max. 2A		初微	初動 Init. Mot.		最大動 Max. 2A		初微	初動 Init. Mot.		最大動 Max. 2A				
		Pre. tr.	E.W.	N.S.	E.W.	N.S.	Pre. tr.	E.W.	N.S.	E.W.	N.S.	Pre. tr.	E.W.	N.S.	E.W.	N.S.			
	h m	s	μ	μ	μ	μ	s	μ	μ	μ	μ	s	μ	μ	μ	μ		km	
	0 28	3.6	− 1	1	10	4	3.4	—	—	15	13	4.0	—	—	2	3	248	14.0	
	1 14	—	—	—	—	2	—	—	—	—	—	—	—	—	—	—	—	—	
	7 06	4.7	—	—	3	3	3.0	—	—	27	11	4.3	—	—	3	10	249	19.6	
	8 47	3.0	—	—	2	2	—	—	—	—	—	—	—	—	—	—	—	—	
	11 16	—	—	—	1	1	—	—	—	—	—	—	—	—	—	—	—	—	
	17 55	6.4	—	—	11	7	2.2	6	− 3	35	13	4.6	—	—	8	7	250	19.0	
	21 00	3.2	—	—	4	3	4.0	—	—	18	10	3.2	—	—	5	5	251	16.5	
	52	3.0	—	—	1	1	5.0	—	—	6	7	3.5	—	—	2	3	252	20.8	
	23 16	3.5	—	—	5	3	—	—	—	—	—	—	—	—	—	—	—	—	
	1 17	5.0	—	—	4	3	2.5	4	− 4	36	15	4.3	—	—	10	14	253	12.0	
	2 43	2 5	− 2	1	13	8	5.0	—	—	8	7	3.2	—	—	3	5	254	17.3	
14	4 47	3.2	—	—	3	3	—	—	—	—	—	—	—	—	—	—	—	—	
	5 57	3.0	9	3	9	9	4.2	—	—	13	13	3.6	—	—	3	4	255	16.4	
	11 25	3.5	—	—	3	2	—	—	—	—	—	—	—	—	—	—	—	—	
	12 36	5.3	—	—	3	3	4.0	—	—	21	14	4.2	—	—	5	10	256	26.8	
	14 18	2.0	—	—	2	2	—	—	—	—	—	—	—	—	—	—	—	—	
	16 21	3.0	−3	2	16	12	—	—	—	—	—	3.0	—	—	—	7	—	—	
	21 20	4.8	—	—	4	3	2.5	—	—	15	20	3.6	—	—	—	7	257	16.5	
	22 02	—	—	—	3	2	—	—	—	—	—	—	—	—	—	—	—	—	
	1 59	2.6	35	23	110	123	3.9	46	−25	100	98	3.5	—	—	—	163	258	9.0	
15	2 17	3.5	− 35	—	1	1	—	—	—	—	—	—	—	—	—	—	—	—	
	20	2.6	—	—	2	2	—	—	—	—	—	—	—	—	—	—	—	—	
	44	4 0	—	—	3	3	3.1	—	—	19	12	3.5	—	—	—	7	259	15.7	
	3 51	3.5	—	—	3	3	4.3	—	—	15	15	3.5	—	—	—	5	260	20.4	
	4 04	3.0	—	—	3	2	4.5	—	—	8	5	3.6	—	—	—	7	261	18.3	
	56	3.6	—	—	2	3	4.0	—	—	7	8	4.2	—	—	—	3	262	18.3	
	10 49	5.0	—	—	8	3	2.3	3	−7	69	105	4.3	—	—	—	15	263	15.6	
	14 36	2.3	—	—	13	11	6.1	—	—	12	10	3.4	—	—	—	5	264	16.4	
	22 21	3.0	—	—	7	8	4.2	—	—	7	12	—	—	—	—	—	—	—	
16	4 52	3.5	—	—	13	10	3.4	− 5	−1	8	11	3.2	—	—	6	5	265	14.0	
	11 39	—	—	—	2	2	—	—	—	—	—	—	—	—	—	—	—	—	
	15 36	—	—	—	?	?	—	—	—	—	—	—	—	—	—	—	—	—	
	17 20	—	—	—	2	2	—	—	—	—	—	—	—	—	—	—	—	—	
	20 57	4.2	3	− 2	102	33	3.0	8	−2	40	25	3.6	−4	−6	30	40	266	17.2	
	57	—	—	—	10	7	—	—	—	—	—	—	—	—	—	—	—	—	

	57	—	—	—	8	6	—	—	—	—	—	—	—	—	—	—	—	—
	21 08	3.1	—	—	2	2	4.4	—	—	8	8	3.3	−5	3	22	23	267	18.5
	22 34	4.5	—	—	67	38	2.8	100	−33	215	302	4.2	−15	−10	165	130	268	12.5
	59	—	—	—	—	—	4.3	—	—	7	5	—	—	—	—	—	—	—
	23 24	—	—	—	1	1	—	—	—	—	—	—	—	—	—	—	—	—
	40	2.6	−2	2	5	4	—	—	—	—	—	—	—	—	—	—	—	—
17	1 17	3.2	—	—	2	2	—	—	—	—	—	—	—	—	—	—	—	—
	53	2.5	—	—	1	1	—	—	—	—	—	—	—	—	—	—	—	—
	13 33	—	—	—	?	?	—	—	—	—	—	—	—	—	—	—	—	—
	15 23	3.7	−1	1	5	3	4.2	—	—	5	3	3.6	—	—	3	3	269	21.4
	27	—	—	—	1	1	3.5	—	—	5	4	—	—	—	2	2	—	—
	44	3.7	−4	5	55	44	4.2	15	−7	87	34	3.5	—	—	48	75	270	21.3
	18 43	3.6	—	—	3	2	—	—	—	5	5	—	—	—	—	—	—	—
	19 43	3.2	—	—	2	1	—	—	—	6	5	—	—	—	—	—	—	—
	23 04	4.0	—	—	2	2	—	—	—	—	—	—	—	—	—	—	—	—
18	5 06	2.7	—	—	2	2	—	—	—	—	—	—	—	—	—	—	—	—
	8 06	2.9	—	—	3	2	—	—	—	—	—	—	—	—	—	—	—	—
	9 39	4.6	—	—	2	2	3.1	—	—	40	30	3.6	—	—	2	3	271	17.8
	11 14	3.0	—	—	1	1	—	—	—	—	—	—	—	—	—	—	—	—
	18 03	4.0	−5	2	23	10	3.3	—	—	45	17	3.0	—	—	7	10	272	14.9
	20 24	7.1	—	—	20	12	3.5	—	—	17	10	7.0	—	—	3	5	273	26.8
	21 27	2.4	—	—	5	6	—	—	—	—	—	—	—	—	—	—	—	—
19	5 10	—	—	—	3	2	—	—	—	—	—	—	—	—	—	—	—	—
	7 18	—	—	—	1	1	—	—	—	—	—	—	—	—	—	—	—	—
	12 25	2.2	−4	2	13	13	—	—	—	—	—	—	—	—	—	—	—	—
	15 25	2.5	—	—	3	2	—	—	—	—	—	—	—	—	—	—	—	—
	19 31	2.6	—	—	6	4	—	—	—	—	—	—	—	—	—	—	—	—
20	5 10	—	—	—	2	2	—	—	—	—	—	—	—	—	—	—	—	—
	49	2.1	−20	8	300	152	6.0	8	−7	35	23	3.6	—	—	70	65	274	17.5
	49	2.0	—	—	14	10	—	—	—	5	5	—	—	—	—	—	—	—
	6 10	2.0	—	—	2	3	—	—	—	—	—	—	—	—	—	—	—	—
	11 50	—	—	—	2	2	—	—	—	—	—	—	—	—	—	—	—	—
21	4 50	5.0	—	—	4	3	2.8	—	—	10	9	3.8	—	—	18	27	275	17.0
	5 32	2.4	—	—	6	6	4.7	—	—	5	6	3.6	—	—	5	7	276	13.0
	11 23	3.1	—	—	11	10	3.8	—	—	13	15	3.3	—	—	8	6	277	14.3
	16 43	3.9	—	—	3	2	3.4	—	—	14	13	3.8	—	—	4	3	278	17.3
	17 21	—	—	—	1	1	—	—	—	—	—	—	—	—	—	—	—	—
22	5 04	—	—	—	2	2	—	—	—	—	—	—	—	—	—	—	—	—
	8 31	4.2	—	—	2	1	—	—	—	—	—	—	—	—	—	—	—	—
	12 31	4.3	−5	1	38	24	3.0	15	8	53	65	4.1	—	—	18	21	279	17.0
	16 31	4.7	—	—	3	2	—	—	—	—	—	—	—	—	—	—	—	—
	22 35	3.4	−1	1	5	4	4.2	—	—	10	11	3.6	—	—	5	5	280	19.4

日時 Time of Occurrence		舞鶴 (Maiduru)					城崎 (Kinosaki)					伊根 (Ine)					震央 Epi-centre	震原の深さ Focal Depth	摘要 Remark
		初微	初動 Init.	初動 Mot.	最大動 Max. 2A		初微	初動 Init.	初動 Mot.	最大動 Max. 2A		初微	初動 Init.	初動 Mot.	最大動 Init.	最大動 Mot.			
	h m	Pre. tr.	E.W.	N.S.	E.W.	N.S.	Pre. tr.	E.W.	N.S.	E.W.	N.S.	Pre. tr.	E.W.	S.N.	E.W.	N.S.			
		s	μ	μ	μ	μ	s	μ	μ	μ	μ	s	μ	μ	μ	μ		km	
April	23 32	7.2	—	—	3	3	3.2	—	—	9	9	6.5	—	—	9	10	281	31.0	
23	0 09	—	—	—	?	?	—	—	—	—	—	—	—	—	—	—	—	—	
	40	3.5	—	—	6	7	4.4	—	—	31	39	3.7	—	—	5	3	282	21.2	
	1 58	2.5	—	—	5	3	—	—	—	—	—	3.6	—	—	—	2	—	—	
	2 00	2.3	—	—	6	5	—	—	—	—	—	3.8	—	—	—	3	—	—	
	6 21	3.0	—	—	2	2	—	—	—	—	—	—	—	—	—	—	—	—	
	7 13	3.5	—	—	2	2	4.2	—	—	3	3	—	—	—	—	—	—	—	
	13 39	3.2	—	—	2	2	—	—	—	—	—	—	—	—	—	—	—	—	
	14 25	2.3	—	—	5	3	—	—	—	—	—	—	—	—	—	—	—	—	
	17 50	3.5	—	—	5	4	—	—	—	—	—	—	—	—	—	—	—	—	
	51	—	—	—	2	2	—	—	—	—	—	—	—	—	—	—	—	—	
	19 19	—	—	—	1	1	—	—	—	—	—	—	—	—	—	—	—	—	
	22 51	3.6	—	—	2	2	—	—	—	—	—	—	—	—	—	—	—	—	
24	1 27	3.0	—	—	1	1	—	—	—	—	—	—	—	—	—	—	—	—	
	2 01	3.6	—	—	23	13	—	—	—	—	—	3.5	—	—	—	5	—	—	
	3 01	4.0	—	—	2	2	—	—	—	—	—	3.5	—	—	—	5	—	—	
	4 14	—	—	—	1	1	—	—	—	—	—	—	—	—	—	—	—	—	
	47	4.0	—	—	1	1	—	—	—	—	—	—	—	—	—	—	—	—	
	13 28	4.3	—	—	3	2	—	—	—	—	—	—	—	—	—	—	—	—	
	15 45	5.3	—	—	3	3	3.0	− 8	3	33	32	4.1	—	—	10	16	283	20.0	
25	5 29	2.6	—	—	2	2	—	—	—	—	—	—	—	—	—	—	—	—	
	7 37	2.1	−6	4	26	25	—	—	—	—	—	3.2	—	—	3	3	284	16.0	
	8 37	2.5	—	—	1	1	—	—	—	—	—	—	—	—	—	—	—	—	
	11 11	—	—	—	2	3	—	—	—	—	—	3.0	—	—	—	5	—	—	
	58	3.0	—	—	1	1	—	—	—	—	—	—	—	—	—	—	—	—	
	19 27	3.1	13	− 5	167	88	3.7	—	− 4	—	143	4.2	−10	−11	25	37	285	8.0	
	20 01	—	—	—	1	1	—	—	—	—	—	—	—	—	—	—	—	—	
	22 08	4.1	−2	2	10	6	3.3	4	—	29	17	3.2	—	—	5	5	286	16.2	
	23 03	4.0	—	—	2	2	—	—	—	—	—	—	—	—	—	—	—	—	
26	2 45	—	—	—	2	1	3.0	8	8	37	36	3.6	—	—	3	2	287	13.5	
	4 36	3.8	—	—	35	8	4.5	—	—	5	5	3.5	—	—	—	8	288	23.2	
	57	3.5	—	—	5	3	—	—	—	—	—	—	—	—	—	—	—	—	
	7 53	2.3	−3	3	6	3	—	—	—	—	—	—	—	—	—	—	—	—	
	8 08	—	—	—	3	3	—	—	—	—	—	—	—	—	—	—	—	—	
	15 53	3.3	—	—	3	3	—	—	—	—	—	3.2	—	—	2	5	—	—	

			57	2 3	—	—	2	1	—	—	—	—	—	3.3	—	—	3	3	—	—
		21	43	—	—	—	2	2	—	—	—	—	—	—	—	—	—	—	—	—
		22	10	3.5	—	—	2	2	3.9	—	—	8	8	3.2	—	—	2	2	289	17.7
		23	38	3.9	—	—	2	2	3.6	—	—	4	3	3.7	—	—	2	2	290	18.8
			38	5.3	—	—	3	2	2.3	—	—	3	5	3.9	—	—	2	5	291	13.0
	27	2	03	5.3	—	—	3	2	2.7	—	—	11	9	3.1	—	—	11	8	292	0
		7	19	—	—	—	—	—	—	—	—	—	—	3.4	—	—	3	4	—	—
			22	3.5	—	—	2	2	—	—	—	—	—	3.7	—	—	4	5	—	—
		8	07	6.3	—	—	3	2	4.0	—	—	25	13	6.1	—	—	3	5	293	32.2
			19	3.9	—	—	4	4	4.1	—	—	12	15	3.6	—	—	4	9	294	21.9
	28	2	04	3.0	—	—	4	5	4.2	—	—	6	7	3.6	—	—	2	3	295	16.3
		8	37	7.5	−3	—	23	28	4.0	−9	−7	193	153	5.3	−2	5	40	102	296	18.6
		16	26	5.5	—	—	4	2	.6	—	—	10	21	3.1	−4	3	9	10	297	9.0
		17	14	4.0	−3	1	40	15	—	—	—	—	—	3.2	—	—	4	3	298	10.0
		18	04	2.6	3	−1	9	9	3.8	—	—	8	8	2.9	—	—	2	4	299	12.0
	29	5	11	—	—	—	—	—	—	—	—	—	—	3.9	—	—	3	2	—	—
		9	03	4.2	—	—	4	5	3.2	—	—	45	50	3.9	—	—	2	2	300	14.7
			21	3.6	−2	1	31	17	3.3	—	—	22	10	3.7	−2	0	6	8	301	14.0
		14	36	3.7	—	—	3	3	—	—	—	—	—	—	—	—	—	—	—	—
		17	34	3.2	—	—	12	12	—	—	—	—	—	—	—	—	—	—	—	—
			38	5.6	—	—	7	4	—	—	—	—	—	—	—	—	—	—	—	—
	30	4	15	2.2	—	—	10	16	6.0	—	—	8	9	—	—	—	—	—	—	—
		7	51	4.2	—	—	4	3	3.0	10	7	36	17	3.2	—	—	5	6	302	15.0
		9	58	—	—	—	2	2	—	—	—	—	—	—	—	—	—	—	—	—
		12	18	3.6	—	—	3	2	3.4	—	—	24	36	3.6	—	—	3	2	303	15.0
		13	30	5.2	—	—	3	2	2.8	—	—	36	13	4.8	—	—	3	3	304	20.5
		14	38	—	—	—	2	2	—	—	—	—	—	—	—	—	—	—	—	—
		22	17	2.8	—	—	2	1	—	—	—	—	—	3.0	—	—	2	1	—	—
May	1	0	28	—	—	—	4	4	—	—	—	—	—	—	—	—	—	—	—	—
			28	3.9	—	—	9	7	3.6	—	—	8	5	3.6	—	—	2	2	305	19.0
		2	46	3.1	—	—	3	2	3.1	—	—	18	20	4.0	—	—	7	16	306	0
		3	09	—	—	—	2	2	3.1	—	—	7	8	3.6	—	—	4	5	—	—
			26	4.6	—	—	3	4	5.9	—	—	5	5	5.6	—	—	5	6	307	33.6
		8	48	3.8	−2	1	14	9	4.2	—	—	11	8	3.8	—	—	9	8	308	22.0
		10	53	3.5	—	—	5	5	3.9	—	—	6	6	—	—	—	—	—	—	—
		18	20	2.6	—	—	4	4	4.4	—	—	18	11	—	—	—	—	—	—	—
		20	09	2.5	—	—	26	20	4.3	—	—	10	17	2.9	—	—	2	3	309	13.2
			31	—	—	—	2	1	4.2	—	—	3	3	—	—	—	—	—	—	—
			32	3.2	—	—	3	2	—	—	—	—	—	—	—	—	—	—	—	—
			37	3.0	—	—	2	2	—	—	—	—	—	4.0	—	—	10	10	—	—
			47	—	—	—	2	1	—	—	—	—	—	—	—	—	—	—	—	—
	2	8	24	3.6	—	—	3	2	—	—	—	—	—	3.7	—	—	2	2	—	—

日時 Time of Occurrence	舞鶴 (Maiduru)					城崎 (Kinosaki)					伊根 (Ine)					震央 Epi-centre	震原の深さ Focal Depth	摘要 Remark
	初微	初動 Init.		最大動 Max. 2A		初微	初動 Init.		最大動 Max. 2A		初微	初動 Init.		最大動 Max. 2A				
	Pre. tr.	E.W.	N.S.	E.W.	N.S.	Pre. tr.	E.W.	N.S.	E.W.	N.S.	Pre. tr.	E.W.	N.S.	E.W.	N.S.			
h m	s	μ	μ	μ	μ	s	μ	μ	μ	μ	s	μ	μ	μ	μ		km	
21 06	3.5	−2	2	3	3	3.8	—	—	6	6	3.4	—	—	2	2	310	17.7	
22 27	2.9	—	—	2	2	—	—	—	—	—	—	—	—	—	—	—	—	
23 27	2.3	—	—	3	2	—	—	—	—	—	—	—	—	—	—	—	—	
3 7 15	3.0	—	—	3	3	—	—	—	—	—	—	—	—	—	—	—	—	
11 48	4.5	8	− 3	28	33	2.8	15	− 7	394	112	3.3	—	—	115	80	311	16.6	
48	—	—	—	5	5	—	—	—	—	—	—	—	—	—	—	—	—	
12 21	—	—	—	1	1	4.5	—	—	10	13	—	—	—	—	—	—	—	
4 3 36	2.0	—	—	7	4	—	—	—	—	—	—	—	—	—	—	—	—	
9 01	3.1	—	—	18	16	3.9	—	—	10	8	3.0	—	—	5	10	312	15.1	
28	—	—	—	—	—	3.0	—	—	21	8	3.5	—	—	3	5	—	—	
10 57	4.0	—	—	3	2	3.8	—	—	20	12	3.7	—	—	3	3	313	21.2	
5 6 13	4.3	—	—	3	2	3.0	—	—	23	12	3.5	—	—	5	3	314	16.4	
7 04	5.7	—	—	10	5	1.6	− 9	2	208	205	5.4	—	—	10	5	315	7.0	
6 6 33	4.1	—	—	6	3	3.3	—	—	23	13	3.5	—	—	13	11	316	17.5	
17 19	3.6	−3	1	11	12	3.0	12	−10	108	57	2.9	—	—	13	15	317	10.2	
35	—	—	—	—	—	3.6	—	—	15	15	3.2	—	—	7	15	—	—	
44	1.6	—	—	3	2	—	—	—	—	—	—	—	—	—	—	—	—	
52	—	—	—	2	1	—	—	—	—	—	4.3	—	—	3	2	—	—	
22 47	6.6	—	—	7	6	4.5	—	—	10	13	8.1	—	—	5	4	318	—	Epicentre : near Mt. Myôken.
7 8 13	4.2	—	—	2	2	2.8	—	—	24	17	4.5	—	—	5	10	319	12.7	
54	4.8	—	—	8	12	4.5	—	—	113	60	3.5	−4	−1	29	17	32)	25.0	
9 00	2.4	− 1	—	9	8	5.4	—	—	7	6	3.0	—	—	3	7	321	17.7	
18 12	—	—	—	3	2	—	—	—	—	—	—	—	—	—	—	—	—	
19 28	5.0	—	—	5	2	3.0	—	—	13	10	4.1	—	—	5	9	322	20.0	
39	3.4	—	—	4	4	4.0	—	—	5	3	3.6	—	—	2	2	323	18.2	
21 15	3.0	—	—	3	3	4.3	—	—	7	5	2.9	—	—	3	4	324	16.4	
8 6 02	4.5	− 3	2	14	6	2.5	6	0	83	53	4.0	−3	2	13	15	325	13.9	
9 07	4.5	− 3	1	14	7	2.4	14	−8	100	64	4.3	−4	−3	27	38	326	13.2	
11 44	3.7	—	—	5	3	3.3	—	—	39	10	3.2	—	—	10	10	327	14.5	
47	—	—	—	—	—	3.5	—	—	10	10	2.9	—	—	3	3	—	—	
12 44	3.5	—	—	6	4	3.9	—	—	12	7	3.7	—	—	2	2	328	18.3	
17 06	3.4	—	—	3	2	3.9	—	—	9	6	3.4	—	—	10	7	329	17.3	
43	2.5	—	—	2	2	—	—	—	—	—	—	—	—	—	—	—	—	
9 3 13	1.4	—	—	—	4	6.0	—	—	3	2	3.6	—	—	6	13	330	10.0	
52	—	—	—	1	1	3.6	—	—	7	5	—	—	—	—	—	—	—	

	5 39	4.0	—	—	3	3	3.2	—	—	19	8	3.8	—	—	3	3	331	16.7
	47	—	—	—	2	1	3.6	—	—	12	8	3.9	—	—	2	3	—	—
	7 23	3.6	—	—	20	12	4.8	—	—	6	6	2.9	—	—	4	5	332	21.4
	10 25	2.4	—	—	5.	5	—	—	—	—	—	—	—	—	—	—	—	—
	15 55	2.6	—	—	3	3	4.6	—	—	8	5	2.8	—	—	5	11	333	15.4
	21 01	3.5	—	—	2	1	4.3	—	—	10	7	3.8	—	—	5	7	334	20.5
	22 49	4.0	—	—	2	1	—	—	—	8	10	—	—	—	2	2	—	—
10	1 05	4.2	—	2	8	6	2.6	—	—	17	24	3.9	—	—	8	13	335	13.1
	33	4.4	—	—	6	5	2.5	7	−3	30	23	3.6	—	—	8	3	336	12.8
	35	4.7	—	—	3	2	2.3	—	—	8	9	4.0	—	—	5	5	337	13.8
	56	—	—	—	—	—	—	—	—	—	—	—	—	—	—	—	—	—
	5 07	3.3	—	—	4	3	—	—	—	—	—	3.5	—	—	3	3	—	—
	15 24	2.7	—	—	3	3	—	—	—	—	—	—	—	—	—	—	—	—
11	2 30	3.1	—	—	5	4	4.0	—	—	15	11	3.4	—	—	5	5	338	15.8
	9 28	—	—	—	2	2	—	—	—	—	—	3.3	—	—	6	7	—	—
	14 13	—	—	—	1	1	—	—	—	—	—	—	—	—	—	—	—	—
	23 48	—	—	—	2	2	—	—	—	—	—	—	—	—	—	—	—	—
12	1 30	—	—	—	—	—	3.4	—	—	3	5	—	—	—	2	2	—	—
	3 30	—	—	—	—	—	3.4	—	—	5	6	3.6	—	—	4	6	—	—
	7 40	—	—	—	—	—	—	—	—	—	—	2.9	—	—	8	7	—	—
	13 18	—	—	—	—	—	3.5	—	—	3	3	—	—	—	—	—	—	—
	19 05	3.5	−2	—	11	5	3.5	—	—	4	3	2.8	—	—	8	10	339	14.0
	20 38	—	—	—	—	—	—	—	—	—	—	2.9	—	—	2	2	—	—
13	1 47	3.7	—	—	4	3	—	—	—	—	—	3.4	—	—	2	4	—	—
	7 43	4.0	—	—	3	3	—	—	—	—	—	—	—	—	—	—	—	—
	8 40	—	—	—	2	2	—	—	—	—	—	—	—	—	—	—	—	—
	17 43	4.1	−8	4	107	90	3.6	77	−39	142	150	3.6	−19	−11	50	66	340	19.7
14	0 01	4.2	—	—	7	6	2.7	—	—	7	7	4.5	—	—	3	3	341	13.8
	2 53	—	—	—	3	2	—	—	—	—	—	3.8	—	—	3	6	—	—
	8 31	4.2	—	—	2	2	—	—	—	—	—	—	—	—	2	2	—	—
	11 08	3.1	—	—	7	4	—	—	—	—	—	3.3	—	—	4	6	—	—
	43	—	—	—	2	2	—	—	—	—	—	—	—	—	—	—	—	—
	19 24	5.0	—	—	15	15	5.0	—	—	20	18	3.8	—	—	21	52	342	28.0
15	2 24	—	—	—	2	1	—	—	—	—	—	—	—	—	—	—	—	—
	3 56	4.0	—	—	3	3	—	—	—	—	—	3.4	—	—	5	5	—	—
	5 34	3.9	—	—	3	2	—	—	—	—	—	3.2	—	—	2	3	—	—
	12 31	3.8	—	—	3	3	—	—	—	—	—	—	—	—	—	—	—	—
	15 15	3.2	—	—	2	2	—	—	—	—	—	—	—	—	—	—	—	—
	17 55	—	—	—	2	2	—	—	—	—	—	3.9	—	—	2	2	—	—
16	3 39	3.2	−2	2	6	5	3.2	4	0	12	12	3.8	—	—	5	8	343	6.8
	11 25	2.7	−2	4	33	16	4.5	—	—	37	22	2.9	—	—	10	18	344	15.8
	14 17	4.2	—	—	9	4	—	—	—	—	—	—	—	—	—	—	—	—

日時 Time of Occurrence		舞鶴 (Maiduru)					城崎 (Kinosaki)					伊根 (Ine)					震央 Epi-centre	震原の深さ Focal Depth	摘要 Remark
		初微	初動 Init. Mot.		最大動 Max. 2A		初微	初動 Init. Mot.		最大動 Max. 2A		初微	初動 Init. Mot.		最大動 Max. 2A				
		Pre. tr.	E.W.	N.S.	E.W.	N.S.	Pre. tr.	E.W.	N.S.	E.W.	N.S.	Pre. tr.	E.W.	N.S.	E.W.	N.S.			
	h m	s	μ	μ	μ	μ	s	μ	μ	μ	μ	s	μ	μ	μ	μ		km	
May	22 57	2.1	−6	3	30	31	5.0	—	—	10	12	2.9	—	—	5	9	345	14.0	
17	21 56	3.1	—	—	3	3	—	—	—	10	8	—	—	—	—	—	—	—	
	42	4.2	—	—	2	2	3.0	—	—	19	23	3.4	—	—	3	2	346	15.7	
	23 01	—	—	—	2	2	—	—	—	—	—	—	—	—	—	—	—	—	
	52	3.1	—	—	8	9	4.2	—	—	32	11	2.6	—	—	3	3	347	15.3	
18	20 47	—	—	—	2	2	—	—	—	—	—	—	—	—	—	—	—	—	
19	9 04	3.6	—	—	3	2	—	—	—	—	—	—	—	—	—	—	—	—	
	14 07	—	—	—	2	2	—	—	—	—	—	—	—	—	—	—	—	—	
	15 57	3.6	—	—	2	2	—	—	—	—	—	3.5	—	—	3	2	—	—	
	21 53	4.0	—	—	2	2	—	—	—	—	—	—	—	—	—	—	—	—	
20	9 12	3.8	—	—	2	1	—	—	—	—	—	—	—	—	—	—	—	—	
	15 12	3.4	—	—	3	2	—	—	—	—	—	3.6	—	—	2	3	—	—	
	16 51	5.8	—	—	5	3	3.0	5	− 5	50	42	4.2	—	—	10	8	348	18.0	
	52	6.2	—	—	7	9	2.5	—	—	163	91	4.3	—	—	7	17	349	9.4	
	19 21	5.8	—	—	6	3	2.2	4	− 3	22	13	5.2	—	—	2	2	350	18.0	
21	9 06	3.0	—	—	2	2	—	—	—	—	—	—	—	—	—	—	—	—	
	14 11	4.0	—	—	2	2	—	—	—	—	—	—	—	—	—	—	—	—	
	15 29	—	—	—	—	—	2.3	—	—	10	8	—	—	—	—	—	—	—	
	39	2.2	—	—	3	3	—	—	—	—	—	—	—	—	—	—	—	—	
	49	—	—	—	2	2	—	—	—	—	—	—	—	—	—	—	—	—	
22	14 21	4.0	—	—	2	2	—	—	—	—	—	—	—	—	—	—	—	—	
	18 35	—	—	—	2	2	2.4	—	—	6	5	3.6	—	—	2	2	—	—	
	21 43	—	—	—	2	2	3.4	—	—	12	17	—	—	—	—	—	—	—	
23	1 36	4.7	—	—	8	20	3.2	14	− 2	100	100	3.4	—	—	17	24	351	17.3	
	55	4.7	—	—	4	4	2.7	3	− 1	17	16	3.3	—	—	5	7	352	12.7	
	55	—	—	—	3	2	—	—	—	10	17	2.9	—	—	3	4	—	—	
	55	—	—	—	3	2	—	—	—	8	7	—	—	—	3	3	—	—	
	12 27	—	—	—	2	2	—	—	—	—	—	—	—	—	—	—	—	—	
	21 46	4.4	—	—	3	3	2.7	—	—	5	5	—	—	—	—	—	—	—	
	22 18	2.4	—	—	5	4	5.1	—	—	10	7	2.8	—	—	3	4	353	16·3	
24	21 08	6.0	—	—	6	6	3.2	−10	− 6	100	84	4.7	—	—	8	8	354	13.0	
	08	—	—	—	5	4	—	—	—	24	33	—	—	—	3	3	—	—	
	23 01	6.0	—	—	2	2	2.1	—	—	13	15	5.2	—	—	3	2	355	16.0	
25	3 27	3.2	—	—	3	2	4.1	—	—	5	5	3.1	—	—	3	4	356	16.9	
	14 54	—	—	—	2	2	—	—	—	—	—	3.6	—	—	2	2	—	—	

			57	2.9	—	—	—	11	—	—	—	—	—	3.7	—	—	2	4	—	—
		16	07	3.1	—	—	—	3	—	—	—	—	—	3.6	—	—	4	5	—	—
	26	8	25	—	—	—	2	2	—	—	—	—	—	—	—	—	—	—	—	—
			36	5.0	—	—	3	2	—	—	—	—	—	4.2	—	—	2	2	—	—
		13	37	—	—	—	2	2	—	—	—	—	—	3.6	—	—	3	5	—	—
			—	—	—	—	—	—	—	—	—	—	—	—	—	—	—	—	—	—
	27	1	00	3.5	—	—	2	3	—	—	—	—	—	—	—	—	—	—	—	—
		6	34	6.0	—	—	2	2	1.1	2	-1	43	19	5.3	—	—	3	7	357	9.0
		11	15	3.9	-1	1	3	3	3.4	—	—	10	10	3.6	—	—	6	8	358	16.4
		17	35	5.9	—	—	4	3	1.3	—	—	31	18	5.0	—	—	3	3	359	9.4
	28	1	41	4.0	—	—	3	3	3.2	—	—	6	6	3.8	—	—	2	1	360	16.6
	29	1	30	6.1	-3	1	6	5	1.1	-10	0	477	222	5.0	-13	2	10	12	361	7.7
			30	3.4	-5	-3	13	9	3.5	4	-2	24	21	3.8	—	—	5	7	362	13.3
		4	32	5.9	-4	3	19	21	1.1	57	0	>1000	780	5.6	—	—	43	48	363	4.0
		12	06	—	—	—	2	2	2.3	—	—	14	12	—	—	—	—	—	—	—
			16	—	—	—	1	1	—	—	—	—	—	—	—	—	—	—	—	—
	30	6	35	3.0	—	—	10	10	4.2	—	—	4	3	—	—	—	—	—	—	—
		10	05	—	—	—	—	—	—	—	—	—	—	—	—	—	—	—	—	—
		11	23	—	—	—	—	—	1.6	—	—	22	20	—	—	—	—	—	—	—
			25	—	—	—	—	—	1.5	—	—	20	20	—	—	—	—	—	—	—
	31	14	28	4.2	—	—	2	2	—	—	—	—	—	—	—	—	—	—	—	—
			52	—	—	—	2	2	—	—	—	—	—	—	—	—	—	—	—	—
June	1	3	45	4.0	—	—	3	2	3.0	—	—	5	5	—	—	—	—	—	—	—
	2	0	02	4.2	—	—	4	4	3.2	—	—	5	5	3.6	—	—	2	3	—	—
		22	34	2.8	—	—	4	3	—	—	—	—	—	—	—	—	—	—	—	—
	3	5	12	3.0	—	—	2	2	—	—	—	—	—	—	—	—	—	—	—	—
	4	5	15	2.6	—	—	4	4	—	—	—	—	—	4.3	—	—	3	3	—	—
	5	7	10	5.0	—	—	3	2	—	—	—	—	—	—	—	—	—	—	—	—
		11	26	3.2	—	—	3	2	4.0	—	—	25	13	—	—	—	2	3	—	—
	6	5	07	—	—	—	2	2	—	—	—	—	—	—	—	—	—	—	—	—
		9	12	6.0	—	—	11	6	2.6	-13	13	113	90	4.8	—	—	9	14	364	20.7
		10	45	4.4	—	—	8	6	3.2	—	—	16	18	3.7	—	—	9	5	365	16.5
		12	08	4.5	—	—	3	3	3.4	—	—	—	—	3.9	—	—	2	3	—	—
	7	3	12	4.9	-5	0	8	12	2.9	15	-10	48	20	4.3	—	—	11	50	366	19.0
	8	8	03	—	—	—	2	2	2.8	—	—	2	—	—	—	—	—	—	—	—
		12	25	—	—	—	—	—	2.3	—	—	3	3	—	—	—	—	—	—	—
	29	3	32	4.2	—	—	9	10	—	—	—	—	—	3.5	—	—	2	2	—	—
		9	28	3.6	—	—	6	4	—	—	—	—	—	—	—	—	—	—	—	—
			54	4.0	—	—	5	6	—	—	—	—	—	3.7	—	—	10	12	—	—
July	1	7	10	3.0	—	—	2	1	—	—	—	—	—	—	—	—	—	—	—	—
		22	38	—	—	—	—	—	2.2	—	—	10	8	—	—	—	—	—	—	—
	2	0	27	6 4	-3	1	5	6	3.0	13	-5	146	272	5.7	—	—	6	7	381	25.0

日時 Time of Occurrence		舞鶴 (Maiduru)					城崎 (Kinosaki)					伊根 (Ine)					震央 Epi-centre	震原の深さ Focal Depth	摘要 Remark
		初微	初動 Init. Mot.		最大動 Max. 2A		初微	初動 Init. Mot.		最大動 Max. 2A		初微	初動 Init. Mot.		最大動 Max. 2A				
		Pre. tr.	E.W.	N.S.	F.W.	S.N.	Pre. tr.	E.W.	N.S.	E.W.	N.8.	Pre. tr.	E.W.	N.S.	E.W.	N.S.			
	hm	s	μ	μ	μ	μ	s	μ	μ	μ	μ	s	μ	μ	μ	μ		km	
	19 16	—	—	—	—	—	3.1	—	—	11	12	—	—	—	—	—	—	—	
4	4 42	5.4	—	—	7	9	2.1	3	−3	26	63	4.9	—	—	10	12	382	16.0	Near Wadayama
5	0 54	8.6	−4	−3	37	31	9.3	8	8	92	66	10.0	—	—	23	15	—	—	
	23 50	3.5	−6	2	25	15	3.6	11	—	14	5	3.2	—	—	12	10	383	11.7	
6	3 05	3.8	−3	1	26	10	2.9	—	—	21	11	3.0	—	—	3	5	384	11.3	
	6 41	4.5	—	—	2	2	3.2	—	—	15	10	5.3	—	—	3	4	385	11.6	
	10 11	—	—	—	2	2	—	—	—	—	—	—	—	—	—	—	—	—	
	11 14	—	—	—	2	2	—	—	—	—	—	—	—	—	—	—	—	—	
7	5 24	2.4	−2	1	8	5	5.3	—	—	4	4	2.7	—	—	2	3	386	16.6	
	34	5.1	5	−5	23	12	2.7	48	15	264	91	4.1	−5	3	148	230	387	18.2	
	17 42	2.3	−3	2	17	20	4.9	—	—	33	22	2.8	—	—	7	9	388	14.8	
8	21 40	—	—	—	2	2	—	—	—	—	—	—	—	—	—	—	—	—	
9	4 38	3.6	—	—	2	2	—	—	—	—	—	—	—	—	—	—	—	—	
	22 14	2.6	—	—	2	2	—	—	—	2	4	2.8	—	—	3	3	—	—	
10	14 33	—	—	—	—	—	—	—	—	—	—	3.7	—	—	2	3	—	—	
11	17 09	—	—	—	2	2	—	—	—	—	—	—	—	—	—	—	—	—	
	22 37	5.0	−1	—	15	15	4.4	—	—	19	22	3.3	−12	5	65	12	389	22.0	
12	13 24	8.0	—	—	2	2	8.7	—	—	3	5	—	—	—	—	—	—	—	
13	0 46	5.0	—	—	3	3	—	—	—	—	—	4.8	—	—	2	3	—	—	
	1 02	5.5	−1	—	7	6	4.4	—	—	10	12	3.5	—	—	13	20	390	22.0	
14	5 53	—	—	—	2	2	—	—	—	—	—	—	—	—	—	—	—	—	
15	0 59	3.9	—	—	4	3	—	—	—	—	—	—	—	—	—	—	—	—	
	4 56	7.8	—	—	3	3	—	—	—	—	—	—	—	—	—	—	—	—	
	6 00	3.2	—	—	3	3	—	—	—	—	—	—	—	—	—	—	—	—	
16	12 28	6.9	—	—	5	3	3.9	—	—	—	—	6.2	—	—	2	3	391	32.0	
17	5 51	—	—	—	—	—	—	—	—	—	—	—	—	—	—	—	—	—	
18	22 26	—	—	—	6	3	—	—	—	—	—	3.4	—	—	7	7	—	—	
19	3 13	—	—	—	2	2	—	—	—	—	—	3.7	—	—	2	2	—	—	
	16	—	—	—	—	—	—	—	—	—	—	—	—	—	2	2	—	—	
20	7 20	6.9	—	—	3	3	3.9	—	—	—	—	6.2	—	—	5	4	292	32.0	
21	0 57	4.3	—	—	3	3	2.6	—	—	47	26	3.5	—	—	3	4	393	13.1	
	51	4.4	—	—	3	2	3.4	—	—	35	17	4.0	—	—	5	5	367	20.8	
9	7 58	3.4	—	—	4	3	3.8	—	—	15	10	3.2	—	—	2	4	368	16.5	
	19 24	3.3	—	—	3	2	4.0	—	—	23	19	—	—	—	—	—	—	—	
10	1 21	—	—	—	2	1	4.0	—	—	8	5	—	—	—	—	—	—	—	

	15 52	—	—	—	2	2	—	—	—	—	—	—	—	—	—	—	—	—
11	3 35	5.0	—	—	4	3	3.4	—	—	81	70	4.3	—	—	10	10	369	23.5
	5 14	—	—	—	2	2	—	—	—	—	—	—	—	—	—	—	—	—
	8 52	4.0	—	—	7	10	—	—	—	—	—	3.2	−2	−2	12	14	—	—
13	4 03	3.8	—	—	4	3	3.2	—	—	14	10	3,1	—	—	4	6	370	14.0
	21 48	6.0	—	—	3	3	2 7	—	—	10	15	—	—	—	—	—	—	—
14	2 46	4.2	−1	1	12	11	3.2	—	—	44	32	4.7	—	—	5	9	371	14.5
	10 16	—	—	—	—	—	2.8	—	—	4	5	—	—	—	—	—	—	—
15	3 06	2.8	—	—	7	4	3.6	3	−2	5	5	3.6	—	—	5	6	372	7.8
	8 28	5.9	—	—	2	2	3.8	—	—	12	10	3.9	—	—	3	5	373	18.6
16	14 33	1.8	—	—	5	4	5.0	—	—	3	2	—	—	—	—	—	—	—
17	7 02	5.5	—	—	2	2	—	—	—	—	—	—	—	—	—	—	—	—
	18 30	3.4	−6	2	21	8	3.6	8	−6	40	21	3.1	—	—	8	23	374	15.0
18	2 50	—	—	—	—	—	2.3	—	—	2	2	—	—	—	—	—	—	—
	7 02	4.7	−2	4	11	9	2.6	—	—	8	7	3.7	—	—	10	30	375	15.0
	16 01	—	—	—	2	2	2.5	—	—	35	19	—	—	—	—	—	—	—
19	5 53	—	—	—	—	—	—	—	—	—	—	3.7	—	—	15	20	—	—
	18 33	2.7	−2	1	31	28	4.5	—	—	22	23	3.6	—	—	10	15	376	15.9
	20 04	—	—	—	2	2	—	—	—	—	—	—	—	—	—	—	—	—
	21 24	4.1	—	—	3	3	3.2	4	−5	25	15	3.9	—	—	7	10	377	19.8
	23 29	—	—	—	2	2	—	—	—	—	—	—	—	—	—	—	—	—
20	1 37	—	—	—	—	—	—	—	—	—	—	—	—	—	—	—	—	—
	9 56	—	—	—	2	2	3.2	—	—	10	8	4.0	—	—	4	5	—	—
21	14 27	—	—	—	—	—	—	—	—	—	—	—	—	—	—	—	—	—
22	10 33	3.5	—	—	20	18	3.5	10	−7	42	20	3.9	—	—	10	8	378	15.0
24	19 42	6.0	−1	1	7	6	2.9	4	0	117	62	3.8	—	—	15	12	379	7.0
	23 22	—	—	—	2	2	2.0	—	—	13	4	—	—	—	—	—	—	—
25	15 04	4.2	—	—	—	—	4.1	—	—	10	20	—	—	—	—	—	—	—
	17 02	—	—	—	2	2	4.0	—	—	27	12	—	—	—	—	—	—	—
	20 19	5.8	—	—	4	3	3.7	—	—	23	40	3.2	—	—	26	72	380	0
26	7 37	—	—	—	—	—	4.0	—	—	5	6	—	—	—	—	—	—	—
	22 58	—	—	—	—	—	—	—	—	3	3	—	—	—	—	—	—	—
27	14 25	3.5	—	—	3	3	—	—	—	—	—	—	—	—	—	—	—	—
	12 37	4.3	−30	15	20	20	2.7	35	−18	315	200	3.6	8	−4	32	138	394	14.3
23	1 48	3.3	—	—	4	2	3.8	—	—	8	5	—	—	—	3	5	—	—
	2 28	—	—	—	2	2	3.2	—	—	5	2	—	—	—	2	3	—	—
	7 08	4.6	—	—	3	2	2.6	—	—	19	16	3.6	—	—	2	3	395	14.0
24	9 23	2.8	− 2	1	25	23	4.7	—	—	13	9	2.7	—	—	12	12	396	16.9
	10 22	—	—	—	2	2	3.5	—	—	10	8	4.3	—	—	3	4	—	—
	12 24	2.8	—	—	5	5	4.7	—	—	5	6	2.7	—	—	3	5	397	16.9
	13 55	3.6	—	—	4	4	3.6	—	—	12	6	4.0	—	—	3	6	398	16.3
25	8 17	—	—	—	2	2	—	—	—	—	—	—	—	—	—	—	—	—

日時 Time of Occurrence		舞鶴 (Maiduru)					城崎 (Kinosaki)					伊根 (Ine)					震央 Epi-centre	震原の深さ Focal Depth	摘要 Remark
		初微	初動 Init.		最大動 Max. 2A		初微	初動 Init.		最大動 Max. 2A		初微	初動 Init.		最大動 Max. 2A				
		Pre. tr.	E.W.	N.S.	E.W.	N.S.	Pre. tr.	E.W.	N.S.	E.W.	N.S.	Pre. tr.	E.W.	N.S.	E.W.	N.S.			
	h m	s	μ	μ	μ	μ	s	μ	μ	μ	μ	s	μ	μ	μ	μ		km	
	17 40	3.7	—	—	3	2	3.5	—	—	29	12	—	—	—	—	—	—	—	
	19 45	—	—	—	2	2	—	—	—	—	—	—	—	—	—	—	—	—	
28	1 00	—	—	—	—	—	—	—	—	4	4	—	—	—	—	—	—	—	
30	3 07	3.7	—	—	13	10	3.8	—	—	10	5	—	—	—	—	—	—	—	
	12 17	3.6	—	—	3	2	3.5	—	—	7	6	—	—	—	—	—	—	—	
31	4 09	4.0	—	—	4	2	2.8	—	—	10	12	—	—	—	—	—	—	—	
	7 56	5.1	− 1	2	8	7	—	—	—	—	—	—	—	—	—	—	—	—	
Aug. 1	23 50	4.6	—	—	6	7	2.7	—	—	25	20	—	—	—	—	—	—	—	
3	0 24	—	—	—	2	2	—	—	—	2	3	—	—	—	—	—	—	—	
	13 11	—	—	—	3	3	—	—	—	—	—	—	—	—	—	—	—	—	
	18 53	—	—	—	2	2	3.2	—	—	20	17	—	—	—	—	—	—	—	
4	7 38	4.2	− 4	2	9	8	2.8	2	− 5	32	19	4.4	—	—	5	7	399	13.4	
5	11 44	4.3	—	—	10	6	3.0	16	−11	108	47	3.3	—	—	35	33	400	15.2	
	21 40	5.1	−15	12	153	86	2.6	240	67	>1000	988	4.4	−54	13	590	200	401	18.4	
	22 19	7.3	—	—	3	2	2.3	—	—	8	6	—	—	—	2	3	—	—	
	23 26	3.6	—	—	2	2	—	—	—	—	—	—	—	—	2	2	—	—	
6	10 56	—	—	—	—	—	3.4	—	—	9	5	—	—	—	—	—	—	—	
	13 31	5.1	—	—	2	2	2.6	—	—	19	34	3.3	—	—	2	2	402	9.0	
	16 26	—	—	—	2	1	1.0	—	—	80	30	—	—	—	—	—	—	—	
7	0 21	3.4	− 2	1	14	16	3.3	—	—	59	22	3.4	—	—	9	12	403	12.8	
	31	3.3	—	—	7	4	—	—	—	10	10	4.0	—	—	2	3	—	—	
	19 39	1.6	—	—	20	13	6.3	—	—	6	7	2.9	—	—	3	5	404	12.8	
8	23 02	—	—	—	2	2	—	—	—	—	—	—	—	—	—	—	—	—	
9	5 45	—	—	—	—	—	—	—	—	—	—	3.0	—	—	4	4	—	—	
10	0 33	4.4	—	—	4	3	3.8	—	—	10	13	3.7	—	—	3	3	405	22.5	
	10 31	4.6	—	—	8	5	4.1	—	—	13	11	3.8	—	—	10	12	406	25·2	
12	10 51	8.9	− 5	2	45	17	8.4	0	6	48	25	—	—	—	—	—	—	—	
	14 07	4.1	—	—	5	5	3.8	—	—	12	10	—	—	—	—	—	—	—	
13	8 26	—	—	—	2	2	4.2	—	—	7	4	—	—	—	—	—	—	—	
	14 13	—	—	—	1	1	—	—	—	5	5	—	—	—	—	—	—	—	
15	22 41	—	—	—	2	2	3.8	—	—	19	15	3.6	—	—	2	4	—	—	
16	23 25	8.5	− 1	0	18	8	9.1	0	4	53	33	11.0	—	—	10	13	—	—	
17	12 13	—	—	—	—	—	2.6	—	—	5	5	—	—	—	—	—	—	—	
18	7 24	—	—	—	—	—	3.2	—	—	10	13	—	—	—	—	—	—	—	
19	12 45	5.4	—	—	28	21	2.7	−16	12	381	212	4.6	4	0	17	16	407	19.7	

	23 02	3.0	—	—	3	3	3.9	—	—	12	7	3.9	—	—	5	5	408	12.2
20	15 19	—	—	—	—	—	3.3	—	—	6	13	—	—	—	—	—	—	—
22	13 58	—	—	—	—	—	3.0	—	—	16	10	—	—	—	—	—	—	—
23	19 02	4.3	—	—	5	3	2.7	—	—	62	37	3.2	—	—	9	9	409	12·0
24	5 50	—	—	—	—	—	3.0	—	—	9	14	—	—	—	—	—	—	—
28	9 57	3·1	—	—	11	9	—	—	—	8	3	—	—	—	—	—	—	—
	16 28	4.0	—	—	5	3	3.2	—	—	12	10	—	—	—	—	—	—	—
30	23 03	4.0	—	—	3	2	3.2	—	—	37	17	3.7	—	—	4	5	410	11.8

第 一 圖　四月一日十四時四十九分及七月二十二日十二時三十七分頃の餘震の記象（舞鶴の記象中初動 P の比較的大なるを示す）

April 1, $14^h\ 49^m$ (A, B, C)　　July 22, $12^h\ 37^m$ (A', B', C')

Maiduru Observation

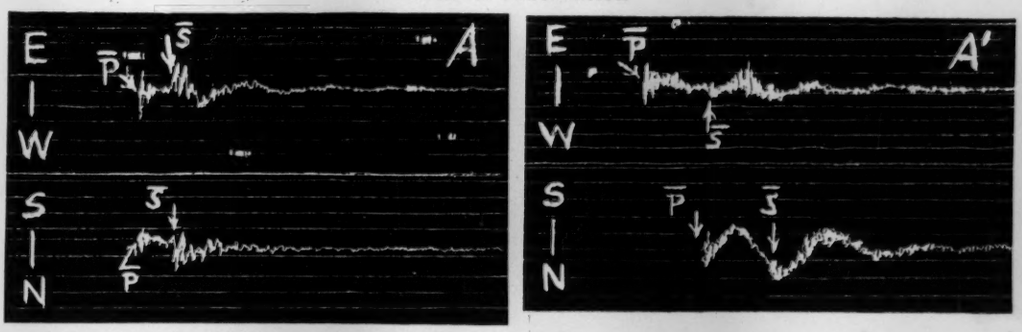

Inemura Observation

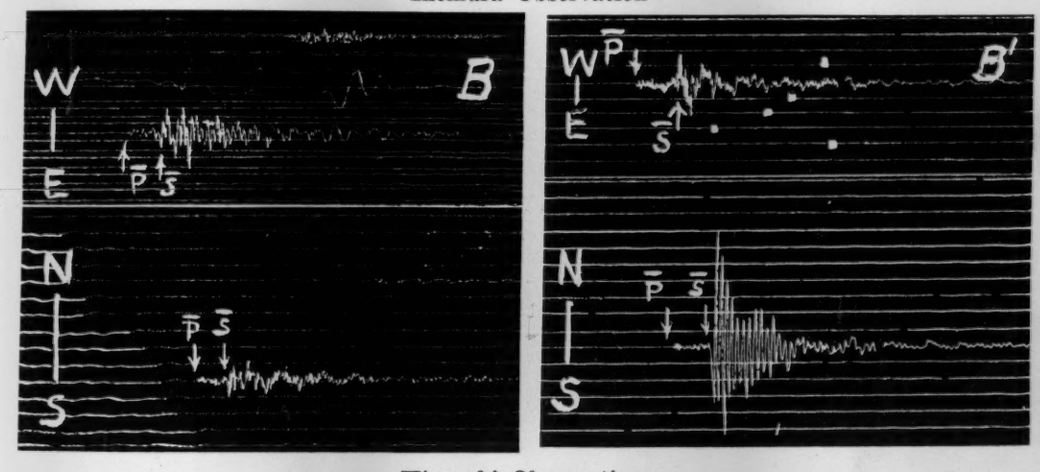

Kinosaki Observation

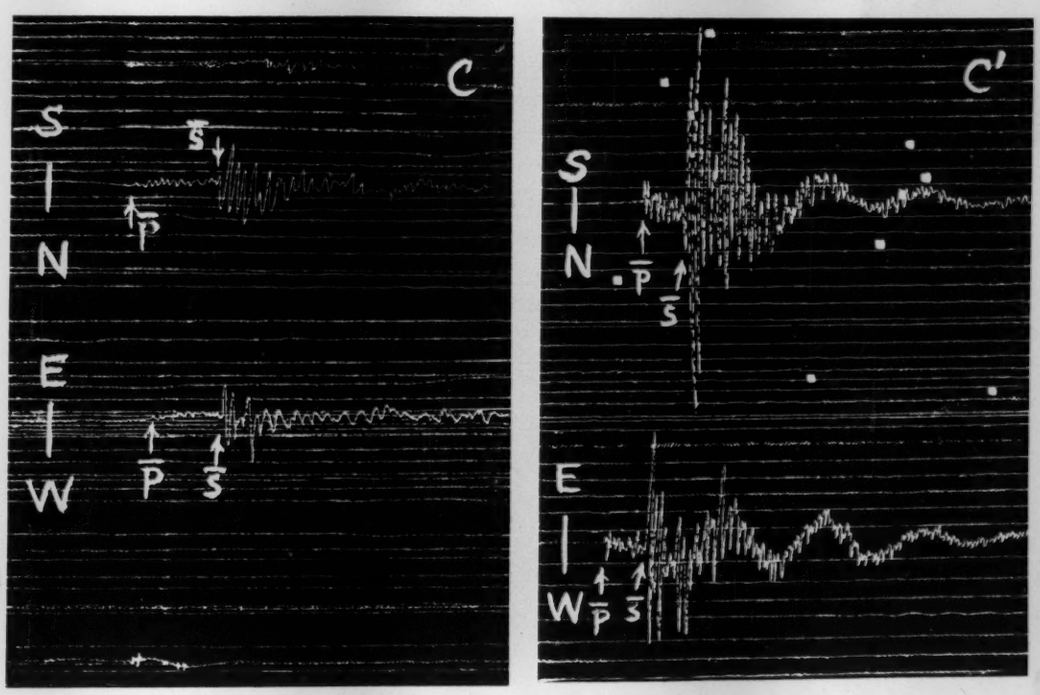

Fig. 1. Seismograms of the aftershocks of April 1, $14^h\ 49^m$ and July 22, $12^h\ 37^m$.
(Notice the initial phase pronounced in Maiduru Observations.)

（震研彙報、第六號、圖版、那須）

A Long Period Fluctuation in Latitude of the Seismic Activity on the Earth.(1)

By **Torahiko TERADA** and **Naomi MIYABE,**

地球上に於ける地震活動地域平均緯度の長期移動

所員　寺田寅彦
同　宮部直巳

地球上に於ける顯著地震の年表から、毎五十年間に起つた地震の地域の緯度の平均値を概算して、其の値の永年變化を調べて見た。此の統計を歐洲大陸、北米、中米、南米、支那、日本等に就き別々に行つて其結果を比較した。

第一圖に示した結果から、勿論餘り確實ではないが、大體次のやうな事が推測される。卽ち、活動地域の平均緯度には二百年前後の程度の長週期をもつた移動がありさうに見える。而して各地方別の變化に多少の相關があるらしいから、此の週期は全然偶然の結果として棄てる事は出來ない。のみならず又上記の結果を、例へば地球自轉速度の永年變化と比較して見ると、多少の相關があるらしく見えるから、此處で想像された地震活動の緯度變化といふ現象には相當なプロバビリチーのあるものと考へなければならない。他のあらゆる方面からの研究を希望したい。

Many investigations have hitherto been made regarding the problem of periodicity of earthquakes. For the most part, however, the periodicity investigated is that of the variation of the frequency of earthquakes as a function of time, while the research concerning the time relation of displacement of seismic activity on the earth has been rarely made. Prof. Omori alluded, indeed, sometimes to an irregular fluctuation in the positions of the epicentres of severe earthquakes occurring successively on a distinct active zone, though he arrived at no definite conclusion on its periodicity. N. F. Drake from his investigation of Chinese earthquakes suggested the existence of a periodic displacement of the activity with a

(1) An abstract of the present note has already been given in Proc. Imp. Acad., 3 (1927), 275; the data have been revised and some correction made for the missed data.

period of about 600 years. His method is, however, connected with the problem of bringing into alignment numerous points scattered on a plane which is often liable to some arbitrary choice. Still, the possibility of such a periodic or irregularly cyclic displacement of the locality frequented by earthquake may scarcely be denied especially by those who have ever made some study on the chronological distribution of earthquakes. The "period" may well be irregular and there may coexist many periods, some long and other short.

Recently, we became incidentally aware of a rather remarkable fact that the epicentres of the following seven destructive earthquakes lie on a nearly straight line inclined about 10° against the parallel of latitude somewhere about 35°N:

Mino-Owari	1891	Kwantô	Sept. 2, 1923
Anegawa	1909	Tazima	1925
Ooigawa	1917	Tango	1927
Kwantô	Sept. 1, 1923		

As a matter of fact, a number of earthquakes are recorded in other parts of Japan during the course of the period above taken, so that the above fact alone may convey no physical significance. Again, on looking a little back in the chronological lists we find the epicentres of the following five severe earthquakes lying on a line, inclined about 20° against the parallel of latitude about one degree, to the north of the former line:

Kanazawa	1799	Sinano	1858
Zenkôzi	1847	Noto	1892
Tôkyô (Yedo)	1855		

Here also, earthquakes in other districts are not wanting in the same epoch, so that just the same objection may be raised here as in the case of Drake's method regarding the physical meaning of the alignment.

The above relation, accidental or not, was at least stimulating and suggested another method of a further study which may give some more insight into the problem. For a trial, we took the chronological lists

compiled by Prof. Imamura and published in "Rika-Nenpyô", 1927, whence all the most severe earthquakes[1] in the Eurasian continent were picked up, which occurred in 1900–26. For these earthquakes we estimated the approximate respective latitudes of the epicentres. As, in many cases, the accurate location of the epicentre is difficult even within a range of few degrees, the latitude evaluated may have generally no meaning other than a kind of very rough index number. We may perhaps have better rounded off the number to each five or ten degree. It is needless to say that the latitudes thus found for a given epoch are widely scattered in values; still, on plotting all the earthquakes in 1900–26 upon a latitude scale, we may remark a conspicuous clustering of the point at about 40°N. On the other hand, a similar statistics was carried out for the preceding epoch 1800–1900 and a maximum of frequency was found at about 35°N. As the conspicuous earthquakes in the Eurasian continents occurs mostly in the well known zone running E–W, the above change in latitude of the zone of maximum frequency may at least suggest an actual secular displacement of the most active zone from N to S in the said succeeding epochs.

The above result led us to take a step further and to investigate the secular fluctuation of the "mean latitudes of earthquakes," in the above sense of the words, and those for different parts of the earth separately. If the time-variation of this mean would show an apparent periodic fluctuation, the *possibility* of such period may be demonstrated. If, again, the fluctuation in different parts of the earth would show some correlation the reality of such a period may appear in some degree *probable*. If, on the other hand, the said fluctuation may show some similarity with the fluctuation of other cosmical phenomena which may theoretically be in some direct or indirect physical relation with the occurrence of earthquake, the probability may be more or less increased. Of course, it is difficult to draw from this kind of investigation any conclusion on the real nature of the fluctuation thus obtained, but it may at least reveal a faint image, so to speak, of what is actually taking place with regard to the secular dis-

(1) Those were chosen of which more than 1000 casualities are reported. The arbitrary choice may be of some use in the present case of statistical investigation.

placement of the zone of activity, provided such thing exists. With these stand points clearly in view, the following may, we hope, be of some interest for many seismologists.

The materials for the further systematic investigation were also taken from the Lists above mentioned. The number of earthquakes recorded decreases necessarily as we go back with the date and, besides, the extent of the geographical area finding entry may also vary with time. All these difficulties are unavoidable, but must and may be taken as they are, when a rough investigation of some gross periodicity is in question, provided the said historical variation in the statistical basis is for the first approximation a continuous one, which may plausibly be assumed.

For the case of Eurasian continent the number of occurrence was large so that we could carry out the separate statistics for the "most

Fig. 1 a.

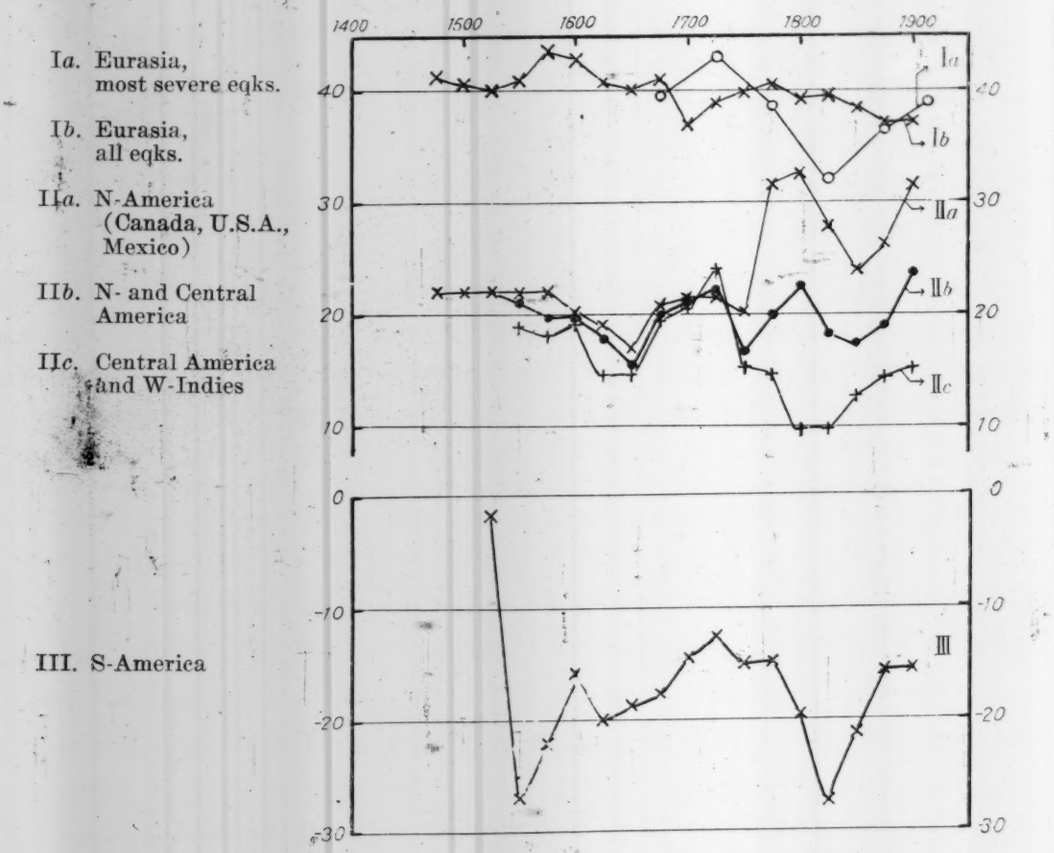

Ia. Eurasia, most severe eqks.

Ib. Eurasia, all eqks.

IIa. N-America (Canada, U.S.A., Mexico)

IIb. N- and Central America

IIc. Central America and W-Indies

III. S-America

Fig. 1 b.

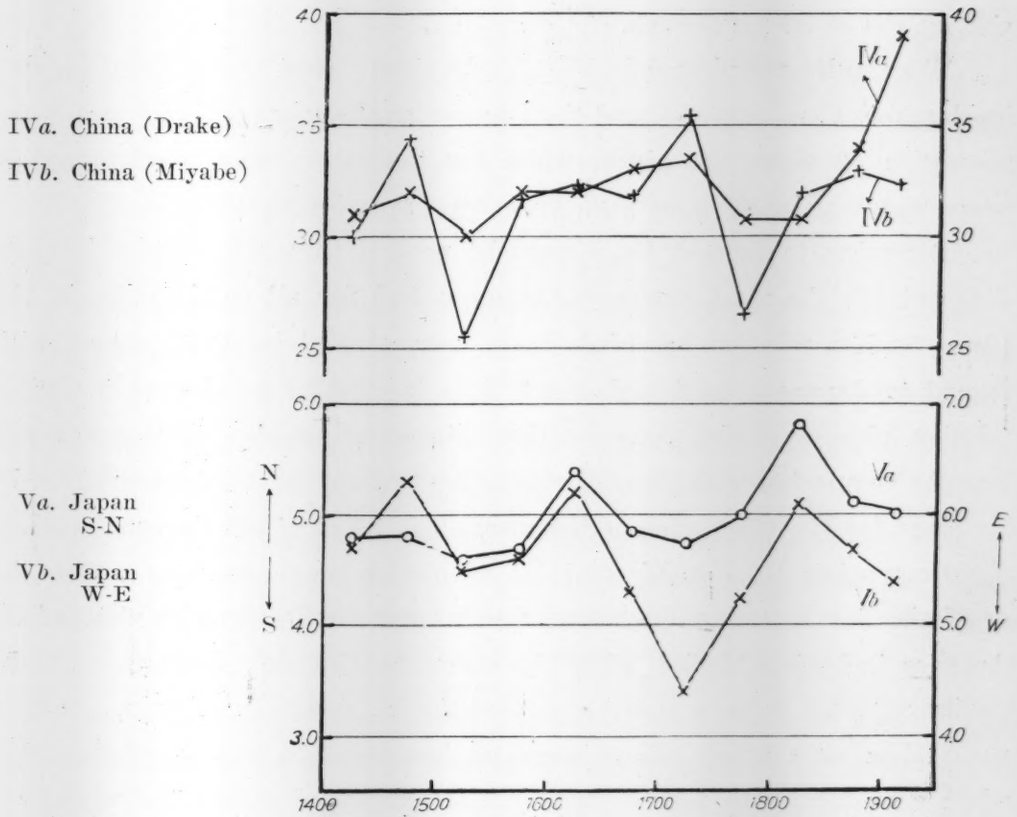

severe earthquakes'' side by side with that for all the earthquakes recorded in the List.[1]

For the other parts of the earth, the following divisions were made:

North America including Mexico.

North America, Mexico and Central America.

Central America and West Indies.

South America.

The data for Chinese earthquakes were taken directly from Drake's paper in which the chronological sequence of earthquakes in separate Provinces are tabulated. We estimated roughly the latitude of the centre of area

(1) The earthquake which occurred within ten years after a severe earthquake in the same district was omitted in the present statistics.

of each Province and then calculated the mean latitude of foci for successive epochs of 50 years each.

The results are plotted in Fig. 1. For the "most severe" earthquakes in Eurasian Continent, I*a*, and the Chinese earthquakes, IV, the means for successive 50 years are given, while for the other cases overlapping 50 years means proceeding with 25 years step are plotted.

Referring to I*a* and I*b*, it may be noticed that the relation is quite different for the most severe earthquakes and for all earthquakes in the List. Such a relation has often been demonstrated by Prof. Omori with regard to Japanese earthquakes and it is interesting to observe a similar relation also appearing here in the data covering the whole continent. For the comparion with the different other regions we must therefore take I*b*, since for the other regions the means are taken of all the earthquakes.

Comparing I*b*, II*a*, II*c* and III with each other, we may notice the graph I*b* for Eurasian Continent shows some similarity with that of N. America including Mexico, while the curve for Central America and West Indies suggests a parallelism with that for S. America. Again, the first pair taken as a whole shows more or less reversed course of variation when compared with the latter pair. II*b* shows of course the mixed influence of II*a* and II*c*. Taking all the curves together a period of some 200 years may be suspected.

Curve IV for Chinese earthquakes shows more resemblance with I*a* or III than with I*b* with which it may be expected to be related. The matter is, therefore, not simple even if the suspected periodicity be real. Still, it may be well possible that a part of continent show an alternative time variation with the entire continent.

On the other hand, a somewhat different method of estimating the variation in position of activity was chosen for the case of historical earthquakes in Japan, which was found most suitable in view of the nature of the data at hand. Thus, the entire region was divided into a net of longitude and latitude with 2.5° mesh. The meshes were numbered 1–10 northwards from 25°N. and 1–8 eastwards from 125°E. This number was taken as an index number for roughly determining the latitude or longitude

of each epicentrum and the mean index number was calculated for each 50 years period. The results are shown in Curves V*a* and *b*.[1] The curves suggest again a period of 150–200 years. Comparing I*b* and V*a* we notice that the Japanese earthquake activity is rather sympathetic with the continental.[2]

Apparent parallelism between V*a* and V*b* may be mainly due to the fact that the Islands of Japan is elongated in the direction SW–NE. On the other hand, one of the authors, N. Miyabe, made an investigation[3] of the fluctuation in position of destructive earthquakes in China, taking the material from the Lists given in "Rika-Nenpyô" as IV*b*. The curve for the latitude-variation obtained shows some similar feature with IV*a* based on Drake's data as is expected. On the other hand, the latitude variation (Fig. 1, IV*b*) obtained by Miyabe shows some remarkable positive correlation with the longitude variation, a fact which means that in China also the displacement of the activity occurs in the direction SW–NE. Moreover, Miyabe's graphs for the latitude and latitude variations in China show some points of agreement with those for Japan. Miyabe also showed that the variation in the frequency of earthquakes shows inverted course for N. and S. China which is in accord with the fact of the latitude variation.

The fluctuations of the mean latitude of seismic activity above described are rather irregular and it will be premature to draw any definite conclusion from such a material. It may, however, not be also denied that there are some points of regularity among these variations. Especially, the parallelism among I*b*, II*a* and V*a* and the inverted course of III may not be hastily passed over as merely accidental, as the former refers to the N. hemisphere while the latter stands for the S. hemisphere.

Leaving the result of statistics as it is, we may now seek after a similar

(1) In Fig. given in the abstract published in Proc. Imp. Acad., loc. cit., the numbers on the right side of the curves are wrong; 4, 5, 6 are to be read 7, 6, 5 for S-N and 6, 5, 4 for W-E direction. The present Fig. is inverted so that N is on the upper side.

(2) The discrepancy remarked in the abstract cited now disappears when we take I*b* for comparion, which is more plausible than I*a* to take.

(3) N. Miyabe, Proc. Imp. Acad., **3** (1927), 659; here also earthquakes within 10 years occurring in the same district is taken as one.

fluctuation in some geophysical or astronomical phenomena which may be in some physical connection with seismic activity.

Recently, the secular change in the length of day has aroused a revived attention among astronomers.(1) De Sitter(2) explains the secular acceleration and fluctuation in the longitudes of the moon, the sun, Venus and Mercury by some actual change in the change of the moment of inertia of the earth, and tidal friction. We reproduce here, in Fig. 2, his graph

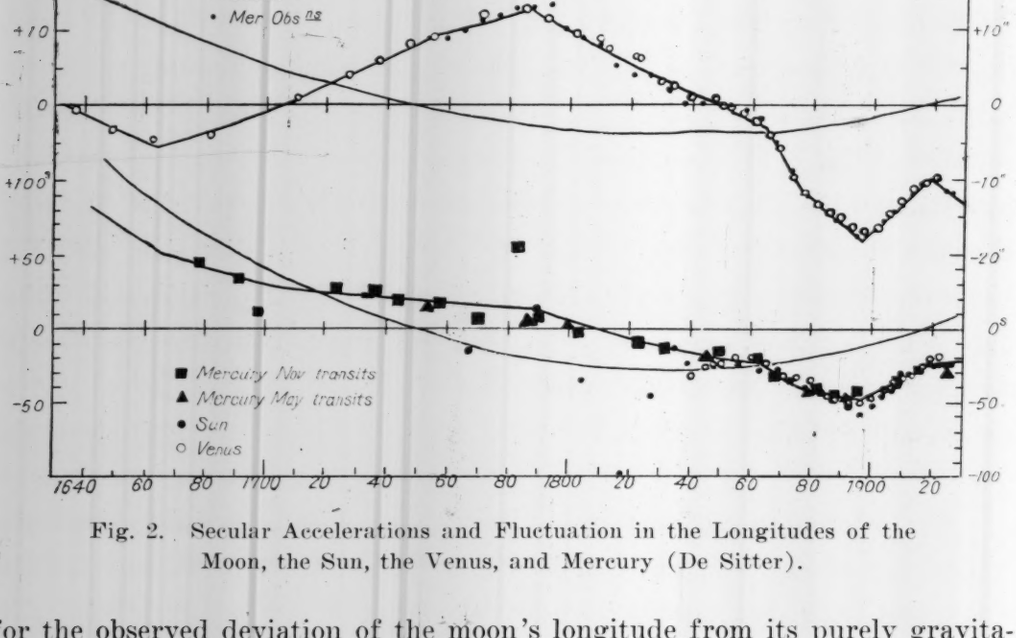

Fig. 2. Secular Accelerations and Fluctuation in the Longitudes of the Moon, the Sun, the Venus, and Mercury (De Sitter).

for the observed deviation of the moon's longitude from its purely gravitational value. The curve shows a conspicuous maximum near 1786 and a minimum at 1897. De Sitter regards the curve as consisting of a series of straight line of which the inclination against the time axis changes sometimes abruptly, corresponding to a sudden change in the length of day.

Comparing Fig. 2 with the graphs given in Fig. 1, we may notice that I*a* and V show some parallelism, while II*c* and III show a roughly inverted

(1) H. Spencer Jones, Monthly Not., **87** (1926), 4; E. W. Brown, Nature, **119** (1927), 200; J. K. Fotheringham, ibid, 318.

(2) W. de Sitter, Nature, **121** (1928), Supplement to No. 3038.

variation (parallel in absolute value of latitude) compared with Fig. 2.

According to De Sitter the maximum and minimum of his curve correspond respectively to some conspicuous increase and decrease in the moment of inertia of the earth. It seems for us more easy to conceive a change in the ellipticity than to assume after him a uniform expansion or shrinkage of an world-wide extent. If the change in ellipticity be chiefly effected by the external crust, while the core is unaffected, the greatest shearing stress will be endured by the intervening plastic "sima" layer near the middle latitude, i.e. at the node of the ellipsoidal deformation. Again, it is highly improbable that such a deformation will not find some expression in the seismic activity of the earth. It is then at least not inconceivable that the change in the ellipticity may in some way be connected with the change in the latitude of the zone thereby placed under the condition favourable for the occurrence of earthquakes. The fact that the curves of Fig. 1, taken as a whole, show a reversed (or similar, in absolute value) course of variation in latitude for the two hemisphere is in some degree favourable for this idea. It will, however, be useless to speculate on the possible mechanism which may give rise to such a kind of correlation between the changes in moment of inertia and the latitude of activity. Still, the relation here pointed out may deserve attention and stimulate a further investigation.

On the other hand, it has been frequently shown that there exists some singular correlation between the frequency of earthquakes and some climatic factor, though the physical meaning of the apparent correlation are for the most cases not clear and for that reason generally regarded with small weight. In our opinion, however, the occurence of earthquakes is physically connected with some meteorological factor, especially with the space and time distribution of atmospheric pressure, as was shown beyond doubt in many respects, especially by the seismologists in this country. On the other hands, all of the climatic factors must theoretically stand in some direct or indirect relation with the barometric pressure. It is well probable that the modes of interrelation are much complicated, so that two factors situated remote from each other in the complicated net-

work of causal connection may reveal a better correlation than some other two which are more closely related in the orders of causal sequence. In view of this consideration, it will not be out of place to compare the secular variation of latitude of earthquake with that of the rate of tree growth, already cited by a previous investigator(1) in an allied problem. Fig. 3*a* and *b* show the rates of growth of *Sequoia washingtoniana* and Arizona pine, the mean values for successive 50 year period being calculated from Douglass's data.(2) Comparing these curves with those in Fig. 1 it may be seen that Fig. 3*a* shows a remarkable parallelism with the curves

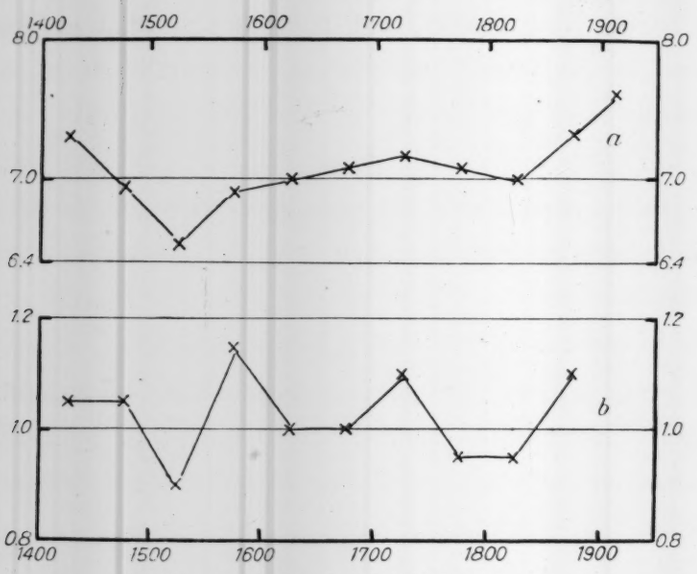

Fig. 3. Tree Growth (Douglass)
(*a*) *Sequoia washingtoniana.*
(*b*) Arizona pine.

for Chinese earthquake, Fig. 1, IV, while Fig. 3*b* has some features common with the variation in position of seismic activity in Japan, V*a* and *b*.

If we tentatively assume that the variation in the seismic activity here concerned is, on one hand, related with the deformation of the earth and, on the other hand, also connected with meteorological factors, we must necessarily admit a possibility of some relation, direct or indirect, between the two latter mentioned phenomena.

(1) H. H. Turner, M. N. R. A. S., **79** (1919), 531; **50** (1920), 617, 793.
(2) E. Huntington, "The Climatic Factor," p. 117, Fig. 20 and p. 327, Table G.

According to De Sitter a general shrinkage of the earth's radius by a few inches is sufficient for explaining the acute change in the length of day as is observed in 1918. In the case of an ellipsoidal deformation, the amount of the necessary change in radius will be somewhat larger, but of the same order of magnitude, as the equatorial zone is predominant. Taking for a rough estimation the case of hydrostatic equilibrium in a meridional canal filled with a liquid with the density of crustal rocks, say 3, a difference of 10 inches in the height of level will correspond to a pressure difference of 56 mm. Hg. As far as the authors are aware of, such a secular transfer of the atmospheric mass between the tropical and arctic zone has not yet been found, though it is well known that the mean or absolute range of variation of annual mean pressure is rather large especially for high latitudes. According to Hann's Handbuch der Meteorologie, the absolute range of January-mean for Paris in an epoch of 120 years amounts to 20.3 mm., which is at least of the same order with the value above calculated. The matter cannot, however, be so simple as here is assumed tentatively. It may suffice here to point out a possibility of actual connections among the phenomena compared statistically. We must wait perhap for a long time, until we can say something more definite about the problem here set forth.

Lastly, it may be pointed ont in passing that if there may exist some physical connection such as is above discussed between the deformation of the crust and some climatic factor, the much disputed problem of the climates in geological ages may be reviewed under a light somewhat different from as usual.

東京帝國大學法學部、文學部及經濟學部講義室鐵骨架構の振動觀測に就いて

内田祥三
齋田時太郎
武藤清

An Investigation of the Vibration of a Steel Frame.

By **Y. UCHIDA, T. SAIDA** and **K. MUTO,**

This Paper describes the result of a vibration test of a steel framing composing a lecture hall of the Tokio Imperial University, carried out in March, 1928. The characteristics of the vibrograph, are as follows:—

Type	Horizontal pendulum
Magnification	30 times
Natural period	1.9 sec. N-S direction.
	2.4 sec. E-W direction.

The periods of the vibrations of the frame found from the vibrograph are as shown below:—

	Frame marked A (Fig. 1) (N-S direction)	Frame marked (Fig. 1) (E-W direction)
The vibration of the first order	0.34 sec.	0.40 sec.
The vibration of the second order	0.15 sec.	0.17 sec.

緒　　言

構造物の固有振動週期は耐震構造上大なる意義を有つものであり、我が國の地震、構造諸學者、構造技術者の等しく重要視せる所である。既に大森博士、今村博士、末廣博士、堀越工學士、齋田理學士、其の他の諸氏が實際の構造物の振動週期を觀測せられたる結果は廣く一般技術者までが興味を以て觀察してゐるのである。本論文は昭和三年三月中旬に行つた東京帝國大學法學部、文學部及經濟學部講義室の鐵骨架構の振動觀測にそいて述ぶるものである。

内田祥三、岸田日出刀、武藤 清

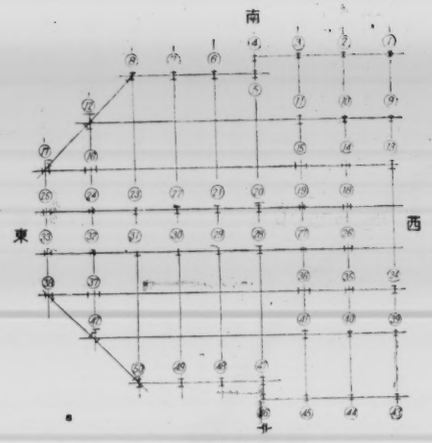

基礎平面圖

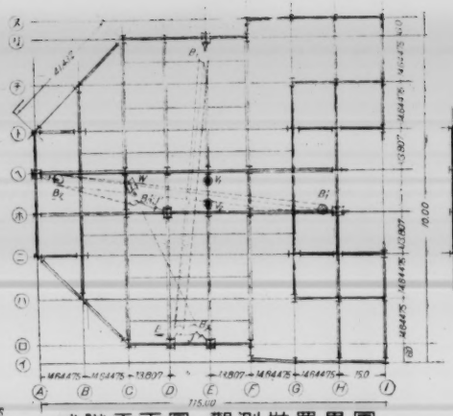

貳階平面圖 觀測裝置略圖

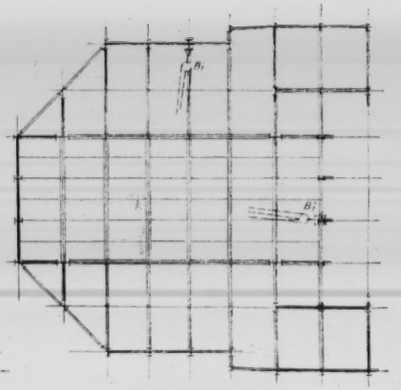

屋根平面圖

鐵骨平面圖

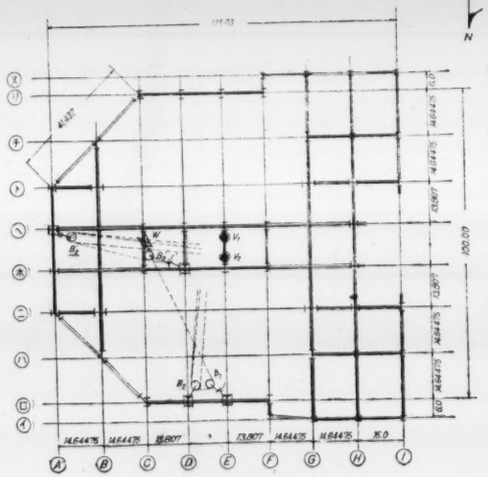

壹階平面圖

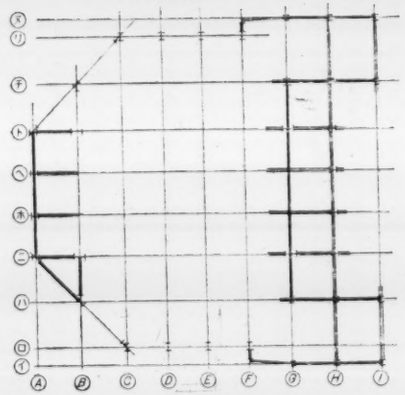

參階平面圖

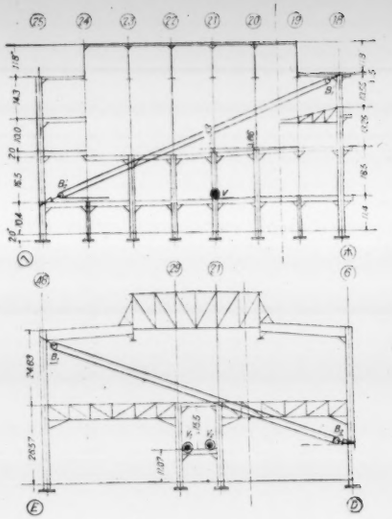

鐵骨縱斷面圖

第一圖　鐵骨立面、平面圖竝に觀測裝置圖

從來の觀測は何れも風或は小震によつて振動せるもの、又は人力によつて振動を與へたものを測定したのであつたが、今回は先づ架構を大規模に引張つて變形を起し、然る後之を突然放して振動せしめ觀測を遂げたのである。その結果從來現れなかつた新なる現象を認め得るに至つた。後に第一次、第二次振動と推論する所のものである。之に關しては、異なる意見を持たるゝ方もあらうし、又觀測方法そのものに就いても更に考慮すべき點なきにもあらずと思はれる。之等に關して同學諸氏の御判斷を得ば最も幸である。

此の觀測に當つて工事を請負つてゐられた大倉土木株式會社が必要な人夫、器具類を寄與せられた事に對し此の機會に於て深く謝意を表するのである。

建築物——鐵骨架構

現在建築中のものは第一圖に示すやうに、その外廓で

東　西　　100 尺

南　北　　112 尺

である。將來更に西側に延びて纏つた建築物となる豫定をもつたものである。高さは地階約 10 尺、第一階約 15 尺、第二階約 24 尺である。第二階は大講堂で、西側には棧敷が出て、特殊な構造になつてゐる。此の鐵骨架構は第一圖に示すやうに可なり不規則な構造である。但し中央部南北方向の架構 D, E, F のみは割合に規則的である。振動の觀則も主として此の架構を目的とした。觀測をなした時は、鐵骨の組立ては終了したのであつたが、屋根トラスの一部分に鋲打の猶終らない所があつたのである。

微動計

觀測には微動計二個を備へたのであるが、その中、良好な結果を記錄せるものは第一圖に示す V_2 であつた。此處にその特性を述べると次のやうである。

形式水平振子式微動計

東京帝國大學工學部建築學教室備品

觀測に使用せる時の

倍　率 ……30

固有振動週期（第二圖參照）東西 …… 1.9 秒

南北 …… 2.4 秒

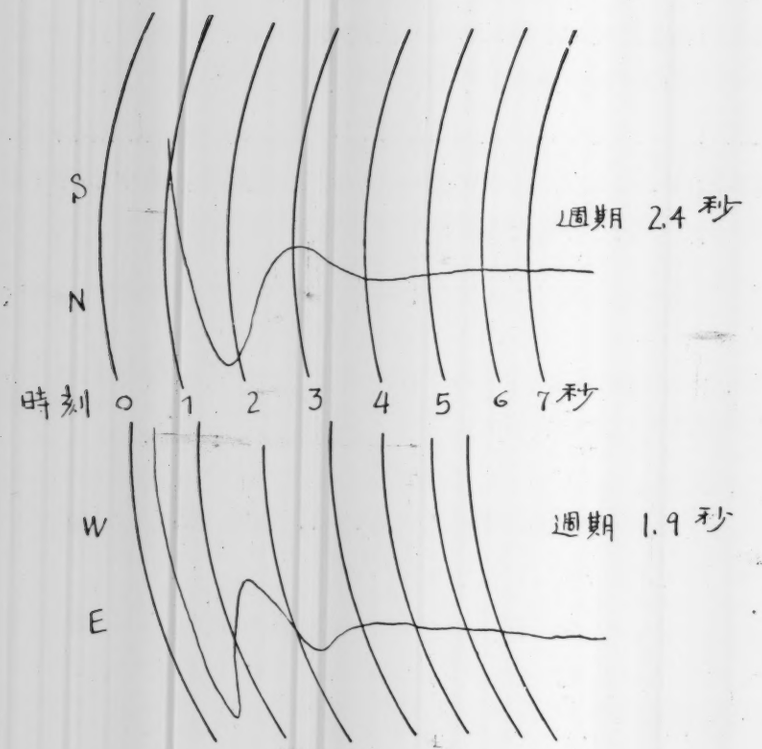

第二圖　微動計 V_2 の固有振動

振動の與へ方

觀測した振動は次の二種である。

第一種 (I)　架構 E を南北に變形せしめて振動を與へたもの、回數　三回。

第二種 (II)　架構 F を東西に變形せしめて振動を與へたもの、回數　一回。

架構に變形を起すためにはウイチを使用した。例へば架構 E を南北に變形せしむるには、第一圖に示すやうに E 柱 6 の屋根と D 柱 49 の第一階床面とに縛着せるブロツク B_1, B_2 とにロープを三回廻し、その端を他のブロツク B_3 を通じてウイチ W に卷いたのである。B_3 と柱 48 とは釣 J を以て引掛け、充分ロープを引張つて後突然釣を外して振動を與へたのである。ウインチは俗に五噸卷と稱するもので人夫五人が之を卷く時にロープ一本につき約一噸の力を出し得る。從つて此の場合には E 架構は約3噸の力がロープの方向に働いたのである。架構木を東西に變形せしめた方針も同樣で第一圖に示す如くである。微動計は柱 29 と 21 とを結ぶ第一階床梁の上に、V_1 は 21 に接し、V_2 は 29 に接して据えたのである。

觀　測　結

觀測の結果を第三、第四圖に示す。第三圖はⅠ即ち架構を南北に變形せしめて放した時の觀測圖である。a は第一回、b は第二回觀測を示す、第四圖は II 即ち架構を東西に變形せしめて放した時の振動記錄を示すのである。

振動圖の分析

第三、第四圖を見るに、その大搖れの部分が微動計の固有振動の現れなる事は明瞭に認められる。從つて架構の自由振動は、之等の記錄から微動計の固有振動を除いたものである。第三圖 a, b の南北動の記錄から微動計の固有振動を除く時は、第五圖 (1) の如くになる。第四圖及び第三圖 b の東西動に就いても同樣の操作をなすに第六圖 (1) の如くになる。

之等を視るに、何れに於ても主要な二つの單弦振動が共存せる事が認められる。之

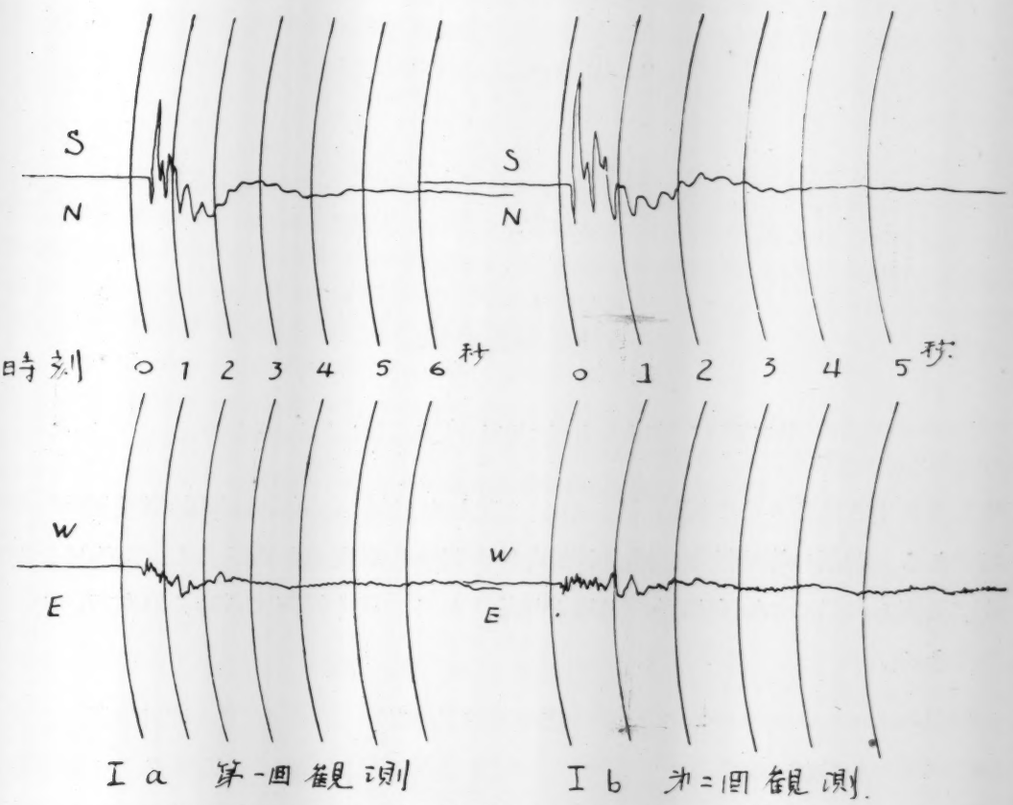

第三圖　Ⅰ架構を南北に變形せしめて放した時の觀測圖

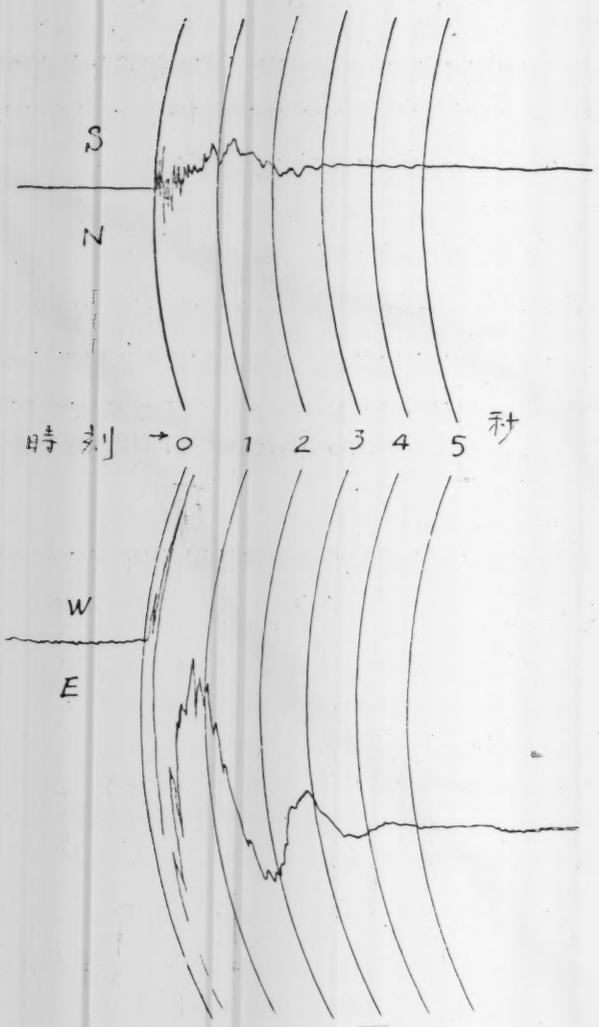

第四圖 II　架構を東西に變形せしめて放した時の觀測圖

等を分析するに各々その圖に (2), (3) と記した二組の、奇麗な減衰單弦振動を得たのである。週期の等時性と、減衰が割合に合理的な事實とから見ると、之等は架構 E 及び架構ホの二つの固有振動の記錄と推論される。斯く解釋する時その週期は次のやうである。

	第一次振動週期	第二次振動週期
架構 E	0.34 秒	0.15 秒
架構 解	0.40 秒	0.17 秒

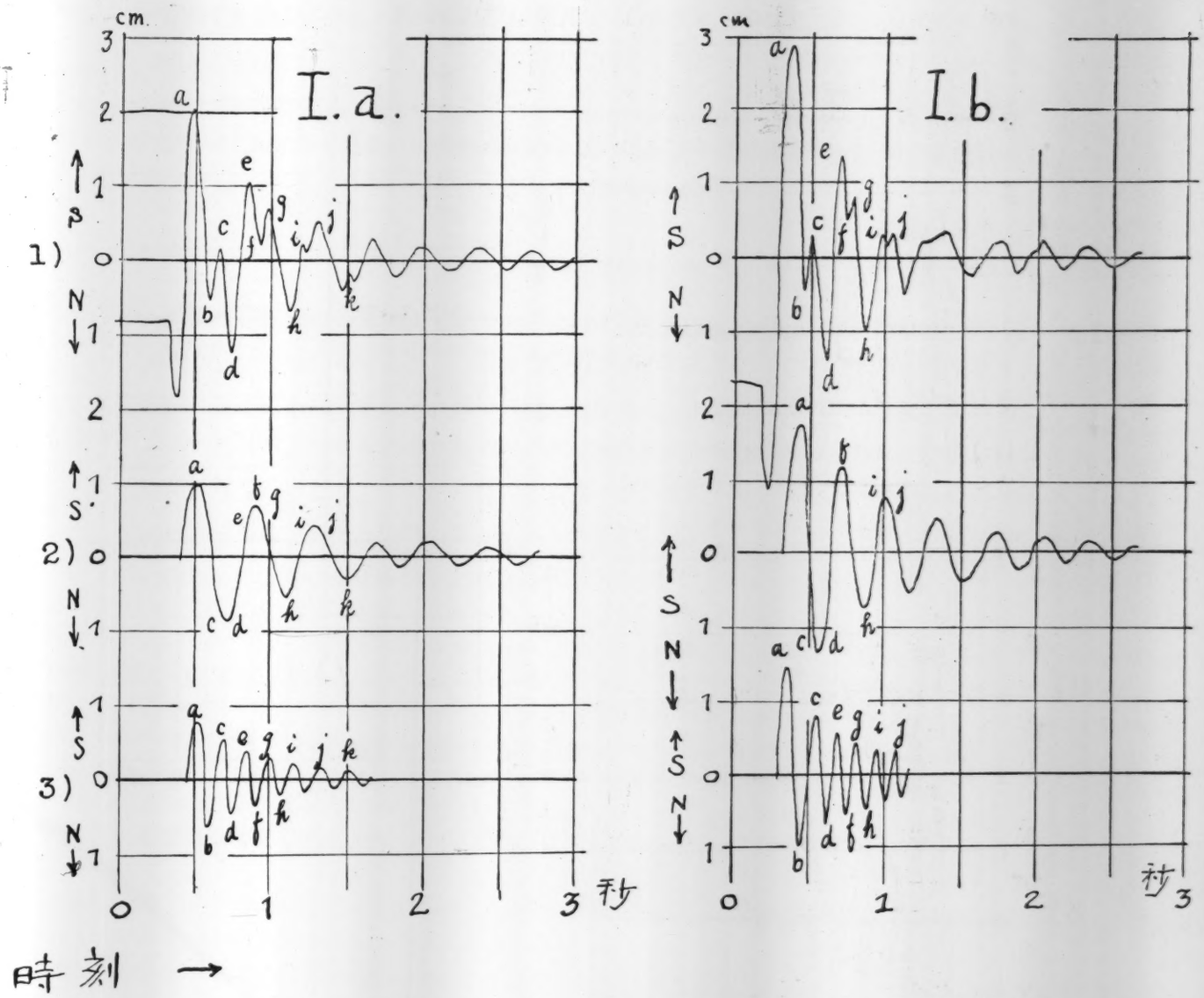

第五圖　架構 E の自由振動記錄の分析　倍率 60

注意　1)　自由振動

2)　第一次固有振動　その週期 0.40 秒

3)　第二次固有振動　その週期 0.17 秒

減衰に就いて

第五、第六圖の (2), (3) を見ると減衰の現象は極めて明瞭である。がその減衰の數値を論ずる事は少くし大膽に過ぐると思はるゝ故省略する。何となれば、此の觀測に使用せる微動計は極く精密なものとは言ひ難いものであるからその振動圖の振幅に

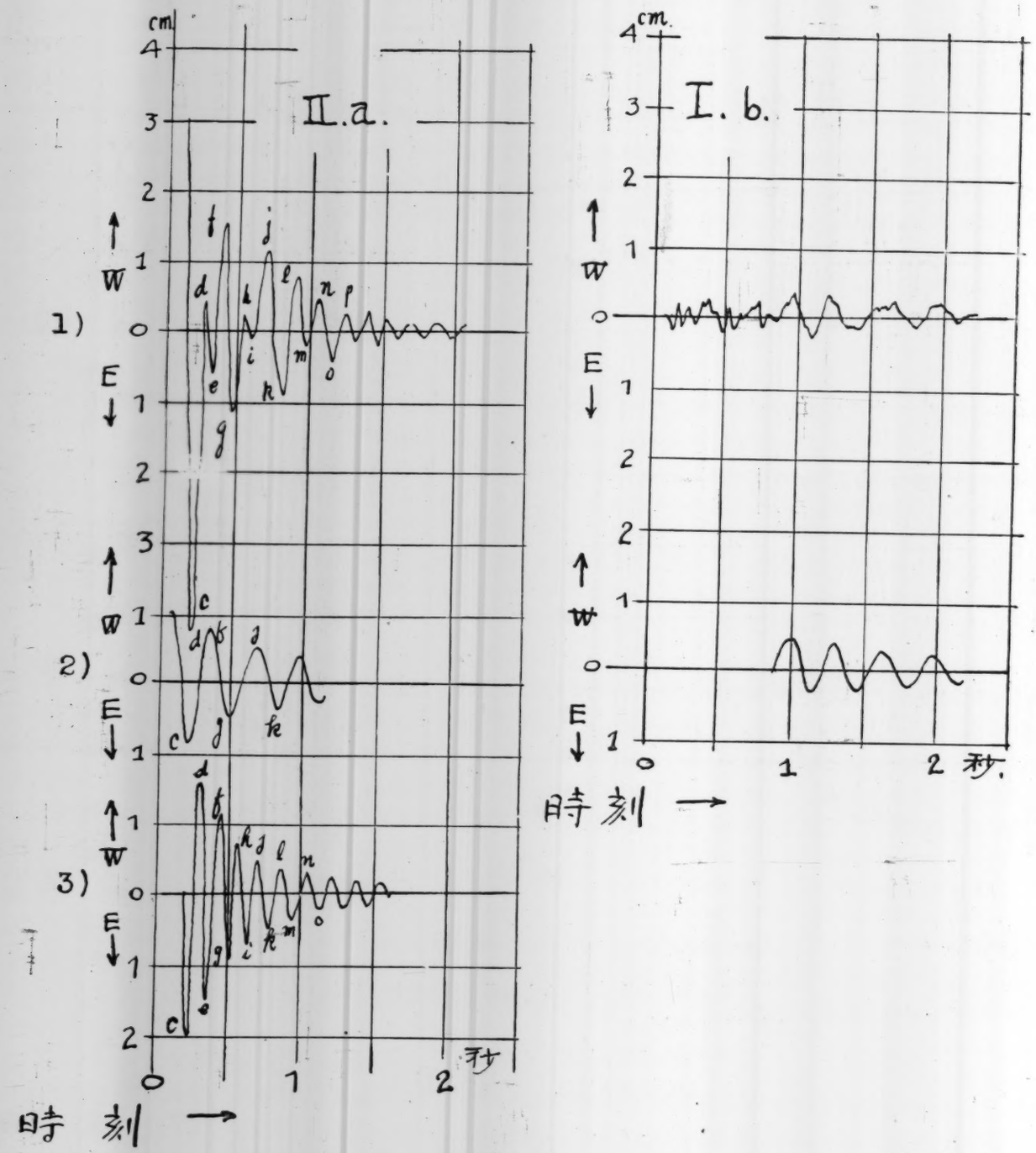

第六圖　架構ホの自由振動記錄の分析　倍率 60

注意　1)　自由振動

2)　第一次固有振動　その週期 0.34 秒

3)　第二次固有振動　その週期 0.15 秒

は可なり疑問があり、更に微動計の固有振動の除去に當つて誤差の入る機會もあり、最後に振動圖の分析に當つて又再び誤差の機會をも加へてゐるが故である。のみならず又一方に於ては、隣接せる架構との連結は柔ではあるがエネルギーの傳導があるだらうから減衰の原因を單に內部外部の抵抗力に歸する事は出來ない。從つて減衰の數値を考究しても決定的の結論は得られないからである。

初期の急振動に就いて

第三、第四圖の振動記錄を視るに、その初期に於て、主なる變形を與へた平面と直角な方向に振幅の相當大きい、急速な振動が認められる、その週期は極めて小さく、振幅は急激に消滅してゐる。此の振動が何物たるかに就いては明確な判斷を與へ得ないのであるが、加力方法の爲めに起つた局部的振動と解釋するより外に途が無いのでは無からうかと思ふ。（附記：微動計に樣々の方法でショツクを與へその振動圖を調べた結果には、斯樣な現象が現れなかつた點から見ると、それが微動計の觀殊な作用に依るものでない事は確かであらう）。

結　　論

之を要するに、此の觀測によつて鐵骨架構の振動性として

第一　固有振動週期の數値を測定し、

第二　著るしき減衰現象を認むる、

事が出來たのである。

以　　上

Monthly Means of the Daily Rates of the Riefler Clock in the Tôkyô Astronomical Observatory and their Bearing on the Occurrence of Earthquakes.

By **Mishio ISHIMOTO** and **Kênosuke TUZI.**

東京天文台に於けるリーフラー時計の遅速度變化と地震發生

所員　石本巳四雄
囑託　辻　光之助

一九一五年十一月より一九二八年十月に至る東京天文台に於けるリーフラー時計の遅速度變化と地震發生との間に多少の關係あるらしく思はれるため報告するものなり。

In the following table are given the monthly means of the daily rates of a Riefler clock maintained in the Tôkyô Astronomical Observatory. These values have been corrected for the effect of the change of pressure inside of the clock vessel according to the empirical formula

$$\frac{\Delta t}{\Delta p} = 0.181 \ \frac{\text{sec.}}{\text{mm.}}$$

and have been reduced to the rates corresponding to a reference pressure. The correction for the effect of the change of length of the clock pendulum caused by its temperature change has not been made, for the rates due to this effect is very small and is only 0.001 sec. for the temperature change of 1°C. When the daily rate of the clock became large, it was adjusted by means of a suitable regulation of the pressure inside of the clock vessel. For each of these cases, the means of the daily rates are given separately in the table corresponding to before and after the adjustment. Small circles marked in the graph denote the time of these adjustments. After the Kwantô great earthquake of 1923, the daily rate of the clock increased gradually until April of 1927 when it was found necessary to made an adjustment on the mass of the pendulum. The clock is now operating under the conditions $p = 656$ mm., $t = 30°$C with the mean daily rate -0.589 sec.

Monthly Means of the Daily Rates of a Riefler Clock in the Tôkyô Astronomical Observatory (from November 1914 to October 1928)

corrected for the pressure change inside of the vessel of the clock.

	1914	1917	1920	1923	1926
I	—	1.460	1.926	2.518	−0.517
II	—	1.502	1.974	2.248	−0.556
III	—	1.493	1.956	2.220	−0.534
IV	—	1.660	1.933	2.059 (1-26) 1.966 (27-29)	−0.475
V	—	1.695	1.972	1.961	−0.446
VI	—	1.854	1.910	2.056	−0.483
VII	—	1.797	1.975	1.777	−0.523
VIII	—	1.792	1.938	1.682	−0.549
IX	—	1.769	1.951	1.084	−0.640
X	— sec.	1.801	1.939	0.247	−0.662
XI	0.069	1.782	1.961	0.692	−0.692
XII	0.163	1.825	2.021	0.421	−0.759

	1915	1918	1921	1924	1927
I	0.423	1.857	2.001	0.379 (1-14) 1.131 (15-23) 1.902 (24-31)	−0.800
II	0.577	1.930	1.991	1.087	−0.781
III	0.705	1.875	2.011	1.177 (1- 8) 1.199 (9-14) 1.047 (14-31)	−0.681
IV	0.889	1.887 (1-18) 1.893 (19-30)	2.005	1.028	−0.677 (2-10) −0.677 (18-30)
V	0.903	1.930	1.967	0.952 (1-19) 0.929	−0.643
VI	0.999	1.889	1.977		−0.582 −0.788
VII	1.160	1.913	1.967		−0.679
VIII	1.172	1.861	1.969	0.175 (1- 6) 0.104 (7-14) 0.091 (16-30)	−0.664
IX	1.066	1.877	1.991	0.040 (1-17) 0.029 (18-30)	−0.656
X	1.064	1.832	2.052	0.003	−0.691
XI	1.170	1.849	2.059	−0.105	−0.719
XII	1.309	1.829	2.160	−0.160	−0.774

	1916	1919	1922	1925	1928
I	1.382	1.856	2.093	−0.119 (1-12) −0.209 (14-31)	−0.855
II	1.343	1.878	2.079	−0.219	−0.885
III	1.383	1.931	2.130	−0.254	−0.887
IV	1.349	1.891	2.107	−0.336	−0.878
V	1.394	1.877	2.033	−0.336	−0.922
VI	1.302	1.823	1.988	−0.406	−0.957
VII	1.314	1.814	1.970	−0.423	−0.850
VIII	1.301	1.891	1.917	−0.472	−0.804
IX	1.371	1.912	1.952	−0.521	−0.819
X	1.386	1.856	1.910	−0.543	−0.828
XI	1.366	1.891	2.028	−0.544	—
XII	1.381	1.901	2.222	−0.505	—

Remarks:—From November 1914 to May 1924—observed at Tôkyô.
From August 1924 to October 1928—observed at Mitaka.

TABLE OF LARGE EARTHQUAKES FELT AT TÔKYÔ DURING THE OBSERVATION.

	Name of earthquake	Date	Position of epicentre
A	Ryûgasaki	Dec. 8, 1921	140°21″E 35°56″N
B	Uraga-suidô	April 26, 1922	139 47 35 11
C	Tukubasan	Jan. 14, 1923	140 03 36 04
D	Kasimaoki	June 2, 1923	140 53 36 05
E	Kwantô	Sept. 1, 1923	139 22 34 59
F	Sagami	Jan. 15. 1924	139 17 35 26
G	Tôkyôwan	Aug. 3, 1926	139 48 35 33
H	Tonegawa	Jan. 1, 1928	139 58 36 03

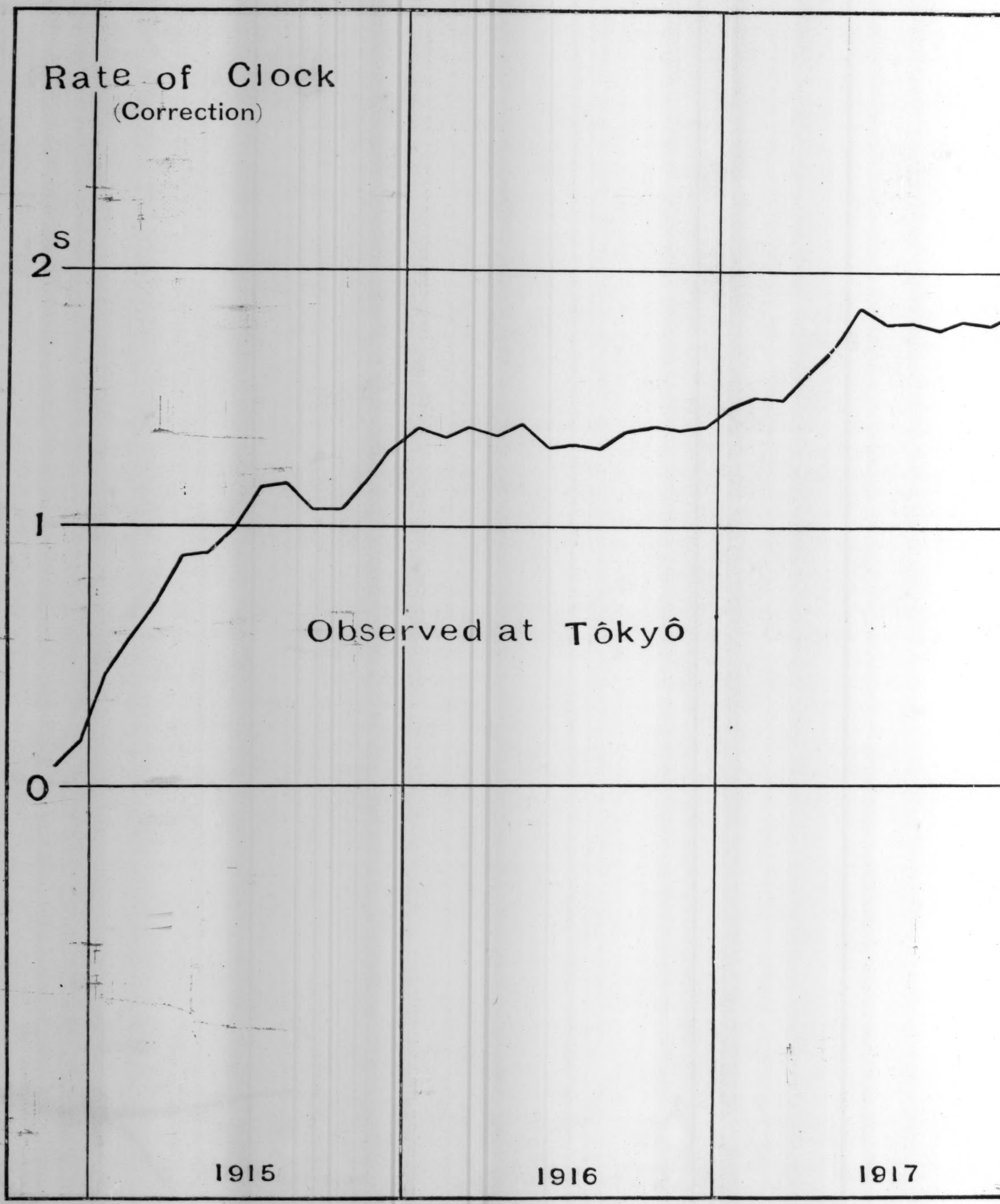

（震研彙報、第六號、圖版、石本、辻）

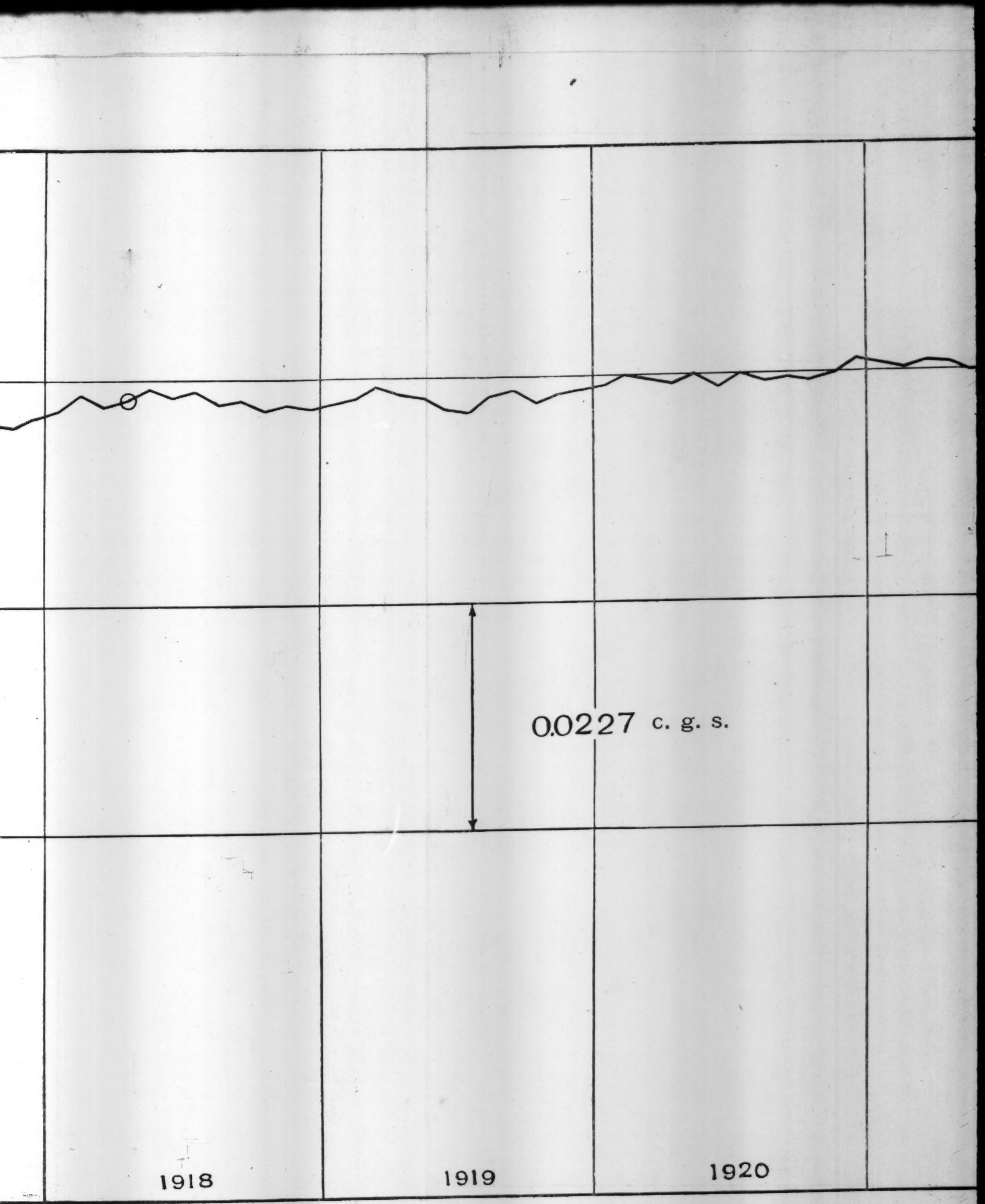
0.0227 c. g. s.
1918
1919
1920

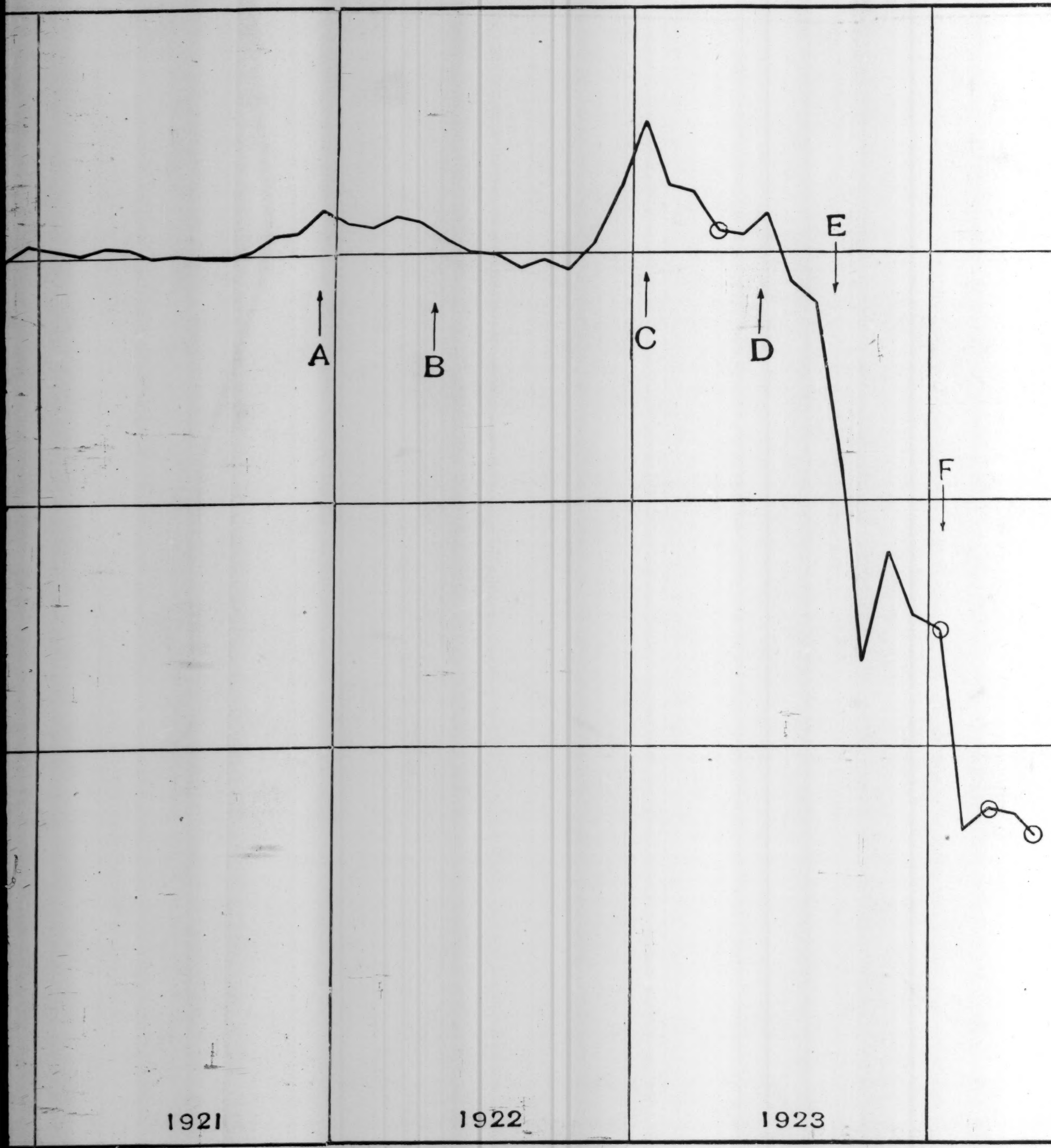
A
B
C
D
E
F
1921
1922
1923

Monthly Means of the Daily Rates of a Riefler's C
in the Tôkyô Astronomical Observatory

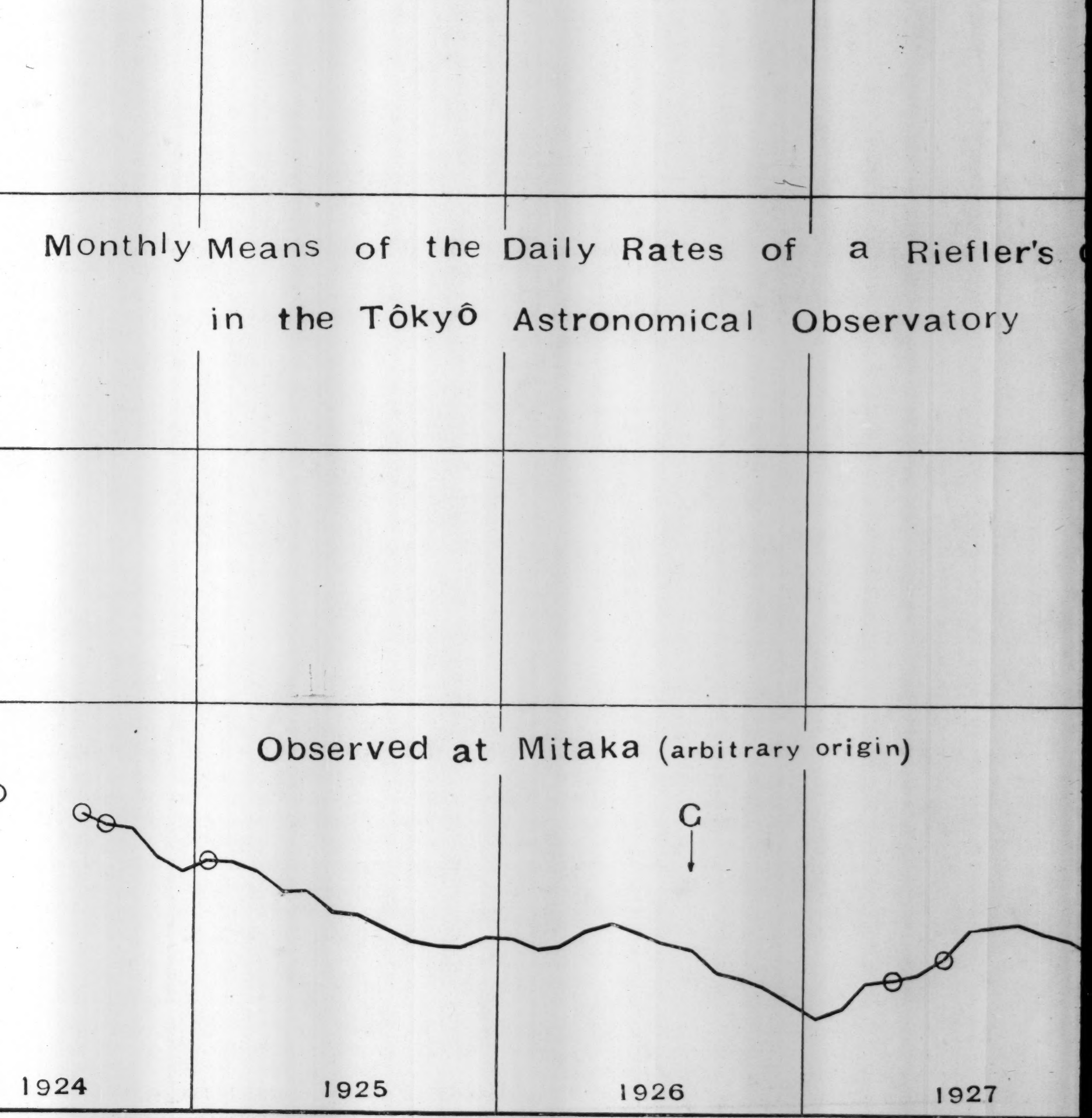

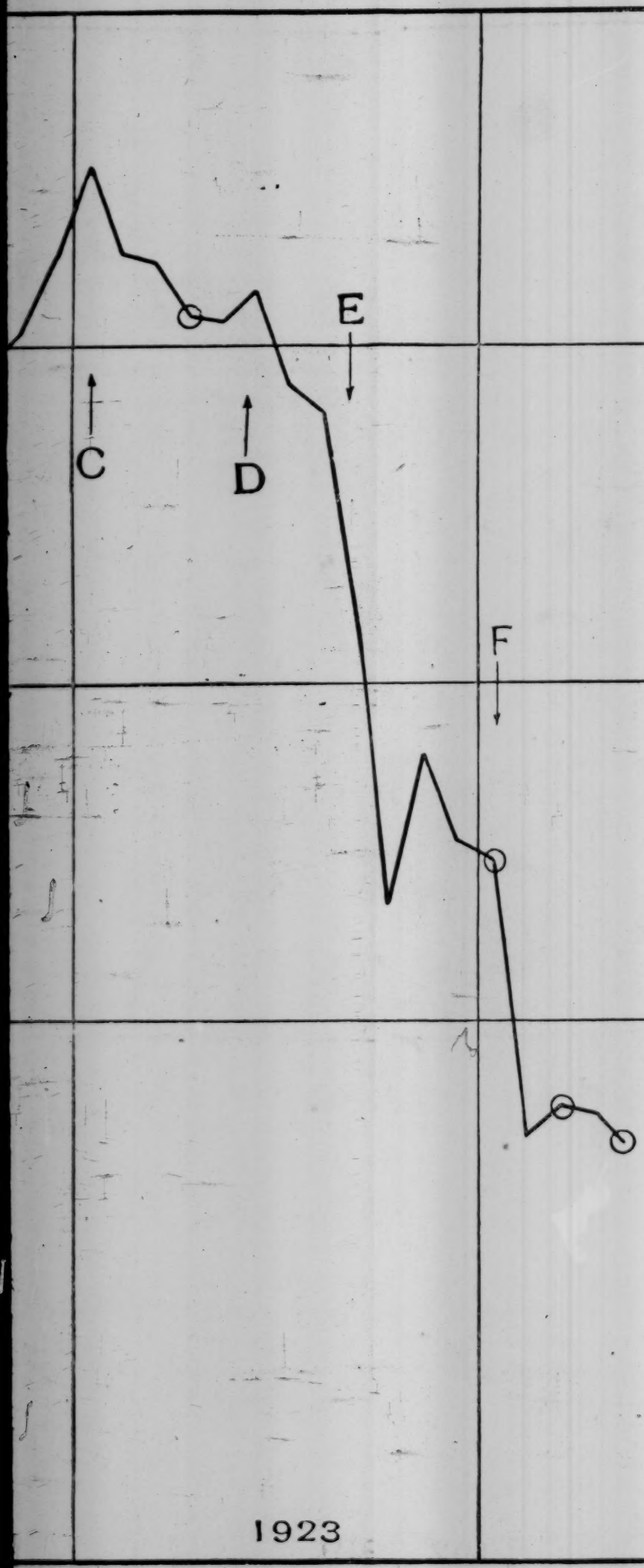

Monthly Means of the Daily

in the Tôkyô Astron

Observed at Mitak

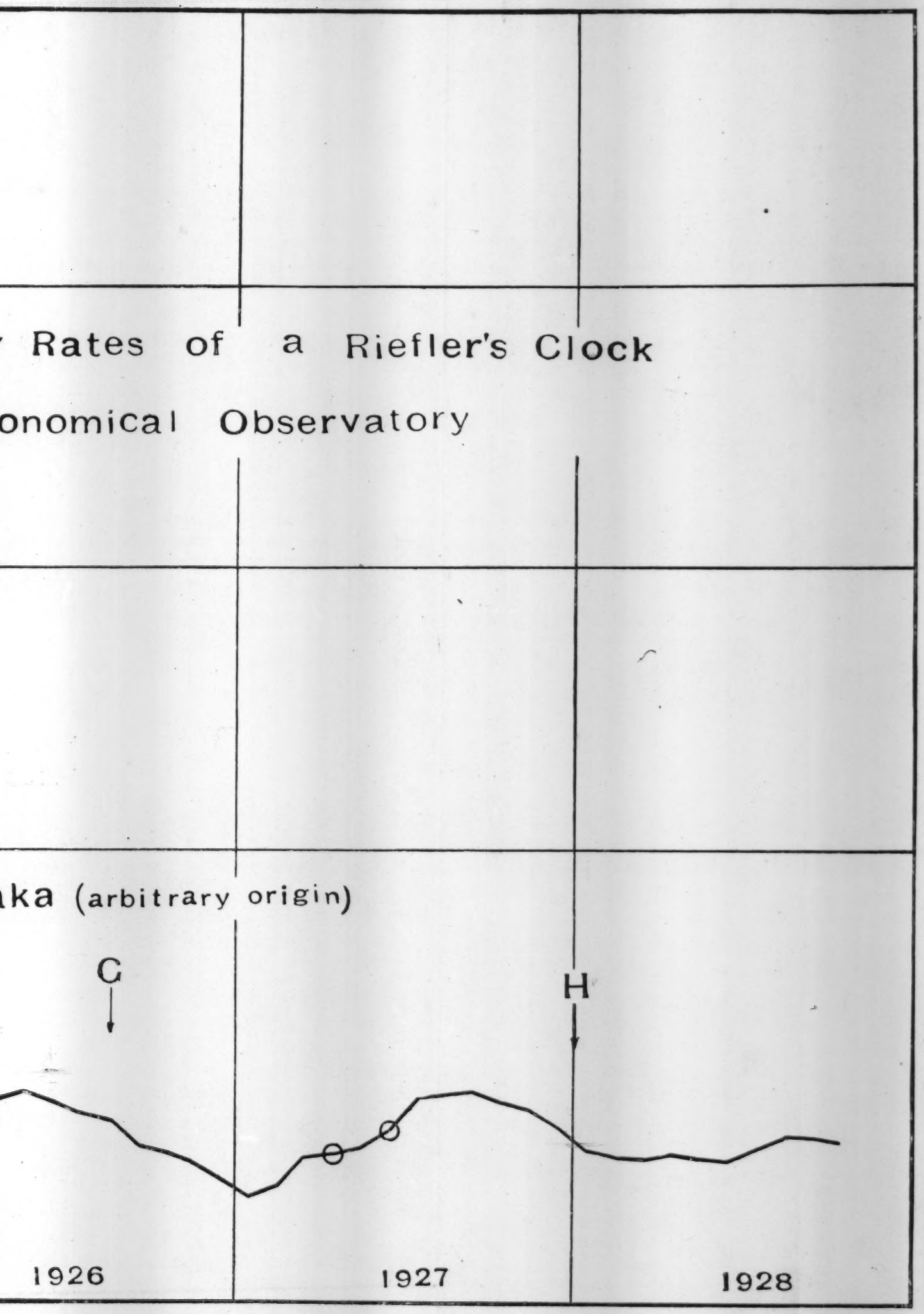
Rates of a Riefler's Clock
onomical Observatory
ka (arbitrary origin)
C
H
1926
1927
1928

═所　報═

○ 談 話 會 記 事

第二十九回談話會 （昭和三年九月十八日）

1. 震源の位置を求める作圖法に就て	中央氣象臺技師	和達清夫
1. 近海の低氣壓と海水面との關係（前回の續き）	囑託	山口生知
1. 丹後地震の水準測量の成果の一解釋	所員	坪井忠二
1. 再び地震發生の機巧に就て	所員	石本巳四雄
1. 安政五年二月廿六日の飛驒、越前、越中地震に就て	所員	今村明恒

第三十回談話會 （昭和三年九月廿五日）

1. 水中衝撃による深水波の生成	所員	妹澤克惟
1. 地震史料の調査（第一報）	所員	寺田寅彦
1. 地震帶に就て	所員	寺田寅彦
1. 初期微動繼續時間と震源距離との一次式に於ける係數の諸數値の意義	所員	松澤武雄
1. 殘存鑛物成生の岩漿分化に及ぼす影響に就て	所員	坪井誠太郎

第三十一回談話會 （昭和三年十月十六日）

1. 鐵骨を入れたる鐵筋コンクリート柱の實驗	囑託	齋田時太郎
1. 方位的及帶狀的に分布せる表面應力を受ける彈性球體の平衡	所員 所員	妹澤克惟 西村源六郎
1. 潮汐の負荷による油壺海岸の傾斜變化	所員	高橋龍太郎
1. 震動分解器による地震觀測の結果	所長	末廣恭二
1. 關東地方震原分布調査第二報	所員 囑託	今村明恒 小平孝雄

第三十二回談話會 （昭和三年十一月廿日）

1. 太平洋に於ける激震の分布	所員	宮部直巳
1. 一九一四年十一月より一九二八年十月に至る東京天文臺「リーフラー」時計の遲速變化	囑託	辻光之助
1. 内部歪核を有する半無限固體の表面傾斜（第一報）	所員	妹澤克惟
1. 複式水平振動計に就て	所長	末廣恭二
1. 笠置山地塊の運動	所員	多田文男

第三十三回談話會 （昭和三年十二月十八日）

1. 三鷹比較基線の測定結果に就て	陸地測量部三角科長	青柳和夫
1. 關東大地震の驗震的結果	中央氣象臺技師	國富信一
1. 相模灣地震機巧補遺	所員 所員	藤原咲平 高山威雄

1. 地震と地塊運動 — 所員 坪井忠二

1. 上下微動計を用ひたる本研究所建物振動測定 — 所員 石本巳四雄 / 所員 高橋龍太郎

1. 内部歪核を有する半無限固體の表面傾斜（第二報）
1. 水底衝撃による淺海波の生成（第一報）
— 所員 妹澤克惟

第三十四回談話會（昭和四年一月十五日）

1. 水底衝撃ニヨル淺海波ノ生成（第二報） — 所員 妹澤克惟

1. 海上ビルデング新築鐵骨架構振動觀測 — 囑託 齋田時太郎 / 武藤清

1. 近海の低氣壓と海水面との關係（前回の續） — 囑託 山口生知

1. 油壺灣内の副振動に依る地表傾斜運動 — 所員 高橋龍太郎

第三十五回談話會（昭和四年二月十九日）

1. 神戸海洋氣象臺及中央氣象臺「リーフラー」時計のレートに就て — 中央氣象臺技師 關口鯉吉 / 谷本誠

1. 内部の多重原による「レーレー」波の生成
附、内部の歪核による半無限固體の表面傾斜（第三報）
— 所員 妹澤克惟 / 所員 西村源六郎

1. 伊豆神津島火山の地質構造と其の岩石に就て — 所員 津屋弘逵

1. 地表面の高さ及地變の量 — 所員 井上宇胤

1. 大陸移動の原因 — 囑託 長岡半太郎

1. 丹後震災地に於ける其の後の水平異動に就て — 陸地測量部三角科長 青柳和夫

1. 重力狀況の變動に就て（第一報） — 所員 坪井忠二

○ 出張

昭和三年九月一日火山地質調査の爲め山梨縣下へ出張 — 所員 坪井誠太郎

昭和三年九月一日火山地質調査の爲め山梨縣下へ出張 — 理學士 市來政兼

昭和三年九月廿日地震事項取調の爲め大阪府及和歌山兵庫二縣下へ出張 — 囑託 那須信治

昭和三年九月廿二日地震事項取調の爲め和歌山三重縣下へ出張 — 囑託 小平孝雄

昭和三年十二月十八日學術上取調の爲め德島、和歌山二縣下へ出張 — 所員 今村明恒

昭和四年一月四日學術上取調の爲め神奈川縣下へ出張 — 所員 石本巳四雄

昭和四年四月二十日印刷
昭和四年四月二十三日發行

編纂兼
發行者　東京帝國大學地震研究所

東京市神田區美土代町二丁目一番地
印刷者　島　連　太　郎

東京市神田區美土代町二丁目一番地
印刷所　三　秀　舍

東京市神田區南神保町十六番地
賣捌所　岩　波　書　店

BULLETIN OF
THE EARTHQUAKE RESEARCH INSTITUTE
TOKYO IMPERIAL UNIVERSITY

April, 1929. Vol. VI.

Contents

Papers Contributed

Further Studies on Rayleigh-waves having Some Azimuthal Distribution. (in English) ..... K. Sezawa

Formation of Deep-Water Waves due to Subaqueous Shocks. (in English) ..... K. Sezawa

Elastic Equilibrium of a Spherical Body under Surface Tractions of a Certain Zonal and Azimuthal Distribution. (in English) ..... K. Sezawa, G. Nishimura

On the Damped Transversal Vibration of Prismatic Bars. (in English) ..... K. Suyehiro

An Interpretation of the Results of the Repeated Precise Levellings in the Tango District after the Tango Earthquake in 1927. (in English) ..... C. Tsuboi

Tilting Motion of the Earth Crust caused by Tidal Loading. (in English) ..... R. Takahashi

Experimental Investigations of the Deformation of Sand Mass by Lateral Pressure. (with an Appendix.) (in English) ..... T. Terada, N. Miyabe

Sur le mécanisme de la production des ondes sismiques. (in Japanese) ..... M. Ishimoto

On the Mechanism of the Great Sagami Bay Earthquake on September 1, 1923. (in English) ..... S. Fujiwhara, T. Takayama

Observation of Some Recent Earthquakes and their Time-distance Curves. (Part II) (in English) ..... T. Matuzawa

Observation of Some Recent Earthquakes and their Time-distance Curves. (Part III) (in English) ..... T. Matuzawa

Observation of Some Recent Earthquakes and their Time-distance Curves. (Part IV) (in English) ..... T. Matuzawa

A Graphical Determination of the Position of the Hypocenter of an Earthquake and the Velocity of the Propagation of the Seismic Waves. (in English) ..... R. Takahashi

On the Aftershocks of the Tango Earthquake. (in Japanese) ..... N. Nasu

A Long Period Fluctuation in Latitude of the Seismic Activity on the Earth. (in English) ..... T. Terada, N. Miyabe

An Investigation of the Vibration of a Steel Frame. (in Japanese) ..... Y. Uchida, T. Saida, K. Muto

Report

Monthly Means of the Daily Rates of the Riefler Clock in the Tokyo Astronomical Observatory and their Bearing on the Occurrence of Earthquakes (in English) ..... M. Ishimoto, K. Tuzi

Institute Notes

(For the papers written in Japanese or in occidental languages, the abstracts are given in occidental languages or in Japanese respectively)